MARINE ENVIRONMENTAL EPIGENETICS

EDITED BY: Jose M. Eirin-Lopez and Hollie Putnam
PUBLISHED IN: Frontiers in Marine Science

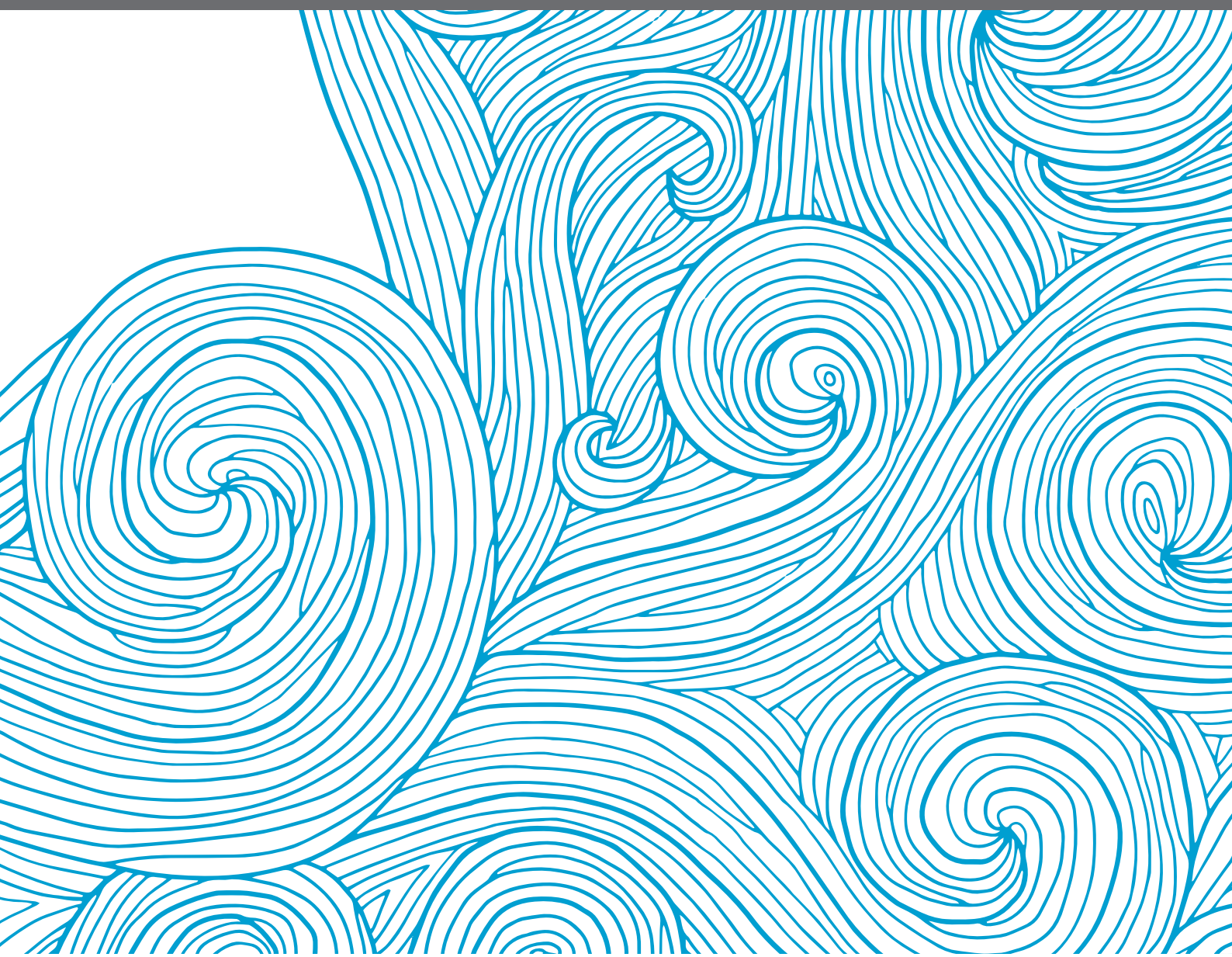

frontiers Research Topics

ISSN 1664-8714
ISBN 978-2-88966-977-6
DOI 10.3389/978-2-88966-977-6

About Frontiers

Frontiers is more than just an open-access publisher of scholarly articles: it is a pioneering approach to the world of academia, radically improving the way scholarly research is managed. The grand vision of Frontiers is a world where all people have an equal opportunity to seek, share and generate knowledge. Frontiers provides immediate and permanent online open access to all its publications, but this alone is not enough to realize our grand goals.

Frontiers Journal Series

The Frontiers Journal Series is a multi-tier and interdisciplinary set of open-access, online journals, promising a paradigm shift from the current review, selection and dissemination processes in academic publishing. All Frontiers journals are driven by researchers for researchers; therefore, they constitute a service to the scholarly community. At the same time, the Frontiers Journal Series operates on a revolutionary invention, the tiered publishing system, initially addressing specific communities of scholars, and gradually climbing up to broader public understanding, thus serving the interests of the lay society, too.

Dedication to Quality

Each Frontiers article is a landmark of the highest quality, thanks to genuinely collaborative interactions between authors and review editors, who include some of the world's best academicians. Research must be certified by peers before entering a stream of knowledge that may eventually reach the public - and shape society; therefore, Frontiers only applies the most rigorous and unbiased reviews.
Frontiers revolutionizes research publishing by freely delivering the most outstanding research, evaluated with no bias from both the academic and social point of view. By applying the most advanced information technologies, Frontiers is catapulting scholarly publishing into a new generation.

What are Frontiers Research Topics?

Frontiers Research Topics are very popular trademarks of the Frontiers Journals Series: they are collections of at least ten articles, all centered on a particular subject. With their unique mix of varied contributions from Original Research to Review Articles, Frontiers Research Topics unify the most influential researchers, the latest key findings and historical advances in a hot research area! Find out more on how to host your own Frontiers Research Topic or contribute to one as an author by contacting the Frontiers Editorial Office: frontiersin.org/about/contact

MARINE ENVIRONMENTAL EPIGENETICS

Topic Editors:
Jose M. Eirin-Lopez, Florida International University, United States
Hollie Putnam, University of Rhode Island, United States

Citation: Eirin-Lopez, J. M., Putnam, H., eds. (2021). Marine Environmental Epigenetics. Lausanne: Frontiers Media SA. doi: 10.3389/978-2-88966-977-6

Table of Contents

frontiers in Marine Science

EDITORIAL
published: 10 May 2021
doi: 10.3389/fmars.2021.685075

Editorial: Marine Environmental Epigenetics

Jose M. Eirin-Lopez[1]* *and Hollie Putnam*[2]*

[1] Biological Sciences, Florida International University, Miami, FL, United States, [2] Biological Sciences, University of Rhode Island, Kingston, RI, United States

Keywords: epigenetics (DNA methylation histone modifications, chromatin remodeling), phenotypic plasticity, ecology, evolution, marine biology

Editorial on the Research Topic

Marine Environmental Epigenetics

During the last decade, the growth of the epigenetics field has accelerated rapidly, particularly driven by the transition from basic laboratory-focused studies to more applied efforts including fieldwork, experimental, and observational components. This has been possible thanks to the advent of molecular technologies, expanding our abilities to develop epigenetic analyses in non-model organisms (and in a cost-effective fashion), as well as to the advancements in knowledge of epigenetic machinery and genetic-epigenetic interactions in ecologically and environmentally relevant taxa. However, the most compelling reason behind such an explosion has been the growing interest in epigenetics by ecologists, evolutionary biologists, environmental scientists, taxonomists, etc., motivated by the role of these mechanisms governing (to a large extent) phenotypic plasticity responses within and across generations. These mechanisms extend far beyond responses to environmental stress (such as pollution and climate change effects) and include developmental effects, life-history traits, pathogenicity, invasiveness, aging, biomarkers, restoration, among others. Such a broad range of effects showcase the fundamental role of epigenetic regulation in transmitting environmental signals to the genome and regulating how the genetic information is subsequently modulated through gene expression (e.g., phenotypic plasticity) to address such signals. Based on these critical aspects and the rate of advancements, we anticipate that the field known as environmental epigenetics will not be slowing down anytime soon.

While the emergence of environmental epigenetic studies is ubiquitous, the impact of global climate change and the Anthropocene in the world's oceans has driven the need to broaden the epigenetic knowledge to diverse marine ecosystems. The marine system provides a suite of very powerful and informative models to study the role of epigenetic modifications regulating gene function across multiple ecologically and economically important taxa. Critically, such studies are laying the foundations for developing solutions that are informed by epigenetic data, notably assisted evolution and development of biomarkers of stress. The relative absence of epigenetic studies on these subjects, along with the many groups actively developing research on this field, led us to propose a session on this topic at the 2019 Aquatic Sciences Meeting of the Association for the Sciences of Limnology and Oceanography (ASLO), held in San Juan, Puerto Rico. The excitement and momentum generated there translated into the present special issue that Frontiers in Marine Science was kind enough to host. With this effort, our goal was to provide a venue where investigators pioneering the field of marine environmental epigenetics could publish their latest research, and also to help establish a solid foundation informing the future of this field. Based on the 37,000 collective views of all papers published in the present special issue at the time of writing this editorial (probably many more now), we believe we have successfully done so!

OPEN ACCESS

Edited and reviewed by:
Ciro Rico,
University of the South Pacific, Fiji

***Correspondence:**
Jose M. Eirin-Lopez
jeirinlo@fiu.edu
Hollie Putnam
hputnam@uri.edu

Specialty section:
This article was submitted to Marine Molecular Biology and Ecology, a section of the journal Frontiers in Marine Science

Received: *24 March 2021*
Accepted: *06 April 2021*
Published: *10 May 2021*

Citation:
Eirin-Lopez JM and Putnam H (2021) Editorial: Marine Environmental Epigenetics. Front. Mar. Sci. 8:685075. doi: 10.3389/fmars.2021.685075

The present special issue consists of 13 research papers gathering more than 60 authors from 25 institutions worldwide. The species studied ranged from microalgae to marine mammals, with a particular emphasis on fish and mollusks. Among the different epigenetic mechanisms, DNA methylation is the most widely studied, although several papers discuss other mechanisms such as chromatin modifiers, histones, and small RNAs. Environmental conditions are challenging organisms in a variety of ways, and this special issue illustrates that by including ocean acidification, thermal stress, seasonal variation, pathogen infection, ocean cycles, among many others, as drivers of the present studies.

Starting with marine algae, Zhao et al. provide a comprehensive study addressing the role of proteins involved in chromatin remodeling (Polycomb and Trithorax groups) using the model diatom *Phaeodactylum tricornutum*. This work provides a genome-wide profiling of histone marks associated with these proteins, and their role in genome function regulation, underscoring the ancestral nature of these mechanisms.

This special issue also includes two papers focused on corals. In the first, Dimond and Roberts investigate changes in the coral *Porites astreoides* DNA methylation in Belize in response to simulated environmental change via transplantation to a novel common garden environment. Their findings indicate subtle shifts in DNA methylation state reflective of the move to the common garden environment. The positive relationship between epigenetic and genetic features indicates potential heritability, which would be necessary for methylation to be implicated as a potential mechanism underlying trans-generational acclimatization. In the second paper, Rodriguez-Casariego et al. investigate the dynamic nature of epigenetic changes in the coral *Acropora cervicornis*. They find temporal changes in genome-wide patterns of DNA methylation, the majority of which are linked to seasonal temperature change. These findings highlight the importance of considering seasonality in field studies to precisely determine the extent of epigenetic responses to environmental stressors.

Several papers use mollusks as model systems to study epigenetic responses to ocean acidification (OA). Bogan et al. quantified global DNA methylation and gene expression over time across different OA regimes in the gasteropod pteropod *Limacina helicina antarctica*, and calculated historical signatures of methylation. They found global DNA methylation responded to low pH and linkage between downregulated genes and high values of calculated methylation. These findings support the potential role of DNA methylation in regulating transcriptomic responses to future ocean acidification. In another paper focused on OA, Venkataraman et al. examined the influence of OA in gonad tissue from the Eastern oyster, *Crassostrea virginica*, detecting DNA methylation primarily in gene bodies and differentially methylated loci between OA treatments. These results again support the role of DNA methylation in transcriptional control in response to OA, with changes in gonad methylation also indicating the potential for these methylation patterns to be inherited by the offspring. In a complementary paper, Downey-Wall et al. studied DNA methylation in calcifying tissues under OA through time in *C. virginica*. They found a small number of OA-induced differentially methylated loci, which corresponded with a weak association between OA-induced changes in genome-wide gene body DNA methylation and gene expression and a subtle response in a large number of genes. These results highlight the value of and need for tissue-specific studies of methylation and expression.

Mollusks were also used as models to study the epigenetic response to pathogens. Johnson et al. combined DNA methylation and gene expression in the Eastern oyster to describe responses to infection by the protistan parasite *Perkinsus marinus* (the cause of the disease commonly known as dermo infection). A network of genes that change in expression in response to infection was discovered, suggesting that gene body DNA methylation is a better predictor of gene expression variation than it is of the overall magnitude of gene expression.

In a more derived marine deuterostome system, Strader et al. explored the epigenetic basis of intra- and inter-generational plasticity in the purple sea urchin by examining relationships between changes in DNA methylation, transcription, and phenotype (embryo spicule length). Here, results suggest that different forms of environmentally induced plasticity are observable across different time scales with a role for DNA methylation, but apparent uncoupling between methylation dynamics in rapid transcriptional responses and whole-organism traits.

Fishes were also well-represented taxa in the present special issue. Accordingly, Fellous and Shama characterized the evolution of the epigenetic machinery involved in key molecular epigenetic pathways including DNA methylation, histone modifications, macroH2A histone, and miRNA biogenesis/turnover in the threespine stickleback, *Gasterosteus aculeatus*. Their results support the need for similar studies across a diversity of taxa, in order to support progress in epigenetic aspects of assisted evolution, conservation, aquaculture, fisheries, and climate change-adaptation studies. Beyond the stickleback model, Beemelmanns et al. investigated the potential for thermal stress and hypoxia to trigger epigenetic changes in the Atlantic salmon, *Salmo salar*. Their examination of a specific suite of genes focused on cellular stress response and metabolism uncovering distinct CpG methylation profiles for fish exposed to different environmental treatment groups. These results support dynamic associations between CpG methylation and transcript expression, supporting wash-in and wash-out temporal dynamics for short-term and long-term acclimatory changes in response to the environment. Intra-generational plasticity and epigenetic inheritance were assessed by Ryu et al. using the reef fish *Acanthochromis polyacanthus* as a model system. While their prior work reported evidence for inter-generational plasticity, the results presented in this paper support that distinct genetic toolkits may be used for intra-generational plasticity to ocean warming in the same species collected from different latitudes. Examination of multi-generational epigenetic signatures in fish by, Major et al. found changes in epigenetic state in young silversides, *Menidia beryllina*, when their parents were exposed to endocrine disrupting chemicals (EDCs). The F1 and some of the F2 generation showed altered methylation in genes

potentially indicative of EDC response providing data for epigenetic inheritance.

Lastly, a study in marine mammals by Beal et al. helps round up the wide taxonomic reach and broad applicability of epigenetic tools representative of the state of the field and in this present special issue. Here, an epigenetic and non-invasive method for aging bottlenose dolphins is defined, building on the known relationship between chronological age and DNA methylation at specific loci. Given that this tool is minimally-invasive, can be implemented at a large-scale using skin biopsy samples, and critically is accurate in estimating dolphin age, it presents a valuable approach to generating age data from free-ranging cetacean populations.

Collectively, this special issue highlights the growing body of knowledge in marine environmental epigenetics. It showcases both strong and subtle epigenetic responses, supports a link between DNA methylation, transcription, and phenotypic plasticity, and highlights many of the potential applications of this emerging field. Interestingly, although DNA methylation is currently the most well-studied mechanism, the lack of substantial and direct linkage with transcriptional state provides the broad message that the key for epigenetic regulation likely resides in the synergistic interaction among multiple types of epigenetic mechanisms. Such integrative work, while challenging, will enrich our understanding of the eco-evolutionary consequences of epigenetics and inform its applications in the marine context.

We hope you enjoy the present special issue and that it brings new inspiration for your future research. We look forward to working with this emerging field to advance our understanding of marine environmental epigenetics under a changing climate.

AUTHOR CONTRIBUTIONS

All authors listed have made a substantial, direct and intellectual contribution to the work, and approved it for publication.

FUNDING

This work was supported by funding from the US National Science Foundation grants EF-1921465 and OCE, IEP, EPSCoR-1756623 to HP and EF-1921402 to JME-L.

Conflict of Interest: The authors declare that the research was conducted in the absence of any commercial or financial relationships that could be construed as a potential conflict of interest.

frontiers in Marine Science

ORIGINAL RESEARCH
published: 26 September 2019
doi: 10.3389/fmars.2019.00561

The Bottlenose Dolphin Epigenetic Aging Tool (BEAT): A Molecular Age Estimation Tool for Small Cetaceans

*Andria P. Beal[1], Jeremy J. Kiszka[2], Randall S. Wells[3] and Jose M. Eirin-Lopez[1]**

[1] Environmental Epigenetics Laboratory, Department of Biological Sciences, Center for Coastal Oceans Research, Institute of Water and Environment, Florida International University, North Miami, FL, United States, [2] Department of Biological Sciences, Florida International University, North Miami, FL, United States, [3] Chicago Zoological Society's Sarasota Dolphin Research Program, c/o Mote Marine Laboratory, Sarasota, FL, United States

Age constitutes a critical parameter for the study of animal populations, providing information about development, environmental effects, survival, and reproduction. Unfortunately, age estimation is not only challenging in large, mobile and legally protected species, but often involves invasive sampling methods. The present work investigates the association between epigenetic modifications and chronological age in small cetaceans. For that purpose, DNA methylation at age-linked genes was characterized in an extensively studied, long-term resident common bottlenose dolphin (*Tursiops truncatus*) community from Sarasota Bay (FL, United States) for which sampled individuals have a known age. Results led to the identification of several CpG sites that are significantly correlated to chronological age in this species with the potential for sex to play a role in the modulation of this correlation. These findings have allowed for the development and validation of the "Bottlenose dolphin Epigenetic Age estimation Tool" (BEAT), improving minimally-invasive age estimation in free-ranging small cetaceans. Overall, the BEAT proved to be accurate in estimating age in these organisms. Given its minimally-invasive nature and potential large-scale implementation using skin biopsy samples, this tool can be used to generate age data from free-ranging small cetacean populations.

Keywords: DNA methylation, population parameter, sex, correlation – regression analysis, pyrosequencing

OPEN ACCESS

Edited by:
Andrew Stanley Mount, Clemson University, United States

Reviewed by:
Charles Rice, Clemson University, United States
Daniel Rittschof, Duke University, United States

***Correspondence:**
Jose M. Eirin-Lopez
jeirinlo@fiu.edu

Specialty section:
This article was submitted to Marine Molecular Biology and Ecology, a section of the journal Frontiers in Marine Science

Received: *04 June 2019*
Accepted: *27 August 2019*
Published: *26 September 2019*

Citation:
Beal AP, Kiszka JJ, Wells RS and Eirin-Lopez JM (2019) The Bottlenose Dolphin Epigenetic Aging Tool (BEAT): A Molecular Age Estimation Tool for Small Cetaceans. Front. Mar. Sci. 6:561. doi: 10.3389/fmars.2019.00561

INTRODUCTION

Dolphins and porpoises are small cetaceans that occur in all marine habitats around the globe, and are threatened by a wide range of human activities (Pompa et al., 2011; Davidson et al., 2012). Common bottlenose dolphins (*Tursiops truncatus*), the model organism used in this study, are wide-ranging animals (Dans et al., 2010; Wells and Scott, 2018) occurring in estuarine, coastal, shelf, and oceanic habitats in temperate, subtropical, and tropical waters around the globe. Unfortunately, because small cetaceans often associate in coastal or near coastal areas, they often are exposed to multiple concurrent anthropogenic stressors (e.g., pollution, boat traffic, bycatch in fishing gears, etc.) with potentially significant impacts on populations. These species are often difficult to study, and access to carcasses to collect biological data is relatively limited, particularly for wild migratory

populations. Such problem has been alleviated by the progressive implementation of remote collection biopsies over the past two decades, improving our understanding of the population structure, feeding ecology, and ecotoxicology of free-ranging small cetacean populations from around the world (Fossi et al., 2000; Torres et al., 2003; Kiszka et al., 2011). Yet, the accurate estimation of chronological age, a critical population parameter, remains elusive from biopsy samples in these organisms.

Age constitutes a critically important parameter for population studies. Within a given population, several aspects of the biology of species can be investigated, including reproductive success, number of individuals of reproductive age, and the age composition of the population (Campana, 2001; Westgate and Read, 2007). In addition, age can be correlated to a variety of parameters, including pollutant loads, foraging tactics, and social structure. However, it is notoriously difficult to determine the age of bottlenose dolphins (as well as many other marine organisms), partly because they do not have conclusive external phenotypic traits that can be visually associated with age (Wilson et al., 1997; Miller et al., 2010; Hartel et al., 2015).

Current methods to estimate age in dolphins and other marine mammals include the use of body size, although this generally provides a rough estimation of the age group in which the animal may be included [e.g., adolescent versus adult (Baker et al., 2018)]. Another very accurate method includes removal of a tooth by a veterinarian, under local anesthesia, longitudinal sectioning, and quantification of growth layer groups in the tooth (International Whaling Commission, 1980; Hohn et al., 1989). This approach requires capture and handling of animals, which may not be feasible or desirable in some cases such as with endangered populations. Cost-effective, efficient, less-invasive alternative methods for obtaining accurate age estimates for large numbers of animals, without the need for capture, would be very useful. Biopsy dart sampling is a well-established technique for obtaining small tissue samples from cetaceans (Barrett-Lennard et al., 1996; Krutzen et al., 2002), and efforts have been made to use such samples for age estimation. Initial work has included the analysis of chromosomal telomere length and lipid accumulation in skin samples of cetaceans (Herman et al., 2009; Olsen et al., 2012). These techniques are limited by the strong influence of environmental conditions and for displaying a very wide range of values across individuals of similar chronological age. More specifically, telomere analyses can also be biased by the high variability in telomere lengths displayed by cetaceans (Olsen et al., 2012), as well as by its correlation with paternal age (Kappei and Arturo Londoño-Vallejo, 2008; Broer et al., 2013).

Complementary to traditional molecular analyses, the study of epigenetics [i.e., the study of phenomena and mechanisms that cause chromosome-bound, heritable (mitotically and/or meiotically) changes to gene expression that are not dependent on changes to DNA sequence (Deans and Maggert, 2015)] is emerging as a very promising framework to estimate chronological and biological age from DNA samples. Epigenetic age estimation (hereinafter referred to as aging) is based on the analysis of DNA methylation (addition of a methyl group to a Cytosine in the DNA sequence to form 5-methylcytosine). This modification is found at 60–80% of CpG sites (where a cytosine, C, is next to a guanine, G, in the DNA sequence) across vertebrate genomes (Jones, 2001, 2012) both at gene bodies and promoters (Deaton and Bird, 2011), participating in the regulation of gene expression in response to developmental and environmental signals (Eirin-Lopez and Putnam, 2018). Most importantly, it has been shown that the %DNA methylation at specific positions of certain genes correlates linearly with chronological age, making age prediction reliable as demonstrated in the case of mammals including humans (Grönniger et al., 2010; Polanowski et al., 2014), as well as in other vertebrates (Paoli-Iseppi et al., 2019). This property has boosted the development of epigenetic aging tools that are now being successfully used in human forensics (Horvath, 2013; Shabani et al., 2018) as well as in marine organisms (Polanowski et al., 2014; Eirin-Lopez and Putnam, 2018).

In the present study we investigate the relationship between epigenetic modifications in age-responsive genes and chronological age in mammals, and their potential to develop an age evaluation tool for bottlenose dolphins and potentially other small cetacean species. For that purpose, genes displaying age-influenced changes in DNA methylation (*GRIA*2, *TET*2, and *CDKN2*A) were examined, in agreement with previous reports on humpback whales (Polanowski et al., 2014). In addition, we explored the potential for sex-specific differences in aging.

MATERIALS AND METHODS

Sample Collection

Skin samples from 39 bottlenose dolphins collected from June 2004 through May 2009 by the Sarasota Dolphin Research Program (Sarasota, FL, United States), as part of capture-release health assessments of the long-term resident Sarasota Bay dolphin community (Wells et al., 2004, 2005) were used. This community has been studied since 1970, through at least six generations, and at any given time includes up to five concurrent generations within a single maternal lineage, and individuals up to 67 years of age (Irvine and Wells, 1972; Wells, 2014). As of 2015, the community was composed of 157.53 ± 43.05 SE dolphins (Tyson and Wells, 2016). In combination, health assessments, tagging and tracking, and monthly systematic photographic identification surveys have provided background information on the members of the resident community, including age, sex, genetic relationships, morphometrics, health, tissue concentrations of environmental contaminants, and reproductive histories (Wells, 2009). Skin samples were chosen as model biological material in the present study given the ability to perform samplings in large numbers of individuals in a minimally-invasive manner. This is further supported by previous reports describing age-related changes in DNA methylation in mammals including humans and humpback whales using skin tissue (Grönniger et al., 2010; Polanowski et al., 2014). Skin samples were obtained as subsamples of wedge-shaped surgical biopsies of blubber and skin collected under local anesthesia. The samples were frozen immediately in liquid nitrogen. Samples were stored at −80°C. Overall, the samples

analyzed were chosen to represent a group consisting of 15 females and 24 males with an even age distribution between sexes ranging from 2 to 36 years of age. However, for both males and females, fewer older animals were sampled than younger. Sex was determined by observation during capture-release efforts (see **Figure 1** and **Supplementary File S1**).

DNA Extraction

DNA was extracted from skin samples using a phenol/chloroform extraction protocol, adapted from Sambrook et al. (1989). Accordingly, a small piece of skin (<2 mm) was cut into small pieces and placed in 500 μL of CTAB lysis buffer (100 mM Tris, 20 mM EDTA, 1.2M NaCl, 2% CTAB, pH 8.0) with 10 μL of proteinase K and 40 μL of Dithiothreitol (DTT). Samples were digested overnight at 50°C in a water bath, and subsequently vortexed and mixed with 600 μL of 4°C phenol/chloroform/isoamyl alcohol (25:24:1 mixture, Fisher BioReagents). Samples were vortexed again and centrifuged at 12,000 *g*, 4°C for 5 min. Approximately, 90% of the supernatant was removed and transferred to a new tube. Two additional cycles of extraction with phenol/chloroform/isoamyl alcohol were performed, placing the resulting supernatant fraction on a new tube and precipitating the DNA using 50 μL of ammonium acetate and 980 μL of 99% isopropyl alcohol at 4°C. After an overnight incubation on ice, samples were vortexed and centrifuged at 12,000 *g*, 4°C for 30 min to form a pellet. The isopropyl alcohol was subsequently removed and the pellet was subject to two consecutive washes using ice-cold 70% ethanol. The precipitate was completely dried using a vacuum centrifuge, DNA quality was assessed using agarose gel electrophoresis, and DNA concentration was calculated using Qubit fluorometric quantitation (Thermo Fisher Scientific).

Quantification of %DNA Methylation at CpG Sites

Freshly extracted DNA was divided into 500 ng aliquots (20 ng/μL) and subsequently subject to bisulfite transformation followed by pyrosequencing (EpigenDx, Hopkinton, MA, United States) to identify the %DNA methylation at individual CpG sites, based on multiple DNA copies. Pyrosequencing yields approximately 20X coverage of each target sequence. Age-responsive candidate genes (*TET2*, *GRIA2*, and *CDKN2A*) were targeted. The selection of these genes was informed by previous reports identifying age-responsive genes in humans and particularly in a large cetacean species, the humpback whale (Polanowski et al., 2014).

Dolphin ortholog sequences for genes *TET2*, *GRIA2*, and *CDKN2A* were retrieved from the dolphin genome database (McGowen et al., 2012; Martinez-Viaud et al., 2019) and used to design primers using PyroMark software (Qiagen), specifically targeting most CpG sites present within the promoter sequences for these target genes (*TET2*, $n = 4$; *GRIA2*, $n = 7$; and *CDKN2A*, $n = 6$). Since *CDKN2A* is not annotated in the bottlenose dolphin genome, the killer whale (*Orcinus orca*) genome was used to verify this ortholog using the target sequence from the HEAA (Polanowski et al., 2014). The target sequences used and the CpG site location in relation to the start codon are detailed in **Table 1** along with an explanation of CpG site labeling for this study. The %DNA methylation of gene promoters was calculated based upon the amount of fluorescence produced by PCR amplifications of pyrosequencing products at the targeted CpG sites. As a result, these analyses provide a final %DNA methylation for each of the samples at each of the CpG sites targeted for the three genes.

Statistical Analyses of BEAT Accuracy and Precision

Simple linear regression analyses were performed for each CpG site of each age-responsive gene using chronological age as the independent known variable and %DNA methylation for each CpG site at the different age-responsive genes as the dependent variable using R software (R Core Team, 2013, Version 3.5.2; R codes are included in **Supplementary File S2**). For each linear regression analysis, the coefficient of determination (R^2) was calculated, representing the percentage of the variation in the dependent variable (%DNA methylation) that is explained by the independent variables. After simple linear regression was performed for all CpG sites, multiple regression analyses were

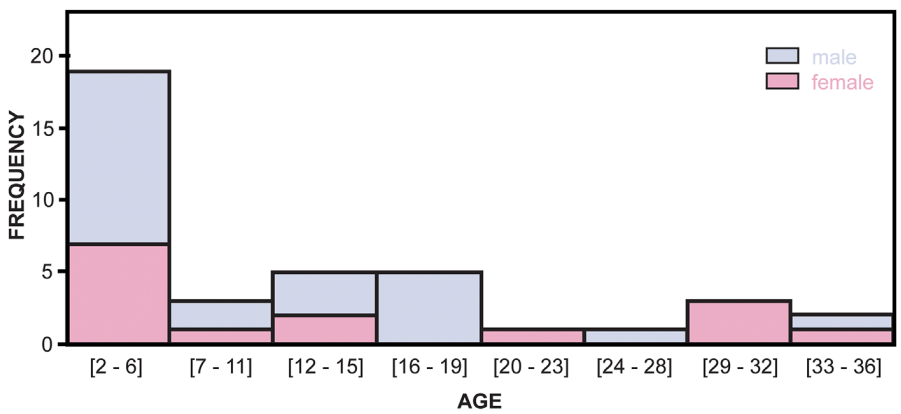

FIGURE 1 | Age distribution of male and female dolphin individuals used for the development of the BEAT tool.

TABLE 1 | Location of the CpG sites identified by the present work at *TET2*, *GRIA2*, and *CDKN2A* genes.

Gene	CpG promoter location
TET2	GGTGGGC **(*TET2_1*, −88384)CG**GGG **(*TET2_2*, −88379)CG**GGGAGAAG **(*TET2_3*, −88369)CG**GGCCTGGGTCAAATTCCTAATTTGT **(*TET2_4*, −88326)CG**AGTCTTTAAAACTA
GRIA2	CCAGTCTC **(*GRIA2_1*, −221)CG**GACTT **(*GRIA2_2*, −213)CG (*GRIA2_3*, −211)CG**AG **(*GRIA2_4*, −207)CG**GGGAC **(*GRIA2_5*, −200)CG**GG **(*GRIA2_6*, −196)CG**CAGGG **(*GRIA2_7*, −189)CG**GCAGCCACCCGCAGGACCTTGGAAA
CDKN2A	**(*CDKN2A_1*, −341)CG**GAGGT **(*CDKN2A_2*, −334)CG**GAGT **(*CDKN2A_3*, −328)CG**GAGACCTCCTCT **(*CDKN2A_4*, −314)CG**G **(*CDKN2A_5*, −311)CG**A **(*CDKN2A_6*, −308)CG**CCTAGGGGGCTCAGGAAGCCACCGGAGGACTGAAAAG

CpG sites are indicated in boldface with their label and location (position of first nucleotide) in parentheses at the promoter region in respect to the transcription initiation site (negative numbers).

conducted. All possible combinations of significantly correlated CpG sites were tested. To avoid the effect of concerted DNA methylation changes among CpG sites on the same gene regions (Grönniger et al., 2010) only one CpG site from each gene was used in the combinations. This approach follows up on the strategy currently used for developing epigenetic age assays in other mammalian species (Koch and Wagner, 2011; Polanowski et al., 2014). Best models were defined based on Akaike information criterion (AIC) and Bayesian information criterion (BIC). The contribution of sex-specific traits to the epigenetic estimation of chronological age was also studied by discriminating between male and female samples in the analysis of %DNA methylation as a function of age. Thus, simple linear regression analyses for male and female datasets were additionally performed (see **Supplementary Files S2**, **S3**). The differences in the best epigenetic aging models obtained for male and female only analyses were evaluated using an analysis of covariance (ANCOVA) using R software ($\alpha = 0.05$). Lastly, the overall epigenetic aging model (including males + females) was validated through multiple regression analysis using the Leave-One-Out Cross Validation (LOOCV) method (Picard and Dennis Cook, 1984). This approach recurrently trains the model using all but one sample each time, until all samples had been left out once thereby predicting a value for each datapoint without using it to train the model.

RESULTS

CpG Methylation at Age-Responsive Genes in Bottlenose Dolphins

Overall, a total of 17 CpG sites were obtained across the three candidate genes targeted (*TET2*, $n = 4$; *GRIA2*, $n = 7$; *CDKN2A*, $n = 6$) using pyrosequencing. The total %DNA methylation for all CpG sites at each of the genes analyzed showed a relatively low %DNA methylation, with gene average methylation falling between 1.6 and 12.2, with the highest percentage at a given site being 24.9 for an individual CpG site at the promoter of *CDKN2A_4*. This was for a 2 year old female. The lowest amount of methylation was the absence of DNA methylation observed at several different sites for some individuals (**Supplementary File S1**). In addition, average %DNA methylation levels were calculated for each individual across all CpG sites for each gene. The individual with the highest average methylation for each gene was as follows: *GRIA2* = female 189 age 32 (10.85 ± 4.40); *CDKN2A* = female 189 age 32 (10.30 ± 2.80); *TET2* = female 217 age 2 (12.25 ± 5.20). Similarly, the lowest averages were: *GRIA2* = male 256 age 2 (1.60 ± 1.60); *CDKN2A* = male 252 age 3 (7.00 ± 3.30); *TET2* = female 193 age 21 (4.30 ± 3.00). The average %DNA methylation was also calculated for each gene, using average values across individuals for each gene. In this case, *CDKN2A* displayed the highest overall average (8.45 ± 3.48; minimum: 4.35, maximum: 13.32), followed by *TET2* (8.10 ± 3.32; minimum: 3.86, maximum: 11.23) and *GRIA2* (3.96 ± 1.78; minimum: 2.12, maximum: 6.91; **Supplementary File S1**). Globally, bottlenose dolphins displayed %DNA methylation levels at CpG sites in *GRIA2* and *CDKN2A* genes similar to those displayed by humpback whales (Polanowski et al., 2014). Oppositely, %DNA methylation at *TET2* CpG sites were lower by almost an order of magnitude in bottlenose dolphins (8.03 ± 1.850, compared with humpback whales 14.630 ± 4.070; **Table 2**).

Correlation Between DNA Methylation and Chronological Age

Simple regression analyses of CpG methylation as a function of chronological age revealed that, out of the 17 CpG sites identified, only 4 of them (*TET2*_4, *CDKN2A*_2, *CDKN2A*_4, *CDKN2A*_6) were not significantly correlated with age, and therefore excluded from subsequent analyses (see **Table 3** for all R^2 values, see **Figure 2** for top correlated CpG site graphs). Multiple regression analyses were then conducted for all possible combinations of CpG sites displaying significant correlation with age, using one CpG site from each of the genes to ensure that independent age estimates were being made. This approach was implemented to account for the observations made in other mammals that CpG sites within a gene tend to be strongly correlated to one another, more often than CpG sites from different genes possibly because of similar processes affecting multiple CpG sites across a single gene (Koch and Wagner, 2011; Polanowski et al., 2014).

Following multiple linear regression analysis, the top model (based on the lowest AIC and BIC and highest R^2 values, $R^2 = 0.779$, residual error = 4.83, $p < 0.001$; **Table 4**) included two genes, *GRIA2* CpG site 5 (*GRIA2*_5) and *TET2* CpG site 2 (*TET2*_2), and is hereafter referred to as the BEAT (Bottlenose dolphin Epigenetic Aging Tool). These two CpG sites displayed the strongest correlation with chronological age among all CpG sites studied in these two genes (**Figure 2**). Full details on the other top models from multiple regression analysis (along with AIC and BIC scores), are shown in **Table 4**. The validation of the best model using the LOOCV method yielded predicted points at $R^2 = 0.740$ (root mean square error = 5.14) which were then plotted against the known age values, and had a strong correlation ($R^2 = 0.780$; **Figure 3**).

TABLE 2 | Comparison between %DNA methylation levels at studied CpG sites in the BEAT and the HEAA models.

	BEAT			HEAA		
	Average %DNA methylation[1]	Minimum	Maximum	Average %DNA methylation[1]	Minimum	Maximum
TET2	8.03	4.70	13.1	14.63	7.51	25.7
GRIA2	5.75	1.60	19.3	1.91	1.07	3.06
CDKN2A	4.41	0.00	6.7	2.39	1.03	4.83

[1]*Averages were calculated by combining %DNA methylation at each individual for the top CpG site correlated to age and then dividing by the total number of individuals.*

TABLE 3 | CpG sites identified at *TET2*, *GRIA2*, and *CDKN2A* genes, along with R^2 and *p*-values obtained in simple linear regression analyses.

CpG site	R^2	*p*-value
TET2_1	0.0878	0.0669
TET2_2	0.2962	0.0003
TET2_3	0.3791	3.02×10^{-5}
TET2_4	0.0642	0.1196
GRIA2_1	0.7310	4.26×10^{-12}
GRIA2_2	0.6082	4.87×10^{-9}
GRIA2_3	0.6082	4.87×10^{-9}
GRIA2_4	0.5933	9.83×10^{-9}
GRIA2_5	0.7556	7.10×10^{-13}
GRIA2_6	0.4806	1.00×10^{-6}
GRIA2_7	0.6887	6.54×10^{-11}
CDKN2A_1	0.3392	0.0001
CDKN2A_2	0.0005	0.8870
CDKN2A_3	0.4428	3.81×10^{-6}
CDKN2A_4	0.0076	0.5956
CDKN2A_5	0.3834	2.64×10^{-5}
CDKN2A_6	0.0001	0.9621

TABLE 4 | Ranked list of the models best describing the relationship between %DNA methylation at CpG sites studied for *TET2*, *GRIA2*, and *CDKN2A* genes as a function of chronological age in bottlenose dolphins (male and female combined).

Ranking	Multiple regression	Adjusted R^2	*p*-value	AIC[1]	BIC[1]
1 (the BEAT)	*TET2_2, GRIA2_5*	0.7789	6.05×10^{-13}	238.32	244.98
2	*TET2_2, GRIA2_5, CDKN2A_1*	0.7779	3.78×10^{-12}	239.40	247.72
3	*TET2_2, GRIA2_5, CDKN2A_5*	0.7742	5.03×10^{-12}	240.04	248.36
4	*TET2_2, GRIA2_5, CDKN2A_3*	0.7729	5.55×10^{-12}	240.26	248.58
5	*TET2_3, GRIA2_5, CDKN2A_1*	0.7655	9.66×10^{-12}	241.51	249.82

[1]*AIC, Akaike information criterion; BIC, Bayesian information criterion. The top model is referred as "the BEAT."*

The following equation created from the multiple regression analysis is as follows: Age estimate = 8.602 + 4.392 (%DNA GRIA_5) − 1.149 (%DNA *TET2_2*).

The contribution of the sex of dolphin individuals to the epigenetic estimation of chronological age was evaluated using analysis of covariance (ANCOVA). While the results revealed a lack of significant differences between male and female changes in DNA methylation with age for the BEAT ($p = 0.760$), simple linear regression analyses performed using only female and male datasets revealed differences for the two CpG sites used in the BEAT model (**Figure 4** and **Supplementary File S3** for all other sites). Most importantly, for site *GRIA2_5*, the slopes for males and females deviate from one another at older ages. For site *TET2_2* we see that both male and female slopes are similar but males tend to have much less methylation than females. ANCOVA analyses for simple linear regressions did not find significant differences except for *TET2_2* ($p = 0.006$), however the methylation of CpG sites at this gene did not display interaction with the sex of the individuals analyzed ($p = 0.713$).

DISCUSSION

Dolphins, as well as many other marine mammals, show relatively little to no visible signs of aging, therefore requiring the use of alternative aging methods. Unfortunately, the current methods used to estimate age in dolphins are limited due to logistical constraints including the need to capture and handle individuals (International Whaling Commission, 1980). Such limitation hampers monitoring, assessing, and studying age-dependent

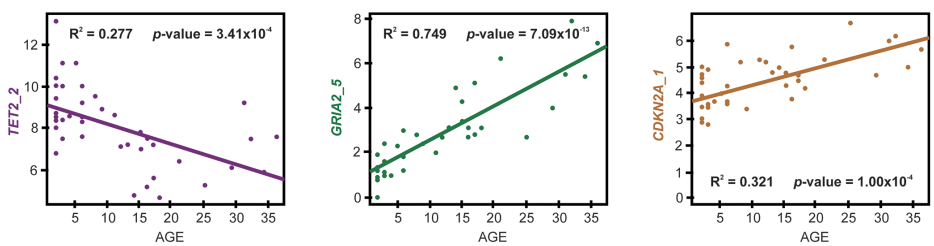

FIGURE 2 | CpG sites displaying the strongest correlation with chronological age across dolphin individuals in each of the three genes studied.

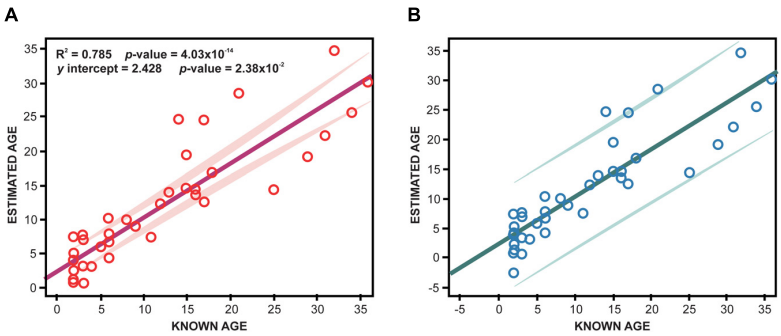

FIGURE 3 | Analysis of the precision of the BEAT model using **(A)** multiple regression analysis (R^2 = 0.785) and **(B)** its validation using LOOCV analysis (bottom graph, R^2 = 0.740). In **(A)**, the estimated age values were calculated for each individual using the equation generated by Multiple Regression analysis using all individuals to generate the model. In **(B)**, estimated age values were calculated for each individual using the equation generated by multiple regression analysis with the individual being estimated left out (see section "Materials and Methods").

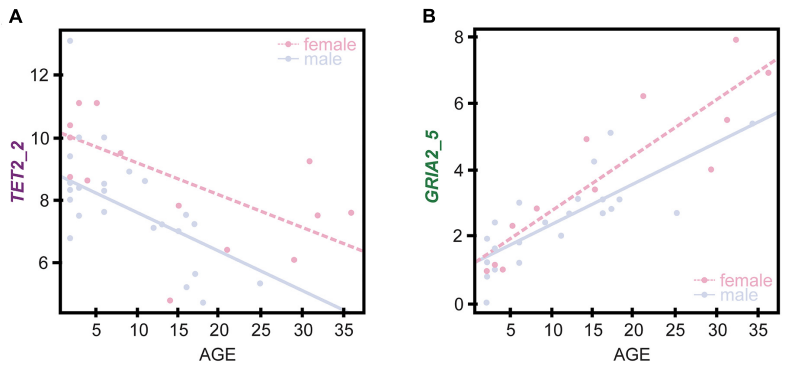

FIGURE 4 | Sex-specific regression analyses between %DNA methylation at the CpG sites defined by the BEAT model in genes *TET2* **(A)** and *GRIA2* **(B)** and chronological age in females (open dots, dashed line) and males (solid dots and line).

effects of environmental stressors at the level of populations (Reeves, 2003; Westgate and Read, 2007; Agusa et al., 2008). Fortunately, studies in cetaceans can easily benefit from ongoing efforts creating more effective molecular aging tools in model systems such as humans or mice (Yi et al., 2014, 2015). In the present work, a similar experimental approach was used to investigate the relationship between epigenetic modifications in age-responsive genes and chronological age in mammals, and their potential to develop the BEAT (Bottlenose dolphin Epigenetic Aging Tool) to efficiently estimate chronological age using skin biopsy samples (Grönniger et al., 2010; Horvath, 2013; Polanowski et al., 2014). The BEAT is very similar to the HEAA [Humpback whale Epigenetic Aging Assay (Polanowski et al., 2014)] on its approach, but requiring only the analysis of CpG sites at two different genes, instead of the three genes required by the HEAA.

Age-Responsive Genes Display Different Levels of CpG Methylation Across Dolphin Age Groups

The BEAT model defined in the present study is based on %DNA methylation information from two age-responsive genes (*GRIA2* and *TET2*) to determine chronological age. These genes were previously (and successfully) used to estimate age in other mammals, including North Atlantic humpback whales and humans (Koch and Wagner, 2011; Buscarlet et al., 2016). *GRIA2* (glutamate receptor 2) belongs to a family of receptors that function in many neurophysiological processes (especially in the brain) and displays hypermethylation in older individuals (Koch and Wagner, 2011). *TET2* (tet methylcytosine dioxygenase 2) encodes an epigenetic regulator mediating the transformation of 5-methylcytosine (5mC) into 5-hydroxymethylcytosine (5hmC) (Buscarlet et al., 2016), also functioning as a tumor suppressor that is heavily methylated in cancer tissues (Grönniger et al., 2010). Surprisingly, *TET2* hypomethylation in older marine mammals contrasts with its hypermethylation in humans (Grönniger et al., 2010; Polanowski et al., 2014), underscoring the effects of the different constraints imposed by the regulatory role of DNA methylation on the function and subsequent long-term evolution of different genes across diverse ecosystems (Hernando-Herraez et al., 2015).

Overall, bottlenose dolphins displayed %DNA methylation levels at CpG sites in *GRIA2* and *CDKN2A* genes similar to those displayed by humpback whales (Polanowski et al., 2014). Oppositely, %DNA methylation at *TET2* CpG sites were

lower by almost an order of magnitude in bottlenose dolphins (8.03 ± 1.850, compared with humpback whales 14.630 ± 4.070; **Table 2**). This difference underscores the importance of doing age assessment studies for different species and even developing species specific aging tools. Discriminating among the CpG sites used in the BEAT, the %DNA methylation at the *GRIA2_5* site displayed a very high coefficient of determination for simple linear regression with age (R^2 = 0.749), which contrasts with the lower value found for *TET2_2* (R^2 = 0.277), suggesting that other factors (besides age) may contribute to DNA methylation in these sites. Although the coefficient of determination obtained for the BEAT (R^2 = 0.779) is not as high as in similar tools developed for human forensics using high-resolution methods [e.g., R^2 = 0.91 (Yi et al., 2014)] this model can still be considered a massive improvement to previous methods used to estimate age in dolphins and small cetaceans, including additional room for improvement as the application of new methods becomes feasible (i.e., affordable) in non-model organisms.

The BEAT Tool Provides Epigenetic Age Estimations Based on Two Age-Responsive Genes

In total, 17 CpG sites located at three age-responsive genes (*GRIA2*, *TET2,* and *CDKN2A*) were studied to develop the BEAT. The best model correlating %DNA methylation with dolphin chronological age used a single CpG site in *TET2* (CpG site 2) and *GRIA2* (CpG site 5) genes (multiple regression R^2 = 0.779; LOOCV validation R^2 = 0.740, **Figure 3**) approximately 78% of the variation observed in %DNA methylation among dolphins is explained by their differences in chronological age. The remainder of the variation (22%) could be potentially due to other environmental factors (e.g., stress exposure) and/or be determined by genetic variability. Contrary to the HEAA assay, the BEAT tool did not require incorporating CpG sites from the *CDKN2A* gene into the model, although this gene was used by the second best correlation model (**Table 4**). Combined, these results suggest that the BEAT model might be less influenced on multiple age proxy markers to produce age estimates, reducing its dependence on genotypic or environmental variation, a key feature supporting its accuracy (Polanowski et al., 2014). Indeed, the methylation at the CpG site used in *GRIA2* confers by itself a very strong correlation to dolphin chronological age (**Figure 2**), which is further improved by the incorporation of an additional CpG site from *TET2*.

The BEAT model displays a high correlation between %DNA methylation and age for the studied CpG sites (**Figure 3** and **Table 4**). Yet, the accuracy of the model decreases slightly as dolphins age, as suggested by the increasing variance of estimated ages for older individuals [the same observation was made by studies attempting to create an age estimation tool for humans (Xu et al., 2015; Yi et al., 2015)]. Nonetheless, this effect does not seem to hamper the ability of the model to produce accurate estimations for a wide range of ages as validated by the LOOCV analysis (**Figure 3**) and by the fact that the error of the BEAT model is never higher than 5 years meaning that age estimates by the model will be within 5 years of the actual age. Obviously, as in every model, the error can be reduced by increasing the sample size (notably by adding older individuals). Nonetheless, its present form constitutes a very important advancement from traditional aging methods used on these organisms (Hohn et al., 1989; Olsen et al., 2012). Further validation of the model using unknown wild specimens was not conducted in this study (but are currently underway) due to the similarity of this model to the HEAA where this type of validation was conducted and was found to be successful (Polanowski et al., 2014). Two different and complementary explanations might account for the observed dispersion. First, in the present study the age distribution of the samples is skewed toward young individuals (2–4 years, n = 14), compared with older individuals (4–36 years, n = 25; **Figure 1** and **Supplementary File S1**). Although such distribution was also a potential problem for the estimations made by the HEAA assay in humpback whales (Polanowski et al., 2014), it can be easily corrected by progressively incorporating older individuals in the dataset to better fit the model. In the present case, the oldest individual incorporated into the BEAT tool was 36 years old, making the model reliable for most dolphins within the boundaries of the lifespan of most individuals (Wells and Scott, 2018).

Sex-Specific Differences Do Not Affect the Age Estimations Made by the BEAT Tool

The second explanation for the wider spread of data points around the regression line for older individuals refers to the potential increasing contribution of sex-specific traits to DNA methylation after dolphins reach sexual maturity. Indeed, mammals display critical differences in gene regulation between females and males, including epigenetic mechanisms [e.g., X chromosome inactivation, imprinting, etc. (Bar et al., 2019; Mutzel et al., 2019)], and their role during aging (Kornack et al., 1991; Berchtold et al., 2008; Arslan-Ergul and Adams, 2014). In the present work, the analysis of younger individuals (either females or males) revealed a better correlation between %DNA methylation and age (**Figures 2**, **3**) when compared with older, sexually mature dolphins (age > 15 years) (Wells and Scott, 2018).

There have been several published studies investigating differences between sexes in aging and many other life functions (Garm et al., 2013; Soares et al., 2014; Fischer and Riddle, 2018). Given the role of epigenetic mechanisms regulating gene expression, it is not surprising that a growing number of studies are reporting sex-specific changes in DNA methylation occurring with age (Horvath, 2013; Horvath et al., 2016), highlighting the importance of including sex in DNA methylation studies. Therefore, in order to ascertain if sex plays a significant role contributing to the BEAT model, additional analyses were performed, discriminating between females (n = 15) and males (n = 24), including similar numbers of 2–4 year old individuals (females n = 6, males n = 8), as well as additional individuals evenly representing all other age groups (see **Figure 1**). The results suggest that the addition of sex to the model does

TABLE 5 | Ranked models best describing the relationship between %DNA methylation at studied CpG sites as a function of chronological age discriminating between female and male bottlenose dolphins.

Ranking	Multiple regression	Adjusted R^2	*p*-value	AIC[1]	BIC[1]
Female 1	*TET2_4, GRIA2_5*	0.8877	7.96×10^{-7}	90.85	93.68
Female 2	*TET2_4, GRIA2_5, CDKN2A_1*	0.8852	4.85×10^{-6}	91.87	95.41
Male 1	*TET2_2, GRIA2_1, CDKN2A_5*	0.9006	8.27×10^{-11}	120.21	126.10
Male 2	*TET2_2, GRIA2_1, CDKN2A_3*	0.8861	3.22×10^{-10}	123.48	129.37

[1]*AIC, Akaike information criterion; BIC, Bayesian information criterion.*

not improve the BEAT's ability to estimate age (ANCOVA, $p = 0.760$, **Figure 4**). Interestingly, when simple and multiple regression analyses were performed separately between females and males, the results revealed the presence of sex-specific differences in the CpG sites displaying higher correlations with %DNA methylation (see **Supplementary File S3**). Similarly, sex-specific multiple regression analyses defined different best models for each sex. Accordingly, the best female-specific model used CpG sites at two different genes (*GRIA2*_5 and *TET2*_4), whereas the male-specific model used CpG sites from all three genes investigated (*GRIA2*_1, *CDKN2A*_5, and *TET2*_2, see **Table 5**).

Overall, although the incorporation of sex does not seem to significantly improve the BEAT model, it does not discard its role in the rate of DNA methylation change between males and females. One possibility is that the small number of reproductive age individuals in the dataset may be hindering such contribution. Indeed, the simple linear regression models for *GRIA2_5* and *TET2_2* discriminating between females and males (**Figure 4**), show that regression lines share similar slopes, with the deviation being more pronounced for older individuals for both CpG sites. As samples from more known-age individuals of greater age become available, sex differences may become more evident and could possibly improve the accuracy of age estimation in cetaceans.

CONCLUSION

The present study investigates the relationship between epigenetic modifications in age-responsive genes and chronological age in bottlenose dolphins, using that information to develop an epigenetic age determination tool, the BEAT. The model underlying the BEAT is based on the %DNA methylation displayed by CpG sites in genes *TET2* (CpG site 2) and *GRIA2* (CpG site 5), estimating chronological age within 4.8 years of accuracy and with a high coefficient of determination ($R^2 = 0.779$). Overall, this tool provides a much needed alternative for feasibly estimating ages for large numbers of individuals in cetacean populations of interest. Furthermore, the ability to train the model with additional samples, especially older individuals with equal representation of males and females, will foster the further development of the BEAT tool providing a finer estimation of age depending on sex and age-groups, and environmental factors that might influence biological age.

DATA AVAILABILITY

Data corresponding to dolphin age, sex, and %DNA methylation for the different CpG sites studied, R scripts and correlation analyses associated to the BEAT on which the present research is based, are deposited in the repository of the CREST-CAChE NSF Center at Florida International University and publicly available at github.com/eelabfiu/beat.

ETHICS STATEMENT

The animal study was conducted under National Marine Fisheries Service Scientific Research Permits, and approvals under Mote Marine Laboratory's IACUC.

AUTHOR CONTRIBUTIONS

AB designed the study, developed the experiments, analyzed the data, and wrote the manuscript. JK designed the study and wrote the manuscript. RW designed the study, provided the samples, and wrote the manuscript. JE-L designed the study, provided the materials, analyzed the data, and wrote the manuscript.

FUNDING

This work was supported by grants from the National Science Foundation (Grant IOS 1810981 awarded to JE-L, and Grant HRD 1547798 awarded to Florida International University as part of the Centers for Research Excellence in Science and Technology Program) and by awards from FIU's CREST Center for Aquatic Chemistry and Environment (CREST-CAChE) and from FIU Tropics (AB).

ACKNOWLEDGMENTS

Samples from Sarasota Bay dolphins were collected under National Marine Fisheries Service Scientific Research Permits issued to RW, under IACUC approvals through Mote Marine Laboratory. We are thankful to the staff, students, veterinarians, collaborators, and volunteers of the Sarasota Dolphin Research Program for collection of the samples, and to all members and volunteers in the Environmental Epigenetics Lab for their assistance during the development of this work. Primary support for sample collection was provided by Dolphin Quest, Inc. This is contribution #148 from the Center for Coastal Oceans Research and #915 from the Southeast Environmental Research

Center in the Institute of Water and Environment at Florida International University.

SUPPLEMENTARY MATERIAL

The Supplementary Material for this article can be found online at: https://www.frontiersin.org/articles/10.3389/fmars.2019.00561/full#supplementary-material

FILE S1 | Bottlenose dolphin dataset used in the present work, including: age, sex, and %DNA methylation for the different CpG sites studied in genes *TET2*, *GRIA2*, and *CDKN2A* across all individuals analyzed.

FILE S2 | R codes used for the development of the BEAT and tests for normality including outlier analyses. Residual plots and Normality Q–Q plots are also included.

FILE S3 | Individual linear correlation analyses for CpG sites displaying a significant correlation between %DNA methylation and age, calculated from whole dataset and discriminating between females and males.

REFERENCES

Agusa, T., Nomura, K., Kunito, T., Anan, Y., Iwata, H., Miyazaki, N., et al. (2008). Interelement relationships and age-related variation of trace element concentrations in liver of striped dolphins (*Stenella coeruleoalba*) from Japanese coastal waters. *Mar. Pollut. Bull.* 57, 807–815. doi: 10.1016/j.marpolbul.2008.01.039

Arslan-Ergul, A., and Adams, M. M. (2014). Gene expression changes in aging Zebrafish (Danio rerio) brains are sexually dimorphic. *BMC Neurosci.* 15:29. doi: 10.1186/1471-2202-15-29

Baker, I., O'Brien, J., McHugh, K., and Berrow, S. (2018). Female reproductive parameters and population demographics of bottlenose dolphins (*Tursiops truncatus*) in the Shannon Estuary, Ireland. *Mar. Biol.* 165:15. doi: 10.1007/s00227-017-3265-z

Bar, S., Seaton, L. R., Weissbein, U., Eldar-Geva, T., and Benvenisty, N. (2019). Global characterization of X chromosome inactivation in human pluripotent stem cells. *Cell Rep.* 27, 20.e3–29.e3. doi: 10.1016/j.celrep.2019.03.019

Barrett-Lennard, L., Smith, T. G., and Ellis, G. M. (1996). A cetacean biopsy system using lightweight pneumatic darts, and its effect on the behavior of killer whales. *Mar. Mammal Sci.* 12, 14–27. doi: 10.1111/j.1748-7692.1996.tb00302.x

Berchtold, N. C., Cribbs, D. H., Coleman, P. D., Rogers, J., Head, E., Kim, R., et al. (2008). Gene expression changes in the course of normal brain aging are sexually dimorphic. *Proc. Natl. Acad. Sci. U.S.A.* 105, 15605–15610. doi: 10.1073/pnas.0806883105

Broer, L., Codd, V., Nyholt, D. R., Deelen, J., Mangino, M., Willemsen, G., et al. (2013). Meta-analysis of telomere length in 19,713 subjects reveals high heritability, stronger maternal inheritance and a paternal age effect. *Eur. J. Hum. Genet.* 21, 1163–1168. doi: 10.1038/ejhg.2012.303

Buscarlet, M., Tessier, A., Provost, S., Mollica, L., and Busque, L. (2016). Human blood cell levels of 5-hydroxymethylcytosine (5hmC) decline with age, partly related to acquired mutations in TET2. *Exp. Hematol.* 44, 1072–1084. doi: 10.1016/j.exphem.2016.07.009

Campana, S. (2001). Accuracy, precision and quality control in age determination, including a review of the use and abuse of age validation methods. *J. Fish Biol.* 59, 197–242. doi: 10.1006/jfbi.2001.1668

Dans, S. L., Crespo, E. A., Koen-Alonso, M., Markowitz, T. M., Vera, B. B., and Dahood, A. D. (2010). "Dusky dolphin trophic ecology: their role in the food web," in *The Dusky Dolphin: Master Acrobat off Different Shores*, eds B. Würsig, and M. Würsig, (Amsterdam: Elsevier), 49–74.

Davidson, A. D., Boyer, A. G., Kim, H., Pompa-Mansilla, S., Hamilton, M. J., Costa, D. P., et al. (2012). Drivers and hotspots of extinction risk in marine mammals. *Proc. Natl. Acad. Sci.* 109, 3395–3400. doi: 10.1073/pnas.1121469109

Deans, C., and Maggert, K. A. (2015). What do you mean, "epigenetic"? *Genetics* 199, 887–896.

Deaton, A. M., and Bird, A. (2011). CpG islands and the regulation of transcription. *Genes Dev.* 25, 1010–1022. doi: 10.1101/gad.2037511

Eirin-Lopez, J., and Putnam, H. (2018). Marine environmental epigenetics. *Annu. Rev. Mar. Sci.* 11, 335–368.

Fischer, K. E., and Riddle, N. C. (2018). Sex differences in aging: genomic instability. *J. Gerontol. A Biol. Sci. Med. Sci.* 73, 166–174. doi: 10.1093/gerona/glx105

Fossi, M. C., Marsili, L., Neri, G., Casini, S., Bearzi, G., Politi, E., et al. (2000). Skin biopsy of Mediterranean cetaceans for the investigation of interspecies susceptibility to xenobiotic contaminants. *Mar. Environ. Res.* 50, 517–521. doi: 10.1016/s0141-1136(00)00127-6

Garm, C., Moreno-Villanueva, M., Bürkle, A., Petersen, I., Bohr, V. A., Christensen, K., et al. (2013). Age and gender effects on DNA strand break repair in peripheral blood mononuclear cells. *Aging Cell* 12, 58–66. doi: 10.1111/acel.12019

Grönniger, E., Weber, B., Heil, O., Peters, N., Stäb, F., Wenck, H., et al. (2010). Aging and chronic sun exposure cause distinct epigenetic changes in human skin. *PLoS Genet.* 6:e1000971. doi: 10.1371/journal.pgen.1000971

Hartel, E. F., Constantine, R., and Torres, L. G. (2015). Changes in habitat use patterns by bottlenose dolphins over a 10-year period render static management boundaries ineffective. *Aquat. Conserv. Mar. Freshw. Ecosyst.* 25, 701–711. doi: 10.1002/aqc.2465

Herman, D. P., Ylitalo, G. M., Robbins, J., Straley, J. M., Gabriele, C. M., Clapham, P. J., et al. (2009). Age determination of humpback whales Megaptera novaeangliae through blubber fatty acid compositions of biopsy samples. *Mar. Ecol. Prog. Ser.* 392, 277–293. doi: 10.3354/meps08249

Hernando-Herraez, I., Garcia-Perez, R., Sharp, A. J., and Marques-Bonet, T. (2015). DNA methylation: insights into human evolution. *PLoS Genet.* 11:e1005661. doi: 10.1371/journal.pgen.1005661

Hohn, A. A., Scott, M. D., Wells, R. S., Sweeney, J. C., and Blair Irvine, A. (1989). Growth layers in teeth from known-age, free-ranging bottlenose Dolphins. *Mar. Mammal Sci.* 5, 315–342. doi: 10.1111/j.1748-7692.1989.tb00346.x

Horvath, S. (2013). DNA methylation age of human tissues and cell types. *Genome Biol.* 14:R115. doi: 10.1186/gb-2013-14-10-r115

Horvath, S., Gurven, M., Levine, M. E., Trumble, B. C., Kaplan, H., Allayee, H., et al. (2016). An epigenetic clock analysis of race/ethnicity, sex, and coronary heart disease. *Genome Biol.* 17:171. doi: 10.1186/s13059-016-1030-0

International Whaling Commission, (1980). *Age Determination of Toothed Whales and Sirenians*. Cambridge: International Whaling Commission.

Irvine, B., and Wells, R. S. (1972). Results of attempts to tag Atlantic bottlenose dolphins (*Tursiops truncatus*). *Cetology* 13, 1–5. doi: 10.1093/mmy/myw011

Jones, P. A. (2001). The role of DNA methylation in mammalian epigenetics. *Science* 293, 1068–1070. doi: 10.1126/science.1063852

Jones, P. A. (2012). Functions of DNA methylation: islands, start sites, gene bodies and beyond. *Nat. Rev. Genet.* 13, 484–492. doi: 10.1038/nrg3230

Kappei, D., and Arturo Londoño-Vallejo, J. (2008). Telomere length inheritance and aging. *Mech. Ageing Dev.* 129, 17–26. doi: 10.1016/j.mad.2007.10.009

Kiszka, J., Simon-Bouhet, B., Martinez, L., Pusineri, C., Richard, P., and Ridoux, V. (2011). Ecological niche segregation within a community of sympatric dolphins around a tropical island. *Mar. Ecol. Prog. Ser.* 433, 273–288. doi: 10.3354/meps09165

Koch, C. M., and Wagner, W. (2011). Epigenetic-aging-signature to determine age in different tissues. *Aging* 3, 1018–1027.

Kornack, D. R., Lu, B., and Black, I. B. (1991). Sexually dimorphic expression of the NGF receptor gene in the developing rat brain. *Brain Res.* 542, 171–174. doi: 10.1016/0006-8993(91)91015-s

Krutzen, M., Barre, L. M., Moller, L. M., Heithaus, M. R., Simms, C., and Sherwin, W. B. (2002). A biopsy system for small cetaceans: darting success and wound healing in *Tursiops* spp. *Mar. Mammal Sci.* 18, 863–878. doi: 10.1111/j.1748-7692.2002.tb01078.x

Martinez-Viaud, K. A., Lawley, C. T., Vergara, M. M., Ben-Zvi, G., Biniashvili, T., Baruch, K., et al. (2019). New de novo assembly of the Atlantic bottlenose dolphin (*Tursiops truncatus*) improves genome completeness and provides haplotype phasing. *Gigascience* 8:giy168. doi: 10.1093/gigascience/giy168

McGowen, M. R., Grossman, L. I., and Wildman, D. E. (2012). Dolphin genome provides evidence for adaptive evolution of nervous system genes and a

molecular rate slowdown. *Proc. R. Soc. B Biol. Sci.* 279, 3643–3651. doi: 10.1098/rspb.2012.0869

Miller, L. J., Solangi, M., and Kuczaj, S. A. II (2010). Seasonal and diurnal patterns of behavior exhibited by Atlantic Bottlenose Dolphins (*Tursiops truncatus*) in the mississippi sound. *Ethology* 116, 1127–1137. doi: 10.1111/j.1439-0310.2010.01824.x

Mutzel, V., Okamoto, I., Dunkel, I., Saitou, M., Giorgetti, L., Heard, E., et al. (2019). A symmetric toggle switch explains the onset of random X inactivation in different mammals. *Nat. Struct. Mol. Biol.* 26, 350–360. doi: 10.1038/s41594-019-0214-1

Olsen, M. T., Bérubé, M., Robbins, J., and Palsbøll, P. J. (2012). Empirical evaluation of humpback whale telomere length estimates; quality control and factors causing variability in the singleplex and multiplex qPCR methods. *BMC Genet.* 13:77. doi: 10.1186/1471-2156-13-77

Paoli-Iseppi, R. D., De Paoli-Iseppi, R., Deagle, B. E., Polanowski, A. M., McMahon, C. R., Dickinson, J. L., et al. (2019). Age estimation in a long-lived seabird (Ardenna tenuirostris) using DNA methylation-based biomarkers. *Mol. Ecol. Resourc.* 19, 411–425. doi: 10.1111/1755-0998.12981

Picard, R. R., and Dennis Cook, R. (1984). Cross-validation of regression models. *J. Am. Stat. Assoc.* 79, 575–583. doi: 10.2307/2288403

Polanowski, A. M., Robbins, J., Chandler, D., and Jarman, S. N. (2014). Epigenetic estimation of age in humpback whales. *Mol. Ecol. Resour.* 14, 976–987. doi: 10.1111/1755-0998.12247

Pompa, S., Ehrlich, P. R., and Ceballos, G. (2011). Global distribution and conservation of marine mammals. *Proc. Natl. Acad. Sci. U.S.A.* 108, 13600–13605. doi: 10.1073/pnas.1101525108

R Core Team, (2013). *R: A Language and Environment for Statistical Computing*. Vienna: R Foundation for Statistical Computing.

Reeves, R. R. (2003). *Dolphins, Whales and Porpoises: 2002-2010 Conservation Action Plan for the World's Cetaceans*. Gland: IUCN.

Sambrook, J., Fritsch, E. F., and Maniatis, T. (1989). *Molecular Cloning: A Laboratory Manual*. Cold Spring Harbor, NY: Cold Spring Harbor Laboratory Press.

Shabani, M., Borry, P., Smeers, I., and Bekaert, B. (2018). Forensic epigenetic age estimation and beyond: ethical and legal considerations. *Trends Genet.* 34, 489–491. doi: 10.1016/j.tig.2018.03.006

Soares, J. P., Cortinhas, A., Bento, T., Leitão, J. C., Collins, A. R., Gaivão, I., et al. (2014). Aging and DNA damage in humans: a meta-analysis study. *Aging* 6, 432–439.

Torres, L. G., Rosel, P. E., D'Agrosa, C., and Read, A. J. (2003). Improving management of overlapping bottlenose dolphin ecotypes through spatial analysis and genetics. *Mar. Mammal Sci.* 19, 502–514. doi: 10.1111/j.1748-7692.2003.tb01317.x

Tyson, R. B., and Wells, R. S. (2016). *Sarasota Bay/Little Sarasota Bay Bottlenose Dolphin Abundance Estimates: 2015. Prepared for National Marine Fisheries Service Northern Gulf of Mexico Bay, Sound and Estuary Bottlenose Dolphin Stock Blocks B20 and B35, Combined. Southeast Fisheries Science Center Reference Document PRBD-2016-02*. Silver Spring, MD: NOAA.

Wells, R., Rhinehart, H., Hansen, L., Sweeney, J., Townsend, F., Stone, R., et al. (2004). Bottlenose Dolphins as marine ecosystem sentinels: developing a health monitoring system. *EcoHealth* 1, 246–254. doi: 10.1007/s10393-004-0094-6

Wells, R. S. (2009). Learning from nature: bottlenose dolphin care and husbandry. *Zoo Biol.* 28, 1–17. doi: 10.1002/zoo.20252

Wells, R. S. (2014). "Social structure and life history of common bottlenose dolphins near Sarasota Bay, Florida: insights from four decades and five generations," in *Primates and Cetaceans: Field Research and Conservation of Complex Mammalian Societies, Primatology Monographs*, eds J. Yamagiwa, and L. Karczmarski, (Tokyo: Springer), 149–172. doi: 10.1007/978-4-431-54523-1_8

Wells, R. S., and Scott, M. D. (2018). "Bottlenose dolphin: common bottlenose dolphin (*Tursiops Truncatus*)," in *Encyclopedia of Marine Mammals*, 3rd Edn, eds B. Würsig, J. G. M. Thewissen, and K. Kovacs (San Diego, CA: Academic Press/Elsevier), 118–125.

Wells, R. S., Tornero, V., Borrell, A., Aguilar, A., Rowles, T. K., Rhinehart, H. L., et al. (2005). Integrating life-history and reproductive success data to examine potential relationships with organochlorine compounds for bottlenose dolphins (*Tursiops truncatus*) in Sarasota Bay, Florida. *Sci. Total Environ.* 349, 106–119.

Westgate, A. J., and Read, A. J. (2007). Reproduction in short-beaked common dolphins (*Delphinus delphis*) from the western North Atlantic. *Mar. Biol.* 150, 1011–1024. doi: 10.1007/s00227-006-0394-1

Wilson, B., Thompson, P. M., and Hammond, P. S. (1997). Habitat use by bottlenose dolphins: seasonal distribution and stratified movement patterns in the Moray Firth, Scotland. *J. Appl. Ecol.* 34, 1365–1374.

Xu, C., Qu, H., Wang, G., Xie, B., Shi, Y., Yang, Y., et al. (2015). A novel strategy for forensic age prediction by DNA methylation and support vector regression model. *Sci. Rep.* 5:17788. doi: 10.1038/srep17788

Yi, S. H., Jia, Y. S., Mei, K., Yang, R. Z., and Huang, D. X. (2015). Age-related DNA methylation changes for forensic age-prediction. *Int. J. Legal Med.* 129, 237–244. doi: 10.1007/s00414-014-1100-3

Yi, S. H., Xu, L. C., Mei, K., Yang, R. Z., and Huang, D. X. (2014). Isolation and identification of age-related DNA methylation markers for forensic age-prediction. *Forensic Sci. Int. Genet.* 11, 117–125. doi: 10.1016/j.fsigen.2014.03.006

Conflict of Interest Statement: The authors declare that the research was conducted in the absence of any commercial or financial relationships that could be construed as a potential conflict of interest.

frontiers in Marine Science

ORIGINAL RESEARCH
published: 20 November 2019
doi: 10.3389/fmars.2019.00721

Genome Survey of Chromatin-Modifying Enzymes in Threespine Stickleback: A Crucial Epigenetic Toolkit for Adaptation?

Alexandre Fellous and Lisa N. S. Shama*

Coastal Ecology Section, Alfred Wegener Institute, Helmholtz Centre for Polar and Marine Research, Wadden Sea Station Sylt, Bremerhaven, Germany

Ocean environments are changing rapidly and marine organisms need to cope with these changes in order to survive, develop, and reproduce. To do so, organisms can either migrate, adapt *in situ* or acclimate via phenotypic plasticity. In this context, the emerging field of environmental epigenetics investigates the contribution of genetic and epigenetic information to adaptive potential of wild populations. Epigenetic modifications are based on the highly dynamic combination of DNA methylation, histone modifications, and non-coding RNAs, which may facilitate phenotypic plasticity through genotype-epigenotype-environment interactions, and can drive rapid evolution in wild populations. However, while knowledge of epigenetic contributions to phenotypes across different developmental and generational timescales is increasing for medical research model species, the mechanistic and synergistic action of these modifications remain comparatively understudied in ecological models such as teleost fishes. Here, we characterized the evolution of the gene toolkit involved in key molecular epigenetic pathways including DNA methylation, histone modifications, macroH2A histone, and miRNA biogenesis/turnover in threespine stickleback, a model species in evolution and ecology. We then investigated these genes within a phylogenetic context by comparing them in stickleback to human, mouse, chicken, tropical clawed frog, zebrafish, medaka, green spotted puffer, channel catfish, and mangrove rivulus. We found that, in general, conserved domains, in conjunction with their phylogenetic positions, suggest evolutionary conservation of putative enzyme activity in stickleback. However, molecular epigenetic pathways also revealed that teleost gene evolution is diversified and complex. Specifically, the number of genes, gene loss/duplication events, identified conserved domains, and putative protein lengths vary greatly from one species to another, particularly within fishes, which exhibit a potentially new class of histone deacetylases. This suggests different biological functions specific to fish species, and that the action of genes regulating epigenetic modifications in model species are not necessarily applicable to other related species. We integrate our results into recent advances concerning epigenetic mechanisms in teleosts, and conclude by discussing the necessity to delve deeper into the fundamental mechanics of epigenetic modifications in a wide array of taxa, particularly those relevant for assisted evolution, conservation, aquaculture, fisheries, and climate change-adaptation studies.

Keywords: evolution, fish, stickleback, DNA methylation/hydroxymethylation, histone modifications, miRNA, global climate change, aquaculture

OPEN ACCESS

Edited by:
Jose M. Eirin-Lopez, Florida International University, United States

Reviewed by:
James Dimond, University of Washington, United States
Hans J. Lipps, Universität Witten/Herdecke, Germany

****Correspondence:***
Alexandre Fellous
alexandre.fellous@awi.de

Specialty section:
This article was submitted to Marine Molecular Biology and Ecology, a section of the journal Frontiers in Marine Science

Received: *02 September 2019*
Accepted: *07 November 2019*
Published: *20 November 2019*

Citation:
Fellous A and Shama LNS (2019) Genome Survey of Chromatin-Modifying Enzymes in Threespine Stickleback: A Crucial Epigenetic Toolkit for Adaptation? Front. Mar. Sci. 6:721. doi: 10.3389/fmars.2019.00721

INTRODUCTION

Epigenetic modifications are based on the highly dynamic combination of DNA methylation, histone modifications, and non-coding RNAs that control transcription (Best et al., 2018; Eirin-lopez and Putnam, 2019). They can be broadly summarized as potentially heritable molecular mechanisms that change gene expression without necessarily being associated with modifications of the DNA sequence (Fincham, 1997). Importantly, they are known to facilitate phenotypic plasticity through genotype-epigenotype-environment interactions (Cosseau et al., 2017). In the context of anthropogenic climate change, understanding the specific contributions of genetic and epigenetic information to adaptive potential of populations and the underlying mechanisms are crucial to assess species' evolution in fast-changing and often unstable environments, in particular when applied to ecological and aquaculture challenges (Gavery and Roberts, 2017; Eirin-lopez and Putnam, 2019). For instance, recent studies in environmental epigenetics applied to marine species (e.g., bivalves, fish) have brought the concept of assisted evolution via epigenetically mediated adaptation to light for aquaculture and conservation applications. The possibility to generate environment-specific phenotypes mediated through heritable epigenetic-based events has been suggested in several species and for a number of traits (e.g., sex ratio, growth, immunity) relevant for the aquaculture industry, even if the precise mechanisms underlying these are poorly described (Gavery and Roberts, 2017; Le Luyer et al., 2017; Panserat et al., 2017; Balasubramanian et al., 2019; Gavery et al., 2019).

Although fish are widely used as model organisms in aquaculture, medicine, ecology, evolution, and ecotoxicology (Cossins and Crawford, 2005), most of our knowledge of their epigenetic mechanisms is mainly focused on laboratory-cultured zebrafish (Horsfield, 2019). However, studies of enzyme evolution (Best et al., 2018) and epigenetic regulation of fish development (Potok et al., 2013; Fellous et al., 2018; Wang and Bhandari, 2019) support the idea of species-specific mechanisms. For instance, an increasing number of studies show an influence of epigenetic modifications in developmental plasticity of trout and salmon, which have implications for species-specific conservation through hatchery rearing programs (Le Luyer et al., 2017; Gavery et al., 2019). Despite the increasing availability of teleost genomic resources, the comparative biology of teleost epigenetic mechanisms remains limited, particularly for non-model species and wild populations (Metzger and Schulte, 2016; Firmino et al., 2017; Labbé et al., 2017; Best et al., 2018; Fellous et al., 2018, 2019a,b; Todd et al., 2019). Hence, our ability to assess the role of epigenetic modifications in adaptive potential and population persistence of ecologically relevant species is still in its infancy.

An ecologically important fish species of interest for epigenetic studies in wild populations is threespine stickleback (*Gasterosteus aculeatus*), as it has been widely used as a model system to investigate the genetic and non-genetic basis of adaptation to novels environments (Shama and Wegner, 2014; Shama et al., 2016; Shama, 2017; Heckwolf et al., 2018; Metzger and Schulte, 2018; Kitano et al., 2019). After the last glaciation, marine stickleback colonized freshwater habitats of the north temperate zone, leading to local adaptation of populations that exhibit different phenotypes based on, for example, behavior, armor plate number, body shape, and gene expression plasticity (Kitano et al., 2019). Furthermore, whole genome sequence comparisons between freshwater and marine individuals revealed that differential gene expression contributed more to adaptive evolution than protein sequence evolution (Kitano et al., 2019). This, in combination with the ability to study the evolution of sex chromosome systems make stickleback an ideal candidate to elucidate the role of epigenetic mechanisms in reproduction, development, and adaptation in fishes (**Figure 1**). Nevertheless, our knowledge about the importance of epigenetic modifications, their precise mechanistic basis, and the number, conservation, and evolution of enzymes implicated in the regulation of these modifications remains scarce. Several recent studies have indeed suggested that phenotypic divergence observed between marine and freshwater populations (Teigen et al., 2015; Artemov et al., 2017; Metzger and Schulte, 2018; Smith et al., 2018), and transgenerational plasticity in response to environmental change (Shama and Wegner, 2014; Shama et al., 2016; Heckwolf et al., 2018) together with local adaptation of populations (Heckwolf et al., 2019) might be due to underlying differences in DNA methylation patterns, but have not yet explicitly demonstrated how epigenetic modifications are regulated in the species.

One of the key challenges identified for our understanding of marine environmental epigenetics is to generate detailed knowledge of epigenetic mechanisms and understanding of synergistic action among epigenetic actors (Eirin-lopez and Putnam, 2019). This information will help to determine the relative weight of these modifications in adaptation, to understand how epigenetic landscapes are generated according to different environmental conditions, as well as if and how they can be transmitted across multiple generations. Indeed, the role of epigenetic modifications in the organism-environment interface or in response to anthropogenic or natural stressors, their mechanistic basis, and the evolution of genes underlying key pathways have been extensively explored in plant and medical model organisms (Baulcombe and Dean, 2014; Yang, 2015; Wang and Köhler, 2017; Shanmugam et al., 2018). These studies were crucial to advances in cancer diagnostics and prognostics (Costa-pinheiro and Montezuma, 2015), to understanding of plant production and plant responses to the environment (Baulcombe and Dean, 2014; Wang and Köhler, 2017), and to understanding of the mechanistic basis of transgenerational epigenetic inheritance in mammals (Van Otterdijk and Michels, 2016). Importantly, recent studies of the DNA methyltransferase family have also revealed that changes in gene copy numbers and molecular interactions can modulate enzyme activity and their role in transcriptional regulation (Lyko, 2018), and that a vast diversity of epigenetic and transcriptional patterns during development are observed among species (Riviere et al., 2013; Eckersley-maslin et al., 2018; Fellous et al., 2018, 2019c; Horsfield, 2019; Vastenhouw et al., 2019). This diversity, coupled with a variable number of genes

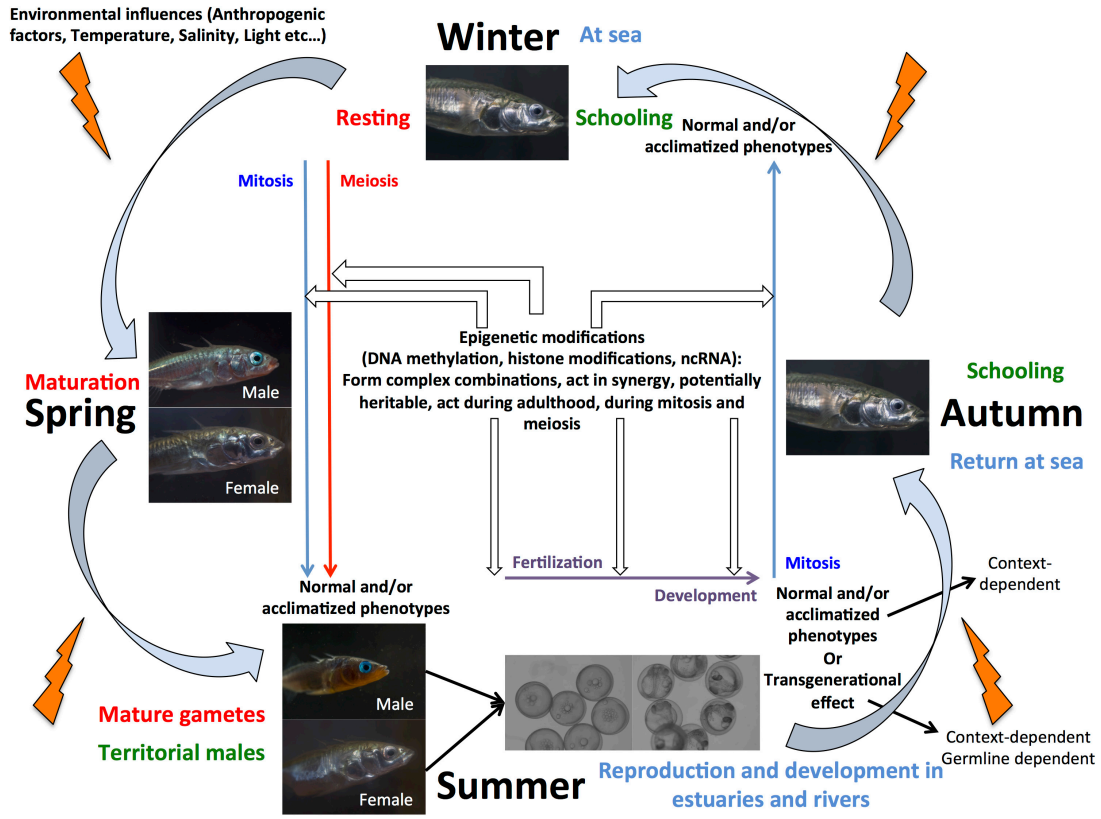

FIGURE 1 | Schmatic view of marine stickleback life cycle illustrating the potential for this species as a model to elucidate the synergistic role of epigenetic mechanisms in aquaculture and eco-evolutionary studies.

and duplication events among species reflects the importance of precisely elucidating species-specific epigenetic toolkits, how the different epigenetic pathways behind are regulated, and how they vary in their biological functions. However, this key knowledge is mostly lacking in fishes (including threespine stickleback; Best et al., 2018; Metzger and Schulte, 2018; Fellous et al., 2019a,b), and marine organisms in general (Gavery and Roberts, 2017).

Here, we performed a genomic survey of genes coding for putative enzymes implicated in key epigenetic pathways: DNA methylation, DNA hydroxymethylation, histone methylation, acetylation, phosphorylation, ubiquitination, sumoylation, poly-ADP ribosylation, and glycosylation, as well as genes coding for putative macroH2A, and genes implicated in the biogenesis/turnover of miRNAs in threespine stickleback. We used *in silico* analyses to identify the epigenetic toolkit in stickleback and characterize the putative proteins molecularly. We then performed phylogenetic analyses of genes potentially implicated in the different known epigenetic pathways by comparing them in stickleback to human, mouse, chicken, tropical clawed frog, zebrafish, medaka, green spotted puffer, channel catfish, and mangrove rivulus. In doing so, we were able to precisely compare the different species' epigenetic toolkits and any duplication/loss events that may have occurred. Finally, based on our results, we discuss the biological role of these putative epigenetic genes in animals, and particularly in other fish species, to provide a fundamental basis for further studies of epigenetic mechanisms potentially underlying adaptive responses of non-model and wild fish populations.

MATERIALS AND METHODS

Identification of Putative Epigenetic Genes Orthologs

Genomic resources of threespine stickleback were screened on the Ensembl genome server[1]. Homology-producing sequences were identified based on the HUGO Gene Nomenclature Committee. Protein conserved domains were identified using Blast[2] and SMART software[3]. All sequences and Ensembl accession numbers are provided in **Supplementary Data Folder 1**.

Phylogenetic Analyses

Sequences encoding the different putative proteins from human (*Homo sapiens*), mouse (*Mus musculus*), chicken (*Gallus gallus*),

[1]http://www.ensembl.org/Gasterosteus_aculeatus
[2]http://blast.ncbi.nlm.nih.gov/Blast.cgi
[3]http://smart.embl-heidelberg.de/

western clawed frog (*Xenopus tropicalis*), zebrafish (*Danio rerio*), medaka (*Oryzias latipes*), mangrove rivulus (*Kryptolebias marmoratus*), green spotted puffer (*Tetraodon nigroviridis*), and channel catfish (*Ictalurus punctatus*) were obtained from the Ensembl genome server[4], and were aligned with the Muscle algorithm (Edgar, 2004). Phylogenetic analyses were performed using a Neighbor-joining method (Bootstrap method: 500 bootstraps, complete or partial deletion of gaps). Results were compared using Minimum Evolution and Maximum Likelihood methods (Bootstrap method: 500 bootstraps, complete or partial deletion of gaps). All analyses were conducted with MEGA software version 7 (Kumar et al., 2016). Sequences used in the analyses and resulting phylogenetic trees are provided in the **Supplementary Data Folder 2**.

RESULTS

Putative Stickleback Enzymes Implicated in DNA Methylation/Hydroxymethylation

Our approach led to the characterization of 14 cDNAs coding for 6 DNA-methyltransferase (DNMT), 5 Methyl DNA-Binding (MDB), and 3 Ten-Eleven Translocated enzyme (TET) putative proteins in stickleback (**Table 1**). While the number of DNMT and TET proteins was fairly constant, the number of MBDs was more variable among the species examined (**Table 2**). DNMT sequences contained a DCM domain that potentially confers methyltransferase activity (**Supplementary Figure 1A**). In addition, they exhibited additional conserved domains such as DNMT1-RFD or PWWP, which recognize and bind the correct residue (**Supplementary Figure 1A**). Phylogenetic analyses (**Supplementary Figure 1B**) revealed that DNMTs cluster into four groups: DNMT1 (maintenance), DNMT3A-DNMT3Bb (*de novo*), DNMT3Ba (*de novo*), and DNMT3l (imprinting). Interestingly, DNMT3A was duplicated once in stickleback, while in zebrafish and medaka, DNMT3A experienced more than one duplication. DNMT3Ab and DNMT3Bb appear to be more closely related to other vertebrate orthologs, whereas DNMT3Aa and DNMT3Ba formed two teleost-specific groups (**Supplementary Figure 1B**). Finally, DNMT3Bb seems to be more closely related to DNMT3A than DNMT3Ba, and no DNMT3l putative proteins were found outside of mammals.

The identified Methyl CpG-binding (MBD) proteins (except Mec2P without conserved domain) contained the MBD domain that binds methylated DNA, while MBD2 and MBD3 had an MBD-C domain known to interact with the NuRD/Mi2 deacetylase complex (**Supplementary Figure 1A**). Stickleback MBD seems to be conserved in vertebrate evolution, whereas the gene coding for the MBD3 protein was duplicated, as also found for the other fish species examined (**Supplementary Figure 1C**). Interestingly, stickleback MDB3a and b are closely related, whereas they form two separate groups in the other fish species examined. The three TET enzymes contained the TET_JBP domain responsible for conversion of 5 methyl-cytosine (5-mC) to 5 hydroxymethyl-cytosine (5 hmC), or further oxidation to 5-formylcytosine (5fC), and 5-carboxylcytosine (5caC) (**Supplementary Figure 1A**). Phylogenetic analyses showed that TETs seem to be highly conserved in vertebrate evolution, and no duplication events occurred in stickleback (or the other fish species examined) (**Supplementary Figure 1D**).

Putative Stickleback Enzymes Implicated in Histone Methylation

In silico analyses revealed 10 *N*-arginine methyltransferase (PRMT) family members in stickleback (**Table 1**), similar to zebrafish, medaka, channel catfish, and mangrove rivulus (**Table 2**). The PRMTs (1-2-3-4-6-8-8b-9) exhibited an AdoMet-MTase conserved domain putatively responsible for methyltransferase activity, while PRMT7 did not contain a conserved domain (**Supplementary Figure 2A**). In contrast to the other PRMTs, PRMT5 had gene-specific domains (PRMT5-TIM, PRMT5, PRMT5-C), which are also responsible for methyltransferase activity (**Supplementary Figures 2A,B**). PRMT4 displayed an additional methyltransferase domain, Carm1, and PRMT2 beared a binding domain, SH3 (**Supplementary Figure 2A**). Stickleback PRMT phylogeny seems to demonstrate that the different classes of enzymes are conserved among vertebrates, with PRMT8 being duplicated in fish (except in the green spotted puffer; **Supplementary Figure 2C**).

Furthermore, 54 cDNAs coding for putative Histone Lysine Methyltransferase (KMTs) were found in stickleback (**Table 1**). While the same number of KMTs was found between human and mouse, it was more variable in the other species examined (**Table 2**). Except for Eef1akmt (Eef1a Lysine methyltransferase) and Dot1 [Histone (H) 3 Lysine (K) 79 *N*-methyltransferase specific], they all contained the conserved domain SET (Su(var)3–9, Enhancer-of-zeste, Trithorax) responsible for methyltransferase activity, but also additional domains such as SANT (Sswi3, Ada2, N-Cor, TFIIIB), or Chromo (CHRomatin Organization Modifier), potentially responsible for chromatin remodeling protein interactions with histones, and chromatin targeting, respectively (**Supplementary Figures 3A,D**). Dot1l contained a Dot1 domain, which is also responsible for methyltransferase activity (**Supplementary Figure 3A**). As seen in **Tables 1**, **2** and **Supplementary Figures 3B,C** KMT subfamilies seem to be conserved in vertebrates, but duplication events differ among the fish species examined. For example, Smyd1 (SET and MYND Domain Containing 1) was duplicated in stickleback, zebrafish, mangrove rivulus and channel catfish, but not in medaka and green spotted puffer (**Supplementary Figure 3B**).

In addition, 32 Histone Lysine Demethylases (KDM) appear to be present in the stickleback genome (**Table 1**). Except for the Kdm1 and Kdm5 enzymes, they all contained the Jumonji-C conserved domain (Jmj-C) (**Supplementary Figure 4A**), putatively responsible for demethylase activity (**Supplementary Figure 4B**). KDMs also had other conserved domains such as JmjN (JumonjiN) or ARID (AT-Rich Interaction Domain), implicated as a co-unit with JmjC and in DNA binding, respectively (**Supplementary Figure 4A**). The different subfamilies of KDMs seem to be conserved in stickleback (**Supplementary Figure 4C**). Interestingly, six KDMs (Kdm1,

[4]http://www.ensembl.org

TABLE 1 | Epigenetic toolkit of threespine stickleback.

Modifications	Type of enzyme	Nbr	Duplication	Conserved domains	No conserved domains
DNA methylation	DNA-methyltransferase	6	DNMT3a and DNMT3b	All	X
	Methyl-DNA binding	5	MBD3	All	MeCp2
DNA hydroxymethylation	TET-Eleven Translocated Enzyme	3	No	All	X
Histone methylation	*N*-arginine methyltransferase	10	Prmt8	All	Prmt7
	Histone lysine demethylase	32	Kdm1, 2a, 2b, 4a, 5b, 6a	All	X
	Histone lysine methyltransferase	54	Ehmt1, Kmt2b, 5a, Prdm1, Smyd1/2	All	X
Histone acetylation	Histone deacetylase	10	No	All	X
	Sirtuin	6	No	All	X
	Histone acetyltransferase	40	Crebbp, Ep300	All	X
Histone phosphorylation	Kinase	40	Fyn, Jak2, Mapk12, Pkn1, Prkcb, Rsp6ka3, Stk24	All	X
Histone ubiquitination	Ligase E1	4	No	All	X
	Ligase E2	27	E2a, E2g1	All	X
	Ligase E3	>21	ARID1A	All	X
	DUBs and Ubiquitin carboxyl-terminal hydrolase	51	Usp6, Usp12, Usp53	All	X
Histone poly-ADP ribolisation	ADP-ribose polymerase	11	No	All	X
	ADP-ribose glycohydrolase	2	No	All	X
Histone glycollisation	Glycosidase	1	No	All	X
	Glycosyltransferase	1	No	All	X
Histone sumoylation	SUMO	3	No	All	X
	SUMO specific protease	5	No	All	X

The modifications and the implicated enzymes are indicated together with the number of enzymes, the ones being duplicated, and the presence of conserved domains or not (in this case, the name of the enzyme is mentioned).

Kdm2a, Kdm2b, Kdm4a, Kdm5b, Kdm6a) were duplicated in stickleback (**Supplementary Figure 4C**), whereas more variability in terms of duplication events was observed for the other fish species examined (**Table 1** and **Supplementary Figure 4C**). Finally, Kdm3a appears to be absent in stickleback and in fish in general (**Supplementary Figure 4C**).

Putative Stickleback Enzymes Implicated in Histone Acetylation

Our genome survey of stickleback revealed 10 genes coding for Histone Deacetylase enzymes (HDAC) and 6 coding for SIlent mating-information Regulation (SIR2)/Sirtuin (**Table 1**). The number of HDAC appears to be lower in stickleback than in the other fish species examined (**Tables 1**, **2**), whereas the number of sirtuins was constant among the examined species (except green spotted puffer) (**Table 2**). Each HDAC member had an Arginase_Hdac superfamily conserved domain, and each SIR2/Sirtuin member exhibited the SIR2 superfamily conserved domain (**Supplementary Figure 5A**), which are both putatively responsible for deacetylase activity (**Supplementary Figure 5B**). Furthermore, Hdac4, Hdac5, and Hdac9b contained a Hdac_Gln (Glutamine Rich N Terminal of Histone Deacetylase) domain that is thought to deacetylate non-histone proteins (**Supplementary Figure 5A**). Phylogenetic analyses of stickleback HDAC/Sirtuin demonstrated that the different classes and subfamilies are conserved in vertebrates and among fish species, with Hdac12 potentially specific to teleosts (**Supplementary Figures 5C,D**). These analyses also showed that Hdac2, Hdac6 (**Supplementary Figure 5C**), and Sirt2 (**Supplementary Figure 5D**) are not present in stickleback, with Hdac2 also absent in zebrafish and mangrove rivulus (**Supplementary Figure 5C**). Interestingly, while Hdac7 was duplicated in medaka and zebrafish, stickleback exhibited only Hdac7b (**Supplementary Figure 5C**).

Forty putative Histone Acetyltransferases (KATs/HATs) were found in the stickleback genome (**Table 1**), as also found in the human genome (**Table 2**). However, specific loss/duplication events occurred in stickleback (**Table 1**) and others fishes (**Table 2**), resulting in a difference between fish and mammals, but also high variability among the teleost species examined. Based on HUGO nomenclature, all KATs/HATs exhibited conserved domains (**Supplementary Figure 6A**) that conferred putative activity and specificity to each member (**Supplementary Figure 6B**). For example, Kat1 (Hat1) contained an acetyltransferase domain, and the Kat2 enzymes displayed the *N*-acetyltransferase domain (Nat) (**Supplementary Figure 6A**). Phylogenetic reconstruction of KATs showed that the different subfamilies are conserved in stickleback, with EP300 and CREBBP being duplicated in teleost species (**Tables 1**, **2** and **Supplementary Figure 6C**). However, Clockb was not duplicated in stickleback, whereas this was the case in zebrafish, medaka, and green spotted puffer (**Tables 1**, **2** and **Supplementary Figure 6C**).

Putative Stickleback Enzymes Implicated in Histone Phosphorylation

Forty sequences coding for putative kinases implicated in histone phosphorylation were characterized in stickleback (**Table 1**), and a variable number of genes and duplication events were observed

TABLE 2 | Epigenetic toolkit of human (*Homo sapiens*, *H. s*), mouse (*Mus musculus*, *M. m*), chicken (*Gallus gallus*, *G. g*), tropical clawed frog (*Xenopus tropicalis*, *X. p*), zebrafish (*Danio rerio*, *D. r*), medaka (*Oryzias latipes*, *O. l*), green spotted puffer (*Tetraodon nigroviridis*, *T, n*), channel catfish (*Ictalurus punctatus*, *I. p*), and mangrove rivulus (*Kryptolebias marmoratus*, *K. m*).

Marks	Enzyme	*H.s*	D	*M. m*	D	*G. g*	D	*X. t*	D	*D. r*	D	*O. l*	D	*T. n*	D	*I. p*	D	*K. m*	D
5 mC	DNMT	5		6		4		3		7	DNMT3a and b	5	DNMT3b	5	DNMT3a and b	5	DNMT3a and b	4	DNMT3a
	MBD	12	Mbdl2	9	Mbdl1 and Mbdl2	5		7		10	MBD1 and 3	7	MBD3	5	MBD3	7	MBD3	7	MBD3
5 hmC	TET	3		3		3		2		3		3		3		3		3	
H me	PRMT	9		9		4		9		10	Prmt8	10	Prmt8	9		10	Prmt8	10	Prmt8
	KDM	33		30		24		24		34	Jarid2, Kdm5a, 4a, 6b, 2a, 7a	28	Kdm2a, 2b, 5b, 6a, 6b	29	Kdm2a, 2b, 4a, 5b	29	Kdm2a, 4a, 5b	27	Kdm2b, 5b, 6b
	KMT	57		57		45		43		54	Smyd1, 2, Prdm1, 2, Setd1b, Setdb1, Kmt2c, 5a, Nsd1, Suv39h1	54	Smyd2, Kmt2b, 5a, Nsd1	44	Smyd2, Prdm1	55	Kmt5a, 5b, SMyd1, Setd1, Ehmt1	50	Smyd1, Nsd1, Prdm1, Kmt5a
H ac	HDAC	11		11		9		9		12	Hdac7	13	Hdac7	11	Hdac7	11	Hdac7	11	Hdac7
	Sirtuin	7		7		7		7	Sirtuin3	7		7		3		7		7	
	KAT	40		39		37	Taf1	38	Taf1	41	Kat7, 5, EP300, Crebbp, Clock	34	Ep300, Clock, Taf1	32	Ep300, Taf1, Clock	36	Ep300, Taf1	36	Ep300
H p	Kinase	39		39		34		34		49	Fyn, Jak2, Mapk8, 12, 14, Pkn1, Prkcb, Stk24, Rsp6k3	41	Jak2, Mapk12, Pkn1, Pak2, Stk24	39	Jak2, Mapk12, 14, Pak2	44	Fyn, Jak2, Mapk12, 14, Pak2, Stk24, Rsp6k3	41	Jak2, Mapk12, Pak2

(Continued)

TABLE 2 | Continued

Marks	Enzyme	*H.s*	D	*M. m*	D	*G. g*	D	*X. t*	D	*D. r*	D	*O. l*	D	*T. n*	D	*I. p*	D	*K. m*	D
H ub	E1	5		5		3		1		5		4		4		2		4	
	E2	39		40		33		24		40	D1, K, L3, N, G1	31		25	E2G1	35	EG1	31	
	E3	>21		>21		>21		>21		>21	Arid1a	>21	Arid1a	>21	Arid1a	>21	Arid1a	>21	Arid1a
	USP	73	Multiple Usp17	56	Multiple Usp17	42		37	Usp12	49	Usp2, 12, 43, 53, 54	47		45	Usp12, 43, 53, 54	44	Usp2, 12, 53, 54	46	Usp2, 12, 43, 53, 54
H rib	PARP	17		12		11		5		14	Parp6, 12	11	Parp6, 12	13	Parp 6 and 12	13	Parp 6 and 12	13	Parp 6 and 12
	PARG	2		2		2		2		3	Parg	2		2		3	Parg	3	Parg
H gly	OGA	1		1		1		1		1		1		1		1		1	
	OGT	1		1		1		1		1		1		1		1		1	
H sum	SUMO	4		3		3		3		5	Sumo2, 3	3		2		4	Sumo2	4	Sumo3
	SENP	7		7		6		4		9	Senp3, 6, 7	5		2		7	Senp6	4	

5 mC (DNA methylation), 5 hmC (DNA hydroxymethylation), H me (histone methylation), H ac (Histone acetylation), H p (Histone phosphorylation), H ub (Histone ubiquitination), H rib (Histone poly-ADP ribolysation), H gly (Histone glycosylation), H sum (Histone sumoylation), and D (Duplication). The modifications and the implicated enzymes are indicated together with the number of enzymes and the ones being duplicated in each examined species.

among species (**Table 2**). Except for Baz1b (Bromodomain adjacent to zinc finger domain protein 1B) and Bub1b ("budding uninhibited by benzimidazoles 1" mitotic checkpoint serine/threonine kinase B), they all exhibited the pKC (Protein Kinase C) domain (**Supplementary Figure 7A**) responsible for serine/threonine phosphorylation (**Supplementary Figure 7B**). Some sequences also contained other conserved domains such as B41 (Band 4.1 homologs) on Jak2 (Janus tyrosine kinases 2), known as a plasma membrane-binding domain, or BROMO (Bromodomain) on Baz1B that recognizes acetylated residues (**Supplementary Figure 7A**). While the main subfamilies of kinases seem to be conserved in vertebrates, some enzymes such as Jak2 appear to be duplicated in the fish species examined (**Table 2** and **Supplementary Figure 7C**). However, there were exceptions, such as Mapk8b (Mitogen-Activated Protein Kinase 8 B), which was only duplicated in zebrafish (**Table 2** and **Supplementary Figure 7C**).

Putative Stickleback Enzymes Implicated in Histone Ubiquitination

In silico analyses revealed genes coding for (at least) 21 ligases E3, 27 ligases E2, and 3 SWI/SNF (Switch/Sucrose Non-Fermentable) E3 proteins (**Table 1**). Four Ubiquitin activating enzymes whose Ube1 containing the conserved catalytic domain Ube1 (**Supplementary Figure 8A**) were detected in stickleback (**Table 1**). All examined stickleback E2s possessed the UbC (Ubiquitin C) domain, putatively active in ubiquitination under stressful conditions (**Supplementary Figure 8A**). While the three ARID (AT-Rich Interactive domain containing) proteins contained the ARID domain implicated in DNA-Protein and/or Protein–Protein interactions, only ARID1aa and ARID1ab had the BAF250 domain responsible of H2B ubiquitination (**Supplementary Figures 8A,C**). The ligases E3 contained a large variety of conserved domains such as the HECTc (Homologous to the E6-AP Carboxyl Terminus c) on E3A (Enzyme Ligase 3A) or Huwe1 (HECT, UBA (Ubiquitin-Associated domain) and WWE domain-containing protein 1) (**Supplementary Figure 8A**), reflecting a diversity of substrates and functions (**Supplementary Figure 8B**). The different ligase subfamilies appear to be conserved in vertebrates (**Supplementary Figures 8C–E**), while, particularly for the E2 ligases, the number of genes and duplication events varied among the vertebrates examined (**Table 2**).

Among the 51 enzymes potentially capable of histone deubiquitination (**Table 1**), 48 were identified as Usp (Ubiquitin carboxyl-terminal hydrolase) (**Supplementary Figure 9**). Thus, all Usp proteins had the peptidase_C19 domain (**Supplementary Figure 9A**), conferring deubiquitination activity against histone and non-histone proteins (**Supplementary Figure 9B**), and many (e.g., Usp25), had additional conserved domains like UBA that bind ubiquitin (**Supplementary Figure 9A**). Finally, the peptidase_C12 domain on BAP1 (BRCA1: Breast cancer type 1 susceptibility protein associated protein 1), MPN (Mpr1, Pad1 N-terminal) on BRCC36 [Lysine-63-specific deubiquitinase BRCC36 (BRCA1/BRCA2-containing complex subunit 36)], and MYSM1 [Histone H2A deubiquitinase MYSM1 (Myb-like,

SWIRM, and MPN domain-containing protein 1)] were also found, and are implicated in deubiquitination (**Supplementary Figure 9A**). The main subfamily classification seems to be conserved in vertebrates (**Supplementary Figures 9C–E**), despite high variability among species in the number of genes and duplication/loss events (**Table 2**).

Putative Stickleback Enzymes Implicated in Histone Poly-ADP Ribosylation

Eleven Poly (ADP-ribose) polymerases (Parp) were found in stickleback (**Table 1**), whereas 17 have been characterized in humans (**Table 2**). Specific loss/duplication events were also observed for the other fish species examined (**Table 2**). Except for Parp9 and Parp14, they all contained the conserved domain Parp responsible for Poly (ADP-ribose) polymerization often implicated in DNA repair (**Supplementary Figure 10A**). Parp9 and Parp14 exhibited a Macro domain that putatively binds ADP-ribose (**Supplementary Figure 10A**). Other conserved domains were also detected, such as the WGR (named after its most conserved motif) domain on Parp1-2-3 (**Supplementary Figure 10A**), which may be a nucleic acid domain. Well-conserved among vertebrates, the different Parp subfamilies were also found in our phylogenetic analyses (**Supplementary Figure 10B**). Interestingly, while most of the discovered Parps were found only once in each species, Parp6 and Parp12 seem to be duplicated in fishes but not in stickleback (**Tables 1**, **2** and **Supplementary Figure 10B**). In addition to the Parps, two Poly (ADP-ribose) glycohydrolases [Parga and Adprhl2 (ADP-ribose glycohydrolase ARH3 (ADP-Ribohydrolase 3)] were found in stickleback (**Table 1**). They both exhibited a conserved domain responsible for poly (ADP-ribose) glycohydrolase (**Supplementary Figure 10A**). Also conserved in vertebrates, Adprhl2 does not seem to be duplicated in fish, whereas Parga may have been duplicated in zebrafish and mangrove rivulus (**Table 2** and **Supplementary Figure 10C**).

Putative Stickleback Enzymes Implicated in Histone Glycosylation

One glycosidase (Oga; nuclear cytoplasmic O-GlcNAcase and acetyltransferase) and one glycosyltransferase (Ogt; UDP -*N*-acetylglucosaminepeptide *N*-acetylglucosaminyltransferase 110 kDa subunit) were found in stickleback (**Table 1**). A catalytic domain was identified for each of the putative proteins (**Supplementary Figure 11**). While the stickleback enzymes seem to be conserved among vertebrates, there were no apparent duplications in the other fish species examined (**Table 2** and **Supplementary Figure 11**).

Putative Stickleback Enzymes Implicated in Histone Sumoylation

The SUMO activating enzyme E1 [SAE1 (SUMO1 activating enzyme subunit 1)], conjugating enzyme E2 (UBC9), and two SUMO ligases E3 (NSE2 and EGR2) were identified (**Supplementary Data Folder 1**). Three Small Ubiquitin-like MOdifers (SUMO) were also found in the stickleback genome (**Table 1**). This number appears to be variable in teleosts (**Table 2**), whereas four SUMOs are known in humans (**Table 2**). The SUMO proteins all exhibited a conserved domain (**Supplementary Figure 12A**), and the different subfamilies appear to be conserved in vertebrates (**Supplementary Figure 12B**). While Sumo2 and/or Sumo3 were duplicated in zebrafish, channel catfish, and mangrove rivulus (**Table 2**), there were no apparent duplications in stickleback (**Supplementary Figure 12B**). Furthermore, five SUMO/Sentrin specific Peptidases (Protease) (SENP), corresponding to each vertebrate subfamilies, were detected in stickleback (**Table 1**), in comparison to seven in mammals and a variable number in the other species examined (**Table 2**). They all exhibited a catalytic domain responsible for peptidase activity (**Supplementary Figure 12C**). Interestingly, outside of human and mouse, this number was also variable among the species examined (**Table 2**). SENP6 and SENP7 were duplicated in zebrafish, whereas they were not duplicated in stickleback (**Supplementary Figure 12D**). Finally, while all of the SENPs clustered with their vertebrate homologs, stickleback SENP6 was found to be more closely related to zebrafish SENP7a (**Supplementary Figure 12D**).

Stickleback H2A

Our *in silico* analyses identified two genes coding for putative H2A proteins [**Supplementary Figure 13(1)**]. Interestingly, while these genes seem to be duplicated in vertebrates for both H2As, this was apparently not the case for stickleback, channel catfish, or green spotted puffer [**Supplementary Figure 13(2)**].

Detection of Stickleback Genes Coding for Proteins Implicated in miRNA Biogenesis/Turnover

Finally, we looked for different putative proteins implicated in miRNA biogenesis and turnover. While all of the genes coding for proteins involved in miRNA biogenesis (**Supplementary Figure 14A**) and turnover (**Supplementary Figure 14B**) pathways were identified in stickleback, no corresponding sequence for *Tut4* (Terminal uridylyltransferase 4) could be retrieved. For each of these genes, no duplication events were detected.

DISCUSSION

We conducted a comprehensive characterization of putative proteins implicated in the large variety of epigenetic pathways in threespine stickleback in order to provide a knowledge base for future studies. Despite stickleback being an excellent candidate fish species for evolutionary and environmental epigenetic studies (Shama et al., 2016; Metzger and Schulte, 2017, 2018; Heckwolf et al., 2018, 2019; Smith et al., 2018), mechanisms underlying different DNA methylation patterns and histone modification profiles, how they are modulated, and how they interact with non-coding RNAs have not yet been described. Here, we showed that stickleback possess a diversified epigenetic toolkit which shares similarities with other fishes and vertebrates, but also differs in the number of genes, loss/duplication events, and putative protein structures, indicating that even if epigenetic

marks seem to be conserved across taxa, they might be differentially regulated among species and/or have potentially unknown functions. Our study underlines the importance of considering species-specific gene regulation pathways, and that patterns observed in model species may not always be applicable to other related species. Below, we discuss the biological role of these epigenetic actors and highlight the potential utility of some in assisted evolution, conservation, aquaculture, and hypothesis testing of species adaptive responses to rapid climate change.

DNA Methylation/Hydroxymethylation

DNA methylation is currently the most studied mechanism in environmental epigenetics. In vertebrates, DNA methylation mainly refers to the transfer of a methyl group to position 5 of cytosine residues to form 5-methylcytosine (5 mC) in a CpG dinucleotide context (Feng et al., 2010). A methyltransferase family, the DNMTs, catalyzes this reaction and is composed of three conserved proteins (DNMT1, DNMT3A, DNMT3B) (Okano et al., 1999; Campos et al., 2012). DNMT1 is called a maintenance enzyme, while DNMT3A and DNMT3B are *de novo* methyltransferases (Li et al., 1992; Okano et al., 1999). DNA methylation also influences chromatin compaction and the associated gene expression via interactions through MBD proteins (six members in vertebrates) (Ballestar and Wolffe, 2001; Lindeman et al., 2010). In addition, DNA 5-hydroxymethylation (5 hmC), a possible stage of DNA demethylation, was recently characterized in vertebrates (Zhao and Chen, 2013), and is catalyzed by the TET enzymes (TET1, TET2, TET3) (Santiago et al., 2014). Nevertheless, the precise relationship between 5 mC and 5 hmC has not yet been established (Kamstra et al., 2015).

Our phylogenetic analyses and the presence of a catalytic domain and additional motifs suggest species-specific differences in genes underlying DNA methylation/hydroxymethylation. As also shown in zebrafish (Campos et al., 2012), bluehead wrasses (Todd et al., 2019), and mangrove rivulus (Fellous et al., 2018), DNMT3A and DNMT3B show duplication events, and DNMT3l is also absent in stickleback. This calls into question the generality of evolutionary conservation of *de novo* methylation and genomic imprinting genes in fishes. Furthermore, the number of MBDs in stickleback suggests a loss of some genes and a duplication of MBD3 due to 3R genome duplication (Best et al., 2018; Balasch and Tort, 2019). In addition, the absence of identified conserved domains on MecP2 questions its functionality (Fatemi and Wade, 2006) in stickleback, since it does exhibit a conserved domain in mangrove rivulus (Fellous et al., 2018). MDBs are still not well known in fishes, and so far, only MeCP2 has been studied in zebrafish (Gao et al., 2015; Nozawa et al., 2017) and mangrove rivulus (Fellous et al., 2018). Furthermore, while the TET family appears to be well conserved in vertebrates, 5 mC/5 hmC patterns during embryonic development and their inheritance are still controversial among fishes (Potok et al., 2013; Fellous et al., 2018; Wang and Bhandari, 2019), illustrating the need to delve deeper into the mechanistic basis of 5 mC/5 hmC regulation.

The biological function of DNMT enzymes appears much more complex than "traditional" maintenance and *de novo* DNA methylation (Lyko, 2018). For example, a recent study supports the role of DNA methylation during reprogramming in the regulation of transposable elements in whitefish that contributes to the survival of nascent species (Laporte et al., 2019). Also, together with an implication of 5 mC in sex ratio determination (Ellison et al., 2015) and environmental sex changes (Todd et al., 2019), a role for DNA methylation in intra- and inter-generational acclimation through *de novo* methylation has been suggested in fish (Fellous et al., 2018) and corals (Putnam and Gates, 2015; Putnam et al., 2016). In stickleback, one study supports this function for *de novo* methylation, but also underlies the possibility of "deleterious" evolution (Mcghee and Bell, 2014), even if the precise regulation of 5 mC remains unknown (Teigen et al., 2015; Artemov et al., 2017; Metzger and Schulte, 2018; Smith et al., 2018; Heckwolf et al., 2019). Thus, future studies would benefit from a more precise understanding of potential interactions between DNMT, MBD, and TET proteins. This, together with investigations of the importance of 5 mC/5 hmC will allow for better mechanistic understanding of the functional significance of the observed DNA methylation patterns in stickleback adaptation and evolution (Metzger and Schulte, 2018; Smith et al., 2018; Heckwolf et al., 2019).

Histone Methylation

Histone methylation is a key element of the "epigenetic code", and regulation of this modification plays important roles in transcription, cell cycles, and genome integrity (Black et al., 2013). Histone proteins can be methylated on arginine (R) (Zhang et al., 2019) or on lysine (K) residues, with lysine potentially mono- (me1), di- (me2), or tri- (me3) methylated (Martin and Zhang, 2005). Arginines are methylated by PRMT enzymes that comprise a group of nine members classified into three types [I (PRMT1-2-3-4-6-8), II (PRMT5-9), III (PRMT7)] with different specificities in vertebrates (Zhang et al., 2019). Lysine methyltransferases (KMTs), specific to different residues, are categorized into two families. The first family contains the SET domain-containing enzymes and is the largest with at least forty members, while the second family has only one member (Dot1l) and is characterized by the lack of a SET domain (Van Leeuwen et al., 2002; Dupret et al., 2017). Both arginine and lysine seem to be demethylated by a major class of enzymes (>100 members), the Jumonji C domain, containing histone demethylases (JHDMs) or Lysine demethylases (KDMs) (Shi et al., 2011) which exhibit a large diversity of substrate and biochemical activities related to the number of methyl groups carried on target residues (Zhang et al., 2019).

Specific knowledge related to PRMT enzymes in fish biology is focused mainly on zebrafish (Lei et al., 2012), and to a lesser extent on channel catfish (Yeh and Klesius, 2012), and our results support the idea that some PRMTs are restricted among metazoans (Wang and Li, 2012). Interestingly, PRMT8, which is duplicated in stickleback, plays a critical role during zebrafish embryonic and neural development (Wang and Li, 2012), and is the only enzyme with tissue-restricted expression. Whereas they are less known outside of other non-model species (Best et al., 2018), the KMTs seem to be conserved in stickleback, as well as in mangrove rivulus (Fellous et al., 2019b), insects (Jiang et al., 2017), and humans (Petrossian and Clarke, 2011), although species-specific loss/duplication events have occurred.

The number of KDMs in stickleback differs slightly from other fish species (Qian et al., 2015; Fellous et al., 2019b). However, despite being well documented in taxa ranging from fruit flies to mammals and crucial in development and adaptation of a number of organisms, as well as being temperature sensitive (Takeuchi et al., 1999; Sasai et al., 2007; Fellous et al., 2014, 2015; Zhang et al., 2019), these fundamental proteins remain understudied in fishes, with the exception of zebrafish (Stewart et al., 2009; Akerberg et al., 2017). Furthermore, the dynamics of histone modifications are particularly important to study in the context of epigenetic inheritance and chromatin configurations in gametes of fishes, but remain largely under studied (Labbé et al., 2017; Best et al., 2018).

Histone Acetylation

Histone acetylation is one of the best studied epigenetic modifications, and plays important roles in the control of chromatin assembly, cell reprogramming, DNA repair, and gene expression (Shin et al., 2018). Histone acetyltransferases (HATs or recently KATs) add acetyl groups to lysine residues and have been classified into two types, A (main chromatin regulator) and B. Type A uses nucleosomal histones only, while type B uses non-nucleosomal histone associated with a partial cytoplasmic localization, and includes five distinct multi-gene families: Myst (*Myst1-2-3-4*), GNAT (*GCN5-related N-acetyltransferase*), Basal transcription/nuclear receptor cofactors, P300-CBP (CREB-binding protein) and Camello (Karmodiya et al., 2014; Sheikh and Akhtar, 2018). While many of these enzymes are well characterized in mammals, some new members are not yet established as real KATs (Sheikh and Akhtar, 2018). On the other hand, histone deacetylases are classified into two families: the "classic" HDAC which is divided into three groups [Class I (HDAC1-2-3-8), Class II (HDAC4-5-6-7-9-10), Class IV (HDAC11)], and the Sirtuins (Class III) (Greiss and Gartner, 2013; Seto and Yoshida, 2014).

The different KAT subfamilies and HDAC/Sirtuins classes are present in stickleback, but the number of genes and loss/duplication events differ among fish species. Interestingly, while sirtuin 1 is mentioned in stickleback by Teigen et al. (2015), no corresponding sequence was detected during our *in silico* analyses. Furthermore, the putative protein structure of HDAC9 questions its specificity toward histones (Petrie et al., 2003), since the arginase-HDAC domain was not found in stickleback, and different biochemical activities were observed in human and western-clawed frog (Petrie et al., 2003). Our analyses also revealed a possible new class of HDAC, HDAC12, which may be specific to teleosts. However, a complete molecular characterization is needed to confirm this. Nevertheless, the presence of a catalytic domain and their protein architecture suggest that these proteins are active, potentially filling a gap of knowledge regarding histone acetylation in fishes (Best et al., 2018). Whereas most studies are primarily focused on zebrafish (He et al., 2014; Román et al., 2018), KAT and HDAC/Sirtuin mRNA expression was recently described in mangrove rivulus during gonad-embryogenesis (Fellous et al., 2019a), and in trout, where histones undergo acetylation during spermatogenesis (Best et al., 2018). In the context of climate-driven range shifts, for species considered to be climate migrants (including stickleback), the precise mechanistic basis of cold acclimation through sirtuin(s) expression (Teigen et al., 2015) should be elucidated, since histone deacetylase activity is known to mediate thermal plasticity in zebrafish (Seebacher and Simmonds, 2019).

Histone Phosphorylation

Response to DNA damage is the best known function of histone phosphorylation, where phosphorylated H2A(X) delimits chromatin domains around the damaged DNA (Rossetto et al., 2012). However, this is not its only function, as it has been shown that a single histone phosphorylation event might be involved in different cellular processes (Rossetto et al., 2012). Histone serine (S) and tyrosine (Y) are part of the target of kinases, but little is known about their specificities (Rossetto et al., 2012; Best et al., 2018). In our study, most of the histone kinases known from mammals were also found in stickleback. However, as for other epigenetic pathways, most of our knowledge comes from zebrafish (Best et al., 2018), and the complexity of this mark is understudied. Thus, the specific loss/duplication of some members of this gene family raises the possibility of additional functions, for example phosphorylation of HDAC1 by aurora in zebrafish embryos (Loponte et al., 2016), or in diapause of the annual killifish (Toni and Padilla, 2016). Finally, phosphorylation of histone H2A.XF, a distinct isoform of H2A only present in very early development of Xenopus and zebrafish (Shechter et al., 2009), suggests a role for this modification in establishing particular transient chromatin conformations necessary for oocyte maturation of rapidly developing aquatic organisms facing environmental changes and/or perturbations.

Histone Ubiquitination

Ubiquitination is one of the main histone post-translational modifications. As in methylation, this mark is associated with both transcriptional activation and repression, whereas, in general, acetylation and phosphorylation are associated with gene expression, and sumoylation with gene repression (Sheng et al., 2014). Histone ubiquitination has been implicated in various cellular processes and cancers (Cao and Yan, 2012), was shown to be crucial to spermatogenesis (Sheng et al., 2014), and is also an aging biomarker (Wang et al., 2019) in mammals. In fish, this mark is largely undescribed (Best et al., 2018), but recent zebrafish studies have demonstrated the importance of ubiquitination in brain patterning (Kumar et al., 2019), and of deubiquination in craniofacial development (Ka and Tse, 2017). The general model of the ubiquitination process requires three enzymes: the ubiquitin activation enzyme E1, the ubiquitin conjugating enzyme (E2), and the ubiquitin ligase enzymes (E3), these last enzymes being very diverse (Sheng et al., 2014; Zheng and Shabek, 2017). Similar to many other epigenetic marks, ubiquitination is reversible, and deubiquitination enzymes (DUBs) deconjugate ubiquitin (Belle and Nijnik, 2014). In stickleback, conserved E1, E2, and E3 enzymes were identified but their enzymatic activity and

biological functions are unknown. The number of characterized E3 may not be fixed, as an increasing number of studies (in mammals) have shown not only new substrates but also new E3 enzymes (Zheng and Shabek, 2017). Our results suggest that many loss/duplication events in DUBs may have occurred in stickleback and in fishes in general (Tse et al., 2009) compared to humans (Nijman et al., 2005).

Histone Poly-ADP Ribosylation

Histone poly-ADP ribosylation is a modification catalyzed by only one known family, the PARP (Poly(ADP-ribose)polymerase) enzymes (Perina et al., 2014). Also called PARylation, this mark is important in many biological processes such as DNA repair, telomere length regulation, apoptosis, aging, and protein degradation (Perina et al., 2014), and can also affect other epigenetic marks such as acetylation (Verdone et al., 2015). Only a small number of eukaryotic species do not possess PARP genes, and the human genome encodes 17 PARP proteins distributed in five classes (Perina et al., 2014). Interestingly, only 11 putative PARPs distributed in four classes were found in stickleback, and only PARP9/PARP14 contain the macro domain, likely reflecting the different evolutionary histories of stickleback and humans (Best et al., 2018). Histone poly-ADP ribosylation is reversible and is degraded by Poly(ADP-ribose)glycohydrolase, which necessitates the complementary action of (ADP-ribosyl)hydrolases (ARHs: two members ARH1/ARH3) (Rack et al., 2018). Thus, while PARGa has a conserved protein architecture, only ARH3 seems to be present in stickleback, suggesting a potential loss of ARH1 in stickleback (Best et al., 2018; Rack et al., 2018). Together, these results suggest that histone poly-ADP ribosylation, implicated in, for example, tumor suppression and defense against bacterial toxins that are specifically associated to ARH1, might be differentially regulated in stickleback compared to humans. Moreover, the biochemical activity of ARH3 should be studied in order to determine if it can compensate for the loss of ARH1 or if different mechanisms occur in stickleback, and if specific interactions with other epigenetic marks occur.

Histone Glycosylation

O-GlcNAcylation seems to contribute greatly to epigenetic reprogramming, and acts as a nutrient sensor implicated in some cancers (Dehennaut et al., 2014). Interests for nutritional programming through, for example, glucose metabolism, are increasing for cultivated fish species, and it has been demonstrated that rainbow trout juveniles may be reprogrammed through epigenetic modifications (DNA methylation and histone acetylation) (Panserat et al., 2017). Nevertheless, O-GlcNAcylation is poorly understood in teleosts, and has so far only been investigated in zebrafish (Sohn and Do, 2005) as a potential mechanism to confer heat resistance (Radermacher et al., 2014). Recent studies have described O-GlcNAcylation as a very important part of the "histone code", and identified OGT as an interacting partner of the TET enzymes (Dehennaut et al., 2014). In stickleback, we identified OGT and OGA regulating O-GlcNAcylation (Dehennaut et al., 2014), and they seem to be conserved among vertebrates. Together with an absence of duplication/loss events, their putative protein architectures suggest strong conservation of their biochemical activity, making them particularly interesting candidates for epigenetically mediated phenotypes used in assisted evolution, aquaculture, and eco-evolutionary studies (Gavery and Roberts, 2017; Eirin-lopez and Putnam, 2019).

Histone Sumoylation

Histone sumoylation has been recently characterized in mammalian cells and is associated with transcriptional repression (Shiio and Eisenman, 2003). This modification is directed by an enzymatic cascade (E1-E2-E3, similar to ubiquitination) that attaches the three known SUMO proteins (Deyrieux and Wilson, 2017) and is crucial for sperm differentiation, oocyte maturation, and embryogenesis (Deyrieux and Wilson, 2017). On the other hand, deSUMOylation is performed by a family of enzymes called SUMO-specific proteases (SENP). While eight members comprise the human SENP, it seems that only six of them are considered true SENPs (Kim and Baek, 2009). SENPs can be separated into two groups: I containing SENP1-2-3-5, and II containing SENP6-7. In humans, SENP3 and SENP4 are identical, and SENP8 is not specific against SUMO (Kim and Baek, 2009). In stickleback, we found that E1 and E2 seem to be conserved, but only two E3 members were identified. Interestingly, the three stickleback SUMO proteins are conserved among the examined vertebrates, even if SUMO3 underwent different duplication events among the fish species examined. In stickleback, the two groups of SENPs were found, but SENP1 (I) or SENP7 (II) may have been lost. In zebrafish development, histone sumoylation is essential but enzymatic activity of each SUMO protein is redundant (Yuan et al., 2010). Consequently, the loss of SENP1/SENP7 in stickleback might be compensated for and/or the underlying molecular mechanisms as well as interactions with other epigenetic pathways may differ.

Stickleback H2A

Histones (H) are small, basic, and conserved proteins, which constitute a key element to pack DNA and to regulate genome accessibility to transcriptional machinery. In eukaryotes, DNA is wrapped around an octamer of histones constituted by H2A, H2B, H3, and H4 to form the nucleosome, the fundamental subunit of chromatin (Biterge and Schneider, 2014). While histones undergo multiple post-translational modifications on their residues, they can also be replaced by variants (Biterge and Schneider, 2014). Some of these variants such as macroH2A have been studied in marine organisms outside of model species (from diatoms to mollusks and fish) and play a role in environmental responses (Eirin-lopez and Putnam, 2019). For instance, a novel H2A variant (H2Af1o) was discovered in fish oocytes (gibel carp, crucian carp, and zebrafish), and its photophosphorylation seems to be implicated in oocyte maturation (Wu et al., 2009). Despite high expression in early embryogenesis and a higher mobility in the nucleosome than other H2A variants, more research is needed to better understand the underlying mechanisms and their

physiological function during gametogenesis and development (Wu et al., 2009). In stickleback, we found multiple genes coding for H2A variants such as H2Afv, while only one gene codes for macroH2A that can give rise to three isoforms. This differs from mammals, where macroH2A was duplicated and gives rise to three isoforms (2 proteins gene 1, 1 protein gene 2) (Kozlowski et al., 2018). This, in conjunction with its duplication in a number of fish species, suggests potential teleost-specific biological functions. Furthermore, in our opinion, macroH2A might be of particular interest for eco-evolutionary studies as it has been linked to embryonic defects in mouse and zebrafish (Kozlowski et al., 2018), and is essential to cold acclimation in fish (Pinto et al., 2005).

Stickleback Genes Coding for Proteins Implicated in miRNA Biogenesis/Turnover

MicroRNAs, or miRNAs, are a class of non-coding RNA found from plants to animals that play important roles in mRNA destabilization and/or translation. With a size of approximately 22 nucleotides and being highly conserved among eukaryotes, they are typically targets for hundreds of genes making them very important for transcription regulation in time and space (Lim et al., 2005). As described in Best et al. (2018), genes implicated in mRNA biogenesis/turnover are well conserved in fish and vertebrates, even though they were unstudied in stickleback at that time. Our genomic survey supports their conclusion, and further shows that all genes implicated in the different miRNA pathways also occur in stickleback. Also, we did not detect any duplication events among the genes observed in the examined fish species, except for *Drosha* which was duplicated in salmonids (Best et al., 2018). Understanding their modulation and role in particular pathways appears to be important, since miRNAs are conserved in zebrafish (Desvignes et al., 2019), and they have a function in species acclimation to freshwater conditions (Rastorguev et al., 2016, 2017). Moreover, an increasing number of studies in different fish species suggest that miRNA are relevant for adaptation, gametogenesis and development (Tse et al., 2016; Baumgart et al., 2017; Gay et al., 2018), making investigations of miRNA biogenesis/turnover important for potential aquaculture applications, eco-evolutionary studies, and in particular, studies of transgenerational plasticity in the context of rapid climate change (Shama et al., 2016; Gavery and Roberts, 2017; Eirin-lopez and Putnam, 2019).

CONCLUSION

Interest in the interplay between genetic and epigenetic components of adaptive potential in marine aquaculture and wild populations is growing fast, and sticklebacks are an excellent model to address these questions. However, as in many other fish species, we suffer from a lack of knowledge concerning the mechanistic basis of epigenetic responses in comparison to well established model organisms. Recent advances using model species (e.g., zebrafish) demonstrate that epigenetic actors, their enzymatic activities, molecular interactions and biological functions are much more diversified and complex than previously thought. Here, we show that the variable number of genes and loss/duplication events among species could have considerable impacts on the different epigenetic pathways, potentially modifying their "traditional" function. Although most of the epigenetic toolbox seems to be evolutionarily conserved, specific loss/duplication events may have occurred, and underlie the need to precisely characterize the mechanistic basis of observed epigenetic variation in order to understand the role of these modifications and their importance in species adaptation. For this, molecular characterization of each enzyme using classic molecular biology tools (sequencing, expression, localization, enzymatic assays, and inhibition) but also new technologies in a collaborative setting are needed to explore the complex synergy of epigenetic mechanisms in teleosts and other taxonomic groups. This will allow us to tease apart the relative contributions of the "general" epigenetic toolkit (which appears to be more complex than previously thought) and species-specific mechanisms, leading to more precise and efficient use of epigenetic modifications in assisted evolution, aquaculture or conservation, and eco-evolutionary studies.

DATA AVAILABILITY STATEMENT

Publicly available datasets were analyzed in this study. This data can be found here: http://www.ensembl.org/Gasterosteus_aculeatus.

ETHICS STATEMENT

This study was conducted in accordance with German animal welfare standards [Schleswig-Holstein Ministerium für Energiewende, Landwirtschaft, Umwelt, Natur und Digitalisierung (Tierschutz), permit no. V244-17922/2018(38-4/18)].

AUTHOR CONTRIBUTIONS

AF conceived, designed, and performed the experiments, and analyzed the data. AF and LS wrote the manuscript.

FUNDING

This study was funded by a Strategy Funds Grant of the Alfred-Wegener-Institut, Helmholtz-Zentrum für Polar- und Meeresforschung awarded to LS.

SUPPLEMENTARY MATERIAL

The Supplementary Material for this article can be found online at: https://www.frontiersin.org/articles/10.3389/fmars.2019.00721/full#supplementary-material

REFERENCES

Akerberg, A. A., Henner, A., Stewart, S., and Stankunas, K. (2017). Histone demethylases Kdm6ba and Kdm6bb redundantly promote cardiomyocyte proliferation during zebrafish heart ventricle maturation. *Dev. Biol.* 426, 84–96. doi: 10.1016/j.ydbio.2017.03.030

Artemov, A. V., Mugue, N. S., Rastorguev, S. M., Zhenilo, S., Mazur, A. M., Tsygankova, S. V., et al. (2017). Genome-Wide DNA methylation profiling reveals epigenetic adaptation of stickleback to marine and freshwater conditions. *Mol. Biol. Evol.* 34, 2203–2213. doi: 10.1093/molbev/msx156

Balasch, J. C., and Tort, L. (2019). Netting the stress responses in fish. *Front. Endrocrinol.* 10:62. doi: 10.3389/fendo.2019.00062

Balasubramanian, S., Raghunath, A., and Perumal, E. (2019). Role of epigenetics in zebrafish development. *Gene* 18:144049. doi: 10.1016/j.gene.2019.144049

Ballestar, E., and Wolffe, A. P. (2001). Methyl-CpG-binding proteins Targeting specific gene repression. *Eur. J. Biochem. FEBS* 6, 1–6. doi: 10.1046/j.1432-1327.2001.01869.x

Baulcombe, D. C., and Dean, C. (2014). Epigenetic regulation in plant responses to the environment. *Cold Spring Harb. Perspect. Biol.* 6, a019471. doi: 10.1101/cshperspect.a019471

Baumgart, M., Barth, E., Savino, A., Groth, M., Koch, P., Petzold, A., et al. (2017). A miRNA catalogue and ncRNA annotation of the short-living fish Nothobranchius furzeri. *BMC Genomics* 18:693. doi: 10.1186/s12864-017-3951-3958

Belle, J. I., and Nijnik, A. (2014). The international journal of biochemistry H2A-DUBbing the mammalian epigenome: expanding frontiers for histone H2A deubiquitinating enzymes in cell biology and physiology. *Int. J. Biochem. Cell Biol.* 50, 161–174. doi: 10.1016/j.biocel.2014.03.004

Best, C., Ikert, H., Kostyniuk, D. J., Craig, P. M., Navarro-martin, L., Marandel, L., et al. (2018). Epigenetics in teleost fish: from molecular mechanisms to physiological phenotypes. *Comp. Biochem. Physiol. B Biochem. Mol. Biol.* 224, 210–244. doi: 10.1016/j.cbpb.2018.01.006

Biterge, B., and Schneider, R. (2014). Histone variants: key players of chromatin. *Cell Tissue Resp.* 356, 457–466. doi: 10.1007/s00441-014-1862-1864

Black, J. C., Rechem, C. V., and Whetstine, J. R. (2013). Histone lysine methylation dynamics: establishment. *Regulation Biol. Impact. Mol. Cell* 48, 1–32. doi: 10.1016/j.molcel.2012.11.006.Histone

Campos, C., Valente, L. M. P., and Fernandes, J. M. O. (2012). Molecular evolution of zebrafish dnmt3 genes and thermal plasticity of their expression during embryonic development. *Gene* 500, 93–100. doi: 10.1016/j.gene.2012.03.041

Cao, J., and Yan, Q. (2012). Histone ubiquitination and deubiquitination in transcription, DNA damage response, and cancer. *Front. Oncol.* 2:26. doi: 10.3389/fonc.2012.00026

Cosseau, C., Wolkenhauer, O., Padalino, G., Geyer, K. K., Hoffmann, K. F., and Grunau, C. (2017). (Epi)genetic Inheritance in Schistosoma mansoni: a systems approach. *Trends Parasitol.* 33, 285–294. doi: 10.1016/j.pt.2016.12.002

Cossins, A. R., and Crawford, D. L. (2005). Fish as models for environmental genomics. *Nat. Rev. Genet.* 6, 324–340.

Costa-pinheiro, P., and Montezuma, D. (2015). Diagnostic and prognostic epigenetic biomarkers in cancer. *Epigenomics* 7, 1003–1015. doi: 10.2217/epi.15.56

Dehennaut, V., Leprince, D., and Lefebvre, T. (2014). O -GlcNAcylation, an epigenetic mark . Focus on the histone code, TET family proteins, and polycomb group proteins. *Front. Endrocrinol.* 5:155. doi: 10.3389/fendo.2014.00155

Desvignes, T., Batzel, P., Sydes, J., Eames, B. F., and Postlethwait, J. H. (2019). miRNA analysis with Prost! reveals evolutionary conservation of organ-enriched expression and post-transcriptional modifications in three-spined stickleback and zebrafish. *Sci. Rep.* 9:3913. doi: 10.1038/s41598-019-40361-40368

Deyrieux, A. F., and Wilson, V. G. (2017). Sumoylation in development and differentiation. *Adv. Exp. Med. Biol.* 963, 197–214. doi: 10.1007/978-3-319-50044-7

Dupret, B., Völkel, P., Vennin, C., Toillon, R., Le, X., and Angrand, P. (2017). The histone lysine methyltransferase Ezh2 is required for maintenance of the intestine integrity and for caudal fin regeneration in zebrafish. *BBA Gene. Regul. Mech.* 1860, 1079–1093. doi: 10.1016/j.bbagrm.2017.08.011

Eckersley-maslin, M. A., Alda-catalinas, C., and Reik, W. (2018). Dynamics of the epigenetic landscape during the maternal-to-zygotic transition. *Nat. Rev. Mol. Cell Biol.* 19, 436–450. doi: 10.1038/s41580-018-0008-z

Edgar, R. C. (2004). MUSCLE: multiple sequence alignment with high accuracy and high throughput. *Nucleic Acids Res.* 32, 1792–1797. doi: 10.1093/nar/gkh340

Eirin-lopez, J. M., and Putnam, H. M. (2019). Marine environmental epigenetics. *Ann. Rev. Mar. Sci.* 11, 335–368. doi: 10.1146/annurev-marine-010318-095114

Ellison, A., Rodrı, C. M., Moran, P., Breen, J., Swain, M., Megias, M., et al. (2015). Epigenetic regulation of sex ratios may explain natural variation in self-fertilization rates. *Proc. R. Soc. B* 282:20151900. doi: 10.1098/rspb.2015.1900

Fatemi, M., and Wade, P. A. (2006). MBD family proteins: reading the epigenetic code. *J. Cell Sci.* 119(Pt 15), 3033–3037. doi: 10.1242/jcs.03099

Fellous, A., Earley, R. L., and Silvestre, F. (2019a). Identification and expression of mangrove rivulus (*Kryptolebias marmoratus*) histone deacetylase (HDAC) and lysine acetyltransferase (KAT) genes. *Gene* 691, 56–69. doi: 10.1016/j.gene.2018.12.057

Fellous, A., Earley, R. L., and Silvestre, F. (2019b). The Kdm / Kmt gene families in the self-fertilizing mangrove rivulus fish, *Kryptolebias marmoratus*, suggest involvement of histone methylation machinery in development and reproduction. *Gene* 687, 173–187. doi: 10.1016/j.gene.2018.11.046

Fellous, A., Franc, L. L. E., Jouaux, A., Goux, D., and Favrel, P. (2019c). Histone methylation participates in gene expression control during the early development of the pacific oyster *Crassostrea gigas*. *Genes* 10:695. doi: 10.3390/genes10090695

Fellous, A., Favrel, P., Guo, X., and Riviere, G. (2014). The Jumonji gene family in *Crassostrea gigas* suggests evolutionary conservation of Jmj-C histone demethylases orthologues in the oyster gametogenesis and development. *Gene* 538, 164–175. doi: 10.1016/j.gene.2013.12.016

Fellous, A., Favrel, P., and Riviere, G. (2015). Temperature influences histone methylation and mRNA expression of the Jmj-C histone-demethylase orthologues during the early development of the oyster *Crassostrea gigas*. *Mar. Genomics* 19, 23–30. doi: 10.1016/j.margen.2014.09.002

Fellous, A., Labed-Veydert, T., Locrel, M., Voisin, A.-S., Earley, R. L., and Silvestre, F. (2018). DNA methylation in adults and during development of the self-fertilizing mangrove rivulus, *Kryptolebias marmoratus*. *Ecol. Evol.* 8, 6016–6033. doi: 10.1002/ece3.4141

Feng, S., Cokus, S. J., Zhang, X., Chen, P.-Y., Bostick, M., Goll, M. G., et al. (2010). Conservation and divergence of methylation patterning in plants and animals. *Proc. Natl. Acad. Sci. U.S.A.* 107, 8689–8694. doi: 10.1073/pnas.1002720107

Fincham, J. (1997). Epigenetic Mechanisms of Gene Regulation. Cold Spring Harbor, NY: Cold Spring Harbor Laboratory Press.

Firmino, J., Carballo, C., Armesto, P., Campinho, M. A., Power, D. M., and Manchado, M. (2017). Phylogeny, expression patterns and regulation of DNA Methyltransferases in early development of the flatfish, *Solea senegalensis*. *BMC Dev. Biol.* 17:11. doi: 10.1186/s12861-017-0154-0

Gao, H., Bu, Y., Wu, Q., Wang, X., Chang, N., Lei, L., et al. (2015). Mecp2 regulates neural cell differentiation by suppressing the Id1 to Her2 axis in zebrafish. *J. Cell Sci.* 128, 2340–2350. doi: 10.1242/jcs.167874

Gavery, M. R., Nichols, K. M., Berejikian, B. A., Tatara, C. P., Goetz, G. W., Dickey, J. T., et al. (2019). Temporal dynamics of DNA methylation patterns in response to rearing juvenile steelhead (*Oncorhynchus mykiss*) in a hatchery versus simulated stream environment. *Genes* 10:E356. doi: 10.3390/genes10050356

Gavery, M. R., and Roberts, S. B. (2017). Epigenetic considerations in aquaculture. *PeerJ* 5:e4147. doi: 10.7717/peerj.4147

Gay, S., Bugeon, J., Bouchareb, A., Henry, L., Delahaye, C., Legeai, F., et al. (2018). MiR-202 controls female fecundity by regulating medaka oogenesis. *LoS Genet.* 14:e1007593. doi: 10.1371/journal.pgen.1007593

Greiss, S., and Gartner, A. (2013). Sirtuin/Sir2 phylogeny, evolutionary considerations and structural conservation. *Mol. Cells* 28, 407–415. doi: 10.1007/s10059-009-0169-x.Sirtuin/Sir2

He, Y., Wu, J., Mei, H., Yu, H., Sun, S., Shou, J., et al. (2014). Histone deacetylase activity is required for embryonic posterior lateral line development. *Cell Prolif.* 47, 91–104. doi: 10.1111/cpr.12081

Heckwolf, M. J., Eizaguirre, C., Meyer, B. S., Döring, T., and Reusch, T. B. H. (2018). Transgenerational plasticity and selection shape the adaptive potential of sticklebacks to salinity change. *Evol. Appl.* 11, 1873–1885. doi: 10.1111/eva.12688

Heckwolf, M. J., Meyer, B. S., Häsler, R., and Höppner, M. P. (2019). DNA methylation facilitates local adaptation and adaptive transgenerational plasticity. *Biorxiv*. [Preprint]. doi: 10.1101/649574

Horsfield, J. A. (2019). Packaging development: how chromatin controls transcription in zebrafish embryogenesis. *Biochem. Soc. Trans.* 47, 713–724. doi: 10.1042/BST20180617

Jiang, F., Liu, Q., Wang, Y., Zhang, J., Wang, H., Song, T., et al. (2017). Comparative genomic analysis of SET domain family reveals the origin, expansion, and putative function of the arthropod-specific SmydA genes as histone modifiers in insects. *Giga Sci.* 6, 1–16. doi: 10.1093/gigascience/gix031

Ka, W., and Tse, F. (2017). Importance of deubiquitinases in zebrafish craniofacial development. *Biochem. Biophys. Res. Commun.* 487, 813–819. doi: 10.1016/j.bbrc.2017.04.132

Kamstra, J. H., Aleström, P., Kooter, J. M., and Legler, J. (2015). Zebrafish as a model to study the role of DNA methylation in environmental toxicology. *Environ. Sci. Pollut. Res.* 22, 16262–16276. doi: 10.1007/s11356-014-3466-7

Karmodiya, K., Anamika, K., Muley, V., Pradhan, S. J., Bhide, Y., and Galande, S. (2014). Camello, a novel family of histone acetyltransferases that acetylate histone H4 and is essential for zebrafish. *Sci. Rep.* 4, 1–9. doi: 10.1038/srep06076

Kim, J. H., and Baek, S. H. (2009). Emerging roles of desumoylating enzymes. *BBA Mol. Basis Dis.* 1792, 155–162. doi: 10.1016/j.bbadis.2008.12.008

Kitano, J., Ishikawa, A., and Kusakabe, M. (2019). Parallel transcriptome evolution in stream threespine sticklebacks. *Dev. Growt. Differ.* 61, 104–113. doi: 10.1111/dgd.12576

Kozlowski, M., Corujo, D., Hothorn, M., Guberovic, I., Mandemaker, I. K., Blessing, C., et al. (2018). MacroH2A histone variants limit chromatin plasticity through two distinct mechanisms. *EMBO Rep.* 19:e44445. doi: 10.15252/embr.201744445

Kumar, A., Anuppalle, M., Maddirevula, S., Huh, L., Choe, J., Rhee, M., et al. (2019). Peli1b governs the brain patterning via ERK signaling pathways in zebrafish embryos. *Gene*. 694, 1–6. doi: 10.1016/j.gene.2018.12.078

Kumar, S., Stecher, G., and Tamura, K. (2016). MEGA7: molecular evolutionary genetics analysis version 7 . 0 for bigger datasets. *Mol. Biol. Evol.* 33, 1870–1874. doi: 10.1093/molbev/msw054

Labbé, C., Robles, V., and Paz, M. (2017). Epigenetics in fish gametes and early embryo. *Aquaculture* 472, 93–106. doi: 10.1016/j.aquaculture.2016.07.026

Laporte, M., Luyer, J., Le Rougeux, C., Krick, M., and Bernatchez, L. (2019). DNA methylation reprogramming, TE derepression, and postzygotic isolation of nascent animal species. *Sci. Adv.* 5, 1–9. doi: 10.1126/sciadv.aaw1644

Le Luyer, J., Laporte, M., Beacham, T. D., Kaukinen, K. H., Withler, R. E., and Leong, J. S. (2017). Parallel epigenetic modifications induced by hatchery rearing in a Pacific salmon. *Proc. Natl. Acad. Sci. U.S.A.* 114, 12964–12969. doi: 10.1073/pnas.1711229114

Lei, L., Zhou, S., Ma, H., and Zhang, L. (2012). Expansion and diversification of the SET domain gene family following whole-genome duplications in Populus trichocarpa. *BMC Evol. Biol.* 12:51. doi: 10.1186/1471-2148-12-51

Li, E., Bestor, T. H., and Jaenisch, R. (1992). Targeted mutation of the DNA methyltransferase gene results in embryonic lethality. *Cell* 69, 915–926. doi: 10.1016/0092-8674(92)90611-f

Lim, L. P., Lau, N. C., Garrett-engele, P., and Grimson, A. (2005). Microarray analysis shows that some microRNAs downregulate large numbers of target mRNAs. *Nature* 292, 288–292.

Lindeman, L. C., Winata, C. L., Aanes, H., Mathavan, S., Aleström, P., and Collas, P. (2010). Chromatin states of developmentally-regulated genes revealed by DNA and histone methylation patterns in zebrafish embryos. *Int. J. Dev. Biol.* 813, 803–813. doi: 10.1387/ijdb.103081ll

Loponte, S., Segré, C. V., Senese, S., Miccolo, C., Santaguida, S., De, G., et al. (2016). Dynamic phosphorylation of histone deacetylase 1 by aurora kinases during mitosis regulates zebrafish embryos development. *Sci. Rep.* 6:30213. doi: 10.1038/srep30213

Lyko, F. (2018). The DNA methyltransferase family: a versatile toolkit for epigenetic regulation. *Nat. Rev. Genet.* 19, 81–92. doi: 10.1038/nrg.2017.80

Martin, C., and Zhang, Y. (2005). The diverse functions of histone lysine methylation. *Mol. Cell Biol.* 6, 838–849. doi: 10.1038/nrm1761

Mcghee, K. E., and Bell, A. M. (2014). Paternal care in a fish: epigenetics and fitness enhancing effects on offspring anxiety. *Proc. R. Soc. B* 281, 2–7.

Metzger, D. C. H., and Schulte, P. M. (2016). Epigenomics in marine fishes. *Mar. Genomics* 30, 43–54. doi: 10.1016/j.margen.2016.01.004

Metzger, D. C. H., and Schulte, P. M. (2017). Persistent and plastic effects of temperature on DNA methylation across the genome of threespine stickleback (*Gasterosteus aculeatus*). *Proc. R. Soc. B* 284:20171667. doi: 10.1098/rspb.2017.1667

Metzger, D. C. H., and Schulte, P. M. (2018). The DNA methylation landscape of stickleback reveals patterns of sex chromosome evolution and effects of environmental salinity. *Genome Biol. Evol.* 10, 1–30. doi: 10.1093/gbe/evy034/4840697

Nijman, S. M. B., Luna-vargas, M. P. A., Velds, A., Brummelkamp, T. R., Dirac, A. M. G., Sixma, T. K., et al. (2005). A genomic and functional inventory of deubiquitinating enzymes. *Cell* 123, 773–786. doi: 10.1016/j.cell.2005.11.007

Nozawa, K., Lin, Y., Kubodera, R., Shimizu, Y., and Tanaka, H. (2017). Zebrafish Mecp2 is required for proper axonal elongation of motor neurons and synapse formation. *Dev. Neurobiol.* 77, 1101–1113. doi: 10.1002/dneu.22498

Okano, M., Bell, D. W., Haber, D. A., and Li, E. (1999). DNA methyltransferases Dnmt3a and Dnmt3b are essential for de novo methylation and mammalian development. *Cell* 99, 247–257. doi: 10.1016/s0092-8674(00)81656-6

Panserat, S., Marandel, L., Geurden, I., Veron, V., Dias, K., Plagnes-juan, E., et al. (2017). Muscle catabolic capacities and global hepatic epigenome are modi fi ed in juvenile rainbow trout fed different vitamin levels at fi rst feeding. *Aquaculture* 468, 515–523. doi: 10.1016/j.aquaculture.2016.11.021

Perina, D., Mikoè, A., Ahel, J., Cetkovi, H., and Ahel, I. (2014). Distribution of protein poly (ADP-ribosyl) ation systems across all domains of life. *DNA Repair.* 23, 4–16. doi: 10.1016/j.dnarep.2014.05.003

Petrie, K., Guidez, F., Howell, L., Healy, L., Waxman, S., Greaves, M., et al. (2003). The histone deacetylase 9 gene encodes multiple protein isoforms. *J. Biol. Chem.* 278, 16059–16072. doi: 10.1074/jbc.M212935200

Petrossian, T. C., and Clarke, S. G. (2011). Uncovering the human methyltransferasome. *Mol. Cell. Proteomics* 10:M110.000976. doi: 10.1074/mcp.M110.000976

Pinto, R., Ivaldi, C., Reyes, M., Mietton, F., Mongelard, F., Alvarez, M., et al. (2005). Seasonal environmental changes regulate the expression of the histone variant macroH2A in an eurythermal fish. *FEBS Lett.* 579, 5553–5558. doi: 10.1016/j.febslet.2005.09.019

Potok, M., Nix, D., Parnell, T., and Cairns, B. (2013). Reprogramming the maternal zebrafish genome after fertilization to match the paternal methylation pattern. *Cell* 153, 759–772. doi: 10.1016/j.cell.2013.04.030

Putnam, H. M., Davidson, J. M., and Gates, R. D. (2016). Ocean acidification influences host DNA methylation and phenotypic plasticity in environmentally susceptible corals. *Evol. Appl.* 9, 1165–1178. doi: 10.1111/eva.12408

Putnam, H. M., and Gates, R. D. (2015). Preconditioning in the reef-building coral Pocillopora damicornis and the potential for trans-generational acclimatization in coral larvae under future climate change conditions. *J. Exp. Biol.* 218, 2365–2372. doi: 10.1242/jeb.123018

Qian, S., Wang, Y., Ma, H., and Zhang, L. (2015). Expansion and functional divergence of jumonji C-Containing histone demethylases: signi fi cance of duplications in ancestral angiosperms and vertebrates. *Plant Physiol.* 168, 1321–1337. doi: 10.1104/pp.15.00520

Rack, J. G. M., Ariza, A., Drown, B. S., Shirai, T., Hergenrother, P. J., Shirai, T., et al. (2018). (ADP-ribosyl) hydrolases: Structural Basis for Differential Substrate Recognition and Inhibition Basis for Differential Substrate Recognition and

Inhibition. *Cell Chem. Biol.* 25, 1533.e12–1546.e12. doi: 10.1016/j.chembiol.2018.11.001

Radermacher, P. T., Myachina, F., Bosshardt, F., Pandey, R., Mariappa, D., and Müller, H. J. (2014). O- GlcNAc reports ambient temperature and confers heat resistance on ectotherm development. *Proc. Natl. Acad. Sci. U.S.A.* 111, 5592–5597. doi: 10.1073/pnas.1322396111

Rastorguev, S. M., Nedoluzhko, A. V., Gruzdeva, N. M., Boulygina, E. S., and Sharko, F. S. (2017). Differential miRNA expression in the three-spined stickleback, response to environmental changes. *Sci. Rep.* 7:18089. doi: 10.1038/s41598-017-18128-w

Rastorguev, S. M., Nedoluzhko, A. V., Sokolov, A. S., Gruzdeva, N. M., Skryabin, K. G., and Prokhortchouk, E. B. (2016). Identification of novel microRNA genes in freshwater and marine ecotypes of the three- spined stickleback (*Gasterosteus aculeatus*). *Mol. Ecol. Resour.* 16, 1491–1498. doi: 10.1111/1755-0998.12545

Riviere, G., Wu, G. C., Fellous, A., Goux, D., Sourdaine, P., and Favrel, P. (2013). DNA methylation is crucial for the early development in the Oyster *C. gigas*. *Mar. Biotechnol.* 15, 739–753. doi: 10.1007/s10126-013-9523-9522

Román, A.-C., Vicente-Page, J., Pérez-Escudero, A., Carvajal-González, J. M., Fernández-Salguero, P. M., and de Polavieja, G. G. (2018). Histone H4 acetylation regulates behavioral inter-individual variability in zebrafish. *Genome Biol.* 19:55. doi: 10.1186/s13059-018-1428-y

Rossetto, D., Avvakumov, N., and Côté, J. (2012). Histone phosphorylation: a chromatin modification involved in diverse nuclear events. *Epigen* 7, 1098–1108. doi: 10.4161/epi.21975

Santiago, M., Antunes, C., Guedes, M., Sousa, N., and Marques, C. J. (2014). Genomics TET enzymes and DNA hydroxymethylation in neural development and function – How critical are they? *Genomics* 104, 334–340. doi: 10.1016/j.ygeno.2014.08.018

Sasai, N., Kato, Y., Kimura, G., and Takeuchi, T. (2007). The *Drosophila* jumonji gene encodes a JmjC-containing nuclear protein that is required for metamorphosis. *FEBS J.* 274, 6139–6151. doi: 10.1111/j.1742-4658.2007.06135.x

Seebacher, F., and Simmonds, A. I. M. (2019). Histone deacetylase activity mediates thermal plasticity in zebrafish (Danio rerio). *Sci. Rep.* 9:8216. doi: 10.1038/s41598-019-44726-x

Seto, E., and Yoshida, M. (2014). Erasers of histone acetylation: the histone deacetylase enzymes. *Cold Spring Harb. Perspect. Biol.* 6, 1–26. doi: 10.1101/cshperspect.a018713

Shama, L. N. S. (2017). The mean and variance of climate change in the oceans: hidden evolutionary potential under stochastic environmental variability in marine sticklebacks. *Sci. Rep.* 7:8889. doi: 10.1038/s41598-017-07140-7149

Shama, L. N. S., Mark, F. C., Strobel, A., Lokmer, A., John, U., and Wegner, K. M. (2016). Transgenerational effects persist down the maternal line in marine sticklebacks: gene expression matches physiology in a warming ocean. *Evol. Appl.* 9, 1096–1111. doi: 10.1111/eva.12370

Shama, L. N. S., and Wegner, K. M. (2014). Grandparental effects in marine sticklebacks: transgenerational plasticity across multiple generations. *J. Evol. Biol.* 27, 2297–2307. doi: 10.1111/jeb.12490

Shanmugam, M. K., Arfuso, F., and Arumugam, S. (2018). Role of novel histone modifications in cancer. *Oncotarget* 9, 11414–11426.

Shechter, D., Chitta, R. K., Xiao, A., Shabanowitz, J., Hunt, D. F., and Allis, C. D. (2009). A distinct H2A.X isoform is enriched in Xenopus laevis eggs and early embryos and is phosphorylated in the absence of a checkpoint. *PNAS* 106, 749–754. doi: 10.1073/pnas.0812207106

Sheikh, B. N., and Akhtar, A. (2018). The many lives of KATs – detectors, integrators and modulators of the cellular environment. *Nat. Rev. Genet.* 20, 7–23. doi: 10.1038/s41576-018-0072-74

Sheng, K., Liang, X., Huang, S., and Xu, W. (2014). The role of histone ubiquitination during spermatogenesis. *Biomed Res. Int.* 2014:870695. doi: 10.1155/2014/870695

Shi, L., Sun, L., Li, Q., Liang, J., Yu, W., Yi, X., et al. (2011). Histone demethylase JMJD2B coordinates H3K4 / H3K9 methylation and promotes hormonally responsive breast carcinogenesis. *Proc. Natl. Acad. Sci. U.S.A.* 108, 7541–7546. doi: 10.1073/pnas.1017374108

Shiio, Y., and Eisenman, R. N. (2003). Histone sumoylation is associated with transcriptional repression. *PNSA* 100, 13225–13230. doi: 10.1073/pnas.1735528100

Shin, J., Kim, J., Park, H., and Kim, J. (2018). Investigating the role of Sirtuins in cell reprogramming. *BMB Rep.* 51, 500–507. doi: 10.5483/bmbrep.2018.51.10.172

Smith, G., Smith, C., Kenny, J. G., Chaudhuri, R. R., and Ritchie, M. G. (2018). Genome-Wide DNA methylation patterns in wild samples of two morphotypes of threespine stickleback (*Gasterosteus aculeatus*). *Mol. Biol. Evol.* 32, 888–895. doi: 10.1093/molbev/msu344

Sohn, K., and Do, S. (2005). Transcriptional regulation and O-GlcNAcylation activity of zebrafish OGT during embryogenesis. *Biochem. Biophys. Res. Commun.* 337, 256–263. doi: 10.1016/j.bbrc.2005.09.049

Stewart, S., Tsun, Z., Carlos, J., and Belmonte, I. (2009). A histone demethylase is necessary for regeneration in zebrafish. *Proc. Natl. Acad. Sci. U.S.A.* 106, 19889–19894. doi: 10.1073/pnas.0904132106

Takeuchi, T., Kojima, M., Nakajima, K., and Kondo, S. (1999). jumonji gene is essential for the neurulation and cardiac development of mouse embryos with a C3H / He background. *Mech. Dev.* 86, 29–38. doi: 10.1016/s0925-4773(99)00100-8

Teigen, L. E., Orczewska, J. I., McLaughlin, J., and O'Brien, K. M. (2015). Cold acclimation increases levels of some heat shock protein and sirtuin isoforms in threespine stickleback. *Comp. Biochem. Physiol. Part A Mol. Integr. Physiol.* 188, 139–147. doi: 10.1016/j.cbpa.2015.06.028

Todd, E. V., Ortega-recalde, O., Liu, H., Lamm, M. S., Rutherford, K. M., Cross, H., et al. (2019). Stress, novel sex genes, and epigenetic reprogramming orchestrate socially controlled sex change. *Sci. Adv.* 5, 1–14.

Toni, L. S., and Padilla, P. A. (2016). Developmentally arrested austrofundulus limnaeus embryos have changes in post-translational modifications of histone H3. *Co. Biol.* 219, 544–552. doi: 10.1242/jeb.131862

Tse, A. C., Li, J., Yuan, S., Chan, T., Po, K., and Wu, R. S. (2016). Hypoxia alters testicular functions of marine medaka through microRNAs regulation. *Aquat. Toxicol.* 180, 266–273. doi: 10.1016/j.aquatox.2016.10.007

Tse, W. K. F., Eisenhaber, B., Ho, S. H. K., Ng, Q., Eisenhaber, F., and Jiang, Y. (2009). Genome-wide loss-of-function analysis of deubiquitylating enzymes for zebrafish development. *BMC Genomics* 15:637. doi: 10.1186/1471-2164-10-637

Van Leeuwen, F., Gafken, P. R., and Gottschling, D. E. (2002). Dot1p modulates silencing in yeast by methylation of the nucleosome core. *Cell* 109, 745–756. doi: 10.1016/S0092-8674(02)00759-756

Van Otterdijk, S. D., and Michels, K. B. (2016). Transgenerational epigenetic inheritance in mammals: how good is the evidence? *FASEB J.* 30, 2457–2465. doi: 10.1096/fj.201500083

Vastenhouw, N. L., Cao, W. X., and Lipshitz, H. D. (2019). The maternal-to-zygotic transition revisited. *Development* 146, dev161471. doi: 10.1242/dev.161471

Verdone, L., Fortezza, M., La Ciccarone, F., and Caiafa, P. (2015). Poly (ADP-Ribosyl) ation affects histone acetylation and transcription. *PLoS One* 3:e0144287. doi: 10.1371/journal.pone.0144287

Wang, G., and Köhler, C. (2017). Epigenetic processes in flowering plant reproduction. *J. Exp. Bot.* 68, 797–807. doi: 10.1093/jxb/erw486

Wang, X., and Bhandari, R. K. (2019). DNA methylation dynamics during epigenetic reprogramming of medaka embryo embryo. *Epigenetics* 0, 1–12. doi: 10.1080/15592294.2019.1605816

Wang, Y., and Li, C. (2012). Evolutionarily conserved protein arginine methyltransferases in non-mammalian animal systems. *FEBS J.* 279, 932–945. doi: 10.1111/j.1742-4658.2012.08490.x

Wang, Y., Liu, Q., Tang, F., Yan, L., and Qiao, J. (2019). Epigenetic regulation and risk factors during the development of human gametes and early embryos. *Annu. Rev. Genomics Hum. Genet.* 20, 1–20. doi: 10.1146/annurev-genom-083118-015143

Wu, N., Yue, H., Chen, B., and Gui, J. (2009). Histone H2A has a novel variant in fish oocytes 1. *Biol. Reprod.* 283, 275–283. doi: 10.1095/biolreprod.108.074955

Yang, X. (2015). MOZ and MORF acetyltransferases: molecular interaction, animal development and human disease. *BBA Mol. Cell Res.* 1853, 1818–1826. doi: 10.1016/j.bbamcr.2015.04.014

Yeh, H., and Klesius, P. H. (2012). Molecular characterization, phylogenetic analysis and expression patterns of five protein arginine

methyltransferase genes of channel catfish, Ictalurus punctatus (Rafinesque). *Fish Physio. Bioch.* 38, 1083–1098. doi: 10.1007/s10695-011-9593-x

Yuan, H., Zhou, J., Deng, M., Liu, X., Le Bras, M., De The, H., et al. (2010). Small ubiquitin-related modifier paralogs are indispensable but functionally redundant during early development of zebrafish. *Cell Res.* 20, 185–196. doi: 10.1038/cr.2009.101

Zhang, J., Jing, L. I., Li, M., He, L., and Guo, Z. (2019). Regulation of histone arginine methylation / demethylation by methylase and demethylase (Review). *Mol. Med. Rep.* 19, 3963–3971. doi: 10.3892/mmr.2019.10111

Zhao, H., and Chen, T. (2013). Tet family of 5-methylcytosine dioxygenases in mammalian development. *J. Hum. Genet.* 58, 421–427. doi: 10.1038/jhg.2013.63

Zheng, N., and Shabek, N. (2017). Ubiquitin ligases: structure, function, and regulation. *Annu. Rev. Biochem.* 86, 129–157. doi: 10.1146/annurev-biochem-060815-014922

Conflict of Interest: The authors declare that the research was conducted in the absence of any commercial or financial relationships that could be construed as a potential conflict of interest.

frontiers in Marine Science

ORIGINAL RESEARCH
published: 08 January 2020
doi: 10.3389/fmars.2019.00792

Convergence of DNA Methylation Profiles of the Reef Coral *Porites astreoides* in a Novel Environment

James L. Dimond[1,2]* *and Steven B. Roberts*[1]

[1] School of Aquatic and Fishery Sciences, University of Washington, Seattle, WA, United States, [2] Shannon Point Marine Center, Western Washington University, Anacortes, WA, United States

Phenotypic acclimatization is an organismal response to environmental change that may be rooted in epigenetic mechanisms. In reef building corals, organisms that are severely threatened by environmental change, some evidence suggests that DNA methylation is an environmentally responsive mediator of acclimatization. We investigated changes in DNA methylation of the reef coral *Porites astreoides* in response to simulated environmental change. Coral colonies were sampled from a variety of habitats on the Belize Barrier Reef and transplanted to a common garden for 1 year. We used restriction site associated DNA sequencing, including a methylation-sensitive variant, to subsample the genome and assess changes in DNA methylation levels after a year in the common garden. Methylation changes among the 629 CpG loci we recovered were subtle, yet coral methylomes were more similar to each other after a year in the common garden together, indicating convergence of methylation profiles in the common environment. Differentially methylated loci showed matches with both coding and non-coding RNA sequences with putative roles in intracellular signaling, apoptosis, gene regulation, and epigenetic crosstalk. There was a positive and significant relationship between genetic and epigenetic variation, providing evidence of methylation heritability. Altogether, our results suggest that DNA methylation in *P. astreoides* is at least somewhat responsive to environmental change, reflective of the environment, and heritable, characteristics necessary for methylation to be implicated as part of potential transgenerational acclimatization responses.

Keywords: coral, epigenetic, *Porites astreoides*, DNA methylation, acclimatization

OPEN ACCESS

Edited by:
Andrew Stanley Mount, Clemson University, United States

Reviewed by:
Iliana B. Baums, Pennsylvania State University (PSU), United States
Kevin Marquez Johnson, Louisiana State University, United States

***Correspondence:**
James L. Dimond
jdimond@gmail.com

Specialty section:
This article was submitted to Marine Molecular Biology and Ecology, a section of the journal Frontiers in Marine Science

Received: *27 August 2019*
Accepted: *09 December 2019*
Published: *08 January 2020*

Citation:
Dimond JL and Roberts SB (2020) Convergence of DNA Methylation Profiles of the Reef Coral Porites astreoides in a Novel Environment. Front. Mar. Sci. 6:792. doi: 10.3389/fmars.2019.00792

INTRODUCTION

Epigenetic processes, which contribute to gene regulation without affecting underlying DNA sequences, are increasingly recognized as molecular mechanisms that shape phenotypic responses (Duncan et al., 2014). Moreover, epigenetic signatures of organisms can change over their lifetimes, acting as potential records of, and responses to, environmental changes (Duncan et al., 2014; Hofmann, 2017; Eirin-Lopez and Putnam, 2019). The expanding evidence for both consequential functions of epigenetic processes and their plasticity is therefore driving interest among environmental and evolutionary biologists in search of the molecular basis of phenotypic plasticity, local adaptation, and acclimatization to climate change (Duncan et al., 2014; Hofmann, 2017; Eirin-Lopez and Putnam, 2019).

Although epigenetics encompasses a suite of molecular processes that appear to interact together, DNA methylation is the best understood and most widely studied of these processes (Eirin-Lopez and Putnam, 2019). In the animal kingdom, 5-methylcytosine is the most common form of DNA methylation and is almost exclusively associated with CpG motifs. Invertebrate genomes are generally more sparsely methylated than vertebrate genomes, and methylation tends to be concentrated within gene bodies (i.e., introns and exons) of housekeeping genes (Sarda et al., 2012). While our understanding of the function of gene body methylation is only in its infancy, current evidence suggests that it helps ensure transcriptional fidelity, consistency, and efficiency, and may also be involved in alternative mRNA splicing (Flores et al., 2012; Neri et al., 2017).

Stable yet labile, epigenetic marks like DNA methylation can persist over generations, but they can also be primed and altered by environmental changes. In this way, epigenetic processes are thought to impart environmental "memories" in organisms (Iwasaki and Paszkowski, 2014). Environmental memories may be particularly relevant in organisms such as plants and sessile invertebrates because they must weather any changes in their environment. Indeed, there are numerous examples of environmentally inducible epigenetic modifications in plants (Iwasaki and Paszkowski, 2014; Kinoshita and Seki, 2014). For sessile invertebrates, however, far less is known, and studies are just beginning to emerge.

Tropical reef corals are long-lived, sessile invertebrates that are thought to be particularly reliant on physiological acclimatization and phenotypic plasticity to cope with environmental variation (Gates and Edmunds, 1999; Todd, 2008). The underlying basis of this plasticity could lie, at least in part, in epigenetic mechanisms like DNA methylation (Roberts and Gavery, 2012). However, in order to mediate phenotypic plasticity and acclimatization, DNA methylation itself must be plastic. To date, only a few studies have evaluated the response of DNA methylation to environmental change in corals. In a comparative study of two species of corals, Putnam et al. (2016) found that global methylation levels of *Montipora capitata* did not change in response to reduced pH conditions, while those of *Pocillopora damicornis* were responsive. Within genets of *Acropora palmata*, Durante et al. (2019) showed evidence for microenvironmental influence on methylation. In a study of simulated ocean acidification conditions with *Stylophora pistillata*, Liew et al. (2018b) observed modifications in methylation levels of genes involved in cell cycle and body size pathways that were reflected by phenotypic changes. Finally, in a reciprocal transplant study, Dixon et al. (2018) reported genome-wide changes in methylation in *Acropora millepora* that were correlated with physiological and transcriptional plasticity. In the latter two studies, there was evidence that changes in methylation were associated with acclimatization. However, we still lack sufficient information on the extent to which DNA methylation responds to environmental change.

In this study, we used a common garden transplantation approach to investigate the response of DNA methylation to environmental change in the Western Atlantic reef coral *Porites astreoides*. Corals were resampled after a year in a common garden and methylation levels were assessed using restriction site associated DNA sequencing (RADseq) techniques. We hypothesized that DNA methylation would be responsive to this manipulation and that methylation profiles among colonies would be more similar to each other after a year in a common environment.

MATERIALS AND METHODS

Common Garden Experiment

In November 2015, 19 colonies of *P. astreoides* (approximately 20 cm diameter) were transplanted from their home site to a common garden in the shallow (∼1 m depth) backreef in front of Carrie Bow Cay (CBC; 16° 48′ 9″N, 88° 4′ 55″W), Belize. Coral colonies were haphazardly selected from shallow habitats (1–3 m depth) within a 20 km radius of CBC. Some colonies were collected from windward backreef habitats similar to those of CBC, while others were collected from inshore habitats. Upon collection, colonies were first sampled for DNA by chipping off a small piece of the colony with hammer and chisel, then preserving the fragment in salt-saturated DMSO solution at room temperature until extraction. Colonies were then halved, and one half was brought to the common garden, an approximately 9 m^2 area, where they were reattached to the substratum using A-788 splash zone compound. Fourteen of the original 19 colonies also had their remaining half reattached to the substratum from which they were collected, serving as controls. Numbered aluminum tags were attached adjacent to each coral to permit later identification, and subsurface floats were moored near all control colonies left at their site of origin. Colonies were resampled 1 year later in November 2016, again removing and preserving a small fragment for DNA extraction.

Environmental Analysis

To characterize the surrounding physical environment, remotely sensed data from the AQUA MODIS satellite sensor were used (NASA Goddard Space Flight Center et al., 2016). Previous studies have reported strong correlations between remotely sensed sea surface temperatures (SST) and those recorded from data loggers moored in shallow benthic habitats, suggesting that remotely sensed data is appropriate for studies of shallow benthic environments (Pearce et al., 2006; Smale and Wernberg, 2009). Monthly AQUA MODIS climatology datasets for the period November 2015 to October 2016 were used. For SST, we used the 11 μ band nighttime dataset (NASA Goddard Space Flight Center et al., 2016). For chlorophyll concentration, the OCx algorithm was used (NASA Goddard Space Flight Center et al., 2016). Datasets were imported into R as raster images for analysis. Additionally, Belize basemap (Meerman and Clabaugh, 2017) and coral reef basemap (UNEP-WCMC et al., 2018) shapefiles were used to provide spatial context.

DNA Extraction and Sequencing

DNA extraction and library preparation and sequencing followed methods described in detail by Dimond et al. (2017). Briefly, libraries were prepared according to the double-digest RADseq

(ddRADseq) and EpiRADseq methods of Peterson et al. (2012) and Schield et al. (2016), respectively. This created tandem libraries for each sample; the ddRADseq library used a methylation insensitive common cutter (*Msp*I) targeting 5′-CCGG-3′ motifs, while the EpiRADseq library used a methylation sensitive common cutter (*Hpa*II, also targeting 5′-CCGG-3′). ddRADseq and EpiRADseq rely on a size-selection step to ensure targeted sequencing of a small subset of fragments within a narrow size range, with the ultimate goal of sequencing genomic intervals that will be present across many samples (Peterson et al., 2012). A total of 96 samples, half ddRADseq and half EpiRADseq, were prepared as a single library; some of these samples were used in a separate study. Paired-end, 100 bp reads were sequenced on a single lane of the Illumina HiSeq 4000 at the Vincent J. Coates Genomics Sequencing Laboratory at the University of California, Berkeley.

Symbiont Genotyping

Most reef corals engage in obligate symbiotic associations with dinoflagellates of the family Symbiodiniaceae (LaJeunesse et al., 2018). To inform the sequence assembly workflow described below regarding the choice of symbiont genome used to subtract symbiont reads, symbiont genotypes for each sample were determined at the genus (formerly clade) level via NCBI BLAST (v. 2.6.0) queries of ddRADseq libraries. A custom BLAST database was generated by searching for all *Symbiodinium* (formerly *Symbiodinium* clade A), *Breviolum* (*Symbiodinium* clade B), *Cladocopium* (*Symbiodinium* clade C), and *Durusdinium* (*Symbiodinium* clade D) records in the NCBI nucleotide database. Search terms were as follows: ("*Symbiodinium*" [Organism] AND "*Symbiodinium* sp. clade A" [Organism]) OR "*Symbiodinium* sp. clade B" [Organism]) OR "*Symbiodinium* sp. clade C"[Organism]) OR "*Symbiodinium* sp. clade D" [Organism]. Due to wide variation in the number of records for each taxon, the full dataset was standardized by random sampling to retain 20,000 records per taxon (80,000 total records retained out of the original 447,000). The resulting sequences were used as a BLAST database against which each ddRADseq library was queried with BLASTN using max_target_seqs = 1 and an *e*-value of 1e−20. Reads that aligned to more than one taxon were removed, and any reads mapping to 18S rDNA were also removed since this gave many ambiguous matches.

The efficacy of this approach was tested using a prior dataset for which symbiont genotyping had also been performed using PCR amplification and Sanger sequencing of cp23S rDNA amplicons (methods described and data reported in Dimond et al., 2017). Ten samples of branching *Porites* spp. were tested for correspondence between symbiont identities determined via BLAST searches of ddRADseq reads to those determined via cp23S amplicon sequencing.

Coral Sequence Assembly

Coral ddRADseq and EpiRADseq sequences were assembled with *ipyrad* v.0.5.15 (Eaton, 2014), using the "*de novo* – reference" assembly method to exclude symbiont reads from the assembly. Given the results of the symbiont genotyping analysis identifying the dominant symbiont taxon as *Symbiodinium* (formerly *Symbiodinium* clade A; see section "Results") in all corals, the *Symbiodinium microadriaticum* (GenBank Accession no. GCA_001939145.1; Aranda et al., 2016) genome was used as a reference to exclude symbiont reads. Reads were first demultiplexed by identifying restriction overhangs and barcode sequences associated with each sample; zero barcode mismatches were tolerated. Reads were then edge trimmed of barcodes and adapters and quality filtered using a q-score threshold of 20, with bases below this score converted to Ns and any reads with more than 5 Ns excluded. Next, reads were mapped to the symbiont reference genome with bwa mem using default settings and any mapped reads were excluded from further analysis. Clusters of the remaining reads were then aligned using a threshold of 90% similarity, followed by joint estimation of heterozygosity and error rate (Lynch, 2008) based on a diploid model assuming a maximum of two consensus alleles per individual. These parameters were used to determine consensus bases calls for each allele, removing consensus sequences with >5 Ns per end of paired-end reads. With consensus sequences identified, reads for each sample were clustered and aligned to consensus sequences. Lastly, the data were filtered according to maximum number of indels allowed per read end (8 indels), maximum number of SNPs per locus (20), maximum proportion of shared heterozygous sites per locus (0.3) and minimum number of samples for a locus to be reported (20). From this final dataset, which included monomorphic loci, a subset of the data was chosen that maximized the number of resampled individuals (sampled in both 2015 and 2016) with a robust set of shared loci (i.e., loci with missing data were excluded). Several samples were excluded from analysis if either one or both of the years in which they were sampled had low data yield (e.g., due to low starting DNA quality). See Results for details on the number of samples included in the final assembly.

As a definition of terms used here, the term locus to refers to a consensus paired-end read. The term SNP refers to a single nucleotide polymorphism on a locus, while the term CpG refers to a cytosine-guanine dinucleotide pair that can be either methylated or non-methylated at the 5′-CCGG-3′ restriction site of each locus.

Genetic Analysis

Unlinked SNPs were scored by *ipyrad* at 1 SNP per locus with the least amount of missing data; SNPs were sampled randomly if they had equal amounts of missing data. The SNP error rate, defined as the proportion of SNP mismatches between pairs of datasets from identical individuals (Mastretta-Yanes et al., 2015), was estimated by treating ddRADseq and EpiRADseq libraries as technical replicates and calculating pairwise differences between individuals using the *dist.gene* function in the R package *ape* (Paradis et al., 2004).

Epigenetic Analysis

Analysis of DNA methylation using EpiRADseq data relies on read count information, as read counts of loci using this technique are inversely related to their methylation frequency (Schield et al., 2016). The analysis followed methods described in

detail by Dimond et al. (2017) using a tandem ddRAD/EpiRAD approach in which reads that were present in the ddRAD library but absent in the EpiRAD library were considered methylated. Briefly, a minimum read count threshold of 15 reads in the ddRAD library was used to exclude loci with low coverage; given that ddRAD and EpiRAD reads are strongly correlated (Dimond et al., 2017), exclusion of low coverage loci in the ddRAD library effectively reduces false methylation calls in the EpiRAD data. Read counts for each locus were then standardized according to library size for each sample using the R package *edgeR* (Robinson et al., 2010). As in Dimond et al. (2017), the residuals from linear regression of ddRAD vs. EpiRAD read counts were then used to ascertain methylation status, however, instead of manually setting the methylated/unmethylated threshold for a locus, k-means clustering was used to differentiate methylated from unmethylated loci using $k = 2$. The *superheat* R package was used for heatmap visualization of methylation patterns (Barter and Yu, 2018). The potential functions of differentially methylated loci were determined via a web-based BLASTN search using the default "nr" nucleotide database and an *e*-value threshold of e^{-5}.

Relationships Between Genetic and Epigenetic Variation

Pairwise genetic and epigenetic distance were computed using the *dist.gene* function in the R package *ape* (Paradis et al., 2004). Comparisons between different fragments of the same individual (experimentally generated clones) were excluded. A Mantel test was used to test the hypothesis that pairwise genetic and epigenetic variation were positively related.

RESULTS

Sample Recovery and Data Yield

Of the 19 colony halves transplanted to the common garden, only one was not recovered a year later. Of the 14 control halves left at their site of origin, three were not relocated, while a fourth had been overtaken and killed by a damselfish garden. Although many samples were submitted for sequencing, low sequencing yield from several samples effectively excluded them from the final analysis due to insufficient data. Sequencing yield was highly variable, producing an average of 3.4 (sd = 3.0) million reads per sample. For the samples included in the final assembly, sequencing yield was 4.1 (sd = 3.2) million reads per sample. An average of 7,539 (sd = 4799) consensus loci per sample were included in the final assembly. If data were insufficient (based on summary statistics given by *ipyrad*) for one or both sampling years for a given coral colony, the colony was excluded from analysis. Unfortunately, only two control samples remained in the final analysis. The optimal balance between colony sample size and number of shared loci was achieved with $N = 8$ colonies sampled in both 2015 and 2016, plus two controls, sharing 629 loci. Thus, 629 SNPs and CpGs shared across all samples were analyzed.

Environmental Analysis

Of the eight colonies included in the final analysis, four (colonies 5, 6, 10, and 11) originated from inshore environments approximately 6–8 km west of the barrier reef, while the other four (colonies 2, 3, 8, and 9) were collected from offshore environments just shoreward (within 500 m) of the barrier reef (**Figure 1**). Inshore reefs were characterized by slightly cooler annual temperatures, a larger seasonal temperature range, and higher chlorophyll a concentration (**Figures 1A–C**). These effects likely reflect the relatively shallow depth and longer residence time of water in the lagoon and its greater susceptibility to seasonal variation in solar heating and wind patterns, in addition to freshwater runoff and terrestrial nutrient sources. Most corals brought to the common garden originated in habitats with a greater seasonal temperature range and high chlorophyll concentration; the slightly lower mean temperature of these habitats was probably not biologically meaningful (**Figure 1D**).

Symbiont Genotyping

For the branching *Porites* spp. test dataset evaluating the efficacy of symbiont genotyping via BLAST searches using ddRADseq reads, the dominant symbiont taxon detected via BLAST search was identical to the dominant symbiont taxon detected via cp23S Sanger sequencing in all cases (**Figure 2**). Given these results, we proceeded with the BLAST approach with ddRADseq reads from *P. astreoides*. Among the *P. astreoides* samples, all individuals hosted ≥98% *Symbiodinium* (formerly *Symbiodinium* clade A) across both years. This justified the use of the *S. microadriaticum* genome to subtract symbiont sequences during *de novo* assembly of the RADseq data.

Genetic Analysis

Based on genotyping and analysis of genetic distance among technical replicates (ddRAD and EpiRAD libraries combined), the SNP error rate was estimated to be 1.2% (sd = 0.7%), well below previously published estimates of reduced representation sequencing data (**Figure 3**; Mastretta-Yanes et al., 2015; Recknagel et al., 2015; Dimond et al., 2017). In other words, genotyping was 98.8% accurate. Genetic distance analysis also indicated that resampling of corals from 2015 to 2016 was accurate and no errors (e.g., sampling, misidentification) were made, showing SNP calling error comparable to the SNP error rate reported above for technical replicates (1.7%, sd = 0.9%). Chimerism (within-colony genetic variation resulting from fusion of juvenile colonies) and mosaicism (within-colony genetic variation arising from somatic mutations) is also not uncommon among scleractinian corals (Schweinsberg et al., 2015; Devlin-Durante et al., 2016), and this analysis shows no evidence for these phenomena among the colonies sampled here. By contrast, genetic distance among all non-replicate and non-resampling pairwise comparisons between individuals was much greater, averaging 16.3% (sd = 1.4%). No clones were identified.

Epigenetic Analysis

Across all samples and years, an average of 18.6% (sd = 0.9%) of CpGs were methylated (**Figure 4**). As indicated by the low

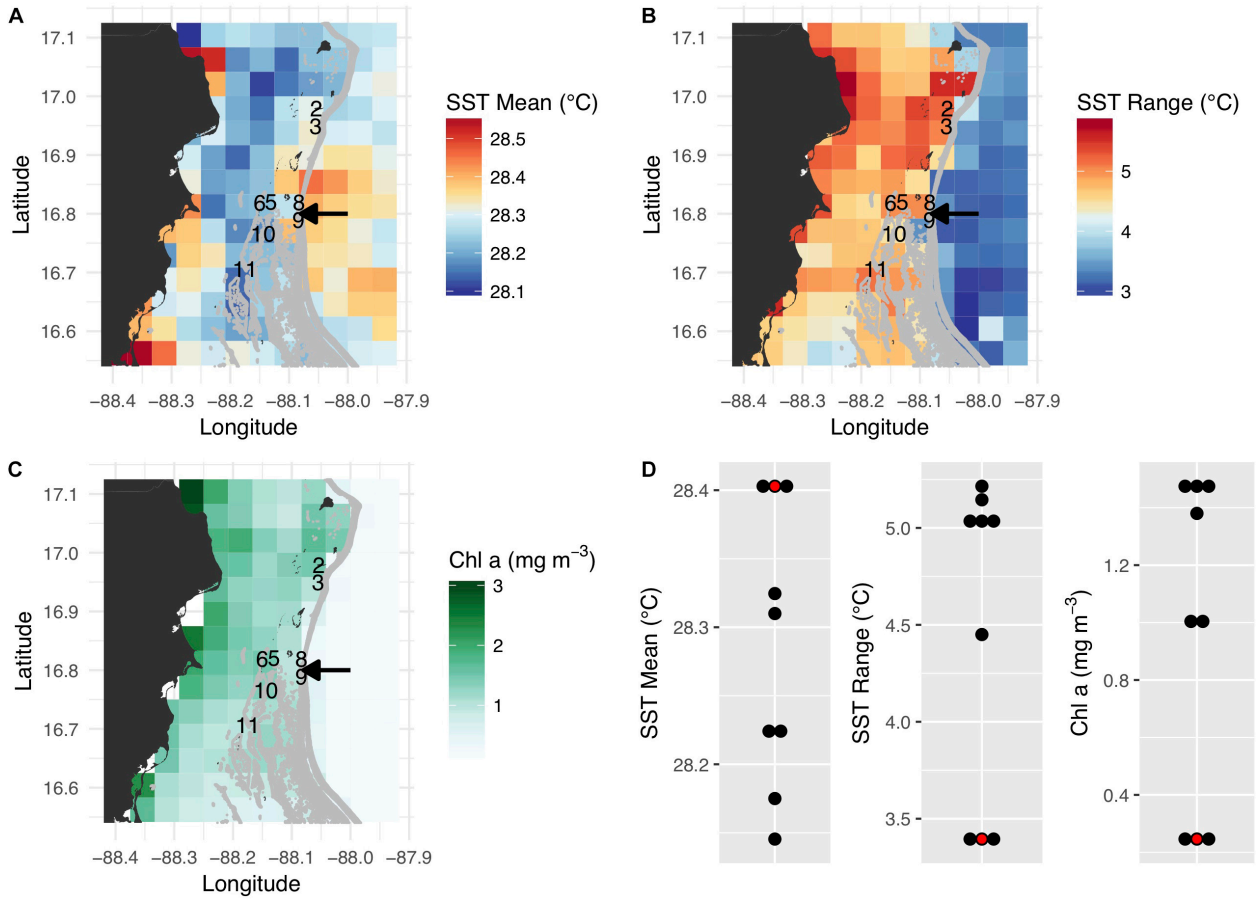

FIGURE 1 | Satellite-derived environmental conditions associated with coral collection sites and the common garden along the Belize Barrier Reef. **(A–C)** Mean annual sea surface temperature (SST), annual SST range, and annual mean chlorophyll a concentration. The collection sites of the eight analyzed coral colonies are depicted by colony numbers, and the arrows show the location of the common garden (colonies 8 and 9 originated from just north of the common garden site). **(D)** Summary of native habitat and common garden environmental conditions. The common garden is depicted in red.

variance, most loci were either methylated or unmethylated across all samples and years; 73% of loci were constitutively unmethylated across samples and years, 12% were constitutively methylated, and 15% were differentially methylated (**Figure 4**). The low SNP error rate reported above also adds confidence to the epigenetic analysis as it indicates that reads were correctly assigned to consensus loci at the level of each sample.

All corals underwent some degree of change in their methylation status, including the two controls (**Figure 5**). The mean percentage of loci changing methylation state per colony was 2.0% (sd = 0.9%). Among the two colonies with controls, the percentage of loci that changed methylation state was equivalent for colony pa11 and its control (2.9%), while for colony pa5, percent change was 1.0 and 1.7% for the common garden and control, respectively. Although there was no significant overall change in percent CpG methylation from 2015 to 2016 (paired *t*-test, df = 7, $p = 0.511$; **Figure 6A**), there was evidence for convergence of the methylation status among colonies toward a more similar methylome after a year in the common garden together, as pairwise differences between colonies were significantly lower in 2016 (paired *t*-test, df = 27, $p < 0.001$; **Figure 6B**). Twenty-eight pairwise comparisons from 8 samples were computed per year ($N-1 \times N/2 = 7 \times 8/2 = 28$) for the latter analysis, hence the higher degrees of freedom. Lastly, there were also significantly lower pairwise differences among transplanted corals (all 2016 samples compared to pa11 and pa5 transplants) compared to controls (all 2016 samples compared to pa11 and pa5 controls; paired *t*-test, df = 13, $p < 0.001$; **Figure 6C**). For this analysis, there were 14 pairwise comparisons for each treatment.

Of the differentially methylated loci, most (76 of 95 = 80%) were differentially methylated in only one colony. To further evaluate differentially methylated loci with some degree of confidence, only loci differentially methylated in more than one colony were considered further. Nineteen loci (19 of 95 = 20%) met this criterion and eight returned BLASTN hits. All matches were coral RNA sequences; six were mRNA sequences, while two were non-coding (nc) RNA sequences (**Table 1**). Four of the sequences had predicted products, including a protein kinase, a helicase-like ribonucleoprotein, a FAM98A-like protein, and a tax-1 binding protein homolog.

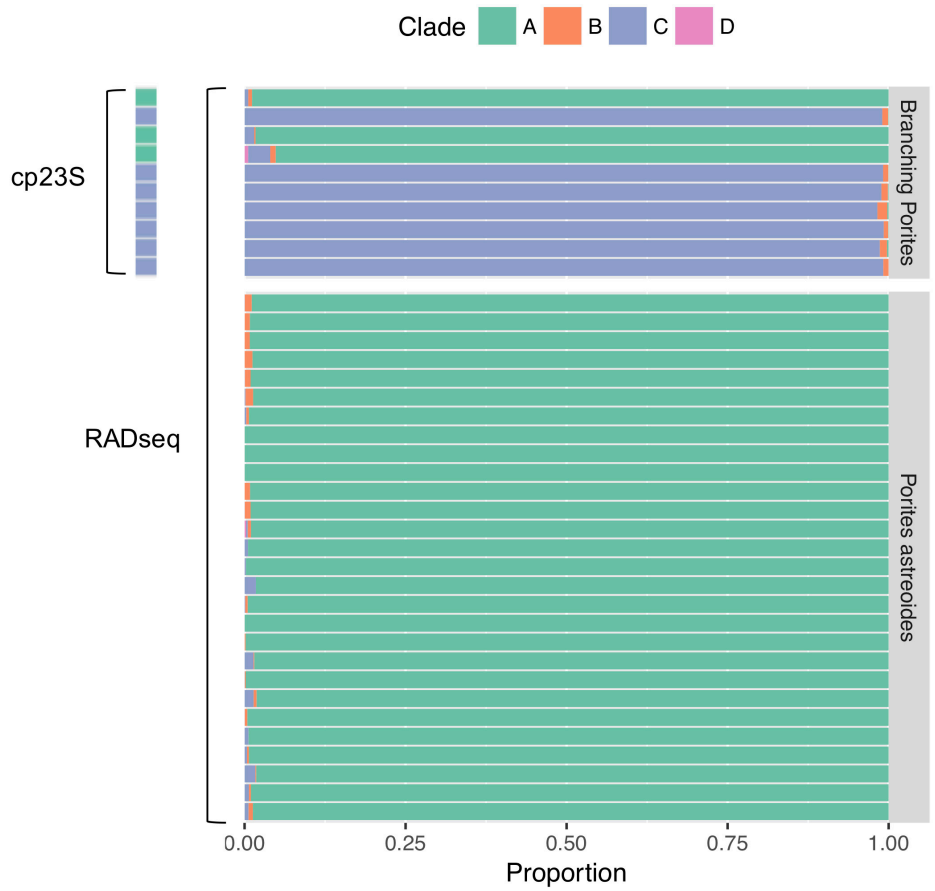

FIGURE 2 | Symbiont identification using BLAST searches of ddRADseq data against custom databases of *Symbiodinium* (formerly *Symbiodinium* clade A), *Breviolum* (*Symbiodinium* clade B), *Cladocopium* (*Symbiodinium* clade C), and *Durusdinium* (*Symbiodinium* clade D). Top panel shows symbionts of branching *Porites* spp. collected for a prior study (Dimond et al., 2017); the dominant symbiont found in BLAST searches was identical to the dominant symbiont identified via cp23S Sanger sequencing. Bottom panel shows results from analysis of the *P. astreoides* colonies that are the primary subject of this study.

Relationships Between Genetic and Epigenetic Variation

There was significant positive relationship between pairwise genetic and epigenetic distance (Mantel test; $r = 0.618$, $p < 0.001$), indicating that corals that are more similar genetically also tend to be more similar epigenetically (**Figure 7**). Genetic distance among colonies was also notably greater than epigenetic distance (**Figure 7**).

DISCUSSION

Our study shows evidence that DNA methylation in *P. astreoides* is at least somewhat responsive to environmental change, reflective of the environment, and heritable. These characteristics of methylation are necessary for it to be implicated as part of potential transgenerational acclimatization responses (Eirin-Lopez and Putnam, 2019). Relatively fast acclimatization responses, along with slower natural selection, are essential, complementary processes that enable coral persistence in the face of climate change (Palumbi et al., 2014).

Transplantation to a new environment for a 1-year period elicited subtle changes in the methylome of *P. astreoides*. Yet, there was also evidence that corals converged toward similar methylomes in the common garden, suggesting that the subtle changes in methylation were reflective of the new environment. Similarly, in a 3-month reciprocal transplant study of *A. millepora* on the Great Barrier Reef, Dixon et al. (2018) found that while DNA methylation was considerably less responsive than gene expression to transplantation, the methylomes of transplants became more similar to native corals. Moreover, methylation changes were correlated with measures of physiological competency in novel environments, with transplanted individuals whose methylomes became more similar to those of native individuals showing more robust physiological profiles (Dixon et al., 2018). The small yet significant convergence of methylation patterns observed after 1 year in the common garden in our study is in agreement with the results of Dixon et al. (2018).

Responsiveness of DNA methylation to changing environmental conditions is not a foregone conclusion, as shown by Putnam et al. (2016) in their study of global

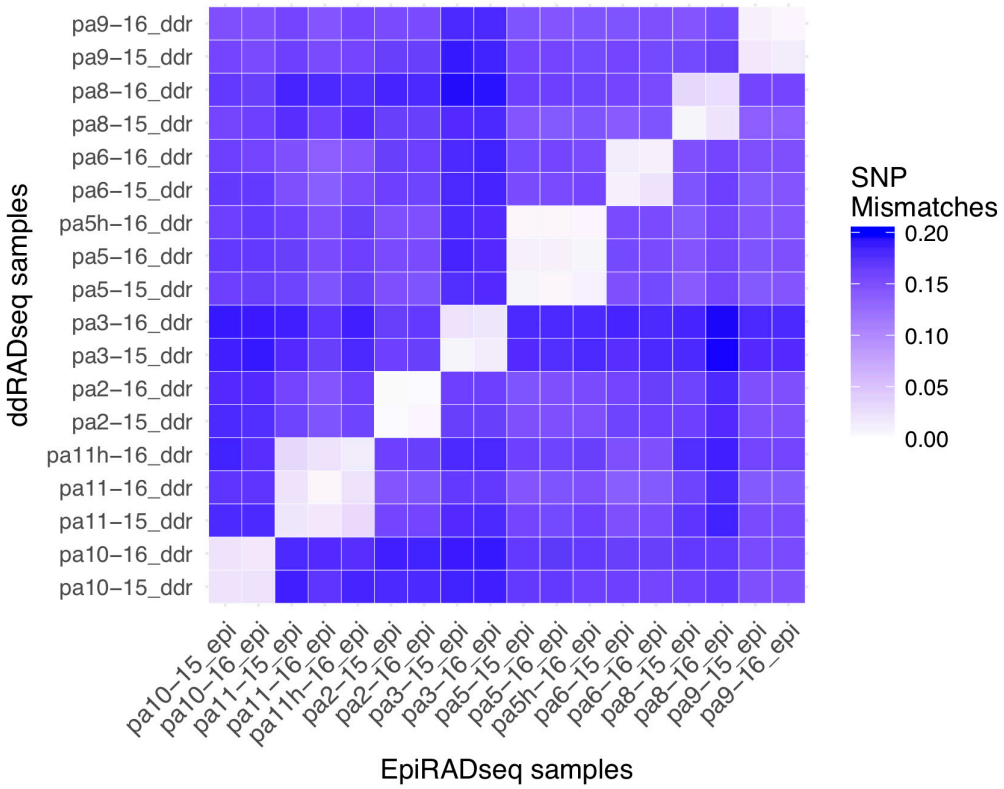

FIGURE 3 | Pairwise SNP mismatches between the *P. astreoides* samples. EpiRADseq samples are shown along the *x*-axis, while ddRADseq samples are shown along the *y*-axis. Values along the diagonal illustrate the SNP error rate using the two libraries as technical replicates, while off-diagonal values show the error associated with resampling corals from 2015 to 2016. Two controls that were left at their site of origin (pa11h and pa5h) are included.

methylation responses of two coral species to low pH. The relatively environmentally sensitive coral *P. damicornis* exhibited significant changes in methylation, while the more robust coral *M. capitata* did not. Interestingly, whereas *P. damicornis* performed poorly and showed limited evidence of acclimatization to the 6-week exposure to experimental conditions, *M. capitata* performed well. This suggests that changes in methylation are not necessarily associated with acclimatization. However, bulk changes in methylated DNA were quantified by Putnam et al. (2016), so it is possible that individual genes in *M. capitata* underwent both increases and decreases in methylation to contribute to homeostasis. Indeed, this is the scenario reported by Dixon et al. (2018) and in our study. Here, approximately 18.5% CpG methylation was maintained before and after transplantation despite an average of 2% of loci changing their methylation state, reflecting a combination of increases and decreases in methylation among individual colonies and loci. Likewise, Dixon et al. (2018) reported no genome-wide increases or decreases in methylation in response to transplantation, but instead that methylation changed in a so-called "seesaw" pattern whereby changes in methylation among hypomethylated genes were mirrored by changes in the opposite direction among hypermethylated genes. Their study, along with a study by Liew et al. (2018b) on pCO_2-mediated changes in methylation and phenotype in *S. pistillata*, have concluded that environmentally induced changes in DNA methylation are associated with homeostatic regulation. The precise mechanisms of this regulation, however, will require further study to fully understand.

The relatively small changes in methylation we detected here could be at least partially attributed to the limited difference in native habitat environmental conditions relative to the common garden. Mean temperature among collections sites and the common garden varied only slightly, while temperature range and chlorophyll concentration were somewhat more variable. It is noteworthy, however, that Dixon et al. (2018) measured relatively small changes in methylation despite much greater environmental differences between transplantation habitats, albeit with only a 3-month experimental duration. On the other hand, small-scale differences in microhabitat were implicated as drivers of methylation variation within genets of *A. palmata* (Durante et al., 2019). Indeed, small-scale variation in water flow conditions or shading may be biologically significant (e.g., Anthony and Hoegh-Guldberg, 2003). Microscale environmental variation and the resulting methylation variation it creates may mean that the epigenetic signatures reported for a given colony reflect the combined signatures of multiple polyps with varied microhabitat exposures. As such, this may be a source of uncharacterized variation in the data.

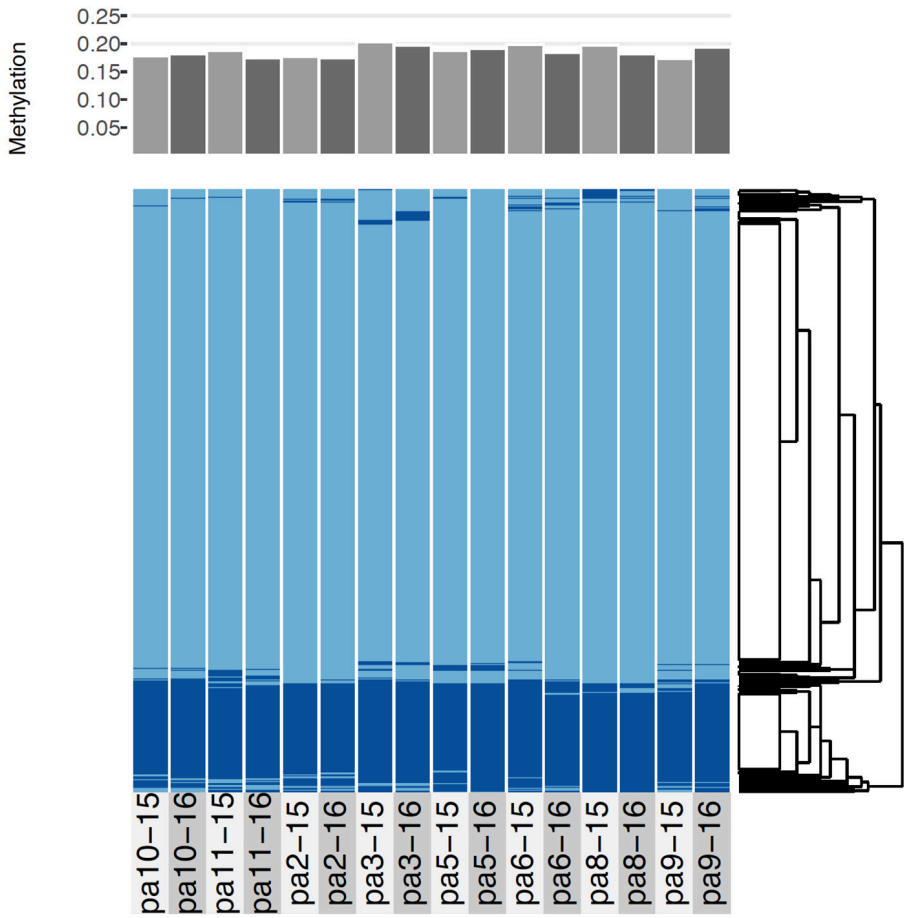

FIGURE 4 | Comparative methylation profiles of the eight *P. astreoides* samples from 2015 to 2016. Every two vertical bars is a single individual, with the first bar showing 2015 methylation and the second showing 2016 methylation. Top panel shows proportion of methylated loci, while bottom panel shows a heatmap with methylated loci in dark blue and unmethylated loci in light blue, ordered via hierarchical clustering.

Were methylation changes truly reflective of common garden conditions? This is worth considering since changes in methylation among the two control colonies that remained at their site of origin were similar in magnitude to the experimental colonies. This could suggest that methylation simply changes temporally as corals age, or that the experimental act of transplantation (halving colonies and reattaching them) caused methylation changes. Age-related changes in methylation, for example, are well-documented among humans and other vertebrates (Horvath, 2013), and there is also some evidence among invertebrates (Lian et al., 2015). Meanwhile, several studies have noted considerable variance in methylation patterns that is incompletely explained by genetics and known environmental conditions (Dimond et al., 2017; Rondon et al., 2017; Durante et al., 2019). However, the significant convergence of colony methylation profiles after a year in the common garden together suggest that methylation was in fact responding to, and reflective of, the common garden environment.

Although epigenetic variation among colonies was considerably smaller than genetic variation, there was a significant positive correlation between these two variables, suggesting that methylation patterns are at least partially heritable. A similar relationship was observed among branching *Porites* spp. by Dimond et al. (2017), and even stronger evidence for heritability of methylation in corals has been reported by several other recent studies (Dixon et al., 2018; Liew et al., 2018a; Durante et al., 2019). While a full appraisal of the potential for methylation to be involved in transgenerational acclimative responses in corals awaits further study, the reports to date are promising.

Lack of an annotated *P. astreoides* genome limited the scope of our analysis and the inferences we were able to draw regarding potential functional implications of changes in methylation, however, a handful of loci exhibiting consistent differences in methylation provide some clues. Most of these loci were apparently associated with coding sequences, which is consistent with gene body methylation as the primary form of methylation among invertebrates (Sarda et al., 2012). One locus was associated with a sequence coding for a calcium-independent protein kinase C-like. Calcium-independent protein kinase C is involved in intracellular signaling, a biological process that is typically associated with the hypomethylated

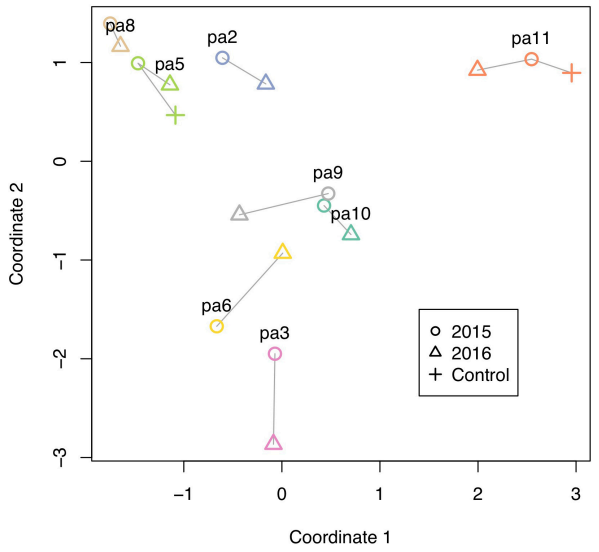

FIGURE 5 | Methylation changes from 2015 to 2016. Multidimensional scaling plot of methylation. Individual colonies are shown with different colors, and vectors show relative direction and magnitude of change from 2015 to 2016, including two controls that were left at their site of origin.

fraction of the genome (Dimond and Roberts, 2016). By contrast with hypermethylated housekeeping genes that tend to exhibit consistent expression across conditions and tissues, hypomethylated genes such as those involved in cell-cell signaling are characterized by their inducibility in response to environmental change (Dimond and Roberts, 2016).

A gene encoding a putative tax1-binding protein homolog was another differentially methylated locus. These proteins are involved in negative regulation of apoptotic processes via negative regulation of NF-κB transcription factor activity. Interestingly, deregulation of host NF-κB is associated with dinoflagellate symbiosis in cnidarians (Mansfield et al., 2017); loss of symbionts (bleaching) is associated with elevated levels of NF-κB. Perhaps differential methylation of a tax1-binding protein gene was associated with symbiotic homeostatic maintenance in the new environment.

Another locus resembled a gene encoding a U5 small nuclear ribonucleoprotein 200 kDa helicase, which is involved in mRNA splicing via its role in the spliceosome. Epigenetic factors are widely implicated in alternative mRNA splicing, which is a major source of protein diversity, and hence, phenotypic variation (Luco et al., 2011). DNA methylation itself has been identified as a modulator of alternative splicing (Lev Maor et al., 2015).

The last mRNA-associated locus coded for a putative FAM98A protein. These proteins have numerous associated biological processes, including positive regulation of cell proliferation and gene expression. However, the most intriguing function involves protein methylation. A study of human colorectal cancer found that FAM98A was required for expression of an arginine methyltransferase (Akter et al., 2017). Protein methylation has been widely studied in histones, and there is ample evidence for

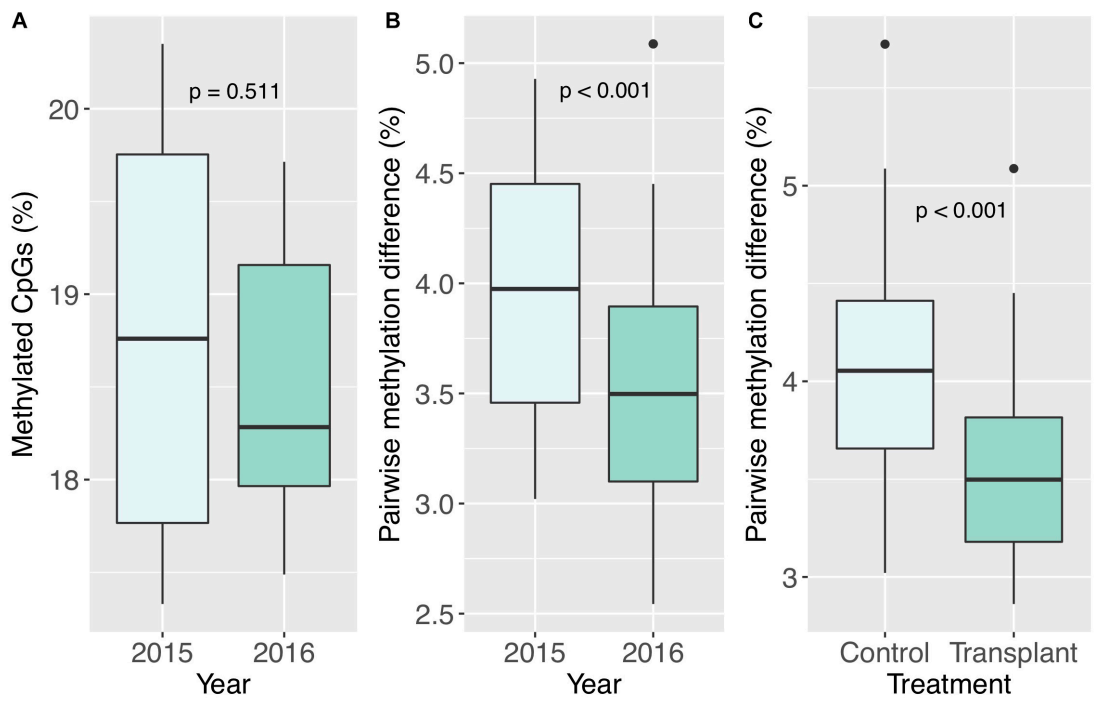

FIGURE 6 | (A) Percent methylated CpGs by year. **(B)** Pairwise methylation difference by year, including all pairwise comparisons between colonies. **(C)** Pairwise methylation differences by treatment, including comparisons of transplanted corals to the two controls, and transplanted corals to the transplanted counterparts of the two controls (pa5 and pa11).

TABLE 1 | BLASTN hits for loci that were differentially methylated in at least two samples.

Locus ID	Description	*e*-value	GenBank accession
20278	PREDICTED: *Orbicella faveolata* uncharacterized LOC110068412, mRNA	1.0E−12	XM_020775789.1
36065	PREDICTED: *Orbicella faveolata* protein FAM98A-like, mRNA	1.0E−06	XM_020762555.1
50692	PREDICTED: *Acropora millepora* taxi-binding protein 1 homolog (LOC114946951), mRNA	2.0E−17	XM_029323598.1
51711	PREDICTED: *Acropora digitifera* uncharacterized LOC107337846 (LOC107337846), mRNA	5.0E−12	XM_015903081.1
66685	PREDICTED: *Orbicella faveolata* U5 small nuclear ribonucleoprotein 200 kDa helicase-like, partial mRNA	1.0E−13	XM_020757069.1
69826	PREDICTED: *Orbicella faveolata* uncharacterized LOC110057897, transcript variant X5, ncRNA	2.0E−16	XR_002297590.1
76792	PREDICTED: *Pocillopora damicornis* uncharacterized LOC113678647, ncRNA	1 OE−05	XR_003446911.1
82175	PREDICTED: *Orbicella faveolata* calcium-independent protein kinase C-like, mRNA	1.0E−18	XM_020748568.1

epigenetic crosstalk between methylated DNA and methylated histones (Du et al., 2015).

Further evidence of epigenetic crosstalk in the loci responsive to transplantation is suggested by two loci associated with putative non-coding RNAs (ncRNAs). Along with DNA methylation and histone modifications, ncRNAs are considered part of the epigenetic machinery. ncRNAs are considerably more abundant than mRNAs and play numerous roles, particularly in processes such as post-transcriptional mRNA silencing (Kornienko et al., 2013). In some cases, they are involved in directing DNA and histone methylation patterns (Kornienko et al., 2013; Miska and Ferguson-Smith, 2016).

CONCLUSION

This work shows that DNA methylation is an environmentally responsive epigenetic process that is reflective of the environment, and is consistent with its putative role in acclimatization. We were able to detect subtle changes in *P. astreoides* methylation associated with experimental transplantation, as well as evidence for heritability of methylation patterns. Loci responding to transplantation were associated with signaling, apoptosis, gene regulation and epigenetic crosstalk, yet much remains to be learned about the function of methylation changes in these differentially methylated genes. This study helps set the stage for further work on both the functional genomics and molecular ecology of acclimatization processes in reef corals.

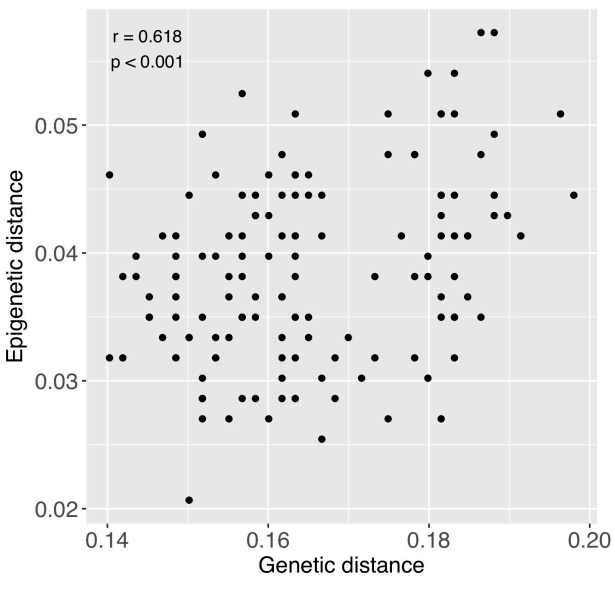

FIGURE 7 | Relationship between pairwise genetic and epigenetic distance. Each point represents a pairwise comparison between each combination of samples, excluding comparisons between fragments of the same individuals. Coefficients in upper left region of figure were obtained from a Mantel test.

DATA AVAILABILITY STATEMENT

The datasets generated for this study can be found in the NCBI Sequence Read Archive, accession number SRP132538. Analysis archive at https://doi.org/10.5281/zenodo.3576526.

AUTHOR CONTRIBUTIONS

JD conceived and designed the study, collected the specimens, prepared the RAD libraries, analyzed the data, and drafted the manuscript. SR contributed reagents, equipment, and analysis tools.

FUNDING

This study was supported by the Hall Conservation Genetics Research Award (UW-CoEnv), the ARCS Foundation Seattle Chapter, and the John E. Halver Fellowship (UW-SAFS).

ACKNOWLEDGMENTS

We thank the Smithsonian Caribbean Coral Reef Ecosystems Program's Carrie Bow Cay Field Station for field support, including Scott Jones, Zach Foltz, Martha Nicholas, Greg and Jo Ann Dramer, and Nick and Marilyn Haren. This is contribution #1034 to the Smithsonian's Caribbean Coral Reef Ecosystems Program. Laboratory support and materials were generously provided by Adam Leaché and Kevin Epperly. Earlier versions of the manuscript were improved by comments from Lorenz Hauser and Ken Sebens.

REFERENCES

Akter, K. A., Mansour, M. A., Hyodo, T., and Senga, T. (2017). FAM98A associates with DDX1-C14orf166-FAM98B in a novel complex involved in colorectal cancer progression. *Int. J. Biochem. Cell Biol.* 84, 1–13. doi: 10.1016/j.biocel.2016.12.013

Anthony, K. R., and Hoegh-Guldberg, O. (2003). Variation in coral photosynthesis, respiration and growth characteristics in contrasting light microhabitats: an analogue to plants in forest gaps and understoreys? *Funct. Ecol.* 17, 246–259. doi: 10.1046/j.1365-2435.2003.00731.x

Aranda, M., Li, Y., Liew, Y. J., Baumgarten, S., Simakov, O., Wilson, M. C., et al. (2016). Genomes of coral dinoflagellate symbionts highlight evolutionary adaptations conducive to a symbiotic lifestyle. *Sci. Rep.* 6:39734. doi: 10.1038/srep39734

Barter, R. L., and Yu, B. (2018). Superheat: an R package for creating beautiful and extendable heatmaps for visualizing complex data. *J. Comput. Graph. Stat.* 27, 910–922. doi: 10.1080/10618600.2018.1473780

Devlin-Durante, M. K., Miller, M. W., Caribbean Acropora Research Group, Precht, W. F., Baums, I. B., Carne, L., et al. (2016). How old are you? Genet age estimates in a clonal animal. *Mol. Ecol.* 25, 5628–5646. doi: 10.1111/mec.13865

Dimond, J. L., Gamblewood, S. K., and Roberts, S. B. (2017). Genetic and epigenetic insight into morphospecies in a reef coral. *Mol. Ecol.* 26, 5031–5042. doi: 10.1111/mec.14252

Dimond, J. L., and Roberts, S. B. (2016). Germline DNA methylation in reef corals: patterns and potential roles in response to environmental change. *Mol. Ecol.* 25, 1895–1904. doi: 10.1111/mec.13414

Dixon, G., Liao, Y., Bay, L. K., and Matz, M. V. (2018). Role of gene body methylation in acclimatization and adaptation in a basal metazoan. *Proc. Natl. Acad. Sci. U.S.A.* 115, 13342–13346. doi: 10.1073/pnas.1813749115

Du, J., Johnson, L. M., Jacobsen, S. E., and Patel, D. J. (2015). DNA methylation pathways and their crosstalk with histone methylation. *Nat. Rev.* 16, 519–532. doi: 10.1038/nrm4043

Duncan, E. J., Gluckman, P. D., and Dearden, P. K. (2014). Epigenetics, plasticity, and evolution: how do we link epigenetic change to phenotype? *J. Exp. Zool. Part B* 322, 208–220. doi: 10.1002/jez.b.22571

Durante, M. K., Baums, I. B., Williams, D. E., Kemp, D. W., and Vohsen, S. (2019). What drives phenotypic divergence among coral clonemates of *Acropora palmata*? *Mol. Ecol.* 28, 3208–3224.

Eaton, D. A. R. (2014). PyRAD: assembly of de novo RADseq loci for phylogenetic analyses. *Bioinformatics* 30, 1844–1849. doi: 10.1093/bioinformatics/btu121

Eirin-Lopez, J. M., and Putnam, H. M. (2019). Marine environmental epigenetics. *Annu. Rev. Mar. Sci.* 11, 335–368. doi: 10.1146/annurev-marine-010318-095114

Flores, K., Wolschin, F., Corneveaux, J. J., Allen, A. N., Huentelman, M. J., and Amdam, G. V. (2012). Genome-wide association between DNA methylation and alternative splicing in an invertebrate. *BMC Genomics* 13:480. doi: 10.1186/1471-2164-13-480

Gates, R. D., and Edmunds, P. J. (1999). The physiological mechanisms of acclimatization in tropical reef corals. *Am. Zool.* 43, 30–43. doi: 10.1093/icb/39.1.30

Hofmann, G. E. (2017). Ecological epigenetics in marine metazoans. *Front. Mar. Sci.* 4:4. doi: 10.3389/fmars.2017.00004

Horvath, S. (2013). DNA methylation age of human tissues and cell types. *Genome Biol* 14:3156.

Iwasaki, M., and Paszkowski, J. (2014). Epigenetic memory in plants. *EMBO J.* 33, 1987–1998. doi: 10.15252/embj.201488883

Kinoshita, T., and Seki, M. (2014). Epigenetic memory for stress response and adaptation in plants. *Plant Cell Physiol.* 55, 1859–1863. doi: 10.1093/pcp/pcu125

Kornienko, A. E., Guenzl, P. M., Barlow, D. P., and Pauler, F. M. (2013). Gene regulation by the act of long non-coding RNA transcription. *BMC Biology* 11:59. doi: 10.1186/1741-7007-11-59

LaJeunesse, T. C., Parkinson, J. E., Gabrielson, P. W., Jeong, H. J., Reimer, J. D., Voolstra, C. R., et al. (2018). Systematic revision of Symbiodiniaceae highlights the antiquity and diversity of coral endosymbionts. *Curr. Biol.* 28, 2570.e–2580.e. doi: 10.1016/j.cub.2018.07.008

Lev Maor, G., Yearim, A., and Ast, G. (2015). The alternative role of DNA methylation in splicing regulation. *Trends Genet.* 31, 274–280. doi: 10.1016/j.tig.2015.03.002

Lian, S., He, Y., Li, X., Zhao, B., Hou, R., Hu, X., et al. (2015). Changes in global DNA methylation intensity and DNMT1 transcription during the aging process of scallop *Chlamys farreri*. *J. Ocean Univers. China* 14, 685–690. doi: 10.1007/s11802-015-2507-2

Liew, Y. J., Howells, E. J., Wang, X., Michell, C. T., Burt, J. A., Idaghdour, Y., et al. (2018a). Intergenerational epigenetic inheritance in reef-building corals. *bioRxiv* [Preprint]. doi: 10.1101/269076

Liew, Y. J., Zoccola, D., Li, Y., Tambutté, E., Venn, A. A., Michell, C. T., et al. (2018b). Epigenome-associated phenotypic acclimatization to ocean acidification in a reef-building coral. *Sci. Adv.* 4:8028. doi: 10.1126/sciadv.aar8028

Luco, R. F., Allo, M., Schor, I. E., Kornblihtt, A. R., and Misteli, T. (2011). Epigenetics in alternative pre-mRNA splicing. *Cell* 144, 16–26. doi: 10.1016/j.cell.2010.11.056

Lynch, M. (2008). Estimation of nucleotide diversity, disequilibrium coefficients, and mutation rates from high-coverage genome-sequencing projects. *Mol. Biol. Evol.* 25, 2409–2419. doi: 10.1093/molbev/msn185

Mansfield, K. M., Carter, N. M., Nguyen, L., Cleves, P. A., Alshanbayeva, A., Williams, L. M., et al. (2017). Transcription factor NF-κB is modulated by symbiotic status in a sea anemone model of cnidarian bleaching. *Sci. Rep.* 7:16025.

Mastretta-Yanes, A., Arrigo, N., Alvarez, N., Jorgensen, T. H., Piñero, D., and Emerson, B. C. (2015). Restriction site-associated DNA sequencing, genotyping error estimation and de novo assembly optimization for population genetic inference. *Mol. Ecol. Resour.* 15, 28–41. doi: 10.1111/1755-0998.12291

Meerman, J., and Clabaugh, J. (2017). *Biodiversity and Environmental Resource Data System of Belize*. Available at: http://www.biodiversity.bz (accessed August 24, 2018)

Miska, E. A., and Ferguson-Smith, A. C. (2016). Transgenerational inheritance: models and mechanisms of non-DNA sequence-based inheritance. *Science* 354, 59–63. doi: 10.1126/science.aaf4945

NASA Goddard Space Flight Center, Ocean Ecology Laboratory, and Ocean Biology Processing Group, (2016). *Moderate Resolution Imaging Spectroradiometer (MODIS) Ocean Color Data, NASA OB.DAAC*. Available at: https://oceancolor.gsfc.nasa.gov/cgi/l3 (accessed August 24, 2018).

Neri, F., Rapelli, S., Krepelova, A., Incarnato, D., Parlato, C., Basile, G., et al. (2017). Intragenic DNA methylation prevents spurious transcription initiation. *Nature* 543, 72–77. doi: 10.1038/nature21373

Palumbi, S. R., Barshis, D. J., Traylor-Knowles, N., and Bay, R. A. (2014). Mechanisms of reef coral resistance to future climate change. *Science* 344, 895–898. doi: 10.1126/science.1251336

Paradis, E., Claude, J., and Strimmer, K. (2004). APE: analyses of phylogenetics and evolution in R language. *Bioinformatics* 20, 289–290. doi: 10.1093/bioinformatics/btg412

Pearce, A., Faskel, F., and Hyndes, G. (2006). Nearshore sea temperature variability off Rottnest Island (Western Australia) derived from satellite data. *Int. J. Remote Sensing* 27, 2503–2518. doi: 10.1080/01431160500472138

Peterson, B. K., Weber, J. N., Kay, E. H., Fisher, H. S., and Hoekstra, H. E. (2012). Double digest RADseq: an inexpensive method for de novo SNP discovery and genotyping in model and non-model species. *PLoS One* 7:e37135. doi: 10.1371/journal.pone.0037135

Putnam, H. M., Davidson, J. M., and Gates, R. D. (2016). Ocean acidification influences host DNA methylation and phenotypic plasticity in environmentally susceptible corals. *Evol. Appl.* 9, 1165–1178. doi: 10.1111/eva.12408

Recknagel, H., Jacobs, A., Herzyk, P., and Elmer, K. R. (2015). Double-digest RAD sequencing using Ion Proton semiconductor platform (ddRADseq-ion) with nonmodel organisms. *Mol. Ecol. Resour.* 15, 1316–1329. doi: 10.1111/1755-0998.12406

Roberts, S. B., and Gavery, M. R. (2012). Is There a Relationship between DNA Methylation and Phenotypic Plasticity in Invertebrates? *Front. Physiol.* 2:116. doi: 10.3389/fphys.2011.00116

Robinson, M. D., McCarthy, D. J., and Smyth, G. K. (2010). edgeR: a bioconductor package for differential expression analysis of digital gene expression data. *Bioinformatics* 26, 139–140. doi: 10.1093/bioinformatics/btp616

Rondon, R., Grunau, C., Fallet, M., Charlemagne, N., Sussarellu, R., Chaparro, C., et al. (2017). Effects of parental exposure to diuron on Pacific oyster spat methylome. *Environ. Epigenet.* 3:dvx004. doi: 10.1093/eep/dvx004

Sarda, S., Zeng, J., Hunt, B. G., and Yi, S. V. (2012). The evolution of invertebrate gene body methylation. *Mol. Biol. Evol.* 29, 1907–1916. doi: 10.1093/molbev/mss062

Schield, D. R., Walsh, M. R., Card, D. C., Andrew, A. L., Adams, R. H., and Castoe, T. A. (2016). EpiRADseq: scalable analysis of genomewide patterns of methylation using next-generation sequencing. *Methods Ecol. Evol.* 7, 60–69. doi: 10.1111/2041-210x.12435

Schweinsberg, M., Weiss, L. C., Striewski, S., Tollrian, R., and Lampert, K. P. (2015). More than one genotype: how common is intracolonial genetic variability in scleractinian corals? *Mol. Ecol.* 24, 2673–2685. doi: 10.1111/mec.13200

Smale, D. A., and Wernberg, T. (2009). Satellite-derived SST data as a proxy for water temperature in nearshore benthic ecology. *Mar. Ecol. Prog. Ser.* 387, 27–37. doi: 10.3354/meps08132

Todd, P. A. (2008). Morphological plasticity in scleractinian corals. *Biol. Rev. Cambridge Philos. Soc.* 83, 315–337. doi: 10.1111/j.1469-185x.2008.00045.x

UNEP-WCMC, WorldFish Centre, WRI, and TNC (2018). *Global Distribution of Warm-water Coral Reefs, Compiled from Multiple Sources Including the Millennium Coral Reef Mapping Project. Version 4.0. Includes contributions from IMaRS-USF and IRD (2005), IMaRS-USF (2005) and Spalding et al. (2001)*. Cambridge: UN Environment World Conservation Monitoring Centre. Available at: http://data.unep-wcmc.org/datasets/1 (accessed August 24, 2018).

Conflict of Interest: The authors declare that the research was conducted in the absence of any commercial or financial relationships that could be construed as a potential conflict of interest.

frontiers in Marine Science

ORIGINAL RESEARCH
published: 22 January 2020
doi: 10.3389/fmars.2019.00788

Changes in Genome-Wide Methylation and Gene Expression in Response to Future pCO_2 Extremes in the Antarctic Pteropod *Limacina helicina antarctica*

*Samuel N. Bogan[1], Kevin M. Johnson[1,2] and Gretchen E. Hofmann[1]**

[1] Department of Ecology, Evolution and Marine Biology, University of California, Santa Barbara, Santa Barbara, CA, United States, [2] Department of Biological Sciences, Louisiana State University, Baton Rouge, LA, United States

OPEN ACCESS

Edited by:
Jose M. Eirin-Lopez, Florida International University, United States

Reviewed by:
Yi Jin Liew, Commonwealth Scientific and Industrial Research Organisation (CSIRO), Australia
Alexandre Fellous, Alfred Wegener Institute Helmholtz Centre for Polar and Marine Research (AWI), Germany

***Correspondence:**
Gretchen E. Hofmann
hofmann@ucsb.edu

Specialty section:
This article was submitted to Marine Molecular Biology and Ecology, a section of the journal Frontiers in Marine Science

Received: *11 October 2019*
Accepted: *06 December 2019*
Published: *22 January 2020*

Citation:
Bogan SN, Johnson KM and Hofmann GE (2020) Changes in Genome-Wide Methylation and Gene Expression in Response to Future pCO_2 Extremes in the Antarctic Pteropod Limacina helicina antarctica. Front. Mar. Sci. 6:788. doi: 10.3389/fmars.2019.00788

Epigenetic processes such as variation in DNA methylation may promote phenotypic plasticity and the rapid acclimatization of species to environmental change. The extent to which an organism can mount an epigenetic response to current and future climate extremes may influence its capacity to acclimatize or adapt to global change on ecological rather than evolutionary time scales. The thecosome pteropod *Limacina helicina antarctica* is an abundant macrozooplankton endemic to the Southern Ocean and is considered a bellwether of ocean acidification as it is highly sensitive to variation in carbonate chemistry. In this study, we quantified variation in DNA methylation and gene expression over time across different ocean acidification regimes. We exposed *L. helicina antarctica* to pCO_2 levels mimicking present-day norms in the coastal Southern Ocean of 255 μatm pCO_2, present-day extremes of 530 μatm pCO_2, and projected extremes of 918 μatm pCO_2 for up to 7 days before measuring global DNA methylation and sequencing transcriptomes in animals from each treatment across time. *L. helicina antarctica* significantly reduced DNA methylation by 29–56% after 1 day of exposure to 918 μatm pCO_2 before DNA methylation returned to control levels after 6 days. In addition, *L. helicina antarctica* exposed to 918 μatm pCO_2 exhibited drastically more differential expression compared to cultures replicating present-day pCO_2 extremes. Differentially expressed transcripts were predominantly downregulated. Furthermore, downregulated genes were enriched with signatures of gene body methylation. These findings support the potential role of DNA methylation in regulating transcriptomic responses by *L. helicina antarctica* to future ocean acidification and *in situ* variation in pCO_2 experienced seasonally or during vertical migration. More broadly, *L. helicina antarctica* was capable of mounting a substantial epigenetic response to ocean acidification despite little evidence of metabolic compensation or recovery of the cellular stress response in this species at future pCO_2 levels.

Keywords: epigenetics, DNA methylation, pteropod, ocean acidification, gene expression, *Limacina helicina antarctica*

INTRODUCTION

Marine ecosystems are already reaching extremes of environmental change on par with projected global climate change over the next century (Hoegh-Guldberg and Bruno, 2010; Harris et al., 2013; Chan et al., 2017; Oliver et al., 2018). Species inhabiting regions such as polar oceans are currently faced with a necessity to acclimatize or adapt to stressors that will only intensify as climate change progresses. Driven by the rapid advancement of extreme physical conditions in ecosystems today and in modeled projections, global change biologists have begun to direct attention to the mechanisms and consequences of species' abilities to rapidly respond to anthropogenic stress via acquired, adaptive traits (Chown et al., 2007; Calosi et al., 2008; Chevin et al., 2010; Nicotra et al., 2010; Beldade et al., 2011; Donelson et al., 2018; Kelly, 2019) and how mechanisms of acclimatization vary within a system between current and projected environmental change (Hennige et al., 2010; Duarte et al., 2018). We examined such a rapidly-acting process – namely, changes in DNA methylation and gene expression in the Antarctic pteropod *Limacina helicina antarctica* during exposure to present and future ocean acidification (OA) levels for the Southern Ocean.

In recent studies of marine metazoans, epigenetic processes have been demonstrated to be associated with the phenotypic plasticity of fitness-related traits in species experiencing climate change-driven stressors (Zhang et al., 2013; Putnam et al., 2016; Clark et al., 2018; Strader et al., 2019; Wong et al., 2019), a relationship that can be explained in part by the link between epigenetic mechanisms, gene expression, translation, and the traits underpinned by these processes (True et al., 2004). For example, experimental manipulation of DNA methylation levels in *Arabidopsis thaliana* has been shown to substantially alter the phenotypic plasticity of key developmental and physiological traits in low- and high-nutrient environments (Bossdorf et al., 2010). In humans, quantitative trait loci at methylated bases are linked to differential gene expression underpinning multiple physiological traits across a diversity of tissue types (Taylor et al., 2019). Overall, understanding how epigenetic processes may promote adaptive responses to environmental stressors will require investigations in diverse, ecologically critical taxa and experimentation across gradients of stress eliciting adaptive and pathological responses.

Among a suite of epigenetic modifications, DNA methylation, the addition of a -CH_3 methyl group to either cytosine or adenine bases, has received considerable focus for its role in regulating gene expression, particularly in vertebrate lineages and plants (Schubeler, 2015; Zhang et al., 2018). Investigations into the role of DNA methylation in invertebrates have uncovered marked differences in methylation's influence on gene expression and performance between phylogenetic lineages and across different environmental contexts (Sarda et al., 2012; Dimond and Roberts, 2016; Hofmann, 2017; Eirin-Lopez and Putnam, 2019). However, studies of DNA methylation and its role in environment-organism interactions in marine invertebrates remain sparse and confined to a small number of species for any given phyla.

Antarctic pteropods offer a valuable system for examining the role of epigenetics in shaping organismal responses to global change in the marine environment. Shelled pteropods or thecosomes have been proposed as a bellwether species for OA (Manno et al., 2017). The Antarctic thecosome *L. helicina antarctica* is a widely distributed and abundant pteropod endemic to the Southern Ocean (Boysen-Ennen et al., 1991; Steinberg et al., 2015; Thibodeau et al., 2019) where it can make up > 50% of total zooplankton measured as individuals per unit volume (Hunt et al., 2008). *Limacina* sp. is also a globally distributed genus spanning both polar and temperate environments (Bernard and Froneman, 2009; Hunt et al., 2010). *L. helicina antarctica* presently experiences a large degree of seasonal variability in seawater pCO_2 and pH, with pH varying by 0.6 units in regions like Prydz Bay (Gibson and Trull, 1999) and the Ross Sea (McNeil et al., 2010). This seasonal variability currently exceeds modeled predictions of an increase in annual mean pH of 0.4 units within the Southern Ocean by 2100 (IPCC, 2013). *L. helicina antarctica* also experiences present-day undersaturation in $\Omega_{aragonite}$ in some regions of the Southern Ocean during the austral winter (Bednaršek et al., 2012b). The frequency and duration of undersaturation events are expected to increase as OA advances in the Southern Ocean (McNeil and Matear, 2008; Hauri et al., 2015; Negrete-García et al., 2019). The onset of month long undersaturation events are predicted in the Southern Ocean within 14–29 years, along with annual mean $\Omega_{aragonite}$ undersaturation as soon as 10–20 years from today (IPCC, 2019).

In the face of future increases in pCO_2, current evidence suggests that *L. helicina antarctica* is poorly poised to acclimatize to predicted OA over the next century (Bednaršek et al., 2012a, 2014b; Gardner et al., 2018). Juvenile *L. helicina antarctica* collected from the McMurdo Sound, Ross Sea, do not appear to alter their metabolic rate over the course of 2-week acclimations to a regional, present-day pCO_2 extreme of 427–513 μatm (Hoshijima et al., 2017). By contrast, acclimation to future pCO_2 extremes of 901–1000 μatm has been shown to significantly alter metabolic rate under near-ambient temperatures (Seibel et al., 2012; Hoshijima et al., 2017). Similarly, gene expression by *L. helicina antarctica* has shown little differential expression in response to intermediate pCO_2 levels of 432 μatm when compared to differential expression under 902 μatm at which pervasive downregulation is apparent among transcripts even after 21 days of acclimation (Johnson and Hofmann, 2017). The dynamic shifts in metabolism and gene expression that arise when *L. helicina antarctica* are exposed to present-day vs. future pCO_2 extremes may be driven or regulated by epigenetic mechanisms such as DNA methylation.

Determining (i) whether DNA methylation in *L. helicina antarctica* varies across exposures to current and future pCO_2 extremes and (ii) whether changes in DNA methylation are associated with differential gene expression may provide valuable insight into molecular mechanisms underpinning this species' performance under OA and its ability to rapidly acclimatize to changing ocean conditions. Findings regarding epigenetic responses by *L. helicina antarctica* to OA may provide translational information for similar studies in other members of *Limacina* sp. and thecosome pteropods, a clade of shelled pteropods considered to be a bellwether for the severity of global OA (Bednaršek et al., 2014a). Furthermore, epigenetic studies

revealing the importance of DNA methylation for biological functions in molluscs (Gavery and Roberts, 2013; Riviere et al., 2013, 2017; Diaz-Freije et al., 2014; Lian et al., 2015; Garcia-Fernandez et al., 2017; Suarez-Ulloa et al., 2019) thus far have been heavily skewed toward bivalves and in particular, oysters, necessitating a broader assessment of diversity in environmental epigenetics across the speciose molluscan phylum.

To this end, we conditioned juvenile *L. helicina antarctica* collected from McMurdo Sound under present-day pCO_2 levels of 255 μatm, present-day pCO_2 extremes of 530 μatm, and future pCO_2 extremes of 918 μatm, resulting in Ωaragnoite undersaturation, for up to 7 days (**Figure 1**). Following this experiment, we quantified the proportion of 5-methylcytosine in *L. helicina limacina* DNA following 1, 3, and 6 days of exposure to each pCO_2 level. Additionally, we sequenced and analyzed the transcriptomes of pteropods sampled from each pCO_2 level after 0.5 and 7 days of conditioning in order to (i) quantify differential expression in response to current and future pCO_2 extremes across time and (ii) test for correlations between differential expression and signatures of DNA methylation among transcribed genes.

MATERIALS AND METHODS

Collection and Conditioning of *L. helicina antarctica*

Juvenile *L. helicina antarctica* were collected in October of 2014 from Cape Evans, McMurdo Sound, via plankton net as previously described (Hoshijima et al., 2017; Johnson and Hofmann, 2017) and transported to the Crary Laboratory, McMurdo Station, where they were held under near-ambient temperature (−0.59°C) in filtered seawater for 24 h before conditioning at different pCO_2 levels. During conditioning, *L. helicina antarctica* were held in 1 L tanks with a flow rate of 2 L h^{-1} at a starting density of 200 animals L^{-1}. *L. helicina antarctica* were not fed at any point during the experiment as the winter-summer transition in the McMurdo Sound is characterized by low phytoplankton abundance (Foster et al., 1987).

Seawater pCO_2 was manipulated using three reservoir containers held at different pCO_2 levels, each connected to three replicate culturing tanks of the volume and flow rate described above. pCO_2 was controlled inside of reservoir tanks by injecting mixtures of filtered, CO_2-scrubbed, dry air and pure CO_2 with seawater. Pure air and CO_2 were mixed using SmartTrak® 100 Series Mass Flow Controllers and Micro-Trak© 101 Series Mass Flow Controllers (Sierra Instruments, United States), respectively. Reservoirs were held in a 1240 L seawater table filled with near-ambient seawater. Culture tanks held a mean temperature of −0.59°C ± 0.11 SD over the course of the 7-day experiment. Seawater temperature, pCO_2, pH, and carbonate chemistry were measured as previously described (Johnson and Hofmann, 2017). Low, intermediate, and high pCO_2 levels averaged 255 μatm ± 3.52 SD, 530 μatm ± 12.03 SD, and 918 μatm ± 19.53 SD. A full report of temperature and seawater chemistry in each culture tank over time is available in **Supplementary Figure S1**.

Quantification and Analysis of Genomic 5-Methylcytosine

DNA was extracted from pooled replicates containing 10 juvenile *L. helicina antarctica* sampled from each pCO_2

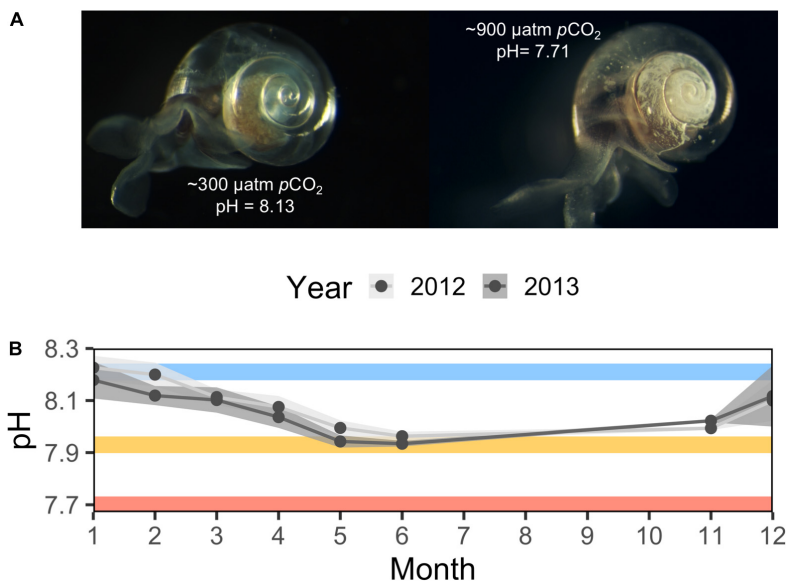

FIGURE 1 | *In situ* and experimental ocean acidification experienced by *Limacina helicina antarctica*. **(A)** Representative images of shell dissolution following exposure to ~300 and ~900 μatm pCO_2 for 14 days. **(B)** Mean surface ocean pH recordings per month from McMurdo Sound taken at McMurdo Station circa 2012 and Cape Evans circa 2013 recorded by Kapsenberg et al., 2015 and Hoshijima et al. (unpublished). Error windows represent ± SD. Mean pH from 255, 530, and 918 μatm pCO_2 experimental conditions are subimposed as blue, yellow, and red lines, respectively.

treatment at 1, 3, and 6 days using a CTAB DNA extraction modified from Worden (2009). The step-by-step DNA extraction protocol is detailed under **Supplementary Data S2**. DNA purity, quality, and concentration were respectively assessed via Nanodrop, agarose gel, and Qubit Broad Range DNA quantification. DNA extractions were performed on five biological replicates per pCO_2 level x timepoint by sampling two pooled replicates from two of the triplicate cultures and one pooled replicate from the third.

The proportion of 5-methylcytosine (5-mC) present in *L. helicina antarctica* DNA was quantified colorimetrically using the ELISA-based MethylFlash DNA 5-mC Quantification Kit (Epigentek, Farmingdale, NY, United States) according to manufacturer guidelines. Contrary to manufacturer instructions, standards and samples were measured in triplicate rather than duplicate in order to improve accuracy. Additionally, the 45 samples were randomly split between two different plates such that 3/5 or 2/5 of replicates for each pCO_2 level x timepoint group would be present on a given plate. Within a single plate, the arrangement of standards, negative controls, and samples was randomized. In keeping with manufacturer instructions, technical replicates remained grouped together within each plate. OD450 was measured using an Epoch Microplate Spectrophotometer (Biotek Instruments, Winooski, VT, United States).

Variation in 5-mC content was modeled as a function of pCO_2 level, exposure time, and their interaction by fitting a linear regression to the data using the lm() function of the R 'stats' package v3.5.1. A full report describing the linear model used to assess changes in 5-mC content is available in **Supplementary Table S1**. Reported *F*-statistics from the fitted model were generated using the anova() function of the R 'stats' package. Cliff's delta estimates, mean effect size estimates, and *post hoc* Mann–Whitney *U*-tests comparing 5-mC content between groups were performed with the 'dabest' package for estimation statistics (Ho et al., 2019).

The presence of outliers within the data was assessed by measuring the non-normality, residual, and leverage of each individual replicate fitted to the linear model using Q–Q plots, residual vs. leverage plots, and Cook's distance estimates executed with the R 'stats' base package. Any sample exhibiting non-normality, high leverage, and high residual was excluded from the linear model, resulting in the removal of a single data point.

RNA Sequencing and Transcriptomic Analyses

RNA was extracted and sequenced from three pooled *L. helicina antarctica* replicates (10 individuals/pool) per treatment for each of the two sampling time points (n = 18 libraries; 2 μg library^{-1}) as previously described (Johnson and Hofmann, 2017). Sequencing was performed at the UC Davis Genome Center on an Illumina HiSeq4000 sequencer using paired-end 100 bp reads. Raw sequencing reads were trimmed using Trimmomatic to remove adapter sequences, low quality base pairs (PHRED < 20), and sequences smaller then 75 bp (Bolger et al., 2014). The quality of trimmed reads was assessed using FastQC v0.11.8 (Andrews, 2018). Trimmed reads were mapped to the *L. helicina antarctica* reference transcriptome (Johnson and Hofmann, 2016) and counted using RSEM v1.3.1. RSEM was chosen for its accurate quantification of read counts mapped to *de novo* reference assemblies (Li and Dewey, 2011). Read processing, alignment, and counting was performed with support from the Indiana University Carbonate computing cluster (Stewart et al., 2017). A differential expression analysis was performed using edgeR v3.24.3 (Robinson et al., 2010) set to 'robust' calculation of dispersion and 'robust' fitting of general linear models using the glmQLFit() function of edgeR. Differentially expressed genes (DEGs) were identified using an FDR cutoff < 0.05 and an absolute $\log_2$ foldchange cutoff of > 1.5 (Chen et al., 2016). A principal coordinates analysis was also performed in order to cluster RNAseq samples by inputting $\log_2$-adjusted counts per million (CPM) read counts to the pcoa() function of the R package 'ape' (Paradis et al., 2004). R scripts used to analyze differential gene expression are included in **Supplementary Data S3**. Enriched gene ontologies (GO) were identified among up- and down-regulated genes using Mann–Whitney *U*-tests input with signed, −log *p*-values using the 'Rank Based Gene Ontology Analysis with Adaptive Clustering' method: https://github.com/z0on/GO_MWU (Wright et al., 2015).

Germline gene body methylation levels were estimated within exons by calculating observed over expected CpG frequencies (CpGOE) across each transcript within the *L. helicina antarctica* reference transcriptome (Johnson and Hofmann, 2016) using python scripts written by Dimond and colleagues https://github.com/jldimond/Coral-CpG (Dimond and Roberts, 2016). Means and distributions of transcript CpGOE values were then compared between up- and down-regulated DEGs within treatment groups using permutation tests and Kolmogorov–Smirnov (KS) tests, respectively. A linear model was used to assess variation in transcript CpGOE as a function of foldchange direction, duration of exposure to high pCO_2, and their interaction using the R package 'lmPerm' v2.1.0, which generates *p*-values for linear models using permutation tests (Wheeler and Torchiano, 2016). Residuals within this linear model were bimodal, necessitating a statistical approach such as a permutation test that does not assume a normal distribution. Two-sided KS tests were performed using the ks.test() function of the R package 'dgof' v1.2 (Arnold and Emerson, 2013). The influence of categorical CpGOE bins (bin size = 0.5) on transcriptional variation represented as the CV of logCPM was assessed using the lm() function of R 'stats.'

RESULTS

Genomic Methylation in *L. helicina antarctica* Under Current and Future pCO_2 Extremes

ELISA-based quantification of 5-methylcytosine in *L. helicina antarctica* revealed significant effects of pCO_2 ($F_{1,40} = 10.24$; $p = 0.0027$), and the interaction of pCO_2 and time ($F_{1,40} = 7.74$; $p = 0.0082$) on DNA methylation. Specifically, acute exposure to future pCO_2 extremes induced hypomethylation of the *L. helicina antarctica* genome followed by a return to normal levels over

time. Exposure to current pCO_2 extremes did not induce detectable changes in genomic methylation relative to ambient pCO_2 (**Figure 2**).

Individuals exposed to 918 µatm pCO_2 (future extremes) for 1 day exhibited a 0.42% (0.29–0.56 95% CI) reduction in 5-mC content relative to 255 µatm (Mann–Whitney $p = 0.020$). For context, the mean 5-mC content of the *L. helicina antarctica* genome equaled 0.944 ± 0.17% when animals exposed to 918 µatm pCO_2 were excluded from the mean. 5-mC in 918 µatm cultures remained 0.19% lower than the 255 µatm treatment after 3 days of exposure (Mann–Whitney $p = 0.060$) before converging at a difference of 0.0039% after 6 days. *L. helicina antarctica* showed no differences in 5-mC content between 530 and 255 µatm pCO_2 treatments at any timepoint (**Figure 2**).

One replicate exhibited 2.14-fold greater 5-mC content than the overall mean. The non-normality, residual, and leverage of this replicate were examined in order to determine its status as an outlier using (i) Cook's distance, (ii) quantile–quantile plots to assess deviation from normality and (iii) residual-leverage plots. The replicate exhibited a substantially high residual and leverage and was thus removed from all analyses (**Supplementary Figure S2**). A full report describing the linear model used to assess changes in 5-mC content (**Supplementary Table S1**) and CV values per replicate (**Supplementary Figure S3**) are available in **Supplementary Data S1**.

Transcriptomic Responses to Current and Future pCO_2 Extremes

As genomic methylation influences both magnitude and variation in gene expression in multiple invertebrate lineages, we sought to pair genome-wide methylation data with transcriptomes sequenced for early and late timepoints under low, medium, and high pCO_2. Overall, we found that gene expression in *L. helicina antarctica* varied as a function of pCO_2 and exposure time. A principal coordinates analysis of CPM read counts demonstrated that a coordinate axis associated with pCO_2 level and time explained 32.53% of transcriptional variation. A second axis associated with time alone explained 8.4% (**Figure 3A**).

Limacina helicina antarctica exhibited substantially more differential expression under 918 µatm pCO_2 than under 530 µatm. After 0.5 day of exposure, pteropods in the 530 µatm treatment exhibited only one significant DEG relative to 255 µatm (FDR < 0.05; absolute $\log_2$FC > 1.5). After 7 days at 530 µatm, 3 transcripts were differentially expressed. Additionally, each DEG in the 530 µatm treatment group was upregulated. By contrast, *L. helicina antarctica* differentially expressed 6,649 transcripts after 0.5 day of exposure to 918 µatm and 6,815 transcripts after 7 days. 69.91% of DEGs detected at 0.5 day under

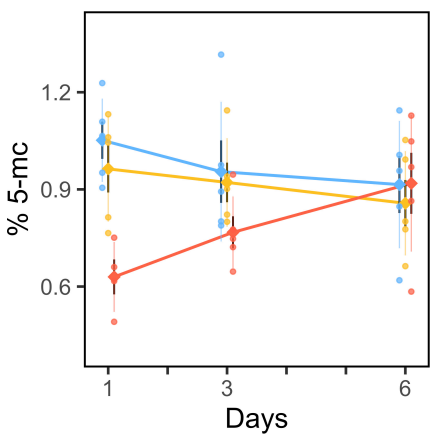

FIGURE 2 | Differential methylation of the *Limacina helicina antarctica* genome during acute exposure to future pCO_2 extremes. Mean values (diamonds) and individual replicates (circles) of percent 5-methylcytosine quantified using ELISA-based methods are plotted for 255 µatm (blue), 530 µatm (yellow), and 918 µatm (red) pCO_2 treatments level across time. ± SE is represented by wide, black error bars. ± SD is represented by narrow, colored error bars.

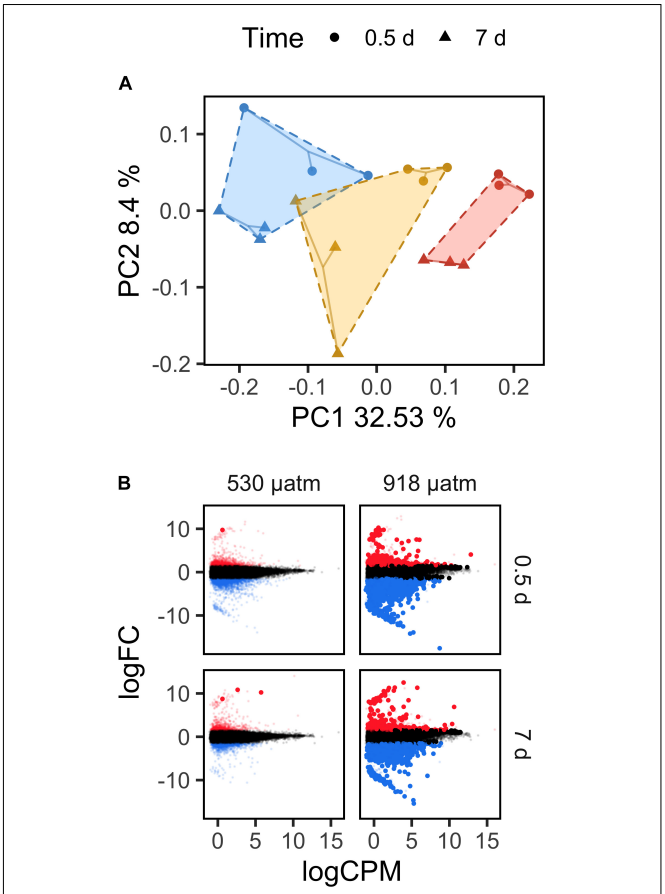

FIGURE 3 | Transcriptomic responses by *Limacina helicina antarctica* to current and future pCO_2 extremes. **(A)** Loading of RNAseq samples to latent variables derived from a principal coordinates analysis of CPM-normalized read counts. Polygons are drawn around pCO_2 255 µatm (blue), 530 µatm (yellow), and 918 µatm (red) pCO_2 treatments. Replicates sampled at different times are denoted by different shapes. **(B)** Differential expression under 530 and 918 µatm pCO_2 relative to 255 µatm. Transcript $\log_2$ foldchanges are plotted against $\log_2$ CPM read counts. Red and blue points denote up- and down-regulated transcripts, respectively, above an absolute $\log_2$ foldchange of 1.5. Large, solid points denote differentially expressed transcripts with an FDR p-value < 0.05.

918 µatm pCO_2 were downregulated. Downregulated transcripts composed 61.20% of DEGs after 7 days of exposure to 918 µatm (**Figure 3B**). 3,607 transcripts were differentially expressed at both 0.5 and 7 days under 918 µatm pCO_2, leaving 3,042 DEGs unique to 0.5 day of exposure and 3,773 DEGs unique to 7 days.

Transcripts that were up- or down-regulated at 0.5 day under 918 µatm pCO_2 were collectively enriched for 88 GO terms while 111 GO terms were enriched among up- and down-regulated transcripts from 7 days of 918 µatm exposure (FDR < 0.01). 81 of these GO terms were commonly enriched among both time points. 56.81% of GO terms enriched at 0.5 day were associated with downregulated transcripts while 54.95% of GO terms enriched at 7 days were associated with downregulation. Ontologies uniquely enriched at 0.5 day pertained to glucose metabolism, protein metabolism, and the oxidative stress response. Ontologies unique to the 7 days timepoint were diverse but included multiple GO terms pertaining to singular functions such as fatty-acid metabolism, antioxidant activity, transcription, trans-membrane transport, and transferase activity for glycosyl and hexosyl groups. Enriched ontologies that were shared between 0.5 and 7 days included functions relating to protein degradation, protein synthesis, cytoskeletal structure, ATP synthesis, and methyltransferase activity (**Supplementary Figures S4, S5**).

Since methyltransferases are of broad interest in an epigenetic context, we queried enriched GO terms for these subsets of genes. We found that 182 and 174 transcripts associated with methyltransferase activity were significantly enriched among down or upregulated genes at 0.5 and 7 days, respectively, under 918 µatm pCO_2. On average, enriched methyltransferases were upregulated at both time points. Sub-ontologies of "methyltransferase activity" (GO:0008168) that were enriched among DEGs at both time points included RNA methyltransferases, tRNA methyltransferases, and SAM-dependent methyltransferases: a class that includes enzymes targeting DNA and/or RNA (**Supplementary Figures S4, S5**). Histone methyltransferases were not enriched among down or upregulated genes, but some were differentially expressed under future pCO_2 extremes. 1 *EZH2* histone-lysine *N*-methyltransferase was upregulated after 0.5 day exposure while four histone-arginine methyltransferases, 1 *UTY* histone demethylase, and 4 histone-lysine *N*-methyltransferases showed downregulation. 1 *SETD8* histone-lysine *N*-methyltransferase was downregulated at both 0.5 and 7 days of exposure to 918 µatm (**Supplementary Figures S6, S7**).

Full lists of transcripts differentially expressed at 918 µatm pCO_2 relative to 255 µatm are available in **Supplementary Data S4, S5**. GO terms significantly enriched among sets of up- and down-regulated genes are visualized in **Supplementary Figures S4, S5**.

Signatures of Gene Body Methylation Among Differentially Expressed Genes

Transcripts that were differentially expressed in response to 918 µatm pCO_2 varied in mean CpGOE ratio depending on fold change direction ($F_{1,13459}$ = 85.05; p < 2e-16). CpGOE is inversely related to germline methylation and, when it is applied to transcripts, demonstrates a signature of gene body methylation. Specifically, downregulated genes were enriched with low CpGOE genes at both 0.5 and 7 days (**Figure 4A**). A significant interaction between foldchange direction and time was also observed ($F_{1,13459}$ = 71.45; p < 2e-16) in which the mean difference in CpGOE between up- and down-regulated DEGs was greater at 0.5 day (Cliff's delta = 0.1409 ± 0.0330) than 7 days (Cliff's delta = 0.0292 ± 0.0296).

As (i) the distribution of CpGOE in the *L. helicina antarctica* transcriptome is bimodal and (ii) the maximum and minimum percentiles of CpGOE distributions were equivalent between up- and down-regulated transcripts, changes in the densities of CpGOE distributions among DEGs served as a more accurate measurement of the frequency of high and low CpGOE values. A Kolmogorov–Smirnov (KS) test demonstrated significant differences in the modality of CpGOE values between up- and

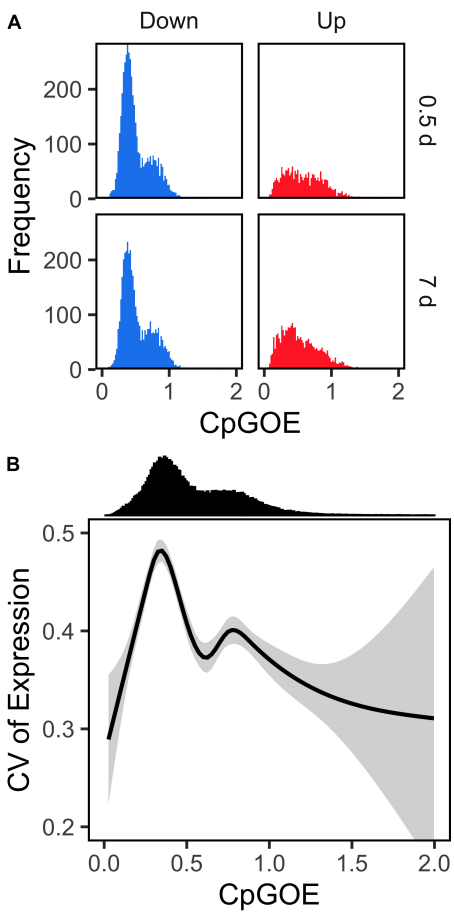

FIGURE 4 | Transcripts downregulated by *Limacina helicina antarctica* in response to future pCO_2 extremes show enriched signatures of gene body methylation. **(A)** CpGOE histograms are plotted for transcripts exhibiting significant downregulation (blue) or upregulation (red) under 918 µatm pCO_2. Bin widths = 0.02 CpGOE. **(B)** Mean CV of expression is plotted across CpGOE. Shaded regions depict ± 95% CI.

down-regulated DEGs at 0.5 day (D = 0.19075; p < 1.0e-15) and 7 days (D = 0.15198; p < 1.0e-15) under 918 μatm pCO_2. Density beneath the low CpGOE mode was 2.44-fold greater among downregulated DEGs compared to upregulated DEGs at 0.5 day and 1.84-fold greater after 7 days (**Figure 4A**). Differences in the modality of CpGOE among DEGs that were downregulated either at 0.5 and 7 days relative to the whole *L. helicina antarctica* transcriptome were significant but less pronounced: KS test D values equaled 0.09318–0.06263 for 0.5 and 7 days, respectively (p < 1.0e-15). Cumulative distributions visualizing the modalities of CpGOE in each of the groups are available in **Supplementary Figure S8**. In contrast to the relationship between genes' CpGOE and differential expression in *L. helicina antarctica*, a negligible association between CpGOE and transcriptional variation was observed. A linear model reported a significant effect of categorical, binned CpGOE (bin size = 0.5) on the CV of expression of transcripts in which the low CpGOE mode exhibited a higher mean CV (**Figure 4B**), albeit with a large degree of variation surrounding the mean.

DISCUSSION

Our analyses of DNA methylation and gene expression in *L. helicina antarctica* showed dynamic changes in both processes following experimental conditioning under future pCO_2 levels predicted for Antarctic coastal waters. Juvenile *L. helicina antarctica* appeared to mount a strong epigenetic response to future pCO_2 extremes, reducing DNA methylation by 29–56% after brief exposure to high pCO_2 before steadily increasing DNA methylation levels over time. In addition, differential gene expression showed an association with DNA methylation as evidenced by an enrichment of low CpGOE transcripts among genes that were significantly downregulated in response to future pCO_2 extremes. Changes in global DNA methylation and differential expression were absent or negligible following exposure to present-day pCO_2 extremes. Taken together, these observations suggest that DNA methylation plays a role in regulating the cellular responses of *L. helicina antarctica* to future OA.

Below, we discuss the functional significance of DNA methylation in the context of marine molecular ecology, compare our findings to studies of DNA methylation in other Antarctic organisms, and discuss the available data on epigenetic responses by other species to OA. Lastly, we point to next steps for the study of epigenetics in polar systems, including future work on *L. helicina antarctica* and other calcifying marine invertebrates.

Hypomethylation Following Acute Exposure to High pCO_2

While *L. helicina antarctica* has exhibited a poor capacity to acclimate to experimental OA as evidenced by a lack of metabolic compensation and upregulation of stress response pathways following 21 days of acclimation to future pCO_2 levels (Hoshijima et al., 2017; Johnson and Hofmann, 2017), in this study, it appears that juvenile *L. helicina antarctica* were capable of mounting a significant epigenetic response to high pCO_2. Our preliminary analyses in *L. helicina antarctica* have identified dynamic change in levels of DNA methylation in response to high pCO_2. This outcome might not be expected if we were to stereotype this species as an Antarctic, cold-adapted invertebrate with diminished cellular responses to environmental change. In fact, studies of environmental epigenetics in two Antarctic marine invertebrates, a benthic polychete and an intertidal gastropod, have both documented differential methylation in response to variation in temperature (Marsh and Pasqualone, 2014; Clark et al., 2018).

It is worth noting that one limit to our approach toward quantifying global patterns of DNA methylation is the non-specific nature of the acquired data. While global levels of methylation provide insight into changes across the whole genome, these measurements are limited in that they (i) provide no indication of functional consequences and (ii) are less sensitive than NGS methods such as bisulfite sequencing. For example, if X methylated CpGs become demethylated in response to a given treatment and are proceeded by methylation at X CpGs that were previously unmethylated, global 5-mC quantification would not detect a change in methylation. For this reason, our results do not rule out the possibility that *L. helicina antarctica* may differentially methylate its genome in response to present-day pCO_2 extremes. Additionally, the large effect strength of 918 μatm pCO_2 on genomic methylation in *L. helicina antarctica* is not unprecedented in the context of acute exposure to stress (Rodrigues et al., 2015; Li et al., 2016; Robinson et al., 2019), but the quantity of this effect should be further evaluated with replicate experiments or similar studies.

Although we did detect changes in total methylation and gene expression, our results are presently not sufficient to directly link differential methylation with the expression of specific genes. However, other studies on invertebrates indicate a relationship between gene expression and genomic methylation in response to variation in multiple abiotic factors. Many invertebrate phyla including molluscs predominantly exhibit DNA methylation within gene coding regions (Zemach et al., 2010; Wang et al., 2014; Jeong et al., 2018; Li et al., 2018; Liew et al., 2018). Hypomethylation at intragenic regions is generally associated with reduced gene expression and increased transcriptional variability and/or spuriousness in both vertebrates (Kobayashi et al., 2012; Neri et al., 2017) and invertebrates (Zemach et al., 2010; Dixon et al., 2014, 2018; Gavery and Roberts, 2014; Li et al., 2018). Many studies have also noted associations between hypomethylation and environmentally-induced or disease-induced pathologies spanning a wide range of taxa including plants, vertebrates, and invertebrates for which hypomethylation was demonstrated in both promoters and/or gene bodies (Aina et al., 2004; Pavet et al., 2006; Pogribny et al., 2006; Rusiecki et al., 2008; Luttmer et al., 2013; Xiu et al., 2019). While mechanistic links between hypomethylation and pathology are unclear, there is strong evidence in support of its role in cellular responses to infection and stress.

Despite extensive research on organismal responses to OA, the cellular mechanisms that contribute to pathological vs. adaptive

responses to pCO_2 stress remain poorly understood (Melzner et al., 2020). It is plausible that hypomethylation of the *L. helicina antarctica* genome in response to high pCO_2 is not adaptive. Rather, it may be related to pathological processes associated with chronic stress seen in *L. helicina antarctica* under OA. The 29–56% reduction in mean 5-mC by *L. helicina antarctica* in response to pCO_2 stress contrasts observations of differential methylation under OA that have been documented in more pCO_2-tolerant calcifying invertebrates. Specifically, scleractinian corals and purple sea urchins of differing life history stages respectively exhibited global hypermethylation or a combination of hypo- and hypermethylation at CpGs in response to elevated levels of pCO_2 (Putnam et al., 2016; Liew et al., 2018; Strader et al., 2019; Strader et al., in review). It is unclear to what extent such variation between these taxa is due to phylogenetic differences, life history or to pCO_2 sensitivity, but they remain noteworthy. Further comparative work exploring differences in the variation of DNA methylation under OA in thecosome pteropods relative to more pCO_2-tolerant calcifying invertebrates could help elucidate mutually exclusive aspects of genomic methylation that contribute to acclimatization and pathology.

Evidence of a Role for DNA Methylation in Differential Expression Under High pCO_2

Limacina helicina antarctica mounted a large transcriptomic response to future pCO_2 extremes that predominantly consisted of downregulated DEGs. This response corroborates our past reporting on differential expression in response to OA among *L. helicina antarctica* collected from the McMurdo Sound (Johnson and Hofmann, 2017). Since (i) gene expression in molluscs and other invertebrates positively correlates with gene body methylation (Zemach et al., 2010; Gavery and Roberts, 2013; Dixon et al., 2014, 2018; Gavery and Roberts, 2014; Li et al., 2018), and (ii) DNA methylation occurs primarily within gene bodies among molluscs and other invertebrates, it is possible that hypomethylation of *L. helicina antarctica* DNA observed in response to high pCO_2 contributed to the differential expression of downregulated genes. Indeed, downregulated DEGs were enriched with low CpGOE transcripts relative to upregulated genes. This demonstrated that downregulated DEGs were likely to have a greater degree of methylation at exons within germline cells, and further, suggested a link between hypomethylation and downregulation across the *L. helicina antarctica* genome.

Despite evidence of DNA methylation's influence on downregulated transcripts, the timing of changes in 5 m-C and differential expression were not synchronized throughout the duration of the experiment. Mean 5-mC levels in *L. helicina antarctica* exposed to 918 μatm became comparable to 530 μatm and 255 μatm cultures by 6 days of exposure while the quantity of downregulation in 918 μatm cultures remained high and relatively unchanged even by 7 days. Thus, DNA methylation and differential expression did not correlate over time despite evidence of their association revealed by CpGOE values. DNA methylation and differential expression do not necessarily correlate throughout time when a causal relationship is present (Secco et al., 2015; Pacis et al., 2019), and have been documented to be unpaired during invertebrate development under high pCO_2 (Strader et al., in review). The relationship between DNA methylation and gene expression in molluscs has proved tenuous in some cases. For example, the offspring of diuron-exposed oysters have exhibited differential expression and DNA methylation relative to offspring from control parents, but only a small number of DEGs were correlated with differentially methylated CpGs (Rondon et al., 2017). Other reports in oysters have documented stronger associations between gene expression and DNA methylation (Olson and Roberts, 2014). The lack of synchronicity in the timing of differential methylation and differential expression in this experiment does not entirely rule out their mutual influence. Rather, it may suggest a more complex relationship that includes other epigenetic factors.

We also observed interesting patterns of differential expression in genes with various functions related to other epigenetic modifications to DNA. For example, the differential expression of histone modifying enzymes by *L. helicina antarctica* correlated strongly with changes in global 5-mC over time under high pCO_2: 1 *EZH2* histone-lysine *N*-methyltransferase was upregulated by *L. helicina antarctica* after 0.5 day exposure to 918 μatm while 4 histone-arginine methyltransferases, 1 *UTY* histone demethylase, and 4 histone-lysine *N*-methyltransferases were downregulated. Only one of these genes remained differentially expressed by 7 days of exposure to 918 μatm, demonstrating an early signature of downregulation in histone methyltransferases. In at least some invertebrates and mammals, gene bodies that exhibit higher levels of baseline DNA methylation are also enriched with H3K36me3, histones with lysine 36 trimethylation (Nanty et al., 2011; Baubec et al., 2015). H3K36me3 can chaperone *de novo* methyltransferases to gene bodies (Baubec et al., 2015). Inversely, the absence of H3K36me3 at gene bodies has been documented to be a predictor of hypomethylation (Hahn et al., 2011). Arginine methylation at H4R3me2 has a similar relationship with *de novo* methyltransferases but ultimately has a more repressive effect on gene expression (Zhao et al., 2009). Therefore, differential methylation of intragenic regions is associated with chromatin accessibility in certain contexts and both of these processes mediate the influence of intragenic regions on differential expression. Overall, our results suggest that differential methylation of DNA and histones may jointly influence persistent transcriptomic responses by *L. helicina antarctica* to future pCO_2 extremes. Histone modifications (e.g., histone methylation) and subsequent changes in transcription have been shown to regulate development and responses to environmental stress in molluscs (Fellous et al., 2015, 2019; Gonzalez-Romero et al., 2017) and other calcifying marine invertebrates (Rodriguez-Casariego et al., 2018). Interactions between chromatin structure and DNA methylation should be explored in greater functional detail in this system in order to substantiate these observations and understand their influence on pervasive and persistent downregulation by *L. helicina antarctica* under OA.

Pervasive downregulation or "dampening" transcriptomic and/or proteomic responses are commonly observed under

high pCO_2 across marine molluscs and other calcifying invertebrates (Todgham and Hofmann, 2009; O'Donnell et al., 2010; Dineshram et al., 2012; Kenkel et al., 2017; De Wit et al., 2018; Kriefall et al., 2018), including some species of *Limacina* pteropods (Koh et al., 2015; Johnson and Hofmann, 2017). Other genera of shelled pteropods have not exhibited dampening transcriptomic responses to OA (Maas et al., 2015; Moya et al., 2016) and strong time-dependent effects on the proportion of upregulated vs. downregulated genes have been documented in *Limacina retroversa* in response to high pCO_2 (Maas et al., 2018). Thus, there does not appear to be a generalizable transcriptional response to OA within Pteropoda or the *Limacina* genus. Studying the potential for phylogenetic variation in epigenetic processes among Pteropods may further explain the contribution of mechanisms such as DNA methylation to cellular responses to OA. Similarly, expanding epigenetic studies of cellular responses to OA across a broader diversity of taxa may reveal mechanistic similarities between evolutionarily distant groups that exhibit similar transcriptional responses to high pCO_2.

CONCLUSION

Perhaps the most important conclusion we can draw from this experiment is that variation in DNA methylation across the *L. helicina antarctica* genome was responsive to ocean acidification and likely yielded consequences for cellular functions due to (i) the magnitude of variation, and (ii) evidence of its influence on gene expression. From a polar biology perspective, our results demonstrate that DNA methylation is dynamic in an otherwise stenothermic Antarctic macrozooplankton. Many Antarctic ectotherms have classically been considered to be specialized to an invariable environment, subsequently lacking phenotypic and physiological plasticity necessary for acclimatizing to environmental shifts on par with future climate change (Peck et al., 2004, 2010, 2014; Beers and Jayasundara, 2015). A growing body of work is beginning to demonstrate, however, that physiological plasticity is retained and sufficient for metabolic recovery under a warmer and/or more acidic ocean in at least some Antarctic ectotherms (Seebacher et al., 2005; Peck et al., 2010; Enzor and Place, 2014; Reed and Thatje, 2015; Huth and Place, 2016a,b; Morley et al., 2016; Enzor et al., 2017; Davis et al., 2018; Hawkins et al., 2018). The responsiveness of DNA methylation in *L. helicina antarctica* to variation in pCO_2 may be linked to this species' environmental experience *in situ*. Recent oceanographic observations suggest that seasonal variation in pCO_2 in coastal waters of the Southern Ocean is substantial (Gibson and Trull, 1999; McNeil et al., 2010; Kapsenberg et al., 2015; Negrete-García et al., 2019). Thus, it is likely that *L. helicina antarctica* is presently faced with low pH conditions that are undersaturated for aragonite calcification during vertical migration.

Lastly, recent modeling efforts have indicated that $\Omega_{aragonite}$ undersaturation in the Southern Ocean will appear at quite shallow depths (∼400 m) by the end of the century (Negrete-García et al., 2019) creating a habitat compression or "squeeze" event for calcifying macrozooplankton such as *L. helicina antarctica*. Thus, quantifying the epigenetic, transcriptional, and physiological plasticity of *L. helicina antarctica* populations is important in assessing their capacity to respond to future changes in ocean carbonate chemistry. With that said, it remains unclear whether or not dynamic changes in DNA methylation are adaptive for *L. helicina* populations experiencing high pCO_2. Future research concerning this ecologically critical species that aims to expand on our findings and past OA experiments will benefit from (i) executing long-term cultures of *L. helicina antarctica* under future pCO_2 extremes for at least 3–6 weeks and (ii) conducting integrated analyses of metabolic rate, calcification, gene expression, and epigenetic profiling. This 3–6 week range has proven to be a metabolic and transcriptional tipping point for other Antarctic ectotherms acclimating to increases in temperature and pCO_2 (Peck et al., 2010; Enzor and Place, 2014; Enzor et al., 2017; Davis et al., 2018). Quantifying DNA methylation at whole-genome or base-by-base levels across long-term acclimations will expand on dynamic epigenetic changes documented in this study and reveal whether or not they associate with or initiate plastic responses to global change. If DNA methylation or other epigenetic mechanisms ultimately do not drive plastic responses to environmental variation in *L. helicina antarctica,* this species still represents a valuable comparative system for studying the contribution of epigenetic mechanisms to adaptive vs. pathological responses to abiotic stress and future OA.

DATA AVAILABILITY STATEMENT

The datasets generated for this study can be found in the Sequence Read Archive (SRA) BioProject PRJNA576909.

AUTHOR CONTRIBUTIONS

GH conceived the aims, scope, and design of the study. GH and KJ collected, cultured, sampled animals for the study, and edited the manuscript. KJ extracted and prepared RNA for sequencing. SB extracted DNA, performed 5-mC quantification, executed downstream 5-mC analyses, and wrote the manuscript. SB and KJ performed transcriptomic analyses.

FUNDING

This work was funded in part by a grant from the U.S. National Science Foundation (NSF) through the U.S. Antarctic Program (PLR-1246202) to GH. KJ was supported by an NSF Graduate Research Fellowship during the time of the experiment. SB was supported by a Graduate Student Fellowship from the Department of Ecology, Evolution, and Marine Biology at UC Santa Barbara throughout his contribution to the study.

ACKNOWLEDGMENTS

The authors would like to thank the late Dr. Umi Hoshijima for his invaluable assistance throughout the experiment, for collecting *in situ* pH data reported in this study, and for his consultation regarding these data. The authors acknowledge both Maddie Housh for her assistance in extracting DNA as well as the Crary Laboratory staff at McMurdo Station, Antarctica, for their support. Additionally, other members of the U.S. Antarctic Program, and of Lockheed's Antarctic Support Corporation (ASC) supported field work for this study. The authors also acknowledge the Indiana University Pervasive Technology Institute for providing computational resources on the Carbonate cluster that have contributed to the results reported within this manuscript.

SUPPLEMENTARY MATERIAL

The Supplementary Material for this article can be found online at: https://www.frontiersin.org/articles/10.3389/fmars.2019.00788/full#supplementary-material

REFERENCES

Aina, R., Sgorbati, S., Santagostino, A., Labra, M., Ghiani, A., and Citterio, S. (2004). Specific hypomethylation of DNA is induced by heavy metals in white clover and industrial hemp. *Physiol. Plant.* 121, 472–480. doi: 10.1111/j.1399-3054.2004.00343.x

Andrews, S. (2018). *FastQC: A Quality Control Tool for High Throughput Sequence Data. (Babraham Bioinformatics)*. Available at: http://www.bioinformatics.babraham.ac.uk/projects/fastqc (accessed August 15, 2019).

Arnold, T. B., and Emerson, J. W. (2013). *Discrete Goodness-of-Fit Tests*. London: Comprehensive R Archive Network.

Baubec, T., Colombo, D. F., Wirbelauer, C., Schmidt, J., Burger, L., Krebs, A. R., et al. (2015). Genomic profiling of DNA methyltransferases reveals a role for DNMT3B in genic methylation. *Nature* 520, 243–247. doi: 10.1038/nature14176

Bednaršek, N., Feely, R. A., Reum, J. C., Peterson, B., Menkel, J., Alin, S. R., et al. (2014a). *Limacina helicina* shell dissolution as an indicator of declining habitat suitability owing to ocean acidification in the California Current Ecosystem. *Proc. R. Soc. B Biol. Sci.* 281:20140123. doi: 10.1098/rspb.2014.0123

Bednaršek, N., Tarling, G. A., Bakker, D. C., Fielding, S., and Feely, R. A. (2014b). Dissolution dominating calcification process in polar pteropods close to the point of aragonite undersaturation. *PLoS One* 9:e109183. doi: 10.1371/journal.pone.0109183

Bednaršek, N., Tarling, G. A., Bakker, D. C. E., Fielding, S., Cohen, A., Kuzirian, A., et al. (2012a). Description and quantification of pteropod shell dissolution: a sensitive bioindicator of ocean acidification. *Glob. Change Biol.* 18, 2378–2388. doi: 10.1111/j.1365-2486.2012.02668.x

Bednaršek, N., Tarling, G. A., Bakker, D. C. E., Fielding, S., Jones, E. M., Venables, H. J., et al. (2012b). Extensive dissolution of live pteropods in the Southern Ocean. *Nat. Geosci.* 5, 881–885. doi: 10.1007/s00227-017-3261-3

Beers, J. M., and Jayasundara, N. (2015). Antarctic notothenioid fish: what are the future consequences of 'losses' and 'gains' acquired during long-term evolution at cold and stable temperatures? *J. Exp. Biol.* 218, 1834–1845. doi: 10.1242/jeb.116129

Beldade, P., Mateus, A. R., and Keller, R. A. (2011). Evolution and molecular mechanisms of adaptive developmental plasticity. *Mol. Ecol.* 20, 1347–1363. doi: 10.1111/j.1365-294X.2011.05016.x

Bernard, K. S., and Froneman, P. W. (2009). The sub-Antarctic euthecosome pteropod, *Limacina retroversa*: distribution patterns and trophic role. *Deep Sea Res. Part I Oceanogr. Res. Pap.* 56, 582–598. doi: 10.1016/j.dsr.2008.11.007

Bolger, A. M., Lohse, M., and Usadel, B. (2014). Trimmomatic: a flexible trimmer for Illumina sequence data. *Bioinformatics* 30, 2114–2120. doi: 10.1093/bioinformatics/btu170

Bossdorf, O., Arcuri, D., Richards, C. L., and Pigliucci, M. (2010). Experimental alteration of DNA methylation affects the phenotypic plasticity of ecologically relevant traits in *Arabidopsis thaliana*. *Evol. Ecol.* 24, 541–553. doi: 10.1007/s10682-010-9372-7

Boysen-Ennen, E., Hagen, W., Hubold, G., and Piatowski, U. (1991). Zooplankton biomass in the ice-covered Weddell Sea, Antarctica. *Mar. Biol.* 111, 227–235. doi: 10.1007/bf01319704

Calosi, P., Bilton, D. T., and Spicer, J. I. (2008). Thermal tolerance, acclimatory capacity and vulnerability to global climate change. *Biol. Lett.* 4, 99–102. doi: 10.1098/rsbl.2007.0408

Chan, F., Barth, J. A., Blanchette, C. A., Byrne, R. H., Chavez, F., Cheriton, O., et al. (2017). Persistent spatial structuring of coastal ocean acidification in the California Current System. *Sci. Rep.* 7:2526. doi: 10.1038/s41598-017-02777-y

Chen, Y., Lun, A. T., and Smyth, G. K. (2016). From reads to genes to pathways: differential expression analysis of RNA-Seq experiments using Rsubread and the edgeR quasi-likelihood pipeline. *F1000Res.* 5:1438. doi: 10.12688/f1000research.8987.2

Chevin, L. M., Lande, R., and Mace, G. M. (2010). Adaptation, plasticity, and extinction in a changing environment: towards a predictive theory. *PLoS Biol.* 8:e1000357. doi: 10.1371/journal.pbio.1000357

Chown, S. L., Slabber, S., McGeouch, M., Janion, C., and Leinaas, H. P. (2007). Phenotypic plasticity mediates climate change responses among invasive and indigenous arthropods. *Proc. R. Soc. B Biol. Sci.* 274, 2531–2537. doi: 10.1098/rspb.2007.0772

Clark, M. S., Thorne, M. A. S., King, M., Hipperson, H., Hoffman, J. I., Peck, L. S., et al. (2018). Life in the intertidal: cellular responses, methylation and epigenetics. *Funct. Ecol.* 32, 1982–1994. doi: 10.1111/1365-2435.13077

Davis, B. E., Flynn, E. E., Miller, N. A., Nelson, F. A., Fangue, N. A., and Todgham, A. E. (2018). Antarctic emerald rockcod have the capacity to compensate for warming when uncoupled from CO_2-acidification. *Glob. Change Biol.* 24, e655–e670. doi: 10.1111/gcb.13987

De Wit, P., Durland, E., Ventura, A., and Langdon, C. J. (2018). Gene expression correlated with delay in shell formation in larval Pacific oysters (*Crassostrea gigas*) exposed to experimental ocean acidification provides insights into shell formation mechanisms. *BMC Genomics* 19:160. doi: 10.1186/s12864-018-4519-y

Diaz-Freije, E., Gestal, C., Castellanos-Martinez, S., and Moran, P. (2014). The role of DNA methylation on *Octopus vulgaris* development and their perspectives. *Front. Physiol.* 5:62. doi: 10.3389/fphys.2014.00062

Dimond, J. L., and Roberts, S. B. (2016). Germline DNA methylation in reef corals: patterns and potential roles in response to environmental change. *Mol. Ecol.* 25, 1895–1904. doi: 10.1111/mec.13414

Dineshram, R., Wong, K. K. W., Xiao, S., Yu, Z., Qian, P. Y., and Thiyagarajan, V. (2012). Analysis of Pacific oyster larval proteome and its response to high-CO_2. *Mar. Pollut. Bull.* 64, 2160–2167. doi: 10.1016/j.marpolbul.2012.07.043

Dixon, G., Bay, L. K., and Matz, M. V. (2014). Bimodal signatures of germline methylation are linked with gene expression plasticity in the coral *Acropora millepora*. *BMC Genomics* 15:1109. doi: 10.1186/1471-2164-15-1109

Dixon, G., Liao, Y., Bay, L. K., and Matz, M. V. (2018). Role of gene body methylation in acclimatization and adaptation in a basal metazoan. *Proc. Natl. Acad. Sci. U.S.A.* 115, 13342–13346. doi: 10.1073/pnas.1813749115

Donelson, J. M., Salinas, S., Munday, P. L., and Shama, L. N. S. (2018). Transgenerational plasticity and climate change experiments: where do we go from here? *Glob. Change Biol.* 24, 13–34. doi: 10.1111/gcb.13903

Duarte, B., Martins, I., Rosa, R., Matos, A. R., Roleda, M. Y., Reusch, T. B. H., et al. (2018). Climate change impacts on seagrass meadows and macroalgal forests: an integrative perspective on acclimation and adaptation potential. *Front. Mar. Sci.* 5:190. doi: 10.3389/fmars.2018.00190

Eirin-Lopez, J. M., and Putnam, H. M. (2019). Marine environmental epigenetics. *Annu. Rev. Mar. Sci.* 11, 335–368. doi: 10.1146/annurev-marine-010318-095114

Enzor, L. A., Hunter, E. M., and Place, S. P. (2017). The effects of elevated temperature and ocean acidification on the metabolic pathways of notothenioid fish. *Conserv. Physiol.* 5:cox019. doi: 10.1093/conphys/cox019

Enzor, L. A., and Place, S. P. (2014). Is warmer better? Decreased oxidative damage in notothenioid fish after long-term acclimation to multiple stressors. *J. Exp. Biol.* 217, 3301–3310. doi: 10.1242/jeb.108431

Fellous, A., Favrel, P., and Riviere, G. (2015). Temperature influences histone methylation and mRNA expression of the Jmj-C histone-demethylase orthologues during the early development of the oyster *Crassostrea gigas*. *Mar. Genomics* 19, 23–30. doi: 10.1016/j.margen.2014.09.002

Fellous, A., Lefranc, L., Jouaux, A., Goux, D., Favrel, P., and Riviere, G. (2019). Histone methylation participates in gene expression control during the early development of the Pacific oyster *Crassostrea gigas*. *Genes* 10:E695. doi: 10.3390/genes10090695

Foster, B. A., Cargill, J. M., and Montgomery, J. C. (1987). Planktivory in *Pagothenia borchgrevinki* (Pisces: Nototheniidae) in McMurdo Sound, Antarctica. *Polar Biol.* 8, 49–54. doi: 10.1007/bf00297164

Garcia-Fernandez, P., Garcia-Souto, D., Almansa, E., Moran, P., and Gestal, C. (2017). Epigenetic DNA methylation mediating *Octopus vulgaris* early development: effect of essential fatty acids enriched diet. *Front. Physiol.* 8:292. doi: 10.3389/fphys.2017.00292

Gardner, J., Manno, C., Bakker, D. C. E., Peck, V. L., and Tarling, G. A. (2018). Southern Ocean pteropods at risk from ocean warming and acidification. *Mar. Biol.* 165:8. doi: 10.1007/s00227-017-3261-3

Gavery, M. R., and Roberts, S. B. (2013). Predominant intragenic methylation is associated with gene expression characteristics in a bivalve mollusc. *PeerJ* 1:e215. doi: 10.7717/peerj.215

Gavery, M. R., and Roberts, S. B. (2014). A context dependent role for DNA methylation in bivalves. *Brief. Funct. Genomics* 13, 217–222. doi: 10.1093/bfgp/elt054

Gibson, J. A. E., and Trull, T. W. (1999). Annual cycle of fCO2 under sea-ice and in open water in Prydz Bay, East Antarctica. *Mar. Chem.* 66, 187–200. doi: 10.1016/s0304-4203(99)00040-7

Gonzalez-Romero, R., Suarez-Ulloa, V., Rodriguez-Casariego, J., Garcia-Souto, D., Diaz, G., Smith, A., et al. (2017). Effects of Florida Red Tides on histone variant expression and DNA methylation in the Eastern oyster *Crassostrea virginica*. *Aquat. Toxicol.* 186, 196–204. doi: 10.1016/j.aquatox.2017.03.006

Hahn, M. A., Wu, X., Li, A. X., Hahn, T., and Pfeifer, G. P. (2011). Relationship between gene body DNA methylation and intragenic H3K9me3 and H3K36me3 chromatin marks. *PLoS One* 6:e18844. doi: 10.1371/journal.pone.0018844

Harris, K. E., DeGrandpre, M. D., and Hales, B. (2013). Aragonite saturation state dynamics in a coastal upwelling zone. *Geophys. Res. Lett.* 40, 2720–2725. doi: 10.1002/grl.50460

Hauri, C., Friedrich, T., and Timmermann, A. (2015). Abrupt onset and prolongation of aragonite undersaturation events in the Southern Ocean. *Nat. Clim. Change* 6, 172–176. doi: 10.1038/nclimate2844

Hawkins, S. J., Evans, A. J., Dale, A. C., Firth, L. B., and Smith, I. P. (2018). Antarctic marine biodiversity: adaptations, environments and responses to change. *Oceanogr. Mar. Biol.* 56, 105–236. doi: 10.1201/9780429454455-3

Hennige, S. J., Smith, D. J., Walsh, S.-J., McGinley, M. P., Warner, M. E., and Suggett, D. J. (2010). Acclimation and adaptation of scleractinian coral communities along environmental gradients within an Indonesian reef system. *J. Exp. Mar. Biol. Ecol.* 391, 143–152. doi: 10.1016/j.jembe.2010.06.019

Ho, J., Tumkaya, T., Aryal, S., Choi, H., and Claridge-Chang, A. (2019). Moving beyond P values: data analysis with estimation graphics. *Nat. Methods* 16, 565–566. doi: 10.1038/s41592-019-0470-3

Hoegh-Guldberg, O., and Bruno, J. F. (2010). The impact of climate change on the world's marine ecosystems. *Science* 328, 1523–1528. doi: 10.1126/science.1189930

Hofmann, G. E. (2017). Ecological epigenetics in marine metazoans. *Front. Mar. Sci.* 4:4. doi: 10.3389/fmars.2017.00004

Hoshijima, U., Wong, J. M., and Hofmann, G. E. (2017). Additive effects of pCO_2 and temperature on respiration rates of the Antarctic pteropod *Limacina helicina antarctica*. *Conserv. Physiol.* 5:cox064. doi: 10.1093/conphys/cox064

Hunt, B., Strugnell, J., Bednarsek, N., Linse, K., Nelson, R. J., Pakhomov, E., et al. (2010). Poles apart: the "bipolar" pteropod species *Limacina helicina* is genetically distinct between the Arctic and Antarctic oceans. *PLoS One* 5:e9835. doi: 10.1371/journal.pone.0009835

Hunt, B. P. V., Pakhomov, E. A., Hosie, G. W., Siegel, V., Ward, P., and Bernard, K. (2008). Pteropods in Southern Ocean ecosystems. *Prog. Oceanogr.* 78, 193–221. doi: 10.1016/j.pocean.2008.06.001

Huth, T. J., and Place, S. P. (2016a). RNA-seq reveals a diminished acclimation response to the combined effects of ocean acidification and elevated seawater temperature in *Pagothenia borchgrevinki*. *Mar. Genomics* 28, 87–97. doi: 10.1016/j.margen.2016.02.004

Huth, T. J., and Place, S. P. (2016b). Transcriptome wide analyses reveal a sustained cellular stress response in the gill tissue of *Trematomus bernacchii* after acclimation to multiple stressors. *BMC Genomics* 17:127. doi: 10.1186/s12864-016-2454-3

IPCC (2013). *Climate Change 2013: the Physical Science Basis. Contribution of Working Group I to the Fifth Assessment Report of the Intergovernmental Panel on Climate Change*, eds T. F. Stocker, D. Qin, G. K. Plattner, M. Tignor, S. K. Allen, J. Boschung, et al. (Cambridge: Cambridge University Press).

IPCC (2019). *IPCC Special Report on the Ocean and Cryosphere in a Changing Climate*, eds H. O. Pörtner, D. C. Roberts, V. Masson-Delmotte, P. Zhai, M. Tignor, E. Poloczanska, et al. (Geneva: IPCC).

Jeong, H., Wu, X., Smith, B., and Yi, S. V. (2018). Genomic landscape of methylation islands in hymenopteran insects. *Genome Biol. Evol.* 10, 2766–2776. doi: 10.1093/gbe/evy203

Johnson, K. M., and Hofmann, G. E. (2016). A transcriptome resource for the Antarctic pteropod *Limacina helicina antarctica*. *Mar. Genomics* 28, 25–28. doi: 10.1016/j.margen.2016.04.002

Johnson, K. M., and Hofmann, G. E. (2017). Transcriptomic response of the Antarctic pteropod *Limacina helicina antarctica* to ocean acidification. *BMC Genomics* 18:812. doi: 10.1186/s12864-017-4161-0

Kapsenberg, L., Kelley, A. L., Shaw, E. C., Martz, T. R., and Hofmann, G. E. (2015). Near-shore Antarctic pH variability has implications for the design of ocean acidification experiments. *Sci. Rep.* 5:9638.

Kelly, M. (2019). Adaptation to climate change through genetic accommodation and assimilation of plastic phenotypes. *Philos. Trans. R. Soc. Lond. B Biol. Sci.* 374:20180176. doi: 10.1098/rstb.2018.0176

Kenkel, C. D., Moya, A., Strahl, J., Humphrey, C., and Bay, L. K. (2017). Functional genomic analysis of corals from natural CO_2-seeps reveals core molecular responses involved in acclimatization to ocean acidification. *Glob. Change Biol.* 24, 158–171. doi: 10.1111/gcb.13833

Kobayashi, H., Sakurai, T., Imai, M., Takahashi, N., Fukuda, A., Yayoi, O., et al. (2012). Contribution of intragenic DNA methylation in mouse gametic DNA methylomes to establish oocyte-specific heritable marks. *PLoS Genet.* 8:e1002440. doi: 10.1371/journal.pgen.1002440

Koh, H. Y., Lee, J. H., Han, S. J., Park, H., Shin, S. C., and Lee, S. G. (2015). A transcriptomic analysis of the response of the arctic pteropod *Limacina helicina* to carbon dioxide-driven seawater acidification. *Polar Biol.* 38, 1727–1740. doi: 10.1007/s00300-015-1738-4

Kriefall, N. G., Pechenik, J. A., Pires, A., and Davies, S. W. (2018). Resilience of Atlantic slippersnail *Crepidula fornicata* larvae in the face of severe coastal acidification. *Front. Mar. Sci.* 5:312. doi: 10.3389/fmars.2018.00312

Li, B., and Dewey, C. N. (2011). RSEM: accurate transcript quantification from RNA-Seq data with or without a reference genome. *BMC Bioinformatics* 12:323. doi: 10.1186/1471-2105-12-323

Li, S., Papale, L. A., Zhang, Q., Madrid, A., Chen, L., Chopra, P., et al. (2016). Genome-wide alterations in hippocampal 5-hydroxymethylcytosine links plasticity genes to acute stress. *Neurobiol. Dis.* 86, 99–108. doi: 10.1016/j.nbd.2015.11.010

Li, Y., Liew, Y. J., Cui, G., Cziesielski, M. J., Zahran, N., Michell, C. T., et al. (2018). DNA methylation regulates transcriptional homeostasis of algal endosymbiosis in the coral model *Aiptasia*. *Sci. Adv.* 4:eaat2142. doi: 10.1126/sciadv.aat2142

Lian, S., He, Y., Li, X., Zhao, B., Hou, R., Hu, X., et al. (2015). Changes in global DNA methylation intensity and DNMT1 transcription during the aging process of scallop *Chlamys farreri*. *J. Ocean Univ. China* 14, 685–690. doi: 10.1007/s11802-015-2507-2

Liew, Y. J., Didier, Z., Li, Y., Tamubtté, E., Venn, A. A., Michell, C. T., et al. (2018). Epigenome-associated phenotypic acclimatization to ocean acidification in a reef-building coral. *Sci. Adv.* 4:eaar8028. doi: 10.1126/sciadv.aar8028

Luttmer, R., Spijkerman, A. M., Kok, R. M., Jakobs, C., Blom, H. J., Serne, E. H., et al. (2013). Metabolic syndrome components are associated with DNA

hypomethylation. *Obes. Res. Clin. Pract.* 7, 106–115. doi: 10.1016/j.orcp.2012.06.001

Maas, A. E., Lawson, G. L., Bergan, A. J., and Tarrant, A. M. (2018). Exposure to CO_2 influences metabolism, calcification and gene expression of the thecosome pteropod *Limacina retroversa*. *J. Exp. Biol.* 221:jeb164400. doi: 10.1242/jeb.164400

Maas, A. E., Lawson, G. L., and Tarrant, A. M. (2015). Transcriptome-wide analysis of the response of the thecosome pteropod *Clio pyramidata* to short-term CO_2 exposure. *Comp. Biochem. Physiol. Part D Genomics Proteomics* 16, 1–9. doi: 10.1016/j.cbd.2015.06.002

Manno, C., Bednaršek, N., Tarling, G. A., Peck, V. L., Comeau, S., Adhikari, D., et al. (2017). Shelled pteropods in peril: assessing vulnerability in a high CO_2 ocean. *Earth Sci. Rev.* 169, 132–145. doi: 10.1016/j.earscirev.2017.04.005

Marsh, A. G., and Pasqualone, A. A. (2014). DNA methylation and temperature stress in an Antarctic polychaete, *Spiophanes tcherniai*. *Front. Physiol.* 5:173. doi: 10.3389/fphys.2014.00173

McNeil, B. I., and Matear, R. J. (2008). Southern Ocean acidification: a tipping point at 450-ppm atmospheric CO_2. *Proc. Natl. Acad. Sci. U.S.A.* 105, 18860–18864. doi: 10.1073/pnas.0806318105

McNeil, B. I., Tagliabue, A., and Sweeney, C. (2010). A multi-decadal delay in the onset of corrosive 'acidified' waters in the Ross Sea of Antarctica due to strong air-sea CO_2 disequilibrium. *Geophys. Res. Lett.* 37:L19607.

Melzner, F., Mark, F. C., Seibel, B. A., and Tomanek, L. (2020). Ocean acidification and coastal marine invertebrates: tracking CO_2 effects from seawater to the cell. *Annu. Rev. Mar. Sci.* 12, 1–25.

Morley, S. A., Berman, J., Barnes, D. K. A., de Juan Carbonell, C., Downey, R. V., and Peck, L. S. (2016). Extreme phenotypic plasticity in metabolic physiology of Antarctic demosponges. *Front. Ecol. Evol.* 3:157. doi: 10.3389/fevo.2015.00157

Moya, A., Howes, E. L., Lacoue-Labarthe, T., Foret, S., Hanna, B., Medina, M., et al. (2016). Near-future pH conditions severely impact calcification, metabolism and the nervous system in the pteropod *Heliconoides inflatus*. *Glob. Change Biol.* 22, 3888–3900. doi: 10.1111/gcb.13350

Nanty, L., Carbajosa, G., Heap, G. A., Ratnieks, F., van Heel, D. A., Down, T. A., et al. (2011). Comparative methylomics reveals gene-body H3K36me3 in *Drosophila* predicts DNA methylation and CpG landscapes in other invertebrates. *Genome Res.* 21, 1841–1850. doi: 10.1101/gr.121640.111

Negrete-García, G., Lovenduski, N. S., Hauri, C., Krumhardt, K. M., and Lauvset, S. K. (2019). Sudden emergence of a shallow aragonite saturation horizon in the Southern Ocean. *Nat. Clim. Change* 9, 313–317. doi: 10.1038/s41558-019-0418-8

Neri, F., Rapelli, S., Krepelova, A., Incarnato, D., Parlato, C., Basile, G., et al. (2017). Intragenic DNA methylation prevents spurious transcription initiation. *Nature* 543, 72–77. doi: 10.1038/nature21373

Nicotra, A. B., Atkin, O. K., Bonser, S. P., Davidson, A. M., Finnegan, E. J., Mathesius, U., et al. (2010). Plant phenotypic plasticity in a changing climate. *Trends Plant Sci.* 15, 684–692. doi: 10.1016/j.tplants.2010.09.008

O'Donnell, M. J., Todgham, A. E., Sewell, M. A., Hammond, L. M., Ruggiero, K., Fangue, N. A., et al. (2010). Ocean acidification alters skeletogenesis and gene expression in larval sea urchins. *Mar. Ecol. Prog. Ser.* 398, 157–171. doi: 10.3354/meps08346

Oliver, E. C. J., Donat, M. G., Burrows, M. T., Moore, P. J., Smale, D. A., Alexander, L. V., et al. (2018). Longer and more frequent marine heatwaves over the past century. *Nat. Commun.* 9:1324. doi: 10.1038/s41467-018-03732-9

Olson, C. E., and Roberts, S. B. (2014). Genome-wide profiling of DNA methylation and gene expression in *Crassostrea gigas* male gametes. *Front. Physiol.* 5:224. doi: 10.3389/fphys.2014.00224

Pacis, A., Mailhot-Leonard, F., Tailleux, L., Randolph, H. E., Yotova, V., Dumaine, A., et al. (2019). Gene activation precedes DNA demethylation in response to infection in human dendritic cells. *Proc. Natl. Acad. Sci. U.S.A.* 116, 6938–6943. doi: 10.1073/pnas.1814700116

Paradis, E., Claude, J., and Strimmer, K. (2004). APE: analyses of phylogenetics and evolution in R language. *Bioinformatics* 20, 289–290. doi: 10.1093/bioinformatics/btg412

Pavet, V., Quintero, C., Cecchini, N. M., Rosa, A. L., and Alvarez, M. E. (2006). *Arabidopsis* displays centromeric DNA hypomethylation and cytological alterations of heterochromatin upon attack by *Pseudomonas syringae*. *Phytopathology* 19, 577–587. doi: 10.1094/mpmi-19-0577

Peck, L. S., Morley, S. A., and Clark, M. S. (2010). Poor acclimation capacities in Antarctic marine ectotherms. *Mar. Biol.* 157, 2051–2059. doi: 10.1007/s00227-010-1473-x

Peck, L. S., Morley, S. A., Richard, J., and Clark, M. S. (2014). Acclimation and thermal tolerance in Antarctic marine ectotherms. *J. Exp. Biol.* 217, 16–22. doi: 10.1242/jeb.089946

Peck, L. S., Webb, K. E., and Bailey, D. M. (2004). Extreme sensitivity of biological function to temperature in Antarctic marine species. *Funct. Ecol.* 18, 625–630. doi: 10.1111/j.0269-8463.2004.00903.x

Pogribny, I. P., Ross, S. A., Wise, C., Pogribna, M., Jones, E. A., Tryndyak, V. P., et al. (2006). Irreversible global DNA hypomethylation as a key step in hepatocarcinogenesis induced by dietary methyl deficiency. *Mutat. Res.* 593, 80–87. doi: 10.1016/j.mrfmmm.2005.06.028

Putnam, H. M., Davidson, J. M., and Gates, R. D. (2016). Ocean acidification influences host DNA methylation and phenotypic plasticity in environmentally susceptible corals. *Evol. Appl.* 9, 1165–1178. doi: 10.1111/eva.12408

Reed, A. J., and Thatje, S. (2015). Long-term acclimation and potential scope for thermal resilience in Southern Ocean bivalves. *Mar. Biol.* 162, 2217–2224. doi: 10.1007/s00227-015-2752-3

Riviere, G., He, Y., Tecchio, S., Crowell, E., Gras, M., Sourdaine, P., et al. (2017). Dynamics of DNA methylomes underlie oyster development. *PLoS Genet.* 13:e1006807. doi: 10.1371/journal.pgen.1006807

Riviere, G., Wu, G. C., Fellous, A., Goux, D., Sourdaine, P., and Favrel, P. (2013). DNA methylation is crucial for the early development in the oyster *C. gigas*. *Mar. Biotechnol.* 15, 739–753. doi: 10.1007/s10126-013-9523-2

Robinson, M. D., McCarthy, D. J., and Smyth, G. K. (2010). edgeR: a Bioconductor package for differential expression analysis of digital gene expression data. *Bioinformatics* 26, 139–140. doi: 10.1093/bioinformatics/btp616

Robinson, N. A., Johnsen, H., Moghadam, H., Andersen, O., and Tveiten, H. (2019). Early developmental stress affects subsequent gene expression response to an acute stress in Atlantic salmon: an approach for creating robust fish for aquaculture? *G3* 9, 1597–1611. doi: 10.1534/g3.119.400152

Rodrigues, G. M. Jr., Toffoli, L. V., Manfredo, M. H., Francis-Oliveira, J., Silva, A. S., Raquel, H. A., et al. (2015). Acute stress affects the global DNA methylation profile in rat brain: modulation by physical exercise. *Behav. Brain Res.* 279, 123–128. doi: 10.1016/j.bbr.2014.11.023

Rodriguez-Casariego, J. A., Ladd, M. C., Shantz, A. A., Lopes, C., Cheema, M. S., Kim, B., et al. (2018). Coral epigenetic responses to nutrient stress: histone H2A.X phosphorylation dynamics and DNA methylation in the staghorn coral *Acropora cervicornis*. *Ecol. Evol.* 8, 12193–12207. doi: 10.1002/ece3.4678

Rondon, R., Grunau, C., Fallet, M., Charlemagne, N., Sussarellu, R., Chaparro, C., et al. (2017). Effects of a parental exposure to diuron on Pacific oyster spat methylome. *Environ. Epigenet.* 3:dvx004. doi: 10.1093/eep/dvx004

Rusiecki, J. A., Baccarelli, A., Bollati, V., Tarantini, L., Moore, L. E., and Bonefeld-Jorgensen, E. C. (2008). Global DNA hypomethylation is associated with high serum-persistent organic pollutants in Greenlandic Inuit. *Environ. Health Perspect.* 116, 1547–1552. doi: 10.1289/ehp.11338

Sarda, S., Zeng, J., Hunt, B. G., and Yi, S. V. (2012). The evolution of invertebrate gene body methylation. *Mol. Biol. Evol.* 29, 1907–1916. doi: 10.1093/molbev/mss062

Schubeler, D. (2015). Function and information content of DNA methylation. *Nature* 517, 321–326. doi: 10.1038/nature14192

Secco, D., Wang, C., Shou, H., Schultz, M. D., Chiarenza, S., Nussaume, L., et al. (2015). Stress induced gene expression drives transient DNA methylation changes at adjacent repetitive elements. *eLife* 4:e09343. doi: 10.7554/eLife.09343

Seebacher, F., Davison, W., Lowe, C. J., and Franklin, C. E. (2005). A falsification of the thermal specialization paradigm: compensation for elevated temperatures in Antarctic fishes. *Biol. Lett.* 1, 151–154. doi: 10.1098/rsbl.2004.0280

Seibel, B. A., Maas, A. E., and Dierssen, H. M. (2012). Energetic plasticity underlies a variable response to ocean acidification in the pteropod, *Limacina helicina antarctica*. *PLoS One* 7:e30464. doi: 10.1371/journal.pone.0030464

Steinberg, D. K., Ruck, K. E., Gleiber, M. R., Garzio, L. M., Cope, J. S., Bernard, K. S., et al. (2015). Long-term (1993–2013) changes in macrozooplankton off the Western Antarctic Peninsula. *Deep Sea Res. Part I Oceanogr. Res. Pap.* 101, 54–70. doi: 10.1016/j.dsr.2015.02.009

Stewart, C. A., Welch, V., Plale, B., Fox, G., Pierce, M., and Sterling, T. (2017). *Indiana University Pervasive Technology Institute*. Bloomington: Indiana University.

Strader, M. E., Wong, J. M., Kozal, L. C., Leach, T. S., and Hofmann, G. E. (2019). Parental environments alter DNA methylation in offspring of the purple sea urchin, *Strongylocentrotus purpuratus*. *J. Exp. Mar. Biol. Ecol.* 517, 54–64. doi: 10.1016/j.jembe.2019.03.002

Suarez-Ulloa, V., Rivera-Casas, C., and Michel, M. (2019). Seasonal DNA methylation variation in the flat tree oyster *Isognomon alatus* from a mangrove ecosystem in North Biscayne Bay, Florida. *J. Shellfish Res.* 38, 79–88.

Taylor, D. L., Jackson, A. U., Narisu, N., Hemani, G., Erdos, M. R., Chines, P. S., et al. (2019). Integrative analysis of gene expression, DNA methylation, physiological traits, and genetic variation in human skeletal muscle. *Proc. Natl. Acad. Sci. U.S.A.* 116, 10883–10888. doi: 10.1073/pnas.1814263116

Thibodeau, P. S., Steinberg, D. K., Stammerjohn, S. E., and Hauri, C. (2019). Environmental controls on pteropod biogeography along the Western Antarctic Peninsula. *Limnol. Oceanogr.* 64, S240–S256.

Todgham, A. E., and Hofmann, G. E. (2009). Transcriptomic response of sea urchin larvae *Strongylocentrotus purpuratus* to CO_2-driven seawater acidification. *J. Exp. Biol.* 212, 2579–2594. doi: 10.1242/jeb.032540

True, H. L., Berlin, I., and Lindquist, S. L. (2004). Epigenetic regulation of translation reveals hidden genetic variation to produce complex traits. *Nature* 431, 184–187. doi: 10.1038/nature02885

Wang, X., Li, Q., Lian, J., Li, L., Jin, L., Cai, H., et al. (2014). Genome-wide and single-base resolution DNA methylomes of the Pacific oyster *Crassostrea gigas* provide insight into the evolution of invertebrate CpG methylation. *BMC Genomics* 15:1119. doi: 10.1186/1471-2164-15-1119

Wheeler, R., and Torchiano, M. (2016). *Permutation Tests for Linear Models*. London: Comprehensive R Archive Network.

Wong, J. M., Kozal, L. C., Leach, T. S., Hoshijima, U., and Hofmann, G. E. (2019). Transgenerational effects in an ecological context: conditioning of adult sea urchins to upwelling conditions alters maternal provisioning and progeny phenotype. *J. Exp. Mar. Biol. Ecol.* 517, 65–77. doi: 10.1016/j.jembe.2019.04.006

Worden, A. (2009). *DNA Extraction - CTAB Method*. Moss Landing, CA: Monterey Bay Aquarium Research Institute.

Wright, R. M., Aglyamova, G. V., Meyer, E., and Matz, M. V. (2015). Gene expression associated with white syndromes in a reef building coral, *Acropora hyacinthus*. *BMC Genomics* 16:371. doi: 10.1186/s12864-015-1540-2

Xiu, Y., Shao, C., Zhu, Y., Li, Y., Gan, T., Xu, W., et al. (2019). Differences in DNA methylation between disease-resistant and disease-susceptible Chinese tongue sole (*Cynoglossus semilaevis*) families. *Front. Genet.* 10:847. doi: 10.3389/fgene.2019.00847

Zemach, A., McDaniel, I. E., Silva, P., and Zilberman, D. (2010). Genome-wide evolutionary analysis of eukaryotic DNA methylation. *Science* 328, 916–919. doi: 10.1126/science.1186366

Zhang, H., Lang, Z., and Zhu, J. K. (2018). Dynamics and function of DNA methylation in plants. *Nat. Rev. Mol. Cell Biol.* 19, 489–506. doi: 10.1038/s41580-018-0016-z

Zhang, Y. Y., Fischer, M., Colot, V., and Bossdorf, O. (2013). Epigenetic variation creates potential for evolution of plant phenotypic plasticity. *New Phytol.* 197, 314–322. doi: 10.1111/nph.12010

Zhao, Q., Rank, G., Tan, Y. T., Li, H., Moritz, R. L., Simpson, R. J., et al. (2009). PRMT5-mediated methylation of histone H4R3 recruits DNMT3A, coupling histone and DNA methylation in gene silencing. *Nat. Struct. Mol. Biol.* 16, 304–311. doi: 10.1038/nsmb.1568

Conflict of Interest: The authors declare that the research was conducted in the absence of any commercial or financial relationships that could be construed as a potential conflict of interest.

frontiers in Marine Science

ORIGINAL RESEARCH
published: 31 March 2020
doi: 10.3389/fmars.2020.00189

Probing the Diversity of Polycomb and Trithorax Proteins in Cultured and Environmentally Sampled Microalgae

Xue Zhao[1,2], Anne Flore Deton Cabanillas[3], Alaguraj Veluchamy[4], Chris Bowler[3], Fabio Rocha Jimenez Vieira[3] and Leila Tirichine[1]**

[1] Department of Biology, Université de Nantes, CNRS, UFIP, UMR 6286, Nantes, France, [2] Université Paris-Saclay, CNRS, INRAE, Univ Evry, Institute of Plant Sciences Paris-Saclay (IPS2), Orsay, France, [3] Institut de Biologie de l'Ecolenormale Supérieure (IBENS), Ecole Normale Supérieure, CNRS, INSERM, PSL Université Paris, Paris, France, [4] Biological and Environmental Science and Engineering Division, Laboratory of Chromatin Biochemistry, King Abdullah University of Science and Technology, Thuwal, Saudi Arabia

OPEN ACCESS

Edited by:
Jose M. Eirin-Lopez, Florida International University, United States

Reviewed by:
Daniel Garcia-Souto, University of Vigo, Spain
Chiara Lanzuolo, Institute of Cell Biology and Neurobiology (CNR), Italy

***Correspondence:**
Fabio Rocha Jimenez Vieira
rocha@biologie.ens.fr; fabiorjvieira@gmail.com
Leila Tirichine
tirichine-l@univ-nantes.fr; Leila.Tirichine@univ-nantes.fr

Specialty section:
This article was submitted to Marine Environmental Epigenetics, a section of the journal Frontiers in Marine Science

Received: 09 December 2019
Accepted: 11 March 2020
Published: 31 March 2020

Citation:
Zhao X, Deton Cabanillas AF, Veluchamy A, Bowler C, Vieira FRJ and Tirichine L (2020) Probing the Diversity of Polycomb and Trithorax Proteins in Cultured and Environmentally Sampled Microalgae. Front. Mar. Sci. 7:189. doi: 10.3389/fmars.2020.00189

Polycomb (PcG) and Trithorax (TrxG) complexes are two evolutionarily conserved epigenetic regulatory components that act antagonistically to regulate the expression of genes involved in cell differentiation and development in multicellular organisms. The absence of PcG in both yeast models *Saccharomyces cerevisiae* and *Schizosaccharomyces pombe* suggested that polycomb proteins might have evolved together with the emergence of multicellular organisms. However, high throughput sequencing of several microalgal genomes and transcriptomes reveals an unprecedented abundance and diversity of genes encoding the components of these complexes. We report here the diversity of genes encoding PcG and TrxG proteins in microalgae from the Marine Microbial Eukaryote Transcriptome Sequencing Project database (MMETSP) and detected at broad scale in *Tara* Oceans genomics datasets using a highly sensitive method called eDAF (enhanced Domain Architecture Filtering). Further, we explored the correlation between environmental factors measured during the *Tara* Oceans expedition and transcript levels of PcG and TrxG components. PcG and TrxG are responsible for the deposition of a number of histone marks among which a TrxG associated mark, H3K4me3 which we profiled genome wide in the model diatom *Phaeodactylum tricornutum* to understand its role in microalgae and revisited the previously published histone code and co-occurrence with other histone marks including the antagonizing Polycomb deposited mark H3K27me3.

Keywords: epigenetics, environment, microalgae, diatoms, bioinformatics, *Phaeodactylum tricornutum*, polycomb, trithorax

INTRODUCTION

Polycomb (PcG) and trithorax (TrxG) protein complexes were initially isolated in *Drosophila* as factors responsible for the maintenance of expression of *HOX* genes, important determinants of body patterning (Schuettengruber et al., 2007). Several decades of research has revealed that these two complexes are involved in a plethora of biological processes including X chromosome

inactivation, genomic imprinting, cell cycle control, stem cell biology, and cancer (Schuettengruber et al., 2017). PcG and TrxG complexes have been shown to act antagonistically to modify chromatin via histone-modifying or chromatin-remodeling activities that repress or activate their target genes, respectively (Geisler and Paro, 2015). Both complexes are highly conserved among eukaryotes and their recent discovery in single celled species raises important questions about their function and role in unicellular organisms and in the evolution of multicellularity. Of note, PcG complexes are not found in two widely studied yeast species *Saccharomyces cerevisiae* and *Schizosaccharomyces pombe* and their recent discovery and conservation in several unicellular microalgae points to their ancient origin and importance (Shaver et al., 2010).

In animals and plants, polycomb proteins form at least two distinct complexes, PRC1 and PRC2. In mammals, PRC1 regulates gene expression through controlling chromatin compaction and catalyzing mono-ubiquitylation of histone H2A, whereas PRC2 is responsible for chromatin structure and methylation of lysine 27 of histone H3 (H3K27) (Gil and O'Loghlen, 2014). PRC1 contains four core subunits: polycomb (Pc), posterior sex combs (Psc), polyhomeotic (Ph; absent in plants), sex combs extra (Sce) or dRING (Barrero and Izpisua Belmonte, 2013). The PRC2 complex comprises four core components: a histone methyltransferase, enhancer of zeste E(z), a WD40 domain protein, extra sex combs (ESC), a zinc finger protein, suppressor of zeste 12 (Su(z)12), and another WD40 domain protein, Nurf-55 (Margueron and Reinberg, 2011).

TrxG complex has been classified into three groups based on the function of its members (1) SET domain containing proteins which methylate histones including COMPASS and COMPASS-like involved in the methylation of Lysine 4 of histone H3 for general gene activation as well as methylation of specific genes and methylation of H3K36me3 (2) ATP dependent chromatin remodeling factors with few proteins that can read the histone methylation marks deposited by the SET domain proteins, and (3) TrxG proteins known to bind directly to specific DNA sequences. Our focus here is on the first group of TrxG complex proteins considering their role in antagonizing PcG mediated repression.

Both complexes have been studied intensively in multicellular species but only scarcely investigated in unicellular organisms such as microalgae or yeast model species in which PRC1 and PRC2 complexes do not exist. Here, we draw a comprehensive picture of the diversity and abundance of both complexes in the Marine Microbial Eukaryote Transcriptome Sequencing Project database (MMETSP) and metagenome/metatranscriptome samples from *Tara* Oceans using the enhanced Domain Architecture Framework, eDAF, which is an ensemble of algorithms to process, enhance and expand the output of DAMA (Bernardes J.S. et al., 2016) or any other domain architecture algorithm (Terrapon et al., 2009; Yeats et al., 2010; Ochoa et al., 2011). Since eDAF can improve domain annotations, it is complementary to more prominent tools, such as InterPro (Mitchell et al., 2019). It also strongly improves the abilities of CLADE (Bernardes J. et al., 2016) by allowing it to analyze nucleotide sequences and propose the most probable translation of a given sequence (**Figure 1**).

Both PcG and TrxG complexes are histone writers involved in post translational modifications of histones (PTMs), namely H3K27me3, H2AK119 Ub and H3K4me3/K36me3 and probably more as some recent work points to the involvement of enhancer of zeste in tri-methylation of lysine 9 of histone H3 (Frapporti et al., 2019). Therefore, these complexes play an important role in genome regulation providing a plasticity in mediating genome responses to environmental factors and developmental triggers. In this study, we illustrate the importance of these PTMs in particular a trithorax deposited mark, H3K4me3 using the model diatom *Phaeodactylum tricornutum* where chromatin immunoprecipitation was used with deep sequencing to investigate the pattern of its distribution genome wide and its role in microalgae. Further, we revisited the epigenetic code in *P. tricornutum* (Veluchamy et al., 2015) and compared H3K4me3 mapping profile with the previously investigated Polycomb associated mark H3K27me3 (Veluchamy et al., 2015) to address for the first time their co-occurrence in a unicellular species.

MATERIALS AND METHODS

Material and Growth Conditions

Cells of *P. tricornutum* reference strain Pt1 8.6 CCAP 1055/1 (CCMP2561) were harvested after a week of growth in artificial sea water (Vartanian et al., 2009) at 19°C, under 12/12 light dark period with a light intensity of 75 μmol photons m-2 s-1.

Enhanced Domain Architecture Framework Analysis

eDAF is composed of four different modules: gene prediction (GP), most specific gene ontology terms (SGO), architecture extended information (AEI) and CLADE automation (CA) (**Figure 1**). Each of these modules is detailed below.

Gene Prediction

The gene prediction module allows CLADE to analyze all possible six-frame translations of each uniGene (Carradec et al., 2018). Once CLADE/DAMA predicts a domain architecture for a frame, we use a quadratic regression (Gergonne, 1974) to select the frame with the highest score. The variables of quadratic regression are the coverage, the *e*-value, and the average length of the PFAM domain (El-Gebali et al., 2019). The regression might select the frame with the best domain architecture, that is, with the highest number of conserved regions, the best coverages and *e*-values. Note that we call domain architecture an arrangement of conserved regions (domains) typically found in protein sequences. Since the selected frame can contain more than one gene, we trim it to where start/stop codons are detected; however, we did not consider start and stop codons within domains. We have considered the standard list of start/stop codons and users can change it by adding/removing entries in the eDAF start/stop codon table.

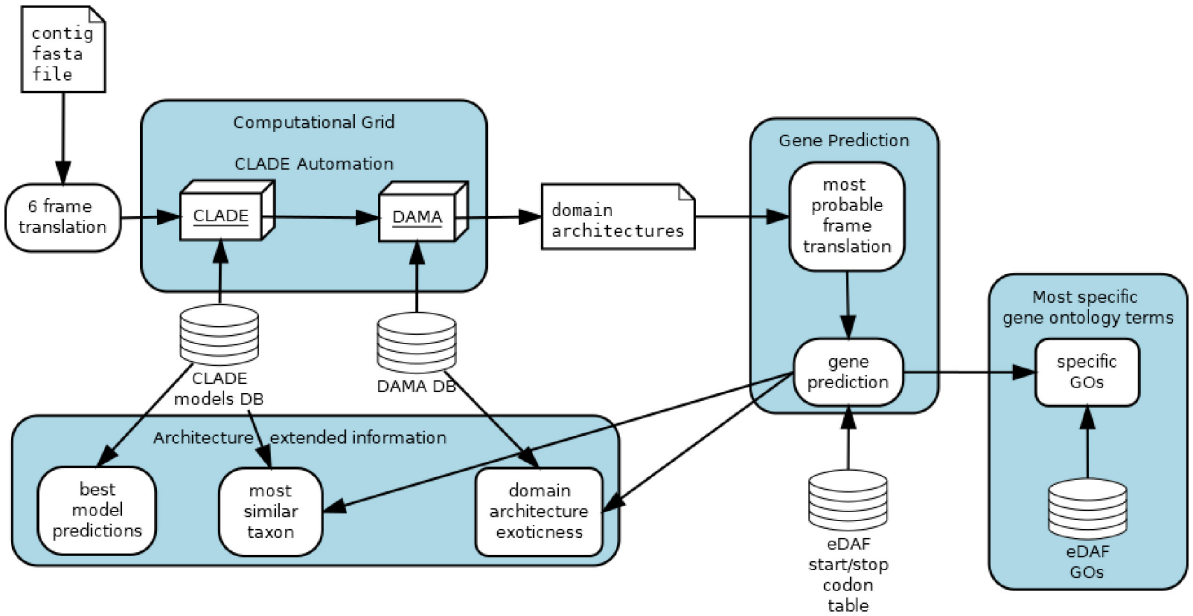

FIGURE 1 | eDAF flow chart.

Most Specific Gene Ontology Terms

After gene predictions, search is performed for their functional annotations. "PFAM2GO" that provides the Gene Ontology terms (Mitchell et al., 2015) for each domain detected by CLADE is used. Domains are represented by a set of GO terms organized in a hierarchical representation. To look for the most specific gene ontology terms of each domain, the postgresql database is used to execute a depth first search (Even, 2011) over the gene ontology tree terms (Carbon and Mungall, 2018). This search algorithm retains only the terms located on the leaves by avoiding generic terms, such as "cellular activity," that do not provide conclusive knowledge of protein function. However, generic terms can also be found on the leaves; thus, only terms whose depth is higher than the three levels are retained. Also, terms that are in the downward path of more profound terms are not retained. To produce the most enriched terms for a gene, all specific domain terms are considered, and only those with a frequency higher than three standard deviations above the mean of all identified terms (0.1% most enriched/frequent terms) are retained. Finally, repetitive/similar terms are grouped and collapsed by an approximate string matching algorithm (Sellers, 1980).

Architecture Extended Information (AEI)

Architecture Extended Information displays some DAMA and CLADE outputs not explored before. Each CLADE prediction is associated with one or more models and each model is associated to a specific taxonomy (species level). AEI recovers the corresponding taxa of each gene prediction and displays them to the user. The frequency of observed domain co-occurrence (internally part of DAMA database) are shown to highlight exotic (rarely observed) composition of conserved regions in the predictions.

CLADE Automation

CLADE is a set of powerful tools that need some expertise to be properly used. To make it user friendly, we implemented an automation. Basically, the user should only call one script and inform the gene fasta file; CLADE automation module will produce the submission files and the corresponding jobs to be sent to the computational grid. Currently, CLADE automation only works with Condor Computational Grid (Thain et al., 2005), but it can be easily adapted to other schedulers.

eDAF Analysis

We conducted an extensive set of scans over more than 11,720 transcriptomes distributed among 414 species (the MMETSP dataset) using eDAF. First, we used eDAF to interrogate the MMETSP transcripts by first translating each into the 6 possible frame translations. Next, eDAF fed the translations into CLADE and DAMA to identify the conserved domains. Then, eDAF selected the most probable translation of each transcript (as described in the previous sections). eDAF outputs the resulting proteins and the domain architecture of the corresponding MMETSP transcripts. Finally, to identify the true positives among the MMETSP sequences, we used eDAF to identify the domain architecture of both Polycomb and Thrithorax reference proteins (sequences reported as true positives in the literature). We retained only those MMETSP sequences with the same domain architecture of the references.

Phylogenetic Analysis

Both reference sequences and MMETSP true positives were aligned with Clustal Omega (Sievers et al., 2011). The corresponding alignments were used to produce the phylogenetic trees, which were built with MrBayes (Harmanci et al., 2014) using the following parameters (fixed rate model Blosum; mcmc

nruns = 1; ngen = 1000000; samplefreq = 100; sump burnin = 250; sumt burnin = 250).

ChIP-Seq Analysis

ChIP-Seq was performed on the reference strain of *P. tricornutum* Pt1 8.6 as described previously (Veluchamy et al., 2015) using a monoclonal antibody anti-trimethyl histone H3 (Lys4) (H3K4me3, Cell signaling Technology 9751S). Library preparation was performed at Fasteris next generation sequencing facilities (Switzerland), using the Illumina TruSeq kit and sequencing was performed on a HiSeq platform (V4 chemistry) with 1 × 50 bp single-reads. Two replicates with input each around 10 million reads were sequenced. Quality check on reads was done using FASTQC [1]with a cut-off Phred score of 20. Reads with minimum length of 36 bp were retained after trimming using Trimmomatic. Parameters for Trimmomatic were set as follows: Minimum length of 36 bp; Mean Phred quality score greater than 30; leading and trailing bases removal with base quality below 3; sliding window of 4:15. The reads were then mapped onto Phatr3 using Bowtie with unique read mapping parameter (Langmead and Salzberg, 2012).

For peak calling, we used three different peak detection methods such as MUSIC (Harmanci et al., 2014), BCP (Xing et al., 2012) and MACS2 (Zhang et al., 2008). We found a significant overlap between them and took consensus peaks from the three methods. Genome-wide analysis of tag density profile on TSS (transcriptional start sites) was performed using deepTools (Ramirez et al., 2014). Mean and standard deviations of the coverage depth were calculated and plotted using Qualimap and samtools. Analysis and visualization of the data were performed using Integrative genomics viewer from Broad Institute (IGV) (Robinson et al., 2011) and R module ChIP peak annotation.

Co-occurrence and Correlation Analysis

ChIP-seq peaks were annotated with gene annotation from Phatr3 (Rastogi et al., 2018). The intersection of different sets of genes overlapping with individual ChIP-seq peaks was performed using UpSetR (Conway et al., 2017). All combinations of overlap are derived and ordered from most to least overlapping categories. Non-overlapping peak sets are removed from the plot.

The aligned histone modification ChIP-seq dataset was binned for coverage with a window size of 1 kb. Replicate correlation was performed using multiBigwigSummary tools from deepTools. Pearson pairwise correlation coefficients were calculated from tag density. Scatter plot for correlation depicts the tag density for a bin of 1 kb each.

Sequence data were deposited in NCBI Gene Expression Omnibus database (accession number GSE139676).

RESULTS

Unlike in mammals and plants, Polycomb and Trithorax complexes are not well studied in unicellular species. Only a few recent studies of PcG proteins have been reported in microalgae (Shaver et al., 2010). To further investigate the diversity of Polycomb and Trithorax complexes in single-cell species, we first made an extensive scan of the MMETSP database using eDAF (see section "Materials and Methods") and reference sequences (**Supplementary Table S1**). We retained only MMETSP sequences whose corresponding domain architectures were identical to at least one of the reference sequences (see methods for details). Next, we aligned both reference and MMETSP sequences with Clustal Omega (Sievers et al., 2011) and built phylogenetic trees. In total, 203 homologs were identified from the MMESTP database that possess at least one of the components of the PRC1 or PRC2 complexes (**Supplementary Table S2**).

Phylogenetic Distribution of Polycomb Complexes in Marine Unicellular Species

Three core components of PRC2 are discussed here, E(z), Esc and Su(z)12. Nurf55 was not considered in our study because it is ubiquitous and is related to a high number of different biological processes that do not involve PRC2. Phylogenies of E(z), Esc and Suz(12) show similarity to human and plant genes with very conserved domains displaying high support values (above 85%) (**Figure 2**). PRC2 components are in principle very conserved, however, the phylogenetic tree of E(z), Esc and Su(z)12 polypeptides all fail to reconstruct or represent the consensus tree of eukaryotic monophyletic tree, not only because of the normal weakness of individual gene phylogeny, but might also be due to insufficient information in the database. Despite this, diatom and green algae E(z) homologs are well-clustered by their domain architecture (**Figure 2A**), although there is one exception, *Thalassiosira oceanica*, a centric diatom, surprisingly clustered with Alveolata and Rhizaria polypeptides. About 90 E(z) homologs share two conserved regions, CXC domain known as pre-SET domain and the SET domain itself (**Supplementary Table S2**). Esc homologs have two WD-40 repeat domains which can form a platform for protein-protein interactions (**Supplementary Table S2**). Esc transcripts are not as widely distributed as E(z) and Su(z)12 in diatom species. Consequently, the phylogenetic tree of Esc cannot well resolve the relationship among the species for which Esc sequences were detected (**Figure 2B**). Using the VEFS-Box of the polycomb domain to construct the phylogenetic tree of Su(z)12, we found that Chlorophytes and diatom Su(z)12 sequence formed a well-supported cluster like E(z), but with a few exceptions such as some pennate diatoms, *Pseudo-nitzschia delicatissima*, *P. arenysensis* and *Fragilariopsis kerguelensis* which were found to cluster with Rhizaria and Fungi (**Figure 2C**). The high conservation of domain architecture suggests the ancient origin of PRC2 proteins and the important function of this complex during evolution, while the branching of E(z) and Su(z)12 suggests the early divergence of these two genes.

Like in PRC2, PRC1 components show strict conservation in unicellular species (**Figure 3** and **Supplementary Table S3**). RING1 is the catalytic enzyme in the PRC1 complex which deposits H2AK119Ubi. C_3HC_4 type RING finger domain was the only conserved domain found and the proteins containing this

[1]http://www.bioinformaticsbabraham.ac.uk/projects/fastqc/

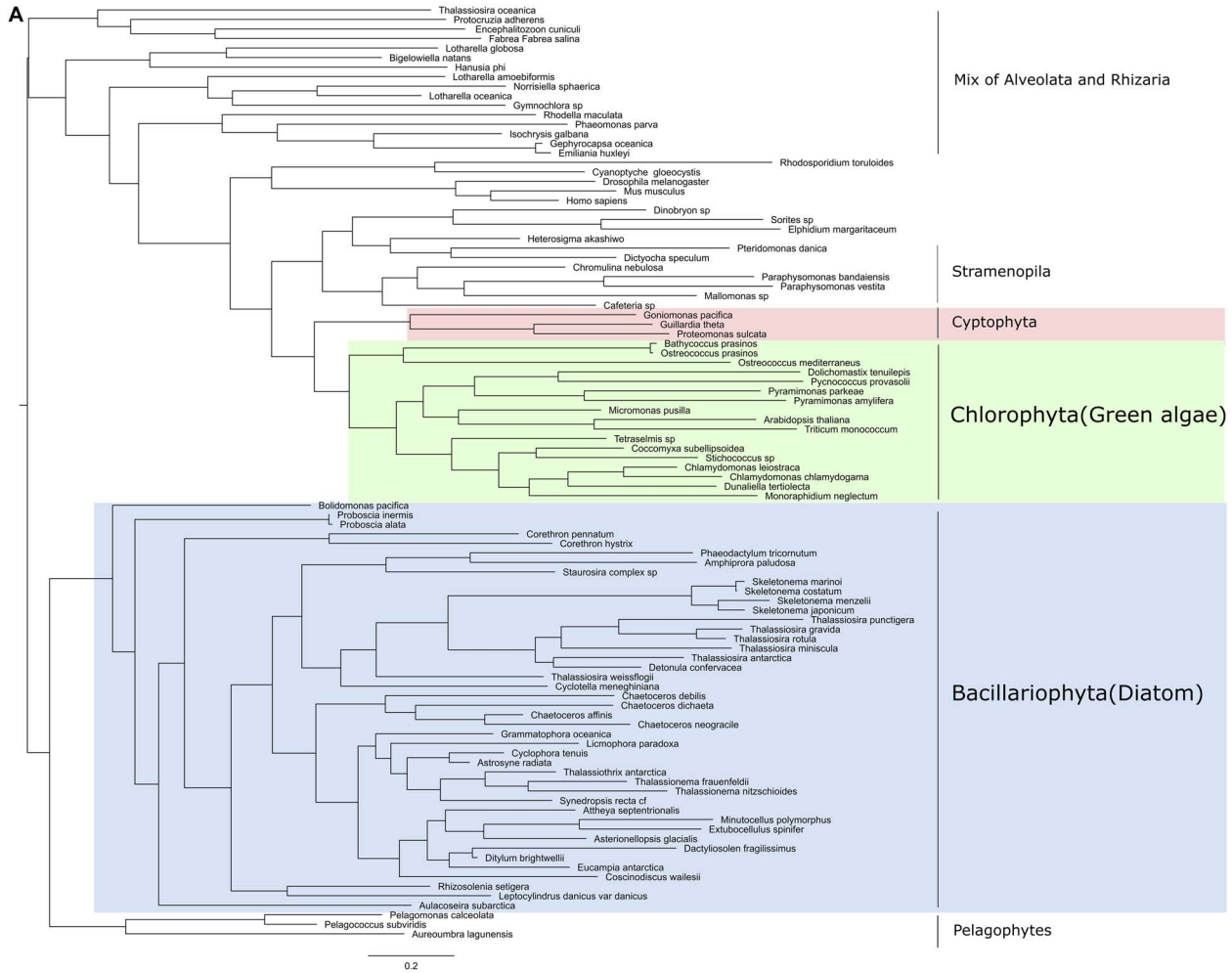

FIGURE 2A | Continued

domain typically play a key role in the ubiquitination pathway (Joazeiro and Weissman, 2000). Psc homologs which consist of two conserved domains, C_3HC_4 type RING finger and RAWUL domains, can function alone or together with RING1 to act as E3 ligase (Vidal, 2019). Phylogenetic tree of Psc was found to cluster well by species. Clusters of diatoms, green algae, Rhizaria and hacrobia species were found (**Figure 3B**). Similar to E(z), diatom homologs of Psc are closer to other Stramenopile species such as Ochrophyta, while green algae are clustered with Hacrobia species. Further, our study shows that Psc and E(z) proteins in Haptophyta are closer to green lineages while Cryptophyta homologs are closer to SAR lineages. Although Haptophyta and Cryptophyta both belong to Hacrobia, several studies support that they do not form a monophyletic group (Baurain et al., 2010; Burki et al., 2012) which is supported by our finding. Psc and RING1 are known to share RING finger and RAWUL domains from plants to mammals, but in our study only Psc have RAWUL domains whereas RING1 homologs do not. Interestingly, our results indicate that Psc and RING1 homologs are found almost mutually exclusively (**Figure 4**), except in four species, *Chrysochromulina brevifilum*, *Emiliania huxleyi*, *Isochrysis galbana* and *Neoparamoeba aestuarina*, suggesting the simplicity of PRC1 complexes or the existence of two types of PRC1 complexes in unicellular species, RING1-Type and Psc-Type. This composition found only in Haptophytes might be an indication of regulation mechanisms more similar to plants and animals compared to the rest of investigated species from the SAR lineage.

Pc homologs have a chromodomain and act as reader of H3K27me3. Yeast two-hybrid experiments show that Psc can directly interact with Pc and Ph through the RING finger domain (Kyba and Brock, 1998) which is in line with our finding that Pc expression always co-occurs with Psc and RING1 (**Figure 4**), whereas Ph was not detected in our study.

To further investigate the coexistence of polycomb complexes within species, we looked at all the ones that have at least one homolog in either PRC1 or/and PRC2 complex (**Figure 4**). It seems that PRC1 proteins are more present in Hacrobia exclusively without PRC2 components. The only exception is *Emiliania huxleyi* and *Isochrysis galbana* which have E(z)

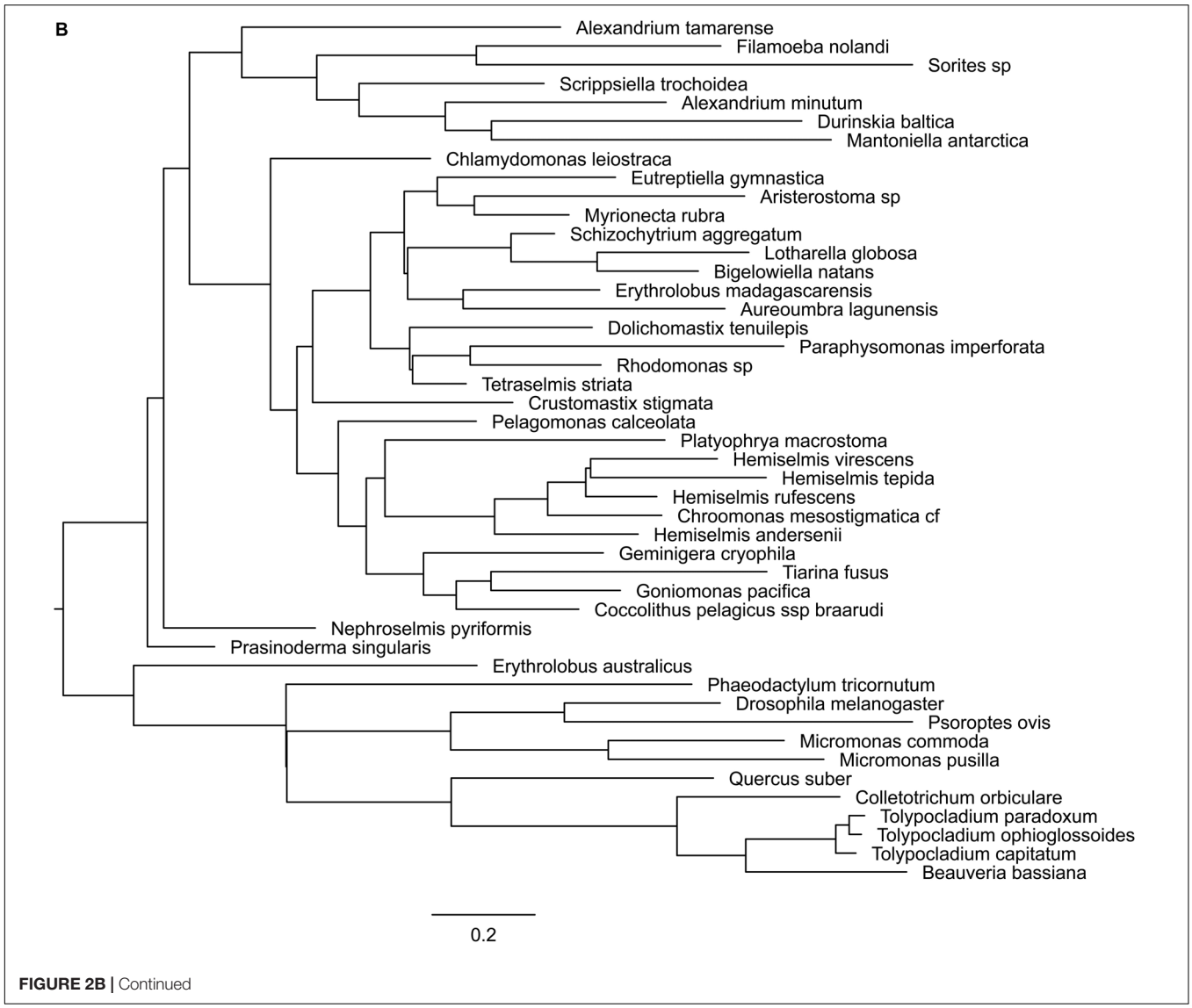

FIGURE 2B | Continued

in PRC2. While PRC2 components are more abundant in Stramenopila and Chlorophyta, which exclusively lack PRC1 subunits, 24 species have both PRC1 and PRC2 core components with two catalytic enzymes from each complex (**Supplementary Table S2** and **Figure 4**). *P. tricornutum* is the only species that contains all the subunits of both complexes PRC1 and PRC2 (**Supplementary Table S3** and **Figure 4**). It is important to note that MMETSP is based on transcripts and most of its species have poorly assembled genomes which means that undetected components might be due to a poor or lack of expression. On the other hand, *P. tricornutum* is one of the rare microalgae species with a fully sequenced high quality genome.

Diversity of Domain Features in the Trithorax Subfamily

TrxG proteins can be divided into 3 classes: histone-modifying SET domain proteins, ATP-dependent chromatin-remodeling factors which can recognize methylated sites by the SET domain, and a third class that includes proteins with specific DNA sequences (Schuettengruber et al., 2011). We chose references from the SET domain TrxG proteins and found that TrxG homologs are more diverse compared to PcG protein homologs, with 54 sequences that can be sorted into 4 clades according to phylogeny and domain structures (**Figures 5A,B**). Clade 1 contains five domains, Bromodomain, PHD finger domain, PHD-like zinc-binding domain, F/Y-rich N-terminus domain and SET domain. Clade 2 is composed of three domains: PHD finger domain, F/Y-rich N-terminus domain and SET domain. Clade 3 is small and can be considered to be a sub-set of either clade 1 without the Bromodomain or clade 2 with extra F/Y-rich N-terminal domains. Clade 4 has the simplest combinations with only PHD finger and SET domains.

To explore the distribution and evolution of TrxG protein homologs, phylogenetic analysis was performed as described above. Interestingly, all diatom species were found to possess

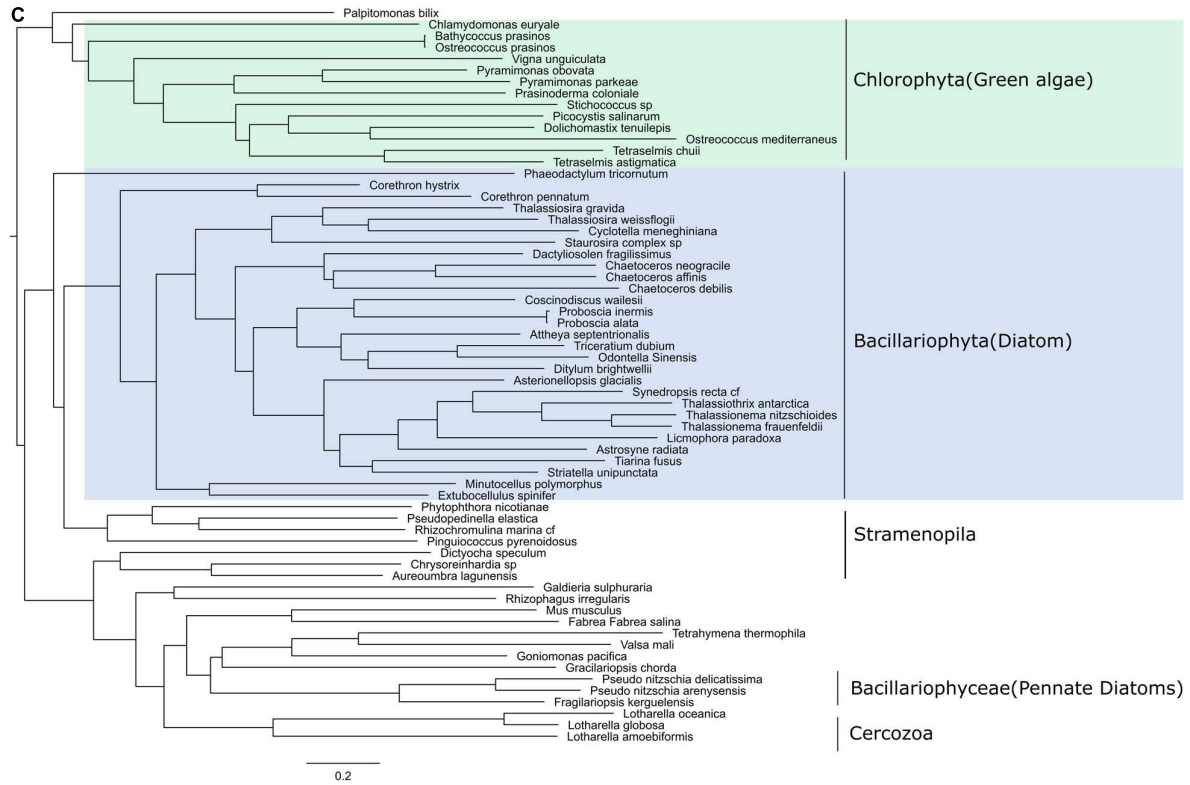

FIGURE 2C | Phylogenetic trees of PRC1 components. **(A)** RING, **(B)** Psc, **(C)** Pc.

a Bromodomain which belongs to Clade 1 and Clade 2, with a clear distinction between pennate diatoms, which are all in Clade 1, while centric diatoms are restricted to Clade 2. Some Stramenopile groups such as Chysophyceae and Pelagophyceae might have lost the Bromodomain during evolution (**Figure 5**). Three cercozoan species were found to have Clade 4-type Trithorax homologs in Rhizaria that lack the Bromodomain. On the other hand, in the Alveolata we found Clade 4-type trithorax as well as Clades 1 and 2.

Compared to the complicated situation in SAR group organisms, green lineage organisms show simpler combinations of domains. All 12 green algae have either Clade 3 or Clade 4 type Trithorax with the following combination: PHD finger domain and SET domain, sometimes with the F/Y-rich N-terminal domain. As expected, a phylogenetic tree of Trithorax homologs shows that sequences from green lineage organisms cluster with the reference sequences ATX1 and ATX2 from the plant model species *Arabidopsis thaliana* (**Figure 6**). Among the five species found in Haptophyta, except for *Chrysoculter rhomboideus*, four have Clade 1-type Trithorax homologs.

Assessment of Polycomb and Trithorax Complexes in Environmentally Sampled Microalgae

To investigate the presence of Polycomb and Trithorax members in the environment, we used metagenomes and metatranscriptomes from *Tara* Oceans and applied eDAF (same procedure described in the Materials and Methods section) to detect all the unigenes. We retained only sequences with the exact same arrangements of conserved regions as the reference sequences (**Supplementary Table S3**), and considered only surface samples in 0.8 to 5, 5 to 20, 20 to 180 and 180 to 2000 μm size fractions.

Both RING and enhancer of zeste genomic sequences were weakly detected in 28 stations (9 and 25, respectively) out of 68 where diatoms were found (Carradec et al., 2018). However, their expression is significant in response to nitrate and phosphate although to a lesser extent than what was observed for the Trithorax complex (**Figure 7B**). This anti-correlation can be explained by the quality of DNA sequence reads, as reported previously in a much wider study of *Tara* Oceans samples (Terrapon et al., 2009). The majority of transcripts from genes encoding Trithorax components belong to Stramenopiles and only a few are shared between Chlorophyta and Haptophyceae. On the other hand, transcripts from genes encoding EZ and RING components are dominated by Dinophyceae (**Supplementary Figure S1**). The proportions of genomic DNA and transcripts for each class of microalgae can be accessed using Krona interactive charts in the following links: (https://ndownloader.figshare.com/files/20019587?private_link=302f866ec48cc9a2e1ed, https://ndownloader.figshare.com/files/20019590?private_link=302f866ec48cc9a2e1ed).

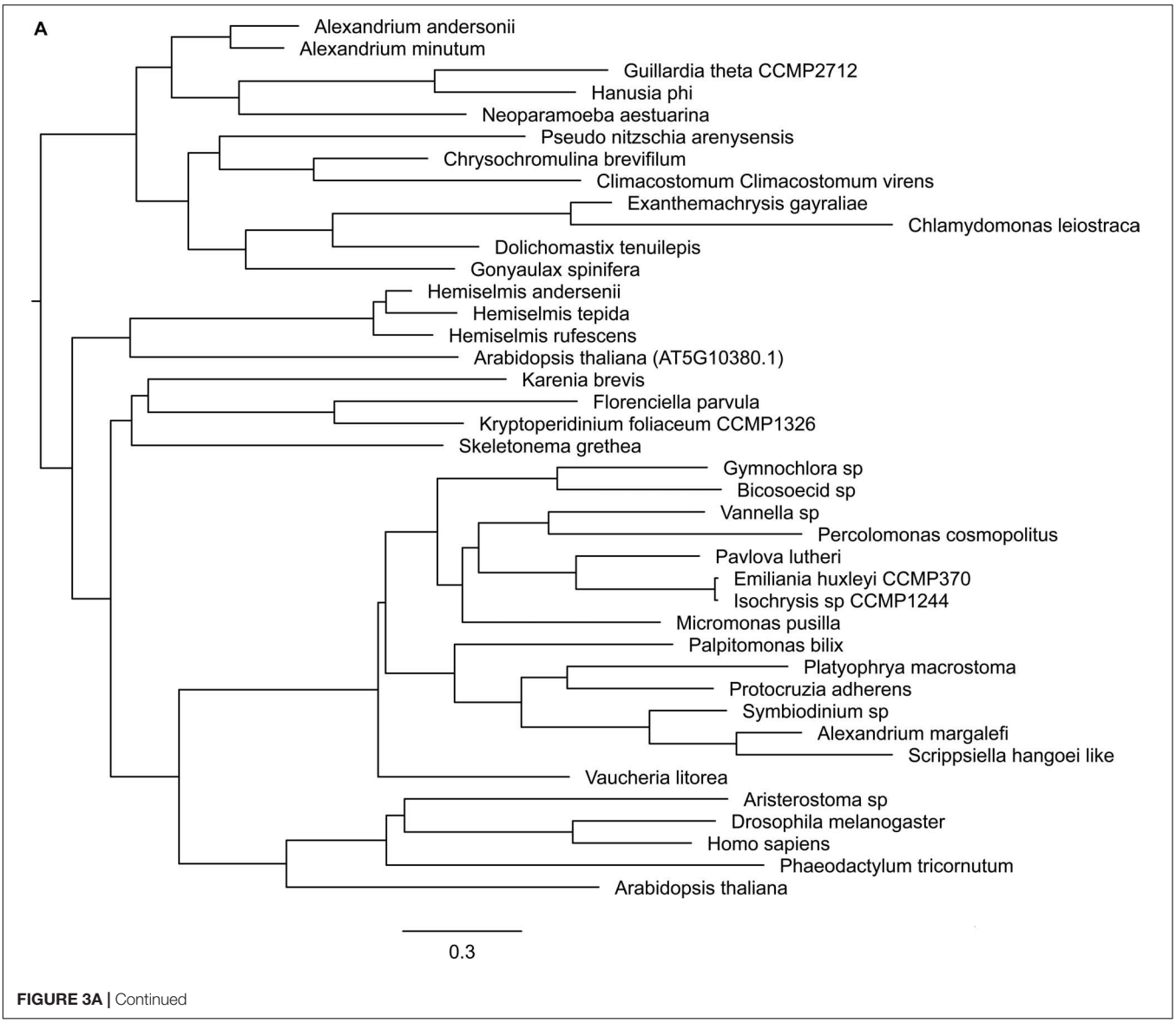

FIGURE 3A | Continued

Several environmental factors were measured during the *Tara* Oceans expedition, so we examined whether there was any correlation with the expression of genes encoding Polycomb and Trithorax components. Only phosphate and nitrate showed significant correlations with enhancer of zeste, RING and Trithorax. Trithorax members were found to be highly expressed in response to increasing levels of nitrate and phosphate. Enhancer of zeste shows the same trend although to a lesser extent. RING was also found to correlate moderately with increasing levels of both nutrient except in TARA Stations 84 and 85 in the South Atlantic Ocean where they respond to lower levels of nitrate and phosphate (**Figures 7A,B**).

Among the other environmental factors measured during the *Tara* Oceans expedition, we observed a weak correlation between salinity and the expression of RING genes in 9 stations (scc: 0.56, *p* value: 0.04). The low number of stations is due to the absence of genes encoding RING proteins in most of the stations. We also obtained a weak correlation between the expression of genes encoding Trithorax components in 46 stations with measured oxygen levels (scc: 0.54 *p* value: 0.47). However, the observed high *p* values prevent us from drawing any conclusions.

Trithorax Deposited H3K4me3 Is an Active Mark Exclusive to Genes in *P. tricornutum*

Phaeodactylum tricornutum is the first and only Stramenopile so far for which a chromatin landscape has been drawn, with the mapping of five histone marks including H3K4me2, H3K9/14Ac, H3K9me2/me3, and H3K27me3 (Veluchamy et al., 2015). To explore the role of H3K4me3, known to be deposited by the Trithorax complex described above, and investigate its relationship to the repressive mark H3K27me3 reported to antagonize H3K4me3 (Aach et al., 2014), we performed

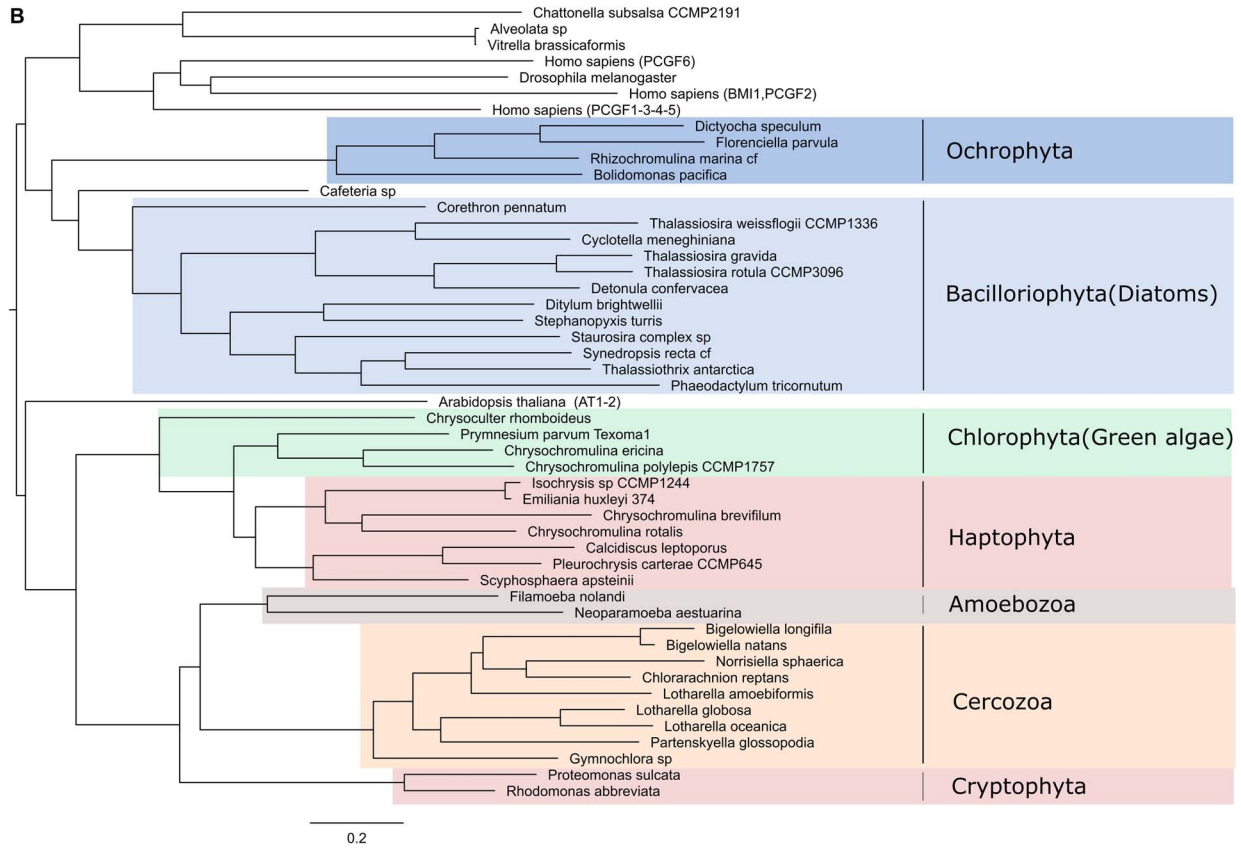

FIGURE 3B | Continued

chromatin immunoprecipitation with deep sequencing on two independent replicates of cultures of the reference strain Pt1 8.6 (**Supplementary Figure S2**).

H3K4me3 was found to cover around 42% of the genome targeting only genes (**Supplementary Table S4**). A total of 8,431 genes out of 12,152 were marked by H3K4me3, which was found mainly on exons (2,109 on exons out of 2,168 total peaks). H3K4me3 localizes at the 5′-end of transcribed regions (TSSs) and shows a similar profile to H3K9 acetylation and H3K4me2 but is different from the broader pattern of repressive marks such as H3K9me3 and H3K27me3 (**Supplementary Figure S3**).

We subsequently investigated the correlation between H3K4me3 distribution and transcript levels using ChIP-Seq from this study and RNA-Seq data generated previously in the same growth conditions (Bernardes J.S. et al., 2016). Analysis using a *t*-test shows significant differences in expression levels between marked and unmarked genes (*t*-test *p*-value:4.6e-08). Analysis of categorization of expression quantiles (10 quantiles) shows that highly expressed quantiles have 956 genes marked and 255 genes unmarked. In the low expression quantiles, 343 genes are marked and 988 genes are unmarked by H3K4me3 (**Supplementary Figure S3**). Furthermore, the genes that are uniquely marked by H3K4me3 show similar levels of gene expression than those marked uniquely by either H3K4me2 or H3K9Ac, which are widely recognized as active marks. Overall, H3K4me3 marked genes show increased levels of expression (FPKM), compared to the H3K4me3 unmarked genes, further confirming that H3K4me3 is an active mark in *P. tricornutum*.

Combinatorial Analysis of Histone Marks in *P. tricornutum*

To investigate the relationship between H3K4me3 and previously characterized histone marks (Schuettengruber et al., 2007), we analyzed the co-marking patterns including five histone marks, namely H3K4me2, H3K9/14Ac, H3K9me2, H3K9me3, H3K27me3, and DNA methylation (**Supplementary Figure S4**). Histone marks and DNA methylation can occur in 40 different combinations (**Figure 8**). Correlation analysis with transcript data defines principally three chromatin states (CS), active, repressive and intermediate. The three active marks of the study localize together on the highest number of genes compared to the rest of the combinations. They predominantly appear together with one repressive mark, H3K9me2. The lowest number of genes are co-marked by H3K9me3, H3K27me3 and DNA methylation, leading to a repressive CS. While co-occurrence of DNA methylation and the three repressive histone marks clearly define a repressive chromatin state, their association with one or more active marks switches to an intermediate or active CS with a particular signature of H3K4me3 which tends to have a

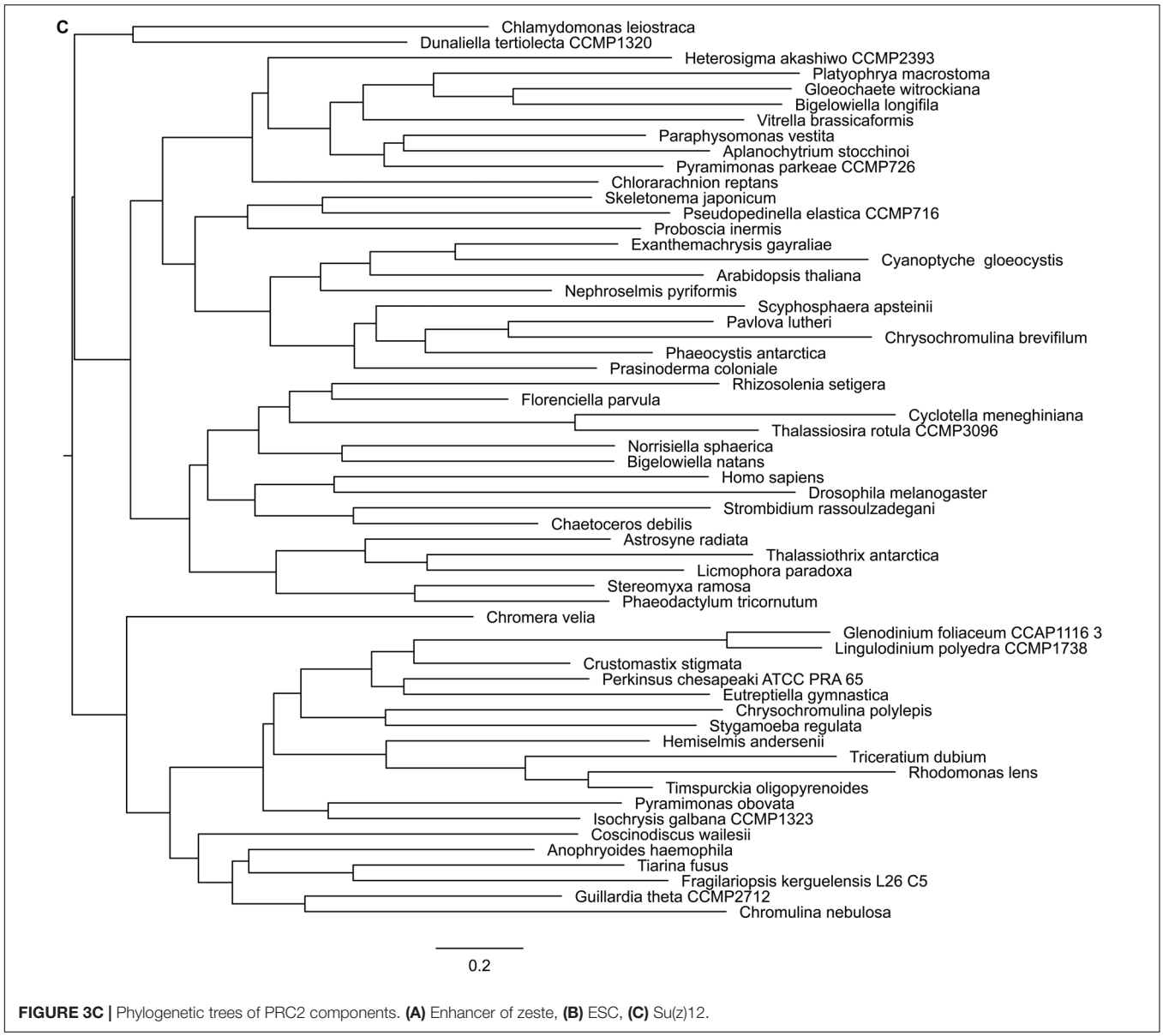

FIGURE 3C | Phylogenetic trees of PRC2 components. **(A)** Enhancer of zeste, **(B)** ESC, **(C)** Su(z)12.

significant effect by itself on the increase of global transcript levels (**Figure 8**). Mapping of an additional active mark does not change the pattern of co-occurrence of four repressive histone marks, which is unique to *P. tricornutum,* suggesting an interdependence or cooperation for transcriptional regulation of genes and TEs.

Considering the antagonistic relationship of both PcG and TrxG complexes in the regulation of several biological processes of the cell reported in plants and animals (Geisler and Paro, 2015; Poynter and Kadoch, 2016), we investigated the expression output when genes are co-marked with H3K27/K4me3. This analysis revealed two scenarios: first, 80 genes were exclusively co-marked with an intermediate level of expression and, second, a total of 814 co-marked genes with higher or lower expression are shared with either acetylation and H3K4m2 (CC6 with 457 genes), acetylation, H3K4m2 and H3K9me2 (CC 13 with 156 genes), only H3K4me2 (CC14 with 152) or H3K4me2 and H3K9me2 (CC25 with 66 genes) (**Figure 8**). Exclusive loci co-marking with both H3K4me3 and H3K27me3 suggests a bivalency that likely maintains genes in a poised state ready for activation or repression in response to relevant signals. These distinct readouts define a new histone code with the co-occurrence of active and repressive marks which likely cooperate or antagonize each other for gene regulation, with a distinct signature of balanced expression when H3K4me3 co-occurs alone with H3K27me3 and higher or lower expression when combined with active or repressive marks, respectively.

GO Functional Categories of H3K4me3 Marked Genes

To gain insights into the functional categories enriched in H3K4me3 marked genes, we performed a GO classification

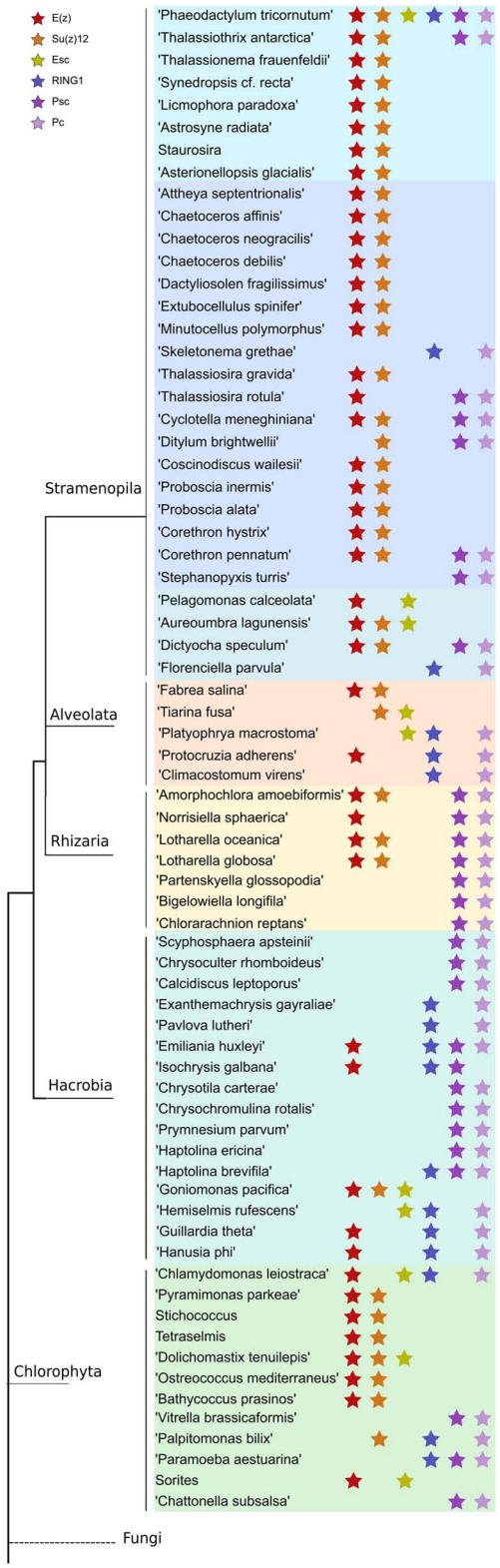

FIGURE 4 | Distribution of PRC1 and PRC2 components in a phylogenetic tree among microalgae species in MMETSP. Each star marks the presence of one component of either PRC1 or PRC2. Different color backgrounds represent species belongs to the same phylum or group.

based on DAMA and CLADE and refined by eDAF results. We found an enrichment mostly in categories such as: (1) tetratricopeptide repeat containing proteins which act as a protein-protein interaction module involved in regulation of different cellular functions including cell cycle, hormone signaling, neurogenesis, protein folding and transport, and transcriptional control (Schapire et al., 2006); (2) mitochondrial carrier proteins the mediate the transport of ions, nucleotides and metabolites across mitochondrial membranes (Palmieri et al., 2011); (3) WD domain, G-beta repeat involved in a variety of functions ranging from signal transduction and transcription regulation to cell cycle control and apoptosis; (4) Aldo/Keto reductase families of proteins which are important intermediates in many metabolic pathways, including sugar metabolism, steroid biosynthesis, amino acid metabolism, and biosynthesis of secondary metabolites (Ellis, 2002); and (5) Kelch motif involved in fundamental cellular activities in multiple cellular compartments such as actin-binding activity, organization of cytoskeletal, plasma membrane and organelle structures (Adams et al., 2000). Overall, functional categories of H3K4me3 marked genes are mostly related to general biological processes involved in house-keeping functions.

The cooperation of two antagonistic marks, H3K4me3 and H3K27me3, for regulation of developmental processes in plants and animals compelled us to analyze the GO categories inherent to these cases. Interestingly, we see developmental and cell differentiation related categories when genes are exclusively co-marked with both H3K27me3/K4me3. When shared with other marks (CC6, CC13, CC14, and CC27), broader GO terms emerge (p-value of 2.52383E-73 for genes only enriched with H3K4me3 versus H3K4me3/K27me3 and no matter the others, p-value 4.54346E-98 for genes only co-marked by H3K4me3/K27me3 versus genes marked only by H3K27me3 or H3K4me3, p-value of 1.094673-123 for genes only marked by H3K4me3 or only H3K27me3 versus genes marked only by H3K4me3, **Supplementary Table S4**).

DISCUSSION

In eukaryotes, the life cycle goes through growth/developmental phases characterized by specific spatial and temporal regulation of genome expression. This regulation is not only defined by their DNA sequence which remains constant between cell types but also by their gene expression pattern controlled by epigenetic mechanisms including dynamic chromatin states. Two groups of evolutionary conserved protein complexes known as Polycomb (PcG) and trithorax (TrxG) play a crucial role in such regulation by preventing or promoting gene expression, respectively (Schuettengruber et al., 2017). While TrxG are scarcely documented in only a few microalgae, PcG proteins are reported to be likely present in the last common ancestor of eukaryotes and to subsequently have been lost during evolution in certain single celled lineages such as both yeast model species *S. pombe* and *S. cerevisiae* (Shaver et al., 2010; Margueron and Reinberg, 2011). In the present study, using eDAF, which is an ensemble of modules for gene prediction,

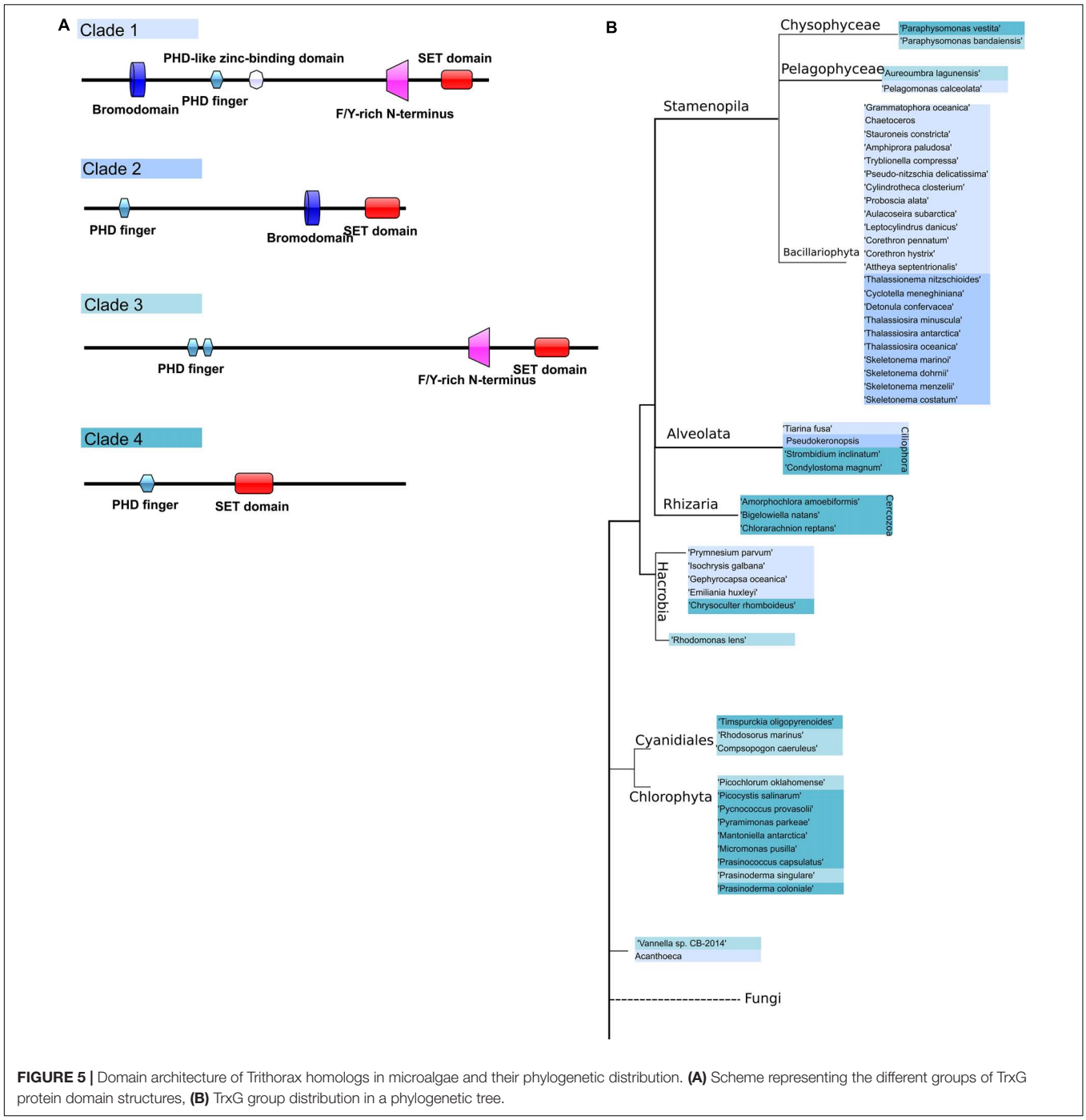

FIGURE 5 | Domain architecture of Trithorax homologs in microalgae and their phylogenetic distribution. **(A)** Scheme representing the different groups of TrxG protein domain structures, **(B)** TrxG group distribution in a phylogenetic tree.

ontology, architecture extended information and automation, we interrogated MMETSP, currently the largest transcriptome reference database for eukaryotic marine microbes, and found that although the coexistence of PcGs and TrxGs is not found frequently in unicellular species (39 out of 203; 19.21%), there are several species that have both PcG catalytic enzymes and TrxGs, including *Bigelowiella natans*, *Corethron hystrix*, *Attheya septentrionalis*, *Pelagomonas calceolate*, and *Proboscia alata* (**Supplementary Table S2**). This number of species might be limited by the nature of the MMETSP database, which contains only transcriptomics sequences, and sequencing more unicellular genomes might reveal additional species with PcG and TrxG complexes.

Recently, studies on PRC2 and its associated epigenetic mark H3K27me3 in microalgae revealed interesting insights on their diversity and role in silencing of genes and transposable elements, which are their main targets (Shaver et al., 2010; Veluchamy et al., 2015; Mikulski et al., 2017; Frapporti et al., 2019). In our

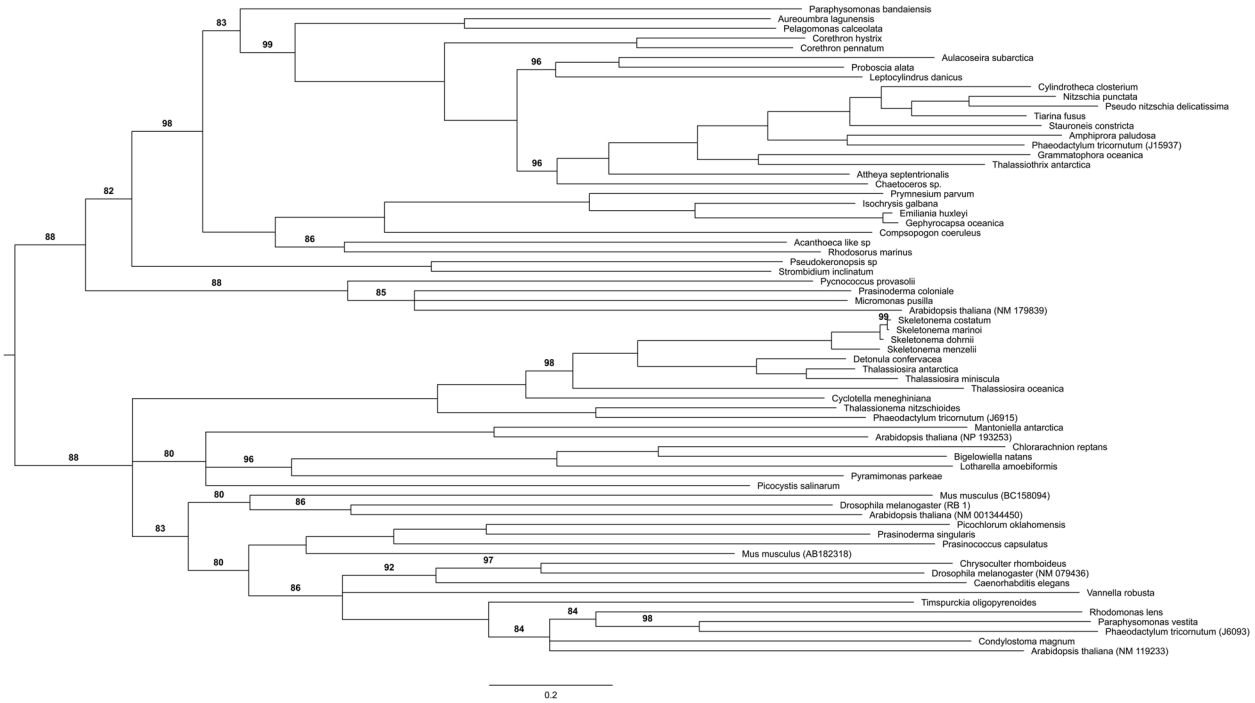

FIGURE 6 | Phylogenetic tree of TrxG components.

study, we found that both PcG and TrxG proteins are not well represented in dinoflagellates. This might reflect the unorthodox nature of histone proteins in dinoflagellates (Marinov and Lynch, 2016) which do not play a major role in genome packaging and heterochromatinization (Gornik et al., 2012). Although previous study show that dinoflagellates have most of the chromatin reader, writer and eraser protein families, including a strikingly large number of SET-domain proteins (Marinov and Lynch, 2016), our search of MMETSP did not yield such examples, except for a few species including *Alexandrium* and *Symbiodinium* which were found to have Esc and/or RING homologs, although no transcripts of other PcGs and TrxGs complex subunits could be found (**Supplementary Table S3**). Possible explanations for the poor representation in dinoflagellates is either the silencing of histone writers in the dinoflagellates contained in MMETSP or it may be a distinctive feature like other epigenetic modifying enzymes such as DNA methyltransferases (DNMTs) that are peculiar and unlike classical DNMTs (de Mendoza et al., 2018).

Trithorax family is a diverse group of proteins involved primarily in gene activation either by nucleosome positioning, histone modifications such as methylating lysine 4 of histone H3 or direct interactions with transcription machineries (Kingston and Tamkun, 2014). Here we focus on MLL/COMPASS complex which has histone methyltransferase activity. MLL family is made up of three pairs of structurally similar proteins, namely MLL1-MLL2, MLL3-MLL4, and SET1A-SET1B (Ruthenburg et al., 2007; Crump and Milne, 2019). Surprisingly, TrxG protein homologs distribution in diatoms is more complicated than expected. They can be divided into two groups: centric and pennates with structure differences that might reflect their evolutionary history with 90 million years of divergence. Green algae TrxG homologs are as simple as the first H3K4 methyltransferase Set1, identified in *S. cerevisiae* (Briggs et al., 2001), only have SET and PHD finger domains, which is similar to SET1A-SET1B group in MLL family. Compared with green algae which possess only clade 3 and 4, diatoms TrxGs are more close to human TrxG genes which reflects the close relationship between stramenopiles and animals.

Using the same reference sequences, we probed the presence of both TrxG and PcG complexes in environmental samples from small size fractions of *Tara* Oceans. Our results point to the presence of TrxG complex including the four constituent proteins, all with SET and PHD finger domains in combination with either Bromodomain or F/Y motifs, which correlate with high concentrations of nitrate and phosphate. Although less important, this correlation is significant for both EZ and RING components of PRC2 and PRC1, respectively. These results suggest a Polycomb and Trithorax mediated regulation in response to nutrient availability. A weak correlation was observed between transcript levels of RING, TrxG and low salinity and oxygen, respectively. To the best of our knowledge, this is the first report of expression of Polycomb and Trithorax genes in environmentally sampled marine eukaryotic microalgae and tehir correlation to macronutrient availability. This may suggest a role of chromatin master regulators in nutrient uptake which is important in nutrient cycling and ultimately primary productivity. Beyond the conservation of Trithorax proteins in unicellular marine microalgae sharing

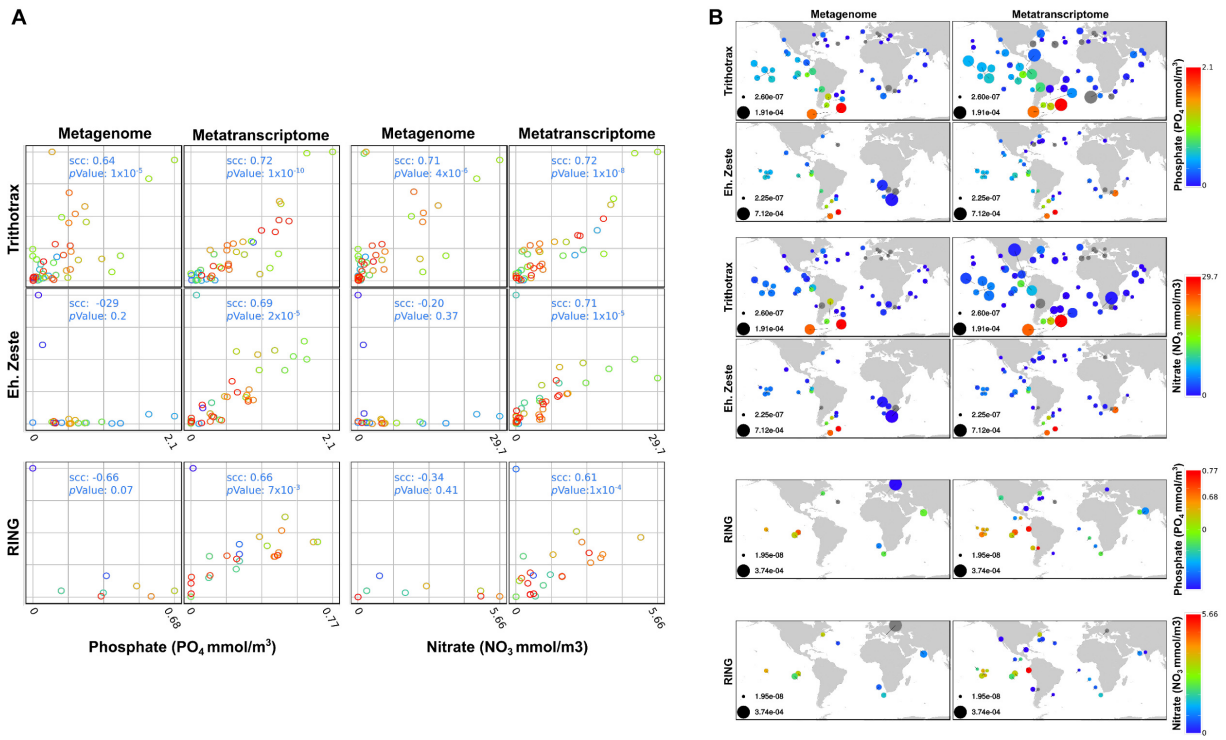

FIGURE 7 | Correlation analysis of Metagenome and metatranscriptome and distribution of PcG and TrxG in TARA stations. **(A)** Correlation of the relative levels of gene presence (Metagenome) and gene expression (Metatranscriptome) detected by TARA station for bacillariophyta sequences when compared with 3 different environmental levels. The relative levels correspond to the abundance in RPKM of each gene/complex at each station normalized by the total abundance in RPKM of bacillariophyta sequences detected at the same station, and then re-scaled to the unit interval (minimum and maximum levels are presented in figure **B**). Abundances at each station were computed by pooling 4 size fractions, namely: 0.8 to 5, 5 to 20, 20 to 180 and 180 to 2000 μm. Spearman correlations coefficients (scc) and *p* values represent statistical association of the environment levels of Phosphate, Nitrate and bioavailable Nitrogen with the relative levels of RING genes, Enhancer of zeste genes and the Trithorax complex. We note that correlations between each respective Metagenome and Metatranscriptome pair were not significant enough to be shown (scc < 0.22) and colors were used to distinguish different stations, for visual clarity. **(B)** Distribution of RING genes, Enhancer of zeste genes and the Trithorax complex among TARA stations. Disk sizes represent the relative levels of gene presence (Metagenome) and gene expression (Metatranscriptome) at each TARA station in RPKM. Color intensities shows the different environment levels of Phosphate, Nitrate and bioavailable Nitrogen according to the corresponding color bars, and gray disks represent relative levels of genes where environmental factors were not available.

conserved domains with animal and plant homologs, the TrxG deposited histone mark H3K4me3 shows similar patterns of distribution in *P. tricornutum* compared to what is described in multicellular species (Barski et al., 2007; Zhang et al., 2009). It is found over genes spanning transcriptional start sites and 5′ promoter regions and correlates with active gene expression, suggesting a ubiquitous role of H3K4me3 as a transcriptionally activating mark.

Analysis of the combinatorial readout of histone PTMs in *P. tricornutum* identified principally three chromatin states that likely reflect a coordinated regulation of genes. Although not exhaustive, this histone code is overall conserved pointing to key PTMs that seem to be important for defining each of the chromatin states confirming previously published study (Veluchamy et al., 2015). Despite the overall conservation of the histone code, unique patterns emerge from the co-occurrences of repressive marks that are not documented in animals and plants, in particular those that combine several repressive marks (e.g., C21 with 91 genes) with a dramatic effect on gene repression compared to the other CS. Our previous work (Veluchamy et al., 2015) has identified such patterns, and profiling a new active histone mark which targets a high number of genes uncovers genes that are uniquely marked with several repressive histone marks and DNA methylation, suggesting a stable pattern of gene regulation that likely involves a crosstalk. This suggests several scenarios of regulation including a cumulative effect or recruitment loop as described in other studies (Strahl and Allis, 2000; Roudier et al., 2011). Genetic studies in model species such as *P. tricornutum* are an important step in elucidating these mechanisms. These chromatin states are an indication of the overall transcriptional output of several marks when they co-occur. However, it needs to be extended to additional key marks which will undoubtedly refine the histone code which is a useful proxy for understanding how chromatin states mediate the regulation of genes in response to developmental and environmental triggers.

Functional annotation of exclusively H3K4me3 marked genes revealed an enrichment in categories such as protein degradation and peptide processing into amino acids, RING finger containing proteins known for their role in diverse cellular processes such

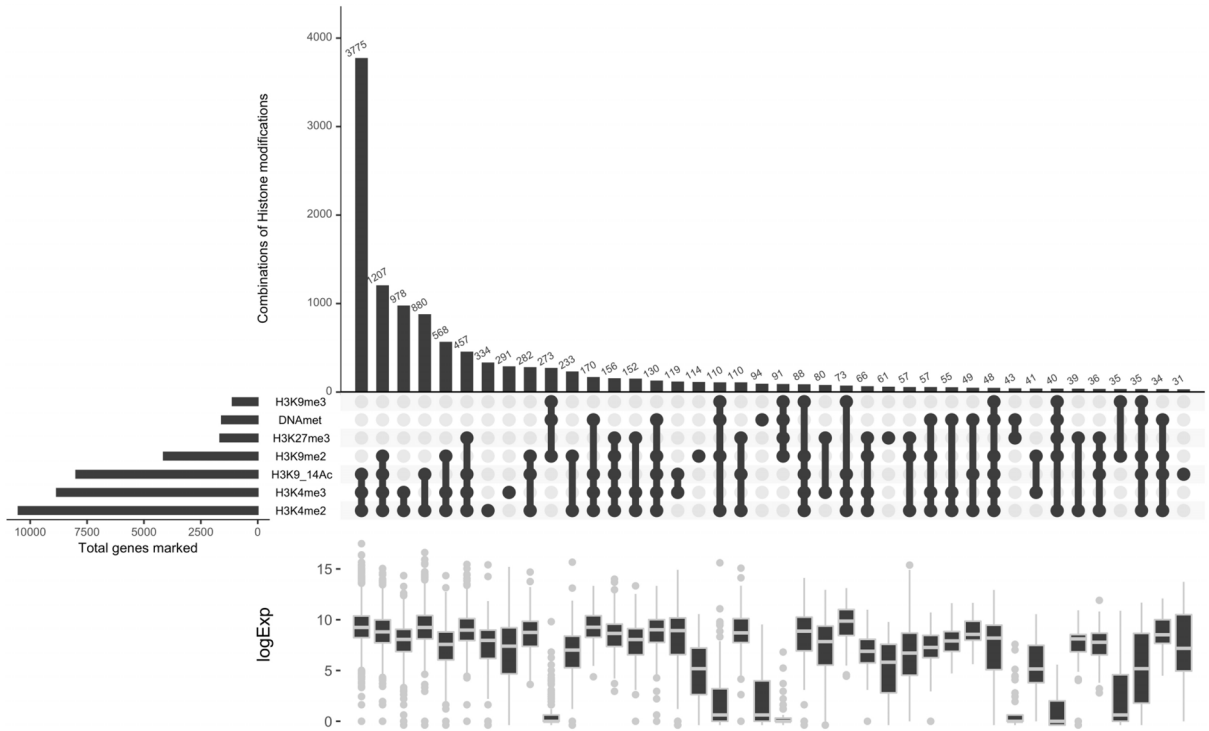

FIGURE 8 | Co-occurrence analysis. A co-occurrence plot for the ChIP-seq peaks of different histone modification. For each set of intersection, a black filled circle is drawn. The size of the intersections is depicted in vertical bar. The vertical black line connects the different dataset that intersect. The number of genes for each chromatin state is shown on the top of the bars.

as regulation of transcription, cell cycle, signaling and secretory pathway (Deshaies, 1999), FYVE domain containing proteins associated to vacuolar protein sorting and endosome function (Leevers et al., 1999; Jensen et al., 2001), proteins with DNA ligase domains with a role in a wide range of DNA transactions (Martin and MacNeill, 2002), all of which are indicative of rather general house-keeping functions. However, gene ontology annotation of H3K4me3/K27me3 loci show enrichment in categories related to cellular architecture with a majority of GO terms referring to regulation of actin polymerization or depolymerization, regulation of cell shape, microtubule cytoskeleton, myosin complex, positive regulation of cellular components organization and peptidyl tyrosine phosphorylation important for cell proliferation, cell cycle progression, metabolic homeostasis, differentiation and development (Hunter, 2009). Although less important, these GO categories are present when genes are marked by H3K3me4/K27me3 and other marks. It is tempting to postulate that co-marking by H3K4me3 and H3K37me3 is a combinatorial action of both marks in transcriptional regulation of genes related to specific functions such as cell differentiation. This analysis is based on the intersection of ChIP-Seq tracks and so it will be important in future studies to perform sequential ChIP to monitor the coexistence of these two marks or the unique co-occurrence of several repressive histone marks within a single nucleosome.

The existence and diversity of PcG and TrxG complexes in eukaryotic unicellular species throughout the tree of life opens a whole range of questions on the molecular mechanisms of their interactions; their role in cell differentiation and other biological processes, how they are recruited to their targets, and understanding their contribution to a fundamental mechanism, the emergence of multicellularity. One particular aspect is understanding the cross talk between these two complexes for gene regulation, especially in a bivalency context where a timely activation is required as well as the maintenance of repression. Future studies in *P. tricornutum* and other emerging unicellular models will undoubtedly bring new insights and deepen our understanding of the evolutionary history of PcG and TrxG complexes.

DATA AVAILABILITY STATEMENT

The datasets generated for this study can be found in the GSE139676.

AUTHOR CONTRIBUTIONS

LT, XZ, and FV conceived and designed the study. AD performed the experimental work. LT, XZ, AV, and FV performed the bioinformatic analysis, analyzed and interpreted the results. LT, XZ, and FV wrote the manuscript with input from all authors. All authors read and approved the manuscript.

FUNDING

LT acknowledges funds from the CNRS and the region of Pays de la Loire (ConnecTalent EPIALG project). CB acknowledges the European Research Council Advanced Award Diatomite. XZ was supported by a Ph.D. fellowship from the Chinese Scholarship Council (CSC-201604910722).

SUPPLEMENTARY MATERIAL

The Supplementary Material for this article can be found online at: https://www.frontiersin.org/articles/10.3389/fmars.2020.00189/full#supplementary-material

FIGURE S1 | Krona Pie charts. **(A–C)** represent metagenomics krona charts of TrxG, EZ and RING. **(D–F)** show meta-transcriptomic Krona charts of TrxG, EZ and RING respectively.

FIGURE S2 | Profile plot of histone marks including H3K4me3 and gene expression levels of H3K4me3 marked versus unmarked genes. **(A)** Averaged tag-density profile for 6 histone modifications are plotted for TSS of 12k genes with 3 kb upstream and 10 kb downstream regions. Regions are ordered and scaled to TSS as reference point. **(B)** Boxplot showing the differences in expression levels of genes with and without histone modifications. Box represents 10–90% of data and the outliers are shown as whiskers. Median of the data is shown in a small dot in the center of the box (*t*-test: *p*-value = 1.581e-08).

FIGURE S3 | H3K4me3 Correlation plot. Pairwise scatterplots showing correlation of the two H3K4me3 ChIP-seq replicates. Genome is split into bins and enrichment scores per bin were calculated. Pearson correlation coefficient for the comparison of enrichment scores is marked.

FIGURE S4 | PTMs distribution. Upper panel shows average ChIPseq profile (read density) over TSS of genes. Lower panel shows heatmaps of ChIPseq data of individual histone modifications and input is shown over TSS.

TABLE S1 | Reference sequences used in this study.

TABLE S2 | List of species found in MMETSP with PRC1 or/and PRC2 components and Trithorax components. The table contains species have at least one PcG proteins with present or absent of TrxG protein which located at the last column. TrxG column also specify the trithorax homologs clade classification which is discussed in this paper, species with both PcG catalytic enzyme (E(z) and RING/Psc) and TrxG were highlight in yellow background.

TABLE S3 | Protein sequences of PRC1, PRC2 and TrxG components. The table shows the PFAM domains, their coordinates within the sequences and score.

TABLE S4 | Gene annotations and functional categories of histone marked genes in *P. tricornutum*. Genes annotated for each histone modification are summarized and tabulated. Histone marked genes are given value 1 and unmarked genes in the genome are given value 0.

REFERENCES

Aach, J., Prashant, M., and George, M. C. (2014). CasFinder flexible algorithm for identifying specific Cas9 targetsin genomes. *bioRxiv* [Preprint]. doi: 10.1101/005074

Adams, J., Kelso, R., and Cooley, L. (2000). The kelch repeat superfamily of proteins: propellers of cell function. *Trends Cell. Biol.* 10, 17–24. doi: 10.1016/s0962-8924(99)01673-6

Barrero, M. J., and Izpisua Belmonte, J. C. (2013). Polycomb complex recruitment in pluripotent stem cells. *Nat. Cell Biol.* 15, 348–350. doi: 10.1038/ncb2723

Barski, A., Cuddapah, S., Cui, K., Roh, T. Y., Schones, D. E., Wang, Z., et al. (2007). High-resolution profiling of histone methylations in the human genome. *Cell* 129, 823–837. doi: 10.1016/j.cell.2007.05.009

Baurain, D., Brinkmann, H., Petersen, J., Rodríguez-Ezpeleta, N., Stechmann, A., Demoulin, V., et al. (2010). Phylogenomic evidence for separate acquisition of plastids in cryptophytes, haptophytes, and stramenopiles. *Mol. Biol. Evol.* 27, 1698–1709. doi: 10.1093/molbev/msq059

Bernardes, J., Zaverucha, G., Vaquero, C., and Carbone, A. (2016). Improvement in protein domain identification is reached by breaking consensus, with the agreement of many profiles and domain co-occurrence. *PLoS Comput. Biol.* 12:e1005038. doi: 10.1371/journal.pcbi.1005038

Bernardes, J. S., Vieira, F. R., Zaverucha, G., and Carbone, A. (2016). A multi-objective optimization approach accurately resolves protein domain architectures. *Bioinformatics* 32, 345–353. doi: 10.1093/bioinformatics/btv582

Briggs, S., Bryk, M., Strahl, B. D., Cheung, W. L., Davie, J. K., Dent, S. Y. D., et al. (2001). Histone H3 lysine 4 methylation is mediated by set1 and required for cell growth and rDNA silencing in *Saccharomyces cerevisiae*. *Genes Dev.* 15, 3286–3295. doi: 10.1101/gad.940201

Burki, F., Okamoto, N., Pombert, J. F., and Keeling, P. J. (2012). The evolutionary history of haptophytes and cryptophytes: phylogenomic evidence for separate origins. *Proc. Biol. Sci.* 279, 2246–2254. doi: 10.1098/rspb.2011.2301

Carbon, S., and Mungall, C. (2018). Gene Ontology Data Archive. Zenodo doi: 10.5281/zenodo.2529950

Carradec, Q., Pelletier, E., Da Silva, C., Alberti, A., Seeleuthner, Y., Blanc-Mathieu, R., et al. (2018). A global ocean atlas of eukaryotic genes. *Nat. Commun.* 9:373. doi: 10.1038/s41467-017-02342-2341

Conway, J. R., Lex, A., and Gehlenborg, N. (2017). UpSetR: an R package for the visualization of intersecting sets and their properties. *Bioinformatics* 33, 2938–2940. doi: 10.1093/bioinformatics/btx364

Crump, N. T., and Milne, T. A. (2019). Why are so many MLL lysine methyltransferases required for normal mammalian development? *Cell Mol. Life Sci.* 76, 2885–2898. doi: 10.1007/s00018-019-03143-z

de Mendoza, A., Bonnet, A., Vargas-Landin, D. B., Ji, N., Li, H., Yang, F., et al. (2018). Recurrent acquisition of cytosine methyltransferases into eukaryotic retrotransposons. *Nat. Commun.* 9:1341. doi: 10.1038/s41467-018-03724-3729

Deshaies, R. J. (1999). SCF and Cullin/Ring H2-based ubiquitin ligases. *Annu. Rev. Cell Dev. Biol.* 15, 435–467. doi: 10.1146/annurev.cellbio.15.1.435

El-Gebali, S., Mistry, J., Bateman, A., Eddy, S. R., Luciani, A., Potter, S. C., et al. (2019). The Pfam protein families database in 2019. *Nucleic Acids Res.* 47, D427–D432. doi: 10.1093/nar/gky995

Ellis, E. M. (2002). Microbial aldo-keto reductases. *FEMS Microbiol. Lett.* 216, 123–131. doi: 10.1111/j.1574-6968.2002.tb11425.x

Even, S. (2011). *Graph Algorithms*. Cambridge: Cambridge University Press.

Frapporti, A., Miró, P. C., Arnaiz, O., Holoch, D., Kawaguchi, T., Humbert, A., et al. (2019). The Polycomb protein Ezl1 mediates H3K9 and H3K27 methylation to repress transposable elements in Paramecium. *Nat. Commun.* 10:2710. doi: 10.1038/s41467-019-10648-10645

Geisler, S. J., and Paro, R. (2015). Trithorax and Polycomb group-dependent regulation: a tale of opposing activities. *Development* 142, 2876–2887. doi: 10.1242/dev.120030

Gergonne, J. D. (1974). The application of the method of least squares to the interpolation of sequences. *Hist. Math. Hist. Math.* 1, 439–447. doi: 10.1016/0315-0860(74)90034-2

Gil, J., and O'Loghlen, A. (2014). PRC1 complex diversity: where is it taking us? *Trends Cell Biol.* 24, 632–641. doi: 10.1016/j.tcb.2014.06.005

Gornik, S. G., Ford, K. L., Mulhern, T. D., Bacic, A., McFadden, G. I., Waller, R. F., et al. (2012). Loss of nucleosomal DNA condensation coincides with appearance of a novel nuclear protein in dinoflagellates. *Curr. Biol.* 22, 2303–2312. doi: 10.1016/j.cub.2012.10.036

Harmanci, A., Rozowsky, J., and Gerstein, M. (2014). MUSIC: identification of enriched regions in ChIP-Seq experiments using a mappability-corrected multiscale signal processing framework. *Genome Biol.* 15:474. doi: 10.1186/s13059-014-0474-473

Hunter, T. (2009). Tyrosine phosphorylation: thirty years and counting. *Curr. Opin. Cell Biol.* 21, 140–146. doi: 10.1016/j.ceb.2009.01.028

Jensen, R. B., La Cour, T., Albrethsen, J., Nielsen, M., and Skriver, K. (2001). FYVE zinc-finger proteins in the plant model Arabidopsis thaliana: identification of

PtdIns3P-binding residues by comparison of classic and variant FYVE domains. *Biochem. J.* 359, 165–173. doi: 10.1042/bj3590165

Joazeiro, C. A., and Weissman, A. M. (2000). RING finger proteins: mediators of ubiquitin ligase activity. *Cell* 102, 549–552. doi: 10.1016/s0092-8674(00)00077-75

Kingston, R. E., and Tamkun, J. W. (2014). Transcriptional regulation by trithorax-group proteins. *Cold Spring Harb. Perspect. Biol.* 6:a019349. doi: 10.1101/cshperspect.a019349

Kyba, M., and Brock, H. W. (1998). The drosophila polycomb group protein Psc contacts ph and Pc through specific conserved domains. *Mol. Cell Biol.* 18, 2712–2720. doi: 10.1128/mcb.18.5.2712

Langmead, B., and Salzberg, S. L. (2012). Fast gapped-read alignment with Bowtie 2. *Nat. Methods* 9, 357–359. doi: 10.1038/nmeth.1923

Leevers, S. J., Vanhaesebroeck, B., and Waterfield, M. D. (1999). Signalling through phosphoinositide 3-kinases: the lipids take centre stage. *Curr. Opin. Cell Biol.* 11, 219–225. doi: 10.1016/s0955-0674(99)80029-80025

Margueron, R., and Reinberg, D. (2011). The Polycomb complex PRC2 and its mark in life. *Nature* 469, 343–349. doi: 10.1038/nature09784

Marinov, G. K., and Lynch, M. (2016). Conservation and divergence of the histone code in nucleomorphs. *Biol. Direct.* 11:18. doi: 10.1186/s13062-016-0119-114

Martin, I. V., and MacNeill, S. A. (2002). ATP-dependent DNA ligases. *Genome Biol.* 3:REVIEWS3005. doi: 10.1186/gb-2002-3-4-reviews3005

Mikulski, P., Komarynets, O., Fachinelli, F., Weber, A. P. M., and Schubert, D. (2017). Characterization of the polycomb-group mark H3K27me3 in unicellular algae. *Front. Plant Sci.* 8:607. doi: 10.3389/fpls.2017.00607

Mitchell, A., Chang, H. Y., Daugherty, L., Fraser, M., Hunter, S., Lopez, R., et al. (2015). The InterPro protein families database: the classification resource after 15 years. *Nucleic Acids Res.* 43, D213–D221. doi: 10.1093/nar/gku1243

Mitchell, A. L., Attwood, T. K., Babbitt, P. C., Blum, M., Bork, P., Bridge, A., et al. (2019). InterPro in 2019: improving coverage, classification and access to protein sequence annotations. *Nucleic Acids Res.* 47, D351–D360. doi: 10.1093/nar/gky1100

Ochoa, A., Llinas, M., and Singh, M. (2011). Using context to improve protein domain identification. *BMC Bioinform.* 12:90. doi: 10.1186/1471-2105-12-90

Palmieri, F., Pierri, C. L., De Grassi, A., Nunes-Nesi, A., and Fernie, A. R. (2011). Evolution, structure and function of mitochondrial carriers: a review with new insights. *Plant J.* 66, 161–181. doi: 10.1111/j.1365-313X.2011.04516.x

Poynter, S. T., and Kadoch, C. (2016). Polycomb and trithorax opposition in development and disease. *Wiley Interdiscip. Rev. Dev. Biol.* 5, 659–688. doi: 10.1002/wdev.244

Ramirez, F., Dundar, F., Diehl, S., Gruning, B. A., and Manke, T. (2014). deepTools: a flexible platform for exploring deep-sequencing data. *Nucleic Acids Res.* 42, W187–W191. doi: 10.1093/nar/gku365

Rastogi, A., Maheswari, U., Dorrell, R. G., Vieira, F. R. J., Maumus, F., Kustka, A., et al. (2018). Integrative analysis of large scale transcriptome data draws a comprehensive landscape of *Phaeodactylum tricornutum* genome and evolutionary origin of diatoms. *Sci. Rep.* 8:4834. doi: 10.1038/s41598-018-23106-x

Robinson, J. T., Thorvaldsdóttir, H., Winckler, W., Guttman, M., Lander, E. S., Getz, G., et al. (2011). Integrative genomics viewer. *Nat. Biotechnol.* 29, 24–26. doi: 10.1038/nbt.1754

Roudier, F., Ahmed, I., Bérard, C., Sarazin, A., Mary-Huard, T., Cortijo, S., et al. (2011). Integrative epigenomic mapping defines four main chromatin states in Arabidopsis. *EMBO J.* 30, 1928–1938. doi: 10.1038/emboj.2011.103

Ruthenburg, A. J., Allis, C. D., and Wysocka, J. (2007). Methylation of lysine 4 on histone H3: intricacy of writing and reading a single epigenetic mark. *Mol. Cell* 25, 15–30. doi: 10.1016/j.molcel.2006.12.014

Schapire, A. L., Valpuesta, V., and Botella, M. A. (2006). TPR proteins in plant hormone signaling. *Plant Signal. Behav.* 1, 229–230. doi: 10.4161/psb.1.5.3491

Schuettengruber, B., Bourbon, H. M., Di Croce, L., and Cavalli, G. (2017). Genome regulation by Polycomb and Trithorax: 70 years and counting. *Cell* 171, 34–57. doi: 10.1016/j.cell.2017.08.002

Schuettengruber, B., Chourrout, D., Vervoort, M., Leblanc, B., and Cavalli, G. (2007). Genome regulation by polycomb and trithorax proteins. *Cell* 128, 735–745. doi: 10.1016/j.cell.2007.02.009

Schuettengruber, B., Martinez, A. M., Iovino, N., and Cavalli, G. (2011). Trithorax group proteins: switching genes on and keeping them active. *Nat. Rev. Mol. Cell Biol.* 12, 799–814. doi: 10.1038/nrm3230

Sellers, P. (1980). The theory and computation of evolutionary distances: pattern recognition. *J. Algorith.* 1, 359–373. doi: 10.1016/0196-6774(80)90016-4

Shaver, S., Casas-Mollano, J. A., Cerny, R. L., and Cerutti, H. (2010). Origin of the polycomb repressive complex 2 and gene silencing by an E(z) homolog in the unicellular alga Chlamydomonas. *Epigenetics* 5, 301–312. doi: 10.4161/epi.5.4.11608

Sievers, F., Wilm, A., Dineen, D., Gibson, T. J., Karplus, K., Li, W., et al. (2011). Fast, scalable generation of high-quality protein multiple sequence alignments using Clustal omega. *Mol. Syst. Biol.* 7:539. doi: 10.1038/msb.2011.75

Strahl, B. D., and Allis, C. D. (2000). The language of covalent histone modifications. *Nature* 403, 41–45. doi: 10.1038/47412

Terrapon, N., Gascuel, O., Marechal, E., and Breehelin, L. (2009). Detection of new protein domains using co-occurrence: application to *Plasmodium falciparum*. *Bioinformatics* 25, 3077–3083. doi: 10.1093/bioinformatics/btp560

Thain, D., Tannenbaum, T., and Livny, M. (2005). Distributed computing in practice: the condor experience. *Concurr. Comput. Pract. Exp.* 17, 323–356. doi: 10.1002/cpe.938

Vartanian, M., Descles, J., Quinet, M., Douady, S., and Lopez, P. J. (2009). Plasticity and robustness of pattern formation in the model diatom *Phaeodactylum tricornutum*. *New Phytol.* 182, 429–442. doi: 10.1111/j.1469-8137.2009.02769.x

Veluchamy, A., Rastogi, A., Lin, X., Lombard, B., Murik, O., Thomas, Y., et al. (2015). An integrative analysis of post-translational histone modifications in the marine diatom *Phaeodactylum tricornutum*. *Genome Biol.* 16:102. doi: 10.1186/s13059-015-0671-678

Vidal, M. (2019). Polycomb assemblies multitask to regulate transcription. *Epigenomes* 3:12. doi: 10.3390/epigenomes3020012

Xing, H., Mo, Y., Liao, W., and Zhang, M. Q. (2012). Genome-wide localization of protein-DNA binding and histone modification by a Bayesian change-point method with ChIP-seq data. *PLoS Comput. Biol.* 8:e1002613. doi: 10.1371/journal.pcbi.1002613

Yeats, C., Redfern, O. C., and Orengo, C. (2010). A fast and automated solution for accurately resolving protein domain architectures. *Bioinformatics* 26, 745–751. doi: 10.1093/bioinformatics/btq034

Zhang, X., Bernatavichute, Y. V., Cokus, S., Pellegrini, M., and Jacobsen, S. E. (2009). Genome-wide analysis of mono-, di- and trimethylation of histone H3 lysine 4 in *Arabidopsis thaliana*. *Genome Biol.* 10:R62. doi: 10.1186/gb-2009-10-6-r62

Zhang, Y., Liu, T., Meyer, C. A., Eeckhoute, J., Johnson, D. S., Bernstein, B. E., et al. (2008). Model-based analysis of ChIP-Seq (MACS). *Genome Biol.* 9:R137. doi: 10.1186/gb-2008-9-9-r137

Conflict of Interest: The authors declare that the research was conducted in the absence of any commercial or financial relationships that could be construed as a potential conflict of interest.

frontiers in Marine Science

ORIGINAL RESEARCH
published: 21 April 2020
doi: 10.3389/fmars.2020.00205

Examining the Role of DNA Methylation in Transcriptomic Plasticity of Early Stage Sea Urchins: Developmental and Maternal Effects in a Kelp Forest Herbivore

Marie E. Strader†, Logan C. Kozal, Terence S. Leach, Juliet M. Wong, Jannine D. Chamorro, Madeline J. Housh and Gretchen E. Hofmann*

Department of Ecology, Evolution and Marine Biology, University of California, Santa Barbara, Santa Barbara, CA, United States

OPEN ACCESS

Edited by:
Hollie Putnam, University of Rhode Island, United States

Reviewed by:
Alexandre Fellous, Alfred-Wegener-Institute Helmholtz Center for Polar and Marine Research (AWI), Germany
Vittoria Roncalli, Stazione Zoologica Anton Dohrn, Italy
Reid S. Brennan, The University of Vermont, United States

***Correspondence:**
Marie E. Strader
stradermarie@gmail.com

†Present address:
Marie E. Strader, Department of Biological Sciences, Auburn University, Auburn, AL, United States

Specialty section:
This article was submitted to Marine Molecular Biology and Ecology, a section of the journal Frontiers in Marine Science

Received: *31 August 2019*
Accepted: *16 March 2020*
Published: *21 April 2020*

Citation:
Strader ME, Kozal LC, Leach TS, Wong JM, Chamorro JD, Housh MJ and Hofmann GE (2020) Examining the Role of DNA Methylation in Transcriptomic Plasticity of Early Stage Sea Urchins: Developmental and Maternal Effects in a Kelp Forest Herbivore. Front. Mar. Sci. 7:205. doi: 10.3389/fmars.2020.00205

Gene expression plasticity can confer physiological plasticity in response to the environment. However, whether epigenetic marks contribute to the dynamics of gene expression is still not well described in most marine invertebrates. Here, we explored the extent and molecular basis of intra- and intergenerational plasticity in the purple sea urchin, *Strongylocentrotus purpuratus,* by examining relationships between changes in DNA methylation, transcription, and embryo spicule length. Adult urchins were conditioned in the lab for 4 months to treatments that represent upwelling (~1200 μatm pCO_2, 13°C) and non-upwelling conditions (~500 μatm pCO_2, 17°C). Embryos spawned from conditioned adults were reared in either the same adult treatment or the reciprocal condition. Maternal conditioning resulted in significantly differentially methylated CpG sites and differential gene expression in embryos, despite no evidence of maternal effects on embryo spicule length. In contrast, conditions experienced during development resulted in significant differences in embryo spicule length. Intragenerational plasticity in spicule length was strongly correlated to transcriptomic plasticity, despite low levels of intragenerational plasticity in CpG methylation. We find plasticity in DNA methylation and gene expression in response to different maternal environments and these changes have similarities across broad functional groups of genes; yet exhibit little overlap on a gene-by-gene basis. Our results suggest that different forms of environmentally induced plasticity are observable across different time scales and that DNA methylation dynamics may be uncoupled from fast transcriptional responses to the environment and whole organism traits. Overall, this study illuminates the extent to which environmental differences can induce both intra- and intergenerational phenotypic plasticity in a common kelp forest herbivore.

Keywords: gene expression, DNA methylation, intragenerational plasticity, intergenerational plasticity, *Strongylocentrotus purpuratus*

INTRODUCTION

Epigenetics, a suite of biochemical modifications to nucleic acids and proteins, has recently been highlighted as a potential mechanism by which environmental signals might modify transcription and thus drive phenotypic plasticity (Feil and Fraga, 2012). Detailed empirical work in plants indicates that epigenetic variation contributes to complex traits and can shape ecological and evolutionary processes (Richards et al., 2017). In addition, theoretical models suggest the timing and outcome of adaptive evolution can be impacted by epigenetic changes that are stable, assuming epigenetic mutations are heritable (Klironomos et al., 2013; Kronholm and Collins, 2016; Banta and Richards, 2018). In an ecological context, it has been proposed that environmentally responsive epigenetic marks could contribute to adaptive plasticity, a field now termed 'environmental epigenetics' (Johannes et al., 2009; Torda et al., 2017; Eirin-Lopez and Putnam, 2019). In order to explore this, it is critical to understand how environmentally induced trait-based, organismal changes may be causally linked to changes in DNA methylation.

Environmental epigenetics has been examined in few marine invertebrate species (Marsh and Pasqualone, 2014; Ardura et al., 2017; Gavery and Roberts, 2017; Gonzalez-Romero et al., 2017; Li et al., 2017; Dixon et al., 2018; Liew et al., 2018; Baums et al., 2019; Hawes et al., 2019). While epigenetics can encompass a variety of non-genetic mechanisms such as histone modifications and small non-coding RNAs, the majority of marine environmental epigenetics research has focused on DNA methylation, in which cytosines, typically in a CpG dinucleotide context, contain a methyl group (Eirin-Lopez and Putnam, 2019). In invertebrates, DNA methylation is confined to gene regions and associated with broad transcriptional patterns, potentially functioning in controlling spurious transcription or fine-tuning of the transcriptome as a whole (Riviere et al., 2013, 2017; Gavery and Roberts, 2014; Saint-Carlier and Riviere, 2015; Dixon et al., 2018; Liew et al., 2018). Epigenetic marks can arise by spontaneous epimutation during replication or repair, similar to mutation in the DNA sequence itself, and persist across generations within a population, or they can be induced to change in response to the environment (Richards, 2008; Shea et al., 2011). Both population-specific and environmentally inducible DNA methylation are evident in reef-building corals (Dixon et al., 2018; Liew et al., 2018). In response to environmental cues, changes in DNA methylation may link to effects on gene expression that could drive phenotypic plasticity in a manner that could be beneficial or deleterious, although key questions remain on mechanisms that may promote these changes across generations, which are illustrated in Eirin-Lopez and Putnam (2019). If shifts in environmentally induced gene expression can occur from one generation to the next, this could be ecologically significant as organisms "tune" to their respective, dynamic environments. In *S. purpuratus*, there is evidence of intergenerational plasticity in DNA methylation (Strader et al., 2019), indicating a potential link between DNA methylation and phenotypic plasticity in response to environmental changes.

Strongylocentrotus purpuratus are ecologically and environmentally important grazing herbivores in kelp forests (Pearse, 2006). In this ecosystem, the California Current System (CCS) is characterized by considerable variation in temperature, dissolved oxygen, and pH both latitudinally and through upwelling events (Feely et al., 2008; Chan et al., 2017). The dynamics of upwelling are likely to intensify with anthropogenic global change (Sydeman et al., 2014; Bakun et al., 2015), which will occur simultaneously with increased sea surface temperatures and the rapid progression of ocean acidification (Gruber et al., 2012). In the Santa Barbara Channel, long-term oceanographic sensor data have greatly informed the abiotic dynamics of these systems, giving insight into the water conditions within kelp forest ecosystems and how they have changed through time (Kapsenberg and Hofmann, 2016; Rivest et al., 2016; Hofmann and Washburn, 2019; Hoshijima and Hofmann, 2019). These data show seasonal and spatial variability in abiotic conditions, often as a result of upwelling events that bring cold, low pH waters from offshore. Upwelling can occur throughout the year, with events typically reaching their peak frequency, duration and intensity during the late winter and spring months (Kapsenberg and Hofmann, 2016; Hoshijima and Hofmann, 2019). These events can vary in length from days to weeks and are interspersed with relaxed, non-upwelling conditions characterized by ambient pH levels and temperatures. This knowledge of the natural abiotic environment is valuable for understanding the relationships between the environment and resident organisms, facilitating the development of ecologically relevant experiments to examine inter- and intragenerational plasticity.

The combination of the dynamic nature of the CCS and *S. purpuratus* phenology may lead to variable and complex organism–environment interactions. The peak upwelling season overlaps with the reproductive cycle of *S. purpuratus* populations near the Santa Barbara coast, which typically undergo gametogenesis during the fall and winter before spawning in the months between January and July (Strathmann, 1987). Therefore, adult *S. purpuratus* can experience upwelling conditions during gametogenesis, and depending on the timing in which spawning occurs, early development of *S. purpuratus* embryos and larvae is likely to occur during upwelling as well. Furthermore, because upwelling events vary in their duration, the sudden appearance or disappearance of an event will influence the environmental conditions adults and their offspring experience respectively. Simulating upwelling or relaxed, non-upwelling conditions that *S. purpuratus* experience in their kelp forest environment within a laboratory setting is therefore highly pertinent for understanding and predicting inter- and intragenerational plasticity in nature.

Previous studies demonstrate both intra- and intergenerational plasticity in *S. purpuratus* in response to pCO_2 and temperature conditions associated with coastal upwelling. When *S. purpuratus* embryos and larvae developed under different pCO_2 levels, there was substantial intragenerational plasticity in body size (Padilla-Gamiño et al., 2013; Kelly et al., 2016). Some forms of intergenerational plasticity are evident as well. When adult *S. purpuratus* were acclimated to different

temperature and pCO_2 regimes during gametogenesis in the lab and in the field, there were maternal effects on either egg protein and lipid content, larval body size, gene expression, or DNA methylation (Wong et al., 2018, 2019; Hoshijima and Hofmann, 2019; Strader et al., 2019). While these previous studies on purple urchins provided valuable insight into the potential for inter- and intragenerational plasticity, the knowledge of how gene expression and DNA methylation interact within this system has yet to be elucidated.

Given previous work on inter- and intragenerational plasticity in urchins, we hypothesized that variation in DNA methylation patterns would be associated with variation in the transcriptome, either within or across generations, in response to end-member upwelling index conditions naturally experienced in kelp forest ecosystems. We measured the larval methylome and transcriptome in response to two different pCO_2 and temperature regimes experienced both during gametogenesis of the mothers and embryonic development of the offspring. In addition to assessing molecular-level changes that were induced by abiotic conditions, we measured embryonic spicule length as an organismal-level trait that might also vary with the experimental treatments. We found that variation in gene expression was largely driven by differences in developmental environments while variation in DNA methylation was largely driven by differences in maternal environments. Overall, this study identified plasticity of the transcriptome and the methylome as a result of environmental differences, but across different time scales, and maternal effects on DNA methylation and transcription likely target modulation of post-transcriptional and translational processes in the cell.

MATERIALS AND METHODS

Adult Urchin Conditioning

Adult purple sea urchins (*Strongylocentrotus purpuratus*, $N = 83$) were collected on September 20, 2017 off of Goleta Beach, CA, United States (34° 24.840′ N, 119° 49.742′ W), at a subtidal site near the University of California Santa Barbara (UCSB) under California Scientific Collection permit SC-1223. Urchins were transported to UCSB where they were held in flow-through seawater tables at ambient seawater conditions for 6 days. After this initial acclimation period, urchins were randomly assigned to one of two acclimation treatments, upwelling (U: 1390 ± 307 μatm pCO_2 and 12.7 ± 0.5°C) or non-upwelling (N: 631 ± 106 μatm pCO_2 and 16.8 ± 0.2°C) (**Table 1** and **Supplementary Figure 1**). These conditions represent end points of those experienced in their natural environment (Kapsenberg and Hofmann, 2016; Rivest et al., 2016). Each treatment was replicated across three 20-gal flow-through aquarium tanks with each holding 12 urchins. Conditioning of adults was maintained for just over 4 months and animals were fed locally collected kelp (*Macrocystis pyrifera*) once a week.

Adult acclimation conditions were controlled by a flow-through CO_2-mixing system (modified from Fangue et al., 2010) and Delta Star heat pumps regulated by Nema 4x digital temperature controllers (AquaLogic San Diego, CA, United States). Each treatment tank was fed water from two 20-gal glass reservoir tanks supplied with 0.35 μm-filtered, UV sterilized seawater (FSW) with a flow rate of 10 L/h (20 L/h total into each tank). Target pCO_2 levels were maintained in the reservoir tanks using mass-flow controllers (Sierra Instruments, United States) that mixed pure CO_2 with dry air that was filtered and CO_2 scrubbed.

TABLE 1 | Carbonate chemistry parameters for adult (U and N) and developmental (U and N) conditions.

	pH_{total}	pCO_2 (μatm)	Ω_{Arg}	Temperature (°C)
Adult Treatment Non-Upwelling (N)	7.89 ± 0.06	631 ± 106	1.92 ± 0.23	16.8 ± 0.2
Upwelling (U)	7.57 ± 0.09	1390 ± 307	0.92 ± 0.17	12.7 ± 0.5
Developmental Treatment				
Non-Upwelling (N)	7.94 ± 0.02	537 ± 28	2.18 ± 0.06	17.2 ± 0.3
Upwelling (U)	7.64 ± 0.03	1145 ± 87	1.07 ± 0.07	13.3 ± 0.3

The pCO_2 and Ω_{Arg} were calculated using measured pH, temperature, salinity and total alkalinity (TA). Average salinity and TA for the duration on the adult acclimation and culturing period was 33.2 ± 0.1 ppt and 2219.75 ± 6.41 μmol k^{-1}, respectively.

Seawater chemistry measurements in each tank were taken every 1–2 days throughout the adult acclimation period (**Table 1** and **Supplementary Figure 2**). Temperature and salinity were measured daily using an Omega HH81A thermocouple and YSI-3100 conductivity meter, respectively. pH was measured using a UV spectrophotometer (Shimadzu UV-1800) and *m*-cresol purple indicator dye (Sigma Aldrich) according to standard operating procedure (SOP) 6b (Dickson et al., 2007). Total Alkalinity (TA) was measured by titration following SOP 3b (Dickson et al., 2007). Water samples for total alkalinity were preserved prior to titration with 0.02% saturated mercuric chloride. CO_2 calc (Robbins et al., 2010) was used to calculate the carbonate chemistry parameters *p*CO2, Ωara, and Ωcal with the equilibrium constants from Hansson (1973) refit by Dickson and Millero (1987; **Table 1**).

Spawning and Developmental Culturing

On January 30th, 2018 spawning of the acclimated adult urchins was induced by injection of 0.53 M KCl into the coelom. Sperm was collected by pipetting from the area around the gonopores of male urchins kept out of water and stored dry in 1.5 mL tubes on ice until activation. Eggs were collected from each female by inverting the female over a beaker filled with FSW so that the gonopores were submerged. Eggs were checked visually for quality under a microscope and counted. Females with eggs of abnormal shape or color or significant numbers of eggs containing visible germinal vesicles were excluded. Sperm from potential males was activated in FSW, checked for motility, and then used to fertilize a subset of eggs from each female to ensure male-female compatibility. Eggs from 9 females per treatment (N or U) were pooled in equal numbers and fertilized with the sperm from one high quality non-upwelling conditioned male (**Supplementary Figure 1**).

As this study focused solely on maternal contributions to intergenerational plasticity, one male was used to sire all offspring to minimize the genetic diversity that might generate noise in the analysis. As such, all larvae in the experiment were a mix of full and half siblings. Dilute, activated sperm was slowly added to each pool of eggs until at least 95% fertilization was reached. The embryos from each treatment pool were divided into 3 non-upwelling culture vessels (N: 537 ± 28 μatm and 17.2 ± 0.3°C) and 3 upwelling culture vessels (U: 1145 ± 87 μatm and 13.3 ± 0.3°C) (**Table 1** and **Supplementary Figures 1, 2**) in a flow-through seawater system for a final concentration of 10 embryos/mL (120,000 embryos/vessel). Therefore, embryos were raised either in the same treatment as the maternal acclimation or the reciprocal condition. This yielded four treatment groups, each with 3 replicate culture vessels: embryos from mothers conditioned to non-upwelling raised under non-upwelling (NN), embryos from mothers conditioned to non-upwelling raised under upwelling (NU), embryos from mothers conditioned to upwelling raised under non-upwelling (UN), embryos from mothers conditioned to upwelling raised under upwelling (UU).

Temperature and pCO_2 conditions under which the embryos developed were maintained with the same CO_2 mixing system and heat pumps used in the adult acclimation. Two reservoir tanks fed 6 culture vessels per treatment (non-upwelling or upwelling developmental conditions) at a rate of 6 L/hr using irrigation drippers (DIG Corporation). Each culture vessel consisted of two nested buckets with a 12L capacity in which the inner bucket had holes covered with 30 μm mesh, allowing water to flow from the inner to the outer bucket and overflow without losing any embryos. Flow-through and mixing was aided in each bucket by an acrylic paddle attached to a 12V motor. Following the same methods outlined for the adult acclimation treatments, temperature and pH were measured daily for each culture vessel to confirm uniform conditions across each treatment. Salinity and TA were measured daily as well (**Table 1** and **Supplementary Figure 2**). Embryos were cultured in their respective treatments until the prism stage, an early echinopluteus larval stage, at which point they were sampled to assess morphometrics, DNA methylation, and transcription.

Larval Morphometrics

The prism stage was defined by the archenteron merging to one side of the body and becoming tripartite, the first development of skeletal rods, and a pyramid-like body shape. Prism larvae were preserved for morphometric analysis by adding 4% formalin buffered with 100mM $NaBO_3$ (pH 8.7) to an equal volume of larvae and FSW for a final concentration of 2% formalin. Samples of 1000 larvae were stored at 4°C until measured. Larvae were photographed on a compound microscope (Olympus BX50) with an attached digital camera (Motic 10 MP) using the Motic Images Plus software. Prism larvae were photographed from a lateral view where both the tip of the body rod and postoral rod were in focus. Photographs were calibrated to a stage micrometer. Spicule length was measured as the length from the tip of the body rod to the branching point of the postoral rod (N = 35 larvae/culture vessel) (**Supplementary Figure 4**). The effect of each fixed factor (maternal condition or developmental condition) on spicule length was examined using a 2-way ANOVA.

RRBS Sequencing and Pre-processing

Genomic DNA was extracted using an established CTAB protocol involving phenol chloroform purification. One sample per culture vessel was prepared for sequencing to generate 12 total samples (3 per treatment × 4 treatments). Each sample contained a pool of 6,000 larvae. Therefore, for each treatment, three replicates of 6,000 larvae were extracted and subsequently sequenced, totaling 18,000 larvae per treatment. In the case of the UU treatment, a missing sample from UU2 led us to process two unique pools (6,000 larvae each) of the UU3 culture. Integrity and quality of genomic DNA was assessed using gel electrophoresis and quantified using a Qubit fluorometer 3.0 (Life Technologies). Genomic DNA (∼2 μg per sample) was sent to the UC Davis Genome Center for RRBS library prep using the Diagenode Premium RRBS kit and sequencing on the Illumina 4000 with 50 bp single end reads across one lane of sequencing. Raw fastq sequences were trimmed and filtered using TrimGalore (V0.5.0)[1], which utilizes cutadapt (V1.9.1) (Martin, 2011), specifying the -rrrbs option that trims one additional bp from the 3′ end of the read as is recommended for RRBS data. This trimming package removes low quality base pairs from the 3′ end of the read (Phred score = 20), Illumina adaptors and short reads. Read quality was visualized using FastQC. Bisulfite treated trimmed reads were mapped to a bisulfite converted genome [*Strongylocentrotus purpuratus* genome (V3.1)] using Bismark (V0.19.1) (Krueger and Andrews, 2011). Methylation output files were produced by running the bismark_methylation_extractor command and summary files were produced by the bismark2summary command.

RRBS Analysis

Bismark coverage files were used for the subsequent analysis in the R environment (V3.4.2). Statistical analysis of CpG data was run using the package *methylKit* (Akalin et al., 2012). Samples were filtered by read coverage where base pairs with less than 10X coverage were removed as well as base pairs in the highest percentile (99.9). CpG sites were merged across samples into a methylBase object where base-pair locations were the same across all samples using the *unite* function. Two independent tests were run to identify differential methylation at each CpG site (DMCpG), one to determine DMCpGs by maternal condition (upwelling vs. non-upwelling) and a second by developmental condition (upwelling vs. non-upwelling). DMCpGs were identified using a logistic regression and significance was determined using p-values adjusted to q-values using a sliding linear model method (SLIM) (Akalin et al., 2012). A CpG was considered significantly differentially methylated (DMCpG) if the q-value < 0.01 and the difference in percent methylation was $>25\%$. Multivariate analyses were performed using percent methylation values for each CpG site. Principal coordinates analysis (PCoA) using Manhattan distances was performed using the packages *adegenet* (Jombart, 2008) and

[1]https://www.bioinformatics.babraham.ac.uk/projects/trim_galore/

vegan (Oksanen et al., 2013). To determine the proportion of variance explained by fixed factors a permutational multivariate ANOVA was run using the function *adonis*.

CpG annotation to genome features was performed using a custom R script. A CpG site was considered methylated if its median value across all samples was >1 (the site was methylated in over half of the samples). To examine percent methylation values per gene, genes with sequenced CpGs were filtered for those with at least 5 representative CpG sites within the gene region. The remaining genes had an average of 10.3 total CpGs represented within the gene region and percent methylation was calculated for each gene (methylated CpG sites/total CpG sites). Gene Ontology (GO) functional enrichment was performed using a Fisher's Exact test on genes that contained at least one DMCpG for either experimental treatment (maternal or developmental) compared to all genes using the GO_MWU package (Wright et al., 2015).

RNA Sequencing and Pre-processing

Total RNA was extracted using TRIzol reagent (Invitrogen). One sample per culture vessel was prepared for sequencing to generate 12 total samples (3 per treatment X 4 treatments). Each sample contained a pool of 6,000 larvae. RNA quality and quantity were assessed using the Agilent TapeStation and Qubit fluorometer 3.0 (Life Technologies), respectively, and all samples had RIN values >8.0. Total RNA (∼2 μg per sample) was submitted to the UC Davis Genome Center for poly A enriched, strand specific RNA library preparation and sequencing on the Illumina 4000 with 50bp single end reads across one lane of sequencing. Raw sequences were filtered for quality and adaptor sequences were discarded using TimGalore (V0.5.0)[1] which utilizes cutadapt (V1.9.1) (Martin, 2011). Trimmed reads were mapped to the *Strongylocentrotus purpuratus* genome (V3.1) using hisat2 (V2.0.0) (Kim et al., 2015). Gene counts were determined using *featureCounts*, a component of the subread package (V1.6.2) (Liao et al., 2014).

Differential Gene Expression Analysis and WGCNA

All statistical analyses were performed in R (V3.4.2). The package *arrayQualityMetrics* was used to identify potential sample outliers (Kauffmann et al., 2009). Gene normalization and models for differential gene expression analysis were performed using DESeq2 (Love et al., 2014). A Wald test [design = formula(∼ treat_maternal + treat_dev)] followed by pair-wise contrasts was run to identify differentially expressed genes (DEGs) associated with either maternal condition (upwelling vs. non-upwelling) or developmental condition (upwelling vs. non-upwelling). Multivariate analyses were performed using regularized log transformed gene count data. Principal coordinates analysis (PCoA) using Manhattan distances was performed using the packages *adegenet* (Jombart, 2008) and *vegan* (Oksanen et al., 2013). To determine the proportion of variance explained by fixed factors a permutational multivariate ANOVA was run using the function *adonis*.

Using only highly expressed genes (15,242 genes, mean counts >10), regularized log transformed counts data were used for a weighted gene co-expression network analysis (WGCNA) (Langfelder and Horvath, 2008). WGCNA analysis clusters genes in a manner that is un-biased toward the experimental design. A similarity matrix of gene expression was calculated using Pearson correlations for all gene pairs across samples and a "signed" network was specified, which allows the direction of the expression change to be retained. Using a power adjacency function and a soft thresholding power of 9, connectivities were transformed from the expression correlations. Genes were hierarchically clustered based on topological overlap which identifies groups of genes, or modules, whose expression covaried across samples. The minimum module size was set to 30 and similar modules were merged when their module eigengenes were highly correlated ($R > 0.80$). Experimental conditions and physiological larval trait data were then correlated to expression modules (**Supplementary Figure 5**). Gene Ontology (GO) enrichment analysis was performed for each module using a Fisher's Exact Test, by presence or absence of each gene within a module using the GO_MWU package (Wright et al., 2015).

RESULTS

Developing in Upwelling Conditions Reduced Spicule Length

In order to examine how plasticity in the methylome and transcriptome correlate to a plastic, organismal trait, we measured the effect of different conditions on spicule length, a trait associated with larval fitness that is known to be sensitive to high pCO_2 but not to temperature differences within the range manipulated in this experiment (Byrne et al., 2013; Padilla-Gamiño et al., 2013; Wong et al., 2018). For early life-history stages of echinoderms, the larval skeleton begins to form just following gastrulation (Okazaki, 1975) and is contingent on sufficient Ωara, and Ωcal to support biogenic calcification (Byrne et al., 2013). We found strong evidence that spicule length varied between development treatments ($p_{ANOVA} < 0.001$), but no evidence for intergenerational plasticity (**Supplementary Figure 4**). Specifically, developing under upwelling conditions (higher pCO_2 and lower temperature) reduced average spicule length by 30.8% relative to those that developed under non-upwelling conditions. Thus, in the case of this organismal trait, we observed that abiotic conditions experienced during development were more influential than the environmental history of the mothers during gametogenesis.

Changes in Environmental Conditions Induce Changes in DNA Methylation

To identify the potential for ecologically relevant abiotic conditions to induce changes in DNA methylation, either in an inter- or intragenerational plasticity context, we characterized the larval methylome using RRBS sequencing. DNA methylation sequencing yielded an average of 24,800,247 reads per sample across 12 samples (**Supplementary Table 1**), with an average

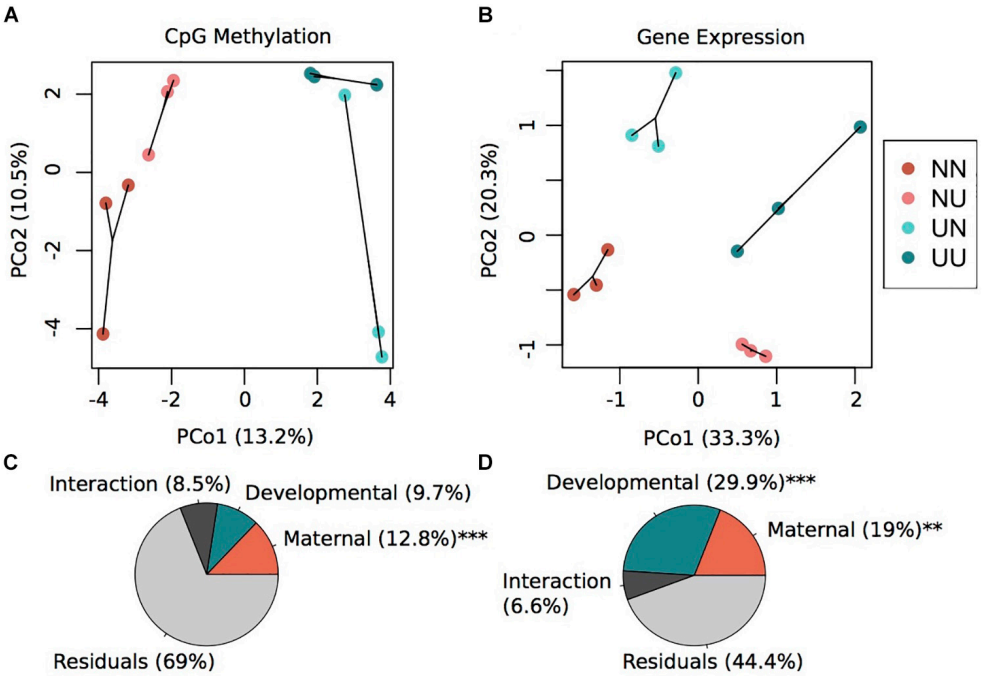

FIGURE 1 | Environmental conditions induce changes in gene expression and DNA methylation. Principal coordinate analysis of CpG methylation **(A)** and gene expression **(B)**. Variance explained by each principal coordinate is specified in the axes labels. Sample labels denote the maternal environment first and the developmental environment second. N, Non-Upwelling, U, Upwelling. Percentage of variation in CpG methylation **(C)** and gene expression **(D)** explained by fixed factors of maternal or developmental rearing environment using a permutational multivariate ANOVA. ***$p < 0.001$ and **$p < 0.01$.

bisulfite conversion rate of 98.92%. After adaptor trimming, read mapping to the bisulfite converted genome resulted in an average of 38.13% uniquely mapped reads and 23.44% ambiguously aligned reads (**Supplementary Table 1**). Bismark revealed 164,062,595 ± 9,335,444 SE total cytosine calls across all sequenced samples. Of these total calls, three different types of cytosine methylation were quantified, CpG (32,803,060 ± 1,885,036 SE), CpH (26,641,240 ± 1,496,753 SE), and CHH (104,619,294 ± 5,954,888 SE). Of these methylation calls, an average of 22.12% of CpGs were methylated, with 1.72% and 1.41% of CpHs and CHHs methylated, respectively (**Supplementary Table 1**). After filtering low coverage and high coverage CpG sites, read coverage per CpG site was 30.26 ± 0.962 SE and percent methylation per base was 22.95% ± 0.3957 SE (**Supplementary Table 1**). After filtering and sample merging, 245,343 CpG sites were shared across all samples, which were used for subsequent analysis.

Using this set of shared CpG sites, we sought to identify whether there were significant changes in the methylome associated with maternal or developmental conditioning. Logistic regression models revealed multiple differentially methylated CpGs. In the context of maternal effects, models found 684 DMCpGs total, with 328 hypermethylated and 356 hypomethylated sites in the methylome when mothers were conditioned in upwelling conditions compared to non-upwelling (**Supplementary Figure 3**). With regard to developmental conditioning, models found 216 DMCpGs total, with 175 hypermethylated and 41 hypomethylated sites when larvae developed in upwelling conditions compared to non-upwelling conditions (**Supplementary Figure 3**). Only 13 of these DMCpGs were significant for both maternal and developmental conditioning of which the majority were hypermethylated with regards to developmental conditioning and hypomethylated with regards to maternal conditioning (**Supplementary Figure 3**).

Principal coordinates analysis revealed that variation in maternal conditioning separated the samples along PCo1 while developmental conditioning separated samples along PCo2 (**Figure 1A**). A permutational multivariate ANOVA revealed that 12.8% ($p < 0.001$) of the variance in percent CpG methylation was explained by maternal condition while 9.7% (not significant) of the variance was explained by developmental condition (**Figure 1C**). The interaction between these two factors explained 8.5% of the variance, but was non-significant (**Figure 1C**). However, the majority of variance was not explained by any of the factors in the model, an outcome that is similar to methylation work in corals (Dixon et al., 2018; Baums et al., 2019), suggesting this remaining epigenetic variance may be driven by genetics or spontaneous epimutations. In summary, we found that maternal conditioning, the abiotic conditions that female urchins experienced during gametogenesis, resulted in more pronounced changes in the methylome than when embryonic development occurred in different abiotic conditions.

Genes With DMCpGs Are Associated With Specific Functions

In order to examine relationships between DMCpGs, transcription and environmental conditioning, we characterized gene bodies containing DMCpG sites. Research on DNA methylation in invertebrates has highlighted patterns between gene body methylation (GBM) and broad transcriptional patterns (Gavery and Roberts, 2013; Dixon et al., 2014, 2018). Therefore, we sought to identify genes with DMCpGs in comparisons of both maternal and developmental conditions. In addition, we performed functional enrichment tests, Gene Ontology (GO), to see if broad functional categories were over-represented in those genes. A total of 95,197 CpG sites were located within gene regions across 9,219 total genes and are further designated as gene specific CpGs (GS-CpGs). Across GS-CpG sites there was a strongly bimodal pattern in the percentage to which each site was methylated (**Supplementary Figure 6A**). For each GS-CpG site, we considered the site methylated if the site had methylated reads in over half of the samples (median > 1), a threshold that resulted in 41,940 methylated GS-CpG sites. Genes were filtered for only those that had at least five GS-CpG sites sequenced per gene, resulting in a total of 5,024 genes. Percentage methylation per gene also showed a bimodal pattern, with the majority of represented genes being 100% methylated (**Supplementary Figure 6B**).

We found a small fraction of total genes that contained DMCpGs. A total of 136 genes contained at least 1 DMCpG for maternal condition while 49 genes contained at least 1 DMCpG for developmental condition. Overall, a total of 258 DMCpGs were also GS-CpGs across 177 unique genes (**Supplementary Table 2**). Notably, the majority of these 177 genes include those that function in protein modification including hydrolase activity (Sp-Vps35, Sp-Abhd3, Sp-Abhd3, Sp-Asah2L3), protein phosphorylation (Sp-Dusp6/7/9, Sp-Mekk4a, Sp-Melkl, Sp-Frap_1, Sp-Ck1g), and ubiquitination (Sp-Ube3cL, Sp-Uba1, Sp-Traf3). In addition to genes with protein modification processes, there were also genes involved in binding (Sp-Myef2, Sp-Z371, Sp-Z163, Sp-Ciz, Sp-Traf3, Sp-Pcbp2) and modification of nucleic acids (Sp-Endrvt33, Sp-Tsen34L_1). Cytoskeletal components such as myosin and kinesin are also represented across all genes containing DMCpGs (Sp-Non/MmyIIhcph, Sp-Unk_109, Sp-Krp85_1, Sp-Kif13A2, Sp-Kif1a, Sp-Kif13BL) as well as DNA binding proteins such as transcription factors (Sp-FoxK, Sp-Mlxip, and Sp-Myc) (**Supplementary Table 2**). GO enrichment tests were run on genes with DMCpGs for maternal condition, developmental condition, and all genes containing a DMCpG. Only tests for maternal DMCpG genes and all genes yielded significant GO enrichments, with the majority of the terms being the same (**Supplementary Table 3**). Among all genes with DMCpGs, there was significant GO enrichment of terms that reflect functions mentioned above including endonuclease activity (GO:0004519), endopeptidase activity (GO:0004175), DNA metabolic processes (GO:0006259), and kinesin complex (GO:0005871), among others (**Supplementary Table 3**). It should be noted that due to the low representation of genic CpGs in our RRBS data, we are missing what could be key information about CpG methylation in gene regions. Therefore, future studies should further examine CpG methylation across gene regions using a whole genome bisulfite sequencing approach. However, this dataset reveals what could be important genes and functional categories associated with DNA methylation in sea urchins. In summary, we identified multiple genic CpGs that varied by environmental context, particularly maternal, with functions indicative of DNA integration, modification and turnover of proteins and nucleic acids as well as cytoskeletal components.

Environmental Conditions Induced Both Intra- and Trans- Generational Plasticity in Gene Expression

To further examine potential connections between environmentally induced changes in DNA methylation and plastic phenotype, such as spicule length, we also sequenced transcriptomes of prism stage embryos. RNA sequencing yielded an average of 29,722,500 reads per sample across 12 samples (**Supplementary Table 1**). After size and quality trimming, an average of 29,713,377 reads per sample remained. Trimmed reads were mapped to the *Strongylocentrotus purpuratus* genome (V3.1) with an average mapping efficiency of 62.1%. Mapped reads were converted to gene counts across 30,284 gene meta-features with an average of 7,897,000 counts per sample (**Supplementary Table 1**). The outlier detection package, *arrayQualityMetrics*, did not detect any sample outliers so all were retained. Genes with low mean counts (less than 3) were discarded from further analysis, leaving 18,015 genes total.

DESeq2 models revealed significant differentially expressed genes for both maternal and developmental conditions. Differences in maternal environment resulted in 1,811 DEGs while developmental environment resulted in 3,765 DEGs (FDR < 0.05), with 645 DEGs overlapping between the two factors (**Supplementary Figure 3**). PCoAs of gene counts revealed strong differences in gene expression between each of the four treatments where developmental condition separated variation along PCo1 and maternal condition separated variation along PCo2 (**Figure 1B**). A permutational multivariate ANOVA revealed that 29.9% ($p = 0.001$) of the variation in gene expression was explained by developmental condition while 19% ($p = 0.002$) was explained by maternal condition (**Figure 1D**). The interaction between the two factors explained 6.6% of the variation, although this was not significant. Overall, a large proportion of the prism-stage transcriptome was responsive to different environmental conditions; this is not likely due to developmental delay as staging was performed using developmental cues not body size.

Gene Expression Modules Strongly Correlated With Environmental Conditions and Spicule Length

To characterize environmentally responsive transcriptional changes, we performed a weighted gene co-expression network analysis (WGCNA). WGCNA revealed 12 gene expression modules with all showing significance for at least one experimental treatment or physiological trait (**Supplementary Figure 5**). Each module contained between

2,676 (turquoise) and 84 genes (royalblue) and the majority of modules showed significant enrichment of GO categories. Significant modules were binned as either strongly representative of changes due to developmental condition (turquoise, pink, red, black, and yellow) (**Figure 2**) or maternal condition (lightyellow, cyan, royalblue, lightgreen, blue, and red) (**Figure 3**). There was a trend for maternal modules to have a higher percentage of genes with DMCpGs in them, although this trend was not significant (**Supplementary Figure 5**). The red module represents genes that show significant correlations for both experimental treatments and therefore represents interaction genes, however, there was no significant enrichment of GO terms within this module (**Supplementary Table 4**).

Developmental modules include those with genes that were up-regulated when embryos were reared in upwelling as compared to non-upwelling conditions (turquoise and pink, **Figure 2**) and those with genes that were down-regulated when reared in upwelling as compared to non-upwelling (black, **Figure 2**). The turquoise and pink modules show enrichment of GO categories associated with RNA processing, methylation and metabolic processes, as well as cellular response to stress and growth. In contrast, genes in the black module show larvae reared under upwelling conditions down-regulated multiple neurological and signaling processes, suggesting these physiological processes are suppressed under upwelling stress. Calcium ion binding genes were also reduced when larvae were reared in upwelling conditions, which correlate strongly with the noticeable reduction in spicule length of these embryos (**Supplementary Figure 4**). The yellow module showed no significant enrichment of GO terms (**Supplementary Table 4**).

Of the modules associated with differences in maternal environment, only two of them showed significant enrichment of GO terms, the cyan and blue modules (**Figure 3**). The cyan module represents genes down-regulated in larvae when mothers were reared in upwelling conditions and includes changes in DNA replication and metabolic processes (**Figure 3B**). The blue module represents genes upregulated in larvae when mothers were reared in upwelling conditions and also includes GO categories associated with DNA metabolism, translation and hydrogen ion transport.

Few Genes Exhibit Both Differential Expression and DMCpGs in Response to Environmental Conditions

Due to environmental effects on DNA methylation, transcription, and spicule length, we further examined patterns that might indicate causality. Percent methylation values per gene were associated with overall gene expression. There was a strong significant correlation between mean gene expression counts and percent methylation (Adjusted R^2 = 0.1836, p_{lm} < 2.2e–16) (**Supplementary Figure 7**). A total of 3,359 genes had >5 sequenced CpG sites and gene expression counts >3. However, there was little association between differences in GS-CpG methylation and differential expression of genes (**Figures 4**, **5**). Differential gene expression was evident in both genes with low methylation as well as high methylation (**Figure 4**); however, DEGs showed higher $\log_2$FC differences amongst lowly methylated genes, particularly when considering differences in maternal treatment (**Figure 4B**). Genes with DMCpGs were almost exclusively those with high methylation, regardless of experimental treatment (**Figure 4**). There was a significant negative relationship between developmental DEGs and percent methylation; lowly methylated genes were more likely to be upregulated when larvae were reared under upwelling conditions (R^2 = 0.11, p_{lm} < 0.001, **Figure 4A**).

There was some overlap between genes with DMCpGs and DEGs from the DESeq2 models in response to the treatments (**Figure 5**). Of the 136 genes with maternal DMCpGs, 12 were differentially expressed with respect to maternal environment and 22 were differentially expressed with respect to developmental environment (**Figure 5** and **Supplementary Table 5**). Of the 49 genes with developmental DMCpGs, 5 were differentially expressed with respect to maternal environment and 12 were differentially expressed with respect to developmental environment (**Figure 5** and **Supplementary Table 5**). Overall, very few individual genes exhibited both differential expression and DMCpGs, suggesting it is unlikely that changes in DNA methylation at the level of gene bodies impart regulatory control on transcription, at least across the time frames examined in this study.

DISCUSSION

Intragenerational and intergenerational plasticity of physiological and molecular traits in response to global change are well characterized in many marine systems (Marshall, 2008; Munday, 2014; Donelson et al., 2017), including in *S. purpuratus* (Wong et al., 2018, 2019; Hoshijima and Hofmann, 2019; Strader et al., 2019). However, molecular pathways that underlie phenotypic plasticity in response to global change are not well understood. We hypothesized that environmentally induced changes in DNA methylation variation may play a role in transcriptional change in response to the environment, and that this would correspond to changes in a known phenotypically plastic trait, spicule length (Byrne, 2011; Byrne et al., 2013). Overall, this study found that environmental differences impacted plasticity of the transcriptome and the methylome, but across different time scales, and that DNA methylation variation within gene bodies is not likely to modulate transcription directly, despite similarities in broad functional categories between DEGs and genes with DMCpGs. To explore the significance of these patterns further, below we discuss: (1) differences in timing of changes and the relationship between DNA methylation and the transcriptome, (2) maternal effects on gene expression and DNA methylation, (3) how conditions during development affect phenotype and gene expression, and (4) potential consequences of epigenetic mechanisms on intergenerational plasticity.

Differences in Time Scale of Response Between GE and DMCpGs

The transcriptome is highly sensitive to environmental differences, ultimately changing organismal traits from the

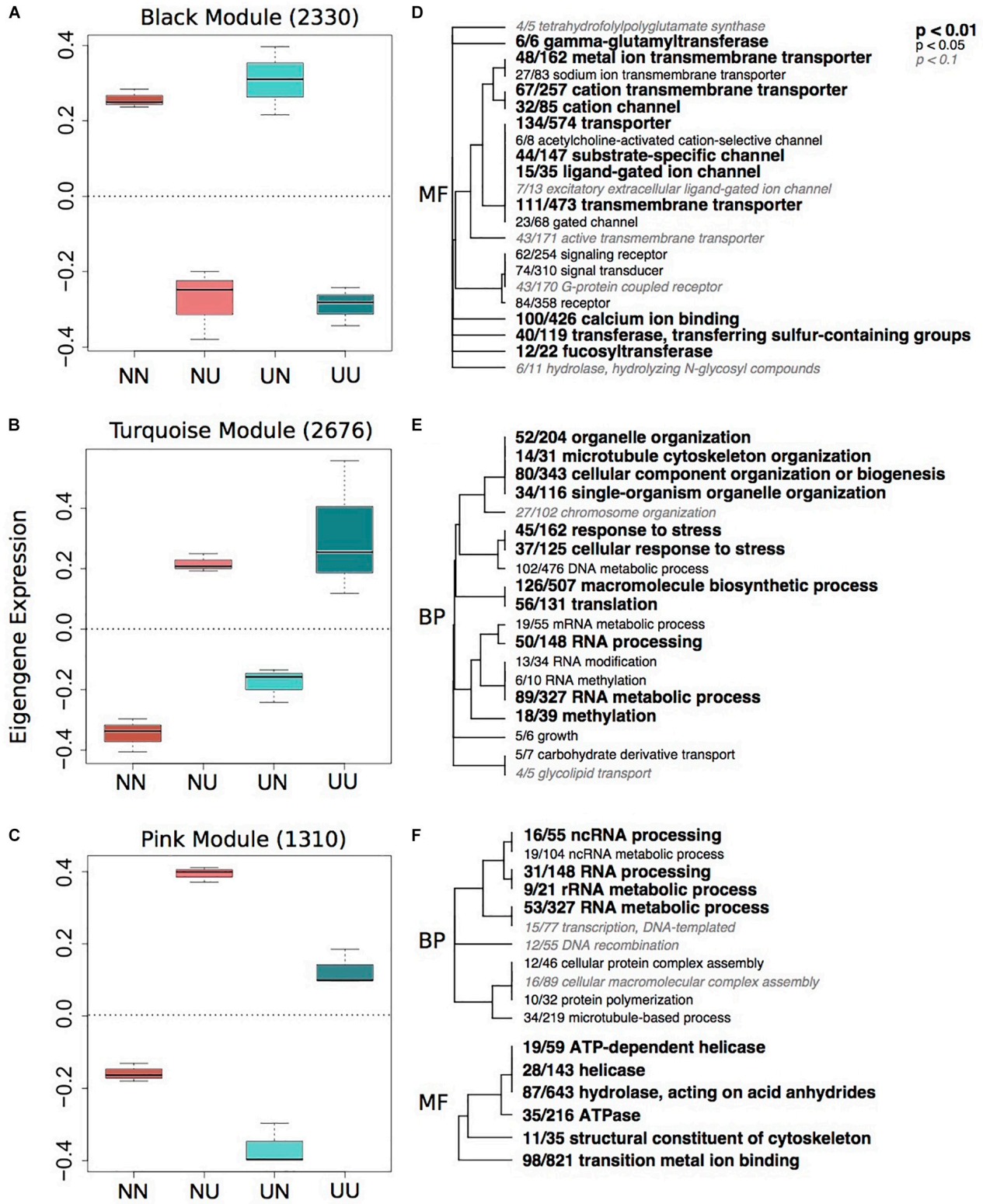

FIGURE 2 | Gene expression modules strongly correlated to developmental environment. Boxplots of eigenegene expression for the black **(A)**, turquoise **(B)**, and pink **(C)** modules. The number of genes represented in each module is in parentheses. Hierarchical clustering of Gene Ontology (GO) terms showing significant enrichment in the black **(D)**, turquoise **(E)** and pink **(F)** modules. Level of significance indicated with bold text. BP, biological processes; MF, molecular function.

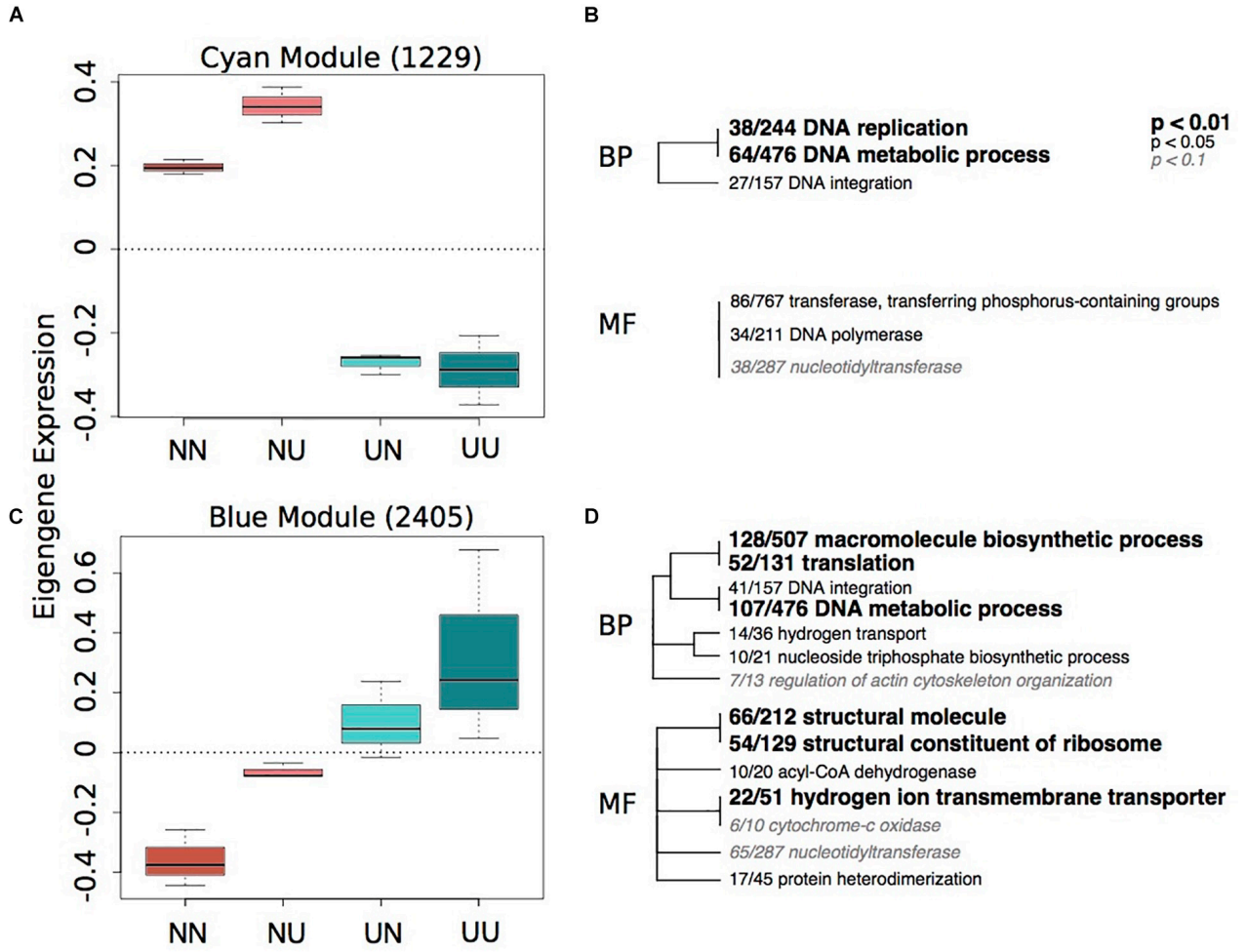

FIGURE 3 | Gene expression modules strongly correlated to maternal environment. Boxplots of eigenegene expression for the cyan **(A)** and blue **(C)** modules. The number of genes represented in each module is in parentheses. Hierarchical clustering of Gene Ontology (GO) terms showing significant enrichment in the cyan **(B)** and blue **(D)** modules. Level of significance indicated with bold text. BP, biological processes; MF, molecular function.

molecular level up to higher-level processes such as behavior. Environmental perturbations can induce substantial changes in the transcriptome within short time frames (on the scale of minutes). These fast reaction times are necessary to alter cellular machinery in response to change. DNA methylation, on the other hand, is relatively stable and while able to change in response to the environment, does so at a lesser magnitude than gene expression and across longer time scales. Therefore, in the context of our experimental design, we see the biggest differences in larval CpG methylation when mothers were conditioned in different environments for 4 months, while the developmental treatment was only ∼72 h. Because of the stability and proposed functions of DNA methylation in gene regions, modulating CpG methylation during periods of short-term environmental differences is not likely to be an evolutionarily favored response, since short-term stress might not be indicative of persistent environmental change. Longer-term chronic environmental differences, such as maternal conditioning in the current experiment, may be more predictive of the future environment, so modulation of DNA methylation in response to this may be an adaptive response that occurs across longer time scales and generations.

In this experiment, we chose to use conditions representative of upwelling, which is variable and periodic in the Santa Barbara Channel. This design employed was intentionally simplified from the *in situ* environmental conditions in an attempt to identify the potential for environmentally induced methylation and gene-expression changes and query any mechanistic relationship between methylation changes driven by the maternal and developmental environment and any corresponding change in transcription. Through field experiments, we know that even variable *in situ* conditions can drive maternal effects (Hoshijima and Hofmann, 2019). Therefore, going forward it will be important to investigate whether offspring DNA methylation patterns are modulated in response to non-static maternal conditioning or if the induction of methylation changes is dependent upon the predictability of the environmental changes (Burgess and Marshall, 2014).

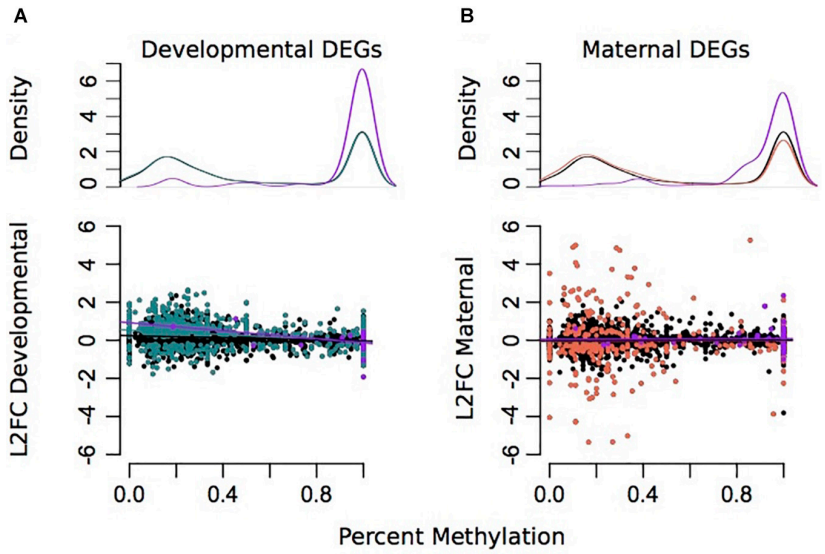

FIGURE 4 | Associations between differential gene expression and percent methylation for comparisons between developmental **(A)** and maternal **(B)** environments. The *Y*-axis represents the log2 fold change for each comparison. The *X*-axis represents the percent methylation for each gene. Gray dots represent each gene. Turquoise genes represent DEGs by developmental environment (FDR < 0.05) and coral genes represent DEGs by maternal environment (FDR < 0.05). Purple genes denote DEGs with differentially methylated CpGs.

Relationship Between DNA Methylation and the Transcriptome

Mechanisms connecting DNA methylation with transcription are less well understood in invertebrates with sparsely methylated genomes as opposed to vertebrate systems where promoter methylation is able to directly alter transcription and downstream phenotypes (reviewed in Li and Zhang, 2014). Generally, gene body methylation is positively correlated with gene expression levels across invertebrate taxa (Zemach et al., 2010) including, bivalves (Gavery and Roberts, 2013; Wang et al., 2014), ascidians (Suzuki et al., 2007), and social insects (Bonasio et al., 2012; Sarda et al., 2012; Wang et al., 2013; Patalano et al., 2015). In corals specifically, it has been suggested that DNA methylation fine tunes gene expression in response to environmental change via reduction in spurious transcription (Li et al., 2017; Liew et al., 2018), genome-wide balance of gene expression (Dixon et al., 2018) and through shaping codon usage over evolutionary time scales (Dixon et al., 2016). Similar studies have been shown in oysters as well (Gavery and Roberts, 2010; Roberts and Gavery, 2012; Wang et al., 2014; Jiang et al., 2015; Saint-Carlier and Riviere, 2015). While these functions are not mutually exclusive, consensus on how actively DNA methylation regulates transcription in response to environmental change is not well agreed upon across many invertebrate systems. That being said, our data is suggestive that DNA methylation changes in genes rarely correspond to gene expression on a gene by gene level, despite broad genome-wide patterns: similarly enriched GO terms are found between DEGs and genes with DMCpGs associated with different maternal environments, highly methylated genes are more likely to be highly transcribed, and genes with DMCpGs are always highly methylated.

There is contention as to whether gene expression or DNA methylation imparts control on the other. While the overall magnitude of gene expression responses to environmental conditions is larger, there was a stronger influence of maternal conditioning on DNA methylation than of the abiotic conditions under which the embryos developed. This might suggest that maternally mediated changes in DNA methylation may translate to differential expression in offspring. However, we found minimal overlap between maternally driven differences in DNA methylation and transcription of those genes in their offspring; the majority of genes with DMCpGs by maternal condition were not differentially expressed. However, genes with DMCpGs showed functional enrichment of DNA metabolic processes and DNA integration (**Supplementary Table 3**), similar to terms enriched in modules showing strong correlation with maternal conditions (**Figure 3** and **Supplementary Table 4**). This is evidence that while there are environmentally inducible changes in both CpG methylation and gene expression, they appear to be only broadly linked. This suggests that environmentally induced changes in DNA methylation may play a different functional role on a cellular level than regulating transcription directly as is observed in vertebrate systems, potentially through controlling spurious transcription. However, it should be noted that the reduced representation approach limits our ability to examine methylation patterns in all genes and a full genomic picture connecting transcription and DNA methylation is warranted.

While the focus of our study was to examine the role of DNA methylation in response to environmental conditions, it is worth noting that DNA methylation is also believed to be necessary to ensure successful development in invertebrates (Regev and Lamb, 1998; Riviere et al., 2013). Indirect evidence of this in sea urchins includes observations that DNA methylation of broad

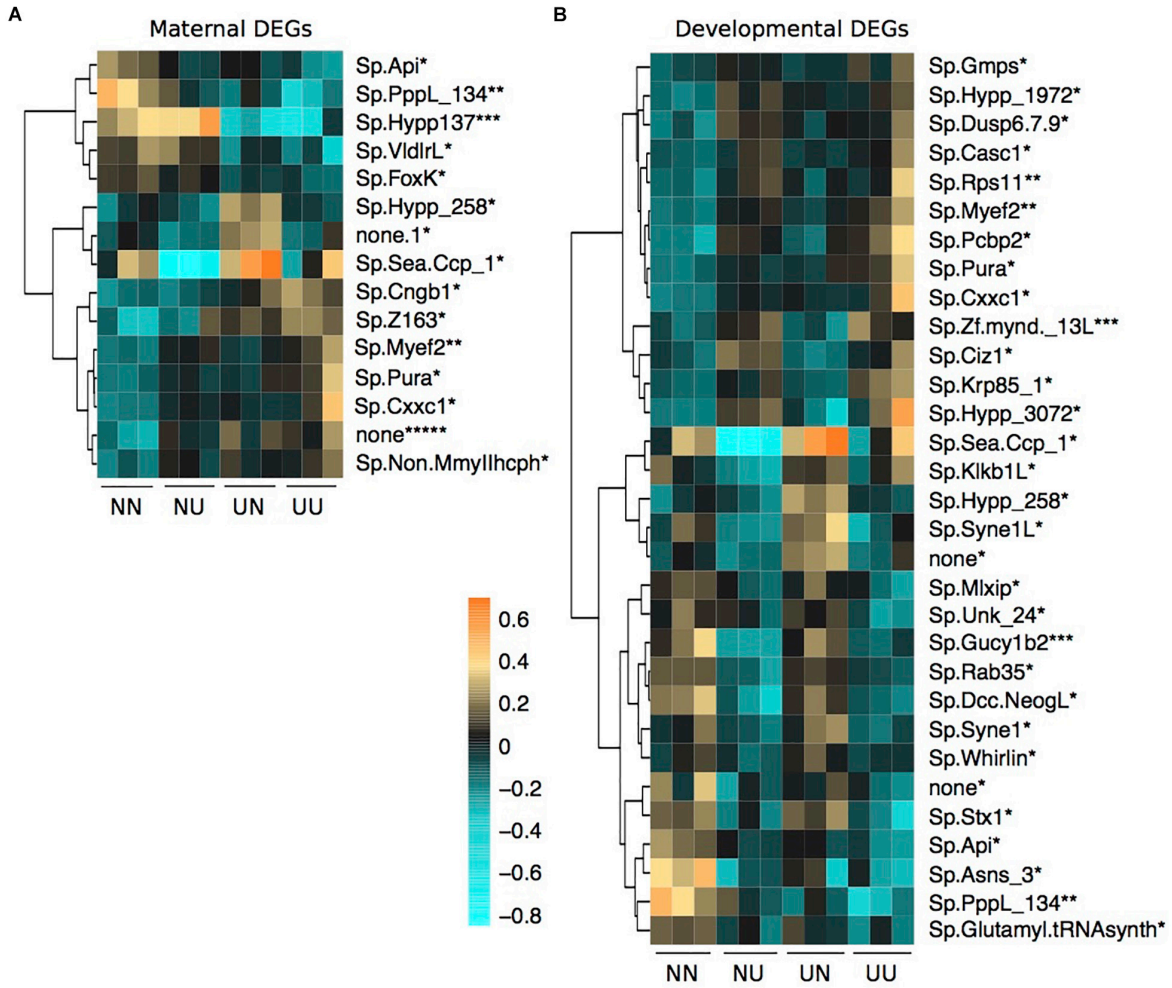

FIGURE 5 | Differentially expressed genes by maternal environment **(A)** and developmental environment **(B)** containing differentially methylated CpGs. Asterisks by each gene name denote the number of DMCpGs within that gene region. Scale is log2fold change relative to the gene mean.

functional groups and developmentally regulated genes vary by life history stage in *S. purpuratus* (Fronk et al., 1992; Strader et al., 2019). Additionally, DNA methyltransferase activity has been shown to change dramatically during the early development of the sea urchin *Sphaerechinus granularis* (Tosi et al., 1995). Treatment with 5-azacytidine, a nuclear methylation inhibitor, at any stage prior to blastula inhibits development beyond the blastula stage in sea urchin embryos, *Paracentrotus lividus* and *Sphaerechinus granularis*, causing embryos to arrest at the blastula stage though some continue to develop spicules with no other morphological change (Crkvenjakov et al., 1970; Maharajan et al., 1986). Although details regarding the specific role that DNA methylation plays in sea urchin development are generally lacking, there is evidence that it is critical to the development of other invertebrates such as the oyster, *Crassostrea gigas* (Riviere et al., 2013), the wasp, *Nasonia vitripennis* (Zwier et al., 2012), and the ascidian, *Phallusia manzmilata* (Maharajan et al., 1986). Thus, in order for development to proceed successfully, we might expect certain limitations on how much DNA methylation can change in developing embryos and larvae. Our previous work showed minimal differential methylation in *S. purpuratus* as a function of developmental conditions (Strader et al., 2019), although the experiment included developmental environments that only varied by pCO_2 level. In this study, the combined temperature and pCO_2 levels of our non-upwelling versus upwelling developmental treatments resulted in differential methylation, but to a lesser extent than the effects of maternal environment on differential methylation. Therefore, some alterations in DNA methylation can occur in response to external factors in spite of potential constraints on methylation during early development, although this likely varies by the multitude and intensity of the environmental stressor(s).

Maternal Effects on Gene Expression and CpG Methylation

The blue module shows an upregulation of genes associated with hydrogen ion transmembrane transporters and hydrogen

transport when larvae had mothers that were reared in upwelling conditions. This suggests that there is a strong maternal effect of these genes, potentially priming these larvae to express more H^+ transporters in the high pCO_2 environment associated with the upwelling treatment. While extracellular tissue in larval urchins maintains the pH of the environment, there is internal control of pH within intracellular compartments, including those surrounding the principal calcifying cells. This internal control is mediated by transporters that regulate the concentrations of H^+ and HCO_3^- ions on either side of the membrane (Evans et al., 2013). Several studies on gene expression responses to high pCO_2 in larval urchins and other marine invertebrates find either no differential expression or downregulation of hydrogen ion transporters (Todgham and Hofmann, 2009; Moya et al., 2012; Evans and Watson-Wynn, 2014). These studies, however, were all performed by exposing early life-history stages to different pCO_2 environments, similar to the developmental treatment in the present study, which found no differential expression of H^+ transporters in response to upwelling developmental conditions (**Figure 2** and **Supplementary Table 5**). This suggests that modulation of H^+ transporters is not likely a fast response to environmental change, as in, within the course of embryonic and larval development. However, longer-term exposure of adult urchins to high pCO_2 and low temperatures (upwelling) can impart an upregulation of these genes that are important in maintaining the balance between H^+ and HCO_3^- ions in offspring. The upregulation of these genes, however, does not seem to generate a benefit to the larvae when exposed to upwelling conditions themselves with regards to larval spicule length (**Supplementary Figure 4**) and expression of cellular stress response genes (**Figure 2**).

Black and cyan modules showed enrichment of genes associated with DNA metabolic processes, macromolecule biosynthetic processes and DNA integration, suggesting overall differential regulation of these processes when mothers are exposed to different conditions. Functional enrichment of genes with DMCpGs, the majority differentially methylated with respect to maternal environment, also reveals enrichment of DNA integration, macromolecule biosynthetic processes, and DNA metabolic processes, among others (**Supplementary Table 3**). Despite similarities in GO terms, maternal modules did not contain more genes with DMCpGs than developmental modules (**Supplementary Figure 5**) and there were very few genes that exhibited both DMCpGs and DEGs by maternal condition (12 genes, **Supplementary Table 5**). The result that maternal responses to upwelling imparted differential methylation and expression in genes with similar functionality suggests that modulating the activity of these genes may be a critical long-term response to upwelling conditions. While there are caveats in extrapolating GO categories from only a subset of genes with sequenced CpGs, in *Aiptasia* sea anemones, similar GO categories are enriched in DM genes, including "DNA-dependent DNA replication" and "DNA integration" (Li et al., 2017), the same top GO category enriched for genes with DMCpGs in this dataset (**Supplementary Table 3**). DNA integration is the process by which one segment of DNA is inserted into another, one example being transposable elements. Epigenetic and transposable elements strongly interact with each other and both can lead to changes in phenotypes and genotypes in response to stress (Rey et al., 2016). For example, epigenetic components are key in repressing transposable element activity. Therefore, it is possible that interactions between DNA methylation and transposable elements can drive rapid changes in phenotypes in response to global change across short time scales in taxa other than vertebrates and plants (Rey et al., 2016). Our results, as well as others reporting differential methylation of genes associated with DNA integration, posit that more research into potential effects of transposable elements on rapid phenotypic change is warranted in marine systems exposed to a global change multi-stressor scenario. In addition, DNA methylation can impact phenotypes by changing the mutability of gene sequences, which has been suggested to impact codon bias evolution (Dixon et al., 2016). These mechanisms might be better representative of downstream effects of environmentally induced changes in DNA methylation than directly changing transcription in invertebrates with sparsely methylated genomes.

Embryonic Development in Upwelling Conditions Imparts Phenotypic and Transcriptomic Signatures of Abiotic Stress

The developmental environment had a more marked impact on spicule length and the transcriptome than did the adult environment during gametogenesis (**Figure 1** and **Supplementary Figure 4**). This is in contrast to a previous study in *S. purpuratus* in which the maternal environmental conditions appeared to have a greater impact on the offspring phenotype and transcriptome than the conditions during development (Wong et al., 2018). This dissimilarity could be in part due to differences in developmental stage, as organismal responses to the environment have been shown to vary greatly by developmental stage (Kurihara, 2008; Ross et al., 2011; Byrne, 2012). Wong et al. (2018) examined the body size and transcriptomic patterns of the gastrula stage, during which major developmental landmarks distinguish this from later larval stages. Another noteworthy distinction is that in Wong et al. (2018), the embryos were raised under two different conditions that only varied by a single abiotic factor: pCO_2 level. In the study presented here, combinations of both temperature and pCO_2, intended to reflect ecologically relevant upwelling or non-upwelling conditions, were manipulated during early development so as to generate similar or reciprocal treatments as the adults experienced. Thus, the dominance of phenotypic and transcriptomic plasticity as a result of developmental conditions may be a result of the inclusion of temperature as a factor during development, or due to the multi-stressor nature of including combinations of different temperature and pCO_2 levels.

Offspring that were reared in upwelling conditions exhibited phenotypic and transcriptomic patterns associated with a response to stress (**Figure 2** and **Supplementary Table 4**). In concert with this stress response, there was an up-regulation

of numerous RNA modification processes as well as processes involved in translation and potentially post-translational modifications (protein polymerization). For example, one gene in the turquoise module, also with a significantly differentially methylated CpG (**Figure 5B**), Sp.Dusp6.7.9, is known to be involved with protein dephosphorylation. Finally, there was also upregulation of genes involved in carbohydrate and lipid transport. These results strongly suggest larvae reared in upwelling conditions exhibit a stress response and a potential reallocation of energy resources, mostly likely to maintain calcification and growth. Larvae reared in upwelling conditions also exhibit a significant reduction in spicule length compared to those reared in non-upwelling conditions (**Supplementary Figure 4**). Differences in RNA metabolic and processing pathways suggest an attempt to modulate cellular functions in response to upwelling stress. In addition, the majority of DMCpGs were hypermethylated in the upwelling condition compared to the non-upwelling condition, which is a similar response to other organisms exposed to pH stress (Liew et al., 2018). Overall, these results show clear compensatory mechanisms in response to upwelling stress.

Stress as a result of developing under the simulated upwelling treatment could be due to low pH, low temperature, or the combination of both. In regards to low pH environments, sea urchin species have generally been shown to display reduced skeletal growth and calcification (Kurihara and Shirayama, 2004; Clark et al., 2009; Dupont et al., 2010; Byrne and Przeslawski, 2013), similar to what we found in this study. The increased expression of genes related to calcium homeostasis has been suggested as a means by which developing sea urchin larvae are able to cope and maintain skeletogenesis in low pH environments (Evans et al., 2013; Evans and Watson-Wynn, 2014). Thus, failure to upregulate calcium-related genes could result in decreased skeletogenesis. Indeed, larvae in this study exhibited a relative downregulation of calcium ion binding genes, a similar pattern to that observed by Todgham and Hofmann (2009) in *S. purpuratus* larvae raised under elevated pCO_2 levels. In regards to temperature effects, sea urchin larvae across a variety of species and latitudes generally exhibit greater growth and calcification when raised under warmer temperatures, which occasionally provides a compensatory effect that helps offset the negative effect of low pH (Sheppard Brennand et al., 2010; Byrne, 2012; Byrne and Przeslawski, 2013; Wangensteen et al., 2013). Throughout upwelling events, however, no such compensatory effect is expected because, in addition to higher pCO_2, cold temperatures are associated with upwelling seawater. Therefore, the down-regulation of calcium ion binding genes and the significant reduction of spicule length under upwelling conditions align with our expectations for larvae developing under low pH and/or low temperature conditions.

Consequences of Epigenetic Inheritance on Intergenerational Plasticity

Epigenetic inheritance, in which epigenetic marks are intergenerationally transmitted through the germline, is a major study question within the field of environmental epigenetics (Verhoeven et al., 2016; Eirin-Lopez and Putnam, 2019), as it may contribute to rapid acclimation and resilience to changing environments, thereby influencing the fitness landscape and resulting evolutionary processes (Bonduriansky and Day, 2009; Bonduriansky et al., 2012). Although this study does not provide direct evidence of this, the pattern in which maternal conditions had a greater influence on differential methylation between larvae than developmental conditions supports the potential for epigenetic inheritance. In this case, epigenetic marks in the form of DMCpGs may have been incorporated by the mothers into their eggs, which then persisted in their offspring during early development despite differences in the environmental conditions under which the embryos and larvae were raised. While further study is required to determine if these epigenetic changes are truly integrated into the germline and are capable of remaining across generations, this study provides support for the potential of epigenetic inheritance in this system.

CONCLUSION

Different environmental conditions revealed plasticity of the transcriptome and the methylome, but across different time scales within the life history of these marine invertebrates. Namely, DNA methylation variation changes over longer time scales, such as between generations, and is not likely to modulate transcription directly in response to abiotic, physical cues. We found significant plasticity in DNA methylation and gene expression in response to different maternal environmental conditions. While this pattern affected similar broad functional groups, there was little overlap between differential methylation and differential expression on a gene-by-gene basis. We did observe potential maternal priming of larvae with enhanced physiological capacity to function in low pH seawater via increased ion transporter activity, although priming was not evident in larval phenotypes: development under upwelling conditions inhibited skeletal growth and activated genes associated with stress response. The over-arching results of the study point to further examination of the connection between changes in the methylome and changes in phenotypes modulated by global change.

DATA AVAILABILITY STATEMENT

Datasets and analysis scripts can be accessed through a Github repository (https://github.com/mariestrader/S.purp_RRBS_RNAseq_2019) and fastq sequences are available through the NCBI Short Read Archive under the accession PRJNA548926.

ETHICS STATEMENT

Adult urchins were collected in the Santa Barbara Channel under the California Scientific Collecting Permit to GEH (SC-1223).

AUTHOR CONTRIBUTIONS

GH designed the study. MS, LK, TL, JW, JC, MH, and GH executed the experiment and generated the samples. MS analyzed the data with contributions from LK, TL, JW, JC, MH, and GH. MS wrote the manuscript with contributions from LK, TL, JW, JC, MH, and GH.

FUNDING

This research was funded by a United States National Science Foundation award (IOS-1656262) to GH. In addition, diving and boating resources were provided by Santa Barbara Coastal Long-Term Ecological Research program (NSF award OCE-1232779; Director: Dr. Daniel Reed).

ACKNOWLEDGMENTS

We thank Clint Nelson of the Santa Barbara Coastal Long-Term Ecological Research (SBC LTER) program for assistance with boating and sea urchin collection. We also thank Christoph Pierre, Director of Marine Operations at the UC Santa Barbara, for kelp collections during the course of the experiment. We also thank Drs. Umi Hoshijima and Groves Dixon for advice on data analysis.

SUPPLEMENTARY MATERIAL

The Supplementary Material for this article can be found online at: https://www.frontiersin.org/articles/10.3389/fmars.2020.00205/full#supplementary-material

REFERENCES

Akalin, A., Kormaksson, M., Li, S., Garrett-Bakelman, F. E., Figueroa, M. E., Melnick, A., et al. (2012). MethylKit: a comprehensive R package for the analysis of genome-wide DNA methylation profiles. *Genome Biol.* 13:R87. doi: 10.1186/gb-2012-13-10-R87

Ardura, A., Zaiko, A., Morán, P., Planes, S., and Garcia-Vazquez, E. (2017). Epigenetic signatures of invasive status in populations of marine invertebrates. *Sci. Rep.* 7:42193. doi: 10.1038/srep42193

Bakun, A., Black, B. A., Bograd, S. J., García-Reyes, M., Miller, A. J., Rykaczewski, R. R., et al. (2015). Anticipated effects of climate change on coastal upwelling ecosystems. *Curr. Clim. Chang. Rep.* 1, 85–93. doi: 10.1007/s40641-015-0008-4

Banta, J. A., and Richards, C. L. (2018). Quantitative epigenetics and evolution. *Heredity* 121, 210–224. doi: 10.1038/s41437-018-0114-x

Baums, I. B., Devlin-Durante, M. K., Williams, D. W., and Kemp, D. W. (2019). What drives phenotypic divergence among coral clonemates? *Mol. Ecol.* 28, 3208–3224. doi: 10.1101/514430

Bonasio, R., Li, Q., Lian, J., Mutti, N. S., Jin, L., Zhao, H., et al. (2012). Genome-wide and caste-specific DNA methylomes of the ants camponotus floridanus and harpegnathos saltator. *Curr. Biol.* 22, 1755–1764. doi: 10.1016/j.cub.2012.07.042

Bonduriansky, R., Crean, A. J., and Day, T. (2012). The implications of nongenetic inheritance for evolution in changing environments. *Evol. Appl.* 5, 192–201. doi: 10.1111/j.1752-4571.2011.00213.x

Bonduriansky, R., and Day, T. (2009). Nongenetic inheritance and its evolutionary implications. *Annu. Rev. Ecol. Evol. Syst.* 40, 103–125. doi: 10.1146/annurev.ecolsys.39.110707.173441

Burgess, S. C., and Marshall, D. J. (2014). Adaptive parental effects: the importance of estimating environmental predictability and offspring fitness appropriately. *Oikos* 123, 769–776. doi: 10.1111/oik.01235

Byrne, M. (2011). Impact of ocean warming and ocean acidification on marine invertebrate life history stages: vulnerabilities and potential for persistence in a changing ocean. *Oceanogr. Mar. Biol. An Annu. Rev.* 49, 1–42. doi: 10.1016/j.marenvres.2011.10.00

Byrne, M. (2012). Global change ecotoxicology: identification of early life history bottlenecks in marine invertebrates, variable species responses and variable experimental approaches. *Mar. Environ. Res.* 76, 3–15. doi: 10.1016/j.marenvres.2011.10.004

Byrne, M., Lamare, M., Winter, D., Dworjanyn, S. A., and Uthicke, S. (2013). The stunting effect of a high CO2 ocean on calcification and development in sea urchin larvae, a synthesis from the tropics to the poles. *Philos. Trans. R. Soc. B Biol. Sci.* 368:20120439. doi: 10.1098/rstb.2012.0439

Byrne, M., and Przeslawski, R. (2013). Multistressor impacts of warming and acidification of the ocean on marine invertebrates' life histories. *Integr. Comp. Biol.* 53, 582–596. doi: 10.1093/icb/ict049

Chan, F., Barth, J. A., Blanchette, C. A., Byrne, R. H., Chavez, F., Cheriton, O., et al. (2017). Persistent spatial structuring of coastal ocean acidification in the California current system. *Sci. Rep.* 7, 1–7. doi: 10.1038/s41598-017-02777-y

Clark, D., Lamare, M., and Barker, M. (2009). Response of sea urchin pluteus larvae (Echinodermata: Echinoidea) to reduced seawater pH: a comparison among a tropical, temperate, and a polar species. *Mar. Biol.* 156, 1125–1137. doi: 10.1007/s00227-009-1155-8

Crkvenjakov, R., Bajkovic, N., and Glisin, V. (1970). The effect of 5-azacytidine on development, nucleic acid and protein metabolism in sea urchin embryos. *Biochem. Biophys. Res. Commun.* 39, 655–660.

Dickson, A. G., and Millero, F. J. (1987). A comparison of the equilibrium constants for the dissociation of carbonic acid in seawater media. *Deep Sea Res.* 34, 1733–1743.

Dickson, A. G., Sabine, C. L., and Christian, J. R. (2007). *Guide to Best Practices for Ocean CO 2 Measurements*. Sidney: North Pacific Marine Science Organization.

Dixon, G., Bay, L. K., Matz, M. V., Biology, M., Science, M., Centre, A. R. C., et al. (2016). Evolutionary consequences of DNA methylation in a basal metazoan. *Mol. Biol. Evol.* 33:043026. doi: 10.1101/043026

Dixon, G., Liao, Y., Bay, L. K., and Matz, M. V. (2018). Role of gene body methylation in acclimatization and adaptation in a basal metazoan. *PNAS* 115, 13342–13346. doi: 10.1073/pnas.1813749115

Dixon, G. B., Bay, L. K., and Matz, M. V. (2014). Bimodal signatures of germline methylation are linked with gene expression plasticity in the coral *Acropora millepora*. *BMC Genomics* 15:1109. doi: 10.1186/1471-2164-15-1109

Donelson, J. M., Salinas, S., Munday, P. L., and Shama, L. N. S. (2017). Transgenerational plasticity and climate change experiments: where do we go from here? *Glob. Chang. Biol.* 24, 13–34. doi: 10.1111/gcb.13903

Dupont, S., Ortega-Martínez, O., and Thorndyke, M. (2010). Impact of near-future ocean acidification on echinoderms. *Ecotoxicology* 19, 449–462. doi: 10.1007/s10646-010-0463-6

Eirin-Lopez, J. M., and Putnam, H. M. (2019). Marine environmental epigenetics. *Ann. Rev. Mar. Sci.* 11, 335–368. doi: 10.1146/annurev-marine-010318-095114

Evans, T. G., Chan, F., Menge, B. A., and Hofmann, G. E. (2013). Transcriptomic responses to ocean acidification in larval sea urchins from a naturally variable pH environment. *Mol. Ecol.* 22, 1609–1625. doi: 10.1111/mec.12188

Evans, T. G., and Watson-Wynn, P. (2014). Effects of seawater acidification on gene expression: resolving broader-scale trends in sea urchins. *Biol. Bull.* 226, 237–254. doi: 10.1086/BBLv226n3p237

Fangue, N. A., O'Donnell, M. J., Sewell, M. A., Matson, P. G., MacPherson, A. C., and Hofmann, G. E. (2010). A laboratory-based, experimental system for the study of ocean acidification effects on marine invertebrate larvae. *Limnol. Oceanogr. Methods* 8, 441–452. doi: 10.4319/lom.2010.8.441

Feely, R. A., Sabine, C. L., Hernandez-Ayon, J. M., Ianson, D., and Hales, B. (2008). Evidence for upwelling of corrosive "acidified" water onto the continental shelf. *Science* 320, 1490–1492. doi: 10.1126/science.1155676

Feil, R., and Fraga, M. F. (2012). Epigenetics and the environment: emerging patterns and implications. *Nat. Rev. Genet.* 13, 97–109. doi: 10.1038/nrg3142

Fronk, J., Tank, G. A., and Langmore, J. P. (1992). DNA methylation pattern changes during development of a sea urchin. *Biochem. J.* 283, 751–753. doi: 10.1042/bj2830751

Gavery, M. R., and Roberts, S. B. (2010). DNA methylation patterns provide insight into epigenetic regulation in the Pacific oyster (*Crassostrea gigas*). *BMC Genomics* 11:483. doi: 10.1186/1471-2164-11-483

Gavery, M. R., and Roberts, S. B. (2013). Predominant intragenic methylation is associated with gene expression characteristics in a bivalve mollusc. *PeerJ* 1:e215. doi: 10.7717/peerj.215

Gavery, M. R., and Roberts, S. B. (2014). A context dependent role for DNA methylation in bivalves. *Brief. Funct. Genomics* 13, 217–222. doi: 10.1093/bfgp/elt054

Gavery, M. R., and Roberts, S. B. (2017). Epigenetic considerations in aquaculture. *PeerJ* 5:e4147. doi: 10.7717/peerj.4147

Gonzalez-Romero, R., Suarez-Ulloa, V., Rodriguez-Casariego, J., Garcia-Souto, D., Diaz, G., Smith, A., et al. (2017). Effects of Florida Red Tides on histone variant expression and DNA methylation in the Eastern oyster *Crassostrea virginica*. *Aquat. Toxicol.* 186, 196–204. doi: 10.1016/j.aquatox.2017.03.006

Gruber, N., Hauri, C., Lachkar, Z., Loher, D., Frolicher, T. L., and Plattner, G.-K. (2012). Rapid progression of ocean acidification in the California current system. *Science* 337, 220–223. doi: 10.1126/science.1216773

Hansson, I. (1973). A new set of acidity constants for carbonic acid and boric acid in sea water. *Deep Sea Res. Oceanogr. Abstr.* 20, 461–478.

Hawes, N. A., Amadorou, A., Tremblay, L. A., Pochon, X., Dunphy, B., Fidler, A. E., et al. (2019). Epigenetic patterns associated with an ascidian invasion: a comparison of closely related clades in their native and introduced ranges. *Sci. Rep.* 9:14275. doi: 10.1038/s41598-019-49813-7

Hofmann, G. E., and Washburn, L. (2019). SBC LTER: Ocean: Time-series: Mid-Water SeaFET pH and CO2 System Chemistry with Surface and Bottom Dissolved Oxygen at Mohawk Reef(MKO), Ongoing Since 2012-01-11. Available online at: https://pasta.lternet.edu/package/eml/knb-lter-sbc/6003/3 (accessed August 2017).

Hoshijima, U., and Hofmann, G. E. (2019). Variability of seawater chemistry in a kelp forest environment is linked to in situ transgenerational effects in the purple sea urchin, *Strongylocentrotus purpuratus*. *Front. Mar. Sci.* 6:62. doi: 10.3389/fmars.2019.00062

Jiang, L., Lei, X.-M., Liu, S., and Huang, H. (2015). Fused embryos and pre-metamorphic conjoined larvae in a broadcast spawning reef coral. *F1000Research* 4:44. doi: 10.12688/f1000research.6136.1

Johannes, F., Porcher, E., Teixeira, F. K., Saliba-colombani, V., Albuisson, J., Heredia, F., et al. (2009). Assessing the impact of transgenerational epigenetic variation on complex traits. *PLoS Genet.* 5:e1000530. doi: 10.1371/journal.pgen.1000530

Jombart, T. (2008). Adegenet: a R package for the multivariate analysis of genetic markers. *Bioinformatics* 24, 1403–1405. doi: 10.1093/bioinformatics/btn129

Kapsenberg, L., and Hofmann, G. E. (2016). Ocean pH time-series and drivers of variability along the northern Channel Islands, California, USA. *Limnol. Oceanogr.* 61, 953–968. doi: 10.1002/lno.10264

Kauffmann, A., Gentleman, R., and Huber, W. (2009). arrayQualityMetrics–a bioconductor package for quality assessment of microarray data. *Bioinformatics* 25, 415–416. doi: 10.1093/bioinformatics/btn647

Kelly, M. W., Padilla-Gamiño, J. L., and Hofmann, G. E. (2016). High pCO2 affects body size, but not gene expression in larvae of the California mussel (*Mytilus californianus*). *ICES J. Mar. Sci.* 73, 962–969. doi: 10.1093/icesjms/fsv184

Kim, D., Langmead, B., and Salzberg, S. L. (2015). HISAT: a fast spliced aligner with low memory requirements. *Nat. Methods* 12, 357–360. doi: 10.1038/nmeth.3317

Klironomos, F. D., Berg, J., and Collins, S. (2013). How epigenetic mutations can affect genetic evolution: model and mechanism. *BioEssays* 35, 571–578. doi: 10.1002/bies.201200169

Kronholm, I., and Collins, A. D. (2016). Epigenetic mutations can both help and hinder adaptive evolution. *Mol. Ecol.* 25, 1856–1868. doi: 10.1111/mec.13296

Krueger, F., and Andrews, S. R. (2011). Bismark: a flexible aligner and methylation caller for Bisulfite-Seq applications. *Bioinformatics* 27, 1571–1572. doi: 10.1093/bioinformatics/btr167

Kurihara, H. (2008). Effects of CO2 driven ocean acidification on the early developmental stages of invertebrates. *Mar. Ecol. Prog. Ser.* 373, 275–284. doi: 10.3354/meps07802

Kurihara, H., and Shirayama, Y. (2004). Effects of increased atmospheric CO2 on sea urchin early development. *Mar. Ecol. Prog. Ser.* 274, 1–9.

Langfelder, P., and Horvath, S. (2008). WGCNA: an R package for weighted correlation network analysis. *BMC Bioinformatics* 9:559. doi: 10.1186/1471-2105-9-559

Li, E., and Zhang, Y. (2014). DNA methylation in mammals. *Cold Spring Harb. Perspect. Biol.* 6:a019133. doi: 10.1101/cshperspect.a019133

Li, Y., Liew, Y. J., Cui, G., Cziesielski, M. J., Zahran, N., Michell, C. T., et al. (2017). DNA methylation regulates transcriptional homeostasis of algal endosymbiosis in the coral model Aiptasia. *Sci. Adv.* 4:eaat2142. doi: 10.1101/213066

Liao, Y., Smyth, G. K., and Shi, W. (2014). FeatureCounts: an efficient general purpose program for assigning sequence reads to genomic features. *Bioinformatics* 30, 923–930. doi: 10.1093/bioinformatics/btt656

Liew, Y. J., Zoccola, D., Li, Y., Tambutté, E., Venn, A. A., Craig, T., et al. (2018). Epigenome-associated phenotypic acclimatization to ocean acidification in a reef-building coral. *Sci. Adv.* 216:188227. doi: 10.1101/188227

Love, M. I., Anders, S., and Huber, W. (2014). *Differential Analysis of Count Data - The DESeq2 Package*. Heidelberg: EMBL.

Maharajan, P., Maharajan, V., Branno, M., and Scarano, E. (1986). Effects of 5 azacytidine on DNA methylation and early development of sea urchins and ascidia. *Differentiation* 32, 200–207.

Marsh, A. G., and Pasqualone, A. A. (2014). DNA methylation and temperature stress in an Antarctic polychaete, *Spiophanes tcherniai*. *Front. Physiol.* 5:173. doi: 10.3389/fphys.2014.00173

Marshall, D. J. (2008). Transgenerational plasticity in the sea: context- dependent maternal effects across the life history. *Ecology* 89, 418–427. doi: 10.1890/07-0449.1

Martin, M. (2011). Cutadapt removes adapter sequences from high-throughput sequencing reads. *EMBnet J.* 17:10. doi: 10.14806/ej.17.1.200

Moya, A., Huisman, L., Ball, E. E., Hayward, D. C., Grasso, L. C., Chua, C. M., et al. (2012). Whole transcriptome analysis of the coral *Acropora millepora* reveals complex responses to CO2-driven acidification during the initiation of calcification. *Mol. Ecol.* 21, 2440–2454. doi: 10.1111/j.1365-294X.2012.05554.x

Munday, P. L. (2014). Transgenerational acclimation of fishes to climate change and ocean acidification. *F1000Prime Rep.* 6, 1–7. doi: 10.12703/P6-99

Okazaki, K. (1975). Spicule formation by isolated micromeres of the sea urchin embryo. *Integr. Comp. Biol.* 15, 567–581. doi: 10.1093/icb/15.3.567

Oksanen, J., Blanchet, F. G., Kindt, R., Legendre, P., Minchin, P. R., O'Hara, R. B., et al. (2013). *Package 'vegan.' Community Ecol. Packag. Version 2*.

Padilla-Gamiño, J. L., Kelly, M. W., Evans, T. G., Hofmann, G. E., Padilla-Gamiño, J. L., Kelly, M. W., et al. (2013). Temperature and CO 2 additively regulate physiology, morphology and genomic responses of larval sea urchins, *Strongylocentrotus purpuratus*. *Proc. R. Soc. B* 280:20130155. doi: 10.1098/rspb.2013.0155

Patalano, S., Vlasova, A., Wyatt, C., Ewels, P., Camara, F., Ferreira, P. G., et al. (2015). Molecular signatures of plastic phenotypes in two eusocial insect species with simple societies. *Proc. Natl. Acad. Sci. U.S.A.* 112, 13970–13975. doi: 10.1073/pnas.1515937112

Pearse, J. S. (2006). Ecological role of purple sea urchins. *Science* 314, 940–941. doi: 10.1126/science.1131888

Regev, A., and Lamb, M. J. (1998). The role of DNA methylation in invertebrates: developmental regulation or genome defense? *Mol. Biol. Evol.* 15, 880–891.

Rey, O., Danchin, E., Mirouze, M., Loot, C., and Blanchet, S. (2016). Adaptation to global change: a transposable element-epigenetics perspective. *Trends Ecol. Evol.* 31, 514–526. doi: 10.1016/j.tree.2016.03.013

Richards, C. L., Alonso, C., Becker, C., Bossdorf, O., Bucher, E., Colomé-Tatché, M., et al. (2017). Ecological plant epigenetics: evidence from model and non-model species, and the way forward. *Ecol. Lett.* 20, 1576–1590. doi: 10.1111/ele.12858

Richards, E. J. (2008). Population epigenetics. *Curr. Opin. Genet. Dev.* 18, 221–226. doi: 10.1016/j.gde.2008.01.014

Rivest, E. B., Brien, M. O., Kapsenberg, L., Gotschalk, C. C., Blanchette, C. A., Hoshijima, U., et al. (2016). Ecological Informatics Beyond the benchtop and the benthos?: dataset management planning and design for time series of ocean carbonate chemistry associated with Durafet ®-based pH sensors. *Ecol. Inform.* 36, 209–220. doi: 10.1016/j.ecoinf.2016.08.005

Riviere, G., He, Y., Tecchio, S., Crowell, E., Sourdaine, P., Guo, X., et al. (2017). Dynamics of DNA methylomes underlie oyster development. *PLoS Genet.* 13:e1006807. doi: 10.1371/journal.pgen.1006807

Riviere, G., Wu, G. C., Fellous, A., Goux, D., Sourdaine, P., and Favrel, P. (2013). DNA methylation Is crucial for the early development in the oyster *C. gigas*. *Mar. Biotechnol.* 15, 739–753. doi: 10.1007/s10126-013-9523-2

Robbins, L. L., Hansen, M. E., Kleypas, J. A., and Meylan, S. C. (2010). *CO2calc: A User-Friendly Seawater Carbon Calculator for Windows, Mac OS X, and iOS (iPhone)*. Reston, VA: USGS.

Roberts, S. B., and Gavery, M. R. (2012). Is there a relationship between DNA methylation and phenotypic plasticity in invertebrates? *Front. Physiol.* 2:116. doi: 10.3389/fphys.2011.00116

Ross, P. M., Parker, L., O'Connor, W. A., and Bailey, E. A. (2011). The impact of ocean acidification on reproduction, early development and settlement of marine organisms. *Water* 3, 1005–1030. doi: 10.3390/w3041005

Saint-Carlier, E., and Riviere, G. (2015). Regulation of Hox orthologues in the oyster Crassostrea gigas evidences a functional role for promoter DNA methylation in an invertebrate. *FEBS Lett.* 589, 1459–1466. doi: 10.1016/j.febslet.2015.04.043

Sarda, S., Zeng, J., Hunt, B. G., and Yi, S. V. (2012). The evolution of invertebrate gene body methylation. *Mol. Biol. Evol.* 29, 1907–1916. doi: 10.1093/molbev/mss062

Shea, N., Pen, I., and Uller, T. (2011). Three epigenetic information channels and their different roles in evolution. *J. Evol. Biol.* 24, 1178–1187. doi: 10.1111/j.1420-9101.2011.02235.x

Sheppard Brennand, H., Soars, N., Dworjanyn, S. A., Davis, A. R., and Byrne, M. (2010). Impact of ocean warming and ocean acidification on larval development and calcification in the sea urchin *Tripneustes gratilla*. *PLoS One* 5:e0011372. doi: 10.1371/journal.pone.0011372

Strader, M. E., Wong, J. M., Kozal, L. C., Leach, T. S., and Hofmann, G. E. (2019). Parental environments alter DNA methylation in offspring of the purple sea urchin, *Strongylocentrotus purpuratus*. *J. Exp. Mar. Biol. Ecol.* 517, 54–64. doi: 10.1016/j.jembe.2019.03.002

Strathmann, M. F. (1987). *Reproduction and development of marine invertebrates of the northern Pacific coast:?: Data and Methods for the Study of Eggs, Embryos, and Larvae*. Seattle: University of Washington Press.

Suzuki, M. M., Kerr, A. R. W., De Sousa, D., and Bird, A. (2007). CpG methylation is targeted to transcription units in an invertebrate genome. *Genome Res.* 17, 625–631. doi: 10.1101/gr.6163007

Sydeman, W. J., García-Reyes, M., Schoeman, D. S., Rykaczewski, R. R., Thompson, S. A., Black, B. A., et al. (2014). Climate change. Climate change and wind intensification in coastal upwelling ecosystems. *Science* 345, 77–80. doi: 10.1126/science.1251635

Todgham, A. E., and Hofmann, G. E. (2009). Transcriptomic response of sea urchin larvae Strongylocentrotus purpuratus to CO2-driven seawater acidification. *J. Exp. Biol.* 212, 2579–2594. doi: 10.1242/jeb.032540

Torda, G., Donelson, J. M., Aranda, M., Barshis, D. J., Bay, L., Berumen, M. L., et al. (2017). Rapid adaptive responses to climate change in corals. *Nat. Clim. Chang.* 7, 627–636. doi: 10.1038/nclimate3374

Tosi, L., Aniello, F., Geraci, G., and Branno, M. (1995). DNA methyltransferase activity in the early stages of a sea urchin embryo Evidence of differential control. *FEBS Lett.* 361, 115–117. doi: 10.1016/0014-5793(95)00160-B

Verhoeven, K. J. F., VonHoldt, B. M., and Sork, V. L. (2016). Epigenetics in ecology and evolution: what we know and what we need to know. *Mol. Ecol.* 25, 1631–1638. doi: 10.1111/mec.13617

Wang, X., Li, Q., Lian, J., Li, L., Jin, L., Cai, H., et al. (2014). Genome-wide and single-base resolution DNA methylomes of the Pacific oyster *Crassostrea gigas* provide insight into the evolution of invertebrate CpG methylation. *BMC Genomics* 15:1119. doi: 10.1186/1471-2164-15-1119

Wang, X., Wheeler, D., Avery, A., Rago, A., Choi, J. H., Colbourne, J. K., et al. (2013). Function and Evolution of DNA methylation in *Nasonia vitripennis*. *PLoS Genet.* 9:e1003872. doi: 10.1371/journal.pgen.1003872

Wangensteen, O. S., Dupont, S., Casties, I., Turon, X., and Palacín, C. (2013). Some like it hot: temperature and pH modulate larval development and settlement of the sea urchin *Arbacia lixula*. *J. Exp. Mar. Bio. Ecol.* 449, 304–311. doi: 10.1016/j.jembe.2013.10.007

Wong, J. M., Johnson, K. M., Kelly, M. W., and Hofmann, G. E. (2018). Transcriptomics reveal transgenerational effects in purple sea urchin embryos: adult acclimation to upwelling conditions alters the response of their progeny to differential pCO2levels. *Mol. Ecol.* 27, 1120–1137. doi: 10.1111/mec.14503

Wong, J. M., Kozal, L. C., Leach, T. S., Hoshijima, U., and Hofmann, G. E. (2019). Transgenerational effects in an ecological context: conditioning of adult sea urchins to upwelling conditions alters maternal provisioning and progeny phenotype. *J. Exp. Mar. Biol. Ecol.* 57, 65–77. doi: 10.1016/j.jembe.2019.04.006

Wright, R. M., Aglyamova, G. V., Meyer, E., and Matz, M. V. (2015). Gene expression associated with white syndromes in a reef building coral, *Acropora hyacinthus*. *BMC Genomics* 16:2. doi: 10.1186/s12864-015-1540-2

Zemach, A., McDaniel, I. E., Silva, P., and Zilberman, D. (2010). Genome-wide evolutionary analysis of eukaryotic DNA methylation. *Science* 328, 916–919. doi: 10.1126/science.1186366

Zwier, M. V., Verhulst, E. C., Zwahlen, R. D., Beukeboom, L. W., and Van De Zande, L. (2012). DNA methylation plays a crucial role during early *Nasonia* development. *Insect Mol. Biol.* 21, 129–138. doi: 10.1111/j.1365-2583.2011.01121.x

Conflict of Interest: The authors declare that the research was conducted in the absence of any commercial or financial relationships that could be construed as a potential conflict of interest.

frontiers in Marine Science

ORIGINAL RESEARCH
published: 22 April 2020
doi: 10.3389/fmars.2020.00225

General DNA Methylation Patterns and Environmentally-Induced Differential Methylation in the Eastern Oyster (*Crassostrea virginica*)

Yaamini R. Venkataraman[1], Alan M. Downey-Wall[2], Justin Ries[2], Isaac Westfield[2], Samuel J. White[1], Steven B. Roberts[1] and Kathleen E. Lotterhos[2]*

[1] School of Aquatic and Fishery Sciences, University of Washington, Seattle, WA, United States, [2] Department of Marine and Environmental Sciences, Northeastern University, Nahant, MA, United States

OPEN ACCESS

Edited by:
Jose M. Eirin-Lopez, Florida International University, United States

Reviewed by:
Linlin Zhang, Institute of Oceanology (CAS), China
Li Li, UT Southwestern Medical Center, United States

****Correspondence:***
Yaamini R. Venkataraman
yaaminiv@uw.edu

Specialty section:
This article was submitted to Marine Molecular Biology and Ecology, a section of the journal Frontiers in Marine Science

Received: *30 December 2019*
Accepted: *24 March 2020*
Published: *22 April 2020*

Citation:
Venkataraman YR, Downey-Wall AM, Ries J, Westfield I, White SJ, Roberts SB and Lotterhos KE (2020) General DNA Methylation Patterns and Environmentally-Induced Differential Methylation in the Eastern Oyster (Crassostrea virginica). Front. Mar. Sci. 7:225. doi: 10.3389/fmars.2020.00225

Epigenetic modification, specifically DNA methylation, is one possible mechanism for intergenerational plasticity. Before inheritance of methylation patterns can be characterized, we need a better understanding of how environmental change modifies the parental epigenome. To examine the influence of experimental ocean acidification on eastern oyster (*Crassostrea virginica*) gonad tissue, oysters were cultured in the laboratory under control (491 ± 49 μatm) or high (2550 ± 211 μatm) pCO_2 conditions for 4 weeks. DNA from reproductive tissue was isolated from five oysters per treatment, then subjected to bisulfite treatment and DNA sequencing. Irrespective of treatment, DNA methylation was primarily found in gene bodies with approximately 22% of CpGs (2.7% of total cytosines) in the *C. virginica* genome predicted to be methylated. In response to elevated pCO_2, we found 598 differentially methylated loci primarily overlapping with gene bodies. A majority of differentially methylated loci were in exons (61.5%) with less intron overlap (31.9%). While there was no evidence of a significant tendency for the genes with differentially methylated loci to be associated with distinct biological processes, the concentration of these loci in gene bodies, including genes involved in protein ubiquitination and biomineralization, suggests DNA methylation may be important for transcriptional control in response to ocean acidification. Changes in gonad methylation also indicate potential for these methylation patterns to be inherited by offspring. Understanding how experimental ocean acidification conditions modify the oyster epigenome, and if these modifications are inherited, allows for a better understanding of how ecosystems will respond to environmental change.

Keywords: eastern oyster, DNA methylation, epigenetics, ocean acidification, *Crassostrea virginica*

INTRODUCTION

As increased anthropogenic carbon dioxide is expected to create adverse conditions for calcifying organisms (IPCC, 2019), efforts have been made to understand how ocean acidification impacts ecologically and economically important organisms like bivalves (Parker et al., 2013; Ekstrom et al., 2015). Bivalve species are sensitive to reduced aragonite saturation associated with ocean

acidification, with larvae being particularly vulnerable (Barton et al., 2012; Waldbusser et al., 2014). Shell structure may be compromised in larvae, juveniles, and adults (Gazeau et al., 2007; Kurihara et al., 2007; Beniash et al., 2010; Ries, 2011). Aside from affecting calcification and shell growth, ocean acidification can impact protein synthesis, energy production, metabolism, antioxidant responses, and reproduction (Tomanek et al., 2011; Timmins-Schiffman et al., 2014; Dineshram et al., 2016; Boulais et al., 2017; Omoregie et al., 2019).

Additionally, adult exposure to ocean acidification may impact their larvae [reviewed in Ross et al. (2016), Byrne et al. (2019)]. For example, adult Manila clams (*Ruditapes philippinarum*) and mussels (*Musculista senhousia*) reproductively conditioned in high pCO_2 waters yield offspring that exhibit significantly faster development or lower oxidative stress protein activity in those same conditions (Zhao et al., 2018, 2019). In contrast, northern quahog (hard clam; *Mercenaria mercenaria*) and bay scallop (*Argopecten irradians*) larvae may be more vulnerable to ocean acidification and additional stressors when parents are reproductively conditioned in high pCO_2 waters (Griffith and Gobler, 2017). Some species exhibit both positive and negative carryover effects [e.g., *Saccostrea glomerata*; (Parker et al., 2012, 2017)]. Intergenerational effects have also been documented when adult exposure to ocean acidification does not coincide with reproductive maturity [e.g., *Crassostrea gigas*; (Venkataraman et al., 2019)]. Although intergenerational carryover effects are now at the forefront of ocean acidification research in bivalve species, the mechanisms responsible for these effects are still unclear.

Epigenetics is the next frontier for understanding how environmental memory may modulate phenotypic plasticity across generations (Eirin-Lopez and Putnam, 2018). Epigenetics refers to changes in gene expression that do not arise from changes in the DNA sequence, with methylation of cytosine bases being the most studied mechanism (Bird, 2002; Deans and Maggert, 2015). Unlike highly methylated vertebrate genomes, marine invertebrate taxa have sparse methylation throughout their genomes, similar to a mosaic pattern (Suzuki and Bird, 2008). Genes that benefit from stable transcription, such as housekeeping genes, tend to be more methylated, while environmental response genes that are less methylated are prone to more spurious transcription and alternative splicing patterns, thereby possibly increasing phenotypic plasticity (Roberts and Gavery, 2012; Dimond and Roberts, 2016; Gatzmann et al., 2018). Increased levels of DNA methylation can also correlate with increased transcription. Several base pair resolution studies in *C. gigas* demonstrate a positive association between DNA methylation and gene expression that is consistent across cell types (Roberts and Gavery, 2012; Gavery and Roberts, 2013; Olson and Roberts, 2014). Since DNA methylation could provide a direct link between environmental conditions and phenotypic plasticity via influencing gene activity, elucidating how invertebrate methylomes respond to abiotic factors is crucial for understanding potential acclimatization mechanisms (Bossdorf et al., 2008; Hofmann, 2017).

While bivalve species have been used as model organisms to characterize marine invertebrate methylomes, how ocean acidification affects bivalve DNA methylation is poorly understood. Methylation responses to ocean acidification have been studied in multiple coral species. When placed in low pH conditions (7.6–7.35), *Montipora capitata* did not demonstrate any differences in calcification, metabolic profiles, or DNA methylation in comparison to clonal fragments in ambient pH (7.9–7.65) (Putnam et al., 2016). DNA methylation increased in another coral species, *Pocillopora damicornis*, in addition to reduced calficiation and more differences in metabolic profiles (Putnam et al., 2016). The coral *Stylophora pistillata* also demonstrates increased global methylation as pH decreases ($pH_{treatment}$ = 7.2, 7.4, 7.8; $pH_{control}$ = 8.0), with methylation reducing spurious transcription (Liew et al., 2018b). Combined whole genome bisulfite sequencing and RNA sequencing revealed differential methylation and expression of growth and stress response pathways controlled differences in cell and polyp size between treatments (Liew et al., 2018b). The association between DNA methylation and phenotypic differences in these corals demonstrates that epigenetic regulation of genes is potentially important for acclimatization and adaptation to environmental perturbation. Recent examination of *C. virginica* methylation patterns in response to a natural salinity gradient suggests that differential methylation may modulate environmental response in this species (Johnson and Kelly, 2019).

There is evidence that suggests that methylation patterns can be inherited in marine invertebrates. For example, purple sea urchin (*Strongylocentrotus purpuratus*) offspring have methylomes that reflect maternal rearing conditions (Strader et al., 2019). Different parental temperature and salinity regimes influence larval methylomes in *Platygyra daedalea* (Liew et al., 2018a). In the Pacific oyster (*C. gigas*), parental exposure to pesticides influence DNA methylation in spat, even though the spat were not exposed to these conditions (Rondon et al., 2017). Methylation changes in gametes are likely the ones that could be inherited, and may play a role in carryover effects. Before determining if DNA methylation is a viable mechanism for altering the phenotypes of offspring or subsequent generations, the epigenome of bivalve reproductive tissue in response to ocean acidification must be characterized.

The present study is the first to determine if ocean acidification induces differential methylation in reproductive tissue in the eastern oyster (*Crassostrea virginica*). Adult *C. virginica* were exposed to control or elevated pCO_2 conditions. We hypothesize that ocean acidification will induce differential methylation in *C. virginica* gonad tissue, and that genes with differentially methylated loci will have biological functions that could allow for acclimatization to environmental perturbation. Understanding how experimental ocean acidification conditions modify the oyster epigenome, and if these modifications are inherited, allows for a better understanding of how ecosystems will respond to environmental change.

MATERIALS AND METHODS

Experimental Design

Adult *C. virginica* (9.55 cm ± 0.45) were collected from an intertidal oyster reef in Plum Island Sound, MA, United States (42.681764, −70.813498) in mid-July 2016. The oysters were transported to the Marine Science Center at Northeastern University (Nahant, MA, United States), where they were cleaned and randomly assigned to one of six flow-through tanks (50 L) maintained at ambient seawater conditions. Oysters were acclimated for 14 days under control conditions (500 μatm; 14–15°C) before initiating a 28-day experimental exposure. Half of the tanks remained at control pCO_2 conditions (500 μatm, $\Omega_{calcite} > 1$), while the other half were ramped up to elevated pCO_2 conditions (2500 μatm, $\Omega_{calcite} < 1$) over 24 h. This elevated treatment is consistent with observations in other estuarine ecosystems that oysters inhabit (Feely et al., 2010), although pH in nature only stays as extreme for short periods of time (e.g., hours). Moreover, the extreme treatment was also chosen to increase precision and therefore power to detect a response (Whitlock and Schluter, 2014).

Treatment conditions were replicated across three tanks, with oysters distributed evenly among tanks (1–2 oysters per tank). Each tank had an independent flow-regulator that delivered fresh, natural seawater at approximately 150 ml min^{-1}. Carbonate chemistry was maintained independently for each tank by mixtures of compressed CO_2 and compressed air at flow rates proportional to the target pCO_2 conditions. Gas flow rates were maintained with *Aalborg* digital solenoid-valve-controlled mass flow controllers (Model GFC17, precision = 0.1 mL/min). Within a treatment, tanks were replenished with fresh seawater and each tank was independently bubbled with its own mixed gas stream, with partial recirculation and filtration with other tanks in the treatment. As a result, the carbonate chemistry (i.e., the independent variable by which the treatments were differentiated) of the replicate tanks were slightly different from each other, which is evidence of their technical independence. Temperature was maintained at 15°C using Aqua Euro United States model MC-1/4HP chillers coupled with 50-watt electric heaters. Average salinity was determined by the incoming natural seawater and reflected ambient ocean salinity of Massachusetts Bay near the Marine Science Center (Latitude = 42.416100, Longitude = −70.907737).

Oysters were fed 2.81 mL/day of a 10% Shellfish Diet 1800 twice daily following Food and Agriculture Organization's best practices for oysters (Helm and Bourne, 2004). Five oysters were collected from each treatment at the end of the 28-day exposure. They were immediately dissected with gonadal tissue harvested and immediately flash frozen. Partial gamete maturation was evident upon visual inspection.

Measurement and Control of Seawater Carbonate Chemistry

The carbonate chemistry of tanks was controlled by bubbling mixtures of compressed CO_2 and compressed air at flow rates proportional to the target pCO_2 conditions. The control pCO_2 treatments were maintained by bubbling compressed ambient air only.

Temperature, pH, and salinity of all replicate tanks was measured three times per week for the duration of the experiment. Temperature was measured using a glass thermometer to 0.1°C accuracy, pH was measured using an *Accumet* solid state pH electrode (precision = 1 mV), salinity was measured using a *YSI 3200* conductivity probe (precision = 0.1 ppt). Every 2 weeks, seawater samples were collected from each replicate tank for analysis of dissolved inorganic carbon (DIC) and total alkalinity (A_T). Samples were collected in 250 mL borosilicate glass bottles sealed with a greased stopper, immediately poisoned with 100 μL saturated $HgCl_2$ solution, and then refrigerated. Samples were analyzed for DIC via coulometry and Alk_T via closed-cell potentiometric Gran Titration with a VINDTA 3C (Marianda Corporation). Other carbonate system parameters, including $\Omega_{calcite}$, pH, and pCO_2, were calculated from DIC, A_T, salinity, and temperature using CO2SYS software version 2.1 (Lewis and Wallace, 1998; Van Heuven et al., 2011), using the seawater pH scale (mol/kg-SW) with K1 and K2 values from Roy et al. (1993), a $KHSO_4$ value from Dickson (1990), and a $[B]_T$ value from Lee et al. (2010).

MBD-BS Library Preparation

DNA was isolated from five gonad tissue samples per treatment using the E.Z.N.A. Mollusc Kit (Omega) according to the manufacturer's instructions. Isolated DNA was quantified using a Qubit dsDNA BR Kit (Invitrogen). DNA samples, ranging from 12.8 to 157 ng/μL, were placed in 1.5 mL centrifuge tubes and sonicated using a QSONICA CD0004054245 (Newtown, CT) in 30 s interval periods over 10 min at 4°C and 25% intensity. Shearing size (350 bp) was verified using a 2200 TapeStation System (Agilent Technologies). Samples were enriched for methylated DNA with the MethylMiner kit (Invitrogen). A single-fraction elution using 400 μL of high salt buffer was used to obtain captured DNA. After ethanol precipitation, 25 μL of buffer was used for the final elution. Library preparation and sequencing was performed by ZymoResearch using Pico Methyl-Seq Library Prep Kit (Cat. #D5455). Libraries were then barcoded and pooled into two lanes (eight samples in one and two in another) to generate 100bp paired-end reads on the HiSeq1500 sequencer (Illumina, Inc.).

Global Methylation Characterization

Sequences were trimmed with 10 bp removed from both the 5′ and 3′ ends using TrimGalore! v.0.4.5 (Martin, 2011). Quality of sequences was assessed with FastQC v.0.11.7 (Andrews, 2010). The *C. virginica* genome (NCBI Accession GCA_002022765.4) was prepared using Bowtie 2-2.3.4 [Linux x84_64 version; (Langmead and Salzberg, 2012)] within the bismark_genome_preparation function in Bismark v.0.19.0 (Krueger and Andrews, 2011). Trimmed sample sequences were then aligned to the genome using Bismark v.0.19.0 (Krueger and Andrews, 2011) with non-directionality specified and alignment score set using -score_min L,0,-1.2. Alignment files (i.e., bam) were deduplicated (deduplicate_bismark), sorted and indexed using SAMtools v.1.9 (Li et al., 2009).

Methylation calls were extracted from deduplicated files using bismark_methylation_extractor.

Various *C. virginica* genome feature tracks were created for downstream analyses using BEDtools v2.26.0 (Quinlan and Hall, 2010). Genes, mRNA, coding sequences, and exons were derived directly from the *C. virginica* genome on NCBI (Gómez-Chiarri et al., 2015). The complement of the exon track was used to identify introns, and coding sequences were subtracted from exons to identify untranslated regions of exons (UTR). Exon locations were removed from the complement of the gene track to define intergenic regions. Putative promoter regions were defined as the 1 kb upstream of transcription start sites. Putative transposable elements were identified using RepeatMasker (v4.07) with RepBase-20170127 and RMBlast 2.6.0 (Smit et al., 2013; Bao et al., 2015). All species available in RepBase-20170127 were used to identify transposable elements.

Overall *C. virginica* gonad methylation patterns were characterized using information from all samples. Individual CpG dinucleotides with at least 5× coverage in each sample were classified as methylated (≥50% methylation), sparsely methylated (10–50% methylation), or unmethylated (<10% methylation). The locations of all methylated CpGs were characterized in relation to putative promoter regions, UTR, exons, introns, transposable elements, and intergenic regions. We tested the null hypothesis that there was no association between the genomic location of CpG loci and methylation status (all CpGs vs.methylated CpGs) with a chi-squared contingency test (chisq.test in R Version 3.5.0).

Methylation islands were determined to characterize overall methylation in the *C. virginica* genome using a sliding window analysis based on (Jeong et al., 2018). Islands were defined as areas of the genome with enriched levels of methylated CpGs (>50% methylation). To define methylation islands, each chromosome was examined using an initial 500 bp window starting at the first methylated CpG. If the proportion of methylated CpGs in the window was greater than 0.2, the window was extended by 50 bp; if not, the analysis proceeded to the next methylated CpG. Windows were continually extended until the proportion of methylated CpGs in the window fell below the 0.2 criteria. The location of methylation islands in the genome were characterized using BEDtools intersect v2.26.0.

Differential Methylation Analysis

Differential methylation analysis for individual CpG dinucleotides was performed using methylKit v.1.7.9 in R (Akalin et al., 2012) using deduplicated, sorted bam files as input. Only CpGs with at least 5× coverage in each sample were considered for analysis. Methylation differences between treatments were obtained for all loci in the CpG background using calculateDiffMeth, a logistic regression built into methylKit. The logistic regression models the log odds ratio based on the proportion of methylation at each locus:

$$log\left(\frac{\pi_i}{1 - \pi_i}\right) = \beta_0 + \beta_1 Treatment_i$$

A differentially methylated locus (DML) was defined as an individual CpG dinucleotide with at least a 50% methylation change between treatment and control groups, and a q-value < 0.01 based on correction for false discovery rate with the SLIM method (Wang et al., 2011). Hypermethylated DML were defined as those with significantly higher percent methylation in oysters exposed to high pCO_2 conditions, and hypomethylated DML with significantly lower percent methylation in the high pCO_2 treatment. A Principal Components Analysis (PCA) was performed for differentially methylated loci (DML) for oyster sample methylation profiles between treatments, then compared to a PCA for all MBD-enriched CpG loci. The location of DML were characterized in relation to putative promoter regions, UTR, exons, introns, transposable elements, and intergenic regions using BEDtools intersect v2.26.0. Loci that did not overlap with the aforementioned genomic features were also identified. A chi-squared contingency test was used to test the null hypothesis of no association between genomic location and methylation status between MBD-enriched CpGs and DML. To describe the location of DML across different gene architectures, the position of DML in the gene was scaled from 0 to 100 bp.

Enrichment Analysis

Functional enrichment analyses were used to determine if any biological processes were overrepresented in genes based on individual CpG methylation levels. Enrichment was conducted with GO-MWU, a rank-based gene enrichment method initially developed for analyzing transcriptomics data (Wright et al., 2015). Instead of only using genes with DML, GO-MWU identifies GO categories that are overrepresented by genes with any CpGs, allowing for more data to contribute to any trends. GO-MWU scripts and a gene ontology database were downloaded from the GO-MWU Github repository[1].

A gene list and table of significance measures were used as GO-MWU analysis inputs. The gene list contained Genbank IDs and all associated gene ontology terms. For the table of significance measures, Genbank IDs were matched with the smallest *P*-value for associated CpGs analyzed by methylKit. To match the Genbank IDs to CpG loci within mRNAs and create the gene list, overlaps between the *C. virginica* mRNA track from NCBI and the CpG background used in methylKit were obtained using BEDtools intersect v2.26.0. The mRNAs were then annotated with Uniprot Accession codes using a BLASTx search [v.2.2.29; (Gish and States, 1993; UniProt Consortium, 2019)]. The Uniprot Swiss-Prot Database (downloaded from SwissProt 2018-06-15) was used to obtain protein information and Uniprot Accession codes. Genbank IDs provided by NCBI were used to match CpG background-mRNA overlaps with the annotated mRNA track. Gene ontology terms were paired to Uniprot Accession codes using the Uniprot Swiss-Prot Database (UniProt Consortium, 2019). All GO-MWU inputs are available in the associated Github repository (Venkataraman, 2020).

[1]https://github.com/z0on/GO_MWU

Once analysis inputs were created, gene ontology terms for each gene were matched with parental terms using default GO-MWU settings. Parental ontology categories with the exact same gene list were combined. Groups were further combined if they shared at least 75% of the same genes. After clustering was complete, a Mann-Whitney *U* test identified gene ontology categories that were significantly enriched by corresponding CpG loci in genes using the default 10% FDR. Genes with DML were mapped to gene ontology subsets (GO Slim terms) for biological processes to further categorize gene functions.

RESULTS

Water Chemistry

All oysters were initially subjected to acclimation pCO_2 conditions (pCO_2 = 521 ± 32 ppm, $\Omega_{calcite}$ = 2.82 ± 0.13) for 14 days. Following acclimation the treatments were initiated. Oysters in control pCO_2 conditions (pCO_2 = 492 ± 50 μatm; $\Omega_{calcite}$ = 3.01 ± 0.25) experienced low pCO_2 and higher $\Omega_{calcite}$ than those in elevated pCO_2 conditions (pCO_2 = 2550 ± 211 μatm; $\Omega_{calcite}$ = 0.72 ± 0.06) (**Table 1**).

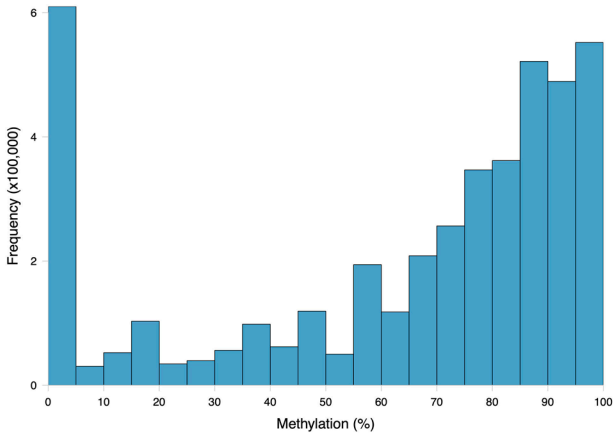

FIGURE 1 | Frequency distribution of methylation ratios for CpG loci in *C. virginica* gonad tissue DNA subjected to MBD enrichment. A total of 4,304,257 CpGs with at least 5× coverage summed across all ten samples were characterized. Loci were considered methylated if they were at least 50% methylated, sparsely methylated loci were 10–50% methylated, and unmethylated loci were 0–10% methylated.

MBD-BS-Seq

DNA sequencing yielded 280 million DNA sequence reads (NCBI Sequence Read Archive: BioProject accession number PRJNA513384). Of 276 million trimmed paired-end reads, 136 million (49.4%) were mapped to the *C. virginica* genome, providing an average of 13.6 million reads per sample. Sequencing efforts provided data for 4,304,257 CpG loci (30.7% of 14,458,703 total CpGs in the *C. virginica* genome) with at least 5× coverage across all samples combined. As expected, the location of CpGs with 5× coverage in the genome differed from the distribution of all CpG motifs (Contingency test; χ^2 = 1,306,900, *df* = 6, *P*-value < 2.2e-16). Of all loci with 5x coverage, 3,255,049 CpGs (75.6%) were found in genic regions in 33,126 out of 38,929 annotated genes in the genome.

The general methylation landscape was defined using all loci with a minimum 5× coverage in each sample. The majority, 3,181,904 (73.9% of MBD-Enriched loci) loci were methylated, with 481,788 (11.2%) sparsely methylated loci and 640,565 (14.9%) unmethylated loci (**Figure 1**). Median values for global percent methylation and sample methylation varied across genome features (**Figure 1**). Based on these parameters and data, we calculated that 22% of all CpGs in the gonads (2.7% of total cytosines) had methylation levels greater than 50%. Loci methylation was characterized in relation to putative promoters, UTR, exons, introns, transposable elements, and intergenic regions (**Figure 2**). Methylated CpGs were found primarily in genic regions, with 2,521,653 loci (79.2%) in 25,496 genes. We rejected the null hypothesis that CpG methylation status was independent of genomic location, as the proportion of methylated CpG loci was different than expected in putative promoters, UTR, exons, introns, transposable elements, and intergenic regions (Contingency test; χ^2 = 1,311,600, *df* = 6, *P*-value < 2.2e-16; **Figure 2**). There was a larger proportion of methylated loci found in exons compared to all CpGs in the genome (**Figure 2**). Methylated loci were also found in introns [with 1,448,786 loci (47.3% of methylated loci) vs.1,013,691 CpGs (31.9%) in exons], although this was not higher than expected based on the distribution of all CpGs. Transposable elements contained 755,222 methylated CpGs (23.7%). Putative promoter regions overlapped with 106,111 loci (3.3%), UTR with 128,585 loci (4.0%), and intergenic regions with 660,197 loci (20.7%). There were 372,047 methylated loci (11.7%) that did not overlap with either exons, introns, transposable elements, or promoter regions.

A total of 37,063 methylation islands were identified in the *C. virginica* genome (Venkataraman, 2020). Methylation islands contained between 11 and 24,777 methylated CpGs, with a median of 30 methylated CpGs per island. Lengths of methylation

TABLE 1 | Summary of water chemistry during the 14-day acclimation period and 28-day experimental exposure.

Experimental Stage	T (°C)	S (PSU)	DIC	A_T	pH_{sw}	pCO_2 (μatm)	$\Omega_{calcite}$
Acclimation	14.6 ± 0.4	31.4 ± 0.1	1978 ± 7	2127 ± 6	7.94 ± 0.00	521 ± 32	2.82 ± 0.13
Control pCO_2 Conditions	14.5 ± 0.4	31.6 ± 0.3	1960 ± 32	2140 ± 15	7.95 ± 0.01	492 ± 50	3.01 ± 0.25
Elevated pCO_2 Conditions	14.5 ± 0.3	31.5 ± 0.3	2173 ± 37	2132 ± 42	7.29 ± 0.01	2550 ± 211	0.72 ± 0.06

Values indicate mean and standard error for temperature (T), salinity (S), dissolved inorganic carbon (DIC), total alkalinity (A_T), calculated pH on seawater scale, calculated pCO_2, and calculated calcite saturation ($\Omega_{calcite}$).

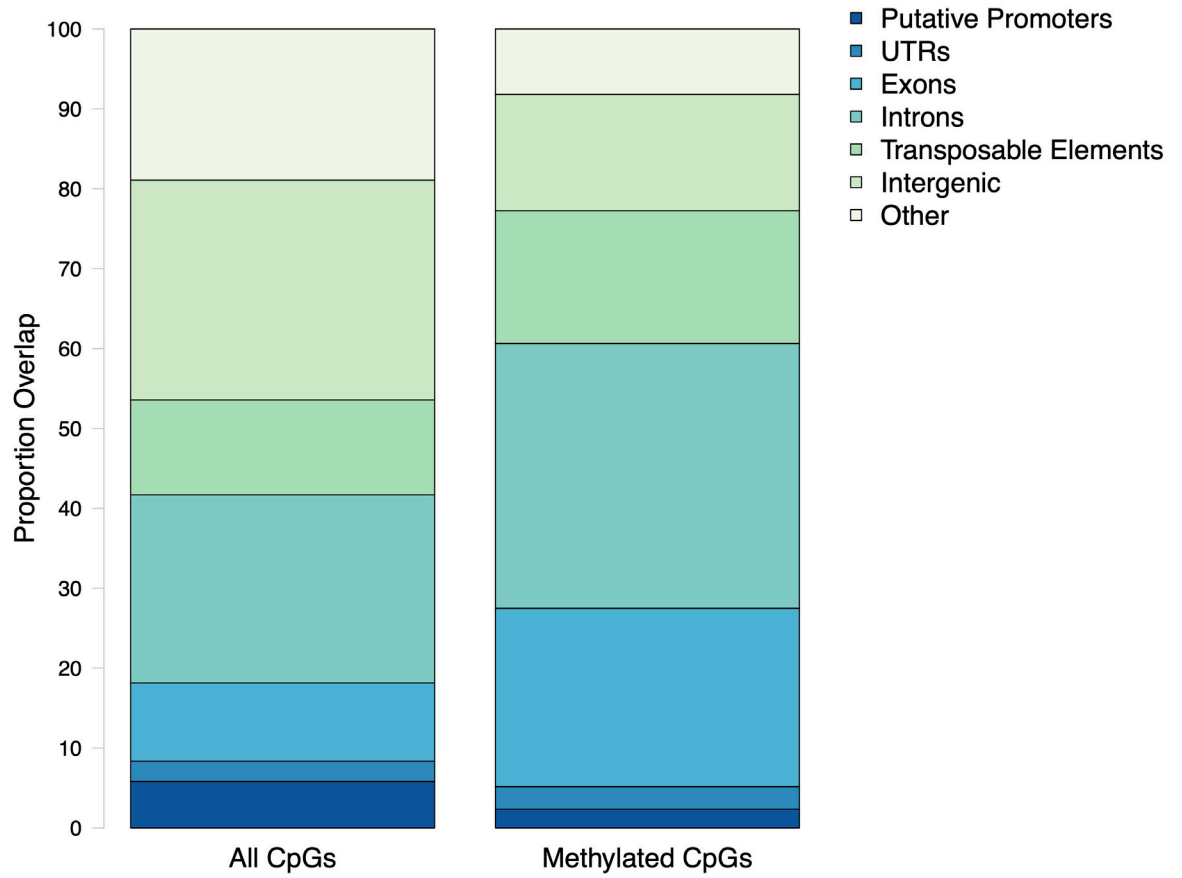

FIGURE 2 | Proportion of CpG loci within genomic features. All CpGs are every dinucleotide in the *C. virginica* genome. Methylated CpGs refers to a dinucleotide with a methylation level of at least 50%.

islands ranged from 500 to 1,236,482 base pairs, with a median length of 1,024 bp. The majority of methylation islands (36,017; 97.2%) were less than 100,000 bp in length. There were 30,773 (83.0%) methylation islands that overlapped with genic regions.

Differential Methylation Analysis

A total of 598 CpG loci were differentially methylated between oysters exposed to control or high pCO_2, with 51.8% hypermethylated and 48.2% hypomethylated between treatments (**Figure 3**; Venkataraman, 2020). When considering a PCA using methylation status of all CpG loci with 5× coverage across all samples, the first two principal components explained 29.8% of sample variation (**Figure 4A**). The first two principal components in a PCA with only differentially methylated loci (DML) explained 57.1% of the variation among treatments (**Figure 4B**). These DML were distributed throughout the *C. virginica* genome (**Figure 5**). The fifth chromosome had the most DML normalized by number of CpGs in the chromosome, and had the most genes; however, this was not the largest chromosome (**Figure 5A**).

Examination of DML within genes revealed that some genes contained multiple DML (**Figures 5B,C**). Of the 481 genes with DML, the majority only contained one DML (**Figure 5B**). There were 48 genes with 2 DML, 16 genes with 3 DML, 6 genes with 4 DML and 1 gene with 5 DML (**Figure 5B**). When multiple DML were found within a gene, they could be methylated in either the same or opposite directions (**Figure 5C**).

Within the genome, DML were mostly present in genic regions, with 560 DML in 481 genes (368 DML in exons and 192 in introns). In addition, 42 DML were found in putative promoter regions, 27 in UTR, 57 in transposable elements, and 38 in intergenic regions. There were 21 DML located outside of exons, introns, transposable elements, and putative promoters. Additionally, 537 DML were found in methylation islands. The distribution of DML in *C. virginica* gonad tissue was higher in exons than expected for MBD-enriched CpG loci with minimum 5× coverage across all samples (Contingency test; χ^2 = 401.09, *df* = 6, *P*-value < 2.2e-16; **Figure 6**). Of the 598 DML, 310 were hypermethylated and 288 were hypomethylated in the high pCO_2 treatment. The number of hyper- and hypomethylated DML was almost evenly split within each genomic feature, with the exception of putative promoter regions that had 44 hypermethylated DML vs. 23 hypomethylated DML. Within a gene, DML did not appear to be concentrated in one particular region. The distribution of hyper- and hypomethylated DML along a gene do not differ from each other (**Figure 7**).

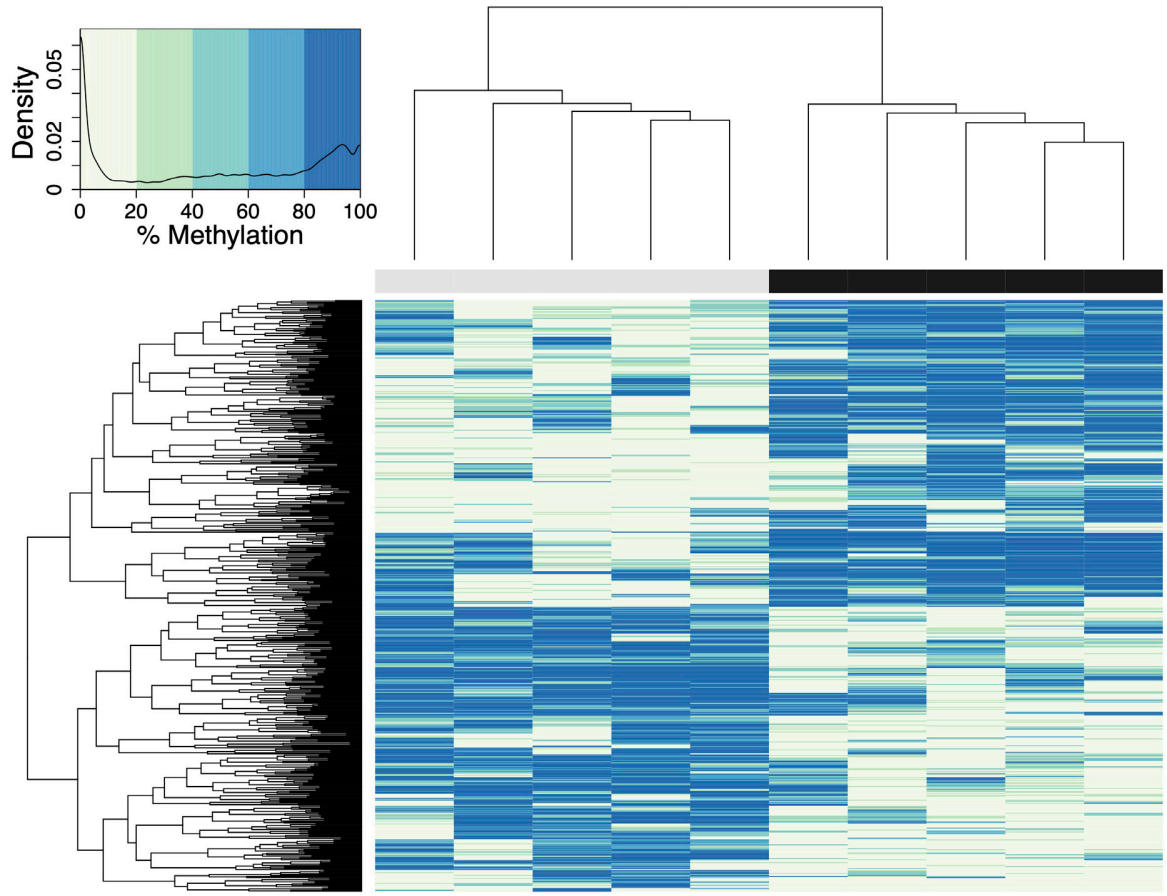

FIGURE 3 | Heatmap of DML in *C. virginica* reproductive tissue created using a euclidean distance matrix. Samples in control pCO_2 conditions are represented by gray, and samples in elevated pCO_2 conditions are represented by a black bar. Loci with higher percent methylation are represented by darker colors. A logistic regression identified 598 DML, defined as individual CpG dinucleotide with at least a 50% methylation change between treatment and control groups, and a q-value < 0.01 based on correction for false discovery rate with the SLIM method. The density of DML at each percent methylation value is represented in the heatmap legend.

The DML were found in genes responsible for various biological processes. However, no gene ontology categories were significantly represented (**Figure 8**). The majority of genes with DML were involved in protein ubiquitination processes. These genes were not consistently hyper- or hypomethylated. Certain biomineralization genes did contain DML. The gene coding for calmodulin-regulated spectrin-associated protein contained three hypomethylated and one hypermethylated DML. Genes coding for EF-hand protein with calcium-binding domain, calmodulin-binding transcription activator, and calmodulin-lysine N-methyltransferase contained one or two hypermethylated DML.

DISCUSSION

The present study is a general description of DNA methylation in *C. virginica*, and is one of the first to examine epigenetic responses to ocean acidification in the gonad tissue of a mollusc species. Five hundred ninety-eight differentially methylated loci (DML) were identified in response to the elevated pCO_2 treatments, most of which were in exons. Not only was DNA methylation of *C. virginica* altered in response to ocean acidification, but changes in gonad methylation indicates potential for these methylation patterns to be inherited by offspring.

Understanding how environmental stressors influence the epigenome is crucial when considering potential acclimatization mechanisms in marine invertebrates. Our finding that high pCO_2 impacts *C. virginica* DNA methylation adds to a growing body of work about ocean acidification's impact on marine invertebrate methylomes. The coral species *P. damicornis* demonstrated an overall increase in DNA methylation when exposed to low pH conditions (7.3–7.6) for 6 weeks, potentially influencing biomineralization (Putnam et al., 2016). Another coral species, *S. pistillata*, also demonstrated an increase in genome-wide DNA methylation when exposed to low pH conditions for 2 years. Changes in the methylome also modified gene expression and altered pathways involved in cell cycle regulation (Liew et al., 2018b). The present study on an oyster, however, did not observe the overall genome-wide increase in methylation

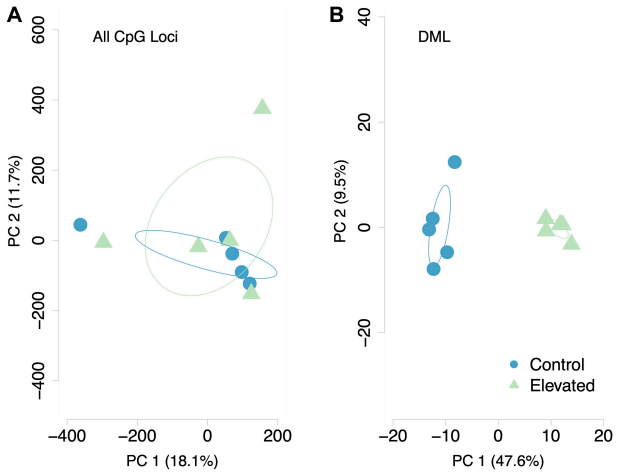

FIGURE 4 | Principal Components Analysis of **(A)** all CpG loci with 5x coverage across samples and **(B)** DML. Methylation status of individual CpG loci explained 29.2% of variation between samples when considering all CpG loci. Methylation status of DML explained 57.1% of sample variation.

that was reported for corals. Instead, we found subtle, but significant, increases or decreases in percent methylation at several hundred individual CpGs distributed across the genome. As *C. virginica* and coral species are adapted to different environments and ecological niches, it is possible that species-specific differences in methylation responses contribute to the observed methylation pattern.

The *C. virginica* methylation landscape suggests a role for methylation in gene activity. Approximately 22% of CpGs in the *C. virginica* gonad genome were methylated, which is consistent with previous studies of marine invertebrate genomes Gavery and Roberts, 2013; Olson and Roberts, 2014; Hofmann, 2017; Dimond and Roberts, 2020). Methylated loci were concentrated in introns for *C. virginica*, followed by exons and transposable elements. This location of methylated CpGs in gene bodies is consistent with what has been reported across similar taxa (Roberts and Gavery, 2012; Eirin-Lopez and Putnam, 2018). The concentration of methylated CpGs in gene bodies corresponds with proposed functionality in influencing gene activity (Roberts and Gavery, 2012; Dixon et al., 2014; Liew et al., 2018b). Our study also found methylation in transposable elements, putative promoters and intragenic regions. In plants, transposable element methylation has been shown to modulate the effect of transposable element insertion in genic regions (Hosaka and Kakutani, 2018). It is possible that methylation of transposable elements in *C. virginica* could also limit the effect of transposable elements. The characterization of methylation islands in the *C. virginica* genome demonstrates the viability of this descriptive tool for future work examining methylation in mollusc species.

The presence of DML suggests that exposure to experimental ocean acidification conditions elicits an epigenetic response. Many studies have documented changes to oyster protein synthesis, energy production, metabolism, antioxidant responses, and reproduction in response to ocean acidification (Tomanek et al., 2011; Timmins-Schiffman et al., 2014; Dineshram et al., 2016; Boulais et al., 2017; Omoregie et al., 2019). Examination of methylation associated with these physiological responses could identify mechanisms that contribute to these changes. For example, our study found a hypomethylated DML in the heat shock protein 75 kDA gene, and gene expression responses to ocean acidification in *C. virginica* have found downregulation in a similar molecular chaperone, heat shock protein 70 kDa (Beniash et al., 2010; Ivanina et al., 2014). Other gene expression studies in bivalves have found changes in oxidative stress proteins such as superoxide dismutase, cytochrome c, peroxiredoxin, and NADH dehydrogenase (Chapman et al., 2011; Clark et al., 2013; Goncalves et al., 2016, 2017). Although we did not find any DML in these genes, combined study of DNA methylation and transcription may reveal how changes in gene expression are regulated in response to environmental stressors.

Although DML were found across various genome features, they were mostly in exons and introns. This is consistent with a recent study of *C. virginica* gill tissue found differentially methylated regions in response to a salinity gradient were primarily in genic regions (Johnson and Kelly, 2019). Interestingly, DML were not found consistently in one particular region of a gene. Similarly, methylated positions in genic regions were evenly distributed after the coral *S. pistillata* was exposed to low pH (Liew et al., 2018b). Examination of another coral, *P. daedalea*, in different temperature and salinity conditions found more frequent methylation at 5′ and 3′ ends of genes (Liew et al., 2018a). We also found several genes with multiple DML. These DML were not consistently hyper- or hypomethylated in the same gene. As hyper- and hypomethylation may result in different transcriptional outcomes, future work should examine the role of multiple DML on alternative splicing and gene expression.

The concentration of DML in gene bodies suggests a role for DNA methylation in gene expression and regulation. A majority of genes with DML were involved in protein ubiquitination. Protein ubiquitination is a post-translational protein modification that is involved in protein synthesis and degradation (Peng et al., 2003; Komander, 2009). Previous studies in which oysters were exposed to experimental ocean acidification conditions have demonstrated changes in this pathway. For example, shotgun proteomic characterization of posterior gill lamellae from adult *C. gigas* exposed to high pCO_2 revealed increased abundance of proteins involved in ubiquitination and decreased protein degradation (Timmins-Schiffman et al., 2014). Elevated pCO_2 levels were also found to upregulate malate dehydrogenase in adult *C. virginica* mantle tissue (Tomanek et al., 2011). Several genes involved in protein ubiquitination, including those for malate dehydrogenase, ubiquitin-protein ligase, RNA polymerase-associated protein, and DNA damage-binding protein, were significantly hypermethylated in gonad tissue exposed to elevated pCO_2. Hypermethylation of these genes may decrease transcriptional opportunities, thus indicating a critical role in the response to ocean acidification.

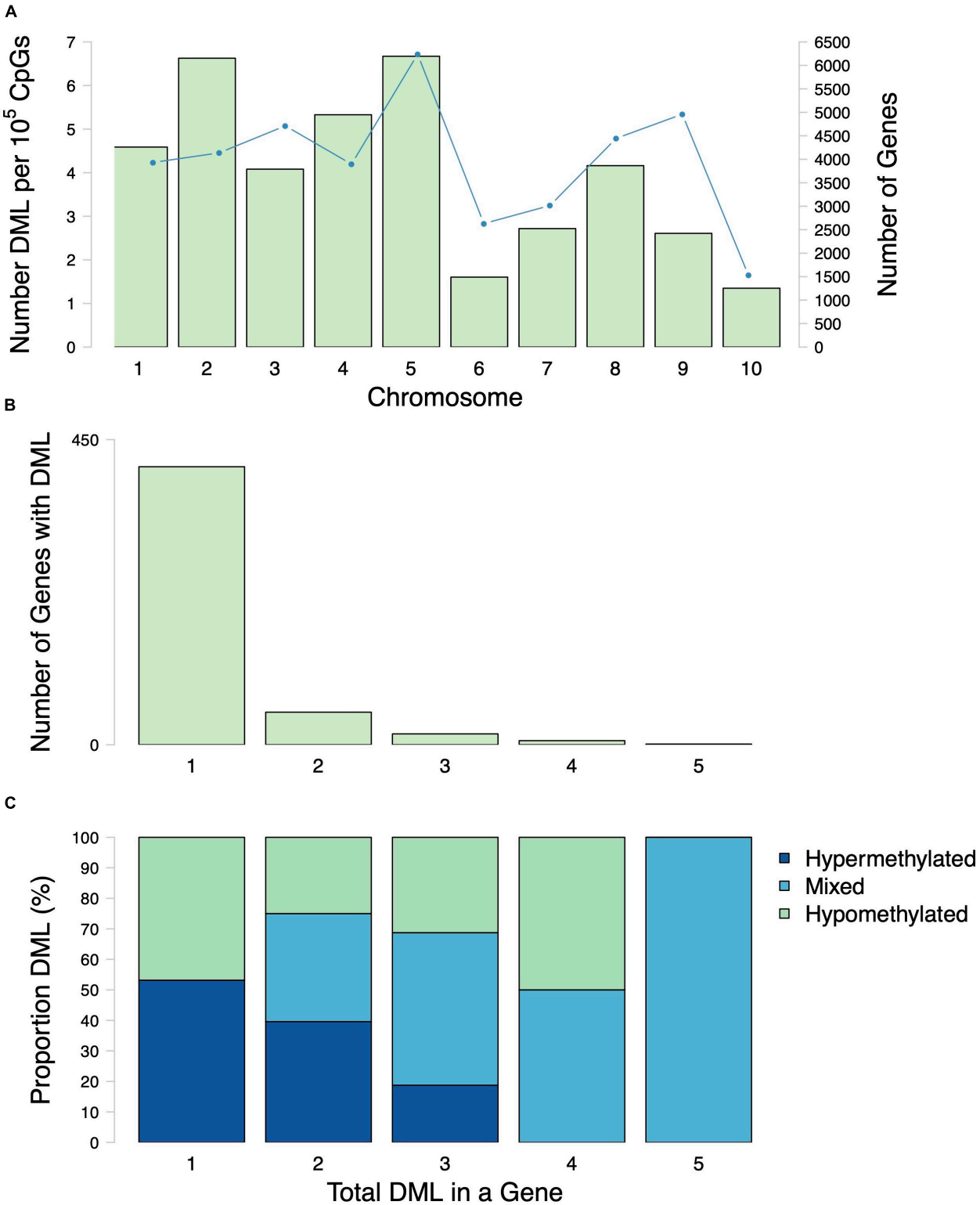

FIGURE 5 | Distribution of DML among chromosomes and genes. **(A)** Number of DML normalized by number of CpG in each chromosome (bars) and number of genes (line) in each *C. virginica* chromosome. **(B)** Number of genes with various numbers of DML per gene (1–5). Most genes that contained DML only had 1 DML. **(C)** Proportion of hypermethylated, hypomethylated DML in genes with various numbers of DML per gene (1–5). Mixed refers to a classification of a gene that has both hypermethylated and hypomethylated DML.

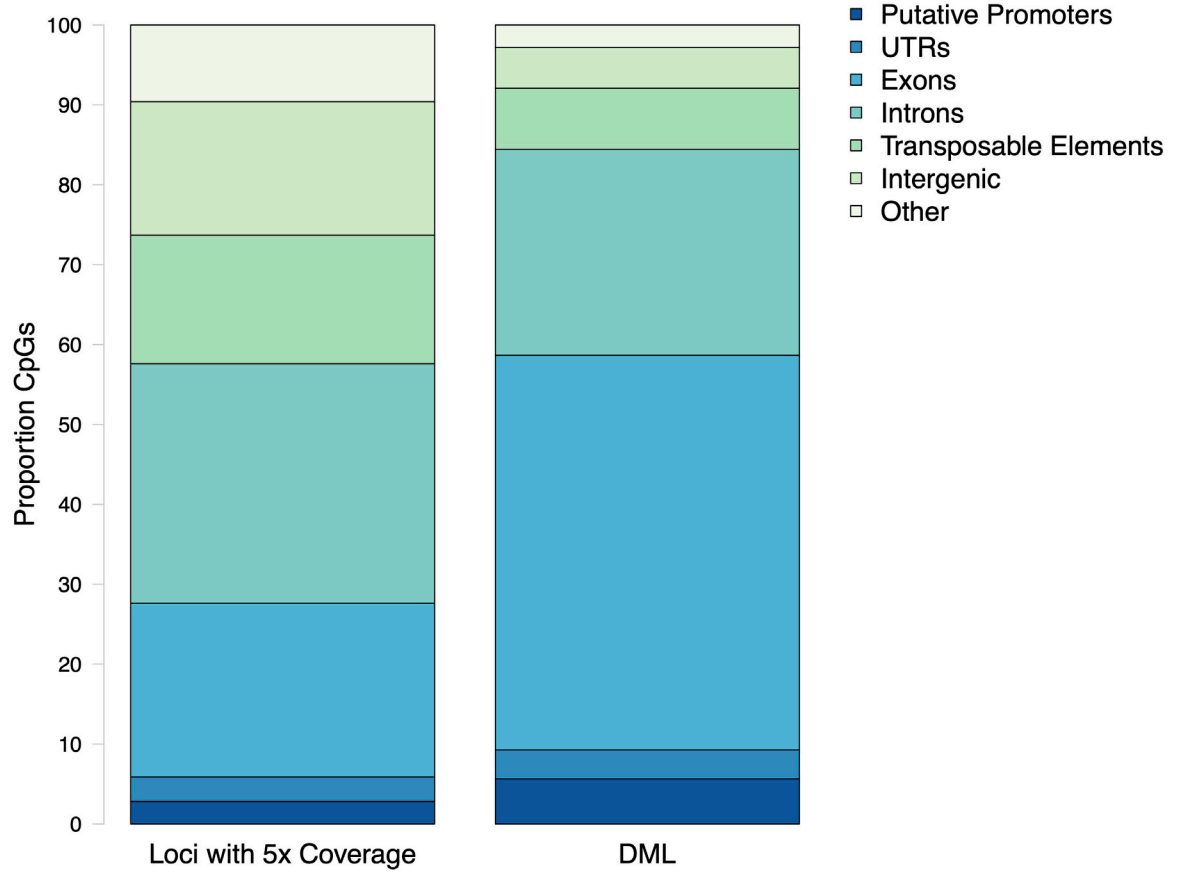

FIGURE 6 | Proportion CpG loci within putative promoters, untranslated regions (UTR), exons, introns, transposable elements, and intergenic regions for MBD-enriched CpGs and differentially methylated loci (DML). The distribution of DML in *C. virginica* gonad tissue in response to ocean acidification differed from distribution of MBD-enriched loci with 5× coverage across control and treatment samples (Contingency test; $\chi^2 = 401.09$, $df = 6$, P-value $< 2.2e\text{-}16$).

Four genes involved in biomineralization contained DML, suggesting these genes can be epigenetically regulated. Upregulation of calcium-binding gene expression has been previously documented in *C. virginica* (Richards et al., 2018). Since the hypermethylated DML in these genes are typically associated with reduced transcriptional opportunities, it is unclear how methylation changes relate to gene expression for biomineralization genes. Many studies examining ocean acidification-induced carryover effects in bivalves note changes to calcification processes. For example, the Sydney rock oyster (*S, glomerata*) larvae exhibit faster shell growth in high pCO_2 conditions when parents mature in those same conditions (Parker et al., 2012, 2015). In contrast, larvae from other species found in the North Atlantic such as northern quahog (hard clam; *M. mercenaria*) and bay scallops (*A. irradians*) developed slower when parents were reproductively conditioned in low pH conditions (Griffith and Gobler, 2017). There is some evidence to suggest that *C. virginica* larvae may be more resilient to high pCO_2 conditions than *M. mercenaria* or *A. irradians* (Gobler and Talmage, 2014). Differential methylation of biomineralization genes in *C. virginica* reproductive tissue could be a mechanism to explain when parental experience impacts larval calcification if in fact these DML are inherited.

Although our work documents significant changes to DNA methylation in reproductive tissue after high pCO_2 exposure, this finding may be confounded by secondary effects of gonad maturation. Specimens collected were from mixed populations, and sampled tissue contained both mature and immature gametes. Reproductive tissue likely contained both gametic and somatic cell types. Sex-specific effects have also been documented in response to ocean acidification in mollusc species (Parker et al., 2018; Venkataraman et al., 2019). Lack of a reproductive phenotype precludes any interpretation of how maturation stage or sex can influence changes DNA methylation, as previous work in *C. gigas* demonstrates these factors as significant influences on baseline methylation patterns (Zhang et al., 2018). Nevertheless, differential methylation in stress response and biomineralization genes suggests that our study does record epigenetic responses to ocean acidification. Future work should pair methylation data with reproductive phenotypes to provide additional information on sex- or stage-specific epigenetic responses to ocean acidification.

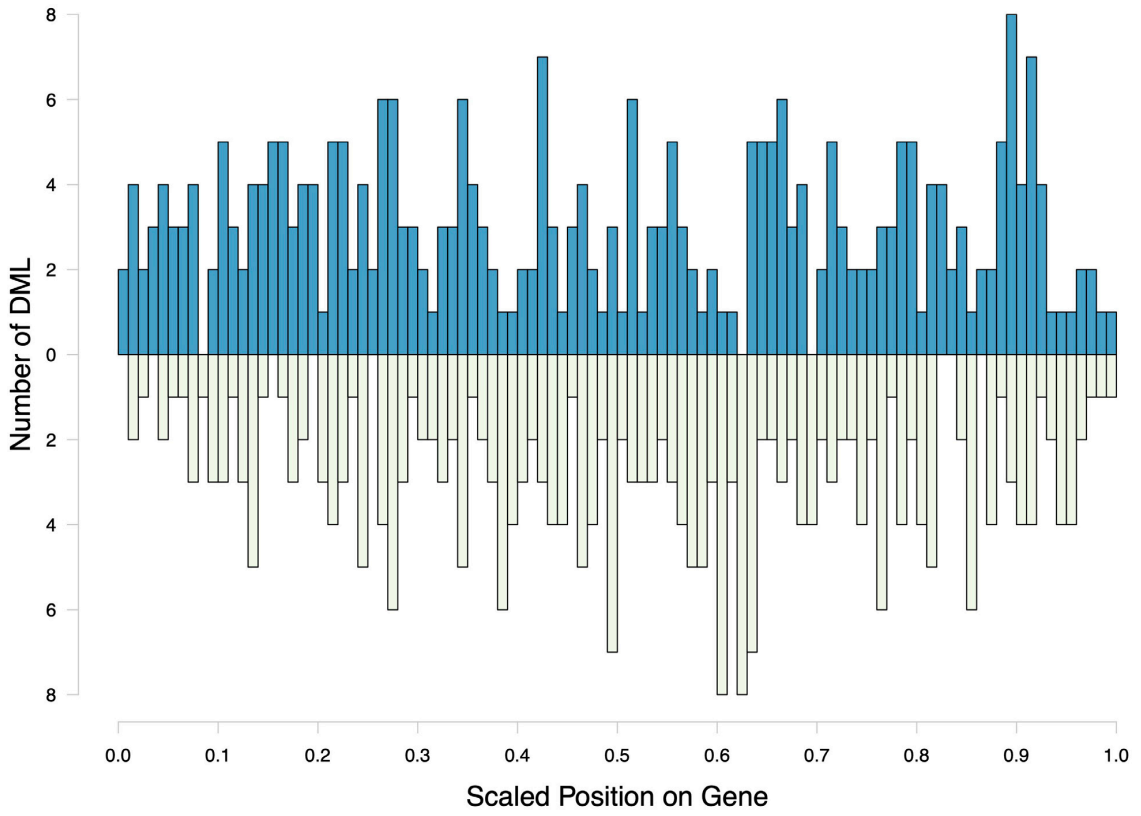

FIGURE 7 | Distribution of hyper- and hypomethylated DML along a hypothetical gene. The scaled position of a DML within a gene was calculated by dividing the base pair position of the DML by gene length. Counts of hypermethylated DML are plotted above the *x*-axis, and hypomethylated DML counts are below the *x*-axis.

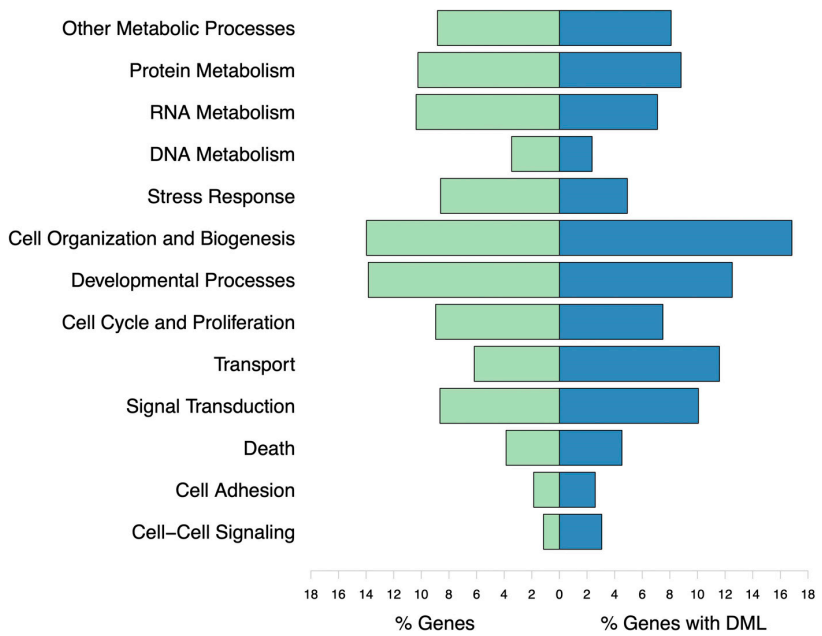

FIGURE 8 | Biological processes represented by all genes used in enrichment background (% Genes) and those with DML (% Genes with DML). Gene ontology categories with similar functions are represented by the same color. Genes may be involved in multiple biological processes. No gene ontologies were significantly enriched.

CONCLUSION

Our study found that *C. virginica* demonstrates a significant epigenetic response to elevated pCO_2 exposure, with 598 DML identified. The concentration of these DML in gene bodies suggests that methylation may be important for transcriptional control in response to environmental stressors. As ocean acidification induced differential methylation in *C. virginica* gonad tissue, there is a potential for intergenerational epigenetic inheritance, which could control the gene activity of processes such as biomineralization. As carryover effects can persist even when stressors are long-removed (Venkataraman et al., 2019), understanding the mechanisms involved in intergenerational acclimatization is crucial. Future work should focus on methylation patterns in adult *C. virginica* fully-formed gametes and larvae exposed to various pCO_2 conditions to determine to what degree a difference in methylation influences gene activity and how this might influence phenotypic plasticity.

DATA AVAILABILITY STATEMENT

Raw sequence data is available at the NCBI Sequence Read Archive under BioProject accession number PRJNA513384, with associated metadata and information also available at Woods Hole Open Access Server: https://hdl.handle.net/1912/25138. Associated information for all analyses and supplemental material can be found in the Github repository which is available in an archival format (Venkataraman, 2020; https://doi.org/10.6084/m9.figshare.11923479).

AUTHOR CONTRIBUTIONS

AD-W, JR, IW, and KL conceived and ran the experiment. YV, SW, and SR performed DNA extractions and methylation analysis. AD-W and KL contributed to analysis. YV and AD-W wrote the initial manuscript draft. All authors reviewed and approved the final manuscript.

FUNDING

This project was funded by National Science Foundation Biological Oceanography award 1635423 to KL, JR, and BR, and a Hall Conservation Genetics Research Award to YV.

ACKNOWLEDGMENTS

We thank Mackenzie Gavery and our two reviewers for their insightful feedback on the manuscript. This work was facilitated through the use of advanced computational, storage, and networking infrastructure provided by the Hyak supercomputer system at the University of Washington.

REFERENCES

Akalin, A., Kormaksson, M., Li, S., Garrett-Bakelman, F. E., Figueroa, M. E., Melnick, A., et al. (2012). methylKit: a comprehensive R package for the analysis of genome-wide DNA methylation profiles. *Genome Biol.* 13:R87.

Andrews, S. (2010). *FastQC: A Quality Control Tool for High Throughput Sequence Data [Online]*. Available online at: http://www.bioinformatics.babraham.ac.uk/projects/fastqc/

Bao, W., Kojima, K. K., and Kohany, O. (2015). Repbase Update, a database of repetitive elements in eukaryotic genomes. *Mob. DNA* 6:11.

Barton, A., Hales, B., Waldbusser, G. G., Langdon, C., and Feely, R. A. (2012). The Pacific oyster, *Crassostrea gigas*, shows negative correlation to naturally elevated carbon dioxide levels: implications for near-term ocean acidification effects. *Limnol. Oceanogr.* 57, 698–710. doi: 10.4319/lo.2012.57.3.0698

Beniash, E., Ivanina, A., Lieb, N. S., Kurochkin, I., and Sokolova, I. M. (2010). Elevated level of carbon dioxide affects metabolism and shell formation in oysters *Crassostrea virginica*. *Mar. Ecol. Prog. Ser.* 419, 95–108. doi: 10.3354/meps08841

Bird, A. (2002). DNA methylation patterns and epigenetic memory. *Genes Dev.* 16, 6–21. doi: 10.1101/gad.947102

Bossdorf, O., Richards, C. L., and Pigliucci, M. (2008). Epigenetics for ecologists. *Ecol. Lett.* 11, 106–115.

Boulais, M., Chenevert, K. J., Demey, A. T., Darrow, E. S., Robison, M. R., Roberts, J. P., et al. (2017). Oyster reproduction is compromised by acidification experienced seasonally in coastal regions. *Sci. Rep.* 7:13276.

Byrne, M., Foo, S. A., Ross, P. M., and Putnam, H. M. (2019). Limitations of cross and multigenerational plasticity for marine invertebrates faced with global climate change. *Glob. Chang. Biol.* 26, 80–102. doi: 10.1111/gcb.14882

Chapman, R. W., Mancia, A., Beal, M., Veloso, A., Rathburn, C., Blair, A., et al. (2011). The transcriptomic responses of the eastern oyster, *Crassostrea virginica*, to environmental conditions. *Mol. Ecol.* 20, 1431–1449. doi: 10.1111/j.1365-294x.2011.05018.x

Clark, M. S., Thorne, M. A. S., Amaral, A., Vieira, F., Batista, F. M., Reis, J., et al. (2013). Identification of molecular and physiological responses to chronic environmental challenge in an invasive species: the Pacific oyster, *Crassostrea gigas*. *Ecol. Evol.* 3, 3283–3297.

Deans, C., and Maggert, K. A. (2015). What do you mean, "Epigenetic"? *Genetics* 199, 887–896. doi: 10.1534/genetics.114.173492

Dickson, A. G. (1990). Standard potential of the reaction : AgCl(s) + 12H2(g) = Ag(s) + HCl(aq), and the standard acidity constant of the ion HSO4- in synthetic sea water from 273.*15* to 318.15 K. *J. Chem. Thermodyn.* 22, 113–127. doi: 10.1016/0021-9614(90)90074-z

Dimond, J. L., and Roberts, S. B. (2016). Germline DNA methylation in reef corals: patterns and potential roles in response to environmental change. *Mol. Ecol.* 25, 1895–1904. doi: 10.1111/mec.13414

Dimond, J. L., and Roberts, S. B. (2020). Convergence of DNA methylation profiles of the reef coral *Porites astreoides* in a novel environment. *Front. Mar. Sci.* 6:792. doi: 10.3389/fmars.2019.00792

Dineshram, R., Chandramouli, K., Ko, G. W. K., Zhang, H., Qian, P.-Y., Ravasi, T., et al. (2016). Quantitative analysis of oyster larval proteome provides new insights into the effects of multiple climate change stressors. *Glob. Chang. Biol.* 22, 2054–2068. doi: 10.1111/gcb.13249

Dixon, G. B., Bay, L. K., and Matz, M. V. (2014). Bimodal signatures of germline methylation are linked with gene expression plasticity in the coral *Acropora millepora*. *BMC Genomics* 15:1109. doi: 10.1186/1471-2164-15-1109

Eirin-Lopez, J. M., and Putnam, H. M. (2018). Marine environmental epigenetics. *Ann. Rev. Mar. Sci.* 11, 335–368. doi: 10.1146/annurev-marine-010318-095114

Ekstrom, J. A., Suatoni, L., Cooley, S. R., Pendleton, L. H., Waldbusser, G. G., Cinner, J. E., et al. (2015). Vulnerability and adaptation of US shellfisheries to ocean acidification. *Nat. Clim. Chang.* 5, 207–214. doi: 10.1038/nclimate2508

Feely, R. A., Alin, S. R., Newton, J., Sabine, C. L., Warner, M., Devol, A., et al. (2010). The combined effects of ocean acidification, mixing, and respiration on pH and carbonate saturation in an urbanized estuary. *Estuar. Coast. Shelf Sci.* 88, 442–449. doi: 10.1016/j.ecss.2010.05.004

Gatzmann, F., Falckenhayn, C., Gutekunst, J., Hanna, K., Raddatz, G., Carneiro, V. C., et al. (2018). The methylome of the marbled crayfish links gene body methylation to stable expression of poorly accessible genes. *Epigenet. Chromatin* 11:57.

Gavery, M. R., and Roberts, S. B. (2013). Predominant intragenic methylation is associated with gene expression characteristics in a bivalve mollusc. *PeerJ* 1:e215. doi: 10.7717/peerj.215

Gazeau, F., Quiblier, C., Jansen, J. M., Gattuso, J.-P., Middelburg, J. J., and Heip, C. H. R. (2007). Impact of elevated CO2 on shellfish calcification. *Geophys. Res. Lett.* 34:L07603.

Gish, W., and States, D. J. (1993). Identification of protein coding regions by database similarity search. *Nat. Genet.* 3, 266–272. doi: 10.1038/ng0393-266

Gobler, C. J., and Talmage, S. C. (2014). Physiological response and resilience of early life-stage Eastern oysters (*Crassostrea virginica*) to past, present and future ocean acidification. *Conserv. Physiol.* 2:cou004. doi: 10.1093/conphys/cou004

Gómez-Chiarri, M., Warren, W. C., Guo, X., and Proestou, D. (2015). Developing tools for the study of molluscan immunity: the sequencing of the genome of the eastern oyster, *Crassostrea virginica*. *Fish Shellfish Immunol.* 46, 2–4. doi: 10.1016/j.fsi.2015.05.004

Goncalves, P., Anderson, K., Thompson, E. L., Melwani, A., Parker, L. M., Ross, P. M., et al. (2016). Rapid transcriptional acclimation following transgenerational exposure of oysters to ocean acidification. *Mol. Ecol.* 25, 4836–4849. doi: 10.1111/mec.13808

Goncalves, P., Thompson, E. L., and Raftos, D. A. (2017). Contrasting impacts of ocean acidification and warming on the molecular responses of CO2-resilient oysters. *BMC Genomics* 18:431. doi: 10.1186/s12864-017-3818-z

Griffith, A. W., and Gobler, C. J. (2017). Transgenerational exposure of North Atlantic bivalves to ocean acidification renders offspring more vulnerable to low pH and additional stressors. *Sci. Rep.* 7:11394.

Helm, M. M., and Bourne, N. (2004). *Hatchery Culture of Bivalves: A Practical Manual*. Rome: Food & Agriculture Org.

Hofmann, G. E. (2017). Ecological epigenetics in marine metazoans. *Front. Mar. Sci.* 4:4. doi: 10.3389/fmars.2017.00004

Hosaka, A., and Kakutani, T. (2018). Transposable elements, genome evolution and transgenerational epigenetic variation. *Curr. Opin. Genet. Dev.* 49, 43–48. doi: 10.1016/j.gde.2018.02.012

IPCC (2019). "Summary for Policymakers," in *IPCC Special Report on the Ocean and Cryosphere in a Changing Climate*, eds H.-O. Pörtner, D. C. Roberts, V. Masson-Delmotte, P. Zhai, M. Tignor, E. Poloczanska, et al. (Geneva: IPCC).

Ivanina, A. V., Hawkins, C., and Sokolova, I. M. (2014). Immunomodulation by the interactive effects of cadmium and hypercapnia in marine bivalves *Crassostrea virginica* and *Mercenaria mercenaria*. *Fish Shellfish Immunol.* 37, 299–312. doi: 10.1016/j.fsi.2014.02.016

Jeong, H., Wu, X., Smith, B., and Yi, S. V. (2018). Genomic Landscape of Methylation Islands in Hymenopteran Insects. *Genome Biol. Evol.* 10, 2766–2776. doi: 10.1093/gbe/evy203

Johnson, K. M., and Kelly, M. W. (2019). Population epigenetic divergence exceeds genetic divergence in the Eastern oyster *Crassostrea virginica* in the Northern Gulf of Mexico. *Evol. Appl.* 00, 1–15. doi: 10.1111/eva.12912

Komander, D. (2009). The emerging complexity of protein ubiquitination. *Biochem. Soc. Trans.* 37, 937–953. doi: 10.1042/bst0370937

Krueger, F., and Andrews, S. R. (2011). Bismark: a flexible aligner and methylation caller for Bisulfite-Seq applications. *Bioinformatics* 27, 1571–1572. doi: 10.1093/bioinformatics/btr167

Kurihara, H., Kato, S., and Ishimatsu, A. (2007). Effects of increased seawater *p*CO2 on early development of the oyster *Crassostrea gigas*. *Aquat. Biol.* 1, 91–98. doi: 10.3354/ab00009

Langmead, B., and Salzberg, S. L. (2012). Fast gapped-read alignment with Bowtie 2. *Nat. Methods* 9, 357–359. doi: 10.1038/nmeth.1923

Lee, K., Tae-Wook, K., Byrne, R., Millero, F. J., Feely, R. A., and Liu, Y.-M. (2010). The universal ratio of boron to chlorinity for the North Pacific and North Atlantic oceans. *Geochim. Cosmochim. Acta* 74, 1801–1811. doi: 10.1016/j.gca.2009.12.027

Lewis, E., and Wallace, D. W. (1998). *R: Program developed for CO2 system calculations ORNL/CDIAC-105*. Oak Ridge: US Department of Energy.

Li, H., Handsaker, B., Wysoker, A., Fennell, T., Ruan, J., Homer, N., et al. (2009). The Sequence Alignment/Map format and SAMtools. *Bioinformatics* 25, 2078–2079. doi: 10.1093/bioinformatics/btp352

Liew, Y. J., Howells, E. J., Wang, X., Michell, C. T., Burt, J. A., Idaghdour, Y., et al. (2018a). Intergenerational epigenetic inheritance in reef-building corals. *bioRxiv* [preprint]. doi: 10.1101/269076

Liew, Y. J., Zoccola, D., Li, Y., Tambutté, E., Venn, A. A., and Michell, C. T. (2018b). Epigenome-associated phenotypic acclimatization to ocean acidification in a reef-building coral. *Sci. Adv.* 4:eaar8028. doi: 10.1126/sciadv.aar8028

Martin, M. (2011). Cutadapt removes adapter sequences from high-throughput sequencing reads. *EMBnet J.* 17, 10–12.

Olson, C. E., and Roberts, S. B. (2014). Genome-wide profiling of DNA methylation and gene expression in *Crassostrea gigas* male gametes. *Front. Physiol.* 5:224. doi: 10.3389/fphys.2014.00224

Omoregie, E., Mwatilifange, N. S. I., and Liswaniso, G. (2019). Futuristic ocean acidification levels reduce growth and reproductive viability in the pacific oyster (*Crassostrea gigas*). *J. Appl. Sci. Environ. Manage.* 23, 1747–1754.

Parker, L. M., O'Connor, W. A., Byrne, M., Coleman, R. A., Virtue, P., Dove, M., et al. (2017). Adult exposure to ocean acidification is maladaptive for larvae of the Sydney rock oyster *Saccostrea glomerata* in the presence of multiple stressors. *Biol. Lett.* 13:20160798. doi: 10.1098/rsbl.2016.0798

Parker, L. M., O'Connor, W. A., Byrne, M., Dove, M., Coleman, R. A., Pörtner, H.-O., et al. (2018). Ocean acidification but not warming alters sex determination in the Sydney rock oyster, *Saccostrea glomerata*. *Proc. R. Soc. B* 285:20172869. doi: 10.1098/rspb.2017.2869

Parker, L. M., O'Connor, W. A., Raftos, D. A., Pörtner, H.-O., and Ross, P. M. (2015). Persistence of positive carryover effects in the Oyster, *Saccostrea glomerata*, following transgenerational exposure to ocean acidification. *PLoS One* 10:e0132276. doi: 10.1371/journal.pone.0132276

Parker, L. M., Ross, P. M., O'Connor, W. A., Borysko, L., Raftos, D. A., and Pörtner, H.-O. (2012). Adult exposure influences offspring response to ocean acidification in oysters. *Glob. Chang. Biol.* 18, 82–92. doi: 10.1111/j.1365-2486.2011.02520.x

Parker, L. M., Ross, P. M., O'Connor, W. A., Pörtner, H. O., Scanes, E., and Wright, J. M. (2013). Predicting the response of molluscs to the impact of ocean acidification. *Biology* 2, 651–692. doi: 10.3390/biology2020651

Peng, J., Schwartz, D., Elias, J. E., Thoreen, C. C., Cheng, D., Marsischky, G., et al. (2003). A proteomics approach to understanding protein ubiquitination. *Nat. Biotechnol.* 21, 921–926. doi: 10.1038/nbt849

Putnam, H. M., Davidson, J. M., and Gates, R. D. (2016). Ocean acidification influences host DNA methylation and phenotypic plasticity in environmentally susceptible corals. *Evol. Appl.* 9, 1165–1178. doi: 10.1111/eva.12408

Quinlan, A. R., and Hall, I. M. (2010). BEDTools: a flexible suite of utilities for comparing genomic features. *Bioinformatics* 26, 841–842. doi: 10.1093/bioinformatics/btq033

Richards, M., Xu, W., Mallozzi, A., Errera, R. M., and Supan, J. (2018). Production of calcium-binding proteins in *Crassostrea virginica* in response to increased environmental CO2 concentration. *Front. Mar. Sci.* 5:203. doi: 10.3389/fmars.2018.00203

Ries, J. B. (2011). A physicochemical framework for interpreting the biological calcification response to CO2-induced ocean acidification. *Geochim. Cosmochim. Acta* 75, 4053–4064. doi: 10.1016/j.gca.2011.04.025

Roberts, S. B., and Gavery, M. R. (2012). Is There a Relationship between DNA Methylation and Phenotypic Plasticity in Invertebrates? *Front. Physiol.* 2:116. doi: 10.3389/fphys.2011.00116

Rondon, R., Grunau, C., Fallet, M., Charlemagne, N., Sussarellu, R., Chaparro, C., et al. (2017). Effects of a parental exposure to diuron on Pacific oyster spat methylome. *Environ. Epigenet.* 3:dvx004. doi: 10.1093/eep/dvx004

Ross, P. M., Parker, L., and Byrne, M. (2016). Transgenerational responses of molluscs and echinoderms to changing ocean conditions. *ICES J. Mar. Sci.* 73, 537–549. doi: 10.1093/icesjms/fsv254

Roy, R. N., Roy, L. N., Vogel, K. M., Porter-Moore, C., Pearson, T., Good, C. E., et al. (1993). The dissociation constants of carbonic acid in seawater at salinities 5 to 45 and temperatures 0 to 45°C. *Mar. Chem.* 44, 249–267. doi: 10.1016/0304-4203(93)90207-5

Smit, A. F. A., Hubley, R., and Green, P. (2013). *RepeatMasker Open-4.0*. Available online at: http://www.repeatmasker.org

Strader, M. E., Wong, J. M., Kozal, L. C., Leach, T. S., and Hofmann, G. E. (2019). Parental environments alter DNA methylation in offspring of the purple sea urchin, *Strongylocentrotus purpuratus*. *J. Exp. Mar. Biol. Ecol.* 517, 54–64. doi: 10.1016/j.jembe.2019.03.002

Suzuki, M. M., and Bird, A. (2008). DNA methylation landscapes: provocative insights from epigenomics. *Nat. Rev. Genet.* 9, 465–476. doi: 10.1038/nrg2341

Timmins-Schiffman, E., Coffey, W. D., Hua, W., Nunn, B. L., Dickinson, G. H., and Roberts, S. B. (2014). Shotgun proteomics reveals physiological response to ocean acidification in *Crassostrea gigas*. *BMC Genomics* 15:951. doi: 10.1186/1471-2164-15-951

Tomanek, L., Zuzow, M. J., Ivanina, A. V., Beniash, E., and Sokolova, I. M. (2011). Proteomic response to elevated PCO2 level in eastern oysters, *Crassostrea virginica*: evidence for oxidative stress. *J. Exp. Biol.* 214, 1836–1844. doi: 10.1242/jeb.055475

UniProt Consortium (2019). UniProt: a worldwide hub of protein knowledge. *Nucleic Acids Res.* 47, D506–D515.

Van Heuven, S., Pierrot, D., Rae, J. W. B., Lewis, E., and Wallace, D. W. R. (2011). *MATLAB program developed for CO2 system calculations. ORNL/CDIAC-105b*. Oak Ridge: US Department of Energy.

Venkataraman, Y. R. (2020). Eastern oyster (*Crassostrea virginica*) gonad DNA methylation data and analysis. *Dataset*. doi: 10.6084/m9.figshare.11923479.v3

Venkataraman, Y. R., Spencer, L. H., and Roberts, S. B. (2019). Larval response to parental low ph exposure in the Pacific Oyster *Crassostrea gigas*. *J. Shellfish Res.* 38:743. doi: 10.2983/035.038.0325

Waldbusser, G. G., Hales, B., Langdon, C. J., Haley, B. A., Schrader, P., Brunner, E. L., et al. (2014). Saturation-state sensitivity of marine bivalve larvae to ocean acidification. *Nat. Clim. Chang.* 5:273. doi: 10.1038/nclimate2479

Wang, H.-Q., Tuominen, L. K., and Tsai, C.-J. (2011). SLIM: a sliding linear model for estimating the proportion of true null hypotheses in datasets with dependence structures. *Bioinformatics* 27, 225–231. doi: 10.1093/bioinformatics/btq650

Whitlock, M., and Schluter, D. (2014). *The Analysis of Biological Data*. Chennai: Roberts & Company.

Wright, R. M., Aglyamova, G. V., Meyer, E., and Matz, M. V. (2015). Gene expression associated with white syndromes in a reef building coral, *Acropora hyacinthus*. *BMC Genomics* 16:371. doi: 10.1186/s12864-015-1540-2

Zhang, X., Li, Q., Kong, L., and Yu, H. (2018). DNA methylation frequency and epigenetic variability of the Pacific oyster *Crassostrea gigas* in relation to the gametogenesis. *Fish. Sci.* 84, 789–797. doi: 10.1007/s12562-018-1214-5

Zhao, L., Liu, L., Liu, B., Liang, J., Lu, Y., and Yang, F. (2019). Antioxidant responses to seawater acidification in an invasive fouling mussel are alleviated by transgenerational acclimation. *Aquat. Toxicol.* 217:105331. doi: 10.1016/j.aquatox.2019.105331

Zhao, L., Yang, F., Milano, S., Han, T., Walliser, E. O., and Schöne, B. R. (2018). Transgenerational acclimation to seawater acidification in the Manila clam *Ruditapes philippinarum*: Preferential uptake of metabolic carbon. *Sci. Total Environ.* 627, 95–103. doi: 10.1016/j.scitotenv.2018.01.225

Conflict of Interest: The authors declare that the research was conducted in the absence of any commercial or financial relationships that could be construed as a potential conflict of interest.

frontiers in Marine Science

ORIGINAL RESEARCH
published: 30 April 2020
doi: 10.3389/fmars.2020.00284

An Epigenetic Signature for Within-Generational Plasticity of a Reef Fish to Ocean Warming

Taewoo Ryu[1,2], Heather D. Veilleux[3,4], Philip L. Munday[3], Imgook Jung[1], Jennifer M. Donelson[3]* and Timothy Ravasi[2]**

[1] APEC Climate Center, Busan, South Korea, [2] Marine Climate Change Unit, Okinawa Institute of Science and Technology Graduate University, Okinawa, Japan, [3] ARC Centre of Excellence for Coral Reef Studies, James Cook University, Townsville, QLD, Australia, [4] Department of Biological Sciences, University of Alberta, Edmonton, AB, Canada

OPEN ACCESS

Edited by:
Jose M. Eirin-Lopez,
Florida International University,
United States

Reviewed by:
Lisa N. S. Shama,
Alfred Wegener Institute Helmholtz Centre for Polar and Marine Research (AWI), Germany
Adam Michael Reitzel,
University of North Carolina at Charlotte, United States

***Correspondence:**
Taewoo Ryu
taewoo.ryu@oist.jp;
dakterl79@gmail.com
Jennifer M. Donelson
jennifer.donelson@jcu.edu.au
Timothy Ravasi
timothy.ravasi@oist.jp

Specialty section:
This article was submitted to Marine Molecular Biology and Ecology, a section of the journal Frontiers in Marine Science

Received: 16 January 2020
Accepted: 07 April 2020
Published: 30 April 2020

Citation:
Ryu T, Veilleux HD, Munday PL, Jung I, Donelson JM and Ravasi T (2020) An Epigenetic Signature for Within-Generational Plasticity of a Reef Fish to Ocean Warming. Front. Mar. Sci. 7:284. doi: 10.3389/fmars.2020.00284

Elevated temperature can have detrimental effects on the physiological performance of many marine organisms. However, phenotypic plasticity may enable some populations to maintain their performance under thermal stress. Two longitudinally separated populations of the coral reef fish, *Acanthochromis polyacanthus* from the Great Barrier Reef have shown differing capacities for thermal plasticity – the southernmost Heron Island population restored aerobic scope within one generation at a higher temperature, whereas the northernmost Palm Island population restored aerobic scope only when two generations were exposed to warmer conditions. We recently discovered an epigenetic signature associated with transgenerational plasticity in the Palm Island population. Here, we aimed to determine if epigenetic changes are also associated with the within-generational plasticity observed in the Heron Island population and, if so, how this epigenetic signature compares to the Palm Island transgenerational epigenome. By sequencing and analyzing the genome-wide DNA methylome of fish reared at control (+0°C) or elevated temperatures (+1.5 and +3°C) since early life, we identified 480 differentially methylated genomic regions and 372 adjacent protein-coding genes associated with within-generational plasticity in the Heron Island population. Functions related to insulin, cardiovascular capacity, development, and heat response were significantly enriched in differentially methylated genes, suggesting that these functions are the core mechanisms for within-generational restoration of aerobic scope. Comparison to the differentially methylated genes identified from F2 Palm Island population revealed little overlap of genes and enriched functions, indicating that distinct genetic toolkits may be used for within- and between-generational plasticity to ocean warming in the same species from different latitudes.

Keywords: climate change, ocean warming, coral reef fish, epigenetics, DNA methylation, phenotypic plasticity

INTRODUCTION

Understanding how organisms respond to rapid environmental change is increasingly important as global climate change intensifies (Scheffers et al., 2016; Pecl et al., 2017; IPCC, 2019). For ectothermic animals, changes in environmental temperature have direct effects on physiological performance, due to a lack of internal thermal regulation, making them especially at risk from future warming (Fry and Hart, 1948; Portner and Farrell, 2008; Sunday et al., 2010). Furthermore,

for many ectotherms, the projected future warming exceeds the current-day thermal performance range and will likely result in the loss of individual performance and potentially increased rate of mortality (Tewksbury et al., 2008; Hughes et al., 2018). However, ectothermic species may be able to buffer the effects of rising temperature on individual performance through phenotypic plasticity and genetic adaptation over the longer-term (Hoffmann and Sgro, 2011; Munday et al., 2013; Reusch, 2014). Therefore, in order to predict the effect of future warming on ectotherm populations it is necessary to understand the adaptive physiological mechanisms that can reduce the impact of elevated environmental temperature over timescales relevant to the pace of climate change.

The capacity for phenotypic plasticity (i.e., environmentally-induced phenotypic variation) to buffer individual responses to higher temperature is likely to be especially advantageous because, for many species, the climate is changing faster than adaption via natural selection can keep up (Gienapp et al., 2008; Reusch, 2014; Fox et al., 2019). Many short-term experiments have demonstrated negative effects of predicted future temperatures on the physiological performance of fish and other marine ectotherms (Wernberg et al., 2012; Hoey et al., 2016). However, new studies are showing that individual performance can be sustained if environmental change is experienced during critical windows within- and between-generations (Donelson et al., 2018). For example, the intertidal copepod, *Tigriopus californicus*, showed a plastic shift in adult upper thermal tolerance when they developed at elevated temperature compared to those developed at control temperature throughout the larval stage (Healy et al., 2019). Similarly, the growth rate of juvenile sheepshead minnow is reduced at elevated temperature, but not when parents were also exposed to elevated temperature (Salinas and Munch, 2012). Nevertheless, our ability to project the extent of thermal phenotypic plasticity beyond the few species that have been studied to date is limited. For example, beneficial plasticity does not always occur (Marshall and Uller, 2007; Bautista and Burggren, 2019) and the magnitude of temperature change can be important in inducing phenotypic change (Grenchik et al., 2013; Shama, 2017). The timing of warming in development can also determine whether phenotypic change occurs, and in some cases development at higher temperature during early life stages is critical for phenotypic adjustment (Shama et al., 2014; Le Roy et al., 2017). The diversity of phenotypic responses to environmental change make projecting future biological responses challenging, but an understanding of the underlying mechanisms could enhance our capacity to predict plasticity in the future.

The coral reef damselfish, *Acanthochromis polyacanthus*, has been extensively studied in terms of within- and between-generational plasticity to elevated temperature. Differing capacities for phenotypic plasticity has been observed between populations of *A. polyacanthus* from the Great Barrier Reef (GBR) (Donelson and Munday, 2012; Donelson et al., 2012). Specifically, restoration of aerobic physiology was observed within a generation in the Heron Island population (near the cold boundary of the species range on the GBR) when fish developed from early life in elevated temperature conditions (Donelson and Munday, 2012). In contrast, there was only partial restoration of aerobic performance within one generation in the Palm Island population (middle of the species range on the GBR) (Donelson and Munday, 2012; Donelson et al., 2012; Veilleux et al., 2015). Full restoration of aerobic scope only occurred when two generations (parents and offspring) were subjected to warmer conditions. The physiological processes involved were also different between the two populations. The Heron Island fish were able to restore aerobic scope by reducing resting metabolic rates (RMR) when reared from early life at +3°C (within-generational treatment) compared to the present-day control group. Conversely, the Palm Island population that were reared at +3°C slightly reduced their RMR, but not enough to restore aerobic scope (Donelson et al., 2011; Donelson and Munday, 2012). However, when Palm Island fish were reared at +3°C for two generations (transgenerational treatment) or reared at +1.5°C for the first generation and then stepped up to +3°C for the second generation (step treatment), fish possessed enhanced aerobic performance through increased maximum metabolic rates (MMR), with the +3°C transgenerational treatment also showing a reduction in RMR (Donelson et al., 2012; Bernal et al., 2018). This implies that underlying molecular mechanisms for thermal physiological plasticity may differ for these populations, and between within- and between-generational plasticity. Understanding the molecular mechanisms governing thermal plasticity in different populations is important for predicting the response of the species to changing climatic conditions across their geographical range.

Epigenetic regulation, a process that can shape heritable phenotypes without changes in the genetic code and can mediate stable gene expression, may be one important mechanism underlying within- and between-generational phenotypic plasticity (Jablonka and Raz, 2009; Ho and Burggren, 2010; Bonduriansky et al., 2012; Duncan et al., 2014). Although epigenetic mechanisms, such as DNA methylation, have been recognized as putatively playing a role in phenotypic plasticity in the context of climate change (Marsh and Pasqualone, 2014; Munday, 2014; Putnam et al., 2016; Anastasiadi et al., 2017; Torda et al., 2017; Ryu et al., 2018), only a handful of studies have addressed relationships among whole genome DNA methylation changes, physiology, and their related gene functions in marine organisms. For example, warm acclimation for 4 weeks in an adult marine polychaete improved mitochondrial performance accompanied by shift of methylation status at 11% of analyzed CpG sites (Marsh and Pasqualone, 2014). An environmentally sensitive coral species subjected to a 6 week CO_2 treatment, which mimics ocean acidification, showed reduced calcification and doubled global methylation level (Putnam et al., 2016). Similarly, sea bass exposed to warm temperatures as larvae showed a distinct global DNA methylation pattern (Anastasiadi et al., 2017). Although these studies identified broad relationships between DNA methylation and phenotype, they were unable to identify detailed mechanisms of DNA methylation and associated gene functions, which can allow a deeper level of understanding about how plasticity is regulated and controlled. This is mainly because previous studies have typically achieved low coverage of

methylation detection due to the methods used (e.g., methylation sensitive amplification polymorphism sequencing or colorimetric assessment of the amount of DNA methylation). We previously studied DNA methylation changes and related genes in the Palm Island population of *A. polyacanthus* with high genome-wide coverage and sequencing depth (Ryu et al., 2018). We found significant changes in methylation among treatments in the F2 generation, and when correlated with the relevant phenotype (adjusted net aerobic scope), we identified genes involved in energy and nutrient homeostasis and cardiovascular functions. This implies these differentially methylated genes play a critical role in between-generational thermal plasticity in the Palm Island population of *A. polyacanthus*.

In this study, we investigated whether DNA methylation in the Heron Island population of *A. polyacanthus* was altered following exposure to elevated water temperatures (+1.5 or +3°C) from the early juvenile stage, as a putative mechanism for within-generational thermal plasticity (Donelson and Munday, 2012). We then compared these Heron Island methylome profiles to those from the F2 Palm Island population that exhibited plasticity in transgenerational and step treatments, as well as the within-generational treatment that showed limited plasticity. Identifying the similar or distinct epigenetic mechanisms associated with within- and between-generational plasticity is important to determine if they rely on similar or different molecular and physiological processes. Establishing if there are fundamentally similar or different processes operating in different examples of thermal plasticity is crucial to making predictions how fish populations will respond to climate change across their geographical range.

MATERIALS AND METHODS

Experimental Design

Recently hatched juveniles of *A. polyacanthus* were collected from February to March 2009 from the reef slope at Heron Island (23°27′ S, 151°57′ E) on the Great Barrier Reef (**Figure 1A**). At this location the average water temperature at 6–8 m depth below sea level was 27°C in summer and 21.8°C in winter (from 1999 to 2008 Australian Institute of Marine Science[1]). Fish were transported to James Cook University's aquarium facility where 120 juvenile fish (<3 months old) were randomly divided into three seasonally-adjusted temperature treatments modeled off the previous 10 years for the collection location: a present-day temperature (control: +0°C) and two within-generational elevated temperature treatments (+1.5 and +3°C above present-day). Fish were maintained in 60 L replicate tanks for each temperature treatment until maturity (11–14 months of age), as previously described (Donelson and Munday, 2012) (**Figure 1B**). Sampling of fish for tissue was completed during the Austral summer of 2009–2010 when water temperature for the three treatments were +0: 27°C, +1.5: 28.5°C, and +3: 30°C.

Liver was the target tissue because it is a major metabolic organ. Liver is an important long-term storage site for excess energy as glycogen, allowing glucose release to the blood and provision of fuel to the body as required (Wasserman, 2009). Liver also synthesizes bile and heme for fat absorption and oxygen delivery, respectively (Campbell, 2006). Adult fish from each treatment were sampled and whole livers immediately dissected, snap-frozen in liquid nitrogen, and then stored at −80°C until further processing. To avoid sex-related epigenome variations we used only liver tissue from male fish.

Nucleotide Extraction and Sequencing

Liver genomic DNA (gDNA) of 8 fish (3, 2, and 3 fish from control, within-generational +1.5°C, and within-generational +3°C groups, respectively) was extracted by homogenizing 100 mg of frozen liver tissue in 700 μL CTAB (hexadecyltrimethylammonium bromide) buffer. After adding proteinase K, the homogenate was incubated overnight at 55°C and then RNase treated for 10 min at room temperature. A standard chloroform/isoamyl alcohol extraction and ethanol precipitation method (Sambrook and Russell, 2001) was used. DNA quality and quantity were checked using NanoDrop Spectrophotometer absorbance readings (Invitrogen, Mulgrave, VIC, Australia) and on a 0.8% agarose gel.

gDNA was bisulfite-converted using Methyl-MaxiSeq™ Kit and sequenced using llumina HiSeq1500/2500 system by Zymo Research (Irvine, CA, United States) as described previously (Ryu et al., 2018). Briefly, 500 ng of genomic DNA was treated with dsDNA Shearase™ Plus (Zymo Research), end-blunted, 3′ A-extended, and purified by DNA Clean & Concentrator™ –5 kit (Zymo Research). DNA fragments were then ligated with adapters and filled in. EZ DNA Methylation–Lightning kit (Zymo Research) was used for bisulfite treatment and DNA fragments were sequenced on Illumina HiSeq1500/2500. All procedures were conducted according to the manufacturer's instructions. 1.26 $\sim$ 1.37 $\times$ 10^9 reads of 101 bp were generated for each sample (**Supplementary Table 1**). The methylomic reads for this study were generated together with those from our previous work (Ryu et al., 2018). The quality of these methylome datasets were validated using targeted bisulfite sequencing assays in the same study.

Analysis of Whole Genome DNA Methylation Patterns

Draft genome assembly and gene models for *A. polyacanthus* from Heron Island were generated as described in our previous work (Veilleux et al., 2018). The assembled genome consisted of 16,609 genomic scaffolds ranging from 500 $\sim$ 3,215,819 bp with N50 of 527,731 bp. Base coverage was 129X on average and assembly completeness measured by CEGMA (Parra et al., 2007) was 99.19%. 23,464 gene models were identified based on *ab initio* and *A. polyacanthus* transcriptome-based gene prediction by Maker2 pipeline (Holt and Yandell, 2011).

Adapters and low quality bases in reads from the whole genome bisulfite sequencing (WGBS) were trimmed by Trim Galore v0.4 (Krueger, 2015). Trimmed reads were mapped to *A. polyacanthus* genome sequences from Heron Island using

[1]http://data.aims.gov.au/

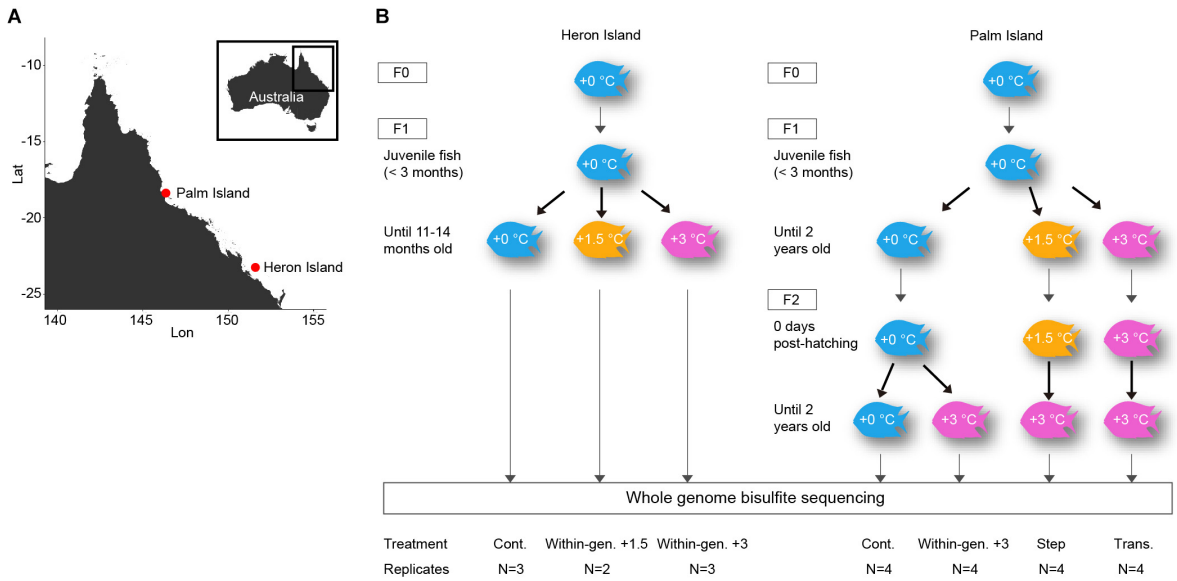

FIGURE 1 | Experimental design to analyze DNA methylation related to thermal plasticity. **(A)** Sampling location of two populations of *A. polyacanthus* on the Great Barrier Reef, Australia. **(B)** Scheme of the fish rearing experiment to study within-generational plasticity (left) and transgenerational plasticity (right).The treatment names and the number of fish samples per treatment (biological replicates) are indicated below.

Bismark v0.13.1 (Krueger and Andrews, 2011) with the '–non-_directional' option. Mapping efficiency was 67.17 ∼ 71.23% per sample. The bisulfite conversion rate is often used as a metric to assess the efficiency of bisulfite treatment and is calculated as numT/(numT +numC) × 100, where numC and numT represent the number of times that cytosines and thymines are observed, respectively at CHG and CHH sites. We used methylKit v.1.2.0 (Akalin et al., 2012) to identify differentially methylated regions (DMRs) as follows. Per base coverage of methylomic reads on the genome was 43 ∼53 × calculated by 'getCoverageStats' function (**Supplementary Table 2**). The 'methRead' function scanned the methylome mapping information and kept cytosines that were covered by a minimum of 10 reads. Highly covered bases (>99.9%) were excluded to remove PCR bias by 'filterByCoverage' function. Variances across entire samples were normalized by 'normalizeCoverage' functions. The genome was broadly categorized as eight functional units (CpG island, CpG shore, promoter, 5′ untranslated region (UTR), exon, introns, 3′ UTR, and repeats), following our previous study (Ryu et al., 2018). Methylation status of individual cytosines in each genomic region were summed per sample by the 'regionCounts' function. Statistical significance of differential methylation between samples was calculated using the Chi-squared test of the 'calculateDiffMeth' function. Multiple testing correction was performed by the Benjamini & Hochberg (BH) method of the 'p.adjust' function from *p*-values from all pairwise comparisons. DMRs for three methylation contexts (CpG, CHH, CHG; H = A, C, T) were identified using the two thresholds: adjusted *p*-value $\leq$ 0.05 and $\geq$ 33.3% methylation difference between two treatments. The adjacent genes to each DMR on the same scaffold were assigned using the 'bedtools closest' v2.23 (Quinlan, 2014).

The 'heatmap.2' function of the 'gplots' package (Warnes et al., 2016) was used to draw heatmaps. For multidimensional scaling analysis, dissimilarity between samples was calculated as '1 – Spearman correlation coefficient' and confidence ellipsoid of each sample was obtained using the 'bootmds' function of the 'smacof' package (De Leeuw and Mair, 2011) with the setting of alpha = 0.05 and 1,000 bootstrap replications. Statistical significance of separation between experimental groups was assessed by ind.ctest function of the 'ICSNP' R package (Nordhausen et al., 2015). *p*-Values were adjusted for multiple testing correction using the BH method.

Functional Analysis

Homologs of *A. polyacanthus* proteins were identified by a BLASTP search against the NCBI non-redundant protein database with e-value of 10^{-4} as a threshold (Altschul et al., 1990). Gene Ontology (GO) terms of homologous proteins were then assigned to *A. polyacanthus* proteins using the NCBI gene2go.gz file[2] and custom script. GO terms were considered when associated with more than two genes. Only Biological Process among the three GO categories (Biological Process, Molecular Function, and Cellular Component) were analyzed to focus on the biological outcome of each gene rather than a specific molecular activity (Molecular Function) or a location relative to cellular structures (Cellular Component) of the gene (Gene Ontology Consortium, 2008). Statistical significance of GO enrichment in DMR genes from all groups or between experimental groups were calculated by cumulative hypergeometric test and adjusted by the BH method using the custom R script respectively.

[2]ftp://ftp.ncbi.nlm.nih.gov/gene/DATA/gene2go.gz

Comparison of Differential Methylation Between Within- and Between-Generational Treatments

To allow comparison of DNA methylation profiles for fish exposed to elevated temperature within- and between-generations, we used the methylome dataset from our previous study (Ryu et al., 2018). This dataset was generated from F2 *A. polyacanthus* from the Palm Island population (central Great Barrier Reef, Australia; 18°37′ S, 146°30′ E) that had been reared at control and elevated temperatures for two generations (**Figure 1A**). Briefly, F1 offspring (<3 months old) of wild-caught adult fish were split between three temperature treatments: a present-day control for the collection location +0°C (mean winter: 23.2°C and summer: 28.5°C) as well as +1.5 and +3°C above present-day (seasonally cycling temperature treatments). Fish were reared in treatment conditions in 40–60 L aquaria until 2 years of age when fish were mature. At this time pairs of fish from unrelated families were randomly mated (Donelson et al., 2012 for more details). F2 offspring from the three F1 parental treatments were divided between two F2 developmental conditions, +0 and +3°C immediately after hatching and remained in treatment until 2 years of age. This produced four F2 treatment groups: control (F1: +0°C, F2: +0°C), within-generational (F1: +0°C, F2: +3°C), step (F1: +1.5°C, F2: +3°C), and transgenerational (F1: +3°C, F2: +3°C) (**Figure 1B**).

To minimize the effect of sex on the downstream analysis, two males and two females were selected for each Palm Island population treatment. DNA extraction from adult liver and WGBS was conducted as written above for Heron Island fish. The methylomic reads were aligned to the genome assembly from Palm Island fish. Each sample has $0.95 \sim 1.36 \times 10^9$ reads of 101 bp and yielded $34 \sim 62\times$ coverage depth after alignment to the genome sequences. The same computational methods used to identify DMRs in Heron Island populations were used except for one parameter: to remove the influence of unbalanced sex ratio in this population, the information of males and females was included as the 'covariates' parameter in the 'calculateDiffMeth' function of methylKit (Akalin et al., 2012). DMRs were identified using the same thresholds (adjusted p-value ≤ 0.05 and $\geq 33.3\%$ methylation difference between two treatments), which resulted in 445 CpG DMR genes.

Orthology was calculated between Heron and Palm Island populations' gene models using Inparanoid (O'brien et al., 2005). This resulted in 17,423 ortholog groups with 17,569 and 17,758 genes from each population, respectively.

RESULTS

Measuring Within-Generational Changes in Whole-Genome Methylation

We extracted methylomes from liver samples that were collected from Heron Island populations of *A. polyacanthus* exposed to control (+0°C) and increased temperatures (+1.5 and +3.0°C) from early life (**Figure 1B**). This resulted in $841.6 \sim 884.8$ million reads that were uniquely mapped, yielding from 67.2 to 71.2% mapping efficiency (**Supplementary Table 2**). Methylated cytosines ranged from 61.1 to 63.4% in the CpG context and from 0.77 to 3.68 in CHG and CHH contexts, across samples (**Supplementary Table 2**). Average bisulfite non-conversion rates were from 0.57 to 2.91% per sample, which is comparable to our previous study (0.84 to 3.46%) (Ryu et al., 2018). Base coverage of methylome reads were $\geq 43\times$ for the three methylation contexts for all Heron Island samples (**Supplementary Table 2**).

Differential methylation in CpG, CHH, and CHG contexts was calculated between pairs of treatments and 480, 88, and 3 DMRs were identified, respectively (**Table 1**). As there were so few CHG DMRs this context was not analyzed further. CpG DMRs were mostly located on exons (22.24%), repeats (21.72%), and introns (20.81%) whilst CHH DMRs were mostly located in repeats (42.66%), introns (16.78%), and CpG shores (13.99%) (**Figure 2C** and **Supplementary Figure 1C**, **Tables 4, 5**).

To determine if within-generational exposure to increased temperatures in the Heron Island population affected global DNA methylation patterns, we performed a multidimensional scaling analysis using the methylation level of DMRs. Individual fish samples were clustered by CpG DMRs and were separated by temperature treatment (**Figures 2A,B**). Statistical tests also showed clear separation of control samples from the elevated temperature treatments (**Supplementary Table 3**). These patterns were less evident for the CHH context (**Supplementary Figures 1A,B** and **Table 3**), which is similar to our previous observation of methylation patterns in control, within-generational, step, and transgenerational in Palm Island fish (Ryu et al., 2018).

Differentially Methylated Gene Functions for Within-Generational Plasticity

We identified 372 CpG DMR genes (nearest genes to any given CpG DMRs, **Supplementary Table 5**) in the Heron Island population. GO enrichment analysis of these 372 genes showed 20 enriched terms (adjusted p-value < 0.05)

TABLE 1 | The number of differentially methylated regions (DMRs) between experimental groups from the Heron Island population.

Context	Comparison		Hyper	Hypo	Unique
CpG	Within-gen. + 1.5°C	vs. cont.	145	119	480
	Within-gen. + 3°C		68	59	
	Within-gen. + 3°C	vs. within-gen. + 1.5°C	130	96	
CHH	Within-gen. + 1.5°C	vs. cont.	28	23	88
	Within-gen. + 3°C		14	16	
	Within-gen. + 3°C	vs. within-gen. + 1.5°C	17	27	
CHG	Within-gen. + 1.5°C	vs. cont.	2	0	3
	Within-gen. + 3°C		0	0	
	Within-gen. + 3°C	vs. within-gen. + 1.5°C	1	0	

Hyper and hypo indicate higher and lower methylation in the left treatment compared to the right treatment in the comparison column, respectively. The unique number of DMRs in each methylation context are shown on the last column.

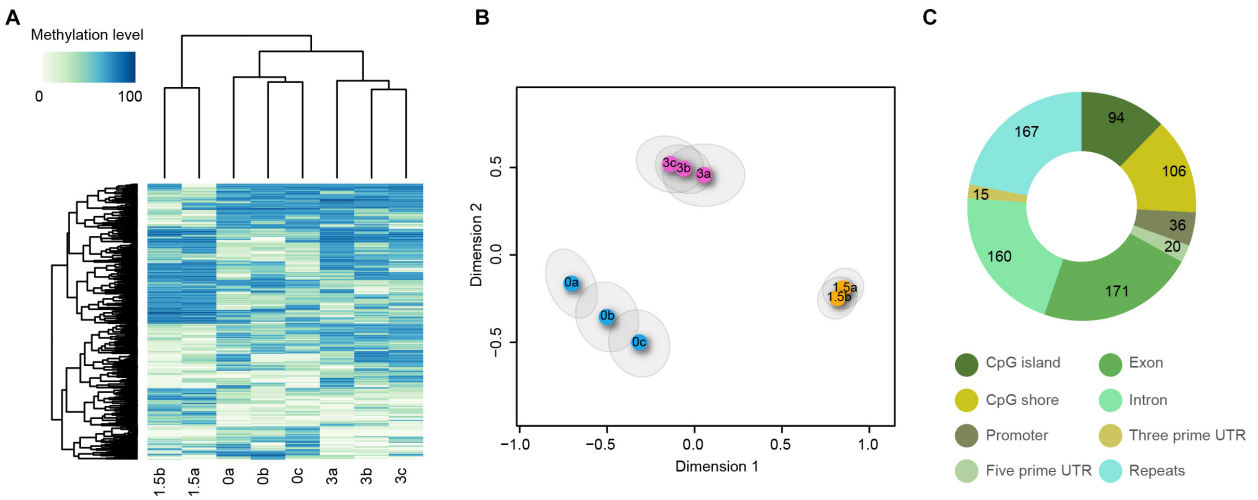

FIGURE 2 | Differential methylation in the CpG context for within-generational plasticity. **(A)** Heatmap of methylation levels for DMRs is shown with the color key in the upper left corner. Column labels indicate the sample code represented by the combination of the increased temperature (0, 1.5, 3) and individual fish number (a, b, and c). **(B)** Multidimensional scaling analysis of DMRs. Each circle corresponds to one fish sample and experimental groups are marked by different colors. 95% confidence ellipses from 1,000 bootstrapping are shown for each sample. No overlap of ellipses for CpG DMRs indicates that CpG methylation patterns are significantly different among experimental groups. **(C)** Distribution of DMRs for CpG contexts across categorized genomic elements.

(**Supplementary Table 6**) mostly related to animal development (e.g., 'cardiac neural crest cell development involved in heart development,' 'central nervous system projection neuron axonogenesis,' and 'retina layer formation') and physiological homeostasis (e.g., 'cellular chloride ion homeostasis,' 'insulin catabolic process,' and 'hypotonic response').

Further investigation of enriched GO terms identified by comparing treatments in a pairwise manner also showed similar but slightly different categories that were treatment-dependent. Most enriched GO terms were related to pathways involved in developmental processes and cardiovascular functions, and the majority of these were found when comparing control to within-generational +1.5°C treated fish (**Figure 3**). GO terms related to diverse developmental processes, such as 'bone morphogenesis,' 'multicellular organism growth,' 'type B pancreatic cell development,' and 'neural retina development' were the most prevalent functions. The enriched terms for cardiovascular physiology included 'cardiac muscle hypertrophy,' 'cardiac myofibril assembly,' and 'regulation of heart rate. Nutrient control and heat stress functions were also noteworthy. 'Insulin catabolic process' was the most significantly enriched GO term in hypomethylated DMR genes from both elevated temperature groups (both +1.5 and +3°C) compared to control. 'Glucose homeostasis' was another enriched term in the comparison between control and within-generational +1.5°C. The GO term 'regulation of cellular response to heat' was enriched among DMR genes that were hypomethylated in within-generational +1.5°C fish compared to control.

This analysis also revealed that functions differed depending on the magnitude of temperature change. The greatest number of enriched GO terms were found when the fish reared in elevated temperatures were compared to control fish, but not when the elevated temperature fish (+1.5 and +3°C groups) were compared to each other (**Figure 3**). For example, the largest number of enriched terms were found among hypomethylated DMR genes in within-generational +1.5°C fish compared to control fish (26 terms), while only two terms were enriched in within-generational +3°C fish compared to within-generational +1.5°C fish. This suggests that major change of physiological functions occurs when a temperature change is experienced during early life, but the magnitude of change, either +1.5 and +3°C, is relatively unimportant.

Comparison of Within- and Between-Generational Epigenetic Signatures

To compare epigenetic mechanisms between within- and between-generational plasticity, we performed the same GO enrichment analysis on the DNA methylome dataset of the F2 population from Palm Island (Ryu et al., 2018). First, we identified 445 CpG DMR genes by pairwise comparison of WGBS data from the four Palm Island treatments (control, within-generational +3°C, step, and transgenerational) (**Supplementary Table 7**). Enrichment analysis on all 445 genes in the F2 Palm Island population identified only three significant GO terms (adjusted p-value < 0.05) (**Supplementary Table 8**), while we identified 20 different GO terms among the 372 CpG DMR genes in the Heron Island population (**Supplementary Table 6**). Enrichment analysis per treatment pair also showed different patterns with regard to the Heron Island population (**Supplementary Figure 2**). Five or fewer GO terms were enriched across treatment pairs and there was no overlap with the enriched terms from the Heron Island population.

Because there was no overlap of GO terms between two populations, we examined if there was similarity between

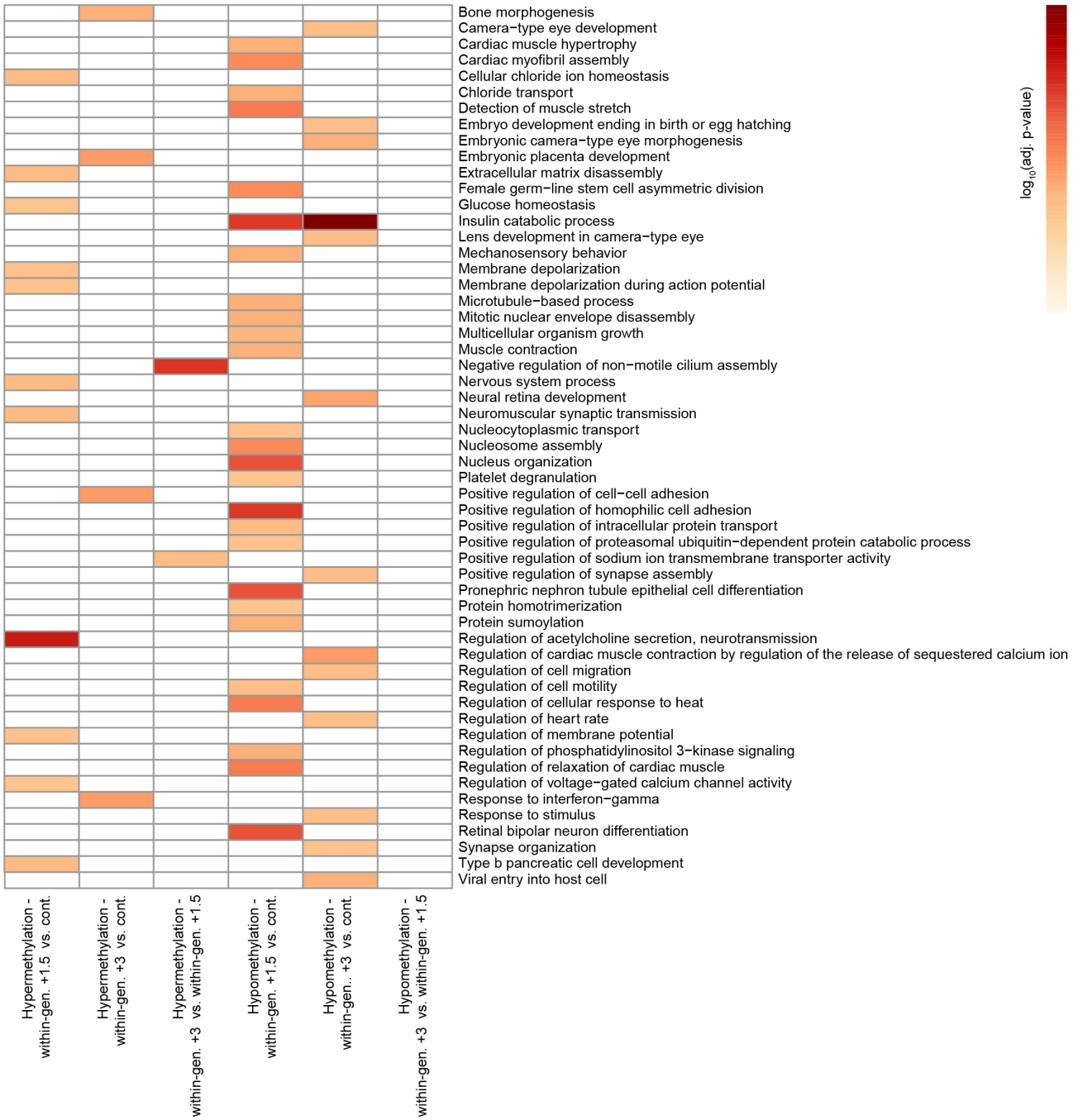

FIGURE 3 | Gene Ontology enrichment of DMR genes related to within-generational plasticity. Significantly enriched GO terms (adjusted $p < 0.05$) between two experimental groups are listed on the right side of the heatmap. Adjusted *p*-values are –log10 transformed and colored as indicated on the color key.

within- and between-generational responses at the individual gene level. Among 372 and 445 DMR genes from Heron and Palm Island populations, respectively, only 12 genes were differentially methylated in both populations (**Figure 4**). These include genes involved in regulation of cell migration (*slit2*), cell volume homeostasis (*znf706*), cytoskeleton organization (*dtnb*), DNA replication (*rfc4*), immune response (*btn1a1*), nutrient metabolism (*grpr*, *ren*, *spon2*, and *srebf1*), sodium channel gating (*unc80*), and transcriptional regulation (*rax2*). Interestingly, all 12 genes that were differentially methylated in at least one of the Heron Island within-generational treatments were also differentially methylated in the Palm Island transgenerational or step treatments compared to control or within-generational treatments.

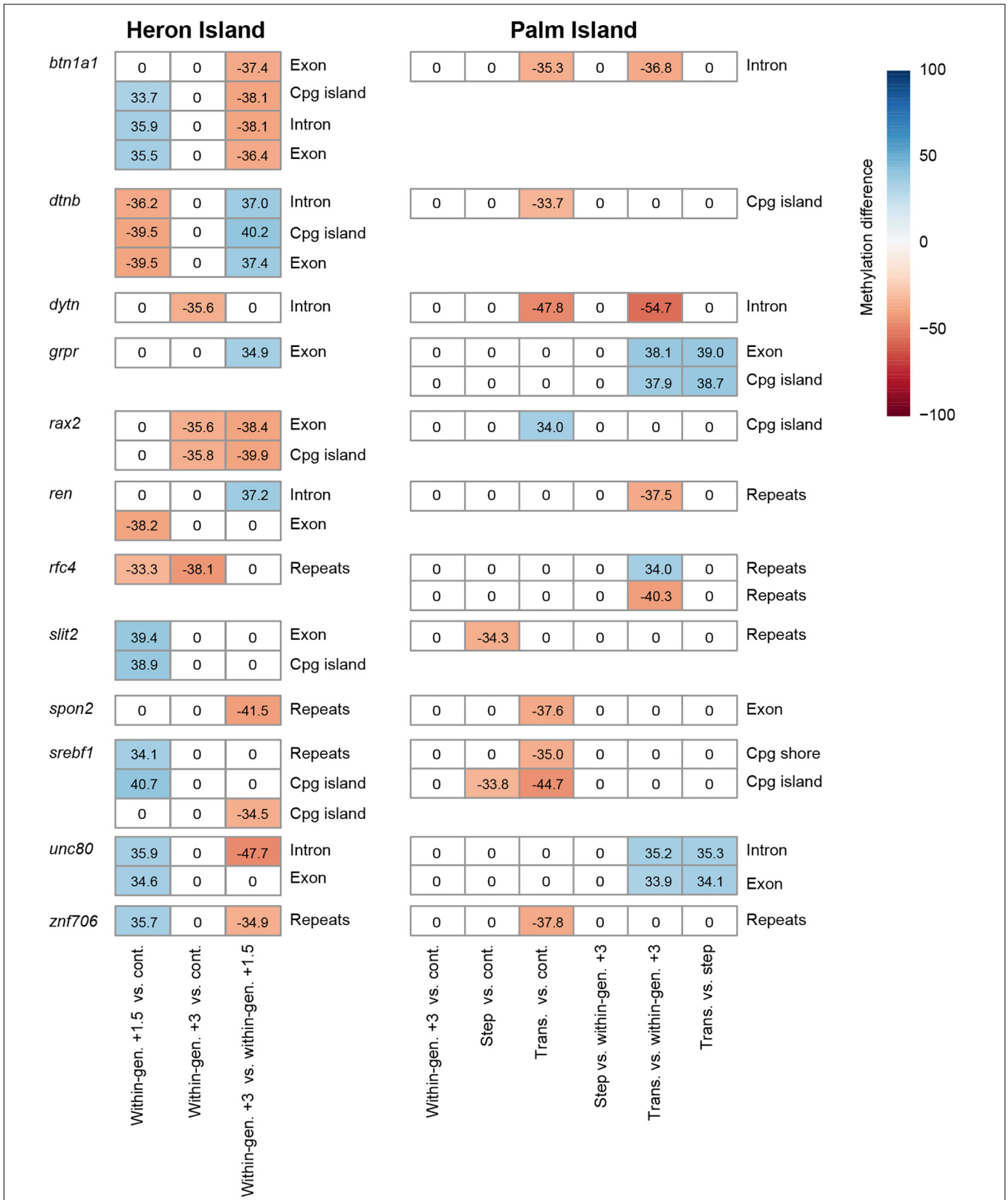

FIGURE 4 | Common DMR genes in Heron and Palm populations. These 12 genes may be involved in both within- and between-generational plasticity to elevated temperatures. Each row and column correspond to one DMR and comparison of two treatments, respectively. The colors and values indicate the percentage differences of methylation level of genomic regions. Methylation differences for non-DMRs are represented as zero.

DISCUSSION

There is ample evidence that environmental experiences during early development can affect phenotypes throughout life; however, the governing cellular mechanisms, especially the role of non-genetic mechanisms in thermal plasticity, are not well-understood. A mechanistic understanding is essential to predict the response of natural populations living in rapidly changing environments. In this study, we investigated if changes in DNA methylation are associated with the capacity for within-generational thermal plasticity of a coral reef fish and compared these methylation patterns to those in a lower latitude population that exhibited between-generational thermal plasticity. In both elevated temperature treatments, the function of DMR genes was related to metabolic control, developmental, cardiovascular, and heat-response functions. However, we found very little overlap between within- and between-generational epigenetic signatures of thermal plasticity from the two populations of the same species; only 3% of the DMR genes from each population were shared.

Exposure to elevated temperatures (+1.5 and +3°C) from the early juvenile stage in the Heron Island population altered the CpG methylation landscape across the genome compared to controls, in addition to differences between the temperature treatments. This suggests that exposure to an altered thermal environment from early life was sufficient to alter the epigenome, which may be related to the phenotype. The strong differentiation of CpG methylation and limited difference for CHH methylation may be explained by their differing maintenance mechanisms. Once established, CpG methylation is preserved with high accuracy; DNA methyltransferases recognize hemimethylated CpG sites generated during DNA replication to re-establish appropriate methylation patterns. However, a maintenance mechanism such as this is unknown for CHH or CHG contexts in animals (Dyachenko et al., 2010). Previously, we obtained similar results for Palm Island *A. polyacanthus* methylomes in that only CpG and not CHH or CHG methylation was affected following within-generational, step, and transgenerational exposure to elevated temperatures (Ryu et al., 2018). Together with the results from this study, our data suggests that CpG methylation is the most appropriate context in which to evaluate either within- or between-generational plasticity in reef fish, at least in *A. polyacanthus*.

Functional analysis of Heron Island DMR genes showed significant enrichment of GO terms related to metabolic control and developmental, cardiovascular, and heat-response functions. In fish, as in other ectotherms, basal metabolic rate increases as ambient temperatures increases (Fry and Hart, 1948; Portner and Farrell, 2008; Clark et al., 2013); hence, maintaining efficient metabolic performance may be critical for normal physiological activities as the oceans warm (Portner, 2010). One metabolic term, 'insulin catabolic process' was enriched among hypomethylated genes in both elevated temperature treatments (+1.5 and +3°C) compared to the current-day control temperature. Insulin serves as a master regulator of energy and metabolic functions, by promoting glucose uptake into cells (Rui, 2014). In heat-stressed animals, basal insulin secretion and sensitivity increases in order to compensate for altered intracellular energetics (Victoria Sanz Fernandez et al., 2015). In our study, the *ceacam1* (carcinoembryonic antigen-related cell adhesion molecule 1) gene, which is hypomethylated in both elevated temperature treatments, encodes a glycoprotein that controls hepatic insulin sensitivity and lipogenesis by mediating insulin clearance and fatty acid synthase activity (DeAngelis et al., 2008; Russo et al., 2016). 'Glucose homeostasis' was enriched in the comparison between +1.5°C and control treatments. An associated 'glucose homeostasis' gene was *gcgr*, which was hypermethylated in +1.5°C fish compared to control fish. Its encoded protein, glucagon receptor, binds to glucagon (a peptide hormone secreted by α cells of the pancreas in response to low blood glucose level) and then promotes the conversion of stored glycogen in liver to glucose and is also involved in gluconeogenesis (Miller and Birnbaum, 2016). The glucagon receptor's mechanisms, which increase the hepatic glucose production and bloodstream glucose levels, are opposite to insulin action that reduces bloodstream glucose levels. Balanced modulation of glucagon and insulin pathways is critical to maintain stable blood glucose level, which is a major cellular energy source. Therefore, epigenetic control of key hepatic metabolic genes may be an important mechanism for within-generational thermal plasticity.

Many enriched functions in the Heron Island elevated temperature treatments were related to developmental processes such as 'multicellular organism growth' and 'type B pancreatic cell development.' The *selenom* and *h3f3a* genes, which encode selenoprotein M and histone H3.3 respectively, were associated with 'multicellular organism growth' and were hypomethylated in +1.5°C fish compared to control fish. Selenium is an essential micronutrient with antioxidant activities and, in chickens, contributes to growth performance and regulation of blood glucose (Zoidis et al., 2018). Selenoprotein M, one of the selenoproteins that chemically incorporate selenium during translation, has regulatory roles in energy metabolism and body weight, identified through a knockout study in mice (Pitts et al., 2013). Moreover, when overexpressed in rats, this protein kept the body in high antioxidant status by altering antioxidant enzyme activity and immune cell composition (Hwang et al., 2008). Thus, epigenetic control of the *selenom* gene may help fish balance cellular redox state and energy usage during juvenile growth when reared in warmer water, potentially contributing to within-generational plasticity. H3.3, which was hypomethylated in the +1.5°C treatment compared to control, is a histone variant that can replace the canonical histones H3.1 and H3.2, and proper replacement among H3 proteins is the frequent target in the epigenetic regulation for multiple processes such as development, fertilization, and somatic growth (Tang et al., 2015). The *wnt5a* gene, associated with the GO term 'type B pancreatic cell development,' was hypermethylated in +1.5°C fish. Type B pancreatic cells (commonly called β cells) are the predominant cell in the islets of Langerhans, where they synthesize insulin. In addition to its close association to a variety of processes such as cell proliferation, cell fate determination, and cardiovascular diseases (Bhatt and Malgor, 2014), the WNT5A protein has been suggested to be an essential molecule for

the formation of pancreatic islets and proliferation of Type B cells in vertebrates (Kim et al., 2005). Differential methylation of genes involved in developmental functions seems counter-intuitive, since we sequenced the epigenome of adult livers; however, recent reports indicate that DNA methylation can reflect the epigenetic history of cellular activities and can be unchanged through development and across tissues (Hon et al., 2013; Huse et al., 2015). Although the possibility that these genes may have additional roles in adult liver cannot be ruled out, DNA methylation of these genes may have been established during early stages of development to maximize the physiological performance in a warmer environment.

Cardiovascular physiology (e.g., enrichment terms 'cardiac myofibril assembly,' 'regulation of heart rate,' and 'regulation of relaxation of cardiac muscle') was also significantly enriched among DMR genes in the Heron Island elevated temperature treatments. Delivering sufficient oxygen to tissues is a limiting factor in the thermal tolerance in fish, as above a critical temperature the cardiovascular system cannot meet the higher demand for oxygen in the tissues (Portner and Farrell, 2008). Thus, enhanced vascular structure may be a central component of thermal plasticity. The titin protein-encoding gene, which was hypomethylated in Heron +1.5°C fish compared to controls, is a key component in the assembly and operation of vertebrate muscles, and is also responsible for the morphogenesis of the vascular network (May et al., 2004). Two genes, *prkaca* and *slc8a1*, were hypomethylated in Heron Island +3°C fish compared to controls and were associated with two enriched terms: 'regulation of heart rate' and 'regulation of cardiac muscle contraction by regulation of the release of sequestered calcium ion.' The *prkaca* gene encodes the catalytic subunit α of protein kinase A that is responsible for post-translational modification to alter various cellular protein activities. Protein kinase A regulates vascular development in vertebrates (Nedvetsky et al., 2016) and mis-regulation of this protein's activities is related to many cardiovascular diseases (Turnham and Scott, 2016). Moreover, protein kinase A serves as the primary mediator of glucagon's effect on hepatic metabolism by phosphorylating many enzymes in the glucoregulatory pathway (Miller and Birnbaum, 2016), implying the possible multifunction of this protein in thermal plasticity. SLC8A1 is a sodium/calcium exchanger protein of cardiomyocytes and is responsible for cardiac contraction (Takimoto et al., 2002). This protein also has a putative role in blood pressure regulation according to the transgenic mouse study (Takimoto et al., 2002; Warren et al., 2017). Thus, modulation of DNA methylation of the genes associated with vascular architecture modification in response to altered metabolic demands could be a key characteristic of within-generational thermal plasticity, and has been similarly reported in transgenerational plasticity (Ryu et al., 2018).

Heat stress can induce negative physiological effects, including protein unfolding, collapse of cytoskeleton networks, mis-localization of organelles, reduced number of mitochondria, aberrant RNA splicing, and changes in membrane morphology (Richter et al., 2010). Therefore, minimizing detrimental effects caused by elevated temperatures is critical to maintain normal physiology. In our study, the GO term 'regulation of cellular response to heat' was enriched among DMR genes that were hypomethylated in +1.5°C fish compared to control. For example, the *nup98* gene associated with this term is found to be associated with heat shock recovery by reactivating the transcription of genes suppressed by the heat shock (Capelson et al., 2010). The alpha-crystallin B chain heat shock protein encoded by the *cryab* gene prevents aggregation of proteins under a variety of stressful conditions and keeps the structural integrity of heart and muscle tissues under heat stress (Wójtowicz et al., 2015; Yin et al., 2019). Methylation control of these genes may help the fish to adjust to the effects of lifelong exposure to increased temperatures.

Epigenetic Signature Shared Between Plastically Adjusted Within- and Between-Generational Treatments

Fish from Heron Island phenotypically adjusted aerobic scope by reducing RMR without a significant change in MMR (Donelson and Munday, 2012). In contrast, the F2 Palm population did not achieve within-generational plasticity, but was able to do so when both parents and offspring were exposed to increased temperatures, either in the step treatment by decreasing RMR or in the transgenerational treatment by increasing MMR and decreasing RMR (Donelson et al., 2012; Bernal et al., 2018). This implies that there could be different physiological mechanisms and underlying genomic responses for within- and between-generational plasticity of aerobic scope, as well as between populations, following exposure to predicted future temperatures. Indeed, we found that each population might employ a different epigenetic toolkit in order to plastically adjust to warmer conditions. Only 12 DMR genes were common among 372 and 445 DMR genes from Heron and Palm Island fish, respectively. However, these 12 genes might be linked to the phenotypic reductions in RMR of both populations. Independent GO analysis for each population also suggested distinct functions may be employed for within- and between-generational plasticity.

These 12 genes shared by the two populations are involved in various regulatory functions for cell migration (*slit2*) (Zeng et al., 2018), cell volume homeostasis (*znf706*) (Dossena et al., 2011), cytoskeleton organization (*dtnb*) (Veroni et al., 2007), DNA replication (*rfc4*) (Kim and Brill, 2001), immune response (*btn1a1*) (Smith et al., 2010), nutrient metabolism (*grpr*, *ren*, *spon2*, and *srebf1*) (Persson et al., 2002; Ferre and Foufelle, 2010; Zhu et al., 2014; Silva et al., 2017), sodium channel gating (*unc80*) (Lear et al., 2013), transcriptional regulation (*rax2*) (Wang et al., 2004), and one had unknown function (*dytn*).

The overlapping differential methylation in genes associated with nutrient delivery and metabolism is not unexpected since these are known to be critical physiological attributes for survival of ectotherms in warming conditions (Portner and Knust, 2007; Portner and Farrell, 2008). The gene *ren* was differentially methylated in both populations (hypomethylated in Heron Island +1.5°C fish vs. controls, hypermethylated in Heron Island +3°C fish vs. +1.5°C fish, and hypomethylated in Palm Island transgenerational fish. vs. +3°C fish) and is

particularly interesting as the encoded protein, RENIN, is the master hormone mediating the volume of extracellular fluid and blood pressure (Persson, 2003). As a component of the renin-angiotensin system, this protein catalyzes angiotensinogen released from the liver, which is eventually converted into angiotensin II, the vasoactive peptide (Persson, 2003). Renin-angiotensin system is also transcriptionally regulated in liver to control glucose and lipid level through hepatic insulin signaling (Silva et al., 2017). We speculate that epigenetic control on this protein may be a key mechanism to improve blood flow and nutrient homeostasis in order to plastically adjust to warmer conditions in *A. polyacanthus.* The *grpr* (gastrin-releasing peptide receptor) gene was hypermethylated in Heron Island +3°C fish vs. +1.5°C fish, hypermethylated in Palm Island transgenerational fish vs. +3°C fish, and hypermethylated in Palm Island transgenerational fish vs. step fish. Its encoded product, GRPR, mediates insulin secretion in pancreatic islet cells (Persson et al., 2002) and regulates glucose metabolism by modulating components of the aerobic glycolysis pathway (Rellinger et al., 2015). A recent mice model study suggested that GRPR may play an important role in hepatic ischemia injury (a status characterized by an insufficient supply of oxygen and nutrients), although the underlying molecular mechanism is yet unclear (Guo et al., 2019). SPON2 (spondin-2), whose encoding gene was hypomethylated in Heron Island +3°C fish vs. +1.5°C fish and also hypomethylated in Palm Island transgenerational fish vs. control, controls hepatic lipid metabolism and insulin resistance in rodents (Zhu et al., 2014). Furthermore, SPON2 is known to protect from cardiovascular diseases (Yan et al., 2011) and function in initiation of innate immunity (He et al., 2004) in rodent studies. SREBF1 (sterol regulatory element-binding protein 1), whose encoding gene was differentially methylated in both populations (hypermethylated in Heron Island +1.5°C fish vs. controls, hypomethylated in Heron Island +3°C fish vs. +1.5°C fish, hypomethylated in Palm Island step fish vs. control, and hypomethylated in Palm Island transgenerational fish vs. control), is the master regulator of the lipogenesis in liver in response to environmental signals such as nutrient demand and mediating the transcription of glycolytic and lipogenic genes in insulin- and sterol-dependent manner (Ferre and Foufelle, 2010; Shao and Espenshade, 2012). Epigenetic control on these regulatory genes involved in cell metabolism might be critical for the strict maintenance of homeostatic status at high temperatures.

There is insufficient data available to understand the likely role in thermal plasticity for the other genes that were differentially methylated in both populations (*slit2, btn1a1*, *dtnb*, *dytn*, *rax2*, *rfc4*, *unc80*, and *znf706*). The *slit2* (slit guidance ligand 2) gene was differentially methylated in treatments where temperature was increased +1.5°C within-generations (Heron Island +1.5°C fish vs. controls and Palm Island step fish vs. control). In mammals, the encoded protein, SLIT2, modulates the migration of hepatic stellate cells, the major cell type involved in fibrogenic activity in the liver in chronically abnormal states such as hepatic fibrosis caused by metabolic disorder (Chang et al., 2015; Zeng et al., 2018). The remaining seven genes are not well-studied in relation to stress responses and/or their function in the liver. Although the role of these genes needs to be investigated further in fish liver following within- and between-generation exposure to increased temperatures, our results suggest that they may be useful as epigenetic markers for thermal plasticity.

The epigenetic patterns of within- and between-generational plasticity for the Heron and Palm Island populations of *A. polyacanthus* could be partially caused by different inheritance mechanisms for DNA methylation. Compared to the epigenomes for within-generational plasticity, which are only transmitted through somatic cell divisions, the epigenomes for between-generational plasticity include transmission through germ and somatic cell division. In mammals, the latter processes include epigenetic reprogramming events during gametogenesis and early embryogenesis, in which DNA methylation marks on the genome are erased and remodeled (Morgan et al., 2005; Messerschmidt et al., 2014). Although not extensively investigated in fish, epigenetic reprogramming differs by fish species. For example, zebrafish did not show global demethylation and recovery, while medaka showed similar reprogramming patterns to mammals (Jiang et al., 2013; Ortega-Recalde et al., 2019; Wang and Bhandari, 2019a,b). If complicated reprogramming event occurs in *A. polyacanthus*, modifications of epigenetic information during reprogramming (e.g., incomplete erasure and recovery) are possible for Palm Island fish (Kearns et al., 2000; Jacob and Moley, 2005). Furthermore, the exposure of Palm Island fish to increased temperatures for longer time frames compared to Heron Island fish (two vs. one generations, respectively) may increase the chances that the genome could be subjected to modification of DNA methylomes, such as replication-dependent passive demethylation or epigenetic drift that can dilute epigenetic memory (Guo et al., 2014; Messerschmidt et al., 2014; Ciccarone et al., 2018). In future studies, it would be of interest to delve more deeply into the cellular mechanisms of methylation inheritance and reprogramming in *A. polyacanthus* and other species that show differing capacities for within- and between-generational plasticity.

CONCLUSION

We performed large scale epigenotyping at the single nucleotide resolution in a reef fish population that can plastically adjust to elevated temperature within a generation. We then compared these epigenetic profiles to those of another population of the same species that failed to plastically adjust within a generation, but which acclimated in the second generation to the same environmental warming. Analysis of genome-wide differential methylation of liver tissue revealed genes involved in nutrient control, developmental processes, cardiovascular functions, and response to heat stress were highly enriched in the population capable of within-generational plasticity compared with the other population. Consequently, these DMR genes might serve as hot spot regions for epigenetic regulation of within-generational plasticity. We also identified 12 shared DMR genes for both types of plasticity, which might serve as part of a general molecular toolkit for thermal plasticity. Exposure to predicted increased

temperatures at early life stages seemed to be imprinted in the form of DNA methylation around genes improving oxygen delivery, nutrient usage, and tolerance to heat stress. Our results indicate that DNA methylation may be an important mechanism associated with buffering the effects of elevated temperature in reef fishes, both within- and between-generations.

DATA AVAILABILITY STATEMENT

Short reads from methylome sequencing have been deposited in GenBank under BioProject ID PRJNA348663.

ETHICS STATEMENT

This project was carried out in accordance with the recommendations of James Cook University Animal Ethics Committee (JCU Ethics A1233 and A1415).

AUTHOR CONTRIBUTIONS

JD and PM managed the fish rearing experiments. HV prepared samples for sequencing. TRy extracted genomic DNA for methylome sequencing. TRy, HV, and JD selected fish samples for sequencing. TRy and TRa designed the computational analysis. TRy performed the analysis, interpreted the results, and drafted the manuscript. IJ contributed on the data analysis. TRy, HV, JD, PM, and TRa completed the manuscript.

FUNDING

This work was supported by the Competitive Research Funds OCRF-2014-CRG3-62140408 from the King Abdullah University of Science and Technology to TRa and PM. TRy acknowledges the support from the APEC Climate Center. PM was supported by the Australian Research Council (ARC) and the ARC Centre of Excellence for Coral Reef Studies. HV and JD were supported by funding from the King Abdullah University of Science and Technology and the ARC Centre of Excellence for Coral Reef Studies.

ACKNOWLEDGMENTS

We thank Eike Joachim Steinig and Clara Ortiz Alvarez (James Cook University) for assisting methylome sequencing.

SUPPLEMENTARY MATERIAL

The Supplementary Material for this article can be found online at: https://www.frontiersin.org/articles/10.3389/fmars.2020.00284/full#supplementary-material

REFERENCES

Akalin, A., Kormaksson, M., Li, S., Garrett-Bakelman, F. E., Figueroa, M. E., Melnick, A., et al. (2012). methylKit: a comprehensive R package for the analysis of genome-wide DNA methylation profiles. *Genome Biol.* 13:R87. doi: 10.1186/gb-2012-13-10-r87

Altschul, S. F., Gish, W., Miller, W., Myers, E. W., and Lipman, D. J. (1990). Basic local alignment search tool. *J. Mol. Biol.* 215, 403–410.

Anastasiadi, D., Díaz, N., and Piferrer, F. (2017). Small ocean temperature increases elicit stage-dependent changes in DNA methylation and gene expression in a fish, the European sea bass. *Sci. Rep.* 7:12401. doi: 10.1038/s41598-017-10861-6

Bautista, N. M., and Burggren, W. W. (2019). Parental stressor exposure simultaneously conveys both adaptive and maladaptive larval phenotypes through epigenetic inheritance in the zebrafish (*Danio rerio*). *J. Exp. Biol.* 222:jeb208918. doi: 10.1242/jeb.208918

Bernal, M. A., Donelson, J. M., Veilleux, H. D., Ryu, T., Munday, P. L., and Ravasi, T. (2018). Phenotypic and molecular consequences of stepwise temperature increase across generations in a coral reef fish. *Mol. Ecol.* 27, 4516–4528. doi: 10.1111/mec.14884

Bhatt, P. M., and Malgor, R. (2014). Wnt5a: a player in the pathogenesis of atherosclerosis and other inflammatory disorders. *Atherosclerosis* 237, 155–162. doi: 10.1016/j.atherosclerosis.2014.08.027

Bonduriansky, R., Crean, A. J., and Day, T. (2012). The implications of nongenetic inheritance for evolution in changing environments. *Evol. Appl.* 5, 192–201. doi: 10.1111/j.1752-4571.2011.00213.x

Campbell, I. (2006). Liver: metabolic functions. *Anaesth. Intensive Care Med.* 7, 51–54. doi: 10.1383/anes.2006.7.2.51

Capelson, M., Liang, Y., Schulte, R., Mair, W., Wagner, U., and Hetzer, M. W. (2010). Chromatin-bound nuclear pore components regulate gene expression in higher eukaryotes. *Cell* 140, 372–383. doi: 10.1016/j.cell.2009.12.054

Chang, J., Lan, T., Li, C., Ji, X., Zheng, L., Gou, H., et al. (2015). Activation of Slit2-Robo1 signaling promotes liver fibrosis. *J. Hepatol.* 63, 1413–1420. doi: 10.1016/j.jhep.2015.07.033

Ciccarone, F., Tagliatesta, S., Caiafa, P., and Zampieri, M. (2018). DNA methylation dynamics in aging: how far are we from understanding the mechanisms? *Mech. Ageing Dev.* 174, 3–17. doi: 10.1016/j.mad.2017.12.002

Clark, T. D., Sandblom, E., and Jutfelt, F. (2013). Aerobic scope measurements of fishes in an era of climate change: respirometry, relevance and recommendations. *J. Exp. Biol.* 216, 2771–2782. doi: 10.1242/jeb.084251

De Leeuw, J., and Mair, P. (2011). *Multidimensional Scaling Using Majorization: SMACOF in R*. Available online at: http://CRAN.R-project.org/package=smacof (accessed March 3, 2020).

DeAngelis, A. M., Heinrich, G., Dai, T., Bowman, T. A., Patel, P. R., Lee, S. J., et al. (2008). Carcinoembryonic antigen-related cell adhesion molecule 1: a link between insulin and lipid metabolism. *Diabetes* 57, 2296–2303. doi: 10.2337/db08-0379

Donelson, J., Munday, P., McCormick, M., and Pitcher, C. (2012). Rapid transgenerational acclimation of a tropical reef fish to climate change. *Nat. Clim. Chang.* 2, 30–32. doi: 10.1038/nclimate1323

Donelson, J. M., and Munday, P. L. (2012). Thermal sensitivity does not determine acclimation capacity for a tropical reef fish. *J. Anim. Ecol.* 81, 1126–1131. doi: 10.1111/j.1365-2656.2012.01982.x

Donelson, J. M., Munday, P. L., McCormick, M. I., and Nilsson, G. E. (2011). Acclimation to predicted ocean warming through developmental plasticity in a tropical reef fish. *Glob. Chang. Biol.* 17, 1712–1719. doi: 10.1371/journal.pone.0097223

Donelson, J. M., Salinas, S., Munday, P. L., and Shama, L. N. (2018). Transgenerational plasticity and climate change experiments: where do we go from here? *Glob. Chang. Biol.* 24, 13–34. doi: 10.1111/gcb.13903

Dossena, S., Gandini, R., Tamma, G., Vezzoli, V., Nofziger, C., Tamplenizza, M., et al. (2011). The molecular and functional interaction between ICln and HSPC038 proteins modulates the regulation of cell volume. *J. Biol. Chem.* 286, 40659–40670. doi: 10.1074/jbc.M111.260430

Duncan, E. J., Gluckman, P. D., and Dearden, P. K. (2014). Epigenetics, plasticity, and evolution: how do we link epigenetic change to phenotype? *J. Exp. Zool. B Mol. Dev. Evol.* 322, 208–220. doi: 10.1002/jez.b.22571

Dyachenko, O. V., Schevchuk, T. V., Kretzner, L., Buryanov, Y. I., and Smith, S. S. (2010). Human non-CG methylation: are human stem cells plant-like? *Epigenetics* 5, 569–572. doi: 10.4161/epi.5.7.12702

Ferre, P., and Foufelle, F. (2010). Hepatic steatosis: a role for de novo lipogenesis and the transcription factor SREBP−1c. *Diabetes Obes. Metab.* 12, 83–92. doi: 10.1111/j.1463-1326.2010.01275.x

Fox, R. J., Donelson, J. M., Schunter, C., Ravasi, T., and Gaitán-Espitia, J. D. (2019). Beyond buying time: the role of plasticity in phenotypic adaptation to rapid environmental change. *Philos. Trans. R. Soc. B Biol.* 374:20180174. doi: 10.1098/rstb.2018.0174

Fry, F. E. J., and Hart, J. S. (1948). The relation of temperature to oxygen consumption in the goldfish. *Biol. Bull.* 94, 66–77. doi: 10.2307/1538211

Gene Ontology Consortium, (2008). The gene ontology project in 2008. *Nucleic Acids Res.* 36, D440–D444. doi: 10.1093/nar/gkm883

Gienapp, P., Teplitsky, C., Alho, J., Mills, J., and Merilä, J. (2008). Climate change and evolution: disentangling environmental and genetic responses. *Mol. Ecol.* 17, 167–178. doi: 10.1111/j.1365-294X.2007.03413.x

Grenchik, M., Donelson, J., and Munday, P. (2013). Evidence for developmental thermal acclimation in the damselfish, *Pomacentrus moluccensis*. *Coral Reefs* 32, 85–90. doi: 10.1007/s00338-012-0949-1

Guo, F., Li, X., Liang, D., Li, T., Zhu, P., Guo, H., et al. (2014). Active and passive demethylation of male and female pronuclear DNA in the mammalian zygote. *Cell Stem Cell* 15, 447–459. doi: 10.1016/j.stem.2014.08.003

Guo, L., Wu, X., Zhang, Y., Wang, F., Li, J., and Zhu, J. (2019). Protective effects of gastrin−releasing peptide receptor antagonist RC−3095 in an animal model of hepatic ischemia/reperfusion injury. *Hepatol. Res.* 49, 247–255. doi: 10.1111/hepr.13315

He, Y.-W., Li, H., Zhang, J., Hsu, C.-L., Lin, E., Zhang, N., et al. (2004). The extracellular matrix protein mindin is a pattern-recognition molecule for microbial pathogens. *Nat. Immunol.* 5, 88–97. doi: 10.1038/ni1021

Healy, T. M., Bock, A. K., and Burton, R. S. (2019). Variation in developmental temperature alters adulthood plasticity of thermal tolerance in *Tigriopus californicus*. *J. Exp. Biol.* 222:jeb213405. doi: 10.1242/jeb.213405

Ho, D. H., and Burggren, W. W. (2010). Epigenetics and transgenerational transfer: a physiological perspective. *J. Exp. Biol.* 213, 3–16. doi: 10.1242/jeb.019752

Hoey, A. S., Howells, E., Johansen, J. L., Hobbs, J.-P. A., Messmer, V., McCowan, D. M., et al. (2016). Recent advances in understanding the effects of climate change on coral reefs. *Diversity* 8:12. doi: 10.3390/d8020012

Hoffmann, A. A., and Sgro, C. M. (2011). Climate change and evolutionary adaptation. *Nature* 470, 479–485. doi: 10.1038/nature09670

Holt, C., and Yandell, M. (2011). MAKER2: an annotation pipeline and genome-database management tool for second-generation genome projects. *BMC Bioinformatics* 12:491. doi: 10.1186/1471-2105-12-491

Hon, G. C., Rajagopal, N., Shen, Y., McCleary, D. F., Yue, F., Dang, M. D., et al. (2013). Epigenetic memory at embryonic enhancers identified in DNA methylation maps from adult mouse tissues. *Nat. Genet.* 45, 1198–1206. doi: 10.1038/ng.2746

Hughes, T. P., Kerry, J. T., Baird, A. H., Connolly, S. R., Dietzel, A., Eakin, C. M., et al. (2018). Global warming transforms coral reef assemblages. *Nature* 556, 492–496. doi: 10.1038/s41586-018-0041-2

Huse, S. M., Gruppuso, P. A., Boekelheide, K., and Sanders, J. A. (2015). Patterns of gene expression and DNA methylation in human fetal and adult liver. *BMC Genomics* 16:981. doi: 10.1186/s12864-015-2066-3

Hwang, D. Y., Sin, J. S., Kim, M. S., Yim, S. Y., Kim, Y. K., Kim, C. K., et al. (2008). Overexpression of human selenoprotein M differentially regulates the concentrations of antioxidants and H2O2, the activity of antioxidant enzymes, and the composition of white blood cells in a transgenic rat. *Int. J. Mol. Med.* 21, 169–179.

IPCC, (2019). *IPCC Special Report on the Ocean and Cryosphere in a Changing Climate*. Geneva: Intergovernmental Panel on Climate Change.

Jablonka, E., and Raz, G. (2009). Transgenerational epigenetic inheritance: prevalence, mechanisms, and implications for the study of heredity and evolution. *Q. Rev. Biol.* 84, 131–176. doi: 10.1086/598822

Jacob, S., and Moley, K. H. (2005). Gametes and embryo epigenetic reprogramming affect developmental outcome: implication for assisted reproductive technologies. *Pediatr. Res.* 58, 437–446. doi: 10.1203/01.PDR.0000179401.17161.D3

Jiang, L., Zhang, J., Wang, J. J., Wang, L., Zhang, L., Li, G., et al. (2013). Sperm, but not oocyte, DNA methylome is inherited by zebrafish early embryos. *Cell* 153, 773–784. doi: 10.1016/j.cell.2013.04.041

Kearns, M., Preis, J., McDonald, M., Morris, C., and Whitelaw, E. (2000). Complex patterns of inheritance of an imprinted murine transgene suggest incomplete germline erasure. *Nucleic Acids Res.* 28, 3301–3309. doi: 10.1093/nar/28.17.3301

Kim, H.-S., and Brill, S. J. (2001). Rfc4 interacts with Rpa1 and is required for both DNA replication and DNA damage checkpoints in *Saccharomyces cerevisiae*. *Mol. Cell. Biol.* 21, 3725–3737. doi: 10.1128/mcb.21.11.3725-3737.2001

Kim, H. J., Schleiffarth, J. R., Jessurun, J., Sumanas, S., Petryk, A., Lin, S., et al. (2005). Wnt5 signaling in vertebrate pancreas development. *BMC Biol.* 3:23. doi: 10.1186/1741-7007-3-23

Krueger, F. (2015). *Trim Galore*. Available online at: http://www.bioinformatics.babraham.ac.uk/projects/trim_galore/ (accessed August 10, 2015).

Krueger, F., and Andrews, S. R. (2011). Bismark: a flexible aligner and methylation caller for Bisulfite-Seq applications. *Bioinformatics* 27, 1571–1572. doi: 10.1093/bioinformatics/btr167

Le Roy, A., Loughland, I., and Seebacher, F. (2017). Differential effects of developmental thermal plasticity across three generations of guppies (*Poecilia reticulata*): canalization and anticipatory matching. *Sci. Rep.* 7:4313. doi: 10.1038/s41598-017-03300-z

Lear, B. C., Darrah, E. J., Aldrich, B. T., Gebre, S., Scott, R. L., Nash, H. A., et al. (2013). UNC79 and UNC80, putative auxiliary subunits of the narrow abdomen ion channel, are indispensable for robust circadian locomotor rhythms in *Drosophila*. *PLoS One* 8:e78147. doi: 10.1371/journal.pone.0078147

Marsh, A. G., and Pasqualone, A. A. (2014). DNA methylation and temperature stress in an Antarctic polychaete, *Spiophanes tcherniai*. *Front. Physiol.* 5:173. doi: 10.3389/fphys.2014.00173

Marshall, D. J., and Uller, T. (2007). When is a maternal effect adaptive? *Oikos* 116, 1957–1963. doi: 10.1111/j.2007.0030-1299.16203.x

May, S. R., Stewart, N. J., Chang, W., and Peterson, A. S. (2004). A Titin mutation defines roles for circulation in endothelial morphogenesis. *Dev. Biol.* 270, 31–46. doi: 10.1016/j.ydbio.2004.02.006

Messerschmidt, D. M., Knowles, B. B., and Solter, D. (2014). DNA methylation dynamics during epigenetic reprogramming in the germline and preimplantation embryos. *Genes Dev.* 28, 812–828. doi: 10.1101/gad.234294.113

Miller, R. A., and Birnbaum, M. J. (2016). Glucagon: acute actions on hepatic metabolism. *Diabetologia* 59, 1376–1381. doi: 10.1007/s00125-016-3955-y

Morgan, H. D., Santos, F., Green, K., Dean, W., and Reik, W. (2005). Epigenetic reprogramming in mammals. *Hum. Mol. Genet.* 14, R47–R58. doi: 10.1093/hmg/ddi114

Munday, P. L. (2014). Transgenerational acclimation of fishes to climate change and ocean acidification. *F1000prime Rep.* 6:99.

Munday, P. L., Warner, R. R., Monro, K., Pandolfi, J. M., and Marshall, D. J. (2013). Predicting evolutionary responses to climate change in the sea. *Ecol. Lett.* 16, 1488–1500. doi: 10.1111/ele.12185

Nedvetsky, P. I., Zhao, X., Mathivet, T., Aspalter, I. M., Stanchi, F., Metzger, R. J., et al. (2016). cAMP-dependent protein kinase A (PKA) regulates angiogenesis by modulating tip cell behavior in a Notch-independent manner. *Development* 143, 3582–3590. doi: 10.1242/dev.134767

Nordhausen, K., Sirkia, S., Oja, H., and Tyler, D. (2015). *ICSNP: Tools for Multivariate Nonparametrics*. Available online at: http://CRAN.R-project.org/package=ICSNP (accessed March 10, 2018).

O'brien, K. P., Remm, M., and Sonnhammer, E. L. (2005). Inparanoid: a comprehensive database of eukaryotic orthologs. *Nucleic Acids Res.* 33(Suppl. 1), D476–D480.

Ortega-Recalde, O., Day, R. C., Gemmell, N. J., and Hore, T. A. (2019). Zebrafish preserve global germline DNA methylation while sex-linked rDNA is amplified and demethylated during feminisation. *Nat. Commun.* 10:3053. doi: 10.1038/s41467-019-10894-7

Parra, G., Bradnam, K., and Korf, I. (2007). CEGMA: a pipeline to accurately annotate core genes in eukaryotic genomes. *Bioinformatics* 23, 1061–1067. doi: 10.1093/bioinformatics/btm071

Pecl, G. T., Araújo, M. B., Bell, J. D., Blanchard, J., Bonebrake, T. C., Chen, I.-C., et al. (2017). Biodiversity redistribution under climate change: impacts on ecosystems and human well-being. *Science* 355:eaai9214. doi: 10.1126/science.aai9214

Persson, K., Pacini, G., Sundler, F., and Ahren, B. (2002). Islet function phenotype in gastrin-releasing peptide receptor gene-deficient mice. *Endocrinology* 143, 3717–3726. doi: 10.1210/en.2002-220371

Persson, P. B. (2003). Renin: origin, secretion and synthesis. *J. Physiol.* 552, 667–671. doi: 10.1113/jphysiol.2003.049890

Pitts, M. W., Reeves, M. A., Hashimoto, A. C., Ogawa, A., Kremer, P., Seale, L. A., et al. (2013). Deletion of selenoprotein M leads to obesity without cognitive deficits. *J. Biol. Chem.* 288, 26121–26134. doi: 10.1074/jbc.M113.471235

Portner, H. O. (2010). Oxygen- and capacity-limitation of thermal tolerance: a matrix for integrating climate-related stressor effects in marine ecosystems. *J. Exp. Biol.* 213, 881–893. doi: 10.1242/jeb.037523

Portner, H. O., and Farrell, A. P. (2008). Ecology, physiology and climate change. *Science* 322, 690–692. doi: 10.1126/science.1163156

Portner, H. O., and Knust, R. (2007). Climate change affects marine fishes through the oxygen limitation of thermal tolerance. *Science* 315, 95–97. doi: 10.1126/science.1135471

Putnam, H. M., Davidson, J. M., and Gates, R. D. (2016). Ocean acidification influences host DNA methylation and phenotypic plasticity in environmentally susceptible corals. *Evol. Appl.* 9, 1165–1178. doi: 10.1111/eva.12408

Quinlan, A. R. (2014). BEDTools: the Swiss-army tool for genome feature analysis. *Curr. Protoc. Bioinform.* 47, 11.12.11–11.12.34. doi: 10.1002/0471250953.bi1112s47

Rellinger, E. J., Romain, C., Choi, S., Qiao, J., and Chung, D. H. (2015). Silencing gastrin−releasing peptide receptor suppresses key regulators of aerobic glycolysis in neuroblastoma cells. *Pediatr. Blood Cancer* 62, 581–586. doi: 10.1002/pbc.25348

Reusch, T. B. (2014). Climate change in the oceans: evolutionary versus phenotypically plastic responses of marine animals and plants. *Evol. Appl.* 7, 104–122. doi: 10.1111/eva.12109

Richter, K., Haslbeck, M., and Buchner, J. (2010). The heat shock response: life on the verge of death. *Mol. Cell* 40, 253–266. doi: 10.1016/j.molcel.2010.10.006

Rui, L. (2014). Energy metabolism in the liver. *Compr. Physiol.* 4, 177–197. doi: 10.1002/cphy.c130024

Russo, L., Ghadieh, H. E., Ghanem, S. S., Al-Share, Q. Y., Smiley, Z. N., Gatto-Weis, C., et al. (2016). Role for hepatic CEACAM1 in regulating fatty acid metabolism along the adipocyte-hepatocyte axis. *J. Lipid Res.* 57, 2163–2175. doi: 10.1194/jlr.m072066

Ryu, T., Veilleux, H. D., Donelson, J. M., Munday, P. L., and Ravasi, T. (2018). The epigenetic landscape of transgenerational acclimation to ocean warming. *Nat. Clim. Chang.* 8, 504–509. doi: 10.1038/s41558-018-0159-0

Salinas, S., and Munch, S. B. (2012). Thermal legacies: transgenerational effects of temperature on growth in a vertebrate. *Ecol. Lett.* 15, 159–163. doi: 10.1111/j.1461-0248.2011.01721.x

Sambrook, J., and Russell, D. W. (2001). *Molecular Cloning : a Laboratory Manual*. New York, NY: Cold Spring Harbor Laboratory Press.

Scheffers, B. R., De Meester, L., Bridge, T. C., Hoffmann, A. A., Pandolfi, J. M., Corlett, R. T., et al. (2016). The broad footprint of climate change from genes to biomes to people. *Science* 354:aaf7671. doi: 10.1126/science.aaf7671

Shama, L. N. (2017). The mean and variance of climate change in the oceans: hidden evolutionary potential under stochastic environmental variability in marine sticklebacks. *Sci. Rep.* 7:8889. doi: 10.1038/s41598-017-07140-9

Shama, L. N., Strobel, A., Mark, F. C., and Wegner, K. M. (2014). Transgenerational plasticity in marine sticklebacks: maternal effects mediate impacts of a warming ocean. *Funct. Ecol.* 28, 1482–1493. doi: 10.1111/1365-2435.12280

Shao, W., and Espenshade, P. J. (2012). Expanding roles for SREBP in metabolism. *Cell Metab.* 16, 414–419. doi: 10.1016/j.cmet.2012.09.002

Silva, A. C. S. E., Miranda, A. S., Rocha, N. P., and Teixeira, A. L. (2017). Renin angiotensin system in liver diseases: friend or foe? *World J. Gastroenterol.* 23, 3396–3406. doi: 10.3748/wjg.v23.i19.3396

Smith, I. A., Knezevic, B. R., Ammann, J. U., Rhodes, D. A., Aw, D., Palmer, D. B., et al. (2010). BTN1A1, the mammary gland butyrophilin, and BTN2A2 are both inhibitors of T cell activation. *J. Immunol.* 184, 3514–3525. doi: 10.4049/jimmunol.0900416

Sunday, J. M., Bates, A. E., and Dulvy, N. K. (2010). Global analysis of thermal tolerance and latitude in ectotherms. *Proc. R. Soc. B Biol. Sci.* 278, 1823–1830. doi: 10.1098/rspb.2010.1295

Takimoto, E., Yao, A., Toko, H., Takano, H., Shimoyama, M., Sonoda, M., et al. (2002). Sodium calcium exchanger plays a key role in alteration of cardiac function in response to pressure overload. *FASEB J.* 16, 373–378. doi: 10.1096/fj.01-0735com

Tang, M. C., Jacobs, S. A., Mattiske, D. M., Soh, Y. M., Graham, A. N., Tran, A., et al. (2015). Contribution of the two genes encoding histone variant h3. 3 to viability and fertility in mice. *PLoS Genet.* 11:e1004964. doi: 10.1371/journal.pgen.1004964

Tewksbury, J. J., Huey, R. B., and Deutsch, C. A. (2008). Putting the heat on tropical animals. *Science* 320, 1296–1297. doi: 10.1126/science.1159328

Torda, G., Donelson, J. M., Aranda, M., Barshis, D. J., Bay, L., Berumen, M. L., et al. (2017). Rapid adaptive responses to climate change in corals. *Nat. Clim. Chang.* 7, 627–636. doi: 10.1038/nclimate3374

Turnham, R. E., and Scott, J. D. (2016). Protein kinase A catalytic subunit isoform PRKACA; history, function and physiology. *Gene* 577, 101–108. doi: 10.1016/j.gene.2015.11.052

Veilleux, H. D., Ryu, T., Donelson, J. M., Munday, P., and Ravasi, T. (2018). Molecular response to extreme summer temperatures differs between two genetically differentiated populations of a coral reef fish. *Front. Mar. Sci.* 5:349. doi: 10.3389/fmars.2018.00349

Veilleux, H. D., Ryu, T., Donelson, J. M., van Herwerden, L., Seridi, L., Ghosheh, Y., et al. (2015). Molecular processes of transgenerational acclimation to a warming ocean. *Nat. Clim. Chang.* 5, 1074–1078. doi: 10.1038/nclimate2724

Veroni, C., Grasso, M., Macchia, G., Ramoni, C., Ceccarini, M., Petrucci, T. C., et al. (2007). β−dystrobrevin, a kinesin−binding receptor, interacts with the extracellular matrix components pancortins. *J. Neurosci. Res.* 85, 2631–2639. doi: 10.1002/jnr.21186

Victoria Sanz Fernandez, M., Johnson, J. S., Abuajamieh, M., Stoakes, S. K., Seibert, J. T., Cox, L., et al. (2015). Effects of heat stress on carbohydrate and lipid metabolism in growing pigs. *Physiol. Rep.* 3:e12315. doi: 10.14814/phy2.12315

Wang, Q.-I., Chen, S., Esumi, N., Swain, P. K., Haines, H. S., Peng, G., et al. (2004). QRX, a novel homeobox gene, modulates photoreceptor gene expression. *Hum. Mol. Genet.* 13, 1025–1040. doi: 10.1093/hmg/ddh117

Wang, X., and Bhandari, R. K. (2019a). DNA methylation dynamics during epigenetic reprogramming of medaka embryo. *Epigenetics* 14, 611–622. doi: 10.1080/15592294.2019.1605816

Wang, X., and Bhandari, R. K. (2019b). The dynamics of DNA methylation during epigenetic reprogramming of primordial germ cells in medaka (Oryzias latipes). *Epigenetics* 15, 483–498. doi: 10.1080/15592294.2019.1695341

Warnes, G. R., Bolker, B., Bonebakker, L., Gentleman, R., Liaw, W. H. A., Lumley, T., et al. (2016). *gplots: Various R Programming Tools for Plotting Data*. Available online at: http://CRAN.R-project.org/package=gplots (accessed February 25, 2020).

Warren, H. R., Evangelou, E., Cabrera, C. P., Gao, H., Ren, M., Mifsud, B., et al. (2017). Genome-wide association analysis identifies novel blood pressure loci and offers biological insights into cardiovascular risk. *Nat. Genet.* 49, 403–415. doi: 10.1038/ng.3768

Wasserman, D. H. (2009). Four grams of glucose. *Am. J. Physiol. Endocrinol. Metab.* 296:E11. doi: 10.1152/ajpendo.90563.2008

Wernberg, T., Smale, D. A., and Thomsen, M. S. (2012). A decade of climate change experiments on marine organisms: procedures, patterns and problems. *Glob. Chang. Biol.* 18, 1491–1498. doi: 10.1111/j.1365-2486.2012.02656.x

Wójtowicz, I., Jabłońska, J., Zmojdzian, M., Taghli-Lamallem, O., Renaud, Y., Junion, G., et al. (2015). *Drosophila* small heat shock protein CryAB ensures structural integrity of developing muscles, and proper muscle and heart performance. *Development* 142, 994–1005. doi: 10.1242/dev.115352

Yan, L., Wei, X., Tang, Q.-Z., Feng, J., Zhang, Y., Liu, C., et al. (2011). Cardiac-specific mindin overexpression attenuates cardiac hypertrophy via blocking AKT/GSK3β and TGF-β1–Smad signalling. *Cardiovasc. Res.* 92, 85–94. doi: 10.1093/cvr/cvr159

Yin, B., Tang, S., Xu, J., Sun, J., Zhang, X., Li, Y., et al. (2019). CRYAB protects cardiomyocytes against heat stress by preventing caspase-mediated apoptosis and reducing F-actin aggregation. *Cell Stress Chaperones* 24, 59–68. doi: 10.1007/s12192-018-0941-y

Zeng, Z., Wu, Y., Cao, Y., Yuan, Z., Zhang, Y., Zhang, D. Y., et al. (2018). Slit2-Robo2 signaling modulates the fibrogenic activity and migration of hepatic stellate cells. *Life Sci.* 203, 39–47. doi: 10.1016/j.lfs.2018.04.017

Zhu, L. H., Wang, A., Luo, P., Wang, X., Jiang, D. S., Deng, W., et al. (2014). Mindin/Spondin 2 inhibits hepatic steatosis, insulin resistance, and obesity via interaction with peroxisome proliferator-activated receptor alpha in mice. *J. Hepatol.* 60, 1046–1054. doi: 10.1016/j.jhep.2014.01.011

Zoidis, E., Seremelis, I., Kontopoulos, N., and Danezis, G. (2018). Selenium-dependent antioxidant enzymes: actions and properties of selenoproteins. *Antioxidants* 7:E66. doi: 10.3390/antiox7050066

Conflict of Interest: The authors declare that the research was conducted in the absence of any commercial or financial relationships that could be construed as a potential conflict of interest.

frontiers in Marine Science

ORIGINAL RESEARCH
published: 24 June 2020
doi: 10.3389/fmars.2020.00471

Early Life Exposure to Environmentally Relevant Levels of Endocrine Disruptors Drive Multigenerational and Transgenerational Epigenetic Changes in a Fish Model

Kaley M. Major[1], Bethany M. DeCourten[1,2], Jie Li[3], Monica Britton[3], Matthew L. Settles[3], Alvine C. Mehinto[4], Richard E. Connon[5] and Susanne M. Brander[1]*

[1] Department of Environmental and Molecular Toxicology, Oregon State University, Corvallis, OR, United States, [2] Department of Biology and Marine Biology, University of North Carolina Wilmington, Wilmington, NC, United States, [3] Bioinformatics Core, Genome Center, University of California, Davis, Davis, CA, United States, [4] Southern California Coastal Water Research Project, Costa Mesa, CA, United States, [5] Department of Anatomy, Physiology & Cell Biology, School of Veterinary Medicine, University of California, Davis, Davis, CA, United States

OPEN ACCESS

Edited by:
Hollie Putnam,
University of Rhode Island,
United States

Reviewed by:
Taewoo Ryu,
Okinawa Institute of Science and Technology Graduate University, Japan
Moises A. Bernal,
Auburn University, United States
Heather Diana Veilleux,
University of Alberta, Canada

***Correspondence:**
Kaley M. Major
kaley.major@gmail.com

Specialty section:
This article was submitted to Marine Molecular Biology and Ecology, a section of the journal Frontiers in Marine Science

Received: 28 January 2020
Accepted: 27 May 2020
Published: 24 June 2020

Citation:
Major KM, DeCourten BM, Li J, Britton M, Settles ML, Mehinto AC, Connon RE and Brander SM (2020) Early Life Exposure to Environmentally Relevant Levels of Endocrine Disruptors Drive Multigenerational and Transgenerational Epigenetic Changes in a Fish Model. Front. Mar. Sci. 7:471. doi: 10.3389/fmars.2020.00471

The inland silverside, *Menidia beryllina*, is a euryhaline fish and a model organism in ecotoxicology. We previously showed that exposure to picomolar (ng/L) levels of endocrine disrupting chemicals (EDCs) can cause a variety of effects in *M. beryllina*, from changes in gene expression to phenotypic alterations. Here we explore the potential for early life exposure to EDCs to modify the epigenome in silversides, with a focus on multi- and transgenerational effects. EDCs included contaminants of emerging concern (the pyrethroid insecticide bifenthrin and the synthetic progestin levonorgestrel), as well as a commonly detected synthetic estrogen (ethinylestradiol), and a synthetic androgen (trenbolone) at exposure levels ranging from 3 to 10 ng/L. In a multigenerational experiment, we exposed parental silversides to EDCs from fertilization until 21 days post hatch (dph). Then we assessed DNA methylation patterns for three generations (F0, F1, and F2) in whole body larval fish using reduced representation bisulfite sequencing (RRBS). We found significant (α = 0.05) differences in promoter and/or gene body methylation in treatment fish relative to controls for all EDCs and all generations indicating that both multigenerational (F1) and transgenerational (F2) effects that were caused by strict inheritance of DNA methylation alterations and the dysregulation of epigenetic control mechanisms. Using gene ontology and pathway analyses, we found enrichment in biological processes and pathways representative of growth and development, immune function, reproduction, pigmentation, epigenetic regulation, stress response and repair (including pathways important in carcinogenesis). Further, we found that a subset of potentially EDC responsive genes (EDCRGs) were differentially methylated across all treatments and generations and included hormone receptors, genes involved in steroidogenesis, prostaglandin synthesis, sexual development, DNA

methylation, protein metabolism and synthesis, cell signaling, and neurodevelopment. The analysis of EDCRGs provided additional evidence that differential methylation is inherited by the offspring of EDC-treated animals, sometimes in the F2 generation that was never exposed. These findings show that low, environmentally relevant levels of EDCs can cause altered methylation in genes that are functionally relevant to impaired phenotypes documented in EDC-exposed animals and that EDC exposure has the potential to affect epigenetic regulation in future generations of fish that have never been exposed.

Keywords: epigenetics, *Menidia beryllina*, endocrine disruptors, transgenerational epigenetic inheritance, multigenerational exposure, DNA methylation, RRBS

INTRODUCTION

Endocrine disrupting chemicals (EDCs) include a variety of compound classes such as pesticides, pharmaceuticals, industrial chemicals, and metals, that are grouped together on the basis of their tendency to alter hormone signaling. Many EDCs enter the aquatic environment through runoff and wastewater, allowing them to move into estuarine and marine systems (Ribeiro et al., 2009; Bayen et al., 2013; Brander, 2013; Cole et al., 2016; DeCourten et al., 2019b; Zhou et al., 2019). Even at low levels (ng/L), EDC exposure during early development has been implicated in causing a variety of effects in fish across biological scales, including changes in growth and development, reproduction, immune function, sex ratio, gene expression, and DNA methylation (Hinck et al., 2008; Schug et al., 2016). For example, a growing body of literature has linked molecular endpoints to physiological and behavioral endpoints of EDC exposure in the ecologically and toxicologically relevant inland silverside, *Menidia beryllina*, an estuarine species common in North America (Brander et al., 2016; Cole et al., 2016; DeCourten and Brander, 2017; DeCourten et al., 2019b; Frank et al., 2019). Multi- and transgenerational effects of EDC exposure have been documented in *M. beryllina*, sometimes with latent effects occurring in the F1 generation (indirectly exposed as primordial germ cells), reinforcing concern for longterm population-level impacts from these ubiquitous environmental chemicals (DeCourten and Brander, 2017; DeCourten et al., 2019a; DeCourten et al., unpublished).

Epigenetic modifications can modulate gene expression stably (i.e., heritably) without alteration to the primary DNA sequence and are now considered to be a common mechanism for transgenerational inheritance of physiological phenotypes (Jablonka and Raz, 2009). Aside from meiotically stable (i.e., germline) modifications, mitotically stable (i.e., somatic) epigenetic modifications are essential to cellular differentiation and development, as well as important in maintaining epigenetically controlled disease phenotypes within an individual (Best et al., 2018). In fact, a variety of disease phenotypes (metabolic syndromes, neurological disorders, infertility, and cancer) originating during development have also been linked to epigenetic mechanisms (Head, 2014; Bhandari, 2016). Some of the most well-studied structural mechanisms of epigenetic control include DNA methylation [the addition of a methyl group to the cytosine in a cytosine-guanine dinucleotide (CpG)] and histone modifications (i.e., acetylation, methylation, ubiquination). Both of these epigenetic mechanisms physically alter the ability of transcriptional machinery to access DNA, thus impacting gene expression (Brander et al., 2017; Alavian-Ghavanini and Ruegg, 2018). The effect of DNA methylation varies with its relative location to genes. DNA methylation near transcription start sites (TSS) often suppresses vertebrate gene expression by blocking transcription machinery, while methylation within the gene body may actually stimulate transcription or alter splice variants (Jones, 2012). The area of environmental epigenomics has arisen to specifically study the effects of environmental exposures, including EDCs, on the perturbation of epigenetic mechanisms. Although EDCs have been well established to alter DNA methylation, particularly in fish (Aniagu et al., 2008; Mirbahai et al., 2011; Olsvik et al., 2014, 2019; Aluru et al., 2018) the mechanism(s) by which that disruption occurs remains under investigation (Xin et al., 2015; Alavian-Ghavanini and Ruegg, 2018).

Altered methylation states may be caused by general epigenetic dysregulation (i.e., changes in the functioning of methylation machinery) or transgenerational epigenetic inheritance. In mammals, there are generally two waves of global genome demethylation associated with development: after fertilization, and again before primordial germ cell (PGC) differentiation. However, fishes differ in their patterns of developmental DNA methylation erasure, with medaka (*Oryzias latipes*), for example, having a pattern that is the same as that of mammals (Wang and Bhandari, 2019), but zebrafish (*Danio rerio*) lacking both reprogramming stages, with embryos eventually harboring the paternal methylome (Jiang et al., 2013; Potok et al., 2013; Ortega-Recalde et al., 2019). In *M. beryllina*, the developmental pattern of DNA methylation erasure has not been established, although its pattern could undoubtedly affect the way that environmental exposures are passed down through methylation. Understanding the linkages between molecular changes caused by environmental EDC exposure and altered phenotypes is essential to strengthening current and informing new adverse outcome pathways (AOPs) for EDCs, which will help define their risk to wild populations (Ankley et al., 2009; Perkins et al., 2019).

Exploring the epigenetic effects of EDC exposure in estuarine fish is essential, not only from a risk assessment perspective, but also from the standpoint of understanding the mechanisms underlying the effects of EDC exposure across a range of different species. To explore how DNA methylation may be influenced by

EDC exposure in estuarine fish, we exposed a parental generation (F0) of *M. beryllina* to a suite of EDCs at environmentally relevant concentrations during early life [8 hours post fertilization (hpf) to 21 days post hatch (dph)]. EDCs included contaminants of emerging concern: the pyrethroid insecticide bifenthrin (Bif) and the synthetic progestin levonorgestrel (Levo), as well as the commonly detected synthetic estrogen ethinylestradiol (EE2), and the synthetic androgen trenbolone (Tren) at exposure levels between 3 and 10 ng/L. These chemicals have been linked to a variety of effects in fish, such as decreased egg production, reproductive impairment, skewed sex ratios, developmental deformities, alterations in behavior, changes in protein and/or gene expression, and DNA methylation (Jobling et al., 1998; Kidd et al., 2007; Jin et al., 2009; Brander et al., 2012; Forsgren et al., 2013; Svensson et al., 2013, 2014; Ellestad et al., 2014; Orlando and Ellestad, 2014; Schwindt et al., 2014; Bertram et al., 2015; Hua et al., 2015; Runnalls et al., 2015; Orn et al., 2016; DeCourten and Brander, 2017; Robinson et al., 2017). In our companion paper, DeCourten et al. (unpublished) demonstrated that EDC exposure caused physiological effects and sometimes changes in gene expression and DNA methylation in a limited analysis of 20 genes. These effects could be measured in the offspring (F1 generation), which were indirectly exposed to EDCs as primordial germ cells, as well as in second-generation offspring (F2), which were never exposed to EDCs. Here we explore the changes in DNA methylation for a larger collection of potentially EDC responsive genes and determine the scope and functional implications of changes in DNA methylation that may underlie physiological changes. We use reduced representation bisulfite sequencing (RRBS) to examine differential methylation in a subset of larval fish across three generations, from the larger study by DeCourten et al. (unpublished). In doing so we capitalize on a unique opportunity to relate apical endpoints, gene expression, and epigenetic modification data to get a fuller picture of the effects of EDC exposure across biological scales. The goals of the present study were to (1) quantify differential methylation caused by exposure to four EDCs across generations of fish that have been directly exposed (F0), indirectly exposed (F1), or unexposed (F2); (2) use focused analyses to determine which biological processes, pathways, and/or select genes are most impacted by differential methylation while relating methylation effects to physiological endpoints measured in larval fish; and (3) determine the extent that differential methylation is present in a multigenerational (F1) or transgenerational (F2) context.

MATERIALS AND METHODS

EDC Exposures, Chemical Analyses, and Multigenerational Rear-Out

A complete account of EDC exposures in the fish analyzed herein will be published elsewhere (DeCourten et al., unpublished). Briefly, embryos were obtained from an adult brood stock and processed according to methods in Porazinski et al. (2010), but without dechorionation. Fish [aged 8 hours post fertilization (hpf) – 21 days post hatch (dph)] in the parental (F0) generation were exposed to environmentally relevant concentrations of each of four chemicals separately: bifenthrin (Bif, 3.02 ng/L; Chem Services, West Chester, PA, United States; 99.5% pure mix of isomers), EE2 (6.79 ng/L; Sigma-Aldrich, St. Louis, MO, United States; CAS 57-63-6, >98% purity), levonorgestrel (Levo, 9.27 ng/L; USP, Rockville, MD, United States; 100% purity) and trenbolone (Tren, 9.60 ng/L; Spectrum Laboratory Products, Gardena, CA, United States; 100% purity). Concentrations for all chemicals are reported as average measured concentrations of exposure water, verified analytically using liquid chromatography-spectrometry described elsewhere (DeCourten et al., unpublished). Control groups were exposed to 10 μL/L of methanol to control for any effects of the solvent used for lipophilic chemicals and five experimental replicates were used for each treatment. New treatment water was mixed just prior to the daily 75% water changes. During periods in the 25 mL beakers (8 hpf-hatch at day 7–10) new water was mixed everyday by adding 10 μL (for BF or EE2) or 20 μL (for levonorgestrel or trenbolone) of EDC stock solutions in MeOH (0.1 mcg/mL). During exposure periods in the 1.4 L jars (hatch-21dph) water was mixed in 2–3 L batches by adding of 5 μL (bifenthrin and EE2) and 10 μL (levonorgestrel and trenbolone) for each liter made of EDC stock solutions in MeOH (1 mcg/L). Each replicate (n = 4–5) was maintained independently as described above throughout the course of the 3-generation study, with EDC exposures continuing until the 21-dph sampling time point (for the F0 generation only; **Figure 1**. After the initial 21-dph sampling time point of the F0 animals, a subset of animals was sampled for molecular endpoints, while the rest of the animals were transferred to clean water and no further EDC exposure occurred. At 21 dph remaining fish were transferred to 6 L glass containers where they were fed a diet of Hikari tropical fish food and live *Artemia nauplii* twice per day, with a 60% water change daily and reared to ∼120 dph. After 120 dph, fish were transferred to 20-gallon recirculating tanks where they were spawned in groups of ∼50 individuals (50:50 sex ratio) by placing strands of dye-free acrylic yarn into tanks overnight, allowing for spawning for roughly 3 h. After spawning, embryos were transferred to the laboratory where they were treated the same as F0 animals, but without chemical exposure, through the F2 generation. Thus, F1 animals were exposed to EDCs indirectly as primordial germ cells within F0 parents, while F2 animals were not exposed to EDCs at all. Any effects noted in the F1 animals would be considered "multigenerational" effects given that both F0 and F1 were either directly or indirectly exposed to the chemicals. Any effects noted in F2 animals, which were never exposed to the chemicals, are considered "transgenerational" effects.

DNA Extraction, Genome Sequencing, RRBS

DNA from fish in the EDC exposure experiment was extracted from two whole 21-dph larvae from each replicate tank (n = 4–5) using the DNeasy Blood & Tissue Kit (Qiagen, Hilden, Germany). Samples were quantified using a Nanodrop 1000

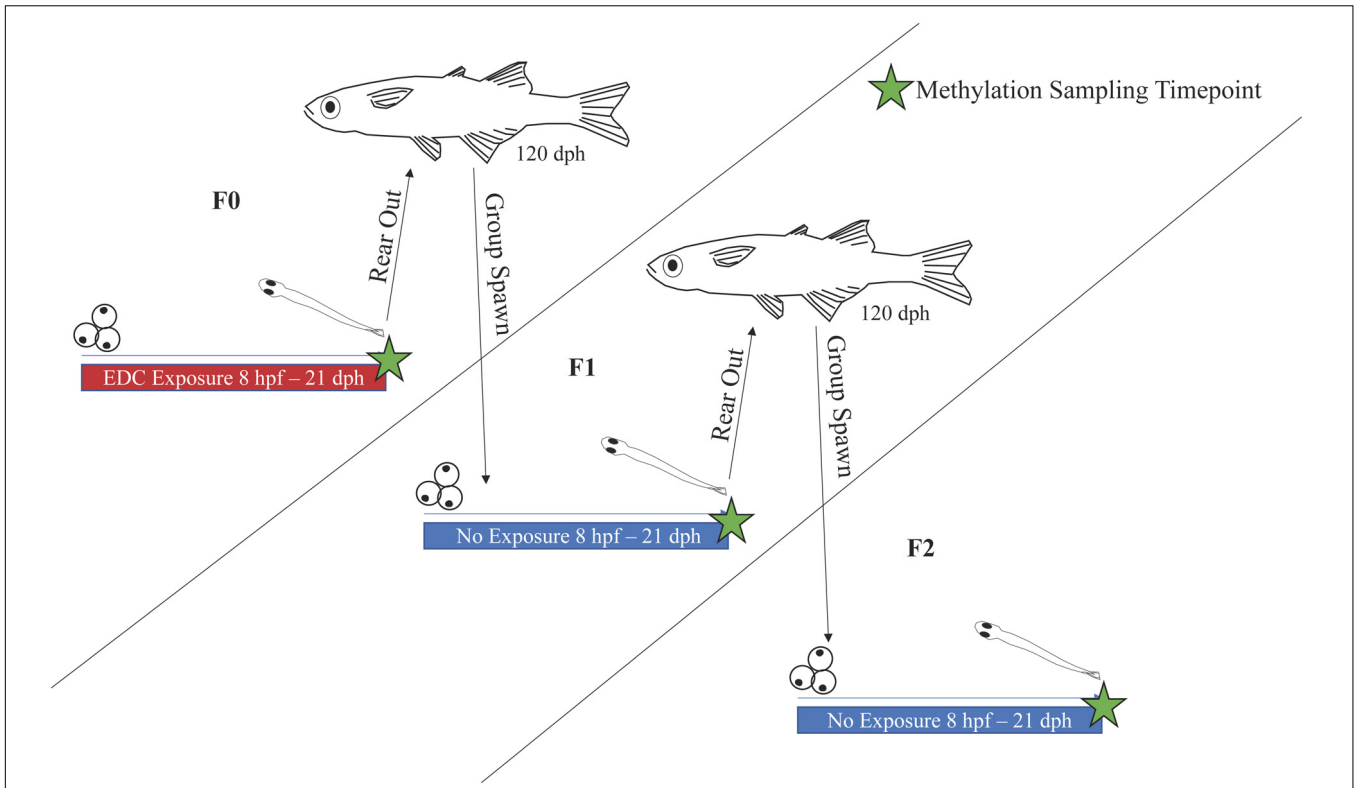

FIGURE 1 | Multigenerational experimental design for *M. beryllina* exposed to one of four different EDCs (Bif, EE2, Levo, or Tren) in the parental generation (F0) from 8 hpf through 21 dph. At 21 dph, a subset of larval fish were sampled for molecular endpoints, while the rest were reared in clean water to approximately 120 dph, after which time they were group spawned (∼50 individuals per tank). Conditions and sampling timepoints remained the same for F1 and F2 generation fish but without chemical exposure during early life.

spectrophotometer (Thermo Fisher Scientific, Waltham, MA, United States) and purity was assessed via electrophoresis on a 1% agarose gel and visualized on a Gel Doc™ XR + Gel Documentation system (Bio-Rad, Hercules, CA, United States). After DNA extraction, approximately 500 ng of genomic DNA was treated with 1 μL of RNAseIF (NEB, Ipswich, MA, United States) for 30 min at 37°C followed by a 0.8X AmPure XP (Beckman Coulter, Carlsbad, CA, United States) clean up.

Genomic DNA was adjusted to a concentration of 1.0 ng/μl, and 1.25 ng of template gDNA was loaded on a Chromium Genome Chip. Whole genome sequencing libraries were prepared using Chromium Genome Library & Gel Bead Kit v.2 (10X Genomics, cat. 120258), Chromium Genome Chip Kit v.2 (10X Genomics, cat. 120257), Chromium i7 Multiplex Kit (10X Genomics, cat. 120262) and Chromium controller according to manufacturer's instructions with one modification. Briefly, gDNA was combined with Master Mix, a library of Genome Gel Beads, and partitioning oil to create Gel Bead-in-Emulsions (GEMs) on a Chromium Genome Chip. The GEMs were isothermally amplified with primers containing an Illumina Read 1 sequencing primer, a unique 16-bp 10x barcode and a 6-bp random primer sequence, and bar-coded DNA fragments were recovered for Illumina library construction. The amount and fragment size of post-GEM DNA was quantified prior using a Bioanalyzer 2100 with an Agilent High sensitivity DNA kit (Agilent, cat. 5067-4626). Prior to Illumina library construction, the GEM amplification product was sheared on an E220 Focused Ultrasonicator (Covaris, Woburn, MA, United States) to approximately 350 bp (55 s at peak power = 175, duty factor = 10, and cycle/burst = 200). Then, the sheared GEMs were converted to a sequencing library following the 10X standard operating procedure. The library was quantified by qPCR with a Kapa Library Quant kit (Kapa Biosystems-Roche) and sequenced on one lane of HiSeq4000 sequencer (Illumina, San Diego, CA, United States) with paired-end 150 bp reads. Using 420M sequencing reads from the genomic library, the *Menidia* genome was assembled using supernova (version 2.0.0) with default parameters, and annotated using GMAP with default parameters[1] and with the *M. beryllina* transcriptome (14,393 genes: **Supplementary File** "transcript_gene_list.txt") established by Jeffries et al. (2015).

Reduced representation bisulfite sequencing (RRBS) libraries were generated using the Premium RRBS Kit from Diagenode (Liege, Belgium) following the manufacturer's instructions. Fragment size distribution of resulting library pools was assessed via micro-capillary gel electrophoresis on a Bioanalyzer 2100 (Agilent, Santa Clara, CA, United States). The library pools were quantified by qPCR with a Kapa Library Quant kit

[1]https://github.com/juliangehring/GMAP-GSNAP/

(Kapa Biosystems/Roche, Basel Switzerland) and each pool was randomized and sequenced on six lanes of an Illumina HiSeq 4000 (Illumina, San Diego, CA, United States) run with single-end 100 bp reads.

Differential Gene Methylation and Functional Enrichment Analyses

Illumina reads were subjected to quality control using trim_galore[2] (version 0.4.5) under RRBS mode. Bases with quality higher than 30 were trimmed from the 3′ end of the reads first, followed by the removal of any adapter sequences from the reads. Reads less than 30 bp in length after trimming were discarded. Bismark (Krueger and Andrews, 2011) (version 0.19.0) with default parameters was used to map all reads that passed the quality control to the *M. beryllina* reference genome that was assembled using 10X linked read technology (not published). Methylated regions were extracted from the alignment using DMRfinder (version 0.3) (Gaspar and Hart, 2017) using default parameters (maximum 500 bp in length with no less than 3 CpG sites within). Differential methylation in each methylated region was analyzed using a binomial test. Multiple test correction was carried out using Benjamini–Hochberg procedure (Benjamini and Hochberg, 1995) which has been applied as an appropriate method for minimizing false positives in methylation datasets (Asomaning and Archer, 2012). We analyzed differential methylation by treatment (Bif, EE2, Levo, Tren) and generation (F0, F1, F2) relative to the control for that generation, and differential methylation was considered significant relative to the control if the Benjamini–Hochberg adjusted *p*-value was less than 0.05 (**Supplementary Data Analysis**). The genomic context of methylated regions with respect to genes of interest was generated by annotating the assembled genome using previously published transcriptomic data (Jeffries et al., 2015; Brander et al., 2016) using gmap (Wu and Watanabe, 2005). The relationship between a methylated region and a gene was generated by overlapping the methylated region with any defined genomic regions. We will focus our discussion on two different regions with respect to genes: (1) Upstream 1000 bp, which we considered generally representative of the gene promoter region and will be referred to as "promoter" for brevity, and (2) within gene body, which comprised the exonic gene region. While the true location of the promoter region varies by individual gene, others have also designated the promoter as 1000 bp upstream of the TSS (Brenet et al., 2011; Wan et al., 2016). Further, in a survey of eukaryotic genomes, vertebrate promoters were frequently identified in less than 1000 bp upstream of the corresponding gene (Yella et al., 2018).

To elucidate the effects of EDCs on differential methylation across generations, we performed three different types of analyses. First, we tracked differential methylation by treatment and generation at the level of the gene, to determine a snapshot of differentially methylated genes overall (promoter and gene body combined) and by region (promoter and gene body analyzed separately).

Next, we performed functional enrichment analyses to determine whether gene ontology (GO) terms or Kyoto Encyclopedia of Genes and Genomes (KEGG) pathways were enriched in the treatment groups based on differential methylation. Genes of interest for each functional enrichment analysis were chosen based on a significant directional change of methylation (hyper, hypo) as well as gene region (promoter versus gene body) relative to controls. GO Term enrichment analyses for biological processes was performed using the R package topGO (version 2.37) (Alexa and Rahnenfuhrer, 2019). GO Term enrichment analyses for cellular component and molecular function were not included in the present work because we chose to focus on the biological processes that were affected by changes in methylation. KEGG Pathways Enrichment analyses were obtained using the R package KEGGREST (version 1.26.1) (Tenenbaum, 2020), based on the *D. rerio* pathways database from the R package org.Dr.eg.db (Carlson, 2019). *D. rerio* Ensembl ID's were converted to KEGG IDs using the bioDBnet database[3] (Mudunuri et al., 2009). Enriched GO terms or KEGG pathways were considered significant at the level of $\alpha = 0.01$ (Fisher's exact test) (**Supplementary Data Analysis**).

Finally, we focused on the differential methylation by gene region for a suite of 109 genes that have either been responsive to EDC exposure or those that have the potential to be responsive based on previous work and phenotypes associated with EDC disruption in *M. beryllina* (Jeffries et al., 2015; Frank et al., 2018; DeCourten et al., 2019a). These genes included hormone receptors, genes essential to osmoregulation and immune function, steroid metabolism, DNA methylation, oxidative stress (**Supplementary Table S1**).

RESULTS AND DISCUSSION

Through RRBS analysis, we found evidence of differential methylation for all four EDC treatments and all generations, indicating direct (F0), multigenerational (F1) and transgenerational (F2) effects of Bif, EE2, Levo, and Tren. Given the abundance of differential methylation and functional enrichment we identified, we focus on the most prominent trends in those data overall, including evidence of both transgenerational epigenetic dysregulation as well as strict epigenetic inheritance.

Genome and RRBS Data Quality

The genome assembly included 52,786 scaffolds that sums up to 568,309,548 base pairs (bp) (**Supplementary Figure S2**). The N50 of the assembly was 4,365,106 bp, in 27 scaffolds. The completeness of the assembly in gene space was assessed using BUSCO (version 3.0.2) with the vertebrate database. Out of 2,586 core BUSCO genes, 82.9% were found to be complete, with 2,023 genes in single copy and 121 genes in duplicated copies. There were 224 fragmented BUSCO genes, and 218 BUSCO genes were missing from the assembly.

[2]http://www.bioinformatics.babraham.ac.uk/projects/trim_galore/

[3]https://biodbnet-abcc.ncifcrf.gov/db/db2db.php

Analysis of RRBS data yielded the number of CpG sites between 1.7 million and 2.3 million in all samples. These CpG sites belonged to 315,410 methylated regions. The coverage information for each sample is summarized as a box plot (**Supplementary Figure S3**). The methylated regions that did not have more than 10 reads covered from at least 146 samples were removed before the differential methylation analysis. This filtering process reduced the number of methylated regions to 66,983.

Overall Trends in Differential Methylation

All treatments (Bif, EE2, Levo, Tren) and generations (F0, F1, F2) showed evidence of differential methylation relative to the control in the analysis of all genes (14,393 genes informed by the *M. beryllina* transcriptome). The percentage of genes that were differentially methylated in their promoter and/or gene body ranged from 6% (Levo F0) to 11% (Bif F2) of all annotated genes (**Figure 2**). Differential methylation at the gene level was nominally higher in the F1and F2 generation animals (8–11% of all annotated genes) of each treatment compared with F0 animals (6–8% of all annotated genes) (**Figure 2**), suggesting a possible increase in multigenerational methylation effects (F1) and transgenerational methylation effects (F2) compared to direct parental effects (F0) caused by all four EDCs. A similar trend has been noted for other EDCs in transgenerational experiments. For an exposure occurring in the parental generation, oviparous fishes, including *M. beryllina* and zebrafish, the F2 generation would be the first generation to display transgenerational effect, compared the F3 generation in viviparous animals (Brander et al., 2017). In one study examining transgenerational epigenetic inheritance in gestating female rats exposed to the agricultural fungicide vinclozin, differential DNA methylation was compared between F3 and F1 generation sperm. Beck et al. (2017) found significantly more DMRs in F3 compared to F1 sperm, with no shared overlap between those DMRs, indicating distinct transgenerational epigenetic methylation patterns. The authors attributed the distinct methylation patterns between generations to the sensitive developmental period of direct exposure in F1s given that these animals were exposed during a period of PGC deprogramming and subsequent reprogramming. Another study on methylmercury-exposed zebrafish also showed more epimutations in F2 (transgenerational effect) compared with embryonically exposed F0 sperm, and most DMRs were unique between the two generations (Carvan et al., 2017). Thus, it seems that transgenerational epigenetic effects of EDCs can be highly variable, and dependent on epigenetic disruption during critical developmental stages. If epigenetic machinery (methylation, histones, ncRNAs, etc.) are disrupted during critical developmental windows in early generations, these perturbations appear to display an exacerbation of epigenetic changes in subsequent generations. Although the pattern of epigenetic erasure and reprogramming post fertilization and PGC differentiation that occurs in medaka (same phylogenetic group – *Atherinomorpha* – as *Menidia*) but not zebrafish (Jiang et al., 2013; Potok et al., 2013; Ortega-Recalde et al., 2019; Wang and Bhandari, 2019) has not been established in *M. beryllina*, evidence of transgenerational epigenetic effects as a result of dysregulation of epigenetic programming appears to be evident in both models (medaka, which shares the pattern with mammals and zebrafish, which does not) as well as in *M. beryllina.*

Aside from the evidence of epigenetic dysregulation driving differential methylation among larval *M. beryllina*, a subset of differential methylation effects (3–5% of all annotated genes, depending on treatment) were shared between F1 and F2 generations, sometimes originating in the F0 generation (**Figure 2**), and can be considered as candidates for evidence of transgenerational epigenetic inheritance in the traditional, strict sense. For example, Rissman and Adli (2014) discuss strict transgenerational epigenetic inheritance as comparable to imprinting, when a specific epimutation is established in the germ line and maintained in subsequent generations. The directional and positional methylation changes at the gene level among EDC treated *M beryllina* would need to be individually verified to confirm this phenomenon. Some genes (∼1% for each treatment) were differentially methylated in the F0 and F2 generations, but not in the F1, thus, the potential for those methylation changes to be directly inherited is unclear. Specific evidence for transgenerational epigenetic inheritance in the strict sense is discussed further below (see Differential Methylation in EDC Responsive Genes).

When distinguishing between gene regions (promoter, gene body), differential methylation was more frequent within the gene body compared with the promoter region for all treatments and generations (**Figure 3**). Despite our use of RRBS to detect differential methylation, which operationally favors promoter regions (Yong et al., 2016), we were still able to detect more gene body differential methylation than promoter methylation. CpG methylation in the promoter region has been correlated with decreased gene expression in fish (Wan et al., 2016). Methylation in the gene body, however, is not correlated with gene repression and has the potential to affect splicing (Laurent et al., 2010) and sometimes lead to increased gene expression (Jones, 2012). It is possible that our definition of the promoter region as only 1 kb upstream was too narrow to capture many of the CpG islands in functional promoters. Gene promoters vary in their proximity relative to TSS by individual gene, so any nominal cutoff for promoters will not accurately represent the functional promoter for any given gene. Further, gene body sizes are typically larger than promoters, which would favor gene body differential methylation detection in our study. Still, we captured a great amount of gene body methylation given our use of RRBS methods. Most differentially methylated genes showed clear evidence of either hypo- or hypermethylation relative to the control, but a minority (<6%) showed evidence of both hypo and hyper methylation in different loci within the same gene region (**Figure 3**), indicating that directional methylation changes were locally specific.

GO Term and KEGG Pathway Enrichment Analyses

GO Term and KEGG pathway enrichment analyses use a standardized classification system and vocabulary to place genes into groups, making it easier to understand the

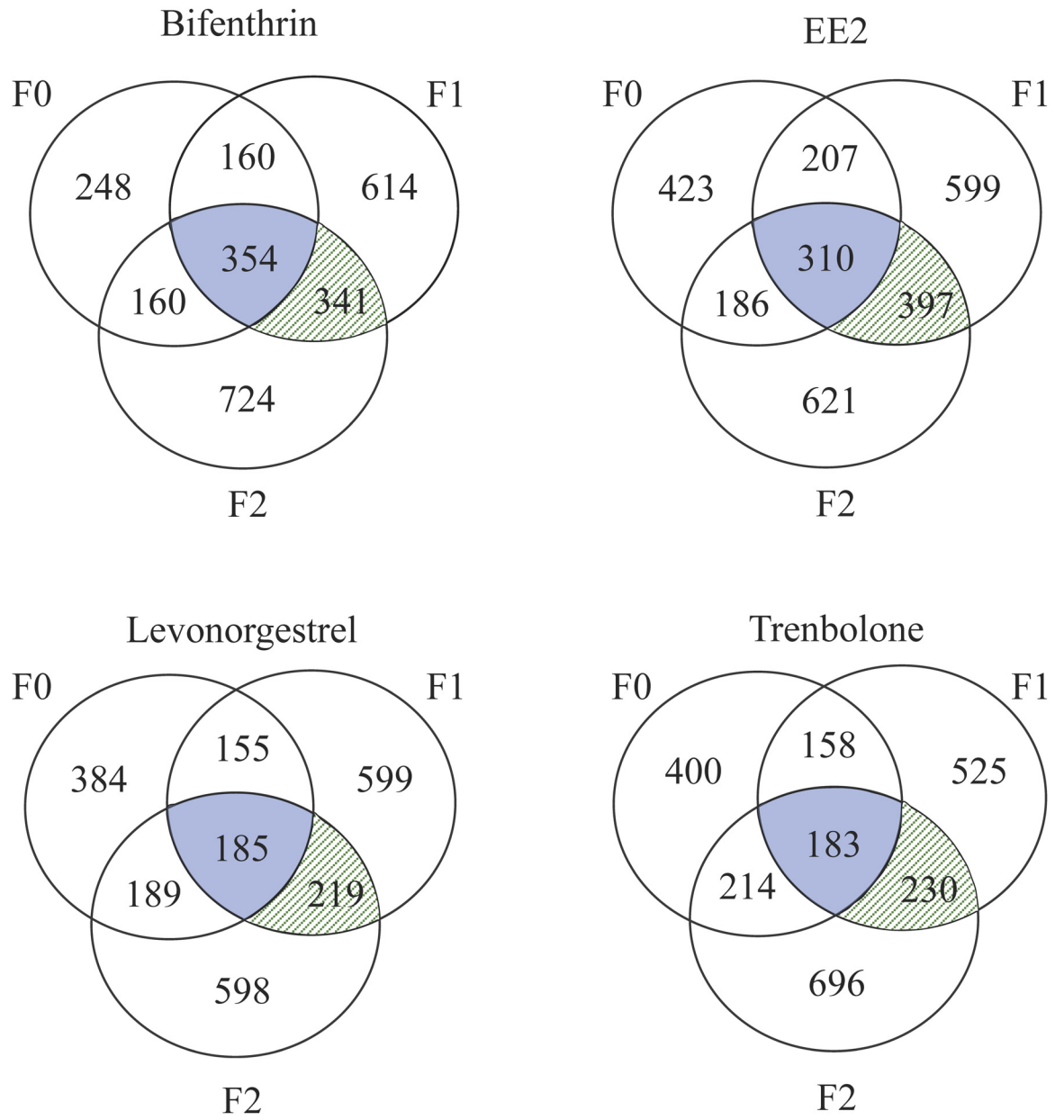

FIGURE 2 | Venn diagrams showing the number of genes (promoter and gene body regions combined) displaying differential methylation relative to control by treatment and generation as informed by the *M. beryllina* transcriptome. F0 animals were treated with an EDC (Bif, EE2, Levo, or Tren) during early development. F1 animals were exposed to these treatments indirectly as primordial germ cells within the F0 animals, and F2 animals were not exposed at all. The differential methylation in F1 animals is indicative of a multigenerational effect of EDCs, while the differential methylation in the F2 generation indicates a transgenerational effect. Differentially methylated genes shared by F1 and F2 (shaded green stripes), sometimes originating in F0 generations (shaded blue), is indicative of potential transgenerational epigenetic inheritance.

overall functional implications of genes that, in this case, are differentially methylated more than would be expected from a random selection of genes. Our GO Term analysis focused on biological processes (and not molecular function or cellular component) while KEGG pathway analysis groups genes by their inclusion in a given pathway (Nguyen et al., 2019; The Gene Ontology Consortium, 2019). Functional analyses of GO term (biological process) enrichment based on differentially methylated gene regions yielded significant enrichment ($\alpha = 0.01$) for a total of 144 GO terms when considering all treatments, generations, directional methylation, gene regions, while KEGG pathway analysis yielded 66 significantly enriched pathways (**Supplementary Tables S4, S5**). Differential gene body methylation produced a greater number of significantly enriched GO terms and KEGG pathways than did differential promoter methylation. As with overall differential

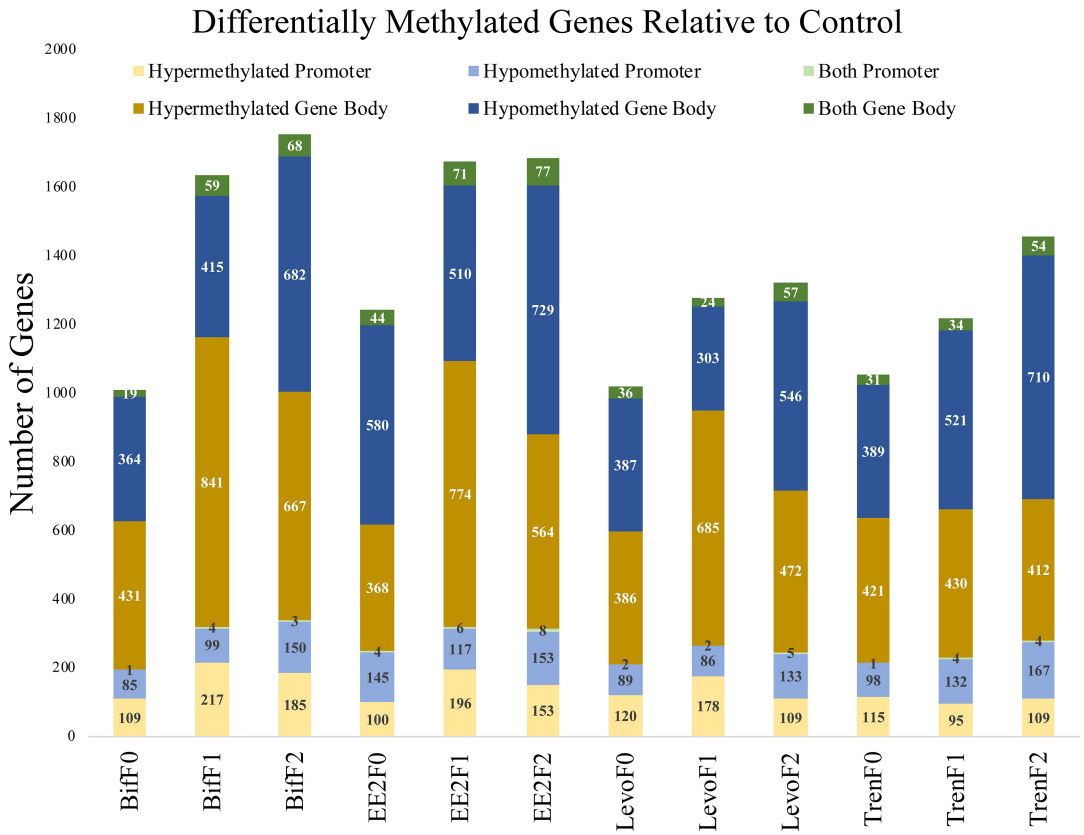

FIGURE 3 | Bar graph depicting the differential methylation relative to control by treatment (Bif, EE2, Levo, Tren), generation (F0, F1, F2), directional methylation change (hyper, hypo) and region (promoter, gene body) for all genes as informed by the *M. beryllina* transcriptome. Differential methylation was more prominent in the gene body than the promoter regions for all treatments and generations. While most genes only showed a singular directional change in methylation by region relative to the control, a minority showed both hypo and hyper methylation at different loci in the same gene.

methylation analyses, this skew may be related to the limited promoter window screened in the present study and the greater length in the gene body compared to the promoter (see above). Enrichment of the same term or pathway sometimes occurred across multiple treatments and generations (**Table 1** and **Figures 4**, **5**). It is important to note, however, that our use of a non-model organism with limited annotation for GO and KEGG enrichment analyses requires cautious interpretation, as enrichment results may be inflated by limited annotation information. Thus, we focus our discussion on enrichment of generalized categories that contain many enriched terms or those in which the number of differentially methylated annotated genes was high compared to the number of background genes expected in those gene ontology groups or pathways.

As part of our larger study, DeCourten et al. (unpublished) found craniofacial and/or skeletal deformities in at least one generation of all four EDC treatments. Our analysis of DNA methylation of enrichment of GO term and KEGG pathways produced changes in methylation for chondrocyte differentiation, cartilage condensation, embryonic morphogenesis, Wnt signaling (which is essential to embryonic development; Steinhart and Angers, 2018), and regulation of actin cytoskeleton (**Figures 4**, **5**), overlapping with all treatments and generations for which craniofacial and/or skeletal deformity phenotypes were measured (Bif F0, EE2 F1, Levo F2, Tren F0 and F1) (DeCourten et al., unpublished). Wnt signaling is essential for embryonic development. Other studies have documented phenotypic growth and development effects caused by EDC exposure linked to changes in DNA methylation. For example, prenatal exposure of the EDC cadmium led to an overrepresentation of DNA methylation in genes that were essential for organ and morphological development and bone mineralization, although only in females (Kippler et al., 2013). Further, DNA methylation has been associated with craniofacial abnormalities (Alvizi et al., 2017). We also found altered cardiovascular deformities in Bif F0, EE2 F1, and Tren F0 animals, some of the same treatments for which we have identified corresponding DNA methylation enrichment in GO terms and KEGG pathways including cardiac conduction (TrenF0) and adrenergic signaling of cardiomyocytes (Bif F2, EE2 F1, Levo F1, and Tren F2 (**Figures 4**, **5**), suggesting that altered methylation of cardiac genes and pathways may be linked to the physical deformities caused by EDC exposure. While we did not find perfect correspondence between the treatments/generations with cardiac deformities and the altered DNA methylation GO terms and KEGG pathways, the overlap suggests that DNA methylation may play a role in altered

TABLE 1 | Most frequently detected functional analysis enrichments considering gene region (promoter and gene body) directional differential methylation relative to the control (hyper, hypo), treatment (Bif, EE2, Levo, Tren), and generation (F0, F1, F2) for Gene Ontology (GO) terms and Kyoto Encyclopedia of Genes and Genomes (KEGG) pathway codes.

Functional enrichment code	Description	Combined instances of diff methyl enrichment (all treatments and generations)
GO Term		
GO:0050919	Negative chemotaxis	9
GO:0006662	Glycerol ether metabolic process	8
GO:0010332	Response to gamma radiation	8
GO:0008630	Intrinsic apoptotic signaling pathway in...	7
GO:0010165	Response to X-ray	5
GO:0043508	Negative regulation of JUN kinase activi...	5
GO:0006978	DNA damage response, signal transduction.	5
GO:0010172	Embryonic body morphogenesis	4
GO:0036071	*N*-glycan fucosylation	4
GO:0034644	Cellular response to UV	4
GO:0060216	Definitive hemopoiesis	4
KEGG pathway code		
path:dre04310	Wnt signaling pathway	12
path:dre04114	Oocyte meiosis	11
path:dre04150	mTOR signaling pathway	10
path:dre04916	Melanogenesis	10
path:dre04261	Adrenergic signaling in cardiomyocytes	9
path:dre03410	Base excision repair	7
path:dre04012	ErbB signaling pathway	7
path:dre04115	p53 signaling pathway	7
path:dre04145	Phagosome	6

Detailed information for all enrichments can be found in the ***Supplementary Tables S4, S5.***

cardiac developmental phenotypes. Although information on the relationship between EDC exposure, cardiac phenotypes, and DNA methylation is lacking, early life exposure to bifenthrin and EE2 has been linked to altered cardiac phenotypes (Jin et al., 2009; Salla et al., 2016). The overlap between the physiological whole organism endpoints resulting from EDC exposure and the functional enrichment of related GO terms and KEGG pathways in our differential methylation analysis suggest that some of the multi- and transgenerational effects observed in DeCourten et al. (unpublished) may be the result of EDC altered epigenetic control, although further work would be needed to mechanistically confirm the connection.

We found evidence of a variety of methylation enriched GO terms and KEGG pathways that are critical to neurodevelopment (e.g., wnt-activated signaling pathway involved in forebrain neuron fate commitment, neural crest cell fate specification, embryonic neurocranium morphogenesis, mTOR signaling pathway, calcium signaling pathway; **Figures 4**, **5**). One study (Frank et al., 2019) found that early life exposure to low (picomolar) concentrations of bifenthrin altered gene expression in calcium signaling pathways, and led to a latent olfactory predator avoidance cue behavioral phenotype in *M. beryllina*. The authors concluded that early-life effects of bifenthrin on neurodevelopment had effects later in life. Negative chemotaxis, or the movement away from chemicals, was the most frequently enriched GO term with differential methylation within the gene body across all treatments, affecting multiple generations within each treatment (**Supplementary Table S1**). It is possible that the alteration of methylation of genes involved in negative chemotaxis is yet another way in which EDCs have impacted neurodevelopmental processes. Others have documented other non-reproductive behavioral effects of estrogens and androgens in fish. Lagesson et al. (2019) exposed eastern mosquitofish (*Gambusia holbrooki*) to environmentally relevant levels (3 ng/L) of trenbolone at one of two temperature regimes for 21 days and found that trenbolone increased fish boldness behavior and altered predator escape behavior (but only at the higher temperature). Three-spined sticklebacks (*Gasterosteus aculeatus*) exposed to EE2 during early development and assayed for behavioral endpoints 8 months after exposures showed a reduction in anxiety behavior related to scototaxis (light/dark preference) (Porseryd et al., 2019). Zebrafish exposed to BPA (0.1 nM to 30 μM) as embryos showed evidence of hyperactivity in mid-range concentrations and altered transcription of genes involved in methylation (dnmt1 and cbs). The authors also found differential DNA methylation in many regions of the genome, primarily within gene bodies, and particularly in genes involved in neurodevelopment, suggesting the potential for differential DNA methylation of neurodevelopmental genes to affect observed differences in swimming behavior (Olsvik et al., 2019).

A number of GO terms and KEGG pathways involved in the regulation of the p53 tumor suppressor gene, generalized response to DNA damage, and regulation of the Wnt signaling pathway were enriched for at least one generation in each treatment. Indeed, Brander et al. (2016) showed that pathways involved in carcinogenesis were differentially expressed within *M. beryllina* exposed to bifenthrin. Further, trenbolone (Boettcher et al., 2011) and binary mixtures of tributyltin and EE2 (Micael et al., 2007) are known genotoxicants in fish. EDCs also play a role in dysregulating DNA methylation for genes important in carcinogenesis (Serman et al., 2014), a finding also supported elsewhere (Mirbahai et al., 2011). One study in mammals showed that most Wnt pathway gene bodies (and not promoters) were differentially methylated in cancer cells (Galamb et al., 2016). We found that Wnt pathway differential methylation was prominent in the gene bodies for all treatments, further strengthening the idea that EDCs may alter methylation in genes and pathways relevant to carcinogenesis. Gene body methylation of TP53 (which encodes p53) in somatic cells contributes to many types of cancer (Rideout et al., 1990; Jones, 2012). We found differential methylation in the gene bodies p53 pathways for all four EDCs. Exposure to EDCs has been widely linked with cancer phenotypes (Soto and Sonnenschein, 2010; Rachon, 2015; Karoutsou et al., 2017), and those cancer phenotypes linked to epigenetic changes (Bhandari, 2016),

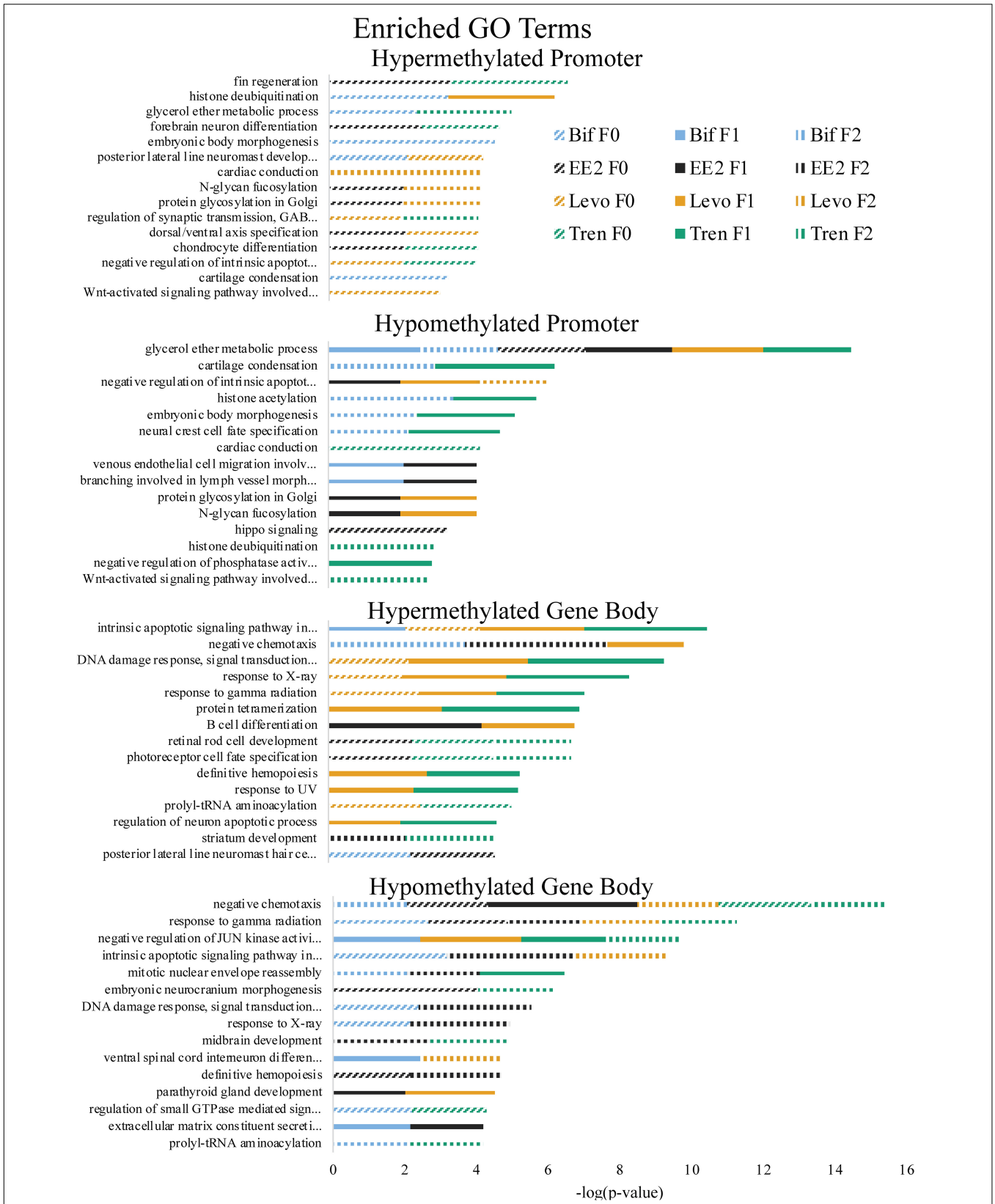

FIGURE 4 | Enriched Gene Ontology (GO) Terms by directional methylation change relative to the control (hyper, hypo), gene region (promoter, gene body), treatment (Bif, EE2, Levo, Tren), and generation (F0, F1, F2) showing level of significance based on Fisher's exact test *p*-values.

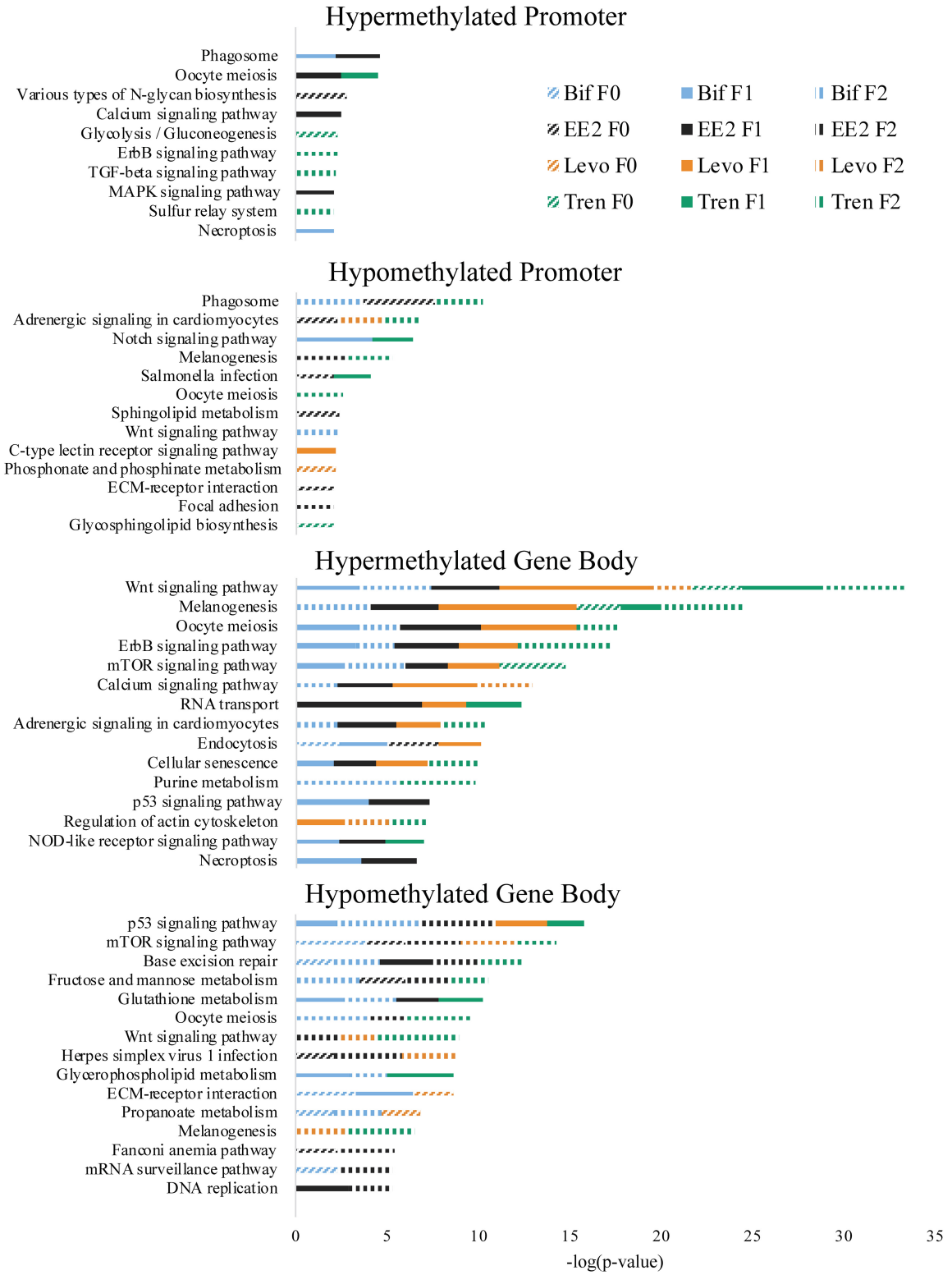

FIGURE 5 | Enriched Kyoto Encyclopedia of Genes and Genomes (KEGG) pathways by directional methylation change relative to the control (hyper, hypo), gene region (promoter, gene body), treatment (Bif, EE2, Levo, Tren), and generation (F0, F1, F2) showing level of significance based on Fishers exact test *p*-values.

providing support that the differential methylation caused by the four EDCs in the present study may play a functional role in carcinogenesis.

Altered DNA methylation in some biological functions may explain the transgenerational transfer of altered methylation patterns. The enriched GO terms related to epigenetic control mechanisms (histone deubiquination, histone acetylation) occurred in F1 or F2 animals for three out of four EDC treatments, suggesting that genes important in epigenetic programming have been dysregulated in these treatments due to early life exposure during sensitive windows, thus potentially perpetuating EDC-induced epigenetic dysregulation in subsequent generations as in Beck et al. (2017) and Carvan et al. (2017).

Another mechanism potentially responsible for the differential DNA methylation that we observed in larval *M. beryllina* may be an EDC-induced change in metabolism, particularly glutathione metabolism. Glutathione conjugation is a common detoxification mechanism for estrogens (Zhu and Conney, 1998) and has been established as a primary pathway involved in bifenthrin (Brander et al., 2016), trenbolone (Evrard and Maghuin-Rogister, 1987), and levonorgestrel metabolism (Stanczyk and Roy, 1990). Adult *M. beryllina* exposed to 0.5, 5, and 50 ng L^{-1} of bifenthrin showed a great deal of differential gene expression for metabolic processes (Brander et al., 2016), in line with our observed GO term and KEGG enrichment for differentially methylated metabolic processes and pathways. We found hypomethylated glutathione metabolism to be enriched in gene bodies for three of four EDC treatments (Bif, EE2, and Tren), which potentially affected glutathione metabolism. Evidence that metabolic alterations can contribute to epigenetic dysregulation is building. For example, more resources diverted to glutathione metabolism may compete with the resources needed by epigenetic machinery to methylate DNA and histones, thereby leading to a generalized hypomethylation (Lee et al., 2009; Oppold and Müller, 2017; Sharma and Rando, 2017). While we found both hyper- and hypomethylation as a result of EDC exposure, it is possible that some of the hypomethylation we observed was produced as a result of the demands of glutathione metabolism. Thus, the general glutathione pathway utilized to detoxify EDCs could be contributing to the differential methylation observed throughout the genome, and/or the differential methylation specific to the glutathione metabolism pathway may also be affecting the balance of methylation/demethylation in other parts of the genome.

Differential Methylation in Potentially EDC-Responsive Genes

The analysis of differential methylation in 109 potentially EDC-responsive genes (EDCRG) yielded 29 genes that were differentially methylated in at least one treatment/generation within their promoter and/or gene body regions. All treatments, generations, and gene regions (promoter, gene body) showed some differentially methylated EDCRGs, with the exception of the Bif F2 promoter region, for which no EDCRG differential methylation was noted (**Supplementary Figures S6, S7**). While a total of 18 EDCRG's were differentially methylated in the promoter and/or gene body across all F0 treatments, 20 EDCRG showed a multigenerational (F1) differential methylation effect while 22 showed a transgenerational (F2) effect depending on treatment and generation (**Supplementary Figures S6, S7**).

Differentially methylated EDCRGs included those involved in calcium signaling (*mtor, ryr1, calr, tgfb*), osmoregulation (*atnb233, atp1a1, atp1a1b, atp1a2*), steroidogenesis (*17ß-hsd, 3ß -hsd*), hormone receptors (*ar, esr2, esr3, gpr30*), immune function and/or inflammation (*cbr1, inha, stat1, tgfb*), structure (*krt13, pdlm1*), DNA methylation (*dnmt3a*), metabolism (*alas2, cyp1a1, smpd3*), sex determination (*dmrt1*), protein translation (*noa1*), proteolysis and degradation (*htra3, usp42*), zinc transport (*slc39a14*), and more general signaling pathway regulation (*ywhab*) (**Supplementary Figures S6**, **S7**). By frequency, the genes with the most alterations to their methylation patterns across all treatments and generations were *dmrt1*, *ar*, *17ß-hsd*, *atp1a1*, *atnb233*, *atp1a1b*, *ywhab*, *gpr30*, *cbr1*, *mtor*, *atp1a2*, *htra3* (**Supplementary Table S8**). The differential methylation we observed in these genes showed concordance with the generalized patterns of altered methylation enrichment in GO term and KEGG pathway analyses. Many of those genes showed differential methylation across generations within the same treatment, primarily within the gene body. Differential methylation occurring across generations was sometimes consistent (e.g., hypomethylation in the promoter of *dmrt1* for Tren F0 through F2 generations), although directional methylation often alternated by generation (e.g., hypomethylation of *atp1a1* within the gene body in EE2 F0 and F2, but hypermethylation of the same gene in F1), with hypomethylation in the gene body prominent in generations F0 and F2, but hypermethylation often prominent in the F1 generation (**Figure 6**). As with the overall analysis of all genes, a subset of EDCRGs showed patterns of both hyper- and hypomethylation, within the same greater region (promoter, gene body), although a singular directional differential methylation was the most common.

The majority of differential gene methylation documented for EDCRGs did not occur at the same sites within a given gene across the generations. Or, if they did, the direction of methylation change relative to the control often alternated (**Supplementary Table S8**), potentially indicating the interplay of epigenetic feedback loops (e.g., Bonasio et al., 2010). However, the same directional methylation changes (hypo, hyper) at the same loci were sometimes noted in F0 and F1 generations of the same treatment (*17ß-hsd* in Tren; *ar* in Bif, EE2, and Levo; *atp1a1* in Bif; *cbr1* in Bif, EE2, and Levo; *dmrt1* in Bif and EE2) indicating identical effects occurring from exposure in both generations or potentially a multigenerational inheritance pattern. Although this phenomenon was less prevalent in F1 and F2 generations of the same treatment (*17ß-hsd* in Bif; *dmrt1* in Tren; *htra3* in Bif and Levo), the maintenance of specific methylation from an exposed generation (F1) to an unexposed generation (F2) indicates a strict form of transgenerational epigenetic inheritance (**Figure 6**). These examples of transgenerational epigenetic inheritance provide evidence of germline-established

Directional Differential Methylation by Gene Region

		Promoter												Gene Body											
		Bif			EE2			Levo			Tren			Bif			EE2			Levo			Tren		
Gene	**Description**	F0	F1	F2	F0	F1	F2	F0	F1	F2	F0	F1	F2	F0	F1	F2	F0	F1	F2	F0	F1	F2	F0	F1	F2
17ß-hsd	17-beta-hydroxysteroid dehydrogenase 14														↑	↑	↓	↑	↓	↓	↑	↑↓	↑	↑	↑
ar	androgen receptor alpha				↓							↓		↑	↑	↓	↑	↑↓	↓	↑	↑↓		↑	↑↓	↓
atnb233	sodium potassium-transporting atpase subunit beta-233			↑			↓						↓				↑		↑↓	↑		↑	↑		
atp1a1	sodium potassium-transporting atpase alpha-1 subunit	↑	↑					↑	↑	↓		↑		↓	↑	↓	↓	↑	↓	↑↓		↓	↓		↓
atp1a1b	sodium potassium atpase alpha subunit													↓	↑	↓	↓	↑	↓	↓		↓	↓		↓
cbr1	carbonyl reductase													↑	↑		↑	↑		↑	↑			↑	
dmrt1	doublesex and mab-3-related transcription factor 3	↓	↓		↓	↓	↑	↓		↑	↓	↓	↓	↓	↓		↓	↓	↑	↓		↑		↓	↓
dnmt3a	dna (cytosine-5)-methyltransferase 3a-like													↑					↓				↑		↓
gpr30	g-protein coupled estrogen receptor 1-like														↑		↓		↑			↓	↓	↑	
htra3	serine protease htra3-like														↑	↑		↑			↑	↑		↑	
mtor	serine threonine-protein kinase mtor													↓	↑	↓		↑	↓			↓			
noa1	nitric oxide-associated protein 1-like														↑	↓		↑			↑	↓			
pdlm1	pdz and lim domain protein 1																							↑	↓
ywhab	14-3-3 protein beta alpha-1-like		↑			↑	↓		↑			↑	↓		↑			↑			↑			↑	

FIGURE 6 | Potential endocrine disrupting compound-responsive genes (EDCRGs) with differential methylation across more than one generation within the same treatment (Bif, EE2, Levo, Tren) relative to the control in **Supplementary Table S1**. Arrows indicate the change in methylation relative to the control (↑ is hypermethylation; ↓ is hypomethylation) in the gene region indicated (promoter or gene body). In instances for which both hyper- and hypo-methylation were noted for different loci in the same gene region, both arrows are indicated (↑↓). A change in methylation in F1 animals indicates a multigenerational effect, while a change in methylation in F2 animals indicates a transgenerational effect of EDC exposure. Methylation changes are shaded in tan the same locus that was differentially methylated across the F0 and F1 generations, indicating identical effects occurring from exposure in both generations or potentially a multigenerational inheritance pattern. Purple shading indicates the maintenance of specific methylation direction and loci from an exposed generation (F1) to an unexposed generation (F2) in support of transgenerational epigenetic inheritance.

differential methylation, in contrast to the evidence of epigenetic programming dysregulation that we also found.

Doublesex And Mab-3 Related Transcription Factor 1 (*dmrt1*) was one of the genes that showed evidence of transgenerational epigenetic inheritance and was the most frequently differentially methylated gene across all treatments and generations. *Dmrt1* is an important gene in sexual determination across many species, including those that exhibit temperature dependent sex determination, as *Menidia* species do (DeCourten and Brander, 2017; Huang et al., 2017) and in the closely related Japanese medaka (Otake et al., 2008). In the marine half-smooth tongue sole (*Cynoglossus semilaevis*), the level of *dmrt1* demethylation was responsible for male gonad development (Shao et al., 2014). It is possible that the skewed sex ratios that are common in EDC exposed populations (Jobling et al., 1998; Kidd et al., 2007; Hua et al., 2015; Orn et al., 2016; DeCourten and Brander, 2017) may be the result of epigenetic reprogramming at the *dmrt1* locus, as evidenced from the differential methylation caused by both estrogenic and androgenic EDCs in the present study.

We found differential methylation in genes involved in calcium signaling (*calr*, *ryr1*, *mtor*, *tgfb*) depending on treatment and generation, although all four EDCs yielded at least one calcium signaling gene with differential methylation (**Supplementary Figures S6, S7**). Alterations in calcium signaling gene expression as a result of bifenthrin exposure in *M. beryllina* and zebrafish have been established (Frank et al., 2018, 2019), and in response to other EDCs as well (Brander, 2013). Early life exposures of EE2 in coho salmon (*Oncorhynchus kisutch*) led to changes in transcription for both *tgfb* and calcium signaling pathways (Harding et al., 2013). The functional significance of the altered methylation in calcium signaling genes requires further study, but our preliminary results suggest that DNA methylation may play a regulatory role in altered calcium signaling pathway function in EDC-exposed fish.

We found differential methylation in the gene body of *dnmt3a*, the DNA methyl transferase responsible for *de novo* methylation (Okano et al., 1999; Hermann et al., 2004), in three different treatments, thus providing a potential mechanism to help explain DNA methylation dysregulation in exposed animals, although more work would need to be performed to confirm the functional relevance of this differential methylation. Other EDCs (TCDD, DES, PCB153) have been shown to alter transcription of Dnmts, which may in turn have direct effects on methylation (Wu et al., 2006).

Hormone receptors and regulators of steroidogenesis play an important role in development and reproduction. A recent multigenerational study with *M. beryllina* showed that exposure to 1 ng/L EE2 produced gene expression (*gpr30*, *17ß-hsd*) changes in directly exposed generations of fish. Exposure to 1 ng/L bifenthrin instead produced latent effects in indirectly exposed F1 generation fish (GPR30) (DeCourten et al., 2019a). We found evidence of differential methylation for *gpr30* in EE2 F0 and F2 and Bif F1 animals, while *17ß-hsd* was differentially methylated in nearly all treatments and generations, indicating that a change in methylation state for these genes may be related to gene expression differences observed previously (DeCourten et al., 2019a). We also documented frequent differential methylation of the *ar*, another hormone receptor, across most treatments and

generations. Casati et al. (2013) found that *ar* expression was modulated by other EDCs (PCBs), and that the altered expression had a basis in epigenetic mechanisms. Changes in *17ß-hsd*, *gpr30*, and *ar* methylation have been correlated with cancer (Bhavani et al., 2008; Tian et al., 2012; Manjegowda et al., 2017), thus there is the potential for differential methylation of these genes to have significant phenotypic effects during both development and later in life.

A limited analysis of differential gene methylation in larval *M. beryllina* from the same treatments as the present study showed little correlation between changes in gene expression and DNA methylation in a suite of twenty genes (measured at 21 dph). In fact, only one gene, *17ß-hsd*, showed hypomethylation within the gene body and significantly decreased expression in EE2 F0 animals (DeCourten et al., unpublished). The lack of concordance between gene expression changes and methylation could indicate that the differential methylation we observed is not functionally relevant and does not, therefore, translate to altered gene expression. Or, the lack of correlation could be a result of the single time point at which gene expression was measured, with epigenetic modifications being more stable than gene expression responses to EDCs. It is also possible that our approach of tracking methylation in the whole body larval fish, rather than specific tissues or cell-types created a dilution effect, making it difficult to track and correlate gene expression and DNA methylation. Future studies involving specific cell types (i.e., gonad) may allow for more prominent differential methylation trends to be revealed on a more mechanistically relevant basis. Other studies have also documented a lack of correspondence between DNA methylation and gene expression, even with tracking tissue-specific methylation (Aluru et al., 2018; Ryu et al., 2018). Further work is needed to determine the functional relationship between EDC-altered gene expression and differential methylation, ideally with multiple timepoint measurements and tissue and/or cell-specific DNA methylation profiling. Still, our detection of differential DNA methylation in all treatments and generations relative to the control provides evidence that EDCs drive changes in methylation on a multi- and transgenerational scale – a phenomenon that has already been established in mouse and human models (Susiarjo et al., 2007).

CONCLUSION

Here, we show that early life exposure to environmentally relevant (low parts per trillion) concentrations of EDCs (Bif, EE2, Tren, or Levo) caused differential methylation of mechanistically relevant genes (in promoter and/or gene body regions) in directly exposed (F0), indirectly exposed (F1), and unexposed (F2) generations of fish. We show evidence of strict epigenetic transgenerational inheritance as well as more generalized epigenetic transgenerational effects that may be driven by dysregulation in epigenetic programming during sensitive windows of development. Our functional and gene level analyses are in accordance with one another as well as with the physiological endpoints measured in DeCourten et al. (unpublished) and elsewhere as a result of EDC exposure. We show that growth and developmental, epigenetic regulation, and carcinogenic pathways are affected by differential methylation, primarily in the gene body compared with the promoter region of genes. All of these data provide evidence that DNA methylation may be altered by EDC exposure in early life, and that more work should be performed to better understand the mechanisms behind epigenetic alteration from exposure to environmentally relevant levels of EDCs.

DATA AVAILABILITY STATEMENT

The datasets presented in this study can be found in online repositories. The names of the repository/repositories and accession number(s) can be found below: NCBI BioSample Accession – SAMN14992539. All data are stored online at: https://datadryad.org/stash/dataset/doi:10.5061/dryad.4f4qrfj8h.

ETHICS STATEMENT

The animal study was reviewed and approved by the UNCW Institutional Animal Care and Use Committee under protocol number A1415-010.

AUTHOR CONTRIBUTIONS

KM was the lead author and performed the RRBS data analysis downstream of DMR identification and statistical analysis. SB and BD designed the original study. BD performed the multi and transgenerational experiments with *M. beryllina*. SB secured funding, advised KM and BD, and facilitated the overall study at UNCW and OSU. AM performed the analytical chemistry to quantify EDC levels in exposure solutions. MB, JL, and MS performed the genome sequencing, assembly and annotation and/or RRBS processing, and primary data analysis. RC assisted with funding the study, advised on research, and served as a liaison between UNCW and the UC Davis genome center.

FUNDING

Funding for this work was provided by the U.S. Environmental Protection Agency, grant no. 835799 (to SB, associate investigators RC and AM) and no. 83950301 (to SB), the California Department of Fish and Wildlife, grant no. P1796002 (to SB and RC), and the Delta Stewardship Council contract no. 18206 (to SB and RC).

ACKNOWLEDGMENTS

We thank colleagues and staff at the University of North Carolina Wilmington and the associated Center for Marine Science for supporting the empirical work that made these analyses possible. We thank the UC Davis Genome Center for sequencing and analysis support and the Oregon State Center for Genome Research and Biocomputing for valuable advice on analyses. We also thank Josh Forbes, Hunter Roark, and

many undergraduate researchers at UNCW, student researchers Jordan Laundry, Yvonne Rericha, and Lindsay Wilson at OSU, as well as Keith Maruya, Ellie Wenger, Wayne Lao (SCCWRP), and Shane Snyder (University of Arizona) for their contributions to the study.

SUPPLEMENTARY MATERIAL

The Supplementary Material for this article can be found online at: https://www.frontiersin.org/articles/10.3389/fmars.2020.00471/full#supplementary-material

REFERENCES

Alavian-Ghavanini, A., and Ruegg, J. (2018). Understanding epigenetic effects of endocrine disrupting chemicals: from mechanisms to novel test methods. *Basic Clin. Pharmacol. Toxicol.* 122, 38–45. doi: 10.1111/bcpt.12878

Alexa, A., and Rahnenfuhrer, J. (2019). *topGO: Enrichment Analysis for Gene Ontology*. Available online at: https://bioconductor.org/packages/release/bioc/html/topGO.html (accessed September 11, 2019).

Aluru, N., Karchner, S. I., Krick, K. S., Zhu, W., and Liu, J. (2018). Role of DNA methylation in altered gene expression patterns in adult zebrafish (*Danio rerio*) exposed to 3, 3', 4, 4', 5-pentachlorobiphenyl (PCB 126). *Environ. Epigenet.* 4:dvy005.

Alvizi, L., Ke, X., Brito, L. A., Seselgyte, R., Moore, G. E., Stanier, P., et al. (2017). Differential methylation is associated with non-syndromic cleft lip and palate and contributes to penetrance effects. *Sci. Rep.* 7:2441.

Aniagu, S. O., Williams, T. D., Allen, Y., Katsiadaki, I., and Chipman, J. K. (2008). Global genomic methylation levels in the liver and gonads of the three-spine stickleback (*Gasterosteus aculeatus*) after exposure to hexabromocyclododecane and 17-beta oestradiol. *Environ. Int.* 34, 310–317. doi: 10.1016/j.envint.2007.03.009

Ankley, G. T., Bencic, D. C., Breen, M. S., Collette, T. W., Conolly, R. B., Denslow, N. D., et al. (2009). Endocrine disrupting chemicals in fish: developing exposure indicators and predictive models of effects based on mechanism of action. *Aquat. Toxicol.* 92, 168–178. doi: 10.1016/j.aquatox.2009.01.013

Asomaning, N., and Archer, K. J. (2012). High-throughput DNA methylation datasets for evaluating false discovery rate methodologies. *Comput. Stat. Data Anal.* 56, 1748–1756. doi: 10.1016/j.csda.2011.10.020

Bayen, S., Zhang, H., Desai, M. M., Ooi, S. K., and Kelly, B. C. (2013). Occurrence and distribution of pharmaceutically active and endocrine disrupting compounds in Singapore's marine environment: influence of hydrodynamics and physical-chemical properties. *Environ. Pollut.* 182, 1–8. doi: 10.1016/j.envpol.2013.06.028

Beck, D., Sadler-Riggleman, I., and Skinner, M. K. (2017). Generational comparisons (F1 versus F3) of vinclozolin induced epigenetic transgenerational inheritance of sperm differential DNA methylation regions (epimutations) using MeDIP-Seq. *Environ. Epigenet.* 3:dvx016.

Benjamini, Y., and Hochberg, Y. (1995). Controlling the flase discovery rate: a practical and powerful approach to multiple testing. *J. R. Stat. Soc. Ser. B* 57, 289–300. doi: 10.1111/j.2517-6161.1995.tb02031.x

Bertram, M. G., Saaristo, M., Baumgartner, J. B., Johnstone, C. P., Allinson, M., Allinson, G., et al. (2015). Sex in troubled waters: widespread agricultural contaminant disrupts reproductive behaviour in fish. *Horm. Behav.* 70, 85–91. doi: 10.1016/j.yhbeh.2015.03.002

Best, C., Ikert, H., Kostyniuk, D. J., Craig, P. M., Navarro-Martin, L., Marandel, L., et al. (2018). Epigenetics in teleost fish: from molecular mechanisms to physiological phenotypes. *Comp. Biochem. Physiol. B. Biochem. Mol. Biol.* 224, 210–244. doi: 10.1016/j.cbpb.2018.01.006

Bhandari, R. K. (2016). Medaka as a model for studying environmentally induced epigenetic transgenerational inheritance of phenotypes. *Environ. Epigenet.* 2:dvv010. doi: 10.1093/eep/dvv010

Bhavani, V., Srinivasulu, M., Ahuja, Y. R., and Hasan, Q. (2008). Role of BRCA1, HSD17B1, and HSD17B2 methylation in breast cancer tissue. *Cancer Biomark.* 5, 207–213. doi: 10.3233/cbm-2009-0105

Boettcher, M., Kosmehl, T., and Braunbeck, T. (2011). Low-dose effects and biphasic effects profiles: Is trenbolone a genotoxicant? *Mutat. Res.* 732, 152–157. doi: 10.1016/j.mrgentox.2011.04.012

Bonasio, R., Tu, S., and Reinberg, D. (2010). Molecular signals of epigenetic states. *Science* 330, 612–616. doi: 10.1126/science.1191078

Brander, S. M. (2013). "Thinking outside the box: assessing endocrine disruption in aquatic life A2," in *Monitoring Water Quality: Pollution Assessment, Analysis, and Remediation*, ed. S. Ahuja (Amsterdam: Elsevier), 103–147.

Brander, S. M., Biales, A. D., and Connon, R. E. (2017). The role of epigenomics in aquatic toxicology. *Environ. Toxicol. Chem.* 36, 2565–2573. doi: 10.1002/etc.3930

Brander, S. M., Cole, B. J., and Cherr, G. N. (2012). An approach to detecting estrogenic endocrine disruption via choriogenin expression in an estuarine model fish species. *Ecotoxicology* 21, 1272–1280. doi: 10.1007/s10646-012-0879-2

Brander, S. M., Jeffries, K. M., Cole, B. J., DeCourten, B. M., White, J. W., Hasenbein, S., et al. (2016). Transcriptomic changes underlie altered egg protein production and reduced fecundity in an estuarine model fish exposed to bifenthrin. *Aquat. Toxicol.* 174, 247–260. doi: 10.1016/j.aquatox.2016.02.014

Brenet, F., Moh, M., Funk, P., Feierstein, E., Viale, A. J., Socci, N. D., et al. (2011). DNA methylation of the first exon is tightly linked to transcriptional silencing. *PLoS One* 6:e14524. 10.1371/journal.pone.0014524 doi: 10.1371/journal.pone.0014524

Carlson, M. (2019). *org.Dr.eg.db: Genome Wide Annotation for Zebrafish*. R package version 3.8.2. Available online at: https://bioconductor.org/packages/org.Dr.eg.db/ (accessed September 11, 2019).

Carvan, M. J. III, Kalluvila, T. A., Klingler, R. H., Larson, J. K., Pickens, M., Mora-Zamorano, F. X., et al. (2017). Mercury-induced epigenetic transgenerational inheritance of abnormal neurobehavior is correlated with sperm epimutations in zebrafish. *PLoS One* 12:e0176155. doi: 10.1371/journal.pone.0176155

Casati, L., Sendra, R., Poletti, A., Negri-Cesi, P., and Celotti, F. (2013). Androgen receptor activation by polychlorinated biphenyls: epigenetic effects mediated by the histone demethylase Jarid1b. *Epigenetics* 8, 1061–1068. doi: 10.4161/epi.25811

Cole, B. J., Brander, S. M., Jeffries, K. M., Hasenbein, S., He, G., Denison, M. S., et al. (2016). Changes in *Menidia beryllina* gene expression and *in vitro* hormone-receptor activation after exposure to estuarine waters near treated wastewater outfalls. *Arch. Environ. Contam. Toxicol.* 71, 210–223. doi: 10.1007/s00244-016-0282-8

DeCourten, B. M., and Brander, S. M. (2017). Combined effects of increased temperature and endocrine disrupting pollutants on sex determination, survival, and development across generations. *Sci. Rep.* 7:9310. doi: 10.1038/s41598-017-09631-1

DeCourten, B. M., Connon, R. E., and Brander, S. M. (2019a). Direct and indirect parental exposure to endocrine disruptors and elevated temperature influences gene expression across generations in a euryhaline model fish. *PeerJ* 7:e6156. doi: 10.7717/peerj.6156

DeCourten, B. M., Romney, A., and Brander, S. (2019b). "The heat is on: complexities of aquatic endocrine disruption in a changing global climate," in *Evaluating Water Quality to Prevent Future Disasters*, ed. S. Ahuja (Amsterdam: Elsevier), 13–49.doi: 10.1016/b978-0-12-815730-5.00002-8

Ellestad, L. E., Cardon, M., Chambers, I. G., Farmer, J. L., Hartig, P., Stevens, K., et al. (2014). Environmental gestagens activate fathead minnow (*Pimephales promelas*) nuclear progesterone and androgen receptors *in vitro*. *Environ. Sci. Technol.* 48, 8179–8187. doi: 10.1021/es501428u

Evrard, P., and Maghuin-Rogister, G. (1987). *In vitro* metabolism of trenbolone: study of the formation of covalently bound residues. *Food Addit. Contam.* 5, 59–65. doi: 10.1080/02652038809373663

Forsgren, K. L., Riar, N., and Schlenk, D. (2013). The effects of the pyrethroid insecticide, bifenthrin, on steroid hormone levels and gonadal development of steelhead (*Oncorhynchus mykiss*) under hypersaline conditions. *Gen. Comp. Endocrinol.* 186, 101–107. doi: 10.1016/j.ygcen.2013.02.047

Frank, D. F., Brander, S. M., Hasenbein, S., Harvey, D. J., Lein, P. J., Geist, J., et al. (2019). Developmental exposure to environmentally relevant concentrations

of bifenthrin alters transcription of mTOR and ryanodine receptor-dependent signaling molecules and impairs predator avoidance behavior across early life stages in inland silversides (*Menidia beryllina*). *Aquat. Toxicol.* 206, 1–13. doi: 10.1016/j.aquatox.2018.10.014

Frank, D. F., Miller, G. W., Harvey, D. J., Brander, S. M., Geist, J., Connon, R. E., et al. (2018). Bifenthrin causes transcriptomic alterations in mTOR and ryanodine receptor-dependent signaling and delayed hyperactivity in developing zebrafish (*Danio rerio*). *Aquat. Toxicol.* 200, 50–61. doi: 10.1016/j.aquatox.2018.04.003

Galamb, O., Kalmar, A., Peterfia, B., Csabai, I., Bodor, A., Ribli, D., et al. (2016). Aberrant DNA methylation of WNT pathway genes in the development and progression of CIMP-negative colorectal cancer. *Epigenetics* 11, 588–602. doi: 10.1080/15592294.2016.1190894

Gaspar, J. M., and Hart, R. P. (2017). DMRfinder: efficiently identifying differentially methylated regions from MethylC-seq data. *BMC Bioinformatics* 18:528. doi: 10.1186/s12859-017-1909-0

Harding, L. B., Schultz, I. R., Goetz, G. W., Luckenbach, J. A., Young, G., Goetz, F. W., et al. (2013). High-throughput sequencing and pathway analysis reveal alteration of the pituitary transcriptome by 17alpha-ethynylestradiol (EE2) in female coho salmon, *Oncorhynchus kisutch*. *Aquat. Toxicol.* 142-143, 146–163. doi: 10.1016/j.aquatox.2013.07.020

Head, J. A. (2014). Patterns of DNA methylation in animals: an ecotoxicological perspective. *Integr. Comp. Biol.* 54, 77–86. doi: 10.1093/icb/icu025

Hermann, A., Gowher, H., and Jeltsch, A. (2004). Biochemistry and biology of mammalian DNA methyltransferases. *Cell. Mol. Life Sci.* 61, 2571–2587. doi: 10.1007/s00018-004-4201-1

Hinck, J. E., Blazer, V. S., Denslow, N. D., Echols, K. R., Gale, R. W., Wieser, C., et al. (2008). Chemical contaminants, health indicators, and reproductive biomarker responses in fish from rivers in the Southeastern United States. *Sci. Total Environ.* 390, 538–557. doi: 10.1016/j.scitotenv.2007.10.026

Hua, J., Han, J., Guo, Y., and Zhou, B. (2015). The progestin levonorgestrel affects sex differentiation in zebrafish at environmentally relevant concentrations. *Aquat. Toxicol.* 166, 1–9. doi: 10.1016/j.aquatox.2015.06.013

Huang, S., Ye, L., and Chen, H. (2017). Sex determination and maintenance: the role of DMRT1 and FOXL2. *Asian J. Androl.* 19, 619–624.

Jablonka, E., and Raz, G. (2009). Transgenerational epigenetic inheritance: prevalence, mechanisms, and implications for the study of heredity and evolution. *Q. Rev. Biol.* 84, 131–176. doi: 10.1086/598822

Jeffries, K. M., Brander, S. M., Britton, M. T., Fangue, N. A., and Connon, R. E. (2015). Chronic exposures to low and high concentrations of ibuprofen elicit different gene response patterns in a euryhaline fish. *Environ Sci. Pollut. Res.* 22, 17397–17413. doi: 10.1007/s11356-015-4227-y

Jiang, L., Zhang, J., Wang, J. J., Wang, L., Zhang, L., Li, G., et al. (2013). Sperm, but not oocyte, DNA methylome is inherited by zebrafish early embryos. *Cell* 153, 773–784. doi: 10.1016/j.cell.2013.04.041

Jin, M., Zhang, X., Wang, L., Huang, C., Zhang, Y., Zhao, M., et al. (2009). Developmental toxicity of bifenthrin in embryo-larval stages of zebrafish. *Aquat. Toxicol.* 95, 347–354. doi: 10.1016/j.aquatox.2009.10.003

Jobling, S., Nolan, M., Tyler, C. R., Brighty, G., and Sumpter, J. P. (1998). Widespread sexual disruption in wild fish. *Environ. Sci. Technol.* 32, 2498–2506. doi: 10.1021/es9710870

Jones, P. A. (2012). Functions of DNA methylation: islands, start sites, gene bodies and beyond. *Nature* 13, 484–492. doi: 10.1038/nrg3230

Karoutsou, E., Karoutsos, P., and Karoutsos, D. (2017). Endocrine disruptors and carcinogenesis. *Arch. Cancer Res.* 5:1. doi: 10.1002/9781118891094.ch1

Kidd, K. A., Blanchfield, P. J., Mills, K. H., Palace, V. P., Evans, R. E., Lazorchak, J. M., et al. (2007). Collapse of a fish population after exposure to a synthetic estrogen. *Proc. Natl. Acad. Sci. U.S.A.* 104, 8897–8901. doi: 10.1073/pnas.0609568104

Kippler, M., Engstrom, K., Mlakar, S. J., Bottai, M., Ahmed, S., Hossain, M. B., et al. (2013). Sex-specific effects of early life cadmium exposure on DNA methylation and implications for birth weight. *Epigenetics* 8, 494–503. doi: 10.4161/epi.24401

Krueger, F., and Andrews, S. R. (2011). Bismark: a flexible aligner and methylation caller for Bisulfite-Seq applications. *Bioinformatics* 27, 1571–1572. doi: 10.1093/bioinformatics/btr167

Lagesson, A., Saaristo, M., Brodin, T., Fick, J., Klaminder, J., Martin, J. M., et al. (2019). Fish on steroids: temperature-dependent effects of 17beta-trenbolone on predator escape, boldness, and exploratory behaviors. *Environ. Pollut.* 245, 243–252. doi: 10.1016/j.envpol.2018.10.116

Laurent, L., Wong, E., Li, G., Huynh, T., Tsirigos, A., Ong, C. T., et al. (2010). Dynamic changes in the human methylome during differentiation. *Genome Res.* 20, 320–331. doi: 10.1101/gr.101907.109

Lee, D. H., Jacobs, D. R. Jr., and Porta, M. (2009). Hypothesis: a unifying mechanism for nutrition and chemicals as lifelong modulators of DNA hypomethylation. *Environ. Health Perspect.* 117, 1799–1802. doi: 10.1289/ehp.0900741

Manjegowda, M. C., Gupta, P. S., and Limaye, A. M. (2017). Hyper-methylation of the upstream CpG island shore is a likely mechanism of GPER1 silencing in breast cancer cells. *Gene* 614, 65–73. doi: 10.1016/j.gene.2017.03.006

Micael, J., Reis-Henriques, M. A., Carvalho, A. P., and Santos, M. M. (2007). Genotoxic effects of binary mixtures of xenoandrogens (tributyltin, triphenyltin) and a xenoestrogen (ethinylestradiol) in a partial life-cycle test with Zebrafish (*Danio rerio*). *Environ. Int.* 33, 1035–1039. doi: 10.1016/j.envint.2007.06.004

Mirbahai, L., Yin, G., Bignell, J. P., Li, N., Williams, T. D., Chipman, J. K., et al. (2011). DNA methylation in liver tumorigenesis in fish from the environment. *Epigenetics* 6, 1319–1333. doi: 10.4161/epi.6.11.17890

Mudunuri, U., Che, A., Yi, M., and Stephens, R. M. (2009). bioDBnet: the biological database network. *Bioinformatics* 25, 555–556. doi: 10.1093/bioinformatics/btn654

Nguyen, T. M., Shafi, A., Nguyen, T., and Draghici, S. (2019). Identifying significantly impacted pathways: a comprehensive review and assessment. *Genome Biol.* 20:203.

Okano, M., Bell, D. W., Haber, D. A., and Li, E. (1999). DNA methyltransferass Dnmt3a and Dnmt3b are essential for de novo methylation and mammalian development. *Cell* 99, 247–257. doi: 10.1016/s0092-8674(00)81656-6

Olsvik, P. A., Whatmore, P., Penglase, S. J., Skjaerven, K. H., Angles d'Auriac, M., Ellingsen, S., et al. (2019). Associations between behavioral effects of Bisphenol A and DNA Methylation in Zebrafish Embryos. *Front. Genet.* 10:184. doi: 10.3389/fgene.2019.00184

Olsvik, P. A., Williams, T. D., Tung, H. S., Mirbahai, L., Sanden, M., Skjaerven, K. H., et al. (2014). Impacts of TCDD and MeHg on DNA methylation in zebrafish (*Danio rerio*) across two generations. *Comp. Biochem. Physiol. C. Toxicol. Pharmacol.* 165, 17–27. doi: 10.1016/j.cbpc.2014.05.004

Oppold, A.-M., and Müller, R. (2017). Epigenetics: a hidden target of insecticides. *Adv. Insect Physiol.* 53, 313–324. doi: 10.1016/bs.aiip.2017.04.002

Orlando, E. F., and Ellestad, L. E. (2014). Sources, concentrations, and exposure effects of environmental gestagens on fish and other aquatic wildlife, with an emphasis on reproduction. *Gen. Comp. Endocrinol.* 203, 241–249. doi: 10.1016/j.ygcen.2014.03.038

Orn, S., Holbech, H., and Norrgren, L. (2016). Sexual disruption in zebrafish (*Danio rerio*) exposed to mixtures of 17alpha-ethinylestradiol and 17beta-trenbolone. *Environ. Toxicol. Pharmacol.* 41, 225–231. doi: 10.1016/j.etap.2015.12.010

Ortega-Recalde, O., Day, R. C., Gemmell, N. J., and Hore, T. A. (2019). Zebrafish preserve global germline DNA methylation while sex-linked rDNA is amplified and demethylated during feminisation. *Nat. Commun.* 10:3053.

Otake, H., Hayashi, Y., Hamaguchi, S., and Sakaizumi, M. (2008). The Y chromosome that lost the male-determining function behaves as an X chromosome in the medaka fish, *Oryzias latipes*. *Genetics* 179, 2157–2162. doi: 10.1534/genetics.108.090167

Perkins, E. J., Gayen, K., Shoemaker, J. E., Antczak, P., Burgoon, L., Falciani, F., et al. (2019). Chemical hazard prediction and hypothesis testing using quantitative adverse outcome pathways. *ALTEX* 36, 91–102. doi: 10.14573/altex.1808241

Porazinski, S. R., Wang, H., and Furutani-Seiki, M. (2010). Dechorionation of medaka embryos and cell transplantation for the generation of chimeras. *J. Vis. Exp.* 46:2055.

Porseryd, T., Larsson, J., Kellner, M., Bollner, T., Dinnetz, P., Hällström, I. P., et al. (2019). Altered non-reproductive behavior and feminization caused by developmental exposure to 17alpha-ethinylestradiol persist to adulthood in three-spined stickleback (*Gasterosteus aculeatus*). *Aquat. Toxicol.* 207, 142–152. doi: 10.1016/j.aquatox.2018.11.024

Potok, M. E., Nix, D. A., Parnell, T. J., and Cairns, B. R. (2013). Reprogramming the maternal zebrafish genome after fertilization to match the paternal methylation pattern. *Cell* 153, 759–772. doi: 10.1016/j.cell.2013.04.030

Rachon, D. (2015). Endocrine disrupting chemicals (EDCs) and female cancer: informing the patients. *Rev. Endocr. Metab. Disord.* 16, 359–364. doi: 10.1007/s11154-016-9332-9

Ribeiro, C., Pardal, M. A., Tiritan, M. E., Rocha, E., Margalho, R. M., Rocha, M. J., et al. (2009). Spatial distribution and quantification of endocrine-disrupting chemicals in Sado River estuary, Portugal. *Environ. Monit. Assess.* 159, 415–427. doi: 10.1007/s10661-008-0639-1

Rideout, W. M. I., Coetzee, G. A., Olumi, A. F., and Jones, P. A. (1990). 5-Methylcytosine as an endogenous mutagen in the human LDL receptor and p53 genes. *Science* 249, 1288–1290. doi: 10.1126/science.1697983

Rissman, E. F., and Adli, M. (2014). Minireview: transgenerational epigenetic inheritance: focus on endocrine disrupting compounds. *Endocrinology* 155, 2770–2780. doi: 10.1210/en.2014-1123

Robinson, J. A., Staveley, J. P., and Constantine, L. (2017). Reproductive effects on freshwater fish exposed to 17alpha-trenbolone and 17alpha-estradiol. *Environ. Toxicol. Chem.* 36, 636–644. doi: 10.1002/etc.3526

Runnalls, T. J., Beresford, N., Kugathas, S., Margiotta-Casaluci, L., Scholze, M., Scott, A. P., et al. (2015). From single chemicals to mixtures–reproductive effects of levonorgestrel and ethinylestradiol on the fathead minnow. *Aquat. Toxicol.* 169, 152–167. doi: 10.1016/j.aquatox.2015.10.009

Ryu, T., Veilleux, H. D., Donelson, J. M., Munday, P. L., and Ravasi, T. (2018). The epigenetic landscape of transgenerational acclimation to ocean warming. *Nat. Clim. Change* 8, 504–509. doi: 10.1038/s41558-018-0159-0

Salla, R. F., Gamero, F. U., Rissoli, R. Z., Dal-Medico, S. E., Castanho, L. M., dos Santos Carvalh, C., et al. (2016). Impact of an environmental relevant concentration of 17alpha-ethinylestradiol on the cardiac function of bullfrog tadpoles. *Chemosphere* 144, 1862–1868. doi: 10.1016/j.chemosphere.2015.10.042

Schug, T. T., Johnson, A. F., Birnbaum, L. S., Colborn, T., Guillette, L. J. Jr., Crews, D. P., et al. (2016). Minireview: endocrine disruptors: past lessons and future directions. *Mol. Endocrinol.* 30, 833–847. doi: 10.1210/me.2016-1096

Schwindt, A. R., Winkelman, D. L., Keteles, K., Murphy, M., Vajda, A. M., Frid, C., et al. (2014). An environmental oestrogen disrupts fish population dynamics through direct and transgenerational effects on survival and fecundity. *J. Appl. Ecol.* 51, 582–591. doi: 10.1111/1365-2664.12237

Serman, L., Nikuseva, T. M., Serman, A., and Vranic, S. (2014). Epigenetic alternations of the Wnt signaling pathway in cancer: a mini review. *Bosn. J. Basic Med. Sci.* 14, 191–194.

Shao, C., Li, Q., Chen, S., Zhang, P., Lian, J., Hu, Q., et al. (2014). Epigenetic modification and inheritance in sexual reversal of fish. *Genome Res.* 24, 604–615. doi: 10.1101/gr.162172.113

Sharma, U., and Rando, O. J. (2017). Metabolic inputs into the epigenome. *Cell Metab.* 25, 544–558. doi: 10.1016/j.cmet.2017.02.003

Soto, A. M., and Sonnenschein, C. (2010). Environmental causes of cancer: endocrine disruptors as carcinogens. *Nat. Rev. Endocrinol.* 6, 363–370. doi: 10.1038/nrendo.2010.87

Stanczyk, F. Z., and Roy, S. (1990). Metabolism of levonorgestrel, norethindrone, and structurally related contraceptive steroids. *Contraception* 42, 67–96. doi: 10.1016/0010-7824(90)90093-b

Steinhart, Z., and Angers, S. (2018). Wnt signaling in development and tissue homeostasis. *Development* 145:dev146589. doi: 10.1242/dev.146589

Susiarjo, M., Hassold, T. J., Freeman, E., and Hunt, P. A. (2007). Bisphenol A exposure in utero disrupts early oogenesis in the mouse. *PLoS Genet.* 3:e5. doi: 10.1371/journal.pgen.0030005

Svensson, J., Fick, J., Brandt, I., and Brunstrom, B. (2013). The synthetic progestin levonorgestrel is a potent androgen in the three-spined stickleback (*Gasterosteus aculeatus*). *Environ. Sci. Technol.* 47, 2043–2051. doi: 10.1021/es304305k

Svensson, J., Fick, J., Brandt, I., and Brunstrom, B. (2014). Environmental concentrations of an androgenic progestin disrupts the seasonal breeding cycle in male three-spined stickleback (*Gasterosteus aculeatus*). *Aquat. Toxicol.* 147, 84–91. doi: 10.1016/j.aquatox.2013.12.013

Tenenbaum, D. (2020). *KEGGREST: Client-Side REST Access to KEGG*. R package version 1.28.0. Available online at: https://bioconductor.org/packages/release/bioc/html/KEGGREST.html

The Gene Ontology Consortium (2019). The gene ontology resource: 20 years and still GOing strong. *Nucleic Acids Res.* 47, D330–D338.

Tian, J., Lee, S. O., Liang, L., Luo, J., Huang, C. K., Li, L., et al. (2012). Targeting the unique methylation pattern of androgen receptor (AR) promoter in prostate stem/progenitor cells with 5-aza-2'-deoxycytidine (5-AZA) leads to suppressed prostate tumorigenesis. *J. Biol. Chem.* 287, 39954–39966. doi: 10.1074/jbc.m112.395574

Wan, Z. Y., Xia, J. H., Lin, G., Wang, L., Lin, V. C., Yue, G. H., et al. (2016). Genome-wide methylation analysis identified sexually dimorphic methylated regions in hybrid tilapia. *Sci. Rep.* 6:35903.

Wang, X., and Bhandari, R. K. (2019). DNA methylation dynamics during epigenetic reprogramming of medaka embryo. *Epigenetics* 14, 611–622. doi: 10.1080/15592294.2019.1605816

Wu, Q., Zhou, Z. J., and Ohsako, S. (2006). Effect of environmental contaminants on DNA methyltransferase activity of mouse preimplantation embryos. *Wei Sheng Yan Jiu* 35, 30–32.

Wu, T. D., and Watanabe, C. K. (2005). GMAP: a genomic mapping and alignment program for mRNA and EST sequences. *Bioinformatics* 21, 1859–1875. doi: 10.1093/bioinformatics/bti310

Xin, F., Susiarjo, M., and Bartolomei, M. S. (2015). Multigenerational and transgenerational effects of endocrine disrupting chemicals: a role for altered epigenetic regulation? *Semin. Cell Dev. Biol.* 43, 66–75. doi: 10.1016/j.semcdb.2015.05.008

Yella, V. R., Kumar, A., and Bansal, M. (2018). Identification of putative promoters in 48 eukaryotic genomes on the basis of DNA free energy. *Sci. Rep.* 8:4520.

Yong, W. S., Hsu, F. M., and Chen, P. Y. (2016). Profiling genome-wide DNA methylation. *Epigenet. Chromatin* 9:26.

Zhou, G. J., Li, X. Y., and Leung, K. M. Y. (2019). Retinoids and oestrogenic endocrine disrupting chemicals in saline sewage treatment plants: removal efficiencies and ecological risks to marine organisms. *Environ. Int.* 127, 103–113. doi: 10.1016/j.envint.2019.03.030

Zhu, B. T., and Conney, A. H. (1998). Functional role of estrogen metabolism in target cells: review and perspectives. *Carcinogenesis* 19, 1–27. doi: 10.1093/carcin/19.1.1

Conflict of Interest: The authors declare that the research was conducted in the absence of any commercial or financial relationships that could be construed as a potential conflict of interest.

frontiers in Marine Science

ORIGINAL RESEARCH
published: 11 August 2020
doi: 10.3389/fmars.2020.00598

Characterizing the Epigenetic and Transcriptomic Responses to *Perkinsus marinus* Infection in the Eastern Oyster *Crassostrea virginica*

Kevin M. Johnson[1], K. A. Sirovy[1], Sandra M. Casas[2], Jerome F. La Peyre[2] and Morgan W. Kelly[1]*

[1] Department of Biological Sciences, Louisiana State University, Baton Rouge, LA, United States, [2] School of Animal Sciences, Louisiana State University Agricultural Center, Baton Rouge, LA, United States

OPEN ACCESS

Edited by:
Hollie Putnam, University of Rhode Island, United States

Reviewed by:
Guillaume Rivière, Université de Caen Normandie, France
Steven Roberts, University of Washington, United States

***Correspondence:**
Kevin M. Johnson
dr.kevin.m.johnson@gmail.com

Specialty section:
This article was submitted to Marine Molecular Biology and Ecology, a section of the journal Frontiers in Marine Science

Received: *31 January 2020*
Accepted: *29 June 2020*
Published: *11 August 2020*

Citation:
Johnson KM, Sirovy KA, Casas SM, La Peyre JF and Kelly MW (2020) Characterizing the Epigenetic and Transcriptomic Responses to Perkinsus marinus Infection in the Eastern Oyster Crassostrea virginica. Front. Mar. Sci. 7:598. doi: 10.3389/fmars.2020.00598

Eastern oysters in the northern Gulf of Mexico are routinely infected with the protistan parasite *Perkinsus marinus*, the cause of the disease commonly known as dermo. Recent experimental challenges among Atlantic coast populations have identified both resistant and susceptible genotypes using comparative transcriptomics. While controlled experimental challenges are essential first assessments, expanding this analysis to field reared individuals provides an opportunity to identify key genomic signatures of infection that appear both in the laboratory and in the field. In this study we combined reduced representation bisulfite sequencing with 3′ RNA sequencing (Tag-seq) to describe two molecular phenotypes associated with infection in oysters outplanted at a common garden field site. These combined approaches allowed us to examine changes in DNA methylation and gene expression for a large number of individuals (n = 40) that developed infections during the course of a common garden outplant experiment. Our epigenetic analysis of DNA methylation identified significant changes in gene body methylation associated with increasing infection intensity, across genes associated with immune responses. There was a smaller transcriptomic response to increasing infection intensities with 32 genes showing differential expression; however, only 40% of these genes were found to also be differentially methylated. While there was no clear pattern between direction of differential methylation and gene expression, there was a significant effect of percent methylation on gene-by-gene expression levels and the coefficient of variation in gene body methylation between treatments. These results show that in *C. virginica*, heavily methylated genes have high levels of gene expression with low levels of variation. Comparing our differential expression results with previously published experimental *P. marinus* challenges identified overlapping expression patterns for genes associated with C1q-domain-containing and V-type proton ATPase proteins. Through our comparative transcriptomic approach using field reared individuals and co-expression network analysis we have also been able to identify a network of genes

that change in expression in response to infection. These combined analyses provide evidence for a conserved response to *P. marinus* infections across infection intensities and suggest that DNA methylation may not be a reliable predictor of differential gene expression in long-term infections.

Keywords: DNA methylation, TagSeq, eastern oyster *Crassostrea virginica*, *Perkinsus marinus* disease, transcriptomics, weighted gene co-expression network analyses

INTRODUCTION

The relationship between tissue-specific DNA methylation and gene expression is an area of interest to a broad research community as these two molecular phenotypes have been proposed as mechanisms of environmental responsiveness and used as biomarkers to describe interactions between organisms and their environment (Roberts and Gavery, 2012; Dixon et al., 2014; Putnam et al., 2016; Hawes et al., 2018; Schmid et al., 2018; Eirin-Lopez and Putnam, 2019; Rubi et al., 2019). The utility of these metrics relies heavily on a well-developed understanding of how a stimulus will modulate either gene expression or DNA methylation levels, and how methylation could in turn modulate gene expression. As a result, the last decade has seen a dramatic increase in the number of studies using whole transcriptome sequencing to describe how non-model species modify their transcriptomes in response to developmental cues, diseases, and shifts in the abiotic environment (Alvarez et al., 2015; De Wit et al., 2018; Jones et al., 2019; Proestou and Sullivan, 2020). Interest in the functional role of DNA methylation has also grown in recent years due to its potential contributions to transgenerational plasticity (Kappeler and Meaney, 2010; Herman and Sultan, 2016; Gavery and Roberts, 2017; Ryu et al., 2018). These studies together have further fueled interest in the mechanisms that control transcriptome variation, with the majority of studies focusing on either DNA methylation or chromatin modifications (Clark et al., 2018; Weinhold, 2018; Eirin-Lopez and Putnam, 2019).

Oysters in the genus *Crassostrea* are both an ecologically and environmentally important keystone species distributed across broad geographic ranges. These widely dispersed species inhabit highly variable environments leading to species with a high degree of phenotypic plasticity (Li et al., 2017). As such, oysters are an ideal organism for exploring how DNA methylation influences phenotypic plasticity. Recent research on this genus has focused on describing the degree to which gene expression contributes to phenotype or how DNA methylation directs gene expression levels. These studies have found strong evidence that environmental variation and/or disease state can have a predictable influence on gene expression (Yan et al., 2017; Jones et al., 2019; Proestou and Sullivan, 2020). In a similar manner, a growing body of literature has provided ample evidence that DNA methylation can shape the transcriptomic phenotype (Rivière et al., 2013; Olson and Roberts, 2014; Song et al., 2017). In the Pacific oyster (*C. gigas*) high levels of methylation in gene bodies are associated with elevated expression, while lowly methylated genes showed higher levels of transcriptomic plasticity (Gavery and Roberts, 2013; Olson and Roberts, 2014). In the eastern oyster (*C. virginica)* DNA methylation is more divergent between populations than single nucleotide polymorphism-based estimates of divergence, suggesting a non-genetic (i.e., environmental) influence on DNA methylation (Johnson and Kelly, 2020). Together, these studies provide some evidence of an association between DNA methylation and transcriptomic expression levels; however, the functional consequences of changes in DNA methylation are still largely unknown in bivalves.

In a similar manner, shifts in gene expression are often essential for responding to infectious diseases in bivalves (Renault et al., 2011; Moreira et al., 2012; Rosani et al., 2015). Previous research investigating the transcriptomic responses of *C. virginica* challenged with *Perkinsus marinus* found significant changes in the regulation of genes involved in immune defense (Tanguy et al., 2004; Wang et al., 2010). Although previous studies have shown that *C. virginica* regulates gene expression in response to *P. marinus*, a major gap remains regarding whether there is a population-specific transcriptomic response to dermo in the northern Gulf of Mexico. Previous research has shown that oyster populations vary in mortality rates in response to dermo, though the molecular basis for this is still unclear (Casas et al., 2017; Leonhardt et al., 2017; La Peyre et al., 2019). A recent study looking at the effect of *P. marinus* infection on the global gene expression pattern of resistant vs susceptible *C. virginica* families found strong acute responses to infection with over 3,000 differentially expressed transcripts with resistant oysters upregulating genes involved with peptidase inhibitor activity and regulation of proteolysis (Proestou and Sullivan, 2020). This response diminished over 28 days after which only 21 differentially expressed genes were observed within the dermo resistant family while the dermo susceptible family differentially expressed over 2,000 genes. These large differences in response to infection in controlled settings provide a base to begin exploring how responses to infections differ in the field.

To this end we present a comparison of 40 individuals with differing levels of *P. marinus* infections following 14 months of outplant at a common-garden field site. We investigated both transcriptomic and epigenetic signatures of these infections to better understand how light vs heavy intensity infections influence molecular phenotypes. Using a combination of reduced representation bisulfite sequencing and 3′ RNA sequencing (TAGseq) we are able to describe two molecular responses to infection intensity in a common garden study. These results also allow us to compare the molecular phenotype of farm-raised oysters with *P. marinus* infections to recent results from a controlled infection (Proestou and Sullivan, 2020). Through a common garden outplant of hatchery reared juveniles we

were able to compare changes in DNA methylation and gene expression for a large number of individuals (n = 40) that were identified as infected with *P. marinus*, but at varying intensities. This allowed us to use a weighted gene co-expression network analysis to identify a collection of genes positively correlated with infection. Furthermore, we were able to explore how changes in DNA methylation related to changes in gene expression on a gene-by-gene basis.

MATERIALS AND METHODS

Oysters

In May 2016, adult oysters (*C. virginica*) were collected by dredging from each of two estuaries; Vermilion Bay, LA (29° 35′ 7.26″ N, 91° 0\2′ 33.92″ W) and Calcasieu Lake, LA (29° 50′ 58.02″ N, 93° 17′ 1.32″ W). These oysters were transported to the Louisiana Department of Wildlife and Fisheries Michael C. Voisin Oyster Hatchery in Grand Isle, LA (29° 14′ 20.3″ N, 90° 00′ 11.2″ W) and placed into off-bottom mesh cages for common garden acclimation. In October 2016, after 5 months of acclimation, oysters were spawned at the MCV oyster hatchery. Oyster spat were reared in an upwelling system, individually tagged, and outplanted in one of three adjustable long-line mesh bags at the Grand Isle Hatchery farm on February 20, 2017. Oysters within each bag were monitored for mortality and cleaned of epibionts approximately every 3 months over a 14-month period.

Sample Collection

On April 24, 2018, after 14 months at the Grand Isle outplant site, 50 individuals were haphazardly sampled. Shell height of each individual was measured from shell umbo to distal edge using a digital caliper (ABS Coolant Proof Calipers, Mituyoto Corporation, Japan). Approximately 1 cm^2 piece of gill tissue was sampled in the field from each individual and preserved with either Invitrogen RNA*later* (gene expression) or 95% ethanol (DNA methylation). The remaining whole animal was placed in a pre-weighed 50 ml test tube in order to measure wet meat weight. Infection intensities were enumerated by adding 0.22 μm filtered seawater (20 ppt) at a concentration of ∼0.4 g ml^{-1} and homogenizing the oyster meat in each 50 ml test tube. One ml of the oyster homogenate was used to measure the number of *P. marinus* hypnospores g^{-1} oyster wet tissue using the whole-oyster procedure (La Peyre et al., 2018). Oyster infections were classified as either very-light (≤1,000 parasites g^{-1} wet tissue), light (1,001–10,000 parasites g^{-1} wet tissue), moderate (10,001–100,000 parasites g^{-1} wet tissue) or moderate-heavy (>100,000 parasites g^{-1} wet tissue). Of the 50 individuals sampled we sequenced 40 individuals that spanned the four different infection categories (**Table 1**).

DNA Methylation Analysis

DNA was extracted using the OMEGA E.Z.N.A. Tissue DNA Kit (D3396-01; Omega bio-tek) with a 2 min RNase A digestion to remove co-purified RNA. DNA purity was assessed based on 260/280 and 260/230 ratios using a nanodrop spectrophotometer (ND1000; Thermofisher Scientific). Presence of high molecular weight DNA was confirmed using a 1.5% agarose gel, and DNA concentration was verified using a Qubit 3.0 Fluorometric dsDNA BR assay kit (Q32850; Life Technologies). The epiGBS library preparation followed previously published methods (Van Gurp et al., 2016; Johnson and Kelly, 2020). Briefly, a total of 500 ng of purified genomic DNA was double digested using the two frequent cutter enzymes *Ase*I and *Nsi*I (NEB-R0127L and NEB-R0526L; Van Gurp 2016). Digested DNA was ligated to custom y-yoked methylated sequencing adapters using a T4 DNA ligase (B9000S; New England Biolabs) with additional rATP to ensure ligation of custom adapters (Glenn et al., 2019). The adapter ligated DNA was bisulfite converted in a 96 well plate using the Zymo Research EZ DNA Methylation-Lightning kit (D5031; Zymo Research) with a 15 min L-desulphonation step. This bisulfite converted DNA was tagged and amplified with Illumina adapters using 16 cycles of PCR. Amplified libraries were size selected to 300–600 base-pairs (bp) using the Zymo Research Select-A-Size DNA clean & concentrator (D4080; Zymo Research). Size selection was confirmed using the Agilent Bioanalyzer DNA high sensitivity chip (5067-4626; Agilent Technologies). Libraries were pooled and sequenced by NovoGene Inc. (R) with a 10% PhiX spike-in on a full flow cell of the Illumina HiseqX with 100 bp paired-end reads.

The epiGBS sequencing reads were adapter trimmed and base pairs with a phred score less than 30 were removed using Trimmomatic (version 0.39) (Bolger et al., 2014). Trimmed reads were mapped to the reference genome (NCBI GCF_002022765.2) and CpG methylation was called using the software package *bismark* (v0.19.0) (Krueger and Andrews, 2011). The *bismark* commands used in the mapping allowed for 1 mismatch in a seed alignment of 10 with a minimum alignment score setting of −0.6 (–score_min L, 0, −0.6). These settings having previously been used in this species and were selected to account for genomic variations between *C. virginica* collected from the northern Gulf of Mexico (nGOM, this study) and the disease-resistant inbred line from the United States East Coast used for the construction of the reference genome (Gómez-Chiarri et al., 2015; Johnson and Kelly, 2020). CpG methylation was extracted from the non-deduplicated mapped reads using the *bismark* command *bismark_methylation_extractor* with the following commands; –ignore_r2 2, –bedGraph, –zero_based, –no_overlap, –cytosine_report, and –report. Differential methylation was conducted on CpG features using the bismark coverage files with methylation across both strands merged and analyzed using the R program *MethylKit* (v.1.2.4) (Akalin et al., 2012). Methylated regions were identified using a tiled window approach with a tile size of 1,000 bp (1 kb) and a step size of 1 kb. The 1 kb regions were filtered using the *filterByCoverage* command to require coverage greater than 10× in at least 8 of the 20 individuals.

Pair-wise differential methylation was measured between individuals with moderate or moderate-heavy (parasites g^{-1} >10,000, n = 15) and very-light (parasites g^{-1} ≤1,000, n = 16) infection intensities. For these analysis, one sample in the high infection group was not included as a result of poor sequence quality. Significantly differentially methylated regions (DMRs)

TABLE 1 | Distribution of the number of individuals sequenced for each infection category, with both mean infections and range of infections for each category.

Infection category	Infection intensity (parasites g^{-1} wet tissue)	Number of individuals	Median infection intensity (parasites g^{-1} wet tissue)	Infection range (parasites g^{-1} wet tissue)	Mean height (mm)	Mean wet tissue weight (g)
Very light	≤1,000	16	138	33–704	94.7 ± 7.8	17.56 ± 4.8
Light	1,001–10,000	8	4,128	1,402–9,474	103.8 ± 6.1	17.60 ± 4.1
Moderate	10,001–100,000	8	42,974	13,918–89,174	106.2 ± 10.3	20.51 ± 5.7
Moderate-heavy	>100,001	8	616,623	194,516–3,049,972	103.3 ± 12.5	19.35 ± 6.0

Mean shell height and mean wet meat weight are also reported with standard deviations.

were identified based on a minimum percent methylation difference between groups of 20% and an adjusted *P*-value (*q*-value) less than or equal to 0.05 (Mathers et al., 2019). Functional enrichment of methylation was assessed using two methods. The first approach explored enrichment in methylation amongst all samples tested using a Mann-Whitney *U*-test to identify enriched ontologies between highly and lowly methylated genes. This test used mean methylation among all individuals for each gene feature with at least a single 1 kb region overlapping a gene's promoter, gene body or downstream region; and, calculated enrichment across each gene ontology (GO) category (MF, Molecular Function; BP, Biological Process, and CC, Cellular Component). The second approach tested for functional enrichment between genes that showed differentially methylated regions using a Fisher's Exact test for each GO category. For both analyses we used a background list consisted of all genes with GO annotations for which DNA methylation was measured ($n = 8{,}624$ of genes passing filter with GO annotations).

TAGseq Analysis

Total RNA was extracted using a E.Z.N.A.® Total RNA Kit I (Omega BIO-TEK Inc., Norcross, GA, United States) following the manufacturer's instructions. The yield and quantity were initially assessed using a NanoDrop 2000 spectrophotometer. Total RNA extracted from the 40 individuals was sent to the University of Texas at Austin's Genomic Sequencing and Analysis Facility where RNA quality control was confirmed using a 2100 Agilent Bioanalyzer on a Eukaryote Total RNA Nano chip and libraries were produced using the 3′ poly-A-directed mRNA-sequencing (TAGseq) method (Meyer et al., 2011). The resulting 40 libraries were sequenced on two lanes of an Illumina HiSeq 2500 platform, with 100 base pair single-end reads. Sequencing reads were trimmed of adapter sequences using Trimmomatic (version 0.39) (Bolger et al., 2014) and base pairs with quality scores below 30 were removed. The trimmed reads were then mapped to the published *C. virginica* reference genome (Gómez-Chiarri et al., 2015) using the single pass option for STAR RNA-seq aligner (version 2.6.0a) (Dobin et al., 2012). We used the default of 10 allowed mismatches for filtering and allowed for multi-mapping. After mapping, we used HTSeq (version 0.11.2) (Anders et al., 2015) to obtain the number of reads mapped to each gene and allowed for multiple alignments to be counted (–non-unique = all). The counts were sorted by alignment position and based on gene features obtained from the *C. virginica* genome assembly on NCBI (version GCF_002022765.2).

Changes in gene expression associated with *P. marinus* infection intensity were tested with two approaches. The first approach assessed pairwise changes in gene expression between individuals with moderate-heavy and very-light infection using the package edgeR (version 3.24.2) (Robinson et al., 2010). For this analysis genes with fewer than three counts per million mapped reads across 50% ($n = 20$) of all samples were removed. The remaining read counts were distributed across 17,439 gene features and were normalized using the trimmed mean of M-values (TMM) normalization method (Robinson and Oshlack, 2010). Broad changes in gene expression were first assessed using a principal coordinate analysis (PCoA) conducted using the R program vegan with Euclidean distances calculated from log2 + 1 transformed normalized counts obtained from the cpm() function in edgeR. These log-transformed counts were also used to test for any significant interactions between gene expression and infection intensity interactions using a PERMANOVA with $1e^6$ permutations. Pairwise differential expression was measured using the genewise negative binomial generalized linear model implemented in the edgeR function glmFit and significantly differentially expressed genes (DEGs) were identified based on FDR rates calculated using benjamini-hochberg method (Benjamini and Hochberg, 1995). Comparisons were made between the lowest infection group (very-light, $n = 16$) and a combination of the two highest infection groups (moderate and moderate-high, $n = 16$). Functional enrichment of differential gene expression for each comparison was tested using a rank-based gene ontology analysis with adaptive clustering that uses a Mann-Whitney *U*-Test to identify enriched ontologies (Wright et al., 2015). For these tests, we tested for enrichment using the log-transformed and signed p-value for each gene in each comparison contrasted using all of the genes that passed the expression filtering for the analysis and had annotated GO terms ($n = 11{,}057$).

The second approach used to assess changes in gene expression associated with *P. marinus* infection intensity was a Weighted Gene Network Analysis (WGCNA). For this component of the analysis we restricted the number of genes to remove lowly expressed features retaining only samples with greater than five counts per million in 75% of all samples ($n = 30$). This additional filtering was included to remove genes with low counts prior to network analysis. WGCNA was run using the 11,998 genes that passed this filter, a soft-threshold of 12, a minimum module size of 30, a signed adjacency matrix, and was correlated to shell height, meat weight, and infection intensity (a continuous variable of counts/g). Functional enrichment was

assessed across 7,398 of the 11,998 genes that had annotated GO terms for the five modules that showed significant correlation with any of the five traits using the GO_MWU methods for WGCNA using eigengene-based module connectivity (kME) as a continuous variable. This method calculates significant enrichment across each gene ontology (GO) category (MF, BP, and CC) for each module, and identifies functional categories in the modules using the Fisher's Exact test. These functional categories were further tested for an association with higher kME values using a within-module MWU test. The product of the resulting *p*-values from the Fisher's Exact and MWU test was then used to calculate false discovery rates with ten permutations of randomly shuffled significance measures among genes.

Methylation and Gene Expression

An important component of this study was the opportunity to examine the interaction between DNA methylation and transcript expression across many individuals. We tested the relationship between percent methylation for moderate-heavy infected individuals vs very-lightly infected individuals and changes in gene expression, as measured by the pairwise differential gene expression analysis. To do this, we summarized each 1 kb region into three categories: 1 kb regions that were located in (i) gene promoter regions (within 2 kb upstream of the first exon), (ii) gene body regions (first exon to last exon), or (iii) downstream regions (within 2 kb downstream of the last exon). For all comparisons if multiple 1 kb regions were present within the annotated feature (promoter, gene body, or downstream region) the mean *p*-value, mean *q*-value, and mean percent difference in methylation was calculated. For each of these three gene regions we explored the association of mean methylation with the log-transformed cpm expression data. For these analyses cpm expression data was distributed into 10 deciles using the *decile* function available in the R package StatMeasures (v.1.0). Significance of the association between mean methylation and expression level deciles was assessed using a Kruskal–Wallis test along with a Dunn *post hoc* test and corrected for multiple comparisons using the Benjamini-Hochberg method.

RESULTS

DNA Methylation

RRBS sequencing produced a total of 878 million reads with an average of 21.4 million reads per sample. Trimming of these reads led to an average of 18.1 million reads per sample, and mapping resulted in an average of 84.6% of reads mapping to the reference genome (range: 77.3–89.1%). Genome tiling in methylkit distributed these reads across 43,085 1-kb regions with a minimum count of 10 in a minimum of 9 individuals in either of the 2 groups (very-light or moderate and moderate-heavy). Of these, 10,741 regions were located along intergenic regions (i.e., greater than 2 kb from any gene feature). The remaining 32,344 1-kb regions were distributed across 15,543 annotated gene features with 13.1% (n = 2,364 genes) found within promoter regions (i.e., 2 kb upstream of first exon), 71.3% (n = 12,781 genes) found within gene bodies, and 15.6% (n = 2,791 genes) found within 2 kb downstream of a gene's final exon. Functional enrichment testing using the rank-based gene ontology analysis with adaptive clustering among all 40 individuals based on mean methylation identified enriched gene functions among both heavily- and lightly methylated genes (relative to the genome-wide average) in each of the three gene ontology categories (14 MF, 6 BP, and 11 CC). We observed higher methylation of key molecular processes such as RNA metabolism, chromosome organization, and general protein binding. While lightly methylated genes were associated with environmentally responsive categories such as enzyme regulation, immune processes and oxidoreductase activity (**Table 2**).

Our pair-wise assessments of differential methylation between the moderately and moderate-heavily and lightly infected groups identified 913 significantly differentially methylated 1-kb regions (DMRs), distributed across 846 genes. Among these, 86 DMRs (10.1%) were found within promoter regions, 666 DMRs (78.8%) were found within gene bodies, and 66 DMRs (8%) were found in downstream regions. Functional enrichment using a Fisher's Exact test for each region (i.e., promoter, gene body, and downstream) did not identify any significant enrichment for hyper/hypo-methylated genes or gene body regions. Examining genes that showed the strongest change in methylation between infection categories identified significant hypomethylation of a uncharacterized long non-coding RNA (−58%), a complement C1q tumor necrosis factor-related protein 4-like gene (−36.5%), a heat shock 70 kDa protein 12A-like isoform (−29.25%), and a caspase-8-like gene (−27.65%) in individuals with higher levels of infection. Gene-body hypermethylation in more infected individuals occurred in UPF0600 protein c5orf51 homolog (+65.1%), two uncharacterized long non-coding RNAs (+52.2%; +48.1%), an organic cation transporter protein (+44.9%), and an ankyrin-2-like isoform (+44.9%).

Gene Expression

Transcriptome sequencing using TAGseq produced a total of 189 million reads, with 4.7 million reads per sample. Trimming of those reads led to a final read count of 4.5 million per sample, which is sufficient for this method (Meyer et al., 2011). Star mapping resulted in 80.20% of reads mapping to the reference genome (range: 75.7–83.1%). Filtering mapped reads based on expression resulted in a total of 17,439 gene features with more than 3 counts per million reads in 20 of the 40 samples. This stringent level of filtering was chosen to avoid including too many genes with low count totals. Principle coordinate analysis revealed significant overlap with the three low-infection groups with separation of these from the single high infection group (**Figure 1**). The PERMANOVA testing expression ∼ infection (parasites g^{-1} wet tissue wet) found a non-significant interaction between infection and gene expression (p-value = 0.09).

Pairwise differential gene expression analysis identified modest levels of differential gene expression between infection intensities. Gene expression changes associated with moderate-heavy vs very-light infections, identified 31 genes up-regulated and 8 genes down-regulated in the moderate-heavy infected individuals (**Figure 2**). A Mann-Whitney *U*-Test of the 11,057 genes in the analysis (regardless of DE status) was run

TABLE 2 | Top results from Mann Whitney *U*-Test enriched gene ontology (GO) terms tested using percent methylation of gene body.

GO category	GO term	Go ID	Percentage of reference	Heavy/lightly methylated	Adjusted *P*-value
MF	Transferase activity	GO:0016740	87.1% (378/434)	Heavy	8.404156e-04
MF	Protein binding	GO:0005515; GO:0008092	94.7% (54/57)	Heavy	8.906802e-03
MF	Oxidoreductase activity	GO:0016491	74.4 % (264/355)	Lightly	7.742907e-09
MF	Enzyme regulator activity	GO:0030234; GO:0098772	65.8% (50/76)	Lightly	8.906802e-03
BP	Immune system process	GO:0002376	67.9% (38/56)	Lightly	2.501468e-05
BP	Chromosome organization	GO:0051276	95.5% (42/44)	Heavy	1.508920e-02
BP	RNA metabolic process	GO:0016070	92.3% (48/52)	Heavy	1.300211e-02
CC	Cytoskeleton	GO:0005856	96.5% (136/141)	Heavy	2.475557e-04
CC	Plasma membrane	GO:0005886; GO:0016020	72.7% (109/150)	Lightly	1.167721e-10

Percent of reference shows the number of genes identified as enriched when compared to the total number of genes for that GO term in the background reference list.

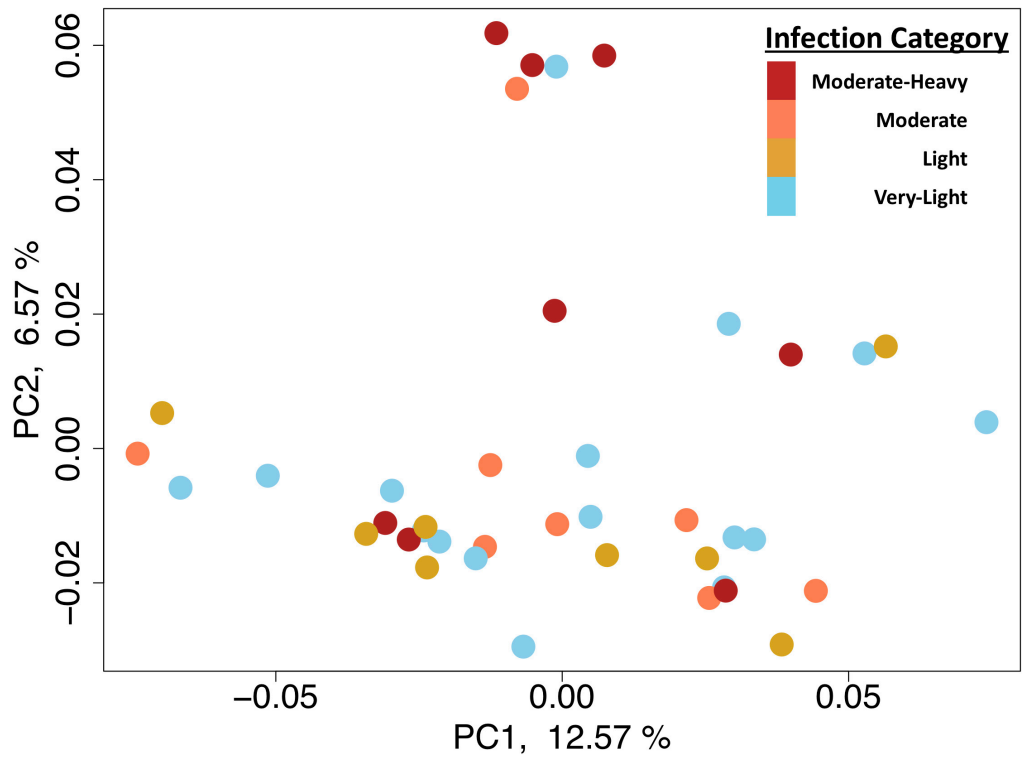

FIGURE 1 | Biplot of the first two principle components from principle coordinate analysis using the gene expression data.

using the log-transformed and signed p-values for genes that passed filtering for the analysis and had annotated GO terms (n = 11,057). This analysis identified 19 enriched categories associated with infection intensity including *G protein-coupled receptor activity*, *ribonucleoprotein complex biogenesis*, and *peptide metabolic process* (**Table 3**). There were three genes significantly differentially expressed (FDR < 0.05) that had predicted enzyme annotations, these genes include a GTP-binding protein GEM-like enzyme (logFC = −1.6; gene18819), a gene coding for a hepatic-like arginase (logFC = + 0.7; gene13511), and a gene coding for uncharacterized protein LOC111128066 that has been functionally annotated as an endonuclease (logFC = +1.5; gene13511). There were five additional genes that were differentially expressed and have previously been found to respond to infection in marine invertebrates (de Lorgeril et al., 2005; Proestou and Sullivan, 2020). These included nijurin 1-like (logFC = +2.1;gene24478); phytanoyl-CoA dioxygenase domain-containing protein 1-like (logFC = +3.0; gene6975), C1q tumor necrosis factor protein 6-like (logFC = −2.6; gene30362), C1q tumor necrosis factor protein protein 7-like (logFC = +2.6; gene10222), a GATA zinc finger domain containing protein 14 (logFC = −6.0; gene 5837), and a nuclear polyadenylated RNA-binding protein 3-like gene (logFC = −3.2; gene5505).

WGCNA Results

The WGCNA analysis identified a total of 12 gene modules; of these, only 1 module was significantly correlated with dermo

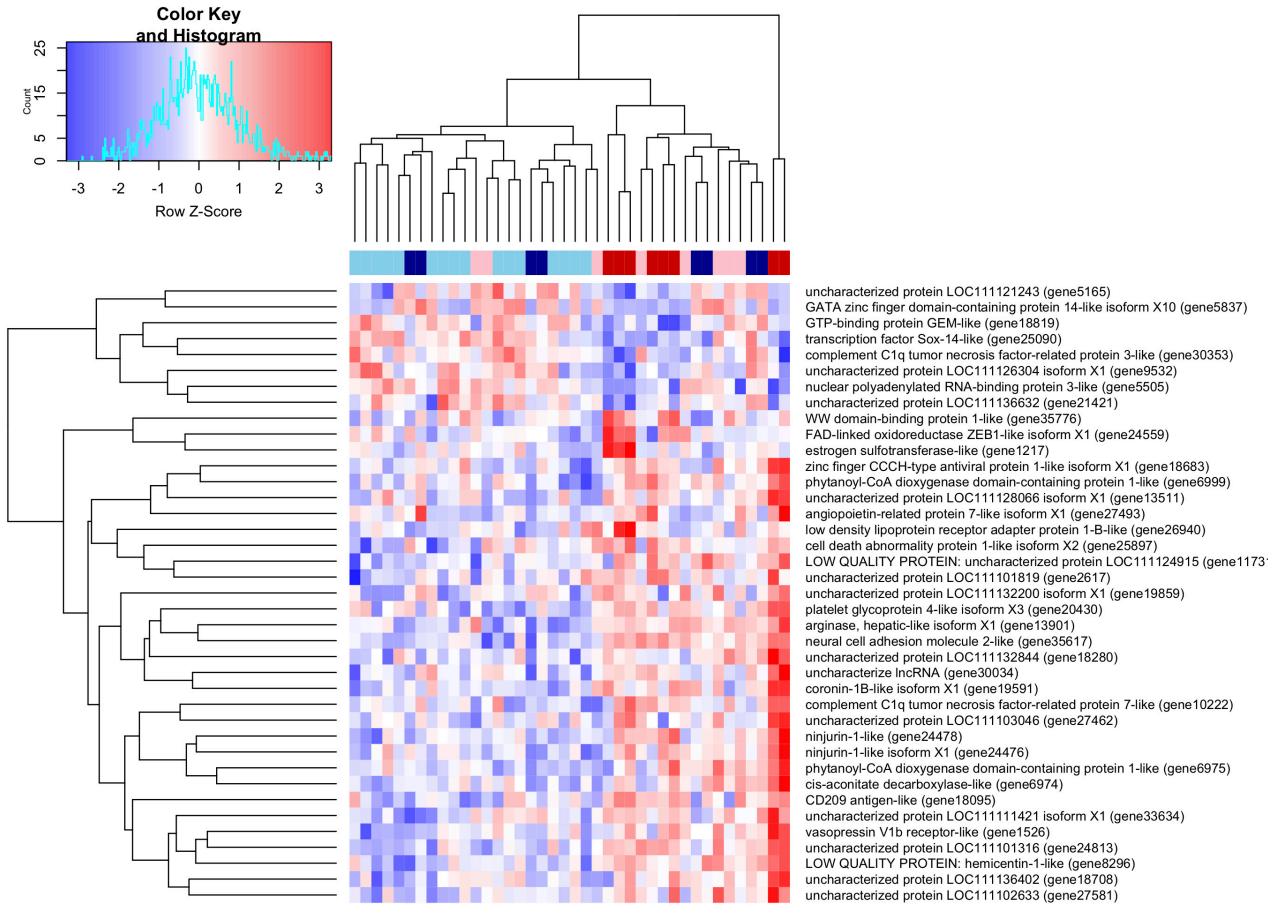

FIGURE 2 | Heatmap and hierarchical clustering of the 39 differentially expressed transcripts between heavily and lightly infected individuals. Top color-coded bar provides individual infection levels with: light blue = very-light infection, blue = light infection, pink = moderate infection, and red = moderate-heavy infection.

infection intensity (**Figure 3A**). Below we discuss the significance of module pink as this module was the only one significantly associated with infection.

Module Pink

Module Pink was comprised of 385 transcripts and was significantly associated with increased intensities of dermo infection. These genes showed a positive correlation between dermo infection and expression levels with the highest infection group showing the strongest association with the module (**Figure 3B**). Of the 24 genes with the highest module membership scores (KmE > 0.75), 2 have been identified in other studies as being involved in immunity in oysters (Wang et al., 2010; Li et al., 2017). In addition, module pink was found to also contain isoform 1 of the ninjurin-1-like gene that was also identified as differentially expressed in the pairwise comparison. Functional enrichment of this module identified enrichment of *supramolecular fiber organization*, *intracellular*, and *cellular carbohydrate metabolic process*. Comparing the list of genes in module Pink and genes identified as differentially expressed in Proestou and Sullivan (2020) identified 16 genes in both datasets. These genes included two isoforms of a multimerin-2-like gene, a calmodulin-2/4-like gene, a HSP70 12A-like gene, and a proline-rich transmembrane protein. This module was also found to have significant GO enrichment for 8 MF terms, 13 BP terms, and 8 CC terms (**Figure 3C**).

Changes in DNA Methylation and Gene Expression

We examined the relationship between gene expression and methylation for gene promoters (2 kb up-stream of first exon), gene bodies, downstream regions (2 kb down stream of last exon), and all intragenic regions combined (e.g., region covered by promoter, gene body, and downstream region). After breaking the expression into deciles, we used a Kruskal–Wallis test to compare mean methylation of each decile. This analysis identified a near-significant association between increasing expression and increased promoter methylation (p-value = 0.065), a significant positive interaction association between expression and gene body methylation (p-value $< 2.2e^{-16}$; **Figure 4A**), and no interaction association between expression and downstream methylation (p-value = 0.11). We also explored the relationship between the mean methylation and the coefficient of gene expression variation for each gene calculated across all samples.

TABLE 3 | Top enriched GO terms for each GO from genes that were differentially expressed between the moderate-heavy and very-light infection intensities.

GO category	GO term	GO ID	Percentage of reference	Up/down-regulated	Adjusted *P*-value
MF	Structural molecule activity	GO:0005198	39.41	Down	4.30E-08
MF	Structural constituent of ribosome	GO:0003735	39.71	Down	1.20E-07
MF	G protein-coupled receptor activity	GO:0004930	39.25	Up	0.012
BP	Macromolecule biosynthetic process	GO:0034645; GO:0009059	40.61	Down	7.07E-08
BP	Peptide metabolic process	GO:0006518	40.22	Down	1.02E-06
BP	Ribonucleoprotein complex biogenesis	GO:0006412;GO:0043043; GO:0043604; GO:0042254;GO:0022613; GO:0044085	38.54	Down	6.32E-06
BP	Cellular component organization or biogenesis	GO:0071840	38.83	Down	0.0042
CC	Ribonucleoprotein complex	GO:1990904	38.61	Down	4.17E-06
CC	Intracellular non-membrane-bounded organelle	GO:0043232; GO:0043228	37.59	Down	6.92E-05
CC	Ribosome	GO:0005840	38.32	Down	8.21E-05

All but one ontology was found to be enriched among downregulated transcripts in the moderate-heavily infected individuals. Percent of reference shows the number of genes identified as enriched when compared to the total number of genes for that GO term in the background reference list.

This analysis identified a significant relationship between decreasing methylation and increasing variation in gene expression (p-value $< 2.2e^{-16}$; **Figure 4B**). However, there was only significant overlap between 2 DMRs and 2 DEGs and a Fisher's Exact test revealed no significant overlap between differential expression and differential methylation (p-value > 0.05).

DISCUSSION

Our study described how *P. marinus* infection intensities influence DNA methylation and gene expression in the eastern oyster *C. virginica*. Through a combination of reduced representation DNA methylation sequencing and 3′-RNA sequencing (TAGseq) we identified significant changes in DNA methylation and subtle changes in gene expression that support previous findings of transcriptomic responses to infection and confirms the relationship between percent DNA methylation and the magnitude and variation in gene expression. The ability to assess these changes across multiple individuals ($n = 40$) strengthened these observations and encourages the use of gene body percent methylation as a proxy for expression and reinforces a potential role for plasticity. However, this study did not find compelling evidence for a relationship between differential methylation and differential expression. This lack of overlap suggests that the majority of changes in DNA methylation in response to infection might occur at any level of infection (i.e., all individuals are exhibiting abroad infection methylome); or, that these changes in DNA methylation are only necessary for acute responses that gradually return to either a seasonally or environmentally responsive methylation pattern. The lack of evidence for this direct connection may derive from the limited knowledge of when infection was initiated, and mechanisms governing changes to gene body methylation. These data suggest much of the observed variation in methylation does not reliably predict the direction of differential gene expression. This observation however, may also be a reflection of the TAGseq approach that is unable to identify changes in splice variant expression. It is therefore quite possible that the changes in DNA methylation are not associated with changes in expression at the gene level, but these changes could be influencing expression at the isoform level.

Changes in DNA Methylation in Response to *P. marinus* Infection

When we then look at the ontologies enriched in the genes that were differentially methylated between the moderate-heavy vs very-light infection categories, we see the regions that were hypomethylated in more heavily infected individuals were enriched for immune response genes, oxidative stress genes, and enzyme regulator activity. The hypomethylation of these regions may increase the plasticity of these genes given that lower methylation was also associated with greater variability in expression in our genome-wide analysis. That this occurs as a function of infection provides some evidence that the plasticity of these genes is being promoted. In contrast, regions hypermethylated in infected individuals were enriched for broad organizational categories associated with cellular structure and replication. If hypermethylation leads to canalization of expression, then it is possible that the increase in percent methylation of the gene bodies reinforces the stability of expression among these genes that may otherwise be altered by the activation of immune responses. The hypomethylation in heavily infected individuals of genes involved in apoptosis (caspase-8), pathogen clearance (C1q tumor necrosis factor-related protein 4), and molecular chaperones (HSP 70 12A-like), suggests that moderate-heavy infections may be promoting higher plasticity of immune response genes (de Lorgeril et al., 2011; Wang et al., 2018). These potential roles are still largely based on the hypothesis that large changes in DNA methylation will drive phenotypic responses. As this still remains untested in

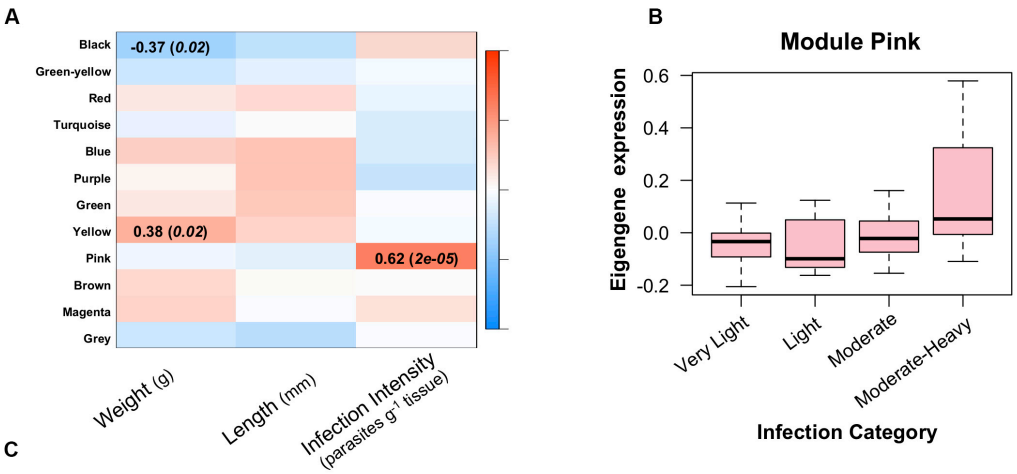

C

GO Category	GO Term	GO ID	% of Reference	Adjusted P-value
MF	Cysteine-type endopeptidase inhibitor	GO:0004869	28.6% (2/7)	0.009
MF	Carbohydrate kinase	GO:0019200	33.3% (2/6)	0.003
BP	Supramolecular fiber organization	GO:0007015 GO:0097435	27.27% (6/22)	<0.0001
BP	Cellular carbohydrate metabolic process	GO:0044262	20.83% (5/24)	<0.0001
BP	Small GTPase mediated signal transduction	GO:0007264	14.29% (6/42)	0.003
CC	Proton-transporting C-type ATPase	GO:0033179	40% (2/5)	<0.0001
CC	Vacuolar part	GO:0044437	60% (3/5)	<0.0001

FIGURE 3 | (A) Weighted Gene Correlated Network Analysis, showing significant relationships between module eigengenes (rows) and oyster traits (columns) in which the color scale (red-blue) represents the strength of the correlation (1 to −1). Only modules with significant correlations to one of the traits are listed. **(B)** Mean eigengene expression levels for genes in module pink across the four infection categories, showing increase expression of module pink among the moderate-heavy infected individuals. **(C)** Enriched gene ontology terms for genes in module pink. Percent of reference shows the number of genes identified as enriched when compared to the total number of genes for that GO term in the background reference list.

bivalves, the community would greatly benefit from controlled studies investigating changes in DNA methylation across time in the same individuals.

Changes in Gene Expression in Response to *P. marinus* Infection Intensity

Differential gene expression analysis identified only 39 genes that showed differential expression between the moderate-heavy (>100,000 parasites g^{-1}) and very-light infected (≤1,000 parasites g^{-1}) individuals (**Figure 2**). This low level of differential gene expression is comparable to the dampened response (21 genes DEG) observed in a dermo resistant family when measured 28-days post-exposure in a controlled experiment (Proestou and Sullivan, 2020). The genes that were differentially expressed in both studies (day 28; Proestou and Sullivan, 2020) included 2 forms of the complement C1q tumor necrosis factor (protein 6-like and protein 7-like) and a nuclear polyadenylated RNA-binding protein 3-like. The fact that these two datasets provide similar findings of a small number of genes being differentially expressed suggests two major takeaways; (1) that the individuals observed in this study were likely suffering from long-term infections of *P. marinus*; and, (2) that the shared differential expression of genes associated with tumor necrosis factors (complement system C1q) means these genes in particular are good candidates for further investigation as potential markers of disease resistance. Assuming that the individuals were suffering from long-term infections is consistent with other observed infection rates at this out-plant site (La Peyre et al., 2018). For the genes identified by both our study and the previous controlled exposure (complement C1q tumor necrosis factor-related protein 7-like and multimerin-2-like) we see an approximate sixfold increase in expression between the moderate-heavy and very-light infection categories. The role of these genes in immune responses is further supported by recent assessments of the functional role of these gene families in bivalve innate immunity (Gerdol et al., 2019). We also observed two versions of a ninjurin

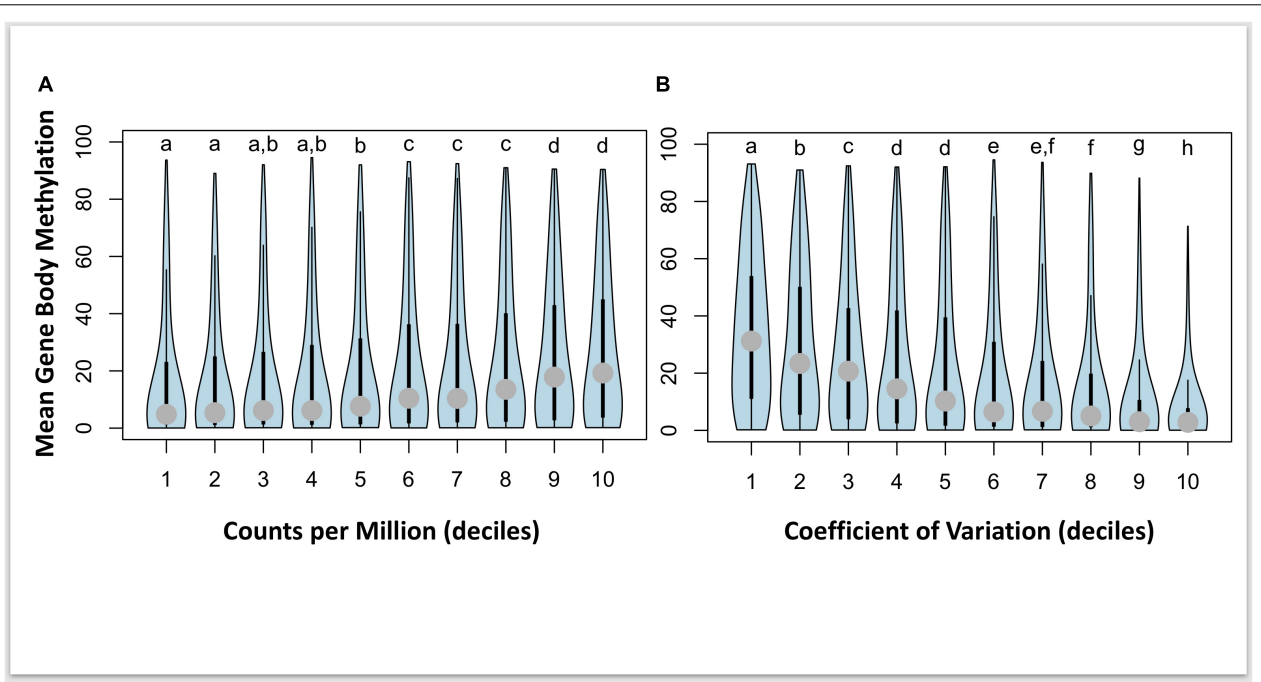

FIGURE 4 | Violin plots of interaction between gene body methylation and gene expression for 5,295 genes with both gene body methylation and expression data. Panel **(A)** plots mean methylation vs normalized counts per million (CPM) expression levels broken into 10 equal sized deciles, and panel **(B)** plots mean methylation vs the coefficient of variation (CV) in expression also broken into 10 equal sized deciles. Letters represent significant differences in mean methylation between deciles calculated separately for CPM and CV of expression.

1-like gene that were both up-regulated in the moderate-heavy infected individuals. Ninjurin-like genes have been found to be upregulated in Pacific Blue Shrimp (*Litopenaeus stylirostris*) that survive infection with *Vibrio penaeicidia* (de Lorgeril et al., 2005). We also found strong upregulation of two forms of a phytanoyl-CoA dioxygenase domain-containing protein 1-like that is putatively involved in peroxisomal lipid metabolism, a potential signal of a prolonged immune response in Manila clams (*Venerupis philippinarum*) responding to *Perkinsus olseni* (Romero et al., 2015). Together, these differential expression data highlight potential gene targets for future selective breeding programs aimed at increasing disease resistance.

WGCNA Module Pink Shows Responses to *P. marinus* Infection Intensity

WGCNA identified 1 module that was significantly correlated with dermo infection (module pink). Comparing the genes in module pink with the results from Proestou and Sullivan (2020) found 18 genes that were identified as DE after 28 days of infection in the dermo susceptible group and 3 genes identified as DE after 28 days in the dermo resistant group in their study. Of these genes the multimerin-2-like gene appears to be associated with angiogenesis and tumor formation (Khan et al., 2017). The positive association of infection of this gene within module Pink may suggest a role of angiogenesis in healing tissues degraded by *P. marinus* secreted proteases (La Peyre et al., 1995). In addition, multimerin-2-like genes have been proposed to have similar domains to complement component C1q genes (Gerdol et al., 2019) that were significantly differentially expressed in the above pairwise analysis of gene expression. In addition, two genes within this module, *Thymosin beta-4* and *kelch-like protein*, have been associated with immune defense against pathogens, *Thymosin beta-4* is also involved in antibacterial activity in *C. gigas* (Nam et al., 2015) and was found to facilitate the clearance of *Vibrio alginolyticus* in *C. hongkongensi* (Li et al., 2017). *Kelch-like proteins* have also been shown to be differentially regulated in *C. virginica* when challenged with dermo (Wang et al., 2010). Our results show that both of these genes are up-regulated as *P. marinus* infection intensity increases. These findings suggest a potential role for both genes in the immune response of *C. virginica* infected with dermo. However, further studies are needed to clarify the role these genes play in defending against dermo infection in oysters. This overlap between groups further supports the module pink as a gene network involved in immune responses and provides additional gene targets for better understanding the variability in susceptibility to *P. marinus* across oyster families. These results also further support the use of weighted gene co-expression network analysis for exploring genomic patterns of expression for disease resistance in marine invertebrates.

Differential Methylation and Differential Expression

Global levels of DNA methylation across gene features revealed some unexpected associations, with limited support for a role of methylation among promoter and downstream regions on gene expression levels. Previous research in the Pacific oyster has

found evidence for a putative role of promoter methylation in regulating gene expression during development (Rivière et al., 2013; Rivière, 2014). In our study, we tested this directly and found a nearly significant association (p-value = 0.065) between gene expression and mean promoter methylation. This lack of significant association is surprising, and it is possible that these differences in observations maybe associated with sampling during development (Rivière et al., 2013) or that only some genes are influenced by promoter methylation leading to a nearly significant result. Other more recent studies have reported that methylation increases at the start of the gene body and not upstream in promoter regions (Song et al., 2017). Rather, gene body methylation showed a strong positive correlation with gene expression (**Figure 4**), a finding that has been previously reported in the Pacific oyster (Gavery and Roberts, 2013; Olson and Roberts, 2014). In our study we found that genes with higher mean methylation have higher overall expression and a lower coefficient of variation of expression. When comparing mean methylation with gene expression, we found that there were four categories (**Figure 4A**) of mean methylation associated with increasing gene expression, but, eight categories (**Figure 4B**) of mean methylation associated with increasing variation in expression. This suggests that mean methylation is a better predictor of gene variation than it is of the magnitude of gene expression. These results align well with previous research in Pacific oyster where it has been proposed that higher levels of gene body methylation are associated with constitutively expressed genes while lower levels of gene body methylation are associated with "environmentally responsive" gene categories (Roberts and Gavery, 2012; Song et al., 2017). As such, it is plausible that genes showing a decrease in gene body methylation (hypomethylated) are modified in a manner that may lead to an increase in plasticity of that gene. This potential increase in plasticity will require additional studies, ideally consisting of time-course observations of a small number of individuals in order to determine if an environmentally induced change in methylation will lead to future changes in the plasticity of that gene. In addition, future studies should further investigate the role of differential methylation on alternative splicing events. Regardless, these data suggest a relatively minor role of differential DNA methylation on observed differences in gene expression among individuals experiencing chronic exposure to infections.

CONCLUSION

This study sought to understand how chronic exposure to sub-lethal infections with the protistan parasite *P. marinus* influenced DNA methylation and gene expression in eastern oysters. Our results have confirmed a relationship between DNA methylation and gene expression such that lower levels of DNA methylation are found among genes with higher variations in expression, while highly methylated genes are found to have higher but less variable constitutive levels of expression. Genes with low gene body methylation included those involved in immune system process and enzyme regulator activity. Gene expression analyses found a limited response to infection, similar to the differential expression levels seen among dermo resistant families after 28 days of exposure (Proestou and Sullivan, 2020). The concordant differential expression results between ours and this previous study for C1q tumor necrosis factor genes suggests additional studies should explore the function of these genes in infection resistance. Finally, the significant but limited overlap in genes showing differential methylation and differential expression is a potential indicator of a limited influence of changes in methylation on changes in expression.

DATA AVAILABILITY STATEMENT

The datasets generated for this study can be found in the NCBI SRA database under BioProject PRJNA604121.

AUTHOR CONTRIBUTIONS

MK and JL conceived of and designed the outplant study. KJ, MK, JL, SC, and KS sampled the animals for this study. SC and JL measured infection intensities. KJ prepared RRBS libraries and performed differential methylation analysis. KS and KJ analyzed the transcriptomic data and wrote the manuscript with input from SC, JL, and MK. All authors contributed to the article and approved the submitted version.

FUNDING

This research was supported by NSF-BioOCE 1731710 to MK and JL, Louisiana Sea Grant award NA14OAR4170099 to MK and JL, and the Alfred P. Sloan Foundation research fellowship awarded to MK. During the project, KJ was supported by an NSF Postdoctoral Fellowship in Biology under Grant No. 1711319; and, KS was supported by an NSF Graduate Research Fellowship under Grant No. 00001414. Portions of this research were conducted with high performance computing resources provided by Louisiana State University (http://www.hpc.lsu.edu).

ACKNOWLEDGMENTS

We thank the Louisiana Department of Fisheries and Wildlife, Dr. John Supan, and Dr. Brian Callam for collecting and spawning the oysters used in this study. We would also like to thank Bennett Thomas and Michelle Gautreaux for their assistance in RNA extractions, Joanna Griffiths for feedback on data analysis. Finally, we thank Alicia Reigel and Megan Guidry for assistance in sampling the oysters used in this study.

SUPPLEMENTARY MATERIAL

The Supplementary Material for this article can be found online at: https://www.frontiersin.org/articles/10.3389/fmars.2020.00598/full#supplementary-material

REFERENCES

Akalin, A., Kormaksson, M., Li, S., Garrett-Bakelman, F. E., Figueroa, M. E., Melnick, A., et al. (2012). MethylKit: a comprehensive R package for the analysis of genome-wide DNA methylation profiles. *Genome Biol.* 13, R87–R87. doi: 10.1186/gb-2012-13-10-r87

Alvarez, M., Schrey, A. W., and Richards, C. L. (2015). Ten years of transcriptomics in wild populations: what have we learned about their ecology and evolution? *Mol. Ecol.* 24, 710–725. doi: 10.1111/mec.13055

Anders, S., Pyl, P. T., and Huber, W. (2015). HTSeq–a Python framework to work with high-throughput sequencing data. *Bioinformatics* 31, 166–169. doi: 10.1093/bioinformatics/btu638

Benjamini, Y., and Hochberg, Y. (1995). Controlling the false discovery rate: a practical and powerful approach to multiple testing. *J. R. Stat. Soc. Ser. B* 57, 289–300. doi: 10.1111/j.2517-6161.1995.tb02031.x

Bolger, A. M., Lohse, M., and Usadel, B. (2014). Trimmomatic: a flexible trimmer for Illumina sequence data. *Bioinformatics* 30, 2114–2120. doi: 10.1093/bioinformatics/btu170

Casas, S., Walton, W., Chaplin, G., Rickards, S., Supan, J., and La Peyre, J. (2017). Performance of oysters selected for dermo resistance compared to wild oysters in northern Gulf of Mexico estuaries. *Aquac. Environ. Interact.* 9, 169–180. doi: 10.3354/aei00222

Clark, M. S., Thorne, M. A. S., King, M., Hipperson, H., Hoffman, J. I., and Peck, L. S. (2018). Life in the intertidal: cellular responses, methylation and epigenetics. *Funct. Ecol.* 32, 1982–1994. doi: 10.1111/1365-2435.13077

de Lorgeril, J., Saulnier, D., Janech, M. G., Gueguen, Y., and Bachere, E. (2005). Identification of genes that are differentially expressed in hemocytes of the Pacific blue shrimp (*Litopenaeus stylirostris*) surviving an infection with *Vibrio penaeicida*. *Physiol. Genom.* 21, 174–183. doi: 10.1152/physiolgenomics.00281.2004

de Lorgeril, J., Zenagui, R., Rosa, R. D., Piquemal, D., and Bachère, E. (2011). Whole transcriptome profiling of successful immune response to *Vibrio* infections in the oyster *Crassostrea gigas* by digital gene expression analysis. *PLoS One* 6:e23142. doi: 10.1371/journal.pone.0023142

De Wit, P., Durland, E., Ventura, A., and Langdon, C. J. (2018). Gene expression correlated with delay in shell formation in larval Pacific oysters (*Crassostrea gigas*) exposed to experimental ocean acidification provides insights into shell formation mechanisms. *BMC Genom.* 19:160. doi: 10.1186/s12864-018-4519-y

Dixon, G. B., Bay, L. K., and Matz, M. V. (2014). Bimodal signatures of germline methylation are linked with gene expression plasticity in the coral *Acropora millepora*. *BMC Genom.* 15:1109. doi: 10.1186/1471-2164-15-1109

Dobin, A., Davis, C. A., Schlesinger, F., Drenkow, J., Zaleski, C., Jha, S., et al. (2012). STAR: ultrafast universal RNA-seq aligner. *Bioinformatics* 29, 15–21. doi: 10.1093/bioinformatics/bts635

Eirin-Lopez, J. M., and Putnam, H. M. (2019). Marine environmental epigenetics. *Annu. Rev. Mar. Sci.* 11, 335–368. doi: 10.1146/annurev-marine-010318-095114

Gavery, M. R., and Roberts, S. B. (2013). Predominant intragenic methylation is associated with gene expression characteristics in a bivalve mollusc. *PeerJ* 1:e215. doi: 10.7717/peerj.215

Gavery, M. R., and Roberts, S. B. (2017). Epigenetic considerations in aquaculture. *PeerJ* 5:e4147. doi: 10.7717/peerj.4147

Gerdol, M., Greco, S., and Pallavicini, A. (2019). Extensive tandem duplication events drive the expansion of the C1q-domain-containing gene family in bivalves. *Mar. Drugs* 17:583. doi: 10.3390/md17100583

Glenn, T. C., Nilsen, R. A., Kieran, T. J., Sanders, J. G., Bayona-Vásquez, N. J., Finger, J. W., et al. (2019). Adapterama I: universal stubs and primers for 384 unique dual-indexed or 147,456 combinatorially-indexed Illumina libraries (iTru & iNext). *PeerJ* 7:e7755. doi: 10.7717/peerj.7755

Gómez-Chiarri, M., Warren, W. C., Guo, X., and Proestou, D. (2015). Developing tools for the study of molluscan immunity: the sequencing of the genome of the eastern oyster, *Crassostrea virginica*. *Fish Shellf. Immunol.* 46, 2–4. doi: 10.1016/j.fsi.2015.05.004

Hawes, N. A., Fidler, A. E., Tremblay, L. A., Pochon, X., Dunphy, B. J., and Smith, K. F. (2018). Understanding the role of DNA methylation in successful biological invasions: a review. *Biol. Invasions* 20, 2285–2300. doi: 10.1007/s10530-018-1703-6

Herman, J. J., and Sultan, S. E. (2016). DNA methylation mediates genetic variation for adaptive transgenerational plasticity. *Proc. R. Soc. B Biol. Sci.* 283:20160988. doi: 10.1098/rspb.2016.0988

Johnson, K. M., and Kelly, M. W. (2020). Population epigenetic divergence exceeds genetic divergence in the Eastern oyster *Crassostrea virginica* in the Northern Gulf of Mexico. *Evolut. Appl.* 13, 945–959. doi: 10.1111/eva.12912

Jones, H. R., Johnson, K. M., and Kelly, M. W. (2019). Synergistic effects of temperature and salinity on the gene expression and physiology of *Crassostrea virginica*. *Integr. Comparat. Biol.* 59, 306–319. doi: 10.1093/icb/icz035

Kappeler, L., and Meaney, M. J. (2010). Epigenetics and parental effects. *Bioessays* 32, 818–827. doi: 10.1002/bies.201000015

Khan, K., Naylor, A., Khan, A., and Mohammed, F. (2017). Multimerin-2 is a ligand for group 14 family C-type lectins CLEC14A, CD93 and CD248 spanning the endothelial pericyte interface. *Oncogene* 36, 6097–6108. doi: 10.1038/onc.2017.214

Krueger, F., and Andrews, S. R. (2011). Bismark: a flexible aligner and methylation caller for Bisulfite-Seq applications. *Bioinformatics* 27, 1571–1572. doi: 10.1093/bioinformatics/btr167

La Peyre, J. F., Casas, S. M., Richards, M., Xu, W., and Xue, Q. G. (2019). Testing plasma subtilisin inhibitory activity as a selective marker for dermo resistance in eastern oysters. *Dis. Aquat. Organ.* 133, 127–139. doi: 10.3354/dao03344

La Peyre, J. F., Casas, S. M., and Supan, J. E. (2018). Effects of controlled air exposure on the survival, growth, condition, pathogen loads and refrigerated shelf life of eastern oyster. *Aquac. Res.* 49, 19–29. doi: 10.1111/are.13427

La Peyre, J. F., Schafhauser, D. Y., Rizkalla, E. H., and Faisal, M. (1995). Production of serine proteases by the oyster pathogen *Perkinsus marinus* (Apicomplexa) in vitro. *J. Eukaryot. Microbiol.* 42, 544–551. doi: 10.1111/j.1550-7408.1995.tb05903.x

Leonhardt, J. M., Casas, S., Supan, J. E., and La Peyre, J. F. (2017). Stock assessment for eastern oyster seed production and field grow-out in Louisiana. *Aquaculture* 466, 9–19. doi: 10.1016/j.aquaculture.2016.09.034

Li, A., Li, L., Song, K., Wang, W., and Zhang, G. (2017). Temperature, energy metabolism, and adaptive divergence in two oyster subspecies. *Ecol. Evol.* 7, 6151–6162. doi: 10.1002/ece3.3085

Mathers, T. C., Mugford, S. T., Percival-Alwyn, L., Chen, Y., Kaithakottil, G., Swarbreck, D., et al. (2019). Sex-specific changes in the aphid DNA methylation landscape. *Mol. Ecol.* 28, 4228–4241. doi: 10.1111/mec.15216

Meyer, E., Aglyamova, G. V., and Matz, M. V. (2011). Profiling gene expression responses of coral larvae (*Acropora millepora*) to elevated temperature and settlement inducers using a novel RNA-Seq procedure. *Mol. Ecol.* 20, 3599–3616.

Moreira, R., Balseiro, P., Planas, J. V., Fuste, B., Beltran, S., Novoa, B., et al. (2012). Transcriptomics of in vitro immune-stimulated hemocytes from the Manila clam *Ruditapes philippinarum* using high-throughput sequencing. *PLoS One* 7:e35009. doi: 10.1371/journal.pone.0035009

Nam, B. H., Seo, J. K., Lee, M. J., Kim, Y. O., Kim, D. G., An, C. M., et al. (2015). Functional analysis of Pacific oyster (*Crassostrea gigas*) β-thymosin: focus on antimicrobial activity. *Fish Shellf. Immunol.* 45, 167–174. doi: 10.1016/j.fsi.2015.03.035

Olson, C. E., and Roberts, S. B. (2014). Genome-wide profiling of DNA methylation and gene expression in *Crassostrea gigas* male gametes. *Front. Physiol.* 5:224. doi: 10.3389/fphys.2014.00224

Proestou, D. A., and Sullivan, M. E. (2020). Variation in global transcriptomic response to *Perkinsus marinus* infection among eastern oyster families highlights potential mechanisms of disease resistance. *Fish Shellf. Immunol.* 96, 141–151. doi: 10.1016/j.fsi.2019.12.001

Putnam, H. M., Davidson, J. M., and Gates, R. D. (2016). Ocean acidification influences host DNA methylation and phenotypic plasticity in environmentally susceptible corals. *Evolut. Appl.* 9, 1165–1178. doi: 10.1111/eva.12408

Renault, T., Faury, N., Barbosa-Solomieu, V., and Moreau, K. (2011). Suppression substractive hybridisation (SSH) and real time PCR reveal differential gene expression in the Pacific cupped oyster, *Crassostrea gigas*, challenged with *Ostreid herpesvirus* 1. *Dev. Comp. Immunol.* 35, 725–735. doi: 10.1016/j.dci.2011.02.004

Rivière, G. (2014). Epigenetic features in the oyster *Crassostrea gigas* suggestive of functionally relevant promoter DNA methylation in invertebrates. *Front. Physiol.* 5:129. doi: 10.3389/fphys.2014.00129

Rivière, G., Wu, G. C., Fellous, A., Goux, D., Sourdaine, P., and Favrel, P. (2013). DNA methylation is crucial for the early development in the Oyster *C. gigas*. *Mar. Biotechnol.* 15, 739–753. doi: 10.1007/s10126-013-9523-2

Roberts, S. B., and Gavery, M. R. (2012). Is there a relationship between DNA methylation and phenotypic plasticity in invertebrates? *Front. Physiol.* 2:116. doi: 10.3389/fphys.2011.00116

Robinson, M. D., and Oshlack, A. (2010). A scaling normalization method for differential expression analysis of RNA-seq data. *Genome Biol.* 11:R25. doi: 10.1186/gb-2010-11-3-r25

Robinson, M. D., McCarthy, D. J., and Smyth, G. K. (2010). edgeR: a Bioconductor package for differential expression analysis of digital gene expression data. *Bioinformatics* 26, 139–140. doi: 10.1093/bioinformatics/btp616

Romero, A., Forn-Cuní, G., Moreira, R., Milan, M., Bargelloni, L., Figueras, A., et al. (2015). An immune-enriched oligo-microarray analysis of gene expression in Manila clam (*Venerupis philippinarum*) haemocytes after a *Perkinsus olseni* challenge. *Fish Shellf. Immunol.* 43, 275–286. doi: 10.1016/j.fsi.2014.12.029

Rosani, U., Varotto, L., Domeneghetti, S., Arcangeli, G., Pallavicini, A., and Venier, P. (2015). Dual analysis of host and pathogen transcriptomes in ostreid herpesvirus 1-positive *Crassostrea gigas*. *Environ. Microbiol.* 17, 4200–4212. doi: 10.1111/1462-2920.12706

Rubi, T. L., Knowles, L. L., and Dantzer, B. (2019). Museum epigenomics: characterizing cytosine methylation in historic museum specimens. *Mol. Ecol. Resour.* 2019, 1–10. doi: 10.1111/1755-0998.13115

Ryu, T., Veilleux, H. D., Donelson, J. M., Munday, P. L., and Ravasi, T. (2018). The epigenetic landscape of transgenerational acclimation to ocean warming. *Nat. Clim. Chang.* 8, 504–509. doi: 10.1038/s41558-018-0159-0

Schmid, M. W., Heichinger, C., Coman Schmid, D., and Grossniklaus, U. (2018). Contribution of epigenetic variation to adaptation in *Arabidopsis*. *Nat. Commun.* 9:4446. doi: 10.1038/s41467-018-06932-5

Song, K., Li, L., and Zhang, G. (2017). The association between DNA methylation and exon expression in the Pacific oyster *Crassostrea gigas*. *PLoS One* 12:e0185224. doi: 10.1371/journal.pone.0185224

Tanguy, A., Guo, X., and Ford, S. E. (2004). Discovery of genes expressed in response to Perkinsus marinus challenge in Eastern (*Crassostrea virginica*) and Pacific (*C. gigas*) oysters. *Gene* 338, 121–131. doi: 10.1016/j.gene.2004.05.019

Van Gurp, T. P., Wagemaker, N. C., Wouters, B., Vergeer, P., Ouborg, J. N., and Verhoeven, K. J. (2016). EpiGBS: reference-free reduced representation bisulfite sequencing. *Nat. Methods* 13, 322–324. doi: 10.1038/nmeth.3763

Wang, L., Song, X., and Song, L. (2018). The oyster immunity. *Dev. Comparat. Immunol.* 80, 99–118. doi: 10.1016/j.dci.2017.05.025

Wang, S., Peatman, E., Liu, H., Bushek, D., Ford, S. E., Kucuktas, H., et al. (2010). Microarray analysis of gene expression in eastern oyster (*Crassostrea virginica*) reveals a novel combination of antimicrobial and oxidative stress host responses after dermo (*Perkinsus marinus*) challenge. *Fish Shellfish Immun.* 29, 921–929. doi: 10.1016/j.fsi.2010.07.035

Weinhold, A. (2018). Transgenerational stress-adaption: an opportunity for ecological epigenetics. *Plant Cell Rep.* 37:3. doi: 10.1007/s00299-017-2216-y

Wright, R. M., Aglyamova, G. V., Meyer, E., and Matz, M. V. (2015). Gene expression associated with white syndromes in a reef building coral, *Acropora hyacinthus*. *BMC Genom.* 16:371. doi: 10.1186/s12864-015-1540-2

Yan, L., Su, J., Wang, Z., Yan, X., Yu, R., Ma, P., et al. (2017). Transcriptomic analysis of *Crassostrea sikamea* × *Crassostrea angulata* hybrids in response to low salinity stress. *PLoS One* 12:e0171483. doi: 10.1371/journal.pone.0171483

Conflict of Interest: The authors declare that the research was conducted in the absence of any commercial or financial relationships that could be construed as a potential conflict of interest.

frontiers in Marine Science

ORIGINAL RESEARCH
published: 30 September 2020
doi: 10.3389/fmars.2020.560424

Genome-Wide DNA Methylation Analysis Reveals a Conserved Epigenetic Response to Seasonal Environmental Variation in the Staghorn Coral *Acropora cervicornis*

*Javier A. Rodríguez-Casariego[1], Alex E. Mercado-Molina[1,2], Daniel Garcia-Souto[3], Ivanna M. Ortiz-Rivera[1,2,4], Christian Lopes[5], Iliana B. Baums[6], Alberto M. Sabat[4] and Jose M. Eirin-Lopez[1]**

[1] Environmental Epigenetics Laboratory, Institute of Environment, Florida International University, Miami, FL, United States, [2] Sociedad Ambiente Marino, San Juan, PR, United States, [3] Genomes and Disease, Centre for Research in Molecular Medicine and Chronic Diseases (CIMUS), Universidad de Santiago de Compostela – IDIS, Santiago de Compostela, Spain, [4] Department of Biology, University of Puerto Rico, San Juan, PR, United States, [5] Seagrass Ecosystems Research Laboratory, Coastlines and Oceans Division, Institute of Environment, Department of Biological Sciences, Florida International University, Miami, FL, United States, [6] Department of Biology, Pennsylvania State University, State College, University Park, PA, United States

Epigenetic modifications such as DNA methylation have been shown to participate in plastic responses to environmental change in a wide range of organisms, including scleractinian corals. Unfortunately, the current understanding of the links between environmental signals, epigenetic modifications, and the subsequent consequences for acclimatory phenotypic changes remain obscure. Such a knowledge gap extends also to the dynamic nature of epigenetic changes, hampering our ability to ascertain the magnitude and extent of these responses under natural conditions. The present work aims to shed light on these subjects by examining temporal changes in genome-wide patterns of DNA methylation in the staghorn coral *Acropora cervicornis* in the island of Culebra, PR. During a 17-month period, a total of 162 polymorphic loci were identified using Methylation-Sensitive Amplified Polymorphism (MSAP). Among them, 83 of these restriction fragments displayed changes in DNA methylation that were significantly correlated to seasonal variation as determined mostly by changes in sea water temperature. Remarkably, the observed time-dependent variation in DNA methylation patterns is consistent across coral genets, coral source sites and site-specific conditions studied. Overall, these results are consistent with a conserved epigenetic response to seasonal environmental variation. These findings highlight the importance of including seasonal variability into experimental designs investigating the role of epigenetic mechanisms such as DNA methylation in responses to stress.

Keywords: staghorn coral, DNA methylation, MSAP, stress response, temperature, seasonality, epigenetics

OPEN ACCESS

Edited by:
Yong Wang,
Institute of Deep-Sea Science and Engineering (CAS), China

Reviewed by:
Alexandre Fellous,
Alfred Wegener Institute Helmholtz Centre for Polar and Marine Research (AWI), Germany
Mikhail V. Matz,
University of Texas at Austin, United States
Hui Huang,
South China Sea Institute of Oceanology (CAS), China

***Correspondence:**
Jose M. Eirin-Lopez
jeirinlo@fiu.edu

Specialty section:
This article was submitted to Marine Molecular Biology and Ecology, a section of the journal Frontiers in Marine Science

Received: *08 May 2020*
Accepted: *07 September 2020*
Published: *30 September 2020*

Citation:
Rodríguez-Casariego JA, Mercado-Molina AE, Garcia-Souto D, Ortiz-Rivera IM, Lopes C, Baums IB, Sabat AM and Eirin-Lopez JM (2020) Genome-Wide DNA Methylation Analysis Reveals a Conserved Epigenetic Response to Seasonal Environmental Variation in the Staghorn Coral Acropora cervicornis. Front. Mar. Sci. 7:560424. doi: 10.3389/fmars.2020.560424

INTRODUCTION

Hermatypic (i.e., reef-building) corals play a critical role as ecosystem foundation species. Hence, it is not surprising that continuous reductions in their populations for the last 30 years have caused the collapse of many coral reef ecosystems worldwide, and a drastic deterioration in the ones still remaining (Pandolfi et al., 2003; Hoegh-Guldberg et al., 2007; Birkeland, 2019). Among the different potential drivers for this decrease, the increase in average temperature in the upper layers of the ocean (Hansen et al., 2012; Abraham et al., 2013) and changes in ocean chemistry (Feely et al., 2009) caused by human-driven global change (Rosenzweig et al., 2008; Hoegh-Guldberg and Bruno, 2010) are considered among the most important factors. It is well known that corals are particularly sensitive to water temperature fluctuations (Cai et al., 2016; Hume et al., 2016), with current conditions provoking frequent bleaching events in reefs worldwide when temperature increases 1–2°C above normal summer maximum (Hoegh-Guldberg, 1999; Hughes et al., 2003). This susceptibility, along with the fast-paced progression of global change has generated concerns about the ability of corals to acclimatize and adapt to these conditions.

Temperature and light represent the main environmental factors responsible for the collapse (i.e., bleaching) of the coral holobiont (the unit formed by the symbiosis between the coral animal and its associated microorganisms, including dinoflagellate algae of the family Symbiodinaceae). In addition, seasonal changes in these parameters also drive subsequent variation in coral physiology (Scheufen et al., 2017). Contrary to the case of random environmental variation, the predictability of seasonal fluctuations can be conducive to the development and inheritance of plastic transcriptional profiles mediating phenotypic responses, regulated by epigenetic mechanisms [e.g., seasonal DNA methylation changes in bivalve mollusks (Suarez-Ulloa et al., 2019), plants (Ito et al., 2019) and birds (Viitaniemi et al., 2019)]. Indeed, seasonality produces dramatic physiological adjustments in corals, including changes in symbiont's abundance and pigmentation (Fitt et al., 2000; Thornhill et al., 2006), modifications of microbial community composition (Sharp et al., 2017), as well as the alteration of transcriptional profiles (Edge et al., 2008; Brady et al., 2011; Parkinson et al., 2018; Brener-Raffalli et al., 2019). On one hand, the different sensitivities to heat stress and bleaching displayed by winter and summer coral phenotypes (Berkelmans and Willis, 1999; Scheufen et al., 2017) seem to support the notion that these changes could prepare corals to respond to increased temperature and light stress during the summer months. On the other hand, recent experiments in *A. cervicornis* have failed to find additional support for this idea (Parkinson et al., 2018). Nevertheless, even if these adjustments were to occur, they may fall short when facing altered seasonal regimes and unprecedented stress events caused by global change. Consequently, understanding the shared mechanisms underlying thermal and seasonal acclimatization in corals will improve our capacity to model coral population trajectories, and enhance coral preconditioning and assisted evolution approaches (van Oppen et al., 2015).

As sessile organisms, corals rely exclusively on phenotypic plasticity to respond to their environment (López-Maury et al., 2008), a response that is largely mediated by the interaction between the coral's genome and intrinsic and extrinsic environmental signals modulating its expression (West-Eberhard, 2003). Although the role of this plasticity is mostly observed during the life of an organism (IntraGenerational Plasticity, IGP), it has been suggested that parents can "prime" their offspring to better respond to changes in their specific environments (InterGenerational Plasticity, ItGP) (e.g., thermal response in fishes; Salinas and Munch, 2012) and even produce phenotypes that will persist for generations even in the absence of the initial stressor triggering that phenotype (TransGenerational Plasticity TGP) (Perez and Lehner, 2019). Based on the current evidence for the inheritance of acquired epigenetic marks, it seems plausible that epigenetic mechanisms play a critical role providing a mechanistic framework for the acquisition and intergenerational inheritance of phenotypes optimized to the prevailing environmental conditions (Vandegehuchte et al., 2009; Navarro-Martín et al., 2011; Marsh and Pasqualone, 2014; Vignet et al., 2015; Eirin-Lopez and Putnam, 2019), increasing the resilience and resistance of corals to global change. However, in order to disentangle the role of epigenetic mechanisms on IGP, ItGP, and TGP, there is an urgent need to better understand how these epigenetic mechanisms interact with environmental factors.

Epigenetic mechanisms display extremely dynamic responses to environmental changes (Cortessis et al., 2012), serving as a "sensory" interface between the environmental condition and the genome function. Therefore, understanding exposure-response relationships of these molecular mechanisms could potentially allow the quantification of the effects of the environment on phenotypic variation (Cortessis et al., 2012; Suarez-Ulloa et al., 2015; Etchegaray and Mostoslavsky, 2016), increasing our capacity to predict population responses after environmental change. While increasing evidence points to a relevant role of DNA methylation and other epigenetic mechanisms in plastic responses to environmental change in corals (Putnam et al., 2016; Dixon et al., 2018; Liew et al., 2018; Dimond and Roberts, 2020) and other marine organisms (Ryu et al., 2018; Eirin-Lopez and Putnam, 2019), there is limited understanding of the factors influencing dynamic epigenetic changes under non-stressed conditions, confounding the ability to determine the magnitude and extent of epigenetic responses under natural conditions (Suarez-Ulloa et al., 2019). In addition, solid baseline data of "natural response" to seasonal and diel cycles in most ecologically important organisms is lacking (Suarez-Ulloa et al., 2019). This gap can be bridged by developing seasonal monitoring of coral epigenetic signatures, helping disentangle the molecular underpinnings of such epigenetic responses, their involvement in seasonal acclimatization, and their capacity to respond to factors driving global change in the Anthropocene. The present work aims to do so by characterizing temporal

Abbreviations: DO, dissolved oxygen; HMM, hemiMethylated target; HPM, hyperMethylated target; ICM, internal cytosine methylation in target; IGP, intraGenerational plasticity; ItGP, interGenerational plasticity; MSAP, methylation-sensitive amplification polymorphism; MSL, methylation-susceptible loci; NML, loci not susceptible to methylation; NMT, non-methylated target; PAR, photosynthetically active radiation; TGP, transGenerational plasticity.

changes in DNA methylation patterns using the staghorn coral *A. cervicornis* as model system.

METHODS

Study Site, Experimental and Sampling Design

A total of $n = 200$ staghorn coral (*Acropora cervicornis*) fragments (naturally generated by hurricanes Irma and Maria between August and October 2017) were collected from 4 reefs around Culebra Island, Puerto Rico (**Figure 1**). Naturally occurring fragments were used to minimize the effect of sampling on standing colonies of *A. cervicornis*. Therefore, sampling effort was not standardized among sites, and analyses on genotypic diversity of the sample pool cannot be extrapolated to compare natural levels of sexual recruitment among sites. Fragments were stabilized by immediate outplanting into two natural reefs located in the Canal Luis Peña No-Take Marine Reserve: Luis Peña (LP: 18°18′45.0″N, 65°20′08.4″W) and Carlos Rosario (CR: 18°19′30.2″N, 65°19′52.7″W) reefs. At the time of outplanting, genotyping information was not available. Thus, in order to homogenize the distribution of putative genets and avoid biases from local adaptation in the site-specific response, fragments from different sources were further subdivided before fixing them to the substrate using nails and plastic ties at two different depths (5 and 15 m). This yielded an equal representation of putative genets at both depths. The outplanting sites were named LP shallow (LPs), LP deep (LPd), CR shallow (CRs), and CR deep (CRd). Coral fragments were organized into 5 × 5 m plots containing 20 fragments per plot, for a total of 5 plots per site ($n = 100$ fragments per site, total = 400 fragments outplanted). The size of outplanted fragments ranged between 10 and 30 cm in length.

The characterization of depth-associated changes in dissolved oxygen, pH, salinity and pressure (tides) was performed by deploying YSI EXO2 multiparameter sondes (YSI, Yellow Springs, OH, United States) and photosynthetically active radiation (PAR) sensors (Sea Bird, Bellevue, WA) at the two studied depths in Luis Peña reef. Sensors were deployed for a month in September 2018 and January 2019 in order to capture summer and winter seasonal peaks. Daily water temperature (3 m below Mean Lower Low Water) records were gathered from NOAA Data Buoy Center, Station CLBP4 located in Culebra, PR, approximately 3.8 and 4 km from LP and CR, respectively (**Figure 1**). Regional light data was obtained from the integration of 25 climatological models (CMIP5 IPCC) for Puerto Rico (San Juan PR, 18°26′24.0″N 66°07′48.0″W).

Tissue samples were clipped from coral fragments using bone cutters at the beginning of the experiment (April 2018), and subsequently stored in 95% non-denatured ethanol for DNA genotyping. Tissue samples were further collected from selected fragments at LP and CR reefs after 3, 5, 6, 9, 12, and 17 months-post-outplanting (hereafter referred to as T + month post outplanting), resampling fragments when possible. Repetitive samples were collected from grown branches, discarding the actively growing tip (generally without symbionts). The selection of specific fragments for sampling was determined based on the

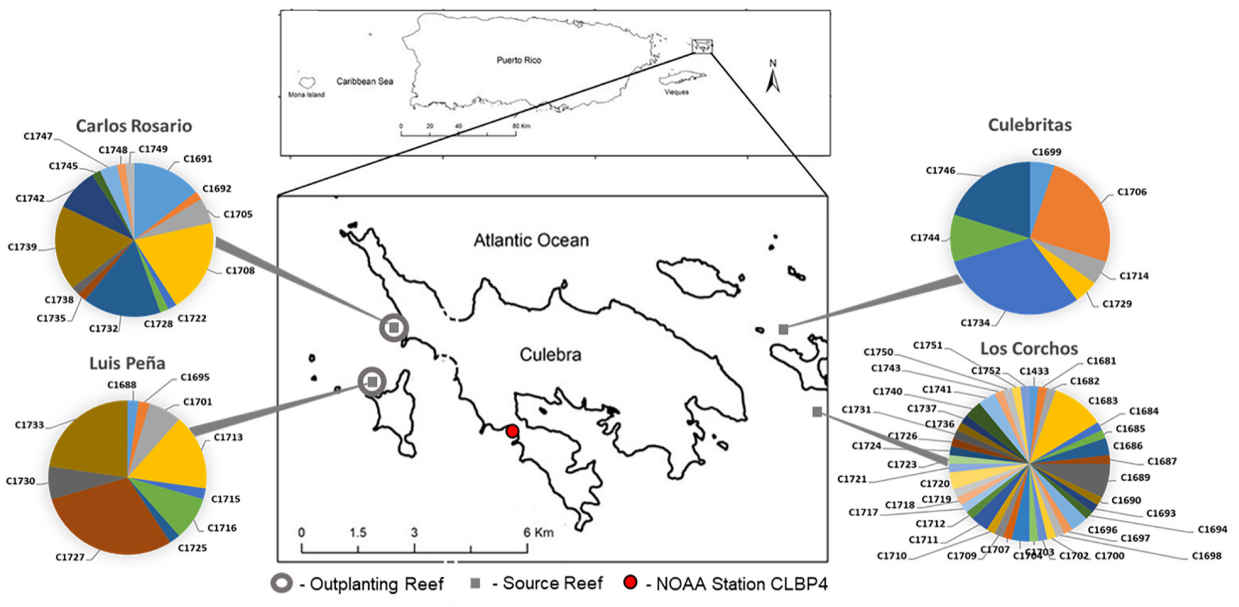

FIGURE 1 | Field experiment locations in Culebra, Puerto Rico. Four source sites are denoted with gray squares, Luis Peña (LP: 18°18′45.0″N, 65°20′08.4″W), Carlos Rosario (CR: 18°19′30.2″N, 65°19′52.7″W), Culebritas (18°19′19.4″N 65°14′14.5″W) and Los Corchos (18°18′33.0″N 65°13′44.3″W). The genotypic composition was obtained using 6 microsatellite loci as in Baums et al. (2005a) and is shown in pie charts. Outplant sites (gray circles) consisted of five 5 m × 5 m plots located at each site at two depths (5 and 15 m). A total of $n = 20$ fragments from each source site were outplanted in each plot for a total of $n = 400$ fragments. Temperature records were gathered from NOAA Data Buoy Center, Station CLBP4 (red circle) located 3.8 and 4 km from LP and CR respectively.

availability of healthy branches not previously disturbed. Coral samples were immediately flash-frozen, shipped on dry ice to Florida International University and stored at −80°C. In order to assess seasonal variation of healthy corals during the study period, only corals that survived the 17-month period and were sampled at least 4 times were included in DNA methylation analysis. This ensured replication at each sampling event. Overall, a total of n = 205 samples from the four outplanting sites were analyzed for DNA methylation (n = 55 for LPs, n = 38 for LPd, n = 64 for CRs, and n = 48 for CRd).

Coral Genotyping and Genomic DNA Isolation

We define a collection of fragments sharing the same multilocus genotype as belonging to the same "genet", and each of the fragments is referred to as a "ramet." Coral host genotyping was based on DNA isolated using a standard phenol-chloroform protocol (Sambrook and Russell, 2006) from the samples collected at the beginning of the experiment. A panel of 6 microsatellite loci was applied (Baums et al., 2005a). Since these markers were demonstrated to be highly heterozygous, the probability of wrongfully identifying ramets as clonemates of the same genet is consequently extremely low (Baums et al., 2005b). Only samples sharing the same alleles at all six loci were classified as ramets of the same genet. The descriptors of coral genotypic structure at the sampled sites, genotypic richness, diversity and evenness were calculated following (Stoddart and Taylor, 1988) and (Baums et al., 2006). Briefly, genotypic richness was calculated as the number of genets (N_g) over the number of colonies sampled (N). Genotypic diversity refers to the diversity of genets in a population. Here, it was calculated as the observed over the expected genotypic diversity (Baums et al., 2006). Observed genotypic diversity (G_o) was calculated as per the equation (Stoddart and Taylor, 1988):

$$G_o = \frac{1}{\sum_i^k g_i^2}$$

where g_i is the relative frequency of each genet. Expected genotypic diversity (Ge) was equal to the total number of colonies analyzed (N), assuming a population with only sexual reproduction. This index of genotypic diversity, therefore, indicates the contribution of sexual reproduction to the population (Baums et al., 2006). Evenness was calculated as the fraction of the observed genotypic diversity (G_o) over the number of genets (N_g).

Coral holobiont's genomic DNA (82.0 ± 41.1 ng/μL, final concentration) was purified from flash-frozen tissue using the Quick DNA/RNA Mini-Prep kit (Zymo Research, Irvine, CA, United States) with some modifications: Briefly, coral fragments were pulverized in liquid nitrogen and approximately 100 mg of the resulting powder was resuspended in 2 mL vials containing 500 mg of Zirconia/Silica beads (0.5 mm diameter) and 1 mL of DNA/RNA Shield (Zymo Research, Irvine, CA, United States). Coral host cells were lysed using two pulses of 30 s in a vortex, in an attempt to leave most of the symbiont cells intact, thus enriching host DNA. However, a significant contribution of symbiont DNA to the final sample was assumed. After centrifugation (12,000 × g for 5 min), the supernatant was carefully transferred to a new tube and DNA isolation continued following the manufacturer's instructions. DNA quality was assessed by gel electrophoresis for integrity and spectrophotometric analysis (NanoVue GE Healthcare, Chicago, IL, United States) for quality as described elsewhere (Rivera-Casas et al., 2017). DNA concentration was measured using a Qubit 2.0 Fluorometer (Thermo Fisher, Waltham, MA, United States) following the instructions provided by the manufacturer. Samples with concentrations under 40 ng/μL or low quality (i.e., ethanol contamination) were processed using a DNA Clean & Concentrator kit (Zymo Research, Irvine, CA, United States) until requirements were met.

Symbiodiniaceae ITS2 Amplicon Sequencing and Analysis

The ITS2 region was sequenced in coral samples in order to assess changes in symbiont community composition throughout the experiment. Accordingly, a total of n = 30 samples, consisting of 10 randomly selected coral fragments from the 4 outplanting and three representative time points (T3, T12 and T17), were used in the analysis. The isolated genomic DNA was quantified using the Qubit 2.0 DNA HS Assay (ThermoFisher, Waltham, MA, United States) and the quality assessed by the Tapestation genomic DNA Assay (Agilent Technologies, Santa Clara, CA, United States). Library preparation and sequencing was performed by Admera Health (South Plainfield, NJ, United States). Briefly, ITS2 spacer regions of the ribosomal DNA of the family Symbiodinaceae were amplified from 50 ng of isolated genomic DNA via PCR, using Symbiodinaceae-specific primers [ITS2alg-F, 5′-GTGAATTGCAGAACTCCGTG-3′; ITS2alg-R, 3′-TTCGTATATTCATTCGCCTCC-5′ (Pochon et al., 2001)] modified to include Illumina® adapters. The resulting libraries were quantified and assessed for quality before sequencing as detailed above, and barcoded for multiplexing using Illumina® 8-nt dual-indices. An equimolar pooling of the libraries was performed based on QC values and sequenced on an Illumina® MiSeq (Illumina, San Diego, CA, United States) with a read length configuration of 2 × 250 for 0.1 M pairs of reads per sample (500K in each direction).

Symbiodinaceae community composition was analyzed using the SymPortal Pipeline (Hume et al., 2019). Briefly, untrimmed demultiplexed forward and reverse sequences (fastq) were submitted directly into SymPortal for quality control and taxonomic assignment as described in Hume et al. (2019). Identified sequence variants per sample was used to characterize ITS2 type profiles (Hume et al., 2019). The abundance of ITS2 type profile and sequencing reads representative of putative Symbiodiniaceae taxa were used to evaluate changes in symbiont communities through time (T3, T12, T17). Differences of ITS2 profiles between collection times was evaluated by Permutational multivariate analysis of variance (PERMANOVA) with the adonis function in vegan (Oksanen et al., 2019), using fragment identity as strata in the model, and performing 9,999 permutations of residuals from Bray-Curtis dissimilarities.

Genome-Wide DNA Methylation Analysis

Genome-wide DNA methylation was assessed on coral host-enriched-DNA samples using an amplified polymorphism approach specific for DNA methylation states (Methylation Sensitive Amplified Polymorphism, MSAP (Reyna-Lopez et al., 1997; Xiong et al., 2013; Covelo-Soto et al., 2015). This method is based on the use of isoesquizomeric endonucleases, *Hpa*II and *Msp*I, with shared sequence targets (CCGG sites) but differential sensitivities to their DNA methylation. More precisely, *Hpa*II cleavage is blocked by either internal cytosine methylation of the target site (i.e., 5′-C^{m}CGG-3′/3′-GG^{m}CC-5′) or its hypermethylation (i.e., 5′-^{m}C^{m}CGG-3′/3′-GG^{m}C^{m}C-5′). *Msp*I, on the other hand, is sensitive to external cytosine methylation, including hemimethylation (i.e., 5′-^{m}CCGG-3′/3′-GGCC-5′) and hypermethylation states. This allows the establishment of global cytosine methylation patterns by comparing both amplified restriction profiles (Díaz-Freije et al., 2014). Accordingly, coral genomic DNA was digested using *Eco*RI/*Hpa*II and *Eco*RI/*Msp*I endonuclease mixes in parallel reactions. In the same step, the resulting fragments were ligated to *Eco*RI and *Hpa*II/*Msp*I adapters (**Table 1**). Digestion-ligation reactions were performed for 2 h at 37°C in a solution consisting of 200 ng DNA, 4 U of *Eco*RI (NEB, Ipswich, MA, United States), 1 U of either *Hpa*II (NEB, Ipswich, MA, United States) or *Msp*I (NEB, Ipswich, MA, United States), 1 U T4 DNA ligase (Thermo Fisher Scientific, Waltham, MA, United States), 1X ligase buffer (Thermo Fisher Scientific, Waltham, MA, United States) and 1X CutSmart Buffer (NEB, Ipswich, MA, United States). The resulting restriction fragments were selectively amplified through two consecutive PCR reactions. First, a pre-selective reaction containing 2 μL of diluted (1:7) restriction-ligation product, 20 pM of each *Hpa*II/*Msp*I and *Eco*RI primers combination (**Table 1**), 1X PCR buffer, 0.5 mM dNTPs (Thermo Fisher Scientific, Waltham, MA, United States), 2.5 mM MgCl2, and 1 U DreamTAQ DNA polymerase (Thermo Fisher Scientific, Waltham, MA, United States). Second, a selective reaction used 0.5 μL of 1:9 of the pre-selective PCR product, 0.83 pM of each labeled selective primer (**Table 1**), 1X PCR buffer, 0.5 mM dNTPs, 2.5 mM $MgCl_2$ and 1 U DreamTaq DNA polymerase. PCR conditions were identical to the original protocol (Reyna-Lopez et al., 1997), and the amplified products (2 per enzyme/sample combination, 4 selective combinations multiplexed, **Table 1**) were diluted to 1:10 for 6-FAM and 1:5 for 6-HEX prior to multiplexing and run on an ABI Prism 310 Genetic Analyzer (Applied Biosystems, Foster City, CA, United States) with a MapMarker 1000 ROX marker at Florida International University's DNA Core facility.

Data and Statistical Analysis

MSAP restriction profiles were scored to a binary matrix for each primer combination with GeneMapper v.3.7 (Applied Biosystems, Foster City, CA, United States), retaining fragments between 50 and 500 bp and above 25 Relative Fluorescent Units for 6-HEX and 50 for 6-FAM. The matrices were filtered utilizing a 5% error rate (loci with one methylation state in more than 95% of the samples) and a 2% occurrence of any DNA methylation state to remove uninformative loci and analyzed using the R-package *msap* (Pérez-Figueroa, 2013). For a given animal, loci were scored according to the presence or absence of *Eco*RI-*Hpa*II and *Eco*RI-*Msp*I bands as either Non-Methylated (NMT, 0/0), Hemimethylated (HMM, 1/0), Internal Cytosine Methylated (ICM, 0/1) or Hypermethylated (HPM, 0/0). Hypermethylation was assumed on 0/0 loci due to the low genetic diversity on our dataset, which comprised the repetitive sampling of ramets of 7 genets. Loci were further classified as susceptible (MSL) or not susceptible to methylation (NML). The resulting data matrix of scored methylation states was subjected to further analysis.

Epigenetic variation on MSL was analyzed with Permutational Multivariate Analysis of Variance [PERMANOVA] (Anderson, 2001), considering genet, outplant site and collection time as grouping variables in the model $genet \times fragment \times time + site$ as implemented on the R-package *vegan* [*adonis* function (Oksanen et al., 2019)]. Fragment identity was included in the

TABLE 1 | Adapters and Primers used for MSAP analysis in *A. cervicornis*.

Step	Adapter/primer	Sequence (5′→ 3′)	Combinations*
Digestion/ligation	*Eco*RI	3′ CTCGTAGACTGCGTACC 5′ 5′ CTGACGCATGGTTAA 3′	DL
	*Hpa*II/*Msp*I	3′ CGACTCAGGACTCAT 5′ 5′ TGAGTCCTGAGTAGCAG 3′	
Pre-selective PCR	*Eco*RI + A	GACTGCGTACCAATTCA	PA
	M/H + T	GATGAGTCTAGAACGGT	
	EcoR1 + C	GACTGCGTACCAATTCC	PB
	M/H + A	GATGAGTCTAGAACGGA	
Selective PCR	SL1-TTG	FAM-GATGAGTCTAGAACGGTTG	SL1
	SL1-TCT	FAM-GATGAGTCTAGAACGGTCT	
	SL2-TCA	FAM-GATGAGTCTAGAACGGTCA	SL2
	SL2-AAC	FAM-GATGAGTCTAGAACGGAAC	
	SL3-TTA	HEX-GATGAGTCTAGAACGGTTA	SL3
	SL3-TAA	HEX-GATGAGTCTAGAACGGTAA	
	SL4-AGT	HEX-GATGAGTCTAGAACGGAGT	SL4
	SL4-ATC	HEX-GATGAGTCTAGAACGGATC	

**Adapters or primers were combined in one PCR reaction for digestion/ligation, pre-selective, and selective combinations.*

model and as a *strata* to assess the effect of repeated measurements. A Euclidean distance matrix was generated with 9,999 permutations. Pairwise PERMANOVA (Martinez-Arbizu, 2019) with Holm's correction (Holm, 1979) was performed to evaluate variables with significant effects on DNA methylation. Statistical significance of each MSL was assessed by means of multiple comparisons between the experimental groups by Fisher's exact tests with Benjamini and Hochberg multi-test corrections (Benjamini and Hochberg, 2000; adjusted $p < 0.05$, pFDR < 0.05), identifying loci with non-random distribution of DNA methylation states for each experimental variable. Using these significant MSL, pairwise distances between all analyzed coral fragments with Gower's Coefficient of Similarity were computed. The resulting distance matrix was clustered with UPGMA (unweighted pair group method with arithmetic mean) and visualized as a heatmap with *ComplexHeatmap* (Gu et al., 2016).

A Discriminant Analysis of Principal Components (DAPC, Pritchard et al., 2000; Jombart et al., 2010; Grünwald and Goss, 2011) was performed to assess the epigenetic discrimination between groups using *adegenet* (Jombart, 2008). The number of principal components (PCs) retained for the analysis was evaluated with two rounds of cross-validation [Xval.dapc function, (Jombart and Collins, 2015)]. All discriminant functions (K-1 = 5) were retained in the analysis. Correlation between the independent variables (Temperature and light) and DAPC coordinates of temporal variation in DNA methylation was evaluated. Appropriate Lag shifts were calculated [*ccf* function, (Brockwell and Davis, 2009)] to determine the cross correlation between each of the univariate series. Next, the lag corrected series (Lag corrected + 1 shift for temperature) were input into a matrix of Pearson's r rank correlation coefficients using *rcorr* in the *Hmisc* library (Harrell and Harrell, 2019).

Non-Metric Multidimensional Scaling Analysis (NMDS) was performed utilizing Gower's distances, and environmental parameters were fitted as vectors in the ordination (*envfit* function) with *vegan* (Oksanen et al., 2019) to represent their effect on DNA methylation. Monthly mean values, maximum, standard deviations and differences for each environmental factor were employed as vectors. For temperature and light irradiance long-term data sets, a coefficient of variation of the previous 3 months (CV3) to each sampling month was calculated and employed as an additional vector to evaluate a possible response to the relative change in the parameter and not the actual magnitude. Significance and coefficient of determination was calculated for each of these parameters.

Fragment Sequencing and Identification

Preselective products from 10 samples with high band representation for each selective (SL1-4) and enzyme (HpaII and MspI) combination were pooled and amplified with non-labeled selective primers. Resulting products ($n = 8$) were cleaned with a DNA Clean & Concentrator kit (Zymo Research, Irvine, CA, United States), quality checked with a TapeStation D1000 ScreenTape (Agilent Technologies Inc., CA, United States) on a Tapestation 4200 system and multiplexed with a Native barcoding expansion kit (EXP-NBD104, Oxford Nanopore Technologies). Libraries for Oxford NanoPore sequencing were constructed with a ligation library kit (SQK-LSK109, Oxford Nanopore Technologies, Oxford, United Kingdom) and sequenced to a total of 20GB on MinION R9.4 flowcells. The resulting sequences were basecalled and demultiplexed with the MinKNOW software, trimmed with Porechop[1] to eliminate PCR adapters, and mapped to the genomes of *A. digitifera* (Shinzato et al., 2011) and *Symbiodinium microadriaticum* (Aranda et al., 2016) using Minimap2 (Li, 2018).

RESULTS

Abiotic Characterization and Seasonality

Hourly data ($n = 824$) was recorded for temperature, photosynthetic active radiation (PAR), dissolved oxygen (DO), and salinity at two sites at a depth of 5 and 15 m (LPs and LPd, respectively) during two monthly deployments to capture peak summer and winter signals in sites representative of studied depths (**Supplementary Table 1**). Greater values (two tailed *t*-test $p < 0.05$) for pH, PAR and Salinity were observed at LPs as opposed to LPd. However, as expected, both depths showed greater values of temperature and PAR as well as lower pH, DO and salinity during the summer (two tailed *t*-test $p < 0.05$). Temperature daily mean for each month was analyzed for seasonality, revealing a trend for the period through 2018 and 2019 (Mann-Kendall trend test $p = 0.007$). This is graphically confirmed (**Supplementary Figure 1**) by applying a moving average to the data set to extract the seasonal component from the trend and error terms assuming an additive model because the variance structure remained homogeneous throughout the periods observed (decompose function in the Stats package R). Solar Radiation is reported as W/m^{-2} with peak values in April and lowest values reported in December.

Genotypic Composition of Source Reefs

A total of $n = 81$ *A. cervicornis* host genets were identified in 186 of the 200 initial fragments analyzed (14 samples failed): 45 from Los Corchos (LC), 15 from Carlos Rosario (CR), 14 from Luis Peña (LP), and 7 from Culebritas (CUL) (**Figure 1**). All genets were exclusive to their corresponding sampling site, and three to four prevalent genets accounted for 67–75% of the collected fragments at each site, with the exception of LC, where most genets had only one or two ramets. The genotypic structure was subsequently described for each site (**Table 2**), resulting in an overall genotypic richness [number of genets (N_g)/number of samples (N)] of 0.38 ± 0.21 for all sites combined. LC showed the highest richness amongst all sampled sites. Genotypic diversity [observed genotypic diversity (G_o)/expected genotypic diversity (G_e)] followed the same pattern with combined values of 0.24 ± 0.16 and 0.47 for LC. For evenness (G_o/N_g) however, both sites in the east of the island (LC and CUL) showed similar values (around 0.68) while the sites on the west were lower (around 0.5).

[1]https://github.com/rrwick/Porechop

TABLE 2 | Genotypic diversity of *A. cervicornis* at source sites around Culebra, PR.

	N	Ng	N_g/N	G_o	G_o/G_e	G_o/N_g
Los Corchos (LC)	60	41	0.683	28	0.467	0.683
Culebrita (CUL)	20	7	0.350	4.762	0.238	0.680
Carlos Rosario (CR)	50	11	0.220	5.438	0.109	0.494
Luis Peña (LP)	56	15	0.268	7.612	0.136	0.507
Average	46.500	18.500	0.380	11.453	0.237	0.591
Std. Dev	18.138	15.351	0.209	11.098	0.163	0.105

N, sample size, N_g, number of genets, G_o, observed genotypic diversity, G_e, expected genotypic diversity.

Symbiodinaceae Community Composition and Dynamic

In order to evaluate symbiotic community dynamics through the duration of the study, ITS2 amplicon sequences for the Symbiodinaceae family were analyzed. The 30 samples generated 5,415,404 sequencing reads, producing 2,707,680 sequences after quality filtering into the SymPortal pipeline (50%). A total of 57 operational taxonomic units were identified from ITS2 sequences, with the majority of filtered ITS2 sequences being of the genus *Symbiodinium* (formerly Clade A), and a minor representation of genuses *Brevolium* (formerly Clade B) and *Cladocopium* (formerly Clade C) (**Supplementary Figure 2**). Four ITS2 type profiles were identified across samples, all uniquely composed by *Symbiodinium* spp. sequences. ITS2 profile shifts were observed in some of the samples. However, no significant dynamic changes were evidenced between collection times (PERMANOVA; F = 0.2552, p = 0.6646; **Supplementary Table 2**).

Global Genome-Wide DNA Methylation Variability

A total of 7 genets were selected among those represented by the transplanted fragments for DNA methylation analyses. Genet selection was based on the number of ramets of each genet surviving the 17-month period, allowing appropriate replication between outplanting sites and source sites. The availability of a minimum of 3 ramets of each genet per outplanting site at the end of the 17-month period were used as criteria for selection. Selected genets were n = 3 from CR (C1708, C1732 and C1739), n = 2 from LP (C1727 and C1733), and n = 2 from CUL (C1706 and C1734), representing most of the highly represented genets at each source site (**Figure 1**). Unfortunately, no genet from LC satisfied the criteria to be included in the DNA methylation analyses.

MSAP analyses were performed to assess changes in whole-genome DNA methylation profiles of corals depending on their outplant site, genet and/or collection time. The four combinations of primers tested yielded a total of n = 199 loci after quality-filtering, among which 192 were categorized as methylation-susceptible loci (MSL, 96%) and the remaining 7 were non-methylated (NML, 4%) loci. Primer combinations SL2 and SL4 (**Table 1**) showed the highest number of methylation-susceptible loci with 93 (46.7%) and 81 (40.7%), respectively. The overall epigenetic diversity within methylation-susceptible loci, based on the occurrence of the different DNA methylation states by means of Shannon's diversity index (SDI), was 0.33 ± 0.22, while non-methylated loci showed a Shannon diversity index of 0.22 ± 0.08. A total of 162 (84%) of the methylation-susceptible loci were characterized as polymorphic, showing at least two occurrences for each DNA methylation state, either NMT, ICM, HMM or HPM. These polymorphic loci were subsequently used for further analyses aimed to describe the influence of collection time, outplant sites, and genet on the DNA methylation patterns.

The results indicate a dynamic fluctuation in coral DNA methylation states over time (**Table 3** and **Supplementary Figure 3**). Accordingly, HPM and NMT trended upward from July 2018 (T3, i.e., 3 months post-outplanting) to April 2019 (T12), then decreased by September 2019 (T17). ICM and HMM showed the opposite trend, with an absolute minimum value by T12 and a subsequent increase by September 2019 (T17). This variation of DNA methylation patterns over time was significant, as revealed by PERMANOVA (**Supplementary Table 3**, F = 4.1524, p < 0.0001). Further *post hoc* analyses (**Table 4**) revealed significantly different DNA methylation patterns between all pairwise sampling time comparisons except for October 2018 with September 2018 (T5-T6, F = 1.6992, p = 0.0994) and October 2018 with Jan 2019 (T6-T9, F = 1.2757, Adjusted p = 0.1782) respectively.

The contribution of genet and outplanting sites to the variability observed in DNA methylation states was also evaluated using PERMANOVA analyses (**Supplementary Table 3**). While no significant differences were observed between outplanting sites (F = 0.8735, p = 0.6637), genets influenced DNA methylation significantly (F = 2.3315, p = 0.0131). Accordingly, *post hoc* analyses (**Table 5**) revealed significant pairwise differences of genet C1739 with C1733 (F = 3.2225, Adjusted p = 0.0084)

TABLE 3 | DNA methylation status of target sequences (percentages) from each time point.

Band pattern (target state)	T3	T5	T6	T9	T12	T17
HPA + /MSP + (Non-methylated)	17.69	15.48	15.75	17.48	17.45	13.49
HPA + /MSP-(Hemimethylated)	10.92	13.15	11.57	9.49	8.64	15.68
HPA-/MSP + (Internal C methylation)	13.39	13.98	13.31	11.45	7.95	15.98
HPA-/MSP-(Hypermethylation)	58.01	57.39	59.38	61.60	65.97	54.85

TABLE 4 | Pairwise PERMANOVA of global DNA methylation patterns between time points.

	T3	T5	T6	T9	T12	T17
T3		**0.0660**	**0.0015**	**0.0015**	**0.0015**	**0.0015**
T5	2.7247		0.0994	**0.0015**	**0.0015**	**0.0015**
T6	5.5726	1.6992		0.1782	**0.0015**	**0.0015**
T9	7.7282	3.5977	1.2757		**0.0015**	**0.0015**
T12	14.6953	9.6050	5.4069	3.4001		**0.0015**
T17	13.3517	9.1919	8.0027	8.4736	16.2329	

Values of F below the diagonal. Adjusted p-values (Holm's method) above the diagonal. Values of p < 0.05 are in bold.

TABLE 5 | Pairwise PERMANOVA of global DNA methylation patterns between coral genets.

	C1706	C1708	C1727	C1732	C1733	C1734	C1739
C1706		0.4536	0.4536	0.2744	0.2744	0.1344	0.2744
C1708	0.9931		0.2744	**0.0494**	0.1837	**0.0440**	0.0765
C1727	1.1813	1.5936		0.1837	0.2744	0.0688	**0.0494**
C1732	1.4882	2.4780	1.9408		0.0765	0.2744	**0.0494**
C1733	1.8353	2.1118	1.7832	2.5051		0.1926	**0.0084**
C1734	1.9702	2.4824	2.2012	1.6745	1.9121		0.0765
C1739	1.7727	2.4298	2.4494	2.5393	3.2224	2.2206	

Values of F below the diagonal. Adjusted p-values (Holm's method) above the diagonal. Values of $p < 0.05$ are in bold.

and marginally significant with C1732 (F = 2.539, Adjusted p = 0.0494) and C1727 (F = 2.449, Adjusted p = 0.0494). Additional marginal significance was found between genets C1732 and C1708 (F = 2.4780, Adjusted p = 0.0494), and between C1734 and C1708 (F = 2.4824, Adjusted p = 0.0440). It is interesting to note that most genet pairs showing significant differences in DNA methylation originated from the same source reefs or from reefs located near each other (i.e., CR and LP), making it less likely that similarities in DNA methylation patterns displayed by most genets were determined by epigenetic memory or local adaptation. Fragment (ramet) identity also had a significant effect on DNA methylation patterns (F = 1.1037, p = 0.0131).

Seasonal Influence on Global DNA Methylation Patterns

Considering the significant fluctuation observed on DNA methylation patterns throughout the studied time series, detailed analyses were performed to ascertain the exact contribution of seasonality to such variation. First, Fisher's exact test analyses were conducted to identify significant MSL, resulting in n = 83 MSL with both significant differences among experimental times (Adjusted $p < 0.05$) and low probability of false positives (pFDR < 0.05). As shown in **Figure 2**, the

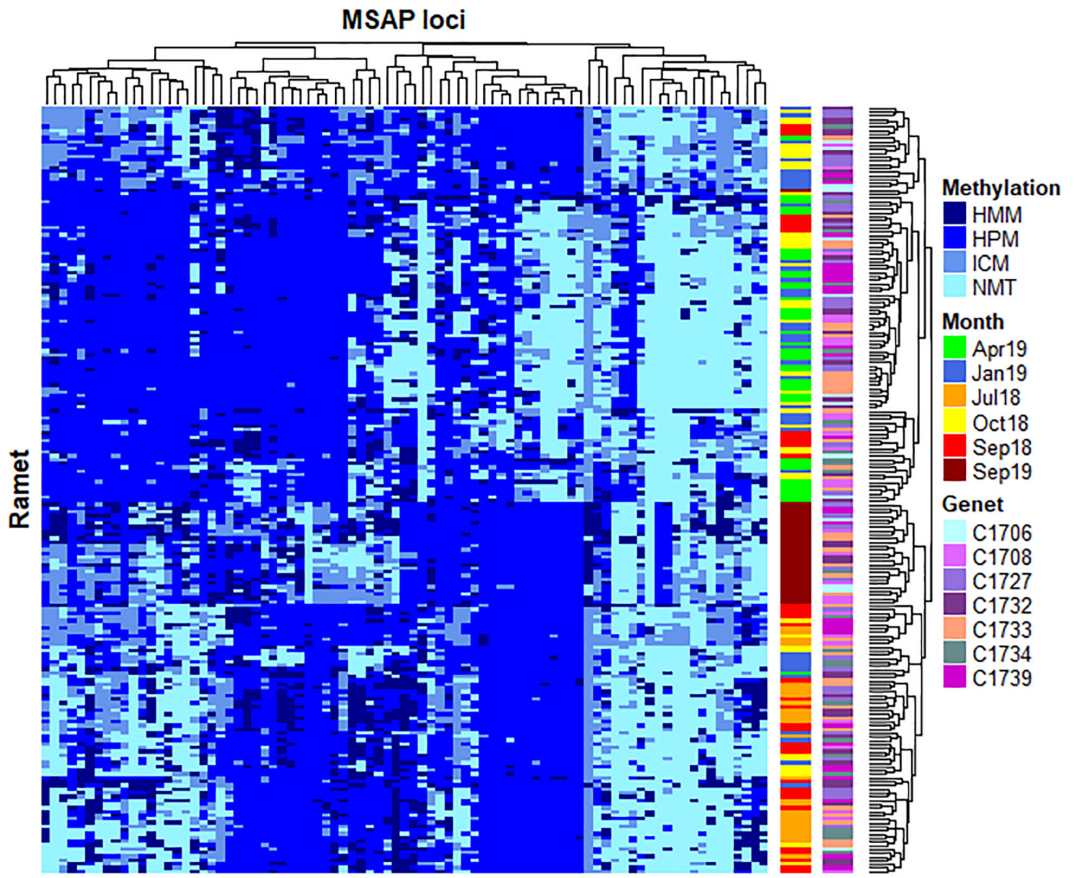

FIGURE 2 | Heatmap representing temporal changes in 83 loci showing a significant non-random distribution of DNA methylation patterns ($p < 0.05$, pFDR < 0.05). Two distinctive clusters separate DNA methylation between cold (April 2019) and warm (July 2018, September 2018 and September 2019) months. Samples from October 2018 and January 2019 show a scattered distribution across these two clusters, while most September 2019 specimens constituted a well-defined sub-cluster within the warm group. No clear clustering is observed for specific genets. Rows (samples) and columns (MSAP loci) were clustered using Gower's Coefficient of Similarity. The methylation status of each locus is indicated in the right margin of the figure: HMM, hemimethylated; HPM, hypermethylated; ICM, internal cytosine methylation; NMT, non-methylated (unmethylated).

clustering analyses of identified loci organized the samples into two major groups based on similar distribution of DNA methylation profiles, discriminating between cold (T12) and warm (T3, T5 and T17) months. Samples from T6 and T9 showed a scattered distribution across these two clusters, while most T17 specimens constituted a well-defined sub-cluster within the warm group.

In order to further assess epigenetic discrimination among sampling times, a Discriminant Analysis of Principal Components (DAPC) analysis was employed (**Figure 3**). As evidenced by the first discriminant function (LD1, *x*-axis, horizontal, **Figures 3A,B**), T17 samples constituted a well-defined cluster with distinct epigenetic signatures respective to the remaining samples. In contrast, the second discriminant function (LD2, *y*-axis, verticals **Figures 3A,C**) split the samples into warm (T3, T5 and T17) and cold (T6, T9 and T12) months, with each of these sampling times forming a discrete cluster. Along this axis, T17 occupied a position between T5 and T6 corresponding to the same period in the previous year. Analysis of the individual

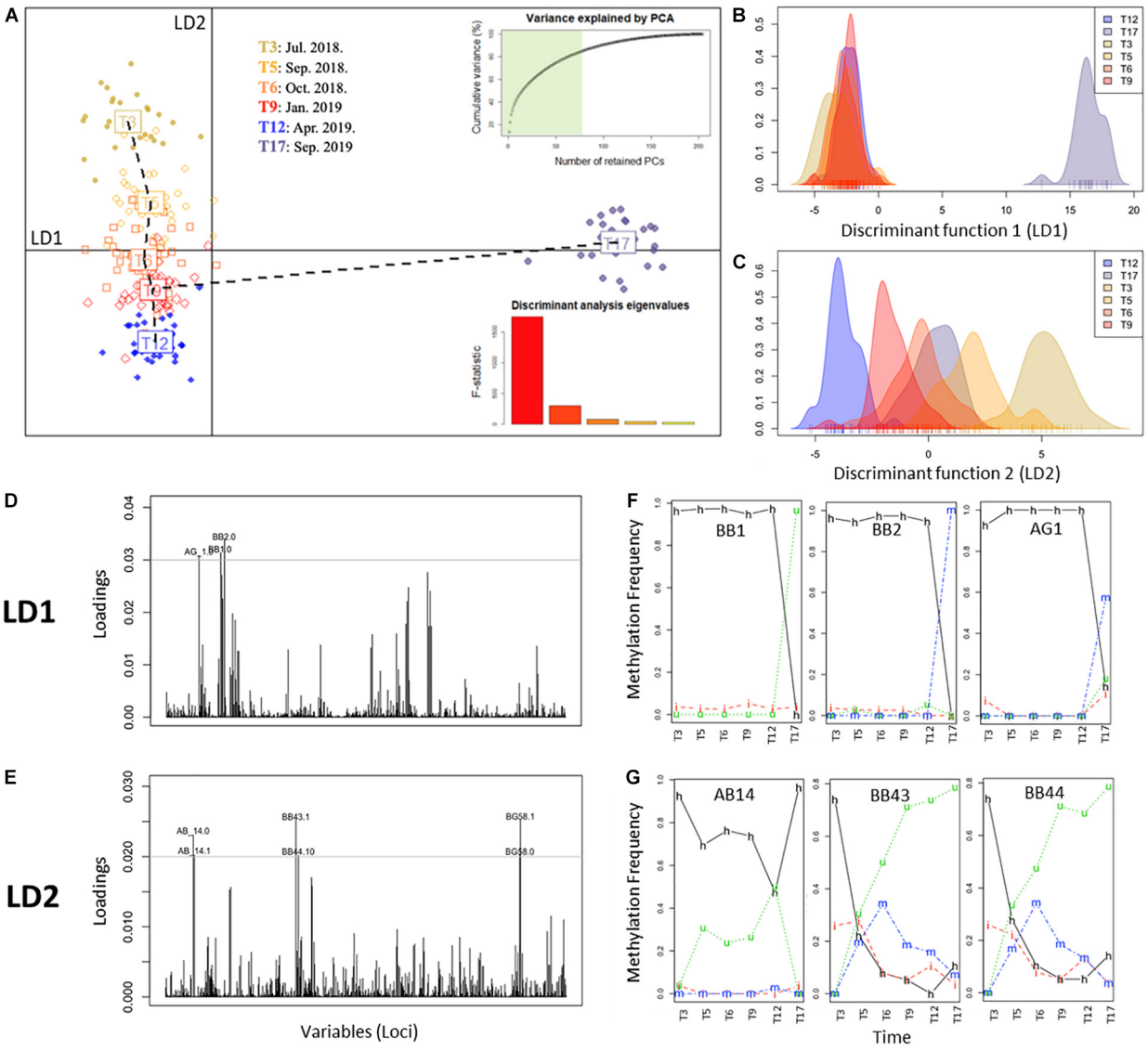

FIGURE 3 | Discriminant analysis of principal components (DAPC) of complete MSAP profiles representing the different groups (i.e., time points). **(A)** Scatterplot of monthly clusters resolved by DAPC. Barplot shows the significance of each of the five discriminant functions retained. In the upper-left corner the variance explained by the 77 PCs retained for the study. Horizontal line: *x*-axis, first discriminant function (LD1) and vertical line: *y*-axis, second discriminant function (LD2). **(B,C)** Density of methylation profiles of each *A. cervicornis* fragment against discriminant function 1 (LD1) and discriminant function 2 (LD2), respectively. **(D,E)** Loading plot of MSAP loci that most contributed to LD1 and LD2 respectively. **(F,G)** Temporal variation of the frequency of each methylation status of loci with high contribution to LD1 (BB1, BB2, AG1) and LD2 (AB14, BB43, BB44), respectively. Methylation status is indicated in the lines of the figure: h, hemimethylated; m, hypermethylated; i, internal cytosine methylation; u, non-methylated (unmethylated).

contribution of each locus to the group separation (Jombart and Collins, 2015; **Figures 3D,E**) resulted in the identification of different groups of loci mediating the separation of each discriminant function. Marked differences in the frequency of occurrence of each DNA methylation status in these loci through time (**Figures 3F,G**) were observed, with loci contributing to LD1 showing stable frequencies with a drastic change at T17, while LD2 loci showed a variable temporal response. These differences could indicate the occurrence of different overlapping responses mediated by DNA methylation changes.

To further investigate this, discriminant 3 (LD3) was also evaluated (**Figure 4**), in spite of its lower discriminant power (hence significant; $F = 76.29$, $p < 0.0001$). In this function, the marked separation of T17 was no longer evident and a clearer seasonal pattern emerged (**Figures 4A,B**). Remarkably, LD3 pattern correlated significantly to Temperature (+1 lag, $r = 0.91$, $p = 0.0310$), but not with irradiance ($r = -0.76$, $p = 0.0783$) that showed significance only for $\alpha = 0.1$. Although LD3 has lower discriminant power (**Figure 4B**), the temporal changes of DNA methylation status in the main contributing loci showed a dynamic variation as in LD2 (**Figure 4C**). Altogether, these results show an orderly transition of DNA methylation profiles during the months after the introduction of corals in their new environment, apparently driven by a warm-cold seasonality, but experiencing a pronounced change from T12 to T17 maybe related with a heat-stress event throughout this period.

Contribution of Coral Host vs. Symbiont to MSAP-Amplified Loci

Considering the limitations to separate symbiont and host DNA efficiently, additional analyses were performed to evaluate the contribution of the symbionts to the methylation pattern observed. Therefore, MSAP products were sequenced and aligned against the genomes of the closely related acroporid coral *A. digitifera* (the *A. cervicornis* genome was not available at the time of this analysis) and a representative symbiont (*S. microadriaticum*, formerly clade A). All MSAP selective-enzyme combinations ($n = 8$) produced a total of 30,519,266 reads after trimming. From those, 27,696,330 reads mapped to the coral genome (90.75%), while only 388,363 reads mapped to the symbiont genome (1.27%). This result indicates that although contamination with symbiont DNA is present, its contribution to MSAP loci is negligible.

Environmental Parameters Driving Seasonal Variability in Global DNA Methylation Patterns

Given the observed seasonal trend in DNA methylation and its link with regional temperature and light irradiance patterns, further analyses were performed to evaluate such relationship. Accordingly, the contribution of different environmental parameters was assessed by conducting non-metric multidimensional scaling (NMDS), fitting vectors to

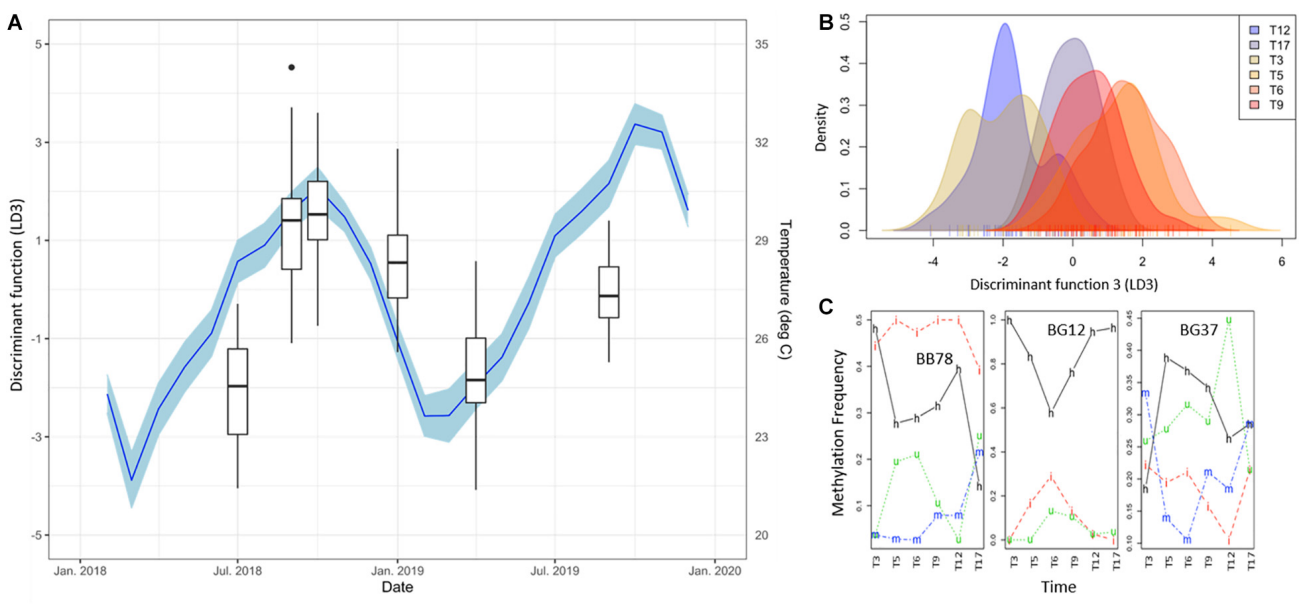

FIGURE 4 | (A) Time series of DNA methylation pattern separation as given by the DAPC discriminant function 3 (LD3, Box Plots). Black dots indicate outliers. Monthly average of daily mean temperature (NOAA Buoy CLBP4, blue line), lagg corrected + 1 as calculated with the *ccf* function in R, is shown as additional *y*-axes. Blue shadings indicate 95% confidence intervals of temperature variability. Note the clear seasonal variation of the DNA methylation patterns evidenced by this discriminant function and its significant correlation with temperature changes (Pearson's rank correlation: $r = 0.91$, $p = 0.0310$). **(B)** Density of DNA methylation profiles of each *A. cervicornis* fragment against discriminant function 3 (LD3). **(C)** Temporal variation of the frequency of each methylation status of three loci with high contribution to LD3 (BB78, BG12, BG37). Methylation status is indicated in the lines of the figure: h, hemimethylated; m, hypermethylated; i, internal cytosine methylation; u, non-methylated (unmethylated).

the ordination using the function *envfit*. Considering the abiotic data available and the lack of difference between the DNA methylation response among outplanting sites, two separate analyses were implemented. First, only samples from T5 (September 2018) and T12 (April 2019) for sites LPs and LPd (where site-specific environmental data was collected) were included (**Figure 5A**). This dataset allowed the evaluation of the contribution of temperature, pH, DO, salinity, and PAR to DNA methylation patterns. Results revealed that temperature, pH and DO correlated significantly with the NMDS ordination of the DNA methylation patterns driven by collection time (**Figure 5B** and **Supplementary Table 4**), while surprisingly PAR did not. Despite clear abiotic differences between depths, these parameters correlate to DNA methylation differences across sampling time points instead of sampling sites, indicating that seasonal variation in these environmental parameters was more relevant than site specific conditions in modulating DNA methylation patterns.

The second analysis fitted regional temperature and light irradiance to the ordination of all sampling times, but only for shallow sites in both reefs. This was performed to determine the influence of these parameters during the duration of the experiment without introducing errors derived by differences in irradiance between depths. We tested the contribution of monthly averages together with the coefficient of variation of the previous 3 months (CV3) for each variable. The NMDS ordination with all the data corroborated the DAPC analysis by showing T17 as an independent cluster (**Figure 5C**). All vectors analyzed showed a significant correlation with the ordination (**Figure 5D** and **Supplementary Table 5**), with temperature mean and CV3 of the irradiance showing the highest coefficients of determination (R^2). Interestingly, it seemed that light and temperature were sensed differently by DNA methylation mechanisms, with rapid responses to temperature and a potentially lagged response to light (**Figure 5D**).

DISCUSSION

This work constitutes the first attempt to characterize seasonal epigenetic changes in stony corals, providing support for the role of DNA methylation during seasonal acclimatization in the coral *A. cervicornis*. The results presented in this work suggest that DNA methylation profiles in this species vary following a season-dependent trend, with similar temporal changes in DNA methylation patterns in all inspected coral fragments, regardless of their genotype, source reef or outplanting site. This concurs with the frequently proposed notion of a seasonal variation in the phenotype of corals, including the presence of winter and summer ecotypes (Scheufen et al., 2017), likely driven by observed transcriptional changes (DeSalvo et al., 2008; Kenkel et al., 2013). These findings underscore the importance of including seasonal variability in environmental epigenetic studies in marine (specially sessile) organisms (Parkinson et al., 2018).

Variability and Seasonal Trends in Environmental Abiotic Parameters

Describing changes in environmental conditions is a prerequisite for the establishment of a seasonal dependence in any organismal response. Since DNA methylation data did not differ among sites, it was possible to use data from NOAA's weather buoy (CLBP4) to describe changes in temperature for all study sites, and data derived from climatological models (CMIP5 IPCC) for light irradiance. A limited *in situ* dataset was used to corroborate the responsiveness of DNA methylation to regional seasonal environmental variation, therefore validating the use of regional data and models to describe the general seasonal patterns as evidenced in temperature correlation with DNA methylation patterns with both datasets (**Figure 5**). Given the resolution of the regional light dataset with a limited sensitivity to differences in depth, it is not possible to categorically invoke interactive effects with depth and season based on the obtained data. Nonetheless, these results strongly support the interest of future research to understand the interactive effects of seasonality and depth differences on global DNA methylation.

Genotypic Composition of Source Reefs

Genotypic variation is correlated with diverse stress responses, disease resistance, epigenetic patterns and reproductive output in Caribbean Acroporids (Baums et al., 2013; Parkinson and Baums, 2014; Drury et al., 2019; Durante et al., 2019). In this experiment, fragments were collected using an opportunistic sampling approach that favors the collection of dominant genets. It is thus encouraging that multiple genets were collected at each site, indicating that the genotypic diversity of *A. cervicornis* around Culebra is not low (**Figure 1** and **Table 2**). Genets were restricted to one collection site each, and thus there was no evidence of long-distance dispersal of asexually derived fragments. This is not surprising, considering that asexual fragmentation (Tunnicliffe, 1981; Drury et al., 2019), restricts dispersion to a few hundred meters under natural conditions (including hurricane impacts), restricting genet distributions. Therefore, genotypic diversity observed on each site was mostly based in sexual recruitment.

Temporal Differences Dominate Patterns of DNA Methylation

Epigenetic landmarks, such as histone variants and DNA methylation, influence phenotypic plasticity in response to changes in environmental conditions and are, therefore, predictors of the general state of the organism in the face of environmental alterations and natural cycles (Rivière, 2014). Emerging evidence suggests that these mechanisms play an important role during responses to environmental changes, likely by regulating gene expression and maintaining DNA integrity throughout the entire lifespan of an organism (Roberts and Gavery, 2012; Dimond and Roberts, 2016; Liew et al., 2018; Rodriguez-Casariego et al., 2018). Recent studies on marine invertebrates [reviewed in Eirin-Lopez and Putnam (2019)] have shown that DNA methylation exerts a role on phenotypic

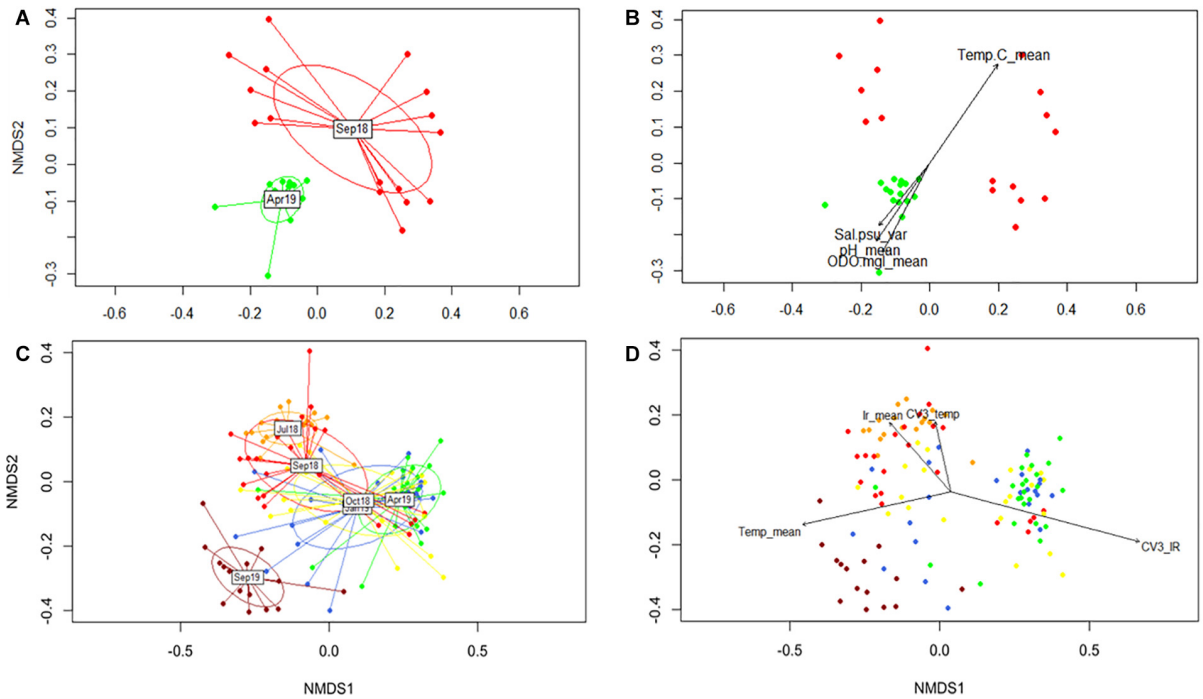

FIGURE 5 | Non-metric multidimensional scaling (NMDS) of global DNA methylation patterns using Gower distances. **(A)** Temporal separation for T5 and T12 for LP sites. **(C)** Representation of all sampling times for both shallow sites (LP and CR). **(B,D)** Significant correlations of environmental parameters to DNA methylation patterns ($P < 0.05$). Colors correspond to collection times.

acclimatization (Putnam et al., 2016; Liew et al., 2018; Durante et al., 2019) by modulating gene expression (Dixon et al., 2018). Moreover, epigenetic marks acquired throughout the lifespan of coral can be inherited intergenerationally, promoting acclimatized phenotypes in the offspring and thus increasing their fitness (Liew et al., 2020; Putnam et al., 2020). In addition, seasonal patterns of DNA methylation have been observed in vertebrates (Stevenson and Prendergast, 2013; Viitaniemi et al., 2019), invertebrates (Pegoraro et al., 2016; Suarez-Ulloa et al., 2019) and plants (Finnegan et al., 1998; Bastow et al., 2004; Ito et al., 2019). Based on these elements, it is not surprising that DNA methylation could play an active role during coral responses to seasonal variation.

The PERMANOVA analysis of all loci susceptible to DNA methylation showed clear differences in DNA methylation patterns between sampled months and genets, while no differences were observed between, sources or outplant sites in this study. This is a remarkable result, considering the significant differences in environmental conditions and habitat type between deep and shallow sites (see **Supplementary Table 1**), although the seasonal variation is larger for most parameters, including temperature. In corals, several studies have also found clear changes in DNA methylation in response to experimental manipulation in environmental conditions (Putnam et al., 2016; Liew et al., 2018; Cziesielski et al., 2019). On the other hand, a study aimed to evaluate the components of phenotypic divergence between clonemates of *A. palmata* under natural conditions (Durante et al., 2019), attributed most of the variation in DNA methylation to difference among genets followed by micro-environmental conditions, rather than between study sites. Nonetheless, this study was still able to observe small differences between sites. In the present work, *A. cervicornis* fragments were transplanted to new locations and only sampled after an acclimation period, hence source-site specific differences in DNA methylation profiles could have been diluted after a rapid acclimation. Still, evidence here suggests that seasonality remains as a stronger modulator of DNA methylation patterns. Coral genotype also exerts a significant effect over DNA methylation variability, although to a lesser extent than the aforementioned temporal influence, as evidenced by PERMANOVA (**Supplementary Table 3**). This observation is consistent with the dependence of DNA methylation on the presence of CpG sites in the DNA, and is further supported by previous evidence that DNA methylation in corals (or in any other eukaryotic organism) directly relies on sequence features of the genome, also supporting its heritability (Dixon et al., 2014; Liew et al., 2018; Durante et al., 2019).

Coral DNA Methylation Displays Seasonal Trends in Response to Environmental Changes

Seasonal environmental variation, similar to diel cycles, triggers the adjustment of physiological functions in corals (Hill and Ralph, 2005; Ulstrup et al., 2008; Brady et al., 2011; Sorek et al., 2014). The obtained results support the role of DNA methylation

on the seasonal acclimatization of *A. cervicornis*, as evidenced by a clear temporal effect over the MSAP methylation patterns. DNA methylation seems to follow seasonal trends in temperature, light, DO and pH, as evidenced by the significant correlation between DNA methylation ordination and the vectors representing mean-value variation of these parameters and coefficient of variations in the case of light and temperature (**Figure 5**), hinting a possible lagged response. However, analysis of the complete dataset with specific methylation patterns (DAPC) showed that temperature (1 + lagged) significantly correlate with changes in DNA methylation, while light was significant only under $\alpha = 0.1$. Yet, interactive effects of light seasonality and depth differences on global DNA methylation require additional analyses. Overall, it seems that seasonal variation in temperature, light, pH and dissolved oxygen modulate DNA methylation patterns.

This seasonal trend, however, seems to be masked by other phenomena occurring in the temporal scale. For example, samples collected during September 2019 have homogeneous DNA methylation profiles, markedly differentiated from the remaining sampling times by the first discriminant function of the DAPC analysis (**Figure 3A**). However, as revealed by the second and third linear discriminant functions (LD2 & LD3) of the DAPC analysis (**Figures 3C**, **4**), these samples are more related to September and October 2018. Although this may sound incompatible with an annual periodicity in DNA methylation profiles (considering there is just one replicated time point in both years), this change may simply reflect either coral acclimation to the experimental environment within the possibilities of its genetic and epigenetic backgrounds, or more likely, a response to stress.

Under an acclimation scenario, the switch in DNA methylation patterns would be immediate and then progressively undergo a resilience period after which the epigenome would be reprogrammed, resulting in the activation (or repression) of genes previously silenced (or activated) under native conditions. Unfortunately, the DNA methylation trends characterized in the present work do not support this notion. While rapid epigenetic changes were observed by our own previous research in coral (Rodriguez-Casariego et al., 2018), the constant change in DNA methylation patterns observed in the present work is not consistent with a linear progression toward an acclimated state. Indeed, several loci follow a seasonal-like pattern returning to DNA methylation values similar to those measured during the same season in the previous year (**Figures 3G**, **4**). This is especially evident in the loci driving the divergence of T17, which display a rather abrupt change instead of a progressive transition toward an acclimated state (**Figure 3F**).

A stress response hypothesis, on the other hand, would be consistent with the occurrence of an abnormal event in September 2019, justifying the dramatic change observed in the aforementioned loci. Abiotic monitoring data seem to validate this idea, including extremely high seawater temperatures during the summer of 2019 (+0.5–1.3°C, between July and October) compared to the same period of 2018. Indeed, a moderate bleaching event was observed in the area in subsequent months following an accumulation of 7 Degree Heat Weaks (Weil et al., 2019). Thermal-stress has been linked to significant changes in coral transcriptional profiles (DeSalvo et al., 2008; Voolstra et al., 2009; Kenkel et al., 2013), and to rapid epigenetic responses (Barshis et al., 2013; Palumbi et al., 2014), even at stress levels not high enough to produce bleaching (Rodriguez-Casariego et al., 2018). However, the anticipation of the response observed in T17 to the heat-stress event opens the possibility that DNA methylation could represent an early indicator of a changing thermal environment.

Overall, the evidence of a seasonal-driven response of DNA methylation presented by this work is in agreement with observed seasonal changes in gene expression in *A. cervicornis* (Parkinson et al., 2018), and phenotypic changes described in the coral holobiont (DeSalvo et al., 2008; Kenkel et al., 2013). Given the proposed role of DNA methylation mediating transcriptional plasticity (Dixon et al., 2014; Dimond and Roberts, 2016), it is not surprising to find such a seasonal response. Previous studies have also highlighted significant responses in the holobiont physiology, supporting seasonal variations (Chen et al., 2005; Ulstrup et al., 2008; Carballo-Bolaños et al., 2019). Bacterial community composition has been also described to follow a certain seasonal pattern in several coral species (Li et al., 2014; Sharp et al., 2017; Cai et al., 2018). Changes in symbiont cell density, pigment composition, and photosynthetic capacity following annual periods have also been reported (Fitt et al., 2000; Warner et al., 2002; Ulstrup et al., 2008). While the proposed role of temperature mediating seasonal changes in coral physiology (Brown et al., 1999; Fitt et al., 2000; Dimond and Carrington, 2007) was confirmed for DNA methylation here, non-conclusive evidence of the significant effect of other environmental factors with seasonal trends like pH, DO and light was obtained and will require further study. Given the marked seasonality observed in calcification rates and photosynthetic production (Hinrichs et al., 2013; Samiei et al., 2016), it is not surprising that these factors would also influence DNA methylation patterns potentially involved in the establishment of these seasonal phenotypes.

CONCLUSION

The present work provides support for the role of DNA methylation during seasonal acclimatization of the coral *A. cervicornis*, based on its correlation with seasonal environmental variation independently of genotypic and site-specific differences. The emergence of these patterns, despite the complexity of DNA methylation responses to environmental stress described in marine invertebrates and the limited resolution of the method employed here (when compared to sequencing techniques), support the relevance of this phenomena for epigenetic regulation in corals. Given the ecological importance of coral acclimatization in the Anthropocene and the potential similarities between seasonal adjustments and heat-stress responses, the evidence generated by the present effort constitutes an initial approach to understanding the dynamicity and the potential for intergenerational inheritance of this epigenetic mechanism. Further studies will be instrumental to decipher the extent in which seasonally driven epigenetic patterns are indicative of IGP, ItGP or even TGP, encompassing

critical implications on the current understanding of the epigenetic regulation of phenotypic plasticity. Overall, the data generated with this work will serve as a baseline to filter the contribution of seasonal-driven DNA methylation changes in studies addressing epigenetic responses to stressors, and as background for the study of environmental disturbances caused by extreme weather episodes (e.g., hurricanes).

DATA AVAILABILITY STATEMENT

Raw sequence data for ITS2 and MSAP analyses are available at the NCBI Sequence Read Archive under BioProjects with accession numbers PRJNA661294 and PRJNA661530, respectively. Additional datasets utilized in the study can be found in the Github repository https://github.com/eelabfiu/seasonal_PR.

AUTHOR CONTRIBUTIONS

JR-C designed the work, performed fieldwork, lab experiments, data analyses, and wrote the manuscript. AM-M designed the work, performed fieldwork, lab experiments, data analyses, and wrote the manuscript. DG-S designed the work, performed data analyses, and wrote the manuscript. IO-R performed lab experiments and data analyses. CL performed data analyses. IB performed lab experiments, data analyses, wrote the manuscript, and provided reagents and funding. AS designed the work, performed fieldwork, wrote the manuscript, and provided reagents and funding. JE-L designed the work, performed fieldwork, wrote the manuscript, and provided reagents and funding. All authors contributed to the article and approved the submitted version.

FUNDING

This work was supported by grants from the National Science Foundation (Grants 1810981 awarded to JE-L, AS, and IB; 1921402 awarded to JE-L, 1537959 awarded to IB; 1547798 awarded to Florida International University as part of the Centers for Research Excellence in Science and Technology Program). DG-S was supported by a postdoctoral contract ED481B/2018/091 (Xunta de Galicia). Corals were collected under Puerto Rico Marine Resources Department's (DERM) permit # 2018-IC-034 O-VS-PVS15-SJ-00980-20042018.

ACKNOWLEDGMENTS

We are thankful to all the volunteers at FIU's Environmental Epigenetics Laboratory, University of Puerto Rico, Rio Piedras and Sociedad Ambiente Marino who assisted during the early stages of this work. Thanks are also due to M. Devlin-Durante who performed the microsatellite genotyping and to FIU's Seagrass lab for providing access to a submersible PAM sensor. This is contribution #204 from the Coastlines and oceans Division of the Institute of Environment at Florida International University.

SUPPLEMENTARY MATERIAL

The Supplementary Material for this article can be found online at: https://www.frontiersin.org/articles/10.3389/fmars.2020.560424/full#supplementary-material

REFERENCES

Abraham, J. P., Baringer, M., Bindoff, N. L., Boyer, T., Cheng, L. J., Church, J. A., et al. (2013). A review of global ocean temperature observations: implications for ocean heat content estimates and climate change. *Rev. Geophys.* 51, 450–483. doi: 10.1002/rog.20022

Anderson, M. J. (2001). A new method for non-parametric multivariate analysis of variance. *Austr. Ecol.* 26, 32–46. doi: 10.1111/j.1442-9993.2001.01070.pp.x

Aranda, M., Li, Y., Liew, Y. J., Baumgarten, S., Simakov, O., Wilson, M. C., et al. (2016). Genomes of coral dinoflagellate symbionts highlight evolutionary adaptations conducive to a symbiotic lifestyle. *Sci. Rep.* 6:39734. doi: 10.1038/srep39734

Barshis, D. J., Ladner, J. T., Oliver, T. A., Seneca, F. O., Traylor-Knowles, N., and Palumbi, S. R. (2013). Genomic basis for coral resilience to climate change. *Proc. Natl. Acad. Sci. U.S.A.* 110, 1387–1392. doi: 10.1073/pnas.1210224110

Bastow, R., Mylne, J. S., Lister, C., Lippman, Z., Martienssen, R. A., and Dean, C. (2004). Vernalization requires epigenetic silencing of FLC by histone methylation. *Nature* 427, 164–167. doi: 10.1038/nature02269

Baums, I. B., Devlin-Durante, M. K., Polato, N. R., Xu, D., and Giri, S. (2013). Genotypic variation influences reproductive success and thermal stress tolerance in the reef building coral, *Acropora palmata*. *Coral Reefs* 32, 703–717. doi: 10.1007/s00338-013-1012-6

Baums, I. B., Hughes, C. R., and Hellberg, M. E. (2005a). Mendelian *Microsatellite loci* for the caribbean coral *Acropora palmata*. *Mar. Ecol. Prog. Ser.* 288, 115–127. doi: 10.3354/meps288115

Baums, I. B., Miller, M. W., and Hellberg, M. E. (2005b). Regionally isolated populations of an imperiled caribbean coral, *Acropora palmata*. *Mol. Ecol.* 14, 1377–1390. doi: 10.1111/j.1365-294x.2005.02489.x

Baums, I. B., Miller, M. W., and Hellberg, M. E. (2006). Geographic variation in clonal structure in a reef-building caribbean coral, *Acropora palmata*. *Ecol. Monogr.* 76, 503–519. doi: 10.1890/0012-9615(2006)076[0503:gvicsi]2.0.co;2

Benjamini, Y., and Hochberg, Y. (2000). On the adaptive control of the false discovery rate in multiple testing with independent statistics. *J. Educ. Behav. Statist.* 25, 60–83. doi: 10.2307/1165312

Berkelmans, R., and Willis, B. L. (1999). Seasonal and local spatial patterns in the upper thermal limits of corals on the inshore central great barrier reef. *Coral Reefs* 18, 219–228. doi: 10.1007/s003380050186

Birkeland, C. (2019). Global status of coral reefs: in combination, disturbances and stressors become ratchets. *World Seas Environ. Eval.* 2019, 35–56. doi: 10.1016/b978-0-12-805052-1.00002-4

Brady, A. K., Snyder, K. A., and Vize, P. D. (2011). Circadian cycles of gene expression in the coral, *Acropora millepora*. *PLoS One* 6:e25072. doi: 10.1371/journal.pone.0025072

Brener-Raffalli, K., Vidal-Dupiol, J., Adjeroud, M., Rey, O., Romans, P., Bonhomme, F., et al. (2019). Gene expression plasticity and frontloading promote *Thermotolerance* in *Pocillopora* corals. *bioRxiv* [Preprint], doi: 10.1101/398602

Brockwell, P. J., and Davis, R. A. (2009). *Time Series: Theory and Methods*. Berlin: Springer.

Brown, B. E., Dunne, R. P., Ambarsari, I., Le Tissier, M. D. A., and Satapoomin, U. (1999). Seasonal fluctuations in environmental factors and variations in

symbiotic algae and chlorophyll pigments in four indo-pacific coral species. *Mar. Ecol. Prog. Ser.* 191, 53–69. doi: 10.3354/meps191053

Cai, L., Tian, R.-M., Zhou, G., Tong, H., Wong, Y. H., Zhang, W., et al. (2018). Exploring coral microbiome assemblages in the south China Sea. *Sci. Rep.* 8:2428.

Cai, W.-J., Ma, Y., Hopkinson, B. M., Grottoli, A. G., Warner, M. E., Ding, Q., et al. (2016). Microelectrode characterization of coral daytime interior pH and carbonate chemistry. *Nat. Commun.* 7:11144.

Carballo-Bolaños, R., Denis, V., Huang, Y.-Y., Keshavmurthy, S., and Chen, C. A. (2019). Temporal variation and photochemical efficiency of species in symbiodinaceae associated with coral *Leptoria phrygia* (*Scleractinia*; *Merulinidae*) exposed to contrasting temperature regimes. *PLoS One* 14:e0218801. doi: 10.1371/journal.pone.00218801

Chen, C. A., Yang, Y.-W., Wei, N. V., Tsai, W.-S., and Fang, L.-S. (2005). Symbiont diversity in scleractinian corals from tropical reefs and subtropical non-reef communities in taiwan. *Coral Reefs* 24, 11–22. doi: 10.1007/s00338-004-0389-7

Cortessis, V. K., Thomas, D. C., Levine, A. J., Breton, C. V., Mack, T. M., Siegmund, K. D., et al. (2012). Environmental epigenetics: prospects for studying epigenetic mediation of exposure-response relationships. *Hum. Genet.* 131, 1565–1589. doi: 10.1007/s00439-012-1189-8

Covelo-Soto, L., Saura, M., and Morán, P. (2015). Does DNA methylation regulate metamorphosis? The case of the sea lamprey (*Petromyzon marinus*) as an example. *Compara. Biochem. Physiol. Part B Biochem. Mol. Biol.* 185, 42–46. doi: 10.1016/j.cbpb.2015.03.007

Cziesielski, M. J., Schmidt-Roach, S., and Aranda, M. (2019). The past, present, and future of coral heat stress studies. *Ecol. Evol.* 9, 10055–10066. doi: 10.1002/ece3.5576

DeSalvo, M. K., Voolstra, C. R., Sunagawa, S., Schwarz, J. A., Stillman, J. H., Coffroth, M. A., et al. (2008). Differential gene expression during thermal stress and bleaching in the caribbean coral *Montastraea faveolata*. *Mol. Ecol.* 17, 3952–3971. doi: 10.1111/j.1365-294x.2008.03879.x

Díaz-Freije, E., Gestal, C., Castellanos-Martínez, S., and Morán, P. (2014). The role of DNA methylation on octopus vulgaris development and their perspectives. *Front. Physiol.* 5:62. doi: 10.3389/fmicb.2014.00062

Dimond, J., and Carrington, E. (2007). temporal variation in the symbiosis and growth of the temperate scleractinian coral *Astrangia poculata*. *Mar. Ecol. Prog. Ser.* 348, 161–172. doi: 10.3354/meps07050

Dimond, J. L., and Roberts, S. B. (2016). Germline DNA methylation in reef corals: patterns and potential roles in response to environmental change. *Mol. Ecol.* 25, 1895–1904. doi: 10.1111/mec.13414

Dimond, J. L., and Roberts, S. B. (2020). Convergence of DNA methylation profiles of the reef coral *Porites astreoides* in a novel environment. *Front. Mar. Sci.* 6:792. doi: 10.3389/fmicb.2014.00792

Dixon, G., Liao, Y., Bay, L. K., and Matz, M. V. (2018). Role of gene body methylation in acclimatization and adaptation in a basal metazoan. *Proc. Natl. Acad. Sci. U.S.A.* 115, 13342–13346. doi: 10.1073/pnas.1813749115

Dixon, G. B., Bay, L. K., and Matz, M. V. (2014). Bimodal signatures of *Germline methylation* are linked with gene expression plasticity in the coral *Acropora millepora*. *BMC Genom.* 15:1109. doi: 10.1186/1471-2156-11-1109

Drury, C., Greer, J. B., Baums, I., Gintert, B., and Lirman, D. (2019). Clonal diversity impacts coral cover in *Acropora cervicornis* thickets: potential relationships between density, growth, and polymorphisms. *Ecol. Evol.* 9, 4518–4531. doi: 10.1002/ece3.5035

Durante, M. K., Baums, I. B., Williams, D. E., Vohsen, S., and Kemp, D. W. (2019). What drives phenotypic divergence among coral clonemates of *Acropora palmata*? *Mol. Ecol.* 28, 3208–3224.

Edge, S. E., Morgan, M. B., and Snell, T. W. (2008). Temporal analysis of gene expression in a field population of the *Scleractinian* coral *Montastraea faveolata*. *J. Exper. Mar. Biol. Ecol.* 355, 114–124. doi: 10.1016/j.jembe.2007.12.004

Eirin-Lopez, J. M., and Putnam, H. M. (2019). Marine environmental epigenetics. *Annu. Rev. Mar. Sci.* 11, 335–368. doi: 10.1146/annurev-marine-010318-095114

Etchegaray, J.-P., and Mostoslavsky, R. (2016). Interplay between metabolism and epigenetics: a nuclear adaptation to environmental changes. *Mol. Cell* 62, 695–711. doi: 10.1016/j.molcel.2016.05.029

Feely, R. A., Doney, S. C., and Cooley, S. R. (2009). Ocean acidification: present conditions and future changes in a high-CO2 world. *Oceanography* 22, 36–47. doi: 10.5670/oceanog.2009.95

Finnegan, E. J., Genger, R. K., Kovac, K., Peacock, W. J., and Dennis, E. S. (1998). DNA Methylation and the promotion of flowering by vernalization. *Proc. Natl. Acad. Sci. U.S.A.* 95, 5824–5829. doi: 10.1073/pnas.95.10.5824

Fitt, W. K., McFarland, F. K., Warner, M. E., and Chilcoat, G. C. (2000). Seasonal patterns of tissue biomass and densities of symbiotic dinoflagellates in reef corals and relation to coral bleaching. *Limnol. Oceanogr.* 45, 677–685. doi: 10.4319/lo.2000.45.3.0677

Grünwald, N. J., and Goss, E. M. (2011). Evolution and population genetics of exotic and re-emerging pathogens: novel tools and approaches. *Annu. Rev. Phytopathol.* 49, 249–267. doi: 10.1146/annurev-phyto-072910-095246

Gu, Z., Eils, R., and Schlesner, M. (2016). Complex heatmaps reveal patterns and correlations in multidimensional genomic data. *Bioinformatics* 32, 2847–2849. doi: 10.1093/bioinformatics/btw313

Hansen, J., Sato, M., and Ruedy, R. (2012). Perception of climate change. *Proc. Natl. Acad. Sci. U.S.A.* 109, E2415–E2423.

Harrell, F. E. Jr., and Harrell, M. F. E. Jr. (2019). *Package 'Hmisc.' CRAN2018 2019: 235-236*.

Hill, R., and Ralph, P. J. (2005). Diel and seasonal changes in fluorescence rise kinetics of three *Scleractinian* corals. *Funct. Plant Biol.* 32, 549–559. doi: 10.1071/fp05017

Hinrichs, S., Patten, N. L., Allcock, R. J. N., Saunders, S. M., Strickland, D., and Waite, A. M. (2013). Seasonal variations in energy levels and metabolic processes of two dominant *Acropora* Species (*A. Spicifera* and *A. Digitifera*) at ningaloo reef. *Coral Reefs* 32, 623–635. doi: 10.1007/s00338-013-1027-z

Hoegh-Guldberg, O. (1999). Climate change, coral bleaching and the future of the world's coral reefs. *Mar. Freshw. Res.* 50, 839–866.

Hoegh-Guldberg, O., and Bruno, J. F. (2010). The impact of climate change on the world's marine ecosystems. *Science* 328, 1523–1528. doi: 10.1126/science.1189930

Hoegh-Guldberg, O., Mumby, P. J., Hooten, A. J., Steneck, R. S., Greenfield, P., Gomez, E., et al. (2007). Coral reefs under rapid climate change and ocean acidification. *Science* 318, 1737–1742.

Holm, S. (1979). A simple sequentially rejective multiple test procedure. *Scand. J. Statist. Theor. Appl.* 6, 65–70.

Hughes, T. P., Baird, A. H., Bellwood, D. R., Card, M., Connolly, S. R., Folke, C., et al. (2003). Climate change, human impacts, and the resilience of coral reefs. *Science* 301, 929–933. doi: 10.1126/science.1085046

Hume, B. C. C., Smith, E. G., Ziegler, M., Warrington, H. J. M., Burt, J. A., LaJeunesse, T. C., et al. (2019). SymPortal: a novel analytical framework and platform for coral algal symbiont next-generation sequencing ITS2 profiling. *Mol. Ecol. Resour.* 19, 1063–1080. doi: 10.1111/1755-0998.13004

Hume, B. C. C., Voolstra, C. R., Arif, C., D'Angelo, C., Burt, J. A., Eyal, G., et al. (2016). Ancestral genetic diversity associated with the rapid spread of stress-tolerant coral symbionts in response to Holocene climate change. *Proc. Natl. Acad. Sci. U.S.A.* 113, 4416–4421. doi: 10.1073/pnas.1601910113

Ito, T., Nishio, H., Tarutani, Y., Emura, N., Honjo, M. N., Toyoda, A., et al. (2019). Seasonal stability and dynamics of DNA methylation in plants in a natural environment. *Genes*. 10:544. doi: 10.3390/genes10070544

Jombart, T. (2008). Adegenet: a R package for the multivariate analysis of genetic markers. *Bioinformatics*. 24, 1403–1405. doi: 10.1093/bioinformatics/btn129

Jombart, T., and Collins, C. (2015). A tutorial for discriminant analysis of principal components (DAPC) using adegenet 2.0. 0. *Imp Coll Lond. MRC Cent Outbreak Anal. Model.* 43, 1–43.

Jombart, T., Devillard, S., and Balloux, F. (2010). Discriminant analysis of principal components: a new method for the analysis of genetically structured populations. *BMC Genet.* 11:94. doi: 10.1186/1471-2156-11-94

Kenkel, C. D., Meyer, E., and Matz, M. V. (2013). Gene expression under chronic heat stress in populations of the mustard hill coral (*Porites astreoides*) from different thermal environments. *Mol. Ecol.* 22, 4322–4334. doi: 10.1111/mec.12390

Li, H. (2018). Minimap2: pairwise alignment for nucleotide sequences. *Bioinformatics* 34, 3094–3100. doi: 10.1093/bioinformatics/bty191

Li, J., Chen, Q., Long, L. J., Dong, J. D., Yang, J., and Zhang, S. (2014). Bacterial dynamics within the mucus, tissue and skeleton of the coral *Porites lutea* during different seasons. *Sci. Rep.* 4:7320.

Liew, Y. J., Howells, E. J., Wang, X., Michell, C. T., Burt, J. A., Idaghdour, Y., et al. (2020). Intergenerational epigenetic inheritance in reef-building corals. *Nat. Clim. Chang.* 10, 254–259. doi: 10.1038/s41558-019-0687-2

Liew, Y. J., Zoccola, D., Li, Y., Tambutté, E., Venn, A. A., Michell, C. T., et al. (2018). Epigenome-associated phenotypic acclimatization to ocean acidification in a reef-building coral. *Sci. Adv.* 4:eaar8028. doi: 10.1126/sciadv.aar8028

López-Maury, L., Marguerat, S. L., and Bähler, J. (2008). Tuning gene expression to changing environments: from rapid responses to evolutionary adaptation. *Nat. Rev. Genet.* 9, 583–593. doi: 10.1038/nrg2398

Marsh, A. G., and Pasqualone, A. A. (2014). DNA Methylation and temperature stress in an antarctic polychaete, *Spiophanes tcherniai*. *Front. Physiol.* 5:173. doi: 10.3389/fmicb.2014.00173

Martinez-Arbizu, P. (2019). *PairwiseAdonis: Pairwise Multilevel Comparison Using Adonis. R Package Version 0. 0 1.*

Navarro-Martín, L., Viñas, J., Ribas, L., Díaz, N., Gutiérrez, A., Di Croce, L., et al. (2011). DNA Methylation of the Gonadal aromatase (cyp19a) promoter is involved in temperature-dependent sex ratio shifts in the European sea bass. *PLoS Genet.* 7:e1002447. doi: 10.1371/journal.pone.0010 02447

Oksanen, J., Blanchet, F. G., Friendly, M., Kindt, R., Legendre, P., McGlinn, D., et al. (2019). *Vegan: Community Ecology Package. 2018. R Package Version 1.17.14.*

Palumbi, S. R., Barshis, D. J., Traylor-Knowles, N., and Bay, R. A. (2014). Mechanisms of reef coral resistance to future climate change. *Science* 344, 895–898. doi: 10.1126/science.1251336

Pandolfi, J. M., Bradbury, R. H., Sala, E., Hughes, T. P., Bjorndal, K. A., Cooke, R. G., et al. (2003). Global trajectories of the long-term decline of coral reef ecosystems. *Science* 301, 955–958. doi: 10.1126/science.1085706

Parkinson, J. E., Bartels, E., Devlin-Durante, M. K., Lustic, C., Nedimyer, K., Schopmeyer, S., et al. (2018). Extensive transcriptional variation poses a challenge to thermal stress biomarker development for endangered Corals. *Mol. Ecol.* 27, 1103–1119. doi: 10.1111/mec.14517

Parkinson, J. E., and Baums, I. B. (2014). The extended phenotypes of marine symbioses: ecological and evolutionary consequences of intraspecific genetic diversity in coral-algal associations. *Front. Microbiol.* 5:445. doi: 10.3389/fmicb. 2014.00445

Pegoraro, M., Bafna, A., Davies, N. J., Shuker, D. M., and Tauber, E. (2016). DNA Methylation changes induced by long and short photoperiods in Nasonia. *Genome Res.* 26, 203–210. doi: 10.1101/gr.196204.115

Perez, M. F., and Lehner, B. (2019). Intergenerational and transgenerational epigenetic inheritance in animals. *Nat. Cell Biol.* 21, 143–151. doi: 10.1038/ s41556-018-0242-9

Pérez-Figueroa, A. (2013). Msap: a tool for the statistical analysis of Methylation-sensitive amplified polymorphism data. *Mol. Ecol. Resour.* 13, 522–527. doi: 10.1111/1755-0998.12064

Pochon, X., Pawlowski, J., Zaninetti, L., and Rowan, R. (2001). High genetic diversity and relative specificity among *Symbiodinium*-like *Endosymbiotic dinoflagellates* in soritid foraminiferans. *Mar. Biol.* 139, 1069–1078. doi: 10. 1007/s002270100674

Pritchard, J. K., Stephens, M., Rosenberg, N. A., and Donnelly, P. (2000). Association mapping in structured populations. *Am. J. Hum. Genet.* 67, 170–181. doi: 10.1086/302959

Putnam, H. M., Davidson, J. M., and Gates, R. D. (2016). Ocean acidification influences host DNA Methylation and phenotypic plasticity in environmentally susceptible corals. *Evol. Appl.* 9, 1165–1178. doi: 10.1111/eva.12408

Putnam, H. M., Ritson-Williams, R., Cruz, J. A., Davidson, J. M., and Gates, R. D. (2020). Environmentally-induced parental or developmental conditioning influences coral offspring ecological performance. *Sci. Rep.* 10:13664. doi: 10. 1038/s41598-020-70605-x

Reyna-Lopez, G. E., Simpson, J., and Ruiz-Herrera, J. (1997). Differences in DNA Methylation patterns are detectable during the dimorphic transition of fungi by amplification of restriction polymorphisms. *Mol. Gen. Genet.* 253, 703–710. doi: 10.1007/s004380050374

Rivera-Casas, C., Gonzalez-Romero, R., Garduño, R. A., Cheema, M. S., Ausio, J., and Eirin-Lopez, J. M. (2017). Molecular and biochemical methods useful for the epigenetic characterization of chromatin-associated proteins in *Bivalve molluscs*. *Front. Physiol.* 8:490. doi: 10.3389/fmicb.2014. 00490

Rivière, G. (2014). Epigenetic features in the oyster *Crassostrea gigas* suggestive of functionally relevant promoter DNA Methylation in invertebrates. *Front. Physiol.* 5:129. doi: 10.3389/fmicb.2014.00129

Roberts, S. B., and Gavery, M. R. (2012). Is there a relationship between DNA Methylation and phenotypic plasticity in invertebrates? *Front. Physiol.* 2:116. doi: 10.3389/fphys.2011.00116

Rodriguez-Casariego, J. A., Ladd, M. C., Shantz, A. A., Lopes, C., Cheema, M. S., Kim, B., et al. (2018). Coral epigenetic responses to nutrient stress: histone H2A. X phosphorylation dynamics and DNA Methylation in the Staghorn coral *Acropora cervicornis*. *Ecol. Evol.* 8, 12193–12207. doi: 10.1002/ece3.4678

Rosenzweig, C., Karoly, D., Vicarelli, M., Neofotis, P., Wu, Q., Casassa, G., et al. (2008). Attributing physical and biological impacts to anthropogenic climate change. *Nature* 453, 353–357. doi: 10.1038/nature06937

Ryu, T., Veilleux, H. D., Donelson, J. M., Munday, P. L., and Ravasi, T. (2018). The epigenetic landscape of transgenerational acclimation to ocean warming. *Nat. Clim. Chang.* 8, 504–509. doi: 10.1038/s41558-018-0159-0

Salinas, S., and Munch, S. B. (2012). Thermal legacies: transgenerational effects of temperature on growth in a vertebrate. *Ecol. Lett.* 15, 159–163. doi: 10.1111/j. 1461-0248.2011.01721.x

Sambrook, J., and Russell, D. W. (2006). Isolation of high-molecular-weight DNA from mammalian cells using proteinase K and phenol. *Cold Spring Harb. Protoc.* 15, 159–163. doi: 10.1101/pdb.prot4036

Samiei, J. V., Saleh, A., Shirvani, A., Fumani, N. S., Hashtroudi, M., and Pratchett, M. S. (2016). Variation in calcification rate of acroporadowningi relative to seasonal changes in environmental conditions in the northeastern Persian gulf. *Coral Reefs* 35, 1371–1382. doi: 10.1007/s00338-016-1464-6

Scheufen, T., Krämer, W. E., Iglesias-Prieto, R., and Enríquez, S. (2017). Seasonal variation modulates coral sensibility to heat-stress and explains annual changes in coral productivity. *Sci. Rep.* 7:4937.

Sharp, K. H., Pratte, Z. A., Kerwin, A. H., Rotjan, R. D., and Stewart, F. J. (2017). Season, but not symbiont state, drives microbiome structure in the temperate Coral *Astrangia poculata*. *Microbiome* 5:120.

Shinzato, C., Shoguchi, E., Kawashima, T., and Hamada, M. (2011). Using the *Acropora digitifera* genome to understand coral responses to environmental change. *Nature* 476, 320–323. doi: 10.1038/nature10249

Sorek, M., Díaz-Almeyda, E. M., Medina, M., and Levy, O. (2014). Circadian clocks in symbiotic corals: the duet between *Symbiodinium* algae and their coral host. *Mar. Genom.* 14, 47–57. doi: 10.1016/j.margen.2014.01.003

Stevenson, T. J., and Prendergast, B. J. (2013). Reversible DNA Methylation regulates seasonal photoperiodic time measurement. *Proc. Natl. Acad. Sci. U.S.A.* 110, 16651–16656. doi: 10.1073/pnas.1310643110

Stoddart, J. A., and Taylor, J. F. (1988). Genotypic diversity: estimation and prediction in samples. *Genetics* 118, 705–711.

Suarez-Ulloa, V., Gonzalez-Romero, R., and Eirin-Lopez, J. M. (2015). Environmental *Epigenetics*: a promising venue for developing next-generation pollution Biomonitoring tools in marine invertebrates. *Mar. Pollut. Bull.* 98, 5–13. doi: 10.1016/j.marpolbul.2015.06.020

Suarez-Ulloa, V., Rivera-Casas, C., and Michel, M. (2019). Seasonal DNA Methylation variation in the flat tree oyster isognomon *Alatus* from a mangrove ecosystem in North Biscayne Bay, Florida. *J. Shellf. Res.* 38:79. doi: 10.2983/035. 038.0108

Thornhill, D. J., LaJeunesse, T. C., Kemp, D. W., Fitt, W. K., and Schmidt, G. W. (2006). Multi-year, seasonal genotypic surveys of coral-algal symbioses reveal prevalent stability or post-bleaching reversion. *Mar. Biol.* 148, 711–722. doi: 10.1007/s00227-005-0114-2

Tunnicliffe, V. (1981). Breakage and propagation of the stony coral *Acropora cervicornis*. *Proc. Natl. Acad. Sci. U.S.A.* 78, 2427–2431. doi: 10.1073/pnas.78. 4.2427

Ulstrup, K. E., Hill, R., van Oppen, M. J. H., Larkum, A. W. D., and Ralph, P. J. (2008). Seasonal variation in the photo-physiology of homogeneous and heterogeneous *Symbiodinium consortia* in two *Scleractinian* corals. *Mar. Ecol. Prog. Ser.* 361, 139–150. doi: 10.3354/meps07360

van Oppen, M. J. H., Oliver, J. K., Putnam, H. M., and Gates, R. D. (2015). Building coral reef resilience through assisted evolution. *Proc. Natl. Acad. Sci. U.S.A.* 112, 2307–2313. doi: 10.1073/pnas.1422301112

Vandegehuchte, M. B., Kyndt, T., Vanholme, B., Haegeman, A., Gheysen, G., and Janssen, C. R. (2009). Occurrence of DNA Methylation in daphnia magna

and influence of multigeneration Cd exposure. *Environ. Intern.* 35, 700–706. doi: 10.1016/j.envint.2009.01.002

Vignet, C., Joassard, L., Lyphout, L., Guionnet, T., Goubeau, M., Le Menach, K., et al. (2015). Exposures of zebrafish through diet to three environmentally relevant mixtures of PAHs Produce behavioral disruptions in unexposed F1 and F2 descendant. *Environ. Sci. Pollut. Res. Intern.* 22, 16371–16383. doi: 10.1007/s11356-015-4157-8

Viitaniemi, H. M., Verhagen, I., Visser, M. E., Honkela, A., van Oers, K., and Husby, A. (2019). Seasonal variation in genome-Wide DNA Methylation patterns and the onset of seasonal timing of reproduction in great tits. *Genome Biol. Evol.* 11, 970–983. doi: 10.1093/gbe/evz044

Voolstra, C. R., Schnetzer, J., Peshkin, L., Randall, C. J., Szmant, A. M., and Medina, M. (2009). Effects of temperature on gene expression in embryos of the coral *Montastraea faveolata*. *BMC Genom.* 10:627. doi: 10.1186/1471-2156-11-627

Warner, M., Chilcoat, G., McFarland, F., and Fitt, W. (2002). Seasonal fluctuations in the photosynthetic capacity of Photosystem II in symbiotic dinoflagellates in the caribbean reef-building coral montastraea. *Mar. Biol.* 141, 31–38. doi: 10.1007/s00227-002-0807-8

Weil, E., Hernández-Delgado, E., Gonzalez, M., Williams, S., Ramos, S. Suleimán, Figuerola, M., et al. (2019). Spread of the new coral disease 'SCTLD' into the Caribbean: implications for Puerto Rico. *Reef Encount.* 34, 38–43.

West-Eberhard, M. J. (2003). *Developmental Plasticity and Evolution*. Oxford: Oxford University Press.

Xiong, W., Li, X., Fu, D., Mei, J., Li, Q., Lu, G., et al. (2013). DNA Methylation alterations at 5'-CCGG sites in the interspecific and intraspecific hybridizations derived from *Brassica rapa* and *B. Napus*. *PLoS One* 8:e65946. doi: 10.1371/journal.pone.0065946

Conflict of Interest: The authors declare that the research was conducted in the absence of any commercial or financial relationships that could be construed as a potential conflict of interest.

frontiers in Marine Science

ORIGINAL RESEARCH
published: 13 November 2020
doi: 10.3389/fmars.2020.566419

Ocean Acidification Induces Subtle Shifts in Gene Expression and DNA Methylation in Mantle Tissue of the Eastern Oyster (*Crassostrea virginica*)

Alan M. Downey-Wall[1], Louise P. Cameron[1], Brett M. Ford[1], Elise M. McNally[1], Yaamini R. Venkataraman[2], Steven B. Roberts[2], Justin B. Ries[1] and Katie E. Lotterhos[1]*

[1] *Department of Marine and Environmental Sciences, Northeastern University, Nahant, MA, United States,* [2] *School of Aquatic and Fishery Sciences, University of Washington, Seattle, WA, United States*

Early evidence suggests that DNA methylation can mediate phenotypic responses of marine calcifying species to ocean acidification (OA). Few studies, however, have explicitly studied DNA methylation in calcifying tissues through time. Here, we examined the phenotypic and molecular responses in the extrapallial fluid and mantle (fluid and tissue at the calcification site) in adult eastern oyster (*Crassostrea virginica*) exposed to experimental OA over 80 days. Oysters were reared under three experimental pCO_2 treatments ("control," 580 μatm; "moderate OA," 1,000 μatm; "high OA," 2,800 μatm) and sampled at 6 time points (24 h–80 days). We found that high OA initially induced an increase in the pH of the extrapallial fluid (pH_{EPF}) relative to the external seawater that peaked at day 9, but then diminished over time. Calcification rates were significantly lower in the high OA treatment compared to the other treatments. To explore how oysters regulate their extrapallial fluid, gene expression and DNA methylation were examined in the mantle-edge tissue of oysters from days 9 and 80 in the control and high OA treatments. Mantle tissue mounted a significant global molecular response (both in the transcriptome and methylome) to OA that shifted through time. Although we did not find individual genes that were significantly differentially expressed under OA, the pH_{EPF} was significantly correlated with the eigengene expression of several co-expressed gene clusters. A small number of OA-induced differentially methylated loci were discovered, which corresponded with a weak association between OA-induced changes in genome-wide gene body DNA methylation and gene expression. Gene body methylation, however, was not significantly correlated with the eigengene expression of pH_{EPF}-correlated gene clusters. These results suggest that OA induces a subtle response in a large number of genes in *C. virginica*, but also indicate that plasticity at the molecular level may be limited. Our study highlights the need to reassess our understanding of tissue-specific molecular responses in marine calcifiers, as well as the role of DNA methylation and gene expression in mediating physiological and biomineralization responses to OA.

Keywords: DNA methylation, gene expression, ocean acidification, acclimatization, *Crassostrea virginica*, oyster, extrapallial fluid

OPEN ACCESS

Edited by:
Andrew Stanley Mount, Clemson University, United States

Reviewed by:
Gary H. Dickinson, The College of New Jersey, United States
Hao Chen, Institute of Oceanology (CAS), China

****Correspondence:***
Alan M. Downey-Wall
adowneywall@gmail.com

Specialty section:
This article was submitted to Marine Molecular Biology and Ecology, a section of the journal Frontiers in Marine Science

Received: *27 May 2020*
Accepted: *09 September 2020*
Published: *13 November 2020*

Citation:
Downey-Wall AM, Cameron LP, Ford BM, McNally EM, Venkataraman YR, Roberts SB, Ries JB and Lotterhos KE (2020) Ocean Acidification Induces Subtle Shifts in Gene Expression and DNA Methylation in Mantle Tissue of the Eastern Oyster (Crassostrea virginica). Front. Mar. Sci. 7:566419. doi: 10.3389/fmars.2020.566419

INTRODUCTION

Ocean acidification (OA), a decrease in seawater pH due to the uptake of anthropogenic CO_2, is expected to have substantial effects on marine species and ecosystems in the near future (Orr et al., 2005; Guinotte and Fabry, 2008; Doney et al., 2009). Specifically, OA is driving a shift in the carbonate system equilibrium, resulting in decreased availability of carbonate ions and lower calcium carbonate saturation state (Feely et al., 2004; Orr et al., 2005). This may be particularly problematic for marine calcifying species, which build their shells and skeletons from calcium and carbonate ions.

Substantial effort has been invested into evaluating the short- and long-term consequences of OA across taxa and life history stages. Prolonged exposure to OA tends to have negative effects on calcification, metabolism, and growth, as observed in corals (e.g., Anthony et al., 2008), pteropods (e.g., Bednaršek et al., 2012), gastropods (e.g., Melatunan et al., 2013), and bivalves (e.g., Talmage and Gobler, 2010). However, these negative effects are not universal, varying in direction (negative or positive) and intensity depending on taxon, severity of OA, and duration of exposure (Ries et al., 2009; Kroeker et al., 2010). Observed non-negative effects may be the result of individual resilience or the capacity of certain species to acclimatize to OA.

One way acclimation may occur is *via* the maintenance of pH homeostasis at the site of calcification, which is a polyphyletic response to OA that has been observed in scleractinian corals (Al-Horani et al., 2002; Ries, 2011; Venn et al., 2011; McCulloch et al., 2012; Holcomb et al., 2014), foraminifera (Rink et al., 1998; Köhler-Rink and Kühl, 2000; de Nooijer et al., 2008, 2009), calcareous green algae (De Beer and Larkum, 2001), coralline red algae (Donald et al., 2017; Anagnostou et al., 2019; Liu et al., 2020), coccolithophores (Liu et al., 2018), and bivalves (Ramesh et al., 2017; Liu et al., 2020). Recent evidence in bivalves suggests that this response may also be affected by other factors, including temperature (Cameron et al., 2019) and life-stage (Ramesh et al., 2017).

Under ambient conditions, adult bivalves tend to maintain their extra-pallial fluid pH (pH_{EPF}) below that of seawater pH ($pH_{seawater}$) (Crenshaw, 1972; Sutton et al., 2018), which has been attributed to the buildup of dissolved CO_2 when the organism's valves are closed (Crenshaw, 1972; Michaelidis et al., 2005; Sutton et al., 2018; Liu et al., 2020). While under OA conditions, some bivalves will actually increase their pH_{EPF} above that of $pH_{seawater}$ (e.g., Liu et al., 2020), potentially enabling them to continue calcifying even under highly acidic scenarios. Only recently have investigators studied the molecular mechanisms that regulate calcification within the mantle tissue (see reviews by Clark, 2020; Rajan and Vengatesen, 2020).

Transcriptomic studies have proven to be a powerful approach for identifying genes and understanding pathways that shape organismal the response to OA, and have been used to help elucidate the potential trade-offs that result from acclimatization (Evans and Hofmann, 2012), including genes associated with biomineralization, acid-base regulation, and metabolic function (Evans et al., 2013; Davies et al., 2016; Li et al., 2016; Goncalves et al., 2017; Wong et al., 2018; Griffiths et al., 2019; Strader et al., 2020). From this literature it has been hypothesized that there is a trade-off between maintaining calcification vs. other core functions (Wood et al., 2008), whereby increased or sustained calcification under continued exposure may become too costly over time. At the transcriptomic level, this cost can manifest as shifts in the expression of both calcification and metabolic genes over time (Li et al., 2016), suggesting that certain acclimatization responses may be unsustainable during extended exposure to OA. The precise mechanisms that mediate these changes in gene expression remain underexplored, but recent studies indicate that DNA methylation, an epigenetic modification, may be an important regulator of these responses (Liew et al., 2018; Bogan et al., 2020).

DNA methylation is an important mediator of gene regulation and physiological response across a diverse range of taxa (see reviews Zilberman et al., 2007; Zemach et al., 2010; Schübeler, 2015; Zhang et al., 2018). DNA methylation refers to the attachment of a methyl group to cytosine, and is most frequently studied in the context of the cytosine-guanine (CpG) motif. These modifications occur on top of the genome without altering the underlying DNA sequence (Richards, 2006; Bonduriansky and Day, 2018) and may be stable enough to be passed from parent to offspring (Jablonka and Lamb, 2002). Previous work has shown they can have an important role in determining an organism's phenotype across a range of species, including fur color and obesity in mice (Dolinoy et al., 2006), rat pup behavior as determined by parental care (Anier et al., 2014), response to phosphate starvation in *Arabidopsis* (Yong-Villalobos et al., 2015), and caste phenotypes in social insects (Lyko et al., 2010). Importantly, the precise manner in which DNA methylation serves to regulate phenotype is taxon-specific.

In invertebrates, association studies have begun to elucidate the relationship between DNA methylation, gene expression, and phenotype (e.g., Gavery and Roberts, 2013; Dixon et al., 2018; Liew et al., 2018). In basal invertebrates (e.g., corals and oysters), genomes are typically only sparsely methylated compared to vertebrates, and DNA methylation tends to be concentrated in CpGs within gene bodies (i.e., exons and introns). In this group, gene body methylation was positively correlated with gene expression and negatively correlated with the variation in expression among individuals (Gavery and Roberts, 2013; Liew et al., 2018). Based on these patterns, DNA methylation may be acting to regulate not only the level of expression, but also the amount of transcriptional noise among individuals (Huh et al., 2013). Furthermore, recent evidence suggests that unlike vertebrates, non-deuterostome invertebrate DNA methylation is not necessarily erased during embryogenesis, opening up the possibility for transmission of marks between generations (Xu et al., 2019).

Understanding the role of environment-induced DNA methylation in regulating gene expression and phenotypic plasticity is of particular interest in the context of marine systems and global change (see reviews Hofmann, 2017; Eirin-Lopez and Putnam, 2019). In corals, early evidence indicates that DNA methylation can be both sensitive to environmental change, including OA in some species (Putnam et al., 2016; Liew et al., 2018), and associated with gene expression (Dixon

et al., 2018) suggesting a potential regulatory role of DNA methylation in coral response to OA. Liew et al. (2018) found OA-sensitive DNA methylation also corresponded with biomineralization-related traits in corals, supporting the idea that DNA methylation may have an important role in phenotypic plasticity and acclimatization to OA. Although these studies examined OA reponses in many different tissues, none of these studies quantified methylation responses to OA at base-pair resolution in calcifying tissue.

Here, we examine the molecular basis of eastern oyster *(Crassostrea virginica)* pH_{EPF} regulation and calcification response to OA. *Crassostrea virginica* is a coastal marine bivalve that provides critical ecosystem services in the form of habitat structure and water filtration, and also serves as an economically important food source (Ekstrom et al., 2015; Gómez-Chiarri et al., 2015). Its genome has been recently sequenced (Gómez-Chiarri et al., 2015) and the species has been the subject of extensive OA studies. Consistent with other bivalve species, *C. virginica* at all life stages exhibit a largely negative calcification response to OA (e.g., Miller et al., 2009; Ries et al., 2009; Beniash et al., 2010; Waldbusser et al., 2011b; Dickinson et al., 2012), while metabolic and physiological responses tend to be more varied and dependent on life stage, experimental condition, and duration of exposure (Beniash et al., 2010; Dickinson et al., 2012; Ivanina et al., 2013; Matoo et al., 2013; Gobler and Talmage, 2014). Like other bivalve species, the chemical composition of *C. virginica* EPF is thought to be regulated *via* the active exchange of ions and other constituents through the mantle epithelium to promote calcification (Crenshaw and Neff, 1969; Crenshaw, 1972). A recent study by Liu et al. (2020) found that *C. virginica* had some ability to moderate their pH_{EPF} in response to OA, however, the mechanisms that regulate this response have not been explored.

The primary goal of the present study was to investigate the molecular mechanisms underlying the biomineralization response of *C. virginica* to short- and long-term OA exposure. Specifically, we studied the role of DNA methylation in physiological and gene expression responses in *C. virginica* mantle-edge tissue. We performed a controlled laboratory experiment in which oysters were exposed to three levels of CO_2-induced OA (control, moderate, and high) for 80 days and monitored the oysters' calcification rate and pH_{EPF}. Based on patterns we observed in the pH_{EPF} response, we examined gene expression and DNA methylation responses in mantle-edge tissue at two time points (days 9 and 80) for oysters exposed to control and high OA treatments. We predicted that the oysters mitigate the effects of OA by regulating pH_{EPF} relative to $pH_{seawater}$ and that this process is associated with a molecular response in the oyster transcriptome and methylome. Specifically, we hypothesized that in *C. virginica* (i) OA will drive differential responses in both the transcriptome and methylome and up-regulation of pH_{EPF} relative to the environment, (ii) pH_{EPF} response will be coupled with the up-regulation of biomineralization related genes, (iii) gene expression will be associated with gene body DNA methylation, and (iv) differential expression will correspond to significant shifts in gene body methylation. By establishing the first integrated dataset on EPF carbonate chemistry, gene expression, and DNA methylation in a mollusk exposed to variable degrees of OA, our study provides new insights into the responses of bivalves to OA over short and long timescales.

MATERIALS AND METHODS

Oyster Collection and Preparation

Adult *C. virginica* were collected from three intertidal sites within Plum Island Sound, Massachusetts, USA (Site 1, 42.751636, −70.837023; Site 2, 42.725186, −70.855022; Site 3, 42.681764, −70.813498) in late April 2017. These sites are all within 8 km of each other and the oysters from these sites are not distinct genetic populations. However, to compensate for any site effects, site was included as a random effect in applicable statistical models (see statistical analysis section for details).

In the lab, oysters were cleaned of epibionts and shell ports were installed over 8 days while being maintained in 50-L flow-through tanks. To measure the carbonate chemistry of the EPF, a 2 mm hole was drilled into the right valve ∼2 cm from the hinge to expose the EPF cavity, without damaging the underlying mantle tissue. The drilled hole was gently rinsed with filtered seawater and patted dry. The barbed end of a nylon luer-lock coupling (McMaster-Carr 51525K123) was trimmed to the length of the shell thickness, inserted into the hole and sealed in place using marine-safe cyanoacrylate (Starbond EM-2000 CA USA). The coupling was then plugged with a nylon cap socket (McMaster-Carr 51525K315) to prevent exchange between seawater and the EPF *via* the port and limit the potential for increased dissolution near the site of the implant. Oysters were allowed to recover for 4 days, after which they were transferred to the experimental tank array (described below) for acclimation and exposure. During the transfer, oysters were assigned one of three pCO_2 treatments: "control" (ca. 580 μatm)—corresponding to near-present-day conditions in the estuary where they were collected; "moderate OA" (ca. 1,000 μatm)—corresponding to end-of-century predictions (Intergovernmental Panel on Climate Change, 2007); and "high OA" (ca. 2,800 μatm)—corresponding to seawater conditions that are undersaturated with respect to calcite ($\Omega_{calcite} < 1$). Importantly, high OA events are already regularly experienced in the coastal marine systems from which these oysters were collected, owing to daily tidal cycles, input of meteoric waters, and seasonal reoxidation of organic matter (**Supplementary Figure 1.1**). This trend is underappreciated in many coastal systems, where local processes are increasing the acidity of the seawater relative to the global average (Reum et al., 2014). The high OA treatment was also used to increase the inferential and statistical power of the study design (Whitlock and Schluter, 2014).

Experimental Design and Water Chemistry

The experiment was conducted at Northeastern University's Marine Science Center, using a flow-through seawater system that draws water from Broad Sound in Nahant, Massachusetts (42.416884, −70.907564). Each pCO_2 treatment was replicated over two blocks, each containing three 42-L acrylic aquaria (total of 6 aquaria per treatment). Tanks within a block were

connected *via* the recirculation and filtration system, while gas mixture, temperature, and incoming filtered seawater were regulated independently for each tank. A blocked randomized design was used to ensure an equal number of oysters from each location were distributed across all treatments and that there were no significant differences in initial oyster size across treatment (mean ± SD shell length: 9.70 ± 2.4 cm). Twelve oysters were placed into each aquarium, four from each location, resulting in 24 oysters per treatment per location (total of 72 oysters per treatment). Oysters were acclimated for 33 days in control pCO_2 conditions at a temperature of 17°C. This extended acclimation period was used to (i) provide time for any acute field-induced changes due to local acidification events to reset, and (ii) ensure that the oysters had sufficient time to recover from the stress of being transported to the laboratory. Following acclimation, the moderate and high OA treatments were ramped up to target pCO_2 over a 12-h period. This 12-h period was the minimum amount of time needed for the experimental OA system to equilibrate with the new pCO_2 conditions and was chosen to simulate the rapid change in OA observed from the field (**Supplementary Figure 1.1**). Treatment conditions were maintained for 80 days.

Target pCO_2 gases were formulated by mixing compressed CO_2 with compressed CO_2-free air (control treatment) or with compressed air (moderate and high OA treatments) using solenoid-valve-controlled mass flow controllers at flow-rates proportional to the target pCO_2 conditions. Filtered seawater was introduced to each aquarium at a flow rate of 150 mL min^{-1}. The temperature of all experimental tanks was maintained at 17°C and was slowly increased to 19.5°C (**Supplementary Figure 1.2**) on days 39–51 of the experiment in an effort to stimulate gonad development for a companion experiment. It should be noted that this is a small temperature shift relative to what these oysters experience seasonally in their native habitats (**Supplementary Figure 1.1**). Oysters were fed 1% Shellfish Diet 1800® twice daily following best practices outlined in Helm and Bourne (2004).

Temperature, pH, and salinity of all tanks were measured three times per week (M,W, and F) for the duration of the experiment. Seawater pH was measured with an Accumet solid state pH electrode (precision = 1 mV) calibrated with pH 7.01 and pH 10.01 NBS buffers (for calibration slope) and Dickson seawater Certified Reference Material (for calibration intercept). Complete carbonate chemistry was determined for each tank every 2 weeks. In brief, seawater samples were collected every 2 weeks in 250 ml borosilicate ground-glass stoppered bottles sealed with vacuum grease from each tank and immediately poisoned with 100 µl saturated $HgCl_2$ solution, then refrigerated until analysis of dissolved inorganic carbon (DIC) and total alkalinity (TA) was performed. DIC, TA, salinity, and temperature were used to calculate calcite saturation state, pH, CO_3^{2-}, HCO_3^-, aqueous CO_2, and pCO_2 of each sample using CO_2SYS version 2.1 (Pierrot et al., 2011). Additional details about the experimental design and calculation of carbonate system parameters is provided in **Supplementary Method 1**.

Oyster EPF and tissue were sampled at six discrete time points (n_{total} = 108, n = 6 per treatment per time point, see **Supplementary Figure 1.3** for a schematic of the experimental design) that decreased in frequency throughout the duration of the experiment (time post 12-h ramp up period: 24, 48 h, 9, 22, 50, and 80 days). This sampling schedule was designed to capture rapid physiological changes that occurred during the onset of exposure and to examine long-term stability of physiological and molecular responses.

Phenotypic Data

Extrapallial Fluid Chemistry

Oyster pH_{EPF} was measured by removing each oyster from its tank, inserting a 5 mL syringe with a flexible 18-gauge polypropylene tip through the luer-lock port into the oyster's extrapallial cavity, and extracting ∼0.5–2 mL of extrapallial fluid. Care was taken to avoid puncturing the mantle tissue and inadvertently sampling either the hemolymph or stomach fluid. The pH_{EPF} was measured immediately after extraction with an Orion 91'10DJWP Double Junction micro-pH probe calibrated with pH 7.01 and 10.01 NBS buffers (for slope) and Dickson seawater Certified Reference Material (for intercept).

Calcification Rate

Net calcification rate was calculated for oysters surviving to either 50 or 80 days ($n_{calcification}$ = 11, 12, and 12 for control, 1,000 ppm, and 2,800 ppm treatments, respectively) from dry weights obtained at the start of the exposure and on day 33 or 34. Dry weights were estimated from buoyant weight measurements using the linear relationship between oyster dry weight and oyster buoyant weight derived empirically for oysters investigated in the present study (see Ries et al., 2009, for details). The average daily change in dry weight was divided by initial dry weight to standardize calcification rate for allometric effects, and multiplied by 100 to convert that fraction into a percent. See **Supplementary Method 2** for a complete description of the buoyant weight measurements and the estimation of the dry weights.

Tissue Collection

Patterns observed in pH_{EPF} over time informed the decision to focus molecular analyses on mantle edge tissue extracted on days 9 and 80 of the exposure in the control and high OA treatments (n_{tissue} = 6 per treatment per time point). For consistency and to minimize potential effects on mantle tissue arising from drilling of the oysters' right valves when installing the EPF extraction ports, mantle tissue was only collected from the left valve of the oysters (i.e., the side opposite of the EPF extraction port). Immediately following extraction of EPF at each time point, the oysters were shucked and the edge of the mantle tissue was sampled. Tissue was immediately flash frozen in liquid nitrogen before being transferred to a −80°C freezer for storage prior to DNA/RNA extraction.

Molecular Data

DNA Methylation Library Preparation and Quantification

DNA was isolated from the oyster mantle edge tissue samples using the E.Z.N.A. Mollusc Kit (Omega) pursuant to the

manufacturer's instructions. Isolated DNA was quantified, sonicated, and fragmentation was verified using a 2200 TapeStation System (Agilent Technologies, Santa Clara, CA, USA). Samples were enriched for methylated DNA using MethylMiner kit (Invitrogen, CA, USA), then sent to Zymo Research (Zymo,CA,USA) for bisulfite-conversion, library preparation, and sequencing. Libraries were sequenced on an Illumina HiSeq1500 platform with paired-end 100 bp sequencing.

Raw sequences were trimmed using TrimGalore! (v0.6.4; Martin, 2011) and aligned using Bismark (v0.22.3; Krueger and Andrews, 2011). Bismark was also used to determine the methylation status, methylated or unmethylated, for all sequenced CpGs. Files were then processed by performing a median based normalization of methylation counts among samples, destranding CpGs loci, and filtering loci that did not have at least 5x coverage for each sample using the R package methylKit (v1.10.0; Akalin et al., 2012). Finally, CpG loci were annotated by feature (e.g., introns, exons, and intergenic regions) and genomic coordinates using feature tracks created based on methods outlined in Venkataraman et al. (2020) and gene annotation file available on NCBI (Accession: GCA_002022765.4). Hereafter, "gene body" is used to reference the transcriptional region of the gene, which includes exons, introns, and untranslated regions, but not promoters. See the **Supplementary Method 3** for a detailed description of this pipeline.

RNA Library Preparation and Quantification

RNA was extracted from the same mantle tissues used for DNA methylation using TRI Reagent Protocol (Applied Biosystems) following manufacturer's instructions. A cDNA library was constructed for each sample using a TruSeq Stranded mRNA kit (Illumina, Cat# RS-122-2101) following manufacturer's instructions. Library fragment size was determined using a BioAnalyzer (RNA 6000 Nano Kit; Agilent, CA, USA) and concentration was quantified on a Qubit (Qubit High Sensitivity RNA Kit; Invitrogen,CA,USA). Samples were sent to Genewiz (NJ,USA) for library preparation and sequencing. Libraries were sequenced on two lanes (12 individuals/lane) of an Illumina HiSeq 3000 platform with paired-end 200 bp sequencing.

RNA reads were trimmed for quality using Trimmomatic (v0.32; Bolger et al., 2014) and mapped to the oyster genome (Accession: GCA_002022765.4) using STAR (v.2.7.0; Dobin et al., 2013). Expression levels for each gene were quantified using RSEM (v1.3.2; Li and Dewey, 2011). Single sample gene count estimates were combined into count matrices (number of samples × number of genes) using a custom shell script (see Data Accessibility for additional script information), then filtered to remove genes that did not contain at least 1 count per million transcripts in at least 80% of individuals within at least one treatment-time experimental level. Expression data was then normalized using the "TMMwsp" method, transformed into log2 counts per million (log2-cpm), and sampled weighted in the R package "limma" (v3.40.6; Ritchie et al., 2015). See the **Supplementary Method 4** for a more detailed description of this pipeline.

Statistical Analyses

All statistical analysis was performed in R (v3.6.0; R Core Team 2019), using the graphical user interface RStudio (v1.2.1335; R Studio Team 2018). See Data Accessibility for R scripts.

Extrapallial Fluid pH (pH_{EPF}) and Calcification Response

We tested the hypothesis that *C. virginica* pH_{EPF} was associated with OA by using a linear mixed model. The full model included the explanatory variables of treatment, time, and their interaction as categorical fixed effects, and tank (nested within block) and oyster collection site as random effects. We conducted two analyses, one for each of the following response variables: (1) the measured value of pH_{EPF} and (2) pH_{EPF} relative to treatment $pH_{seawater}$ [$\Delta pH = pH_{EPF} - pH_{seawater}$; a metric used previously by Liu et al. (2020) as a better indicator of active pH_{EPF} regulation]. Each model was performed in R using the *lme4* package (v1.1-21; Bates et al., 2015). A step-down strategy using likelihood ratio tests (based on the degrees of freedom estimated using the Satterthwaite method) was implemented in *lmerTest*, following the principle of marginality to select the most parsimonious model (v3.1-0; Kuznetsova et al., 2017). To evaluate significant differences in EPF chemistry (both pH_{EPF} and ΔpH) between the moderate and high OA treatments compared to the control treatment for each time point, *post-hoc* comparisons with a Tukey correction were performed using the *multcomp* package (v1.4-10; Hothorn et al., 2008). In addition, single sample *t*-tests were performed to test whether ΔpH was significantly different from 0 (i.e., pH_{EPF} was significantly different than $pH_{seawater}$) for oysters under each treatment at each time point. We corrected for testing multiple hypotheses using a Benjamini-Hochberg correction (Benjamini and Hochberg, 1995).

We examined the effect of pCO_2 on long-term EPF response (both measured pH_{EPF} and ΔpH) using linear mixed effect models. The full models included EPF response (pH_{EPF} or ΔpH) as the response variable, treatment and time and their interaction as categorical fixed effects, and tank (nested within block) and oyster collection site as random effects. Only samples from day-50 and day 80 time points were included in the model in order to investigate long-term trends in EPF response. Model selection and *post-hoc* comparisons were performed using the approach described in the previous paragraph.

We tested the hypothesis that calcification rate was associated with OA or pH_{EPF} using linear-mixed effect models. The full models included calcification rate as the response variable, either pH_{EPF} or treatment as a fixed effect, and tank (nested in block) and collection site as random effects. Time was not included as a fixed effect because calcification rate of oysters was measured across a single time interval (day 0 to day 33 or day 34). Treatment was handled as a continuous variable and was calculated as the average pCO_2 for each tank between days 0 and 33 or 34. Model selection was performed using the approach described in the first paragraph of this section. Regression analysis was used to examine the effect of either treatment or pH_{EPF} on calcification rate.

Genome-Wide Molecular Response

To test the hypothesis that OA-induced changes in the transcriptome and methylome, we examined genome-wide gene expression and gene body DNA methylation using a principal components analysis (PCA) and PERMANOVA approach to visualize and test for differences amongst treatments and time points. The PERMANOVA was based on Manhattan distances and tested the null hypothesis of no effect of treatment, time, or their interaction on global gene expression and DNA methylation patterns using the R package *vegan* (*v2.5-5*; Dixon, 2003). To further investigate the stability of changes in genome-wide variation (gene expression or DNA methylation) induced by OA over time, we used a discriminant analysis of principal components (DAPC) performed with the R package adegenet (v2.1.2; Jombart et al., 2010). For our analysis DAPC was used to generate a discriminant function that maximally differentiated between treatment using samples from day 9, then we predicted where samples from day 80 would fall along this discriminant function to evaluate whether samples exhibited similar patterns of molecular differentiation across time. This allowed us to evaluate if changes that differentiated molecular variation among treatments at day 9 were similarly differentiated at day 80 (i.e., stable through time). See the **Supplementary Method 5** for additional information on specific parameters used for the PERMANOVA and DAPC analyses.

Next, we further examined the hypothesis that OA induced changes in global DNA methylation by using a linear model to look at the effect of treatment, time, and feature (i.e., exon, intron, and intergenic region) on global methylation. Global methylation in this case was summarized as the median methylation across all CpGs within a feature for each sample.

Differential Molecular Response

The hypothesis that individual genes within the transcriptome were sensitive to OA was tested *via* differential gene expression analysis performed using a generalized linear model approach implemented in the R package *limma* (v3.40.6; Ritchie et al., 2015), using treatment, time, and their interaction as fixed effects. Site was not considered in this analysis given that it did not have a significant effect on either the phenotypic or genome-wide responses. Genes with FDR ≤ 0.05 and absolute value of $\log_2$ fold ≥ 2 were considered differentially expressed.

We tested the hypothesis that OA induced changes in DNA methylation at individual CpGs (differentially methylated loci or DML) by performing a logistic regression using treatment as a fixed effect and time as a covariate implemented in the R package methylKit (v1.10.0; Akalin et al., 2012) using the default "slim" method to correct *P*-values. We also performed additional logistic regressions separately for each time point including treatment as a fixed effect. Only CpGs with coverage $\geq$5 for all samples were considered. Loci that had differential methylation of at least 50% between groups being compared and a *q*-value of <0.01 were considered significant. See the **Supplementary Method 6** for additional information on the differential methylation and gene expression analyses.

Gene Co-expression Network Analysis

Clustering genes with similar levels of expression among individuals can help identify groups of genes that may be operating together, such as genes located within the same pathway. The response of these clusters to stress or stimulus can then be evaluated, which can potentially lead to the detection of transcriptomic responses that might otherwise be too subtle to be detected by standard gene-level differential expression analysis. We used a weight gene co-expression network analysis implemented in the R package WGCNA (v1.68; Langfelder and Horvath, 2008) to identify and cluster genes that co-express among individual oysters in order to reexamine the hypothesis that OA induced changes in gene expression and specifically evaluate whether particular clusters of genes respond to OA. We also used these gene clusters to evaluate the hypotheses that OA-induced changes in gene expression are (i) associated with shifts in DNA methylation and (ii) associated with regulation of the pH_{EPF}. In brief, we followed a standard WGCNA pipeline which identified clusters of genes, termed modules, based on their level of dissimilarity among all individuals (regardless of treatment or time point) using the "Ward.D2" method for clustering (Murtagh and Legendre, 2014). Expression of each module for each individual was estimated as the eigenvalue (i.e., the first principal component value for each individual) from a PCA of an expression matrix generated from all genes included in the module for each individual. Similarly, DNA methylation was averaged for all CpGs located within genes included in a module to generate a single methylation value per individual. Linear regressions were used to identify gene expression modules that were significantly associated with EPF response (i.e., ΔpH) and to test whether the expression of these modules was also associated with gene body methylation. See **Supplementary Method 7** for additional details on the steps used in the WGCNA analysis and follow-up statistical analyses.

Functional Enrichment Analysis

As part of the hypothesis that OA induces changes in both gene expression and DNA methylation, we performed a functional enrichment test to investigate whether particular gene ontology (GO) categories were enriched in OA-induced molecular responses (either in gene expression or methylation) using GO-MWU, a rank-based gene enrichment method developed by Wright et al. (2015). We performed this analysis separately for each time point using the $\log_2$-fold change in gene expression and the difference in mean methylation among treatments. Mean methylation was calculated as the mean among all CpG loci within a gene across all individuals within a particular treatment and time point. Only genes with at least 5 CpG loci were considered for the analysis to ensure mean methylation estimates were based on genes with at least moderate CpGs coverage. We also used this analysis to determine if gene modules that were significantly associated with EPF (as determined in the previous section) were enriched in particular GO categories based on the module membership values for each gene within the module. These scores represent a measure of strength for each gene's membership to that module and are used here to determine if particular GO categories are enriched in each module. This

analysis was run separately for GO categories associated with molecular function, biological process, and cellular components. A 10% FDR correction (GO-MWU default) was used to adjust for multiple comparisons. See **Supplementary Method 8** for additional details on the GO-MWU analysis.

Gene-Level Characterization of Gene Expression and DNA Methylation

The hypothesis that DNA methylation correlates gene expression was tested using a PCA-based approach (described in Gavery and Roberts, 2013) to examine the relationship between gene expression, DNA methylation, and gene attributes (e.g., gene length and number of exons). The following variables were used in the input matrix for the PCA: mean gene expression over all treatments (mean log2-cpm values); the coefficient of variation (CV) in gene expression among treatment means; mean DNA methylation level over all treatments; the DNA methylation CV among treatment means, gene length, exon number per gene; and the number of CpGs per gene (scripts for generating each variable within the matrix are available on the github repository). Gene attributes were normalized by log transformation.

RESULTS

Experimental Seawater Chemistry

After a 33-day acclimation period (pCO_2 547.3 ± 20.2 ppm), tanks were incrementally adjusted to the target pCO_2 of the three experimental treatments (mean ± SEM, control: pCO_2 579.1 ± 16.5 ppm, moderate OA: pCO_2 1050.4 ± 47.5 ppm, high OA: pCO_2 2728.6 ± 128.0 ppm, **Supplementary Table 1.1**).

Extrapallial Fluid Chemistry and Calcification Response

We tested the hypothesis that *C. virginica* pH_{EPF} was associated with OA using a linear model that included both fixed effects (treatment and time), their interaction, and the random effect of tank nested within block. There was a significant effect of treatment ($F_{2,14.783=5.8206}$; $P = 0.0137$) and the interaction between time and treatment ($F_{10,74.002=2.412}$; $P = 0.0153$) on pH_{EPF} evaluated across all 6 time points. *Post-hoc* tests revealed a significant decrease in pH_{EPF} within the high OA treatment compared to the control condition at the onset of the exposure (48 h), no difference on days 9–22, and a significant decrease on the final two time points (days 50 and 80; **Figure 1A**).

A slightly different result was found when we examined ΔpH (pH_{EPF} - $pH_{seawater}$) using a model that included both fixed effects (treatment and time), their interaction, and the random effect of tank nested within block. Both treatment ($F_{2,14.818=18.9487}$; $P = 0.0001$) and the interaction between treatment and time ($F_{10,74.036=2.0117}$; $P = 0.0439$) were significant, while the independent effect of time ($F_{5,74.050=0.935}$; $P = 0.4637$) was not significant (**Figure 1B**). *Post-hoc* comparisons between the control treatment and each OA treatment revealed a significant increase in ΔpH under the high OA treatment relative to the control treatment at the onset of the exposure (9–22 days, **Figure 1B**, "Trt"). By days 50 and 80, ΔpH was no longer statistically different amongst treatments, although mean ΔpH in both OA treatments were higher than ΔpH in the control. One-tailed *t*-tests showed that ΔpH of oysters in all treatments was significantly lower than 0 (i.e., the pH_{EPF} was more acidic than the $pH_{seawater}$) at almost all time points of the experiment (**Figure 1B**, "Env"), indicating a strong tendency for oysters to maintain a more acidic EPF fluid relative to their environment. The exception to the trend was the high OA treatment at day 9, where pH_{EPF} was not significantly lower than $pH_{seawater}$ (**Figure 1B**).

We examined the long-term pH_{EPF} and ΔpH responses (i.e., conditions on days 50 and 80) using a model that included treatment as a fixed effect. Treatment was a significant predictor of both pH_{EPF} ($F_{2,29} = 22.438$, $P < 0.0001$) and ΔpH ($F_{2,29} = 7.982$, $P = 0.0018$; **Figures 2A,B**). The *post-hoc* tests revealed a significant decrease in pH_{EPF} in the high OA treatment relative to both the control and moderate OA treatments, and showed an increase in ΔpH in the two OA treatments relative to ΔpH in the control.

Lastly, we found that calcification rate decreased in response to OA ($R^2 = 0.409$, $P = <0.0001$), which was driven largely by the substantial decline in calcification rate between the moderate and high OA treatments (**Figure 2C**). The decline in calcification rate was also associated with a significant decrease in pH_{EPF} ($R^2 = 0.112$, $P = 0.028$, **Figure 2D**).

DNA Methylation Responses to OA

Approximately 1.4 billion paired-end 80 bp reads of MBD-enriched, bisulfite treated DNA were obtained across the all sequenced samples (NCBI BioProject ID: PRJNA594029, see **Supplementary Table 3.1** for sequence coverage details). A total of 622.4 million quality filtered reads mapped to the *C. virginica* genome (88.3% of all CpGs in the genome, **Supplementary Table 3.2**). A single individual within the control treatment on day 9 was removed from downstream analysis due to poor sequencing depth and a high rate of gene duplication error after mapping ($n_{tissue} = 23$). After filtering, we retained 403,976 CpGs with at least 5x coverage for each of the remaining 23 samples (**Supplementary Table 3.2**). Of the CpGs with at least 5x coverage, 94.1% were located within gene bodies, with 59.9% CpGs located in exons among 27,932 genes (**Figure 3A**; "$CpGs_5$"). CpGs with a minimum of 5x coverage in each sample were used for the downstream analyses.

We used a PERMANOVA to test the hypothesis that OA induced changes in genome-wide gene body methylation. We found significant differences in global methylation due to treatment (*Adonis* $P_{Trt} = 0.027$), but not due to time (*Adonis* $P_{Time} = 0.235$) or the interaction between treatment and time (*Adonis* $P_{TimexTrt} = 0.364$; **Figure 3B**). This was supported by the DAPC, which found gene body methylation that was differentiated at day 9 was not maintained at day 80 (**Figure 3C**). Moreover, global median methylation was significantly lower in the high OA treatment compared with the control treatment (hypomethylation, **Figure 3D**, $P_{Trt} < 0.0001$), but significantly increased through time (hypermethylation, $P_{Time} = 0.001$). However, this increase through time only led to a 1–5% shift in methylation when averaged over all loci in the genome. Feature

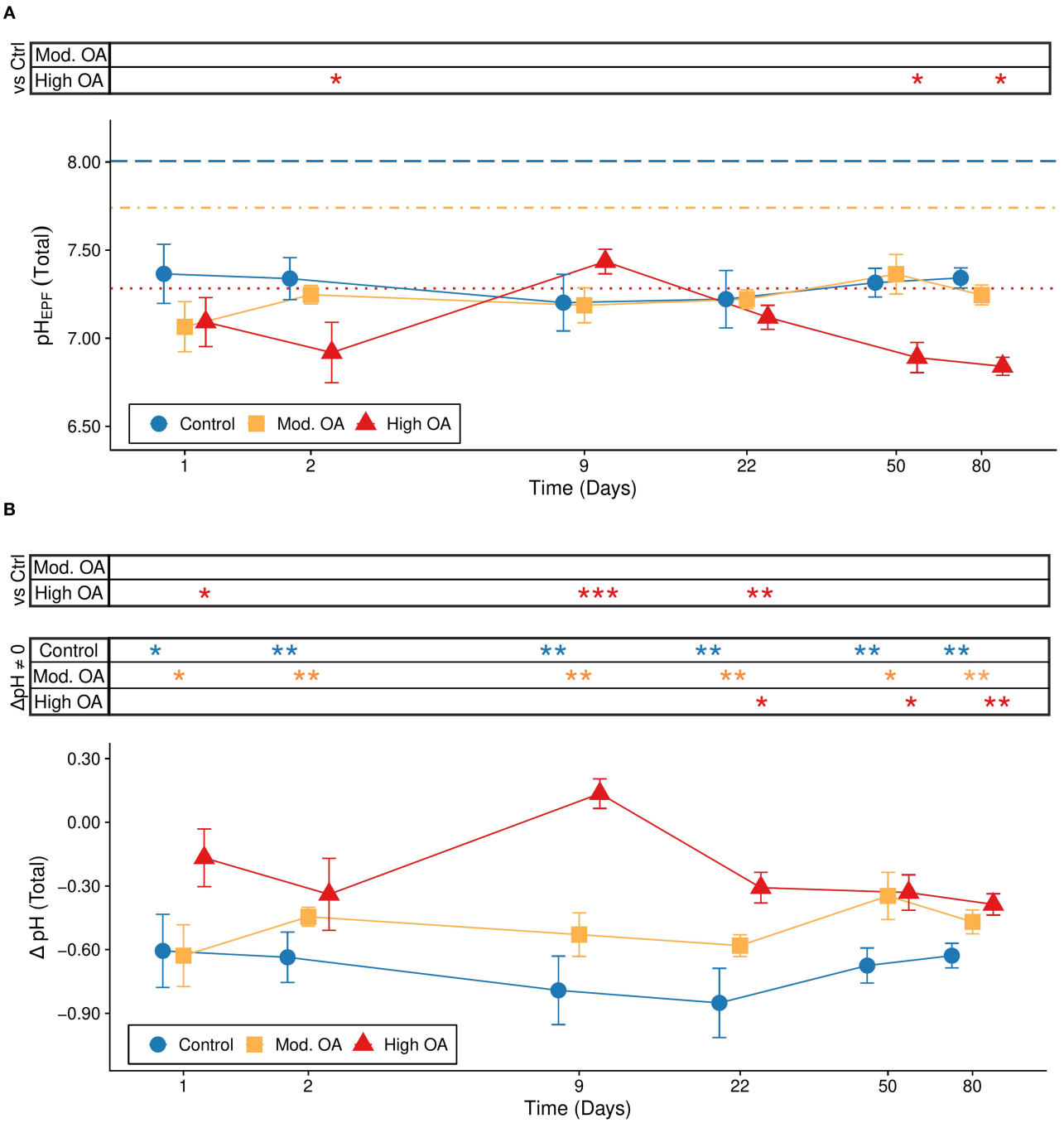

FIGURE 1 | Extrapallial fluid pH over the 80 day experiment. **(A)** pH_{EPF} (total scale) and **(B)** ΔpH (pH_{EPF} – $pH_{seawater}$) across time with standard error bars. **(A)** Colored lines represent each treatment level averaged over the duration of the exposure (dashed: control, dot-dashed: moderate OA, dotted: high OA) and symbols at the top of the graph indicate if the pH_{EPF} in one of the OA treatments ("Mod. OA", 1,000 μatm; "High OA", 2,800 μatm) was significantly different from the pH_{EPF} in the control treatment ("Control", 580 μatm) for each time point (e.g., H_0: Control pH_{EPF} = High OA pH_{EPF}). **(B)** Symbols at the top of the graph indicate significant post hoc tests. The "vs. Ctrl" comparisons indicate time points where ΔpH in one or both of the OA treatments was significantly different from the ΔpH in the control treatment (e.g., H_0: Control ΔpH = High OA ΔpH), while "ΔpH ≠ 0" comparisons indicate time points where ΔpH in one of the treatments was significantly different from 0 (e.g., H_0: Control ΔpH = 0). The latter comparison is equivalent to evaluating whether pH_{EPF} of a particular treatment is significantly different from its respective $pH_{seawater}$. Statistical significance is denoted by asterisks ($^{***}P < 0.001$, $^{**}P < 0.01$, $^{*}P < 0.05$). Time points are presented on a non-linear scale and treatment points within time points were staggered along the x-axis to improve visualization.

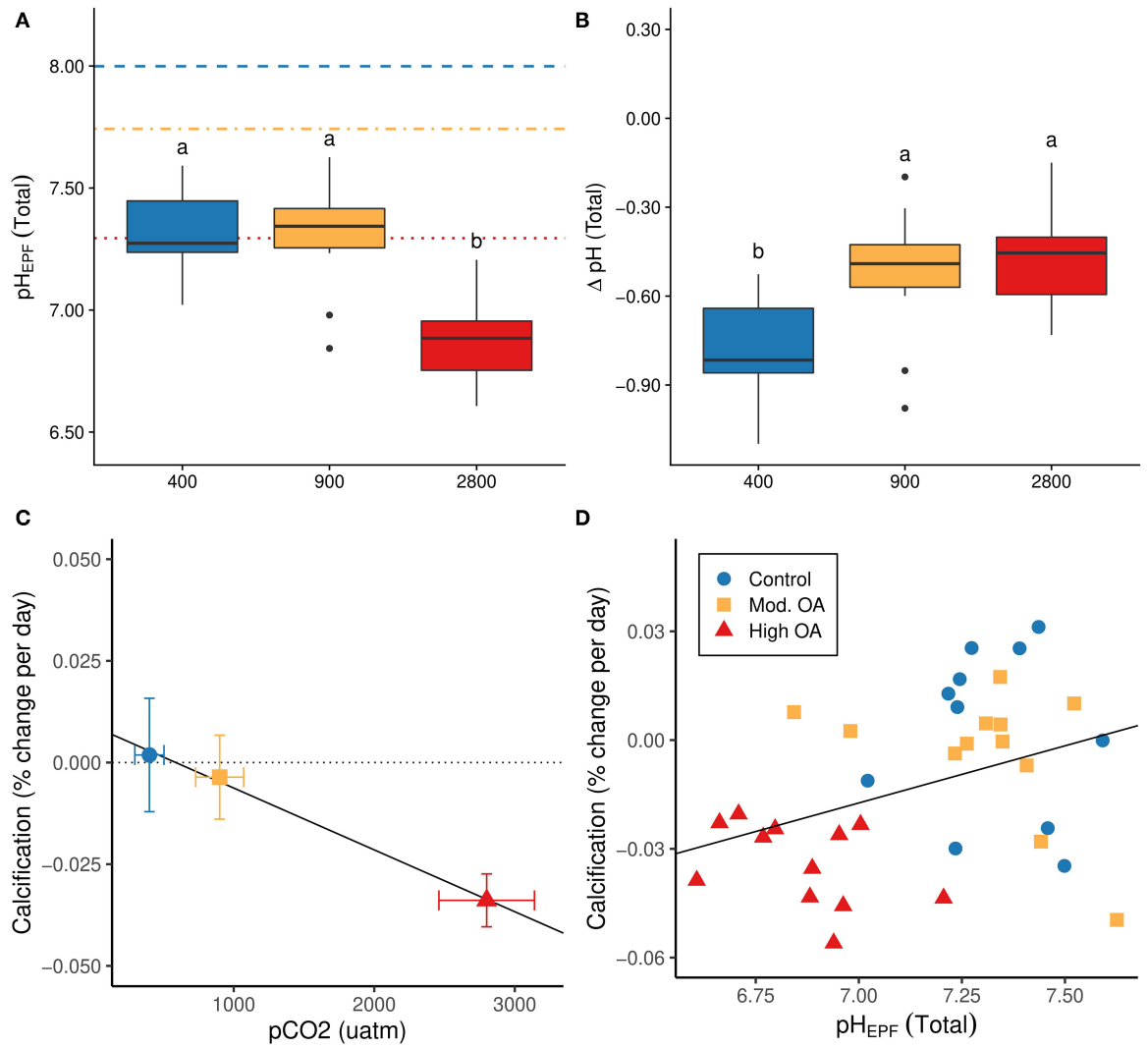

FIGURE 2 | Long term trends in pH_{EPF}, ΔpH, and calcification. **(A)** Long-term average pH_{EPF} (total scale) by treatment; horizontal lines indicate mean seawater pH for the three treatments (dashed: control, dot-dashed: moderate OA, dotted: high OA). **(B)** Long-term average ΔpH (pH_{EPF} – $pH_{seawater}$; total scale) by treatment. **(C)** Percent daily calcification rate (%-change in shell mass/day) by treatment (*slope* = −1.751e-05, $P < 0.0001$, $R^2 = 0.409$), dotted line indicates calcification rate of zero percent and solid black line represents fitted regression. **(D)** Calcification rate vs. pH_{EPF} (*slope* = 0.032, $P = 0.028$, $R^2 = 0.112$); solid black line represents fitted regression. pH_{EPF} measured on day 50 or 80 ($n = 35$). Letters on first two panels **(A,B)** represent levels of significance based on *post hoc* testing, while bars on **(C)** represent standard errors.

had the greatest effect on global median methylation ($P_{Feature} <$ 0.0001), with exons exhibiting the highest levels of methylation.

The hypothesis that OA induced changes in the DNA methylation of specific CpGs was evaluated using a logistic regression approach implemented in methylKit. The initial model contained all samples and included treatment as the main effect and time as a covariate (**Figure 3A**; "DML_{Trt}"). Only 2 CpGs were found to be differentially methylated by treatment, both located in gene bodies. Next, we looked at each time point separately including only treatment as the main effect (**Figure 3A**; day 9—"DML_{Trt_D09};" day 80—"DML_{Trt_D80}"). This led to the additional discovery of 83 DMLs by treatment (25 DML on day 9 and 58 DML on day 80; **Figure 3A**). An additional 50 DML were significant through time in the control treatment, although there was little overlap between these DML and those responding to OA (**Figure 3E**). Additionally, we saw no overlap of specific DML by treatment among days (**Figure 3E**), further illustrating that the loci induced by OA shifted through time as indicated by the DAPC (**Figure 3C**).

Of the 85 DML there was little functional overlap among DML at each time point, with the exception of several genes associated with the THO complex, a nuclear structure composed of multiple proteins involved in transcription elongation and mRNA maturation (**Supplementary Table 3.3**). On day 80, we found DML in several biomineralization and/or stress response related genes, including cadherin, protein ubiquitination, and

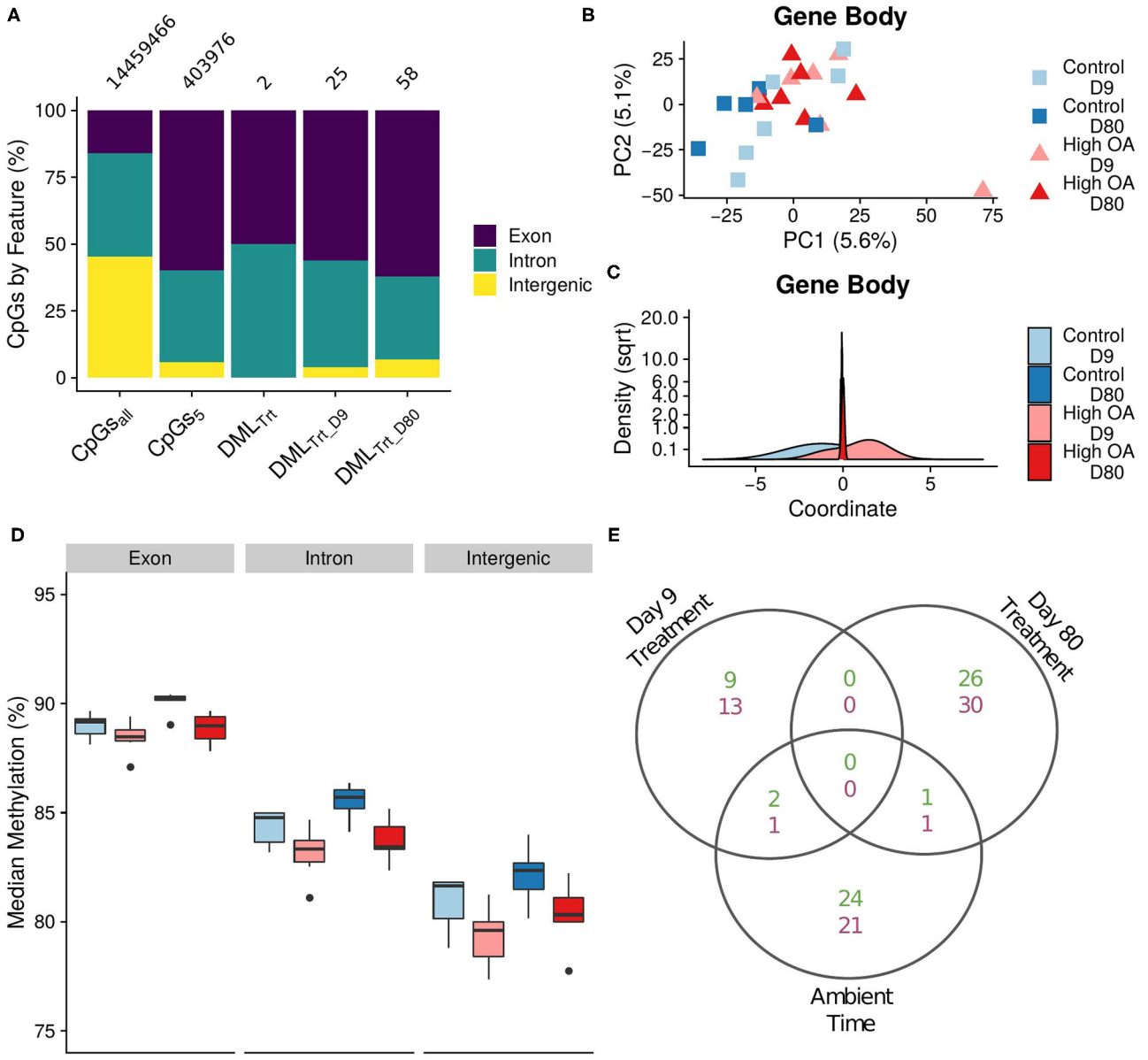

FIGURE 3 | DNA methylation responses to OA. **(A)** Proportion of CpGs by feature across data subsets. $CpGs_{all}$: all CpGs in genome; $CpGs_5$: CpGs with at least 5X coverage for each individual; DML_{Trt}: differentially methylated loci (DMLs) between control and OA treatments across both time points; DML_{Trt_09} and DML_{Trt_80}: DMLs between treatments on day 9 and 80, respectively. Numbers above the bars represent the total number of CpGs for each group. **(B)** Boxplot of median global methylation for each sample by genome feature ($P_{Trt} < 0.0001$, $P_{Time} = 0.001$, $P_{Feature} < 0.0001$). **(C)** Plot of the first two principal components from a principal components analysis ($P_{Trt} = 0.027$, $P_{Time} = 0.235$, $P_{TimexTrt} = 0.364$), and **(D)** density plot of the discriminant values from a DAPC based on gene body methylation (exons and introns). Discriminant values were determined by a function that maximally discriminates between treatment using samples from day 9, then the discriminant value for each sample from day 80 was predicted using the same discriminant function. **(E)** Venn diagram of DMLs among treatments for each day (Day 9 Treatment and Day 80 Treatment) and among time points in the control treatment (Control Time). Overlapping regions indicate DMLs shared among comparisons. Hypermethylated DMLs in green (top number), hypomethylated DMLs in purple (bottom number).

death effector domain-containing genes. Two GO categories were enriched in hypomethylated CpGs, the cellular component "amidotransferase complex" on day 9 and the biological process "biosynthetic process" on day 80 (**Table 1**). No categories were shared among time points.

Gene Expression Responses to OA

RNA sequencing yielded a total of 955 million paired-end reads (NCBI BioProject ID: PRJNA594029) from all sequenced samples (see **Supplementary Table 4.1** for read coverage and mapping details). Reads mapped to 37,098 genes, of which

TABLE 1 | Gene ontology (GO) categories enriched in differentially responsive genes by treatment, summarized by molecular function (MF), biological process (BP), and cellular component (CC).

Category	Day	Direction in OA treatment	Name	Delta rank	P (adj)
Gene expression					
BP	9	Down regulated	Signal transduction	−192	0.0058
BP	9	Up regulated	Biosynthetic process	235	0.0058
BP	9	Up regulated	**Cellular nitrogen compound metabolic process**	164	0.0315
BP	9	Down regulated	G protein-coupled receptor signaling pathway	−227	0.0315
BP	9	Up regulated	**DNA metabolic process**	336	0.0334
BP	80	Down regulated	Macromolecule modification	−374	<0.0001
BP	80	Down regulated	Dephosphorylation	−523	<0.0001
BP	80	Down regulated	Phosphorus metabolic process	−288	<0.0001
BP	80	Up regulated	**DNA metabolic process**	421	0.0008
BP	80	Down regulated	Protein metabolic process	−200	0.0012
BP	80	Up regulated	**Cellular nitrogen compound metabolic process**	178	0.0054
BP	80	Up regulated	DNA recombination	532	0.0211
BP	80	Up regulated	Glutamine family amino acid metabolic process	535	0.0281
BP	80	Up regulated	Glutamate biosynthetic process	1676	0.0443
BP	80	Up regulated	Dicarboxylic acid biosynthetic process	1237	0.0443
BP	80	Up regulated	Macromolecule biosynthetic process	263	0.0474
CC	9	Down regulated	**Transcription factor complex**	−147	0.0170
CC	9	Up regulated	Ribosome	169	0.0431
CC	9	Up regulated	Intracellular non-membrane-bounded organelle	139	0.0454
CC	80	Down regulated	**Transcription factor complex**	−159	0.0045
CC	80	Down regulated	Protein-containing complex	−105	0.0154
MF	80	Up regulated	DNA binding	352	0.0245
MF	80	Up regulated	RNA-DNA hybrid ribonuclease activity	1320	0.0245
MF	80	Up regulated	Oxidoreductase activity	219	0.0245
MF	80	Up regulated	Oxidoreductase activity *	321	0.0245
MF	80	Up regulated	Double-stranded DNA binding	905	0.0487
DNA Methylation					
BP	80	Hypomethylated	Cellular modified amino acid biosynthetic process	−4437	0.0333
CC	9	Hypomethylated	Glutamyl-tRNA(Gln) amidotransferase complex	−8528	0.0179

*Up- and down-regulation refers to the change in gene expression in the high OA treatment relative to the control treatment (i.e., the GO categories enriched in up-regulated genes had higher gene expression under high OA compared to the control treatment). Similarly, hypomethylation indicates the GO category was enriched with CpG loci (DNAm) that were less methylated under high OA relative to the control treatment. Names in bold represent GO categories enriched at both time points. The full category name for "oxidoreductase activity *" is "oxidoreductase activity, acting on paired donors, with incorporation or reduction of molecular oxygen." The "Delta Rank" column provides a summary statistic generated by the Mann Whitney U test, while the "P (adj)" column contains P-values corrected using a Benjamini-Hochberg false discovery rate procedure.*

20,387 remained after filtering (**Supplementary Table 4.2**). An exploratory PCA highlighted a single individual in the day 80 control treatment as an outlier compared to all other samples, which was subsequently removed from downstream analysis ($n_{tissue} = 23$).

The hypothesis that OA induced changes in genome-wide gene expression was evaluated with PERMANOVA. We found that treatment ($R^2 = 0.051$, *Adonis* $P = 0.037$) and time ($R^2 = 0.067$, *Adonis* $P = < 0.001$), but not their interaction (*Adonis* $P = 0.214$), had a subtle but statistically significant impact on genome-wide gene expression (**Figure 4A**). The DAPC showed that the global patterns of gene expression that differentiated the two treatments at day 9 were not maintained at day 80, with the strongest directional change along the discriminant function in the day 80 samples occurring in the high OA treatment (**Figure 4B**).

We also tested the prediction that the transcriptome in oysters is sensitive to OA by looking at the response of individual genes using differential expression analysis. Interestingly, no individual genes were significantly differentially expressed between treatments, including a number of genes known from the literature to be associated with biomineralization (**Supplementary Table 4.3**; **Supplementary Figure 4.1**). However, biomineralization-associated genes tended to be overexpressed relative to the mean expression level for all genes in both control and OA treatments (**Supplementary Figure 4.2**), which suggests that their activity is elevated within the mantle tissue.

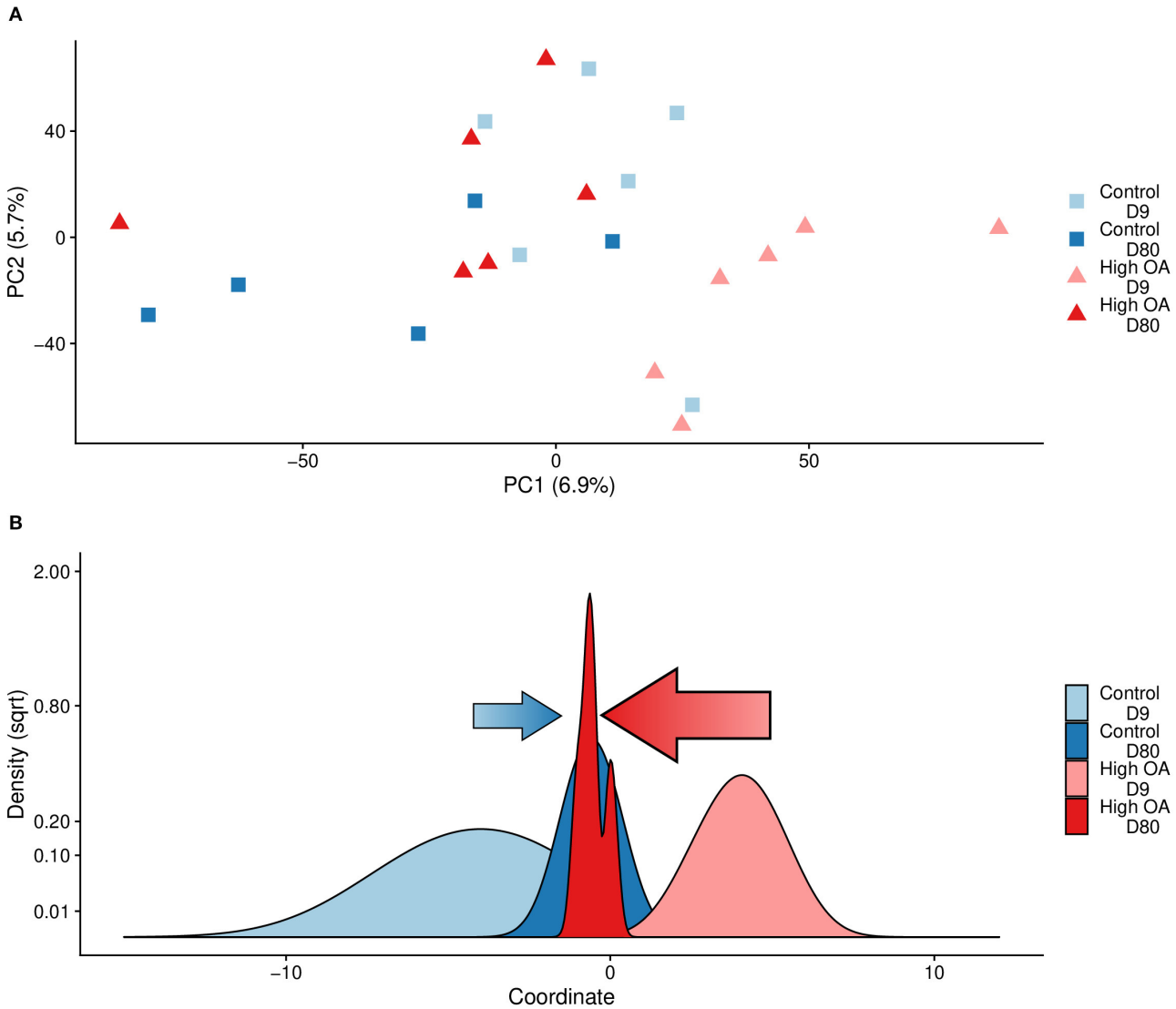

FIGURE 4 | Global transcriptomic responses to OA. **(A)** Plot of the first two principal components from a principal components analysis ($P_{Trt} = 0.037$, $P_{Time} < 0.001$, $P_{TimexTrt} = 0.214$). **(B)** Density plot of the discriminant values from a DAPC. Discriminant values were determined by using the DAPC package to estimate a function that maximally discriminates between treatment using samples from day 9, then the discriminant value for each sample from day 80 was predicted using the same discriminant function. Arrows indicate direction and degree of movement of expression patterns for control (blue) or OA (red) treatments along the discriminant function from day 9 to day 80. Both plots are based on log2-cpm gene expression.

We also tested whether OA induced changes in particular GO categories using a GO enrichment analysis implemented in GO-MWU. Several GO categories were found to be enriched in genes both up- and down-regulated within the high OA treatment relative to the control treatment (**Table 1**), but few GO categories appeared to be shared among time points. The exceptions were two categories enriched in genes up-regulated ("DNA metabolic process" and "cellular nitrogen metabolic processes") and one enriched in genes down-regulated ("transcription factor complex") in the high OA treatment. Overall, more GO categories were enriched on day 80, including several metabolism and biosynthesis related biological processes. Several GO categories associated with oxidoreductase activity were also up-regulated on day 80.

Investigating Associations Between DNA Methylation, Gene Expression, and pH_{EPF}

The following comparative analyses (next two sections) were performed using samples where gene expression and DNA methylation data overlapped ($n_{tissue} = 22$). Only genes with at least 20% coverage of all CpGs were included in the analyses, which represents a reasonable trade-off between maximizing the number of retained genes in the analyses while

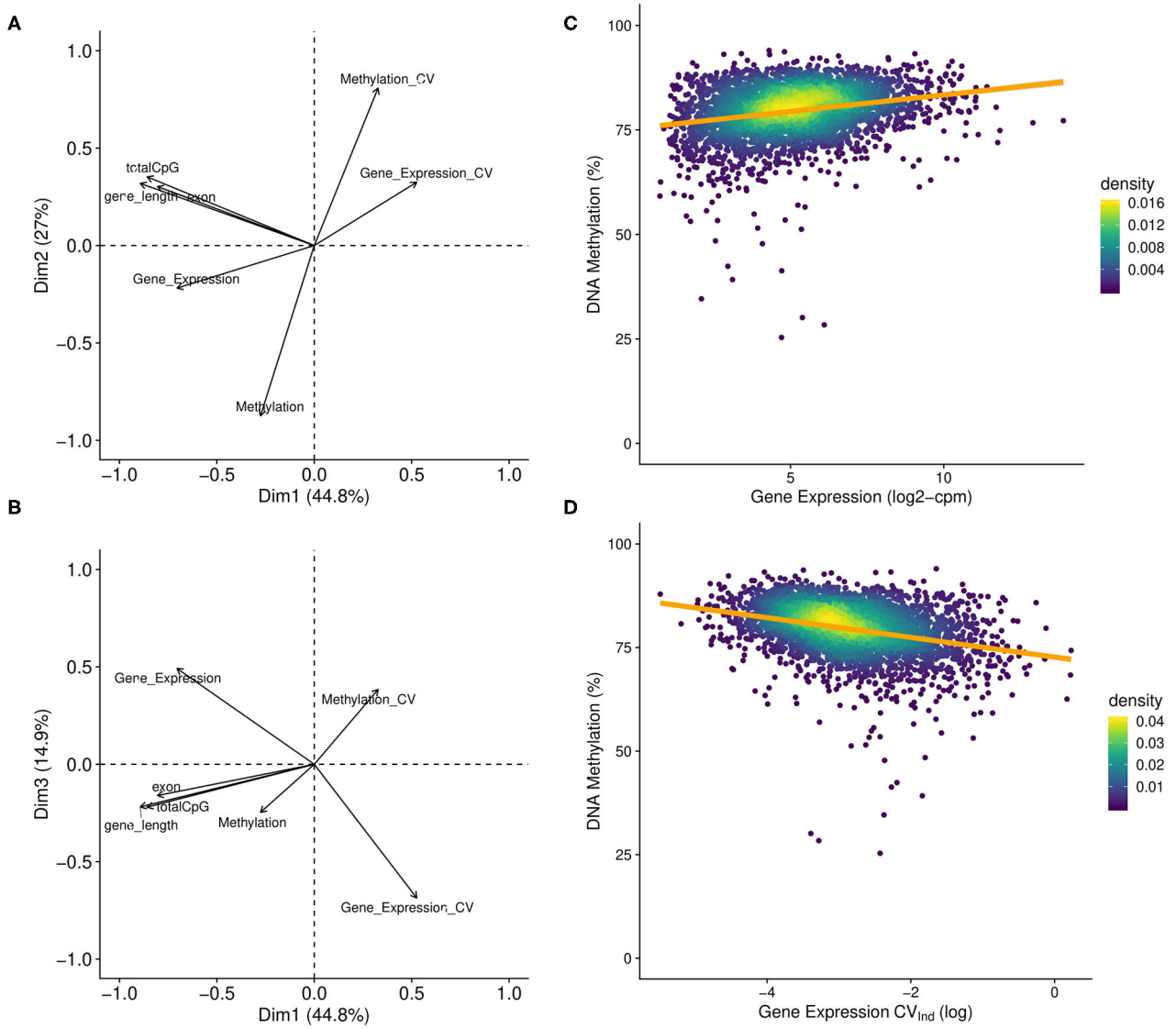

FIGURE 5 | DNA methylation and gene expression correlations. **(A)** First two principal components and **(B)** the first and third components from a principle component analysis that included gene level summary variables for various attributes, expression, and methylation. Variable loadings plotted as arrows, with the length of the arrow corresponding to the relative contribution to PC variance. Significant loadings on the first two PCs included: mean methylation level (Methylation), the coefficient of variance of mean methylation levels among treatments (Methylation_CV), gene expression (Gene_Expression), the number of exons (exon), the number of CpG dinucleotides (totalCpGs), and the gene length in base pairs (gene_length). The CV of gene expression (Expression_CV) was not significant for the first two PCs but was the primary contributor to the third PC (see **Supplementary Material S3.3**) **(C,D)**. Plot of gene level DNA methylation against either **(C)** gene expression or the **(D)** gene expression CV among individuals based samples collected in the control treatment at day 9 (Gene Expression – $R_2 = 0.0624$, $P < 0.0001$; Gene Expression CV_{Ind} – $R_2 = 0.0658$, $P < 0.0001$). Only genes with coverage for at least 20% of all CpGs within the gene were included ($n = 3,604$).

removing genes with limited or no DNA methylation data (**Supplementary Figure 3.1**).

Associations Between DNA Methylation and Gene Expression

To test the hypothesis that DNA methylation is correlated with gene expression, we used a PCA that included measures of DNA methylation, gene expression, and other gene attributes. We found the first three PC axes explained >85% of the variance in the data (**Figures 5A,B**). PC1 was dominated by gene features, including a negative association with the length of the gene (*PC axis loading, percent contribution to PC axis*; gene_length: −0.504, 27%), the number of exons (exon: −0.454, 22%), the number of CpGs (totalCpG: −0.484, 25%). PC2 was loaded positively by mean methylation (−0.636, 40%), and negatively by methylation variation among treatments (Methylation_CV: 0.588, 33%), suggesting a negative relationship between percent methylation and the amount of variation in

methylation among treatments. Finally, PC3 was dominated by gene expression (0.482, 23%), variation in expression among individuals (Gene_Expression_CV: −0.672, 46%), and methylation variation among treatments (Methylation_CV: 0.376, 15%), indicating a positive relationship between variation in methylation and gene expression and a negative relationship between gene expression and gene expression variation. Importantly, these patterns were robust even under increasingly stringent DNA methylation coverage scenarios (**Supplementary Figures 3.2, 3.3**). Finally, simple linear regression found that gene expression exhibited a significant positive relationship with gene body methylation ($R^2 = 0.0624$, $P < 0.0001$; **Figure 5C**), while the variation in expression had a significant negative relationship with gene body methylation ($R^2 = 0.0658$, $P < 0.0001$; **Figure 5D**).

OA-Induced Shifts in DNA Methylation, Gene Expression, and pH_{EPF}

We tested the hypothesis that shifts in DNA methylation were associated with OA-induced changes in gene expression using regression analysis, with log2-fold change in gene expression as the response variable and the percent change in mean gene methylation (i.e., average DNA methylation for all CpGs with coverage in a gene) as a fixed effect. We found there was a significant positive effect of gene methylation changes, but the slope was very small and <2% of the variance in the log2-fold change in gene expression was explained by gene methylation changes (day 9—slope = 0.0121, $P < 0.0001$, $R^2 < 0.012$; day 80—slope = 0.0137, $P < 0.0001$, $R^2 = 0.014$; **Figure 6A**). This indicates that there was a weak but statistically significant relationship between DNA methylation and gene expression.

This weak relationship may have resulted from averaging methylation within each gene body, so regression analysis was used to examine the relationship between the change in methylation for each DML and the log2-fold change in expression of each corresponding gene. While we found a positive association between DML and corresponding log2-fold change in gene expression that explained a higher percent of the variation, the slope was substantially lower ($slope_{Day9} = 0.0005$, $slope_{Day80} = 0.00054$, $P_{Day9} = 0.0005$, $P_{Day80} = 0.0004$, $R^2_{Day9} = 0.406$, $R^2_{Day80} = 0.276$; **Figure 6B**) than in the previous gene-level methylation analysis. Thus, both analyses indicate that differential methylation had a substantially small effect on differential gene expression.

Gene co-expression network analysis identified 52 modules of co-expressed genes (i.e., genes that shared similar expression patterns among all 22 individuals) ranging from 36 to 5,059 genes in size (**Supplementary Table 5.1**). We used these modules to test the hypotheses that (i) pH_{EPF} is associated with the expression of specific gene modules, (ii) the expression of these pH_{EPF}-associated modules is also associated with DNA methylation, and (iii) that DNA methylation within these modules is sensitive to OA. Of the 52 modules, the eigengene expression of four modules was significantly associated with ΔpH (excluding one module that was driven by a single individual outlier; **Figure 7A**). We did not see a significant association between the eigengene expression of any of these four modules and mean gene body DNA methylation (**Figure 7B**). Although, mean gene body DNA methylation within these modules was significantly associated with treatment in three of the four modules, but not time or the interaction of treatment and time (**Figure 7C**). These modules were composed of a diverse collection of genes that were not significantly enriched in specific GO categories. There was, however, evidence of genes involved in pH regulation, ion transport, and other biomineralization-related processes included within the modules (**Supplementary Table 5.1**).

DISCUSSION

We conducted an integrative analysis of physiological, transcriptomic, and methylomic data in the mantle-edge tissue of eastern oysters exposed to a range of pCO_2 conditions to elucidate the oyster's capacity to regulate pH_{EPF} in response to OA and examine the molecular underpinnings of this response. At the physiological level, oysters maintained a pH_{EPF} significantly lower than $pH_{seawater}$ in our control treatments, which is consistent with what has been shown previously in oysters and other species of bivalves (e.g., Crenshaw, 1972; Cameron et al., 2019). This trend was also seen in the OA treatments at most time points, the exception being exposure day 9 in the high OA treatment where oysters maintained pH_{EPF} near $pH_{seawater}$. On day 9 and 22 of the exposure, oysters in the high OA treatment also maintained a ΔpH significantly higher than ΔpH in the control, which resulted in a non-significant difference in the pH_{EPF} between the high OA and control treatment on those days.

At a molecular level, *C. virginica* exhibited a subtle genome-wide response in both the methylome and transcriptome to OA, but surprisingly little response in individual gene expression or methylation. When genes were clustered, we found evidence of a significant association between gene clusters and ΔpH, suggesting subtle shifts in these genes could be responsible for regulating pH_{EPF} in response to OA. However, gene body methylation within these gene clusters was not associated with gene expression, indicating that DNA methylation did not have a significant role in gene regulation. Below, we evaluate the short and long-term effects of OA on both phenotypic and molecular response, examine how these results link together and relate to the current model of EPF fluid regulation, and discuss possible explanations for the surprisingly subtle shifts in both the transcriptome and methylome.

pH_{EPF} Response Through Time

Crassostrea virginica, like other coastal calcifiers, are experiencing OA due to a combination of local (Wallace et al., 2014) and global change-associated processes (e.g., Orr et al., 2005). In particular, local processes, such as excessive nutrient loading (Wallace et al., 2014), input from acidic river water (Salisbury et al., 2008), and upwelling of CO_2 rich groundwater (Feely et al., 2008), are exposing oysters to more intense short-term acidification events well before global, anthropogenic CO_2-induced acidification is predicted to impact these systems. Consistent with these findings, water chemistry data from our collection sites found substantial variation in pCO_2, including intervals of acidification

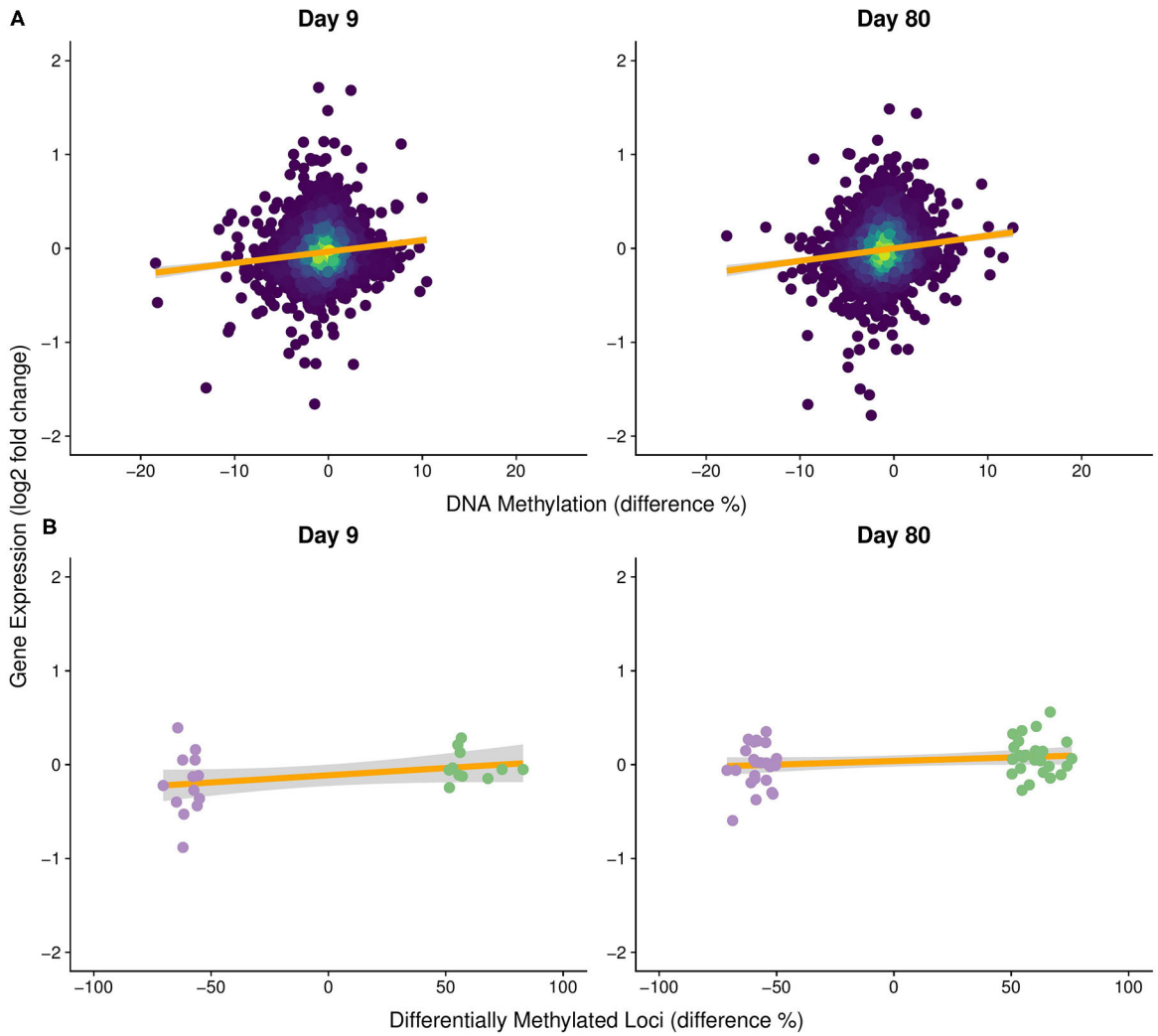

FIGURE 6 | Gene expression change in response to OA as a function of DNA methylation change. Log2-fold change in gene expression compared to % difference in **(A)** mean gene methylation among treatments (Day 9 – slope = 0.0121, $P < 0.0001$, $R^2 = 0.012$; Day 80 – slope = 0.0137, $P < 0.0001$, $R^2 = 0.014$) and **(B)** significantly differentially methylated loci (DML) among treatments (Day 9 – slope = 0.0005, $P = 0.0005$, $R^2 = 0.406$; Day 80 – slope = 0.00054, $P = 0.0004$, $R^2 = 0.276$). Orange line represents the fitted linear model. Colors in **(B)** correspond to DMLs that were significantly hyper- (green) and hypomethylated (purple) in the OA treatment.

near the high OA scenario employed in the present study. Despite the apparent frequency of these short-term acidification events, few studies have examined the response of adult oysters to such high levels of OA (i.e. the high OA treatment in present study), relative to the lower levels of OA-associated with increasing anthropogenic pCO_2 (i.e. the moderate OA treatment in present study).

Bivalve response to OA has received considerable attention over the past two decades (see review Gazeau et al., 2013), with a substantial focus on measuring calcification (Miller et al., 2009; Talmage and Gobler, 2009; Waldbusser et al., 2011a) and physiological responses (Beniash et al., 2010; Ivanina et al., 2013; Matoo et al., 2013; Gobler and Talmage, 2014) in *C. virginica*. Recent research has shown that bivalves can isolate and moderate the fluid at the site of calcification, and elevate the pH of this fluid relative to seawater under OA conditions (Cameron et al., 2019; Liu et al., 2020). It has been hypothesized that this may be a strategy for maintaining calcification even under increasingly acidic conditions. However, the degree to which a species can moderate its calcifying fluid pH under OA scenarios varies across taxa (e.g., McCulloch et al., 2012; Holcomb et al., 2014; Liu et al., 2020), life stage (e.g., Ramesh et al., 2017), and temperature (e.g., Cameron et al., 2019). Previous work with *C. virginica* found that they exhibited a moderate ability to regulate their pH_{EPF} after an extended 60-day experimental exposure, elevating their pH_{EPF} above $pH_{seawater}$ under most OA scenarios (Liu et al., 2020).

We predicted that similar to this previous study, *C. virginica* would increase its pH_{EPF} relative to $pH_{seawater}$ in response to OA. Consistent with our prediction and with previous studies on *C. virginica* (Liu et al., 2020) and adult King scallops *Pectens*

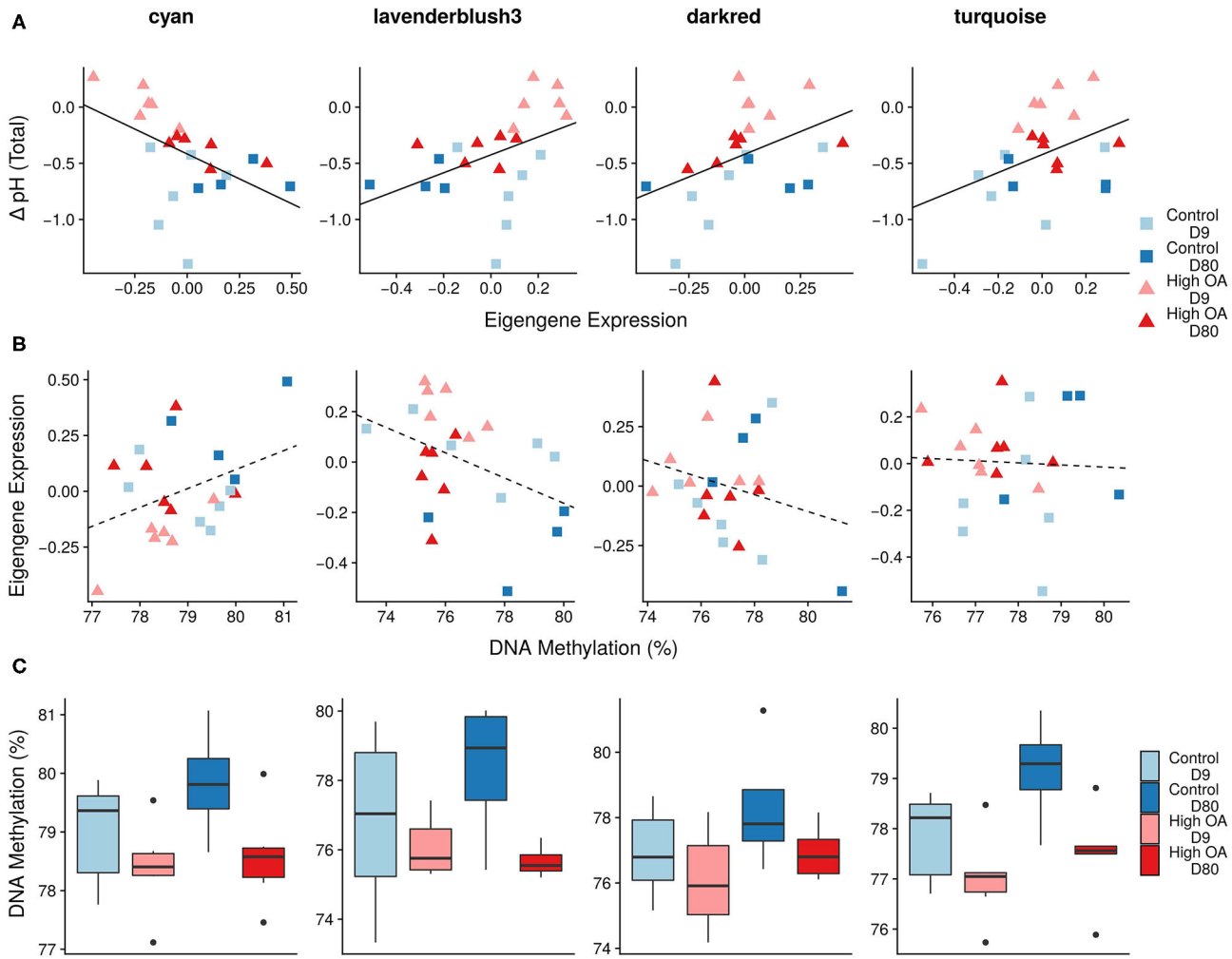

FIGURE 7 | Co-expression and DNA methylation responses to OA. Four of the top five modules associated with oyster ΔpH (colors are randomly assigned by the WGCNA package and have no meaning). Scatterplots of **(A)** ΔpH by eigengene expression ($P_{cyan} = 0.021$, $P_{lavenderblush3} = 0.044$, $P_{darkred} = 0.037$, $P_{turquoise} = 0.042$), **(B)** eigengene expression by mean module methylation ($P_{cyan} = 0.087$, $P_{lavenderblush3} = 0.052$, $P_{darkred} = 0.264$, $P_{turquoise} = 0.833$), and boxplot of **(C)** mean module methylation by treatment and time point. For **(C)** there was a significant effect of treatment in three of the four modules ($P_{cyan} = 0.035$, $P_{lavenderblush3} = 0.038$, $P_{darkred} = 0.123$, $P_{turquoise} = 0.013$), but neither time point or their interaction was significant for any of the modules. Mean module methylation was calculated as the mean methylation for all CpGs for each gene within a module. Solid lines indicate a significant relationship between explanatory (x-axis) and response variable (y-axis) using a linear model, while dotted lines indicate non-significant trends among variables.

maximus (Cameron et al., 2019), we observed an increase in ΔpH under OA conditions. However, pH_{EPF} remained below $pH_{seawater}$ at most time points under the different treatments, which is inconsistent with the prior work on *C. virginica* (Liu et al., 2020) and *P. maximus* (Cameron et al., 2019). One possible explanation for the lower pH_{EPF} and ΔpH in the present study compared with Liu et al. (2020) was the choice of experimental temperatures (~18–19°C in the present study vs. 25°C in the other study), which has been shown in *P. maximus* to impact the relationship between pCO_2 and pH_{EPF} (Cameron et al., 2019). The lower pH_{EPF} in the present study may also reflect increased respiration of CO_2 into the EPF, potentially driven by increased metabolic activity and/or rates of feeding (Crenshaw, 1972; Sutton et al., 2018; Cameron et al., 2019). Comparing among treatments, we found that ΔpH was significantly higher in our high OA treatments relative to the control at days 9 and 22, indicating that OA prompted a response in pH_{EPF}. This short-term response could be the result of stress-induced metabolic depression or increased removal of hydrogen ions from the EPF *via* proton transporters or other ion regulators. Moreover, the short-term elevation of ΔpH in OA treatments was not sufficient to prevent net shell loss (i.e., net dissolution) after 35 days of exposure. However, a prior study on *C. virginica* suggests that gross calcification does occur under comparably high OA conditions, despite net shell loss (Ries et al., 2016). Future studies that specifically consider the deposition rate of calcium carbonate and the impact of the interaction between temperature and OA on the regulation of EPF chemistry in *C. virginica* and other

bivalves will offer substantial insight into the importance of EPF regulation on this species' calcification response to OA.

Biomineralization Response

Recent studies have begun to clarify the role of particular genes, pathways, and associated molecular mechanisms in the biomineralization process, and their responsiveness to OA across a diverse group of marine calcifiers (see review by Clark, 2020). In bivalves, a principal component of the biomineralization process is the transport of ions between the mantle epithelium and the EPF, in particular Ca^{2+} and HCO_3^-, needed for the formation of calcium carbonate. The movement of Ca^{2+} ions into the EPF occurs both passively *via* paracellular pathways and by active transport through transporters in the mantle epithelium membrane (primarily Ca^{2+}-ATPase and Na^+/Ca^{2+} exchangers), while HCO_3^- is shuttled into the EPF *via* HCO_3^- transporters. Additionally, carbonic anhydrase is an important protein in the biomineralization process that catalyzes a reaction that generates HCO_3^- and H^+ ions from CO_2 and water. The H^+ ions produced in this reaction (among many others) serve a critical role in several of the transporter proteins both directly (e.g., Ca^{2+}-ATPase) and indirectly (e.g., Na^+/H^+ exchanger) involved in biomineralization. In addition, reducing the amount of H^+ ions in the EPF (measured as the pH of the fluid) causes HCO_3^- to dissociate to CO_3^{2+}, thereby increasing the calcium carbonate saturation state in support of calcification (Ries, 2011). A number of other marine calcifiers have also exhibited shifts in genes associated with these pathways of ion-transport in response to CO_2-induced OA (Evans et al., 2013; Davies et al., 2016; Johnson and Hofmann, 2017; Griffiths et al., 2019).

We hypothesized that OA would elicit a response in genes involved in biomineralization in the mantle, particularly those involved in ion-transport. Based on the shift in ΔpH from days 9 to 80, we predicted a similar shift in biomineralization-related genes between these same time points. However, we found little evidence of differential gene expression or methylation corresponding to biomineralization or ion transport between these days or across treatments. Despite the lack of differentiation among treatments, biomineralization genes were well-represented in our data and overexpressed relative to all other genes, consistent with current biomineralization models in bivalves. Although carbonic anhydrase and several ion transporter genes were not significantly differentially expressed, they did display a subtle up-regulation in response to OA on day 9 relative to day 80 (**Supplementary Figure 4.1**), indicating that these subtle responses in biomineralization genes could have contributed to the significant global response to treatment that was observed. These results are surprising given the more pronounced gene expression responses seen in other marine calcifiers (Evans et al., 2013; Davies et al., 2016; Johnson and Hofmann, 2017; Griffiths et al., 2019). One possible explanation for the surprisingly weak response observed in the present study was the decision to examine a single tissue type, the mantle, rather than look at the transcriptomic response of the entire organism or multiple tissues (but see Hüning et al., 2013; Li et al., 2016). Moreover, these subtle responses appear to be fairly consistent with previous targeted gene expression studies examining *C. virginica* mantle tissue in response to OA exposure, which also did not find significant differential expression of biomineralization genes (Beniash et al., 2010; Richards, 2018). Thus, biomineralization-associated pathways in *C. virginica* mantle tissue may be relatively canalized compared to other marine calcifiers.

Stress and Metabolic Responses

A broad range of transcriptomic responses related to stress and metabolism have been noted in marine calcifiers in response to OA (see review by Strader et al., 2020). In particular, OA exposure has been shown to elicit an up-regulation of oxidoreductase-related genes and oxygen-stress related enzymes in a broad range of organisms, including corals (Kaniewska et al., 2012), sea urchins (Todgham and Hofmann, 2009), and oysters (Tomanek et al., 2011; Wang et al., 2016). In *C. gigas*, OA exposure led to a delayed antioxidant and oxidative stress response in gill tissue, suggesting that redox homeostasis was possible for short-term (up to 14 days) but not long-term (28 days) exposure to OA (Wang et al., 2016). Consistent with this response in *C. gigas* and paralleling the shift we observed in the partial maintenance of the pH_{EPF}, we found several GO categories associated with metabolic response, in particular oxidative stress. In general, we observed a larger stress response over time, suggesting that OA induced a mild stress response in the mantle tissue, which was exacerbated over time. We did not find evidence of overlap between these GO categories in gene expression and DNA methylation, but we did observe DML within genes corresponding to a number of different stress responses, including hypomethylation of death-effector domain-containing genes and hypermethylation of a protein-ubiquitination related gene on day 80. Both types of genes are involved in cell apoptosis and possibly reflect a stress response to OA. Similar OA-induced responses in protein-ubiquitination genes were found in the gonadal tissue of *C. virginica* (Venkataraman et al., 2020), suggesting OA can induce parallel shifts in DNA methylation in the methylome of different tissues. However, general overlap of OA-induced DNA methylation was low among tissues (2 OA-induced DMLs among 85 identified in the mantle were also induced in the gonadal tissue; **Supplementary Figure 3.4**). Future studies focusing on OA-induced changes in gene expression and DNA methylation among tissues may help clarify if the subtle responses in *C. virginica* are the result of a relatively canalized response in the mantle tissue or represents a pattern unique to the species.

The Molecular Basis for pH_{EPF} Response to OA

Ries (2011) proposed a model to describe the regulation of the calcifying fluid whereby the active pumping of protons out of the calcifying fluid elevates the calcifying fluid pH and maintains a favorable calcium carbonate saturation state ($\Omega > 1$) even under highly acidic conditions. Empirical support for this model within oysters has been provided from shell-based boron-isotope estimates of oyster EPF (e.g., Sutton et al., 2018; Liu et al., 2020), but little is known about the molecular basis of this response. To test the predictions proposed by this model, we hypothesized that regulation of oyster pH_{EPF} would be driven

by changes in gene expression, particularly genes associated with biomineralization, ion transport, and proton pumping. In addition, we also hypothesized that OA-induced shifts in the transcriptome of *C. virginica* would correspond to shifts in the methylome. This was based on growing evidence in the DNA methylation literature indicating that DNA methylation is linked with gene regulation (Zilberman et al., 2007; Zemach et al., 2010; Gavery and Roberts, 2013; Olson and Roberts, 2014; Dixon et al., 2018; Zhang et al., 2020), is induced by OA and other environmental stressors (Putnam et al., 2016; Dixon et al., 2018; Bogan et al., 2020), and corresponds with calcification response to OA in marine invertebrates (Liew et al., 2018).

By clustering genes based on their co-expression, we found that gene expression was associated with EPF response (i.e., ΔpH) in four separate gene modules. This result, coupled with the lack of differential expression in individual genes, suggests that regulation of EPF occurs through subtle changes in a large number of genes. Interestingly, these correlated clusters were composed of a diverse collection of genes which were not significantly enriched in specific GO categories, although they did include genes involved in pH regulation, ion transport, and other biomineralization related processes.

Consistent with previous findings in marine invertebrates (Olson and Roberts, 2014; Liew et al., 2018), gene body DNA methylation in *C. virginica* mantle tissue exhibited a subtle but significant association with both gene expression (positive) and gene expression variation (negative). However, the small R^2-values and slopes from the regressions indicate that changes in gene body DNA methylation had only a small effect on changes in gene regulation in *C. virginica* mantle tissue. Moreover, we found there was a weak positive association between OA-induced log2-fold changes in gene expression and shifts in gene body DNA methylation. Although, we found there was no overlap among enriched GO categories based on gene expression compared to DNA methylation data. We also found no evidence of an association between the eigen gene expression of the four ΔpH-associated modules and gene body DNA methylation, which suggests that an alternative mechanism might be regulating the expression of genes within those modules. Follow-up investigations that use a more targeted, gene-specific approach would clarify whether these weak signals represent an important part of oyster EPF regulation in response to OA.

Subtle Shifts and Constraints

The subtle transcriptomic response of *C. virginica* found in this study contrasted the more pronounced transcriptomic responses exhibited by other marine calcifying taxa in response to OA (e.g., Li et al., 2016). However, other examples of subtle gene expression shifts in response to environmental change do exist (Malik et al., 2020), and these minor shifts can still have phenotypic consequences (Wu et al., 2010). In *C. virginica*, these subtle molecular responses may be the result of: (i) extended evolution under regular extreme OA conditions; (ii) constrained plasticity of the mantle (e.g., an evolved canalization of gene expression in response to OA); and/or (iii) a highly polygenic genetic response architecture.

Crassostrea virginica inhabit coastal estuaries, which can experience regular, unpredictable, and rapid swings in acidity leading to conditions near or above the high OA scenario (Waldbusser and Salisbury, 2014). Since the high OA treatment is not unusual from the oyster's perspective, the subtle molecular responses we observed may reflect that the prescribed high OA treatment in the present study was not different enough from what oysters typically experience on diurnal and/or seasonal cycles to elicit a strong molecular response. On the other hand, highly uncertain environments, in which the frequency of fluctuations is much higher than what the organism can predict or respond to, can lead to the evolution of a single expressed phenotype (in this case, gene expression in the mantle) across all environments that maximizes the geometric mean fitness (Seger and Brockmann, 1987; Starrfelt and Kokko, 2012; Botero et al., 2015). The variable environments inhabited by the oysters in the present study may consequently select for constrained (e.g., canalized) responses in the transcriptome and methylome, in which the expression profile results from the evolution of a nearly fixed bet-hedging strategy, rendering the genome capable of only subtle shifts. From an energetic cost perspective, one would expect selective pressure against increases in mRNA and protein expression due to the costs associated with increased expression (Wagner, 2005; Weiße et al., 2015). Interestingly, calcification genes were associated with higher expression than the genome-wide background in the mantle tissue, suggesting that their expression may be maximized, which could constrain their ability to be further up-regulated in response to OA. Lastly, while we cannot completely exclude the possibility that prior acidification events in the field acclimated the oysters to OA prior to the start of the experiment, thereby limiting differences among treatments. This seems unlikely to completely explain our lack of differences since we performed a one month acclimation at control conditions prior to the experimental exposure. Moreover, if it is true that field-collected oysters show subtle, but significant physiological responses, then the studies that focus on organisms reared in control conditions may be biased toward larger responses than actually exist in nature.

Subtle shifts may also be observed if the traits responding to OA are highly polygenic (Pritchard et al., 2010) and/or there is a redundant genetic architecture (Yeaman, 2015). Although this body of literature is focused primarily on shifts in allele frequencies in response to selection rather than gene expression, the same principles about polygenic traits apply. In the case of plastic polygenic traits, the magnitude of response of individual genes may be relatively small and, therefore, not detectable *via* differential expression analysis. In the case of redundant genetic architecture, theory predicts that high genetic redundancy in a population occurs when individuals can reach a phenotypic outcome by a wide range of genes and pathways (see topic reviewed in Láruson et al., 2020), which could result in very large residual error and limited statistical power to detect differences amongst treatments (i.e., lack of a clear significant response because every individual does something different to achieve the same phenotype). Regardless of whether these results are more influenced by subtle shifts or constraints on gene expression, they show that a marine calcifier's drastic phenotypic responses

to OA (i.e., pH_{EPF} response and reduced calcification rate under high OA) can be associated with only subtle molecular responses within that organism's calcifying tissue.

CONCLUSION

Crassostrea virginica exhibited an overall negative response to long-term OA (e.g., reductions in calcification and pH_{EPF} accompanied by the subtle emergence of stress related transcriptomic responses). Although elevation of ΔpH under the high OA treatment was enhanced at day 9, pH_{EPF} was highly variable within all treatments during the first 22 days of the experiment—which indicates *C. virginica* may have a limited capacity to continue calcifying during ephemeral acidification events, such as those they already experience due to diurnal and seasonal fluctuations in seawater pH. Notably, we did not find a strong association between specific DML and differentially expressed genes or ΔpH, suggesting that the regulation of pH_{EPF} may occur by more subtle or diverse shifts in the methylome and transcriptome or *via* alternative mechanisms. Since the majority of OA transcriptomic studies have not specifically targeted calcifying tissue, our results highlight a need for more studies to focus specifically on calcifying tissues in order to assess how flexible the bivalve calcification process is at the molecular level, particularly in oysters. In contrast to other studies, we did not find strong evidence that DNA methylation acted as a mediator to gene expression or EPF responses to OA, suggesting that the importance of DNA methylation may vary considerably among tissues within the same species, among studies, and among taxa. If the subtle shifts we observed in this study are common in the calcifying tissue of other taxa, it may be difficult to gain an unbiased understanding of this phenomenon due to publication bias against weak or non-significant results. Thus, our study provides a roadmap for others seeking to understand how the calcifying fluid is regulated at the molecular level, even when patterns in the resulting molecular data are relatively weak. Subtle shifts at the molecular level and the capacity for marine calcifiers to maintain these molecular changes provide important context for understanding the capacity of different taxa to respond to long-term OA.

DATA AVAILABILITY STATEMENT

The datasets generated for this study can be found in online repositories. The names of the repository/repositories and accession number(s) can be found below: NCBI BioProject ID - PRJNA594029. Scripts and non-sequence data can be found at the online github repository: https://github.com/epigeneticstoocean/AE17_Cvirginica_MolecularResponse. The data can also be found on Dryad with link: https://doi.org/10.5061/dryad.8cz8w9gnk.

AUTHOR CONTRIBUTIONS

Principle design of the experiment was done by AD-W, SR, JR, and KL. Field collections were done by AD-W, BF, and EM. The experiment was conducted by AD-W. During the experiment, extrapallial fluid was collected and analyzed by LC, while other phenotypic data and tissues were collected by AD-W. Water chemistry was analyzed by AD-W and EM. Tissues were prepared for RNAseq sequencing by BF and prepared for MBD-BSseq by YV and SR. All bioinformatic steps and statistical analyses were performed by AD-W. The manuscript was written by AD-W with assistance from KL, LC, JR, and YV. All authors contributed to editing and approving the final version of the manuscript.

FUNDING

This research was funded by the National Science Foundation (1635423). Resources purchased with funds from the NSF FMSL program (DBI 1722553, to Northeastern University) were used to generate data for this manuscript.

ACKNOWLEDGMENTS

We acknowledge Sara Schaal, Aki Laruson, Isaac Westfield, and other members of the Lotterhos and Ries labs for their helpful comments that improved the manuscript. This research was funded by the National Science Foundation (BIO-OCE 1635423). Resources purchased with funds from the NSF FMSL program (DBI 1722553, to Northeastern University) were used to generate data for this manuscript. We are also thankful for the help of many graduate students, undergraduates, technicians, and volunteers during the experiment, including Andrea Unzueta Martinez, Bodie Weedop, Isabel Gutowski, Jaxine Wolfe, Sandi Scripa, Kevin Wasko, Isaac Westfield, and Camila Cortina.

SUPPLEMENTARY MATERIAL

The Supplementary Material for this article can be found online at: https://www.frontiersin.org/articles/10.3389/fmars.2020.566419/full#supplementary-material

REFERENCES

Akalin, A., Kormaksson, M., Li, S., Garrett-Bakelman, F. E., Figueroa, M. E., Melnick, A., et al. (2012). *methylKit*: a comprehensive R package for the analysis of genome-wide DNA methylation profiles. *Genome Biol.* 13:R87. doi: 10.1186/gb-2012-13-10-r87

Al-Horani, F. A., Al-Moghrabi, S. M., and de Beer, D. (2002). The mechanism of calcification and its relation to photosynthesis and respiration in the scleractinian coral *Galaxea fascicularis*. *Mar. Biol.* 142, 419–426. doi: 10.1007/s00227-002-0981-8

Anagnostou, E., Williams, B., Westfield, I., Foster, G. L., and Ries, J. B. (2019). Calibration of the pH-δ11B and temperature-Mg/Li proxies in the long-lived high-latitude crustose coralline red alga *Clathromorphum compactum* via controlled laboratory experiments. *Geochim. Cosmochim. Acta* 254, 142–155. doi: 10.1016/j.gca.2019.03.015

Anier, K., Malinovskaja, K., Pruus, K., Aonurm-Helm, A., Zharkovsky, A., and Kalda, A. (2014). Maternal separation is associated with DNA methylation and behavioural changes in adult rats. *Eur. Neuropsychopharmacol.* 24, 459–468. doi: 10.1016/j.euroneuro.2013.07.012

Anthony, K. R. N., Kline, D. I., Diaz-Pulido, G., Dove, S., and Hoegh-Guldberg, O. (2008). Ocean acidification causes bleaching and productivity loss in coral reef builders. *Proc. Natl. Acad. Sci. U.S.A.* 105, 17442–17446. doi: 10.1073/pnas.0804478105

Bates, D., Mächler, M., Bolker, B., and Walker, S. (2015). Fitting linear mixed-effects models using *lme4*. *J. Stat. Softw.* 67, 1–48. doi: 10.18637/jss.v067.i01

Bednaršek, N., Tarling, G. A., Bakker, D. C. E., Fielding, S., Jones, E. M., Venables, H. J., et al. (2012). Extensive dissolution of live pteropods in the Southern Ocean. *Nat. Geosci.* 5, 881–885. doi: 10.1038/ngeo1635

Beniash, E., Ivanina, A., Lieb, N. S., Kurochkin, I., and Sokolova, I. M. (2010). Elevated level of carbon dioxide affects metabolism and shell formation in oysters *Crassostrea virginica* (Gmelin). *Mar. Ecol. Prog. Ser.* 419, 95–108. doi: 10.3354/meps08841

Benjamini, Y., and Hochberg, Y. (1995). Controlling the false discovery rate: a practical and powerful approach to multiple testing. *J. of Roy. Stat. Soc. B Met.* 57, 289–300. doi: 10.1111/j.2517-6161.1995.tb02031.x

Bogan, S. N., Johnson, K. M., and Hofmann, G. E. (2020). Changes in genome-wide methylation and gene expression in response to future pCO_2 extremes in the Antarctic pteropod *Limacina helicina antarctica*. *Front. Mar. Sci.* 6:788. doi: 10.3389/fmars.2019.00788

Bolger, A. M., Lohse, M., and Usadel, B. (2014). *Trimmomatic*: a flexible trimmer for illumina sequence data. *Bioinformatics* 30, 2114–2120. doi: 10.1093/bioinformatics/btu170

Bonduriansky, R., and Day, T. (2018). *Extended Heredity: A New Understanding of Inheritance and Evolution*. Princeton University Press. Available online at: https://play.google.com/store/books/details?id=HiNGDwAAQBAJ

Botero, C. A., Weissing, F. J., Wright, J., and Rubenstein, D. R. (2015). Evolutionary tipping points in the capacity to adapt to environmental change. *Proc. Natl. Acad. Sci. U.S.A.* 112, 184–189. doi: 10.1073/pnas.1408589111

Cameron, L. P., Reymond, C. E., Müller-Lundin, F., Westfield, I., Grabowski, J. H., Westphal, H., et al. (2019). Effects of temperature and ocean acidification on the extrapallial fluid pH, calcification rate, and condition factor of the King scallop Pecten maximus. *J. Shellfish Res.* 38:763. doi: 10.2983/035.038.0327

Clark, M. S. (2020). Molecular mechanisms of biomineralization in marine invertebrates. *J. Exp. Biol.* 223, 1–13. doi: 10.1242/jeb.206961

Crenshaw, M. A. (1972). The inorganic composition of molluscan extrapallial fluid. *Biol. Bull.* 143, 506–512. doi: 10.2307/1540180

Crenshaw, M. A., and Neff, J. M. (1969). Decalcification at the mantle-shell interface in molluscs. *Am. Zool.* 9, 881–885. doi: 10.1093/icb/9.3.881

Davies, S. W., Marchetti, A., Ries, J. B., and Castillo, K. D. (2016). Thermal and pCO_2 stress elicit divergent transcriptomic responses in a resilient coral. *Front. Mar. Sci.* 3:112. doi: 10.3389/fmars.2016.00112

De Beer, D., and Larkum, A. W. D. (2001). Photosynthesis and calcification in the calcifying algae *Halimeda discoidea* studied with microsensors. *Plant Cell Environ.* 24, 1209–1217. doi: 10.1046/j.1365-3040.2001.00772.x

de Nooijer, L. J., Toyofuku, T., and Kitazato, H. (2009). Foraminifera promote calcification by elevating their intracellular pH. *Proc. Natl. Acad. Sci. U.S.A.* 106, 15374–15378. doi: 10.1073/pnas.0904306106

de Nooijer, L. J., Toyofuku, T., Oguri, K., Nomaki, H., and Kitazato, H. (2008). Intracellular pH distribution in foraminifera determined by the fluorescent probe HPTS. *Limnol. Oceanogr. Methods* 6, 610–618. doi: 10.4319/lom.2008.6.610

Dickinson, G. H., Ivanina, A. V., Matoo, O. B., Pörtner, H. O., Lannig, G., Bock, C., et al. (2012). Interactive effects of salinity and elevated CO_2 levels on juvenile eastern oysters, *Crassostrea virginica*. *J. Exp. Biol.* 215, 29–43. doi: 10.1242/jeb.061481

Dixon, G., Liao, Y., Bay, L. K., and Matz, M. V. (2018). Role of gene body methylation in acclimatization and adaptation in a basal metazoan. *Proc. Natl. Acad. Sci. U.S.A.* 115, 13342–13346. doi: 10.1073/pnas.1813749115

Dixon, P. (2003). *VEGAN*, a package of R functions for community ecology. *J. Veg. Sci.* 14, 927–930. doi: 10.1111/j.1654-1103.2003.tb02228.x

Dobin, A., Davis, C. A., Schlesinger, F., Drenkow, J., Zaleski, C., Jha, S., et al. (2013). *STAR*: ultrafast universal RNA-seq aligner. *Bioinformatics* 29, 15–21. doi: 10.1093/bioinformatics/bts635

Dolinoy, D. C., Weidman, J. R., Waterland, R. A., and Jirtle, R. L. (2006). Maternal genistein alters coat color and protects Avy mouse offspring from obesity by modifying the fetal epigenome. *Environ. Health Perspect.* 114, 567–572. doi: 10.1289/ehp.8700

Donald, H. K., Ries, J. B., Stewart, J. A., Fowell, S. E., and Foster, G. L. (2017). Boron isotope sensitivity to seawater pH change in a species of Neogoniolithon coralline red alga. *Geochimi Cosmochim. Acta* 217, 240–253. doi: 10.1016/j.gca.2017.08.021

Doney, S. C., Fabry, V. J., Feely, R. A., and Kleypas, J. A. (2009). Ocean acidification: the other CO_2 problem. *Ann. Rev. Mar. Sci.* 1, 169–192. doi: 10.1146/annurev.marine.010908.163834

Eirin-Lopez, J. M., and Putnam, H. M. (2019). Marine environmental epigenetics. *Ann. Rev. Mar. Sci.* 11, 335–368. doi: 10.1146/annurev-marine-010318-095114

Ekstrom, J. A., Suatoni, L., Cooley, S. R., Pendleton, L. H., Waldbusser, G. G., Cinner, J. E., et al. (2015). Vulnerability and adaptation of US shellfisheries to ocean acidification. *Nat. Clim. Change* 5, 207–214. doi: 10.1038/nclimate2508

Evans, T. G., Chan, F., Menge, B. A., and Hofmann, G. E. (2013). Transcriptomic responses to ocean acidification in larval sea urchins from a naturally variable pH environment. *Mol. Ecol.* 22, 1609–1625. doi: 10.1111/mec.12188

Evans, T. G., and Hofmann, G. E. (2012). Defining the limits of physiological plasticity: how gene expression can assess and predict the consequences of ocean change. *Philos. Trans. R. Soc. Lond. B Biol. Sci.* 367, 1733–1745. doi: 10.1098/rstb.2012.0019

Feely, R. A., Sabine, C. L., Hernandez-Ayon, J. M., Ianson, D., and Hales, B. (2008). Evidence for upwelling of corrosive "acidified" water onto the continental shelf. *Science* 320, 1490–1492. doi: 10.1126/science.1155676

Feely, R. A., Sabine, C. L., Lee, K., Berelson, W., Kleypas, J., Fabry, V. J., et al. (2004). Impact of anthropogenic CO_2 on the $CaCO_3$ system in the oceans. *Science* 305, 362–366. doi: 10.1126/science.1097329

Gavery, M. R., and Roberts, S. B. (2013). Predominant intragenic methylation is associated with gene expression characteristics in a bivalve mollusc. *PeerJ* 1:e215. doi: 10.7717/peerj.215

Gazeau, F., Parker, L. M., Comeau, S., Gattuso, J.-P., O'Connor, W. A., Martin, S., et al. (2013). Impacts of ocean acidification on marine shelled molluscs. *Mar. Biol.* 160, 2207–2245. doi: 10.1007/s00227-013-2219-3

Gobler, C. J., and Talmage, S. C. (2014). Physiological response and resilience of early life-stage Eastern oysters (*Crassostrea virginica*) to past, present and future ocean acidification. *Conserv. Physiol.* 2:cou004. doi: 10.1093/conphys/cou004

Gómez-Chiarri, M., Warren, W. C., Guo, X., and Proestou, D. (2015). Developing tools for the study of molluscan immunity: the sequencing of the genome of the eastern oyster, *Crassostrea virginica*. *Fish Shellfish Immun.* 46, 2–4. doi: 10.1016/j.fsi.2015.05.004

Goncalves, P., Jones, D. B., Thompson, E. L., Parker, L. M., Ross, P. M., and Raftos, D. A. (2017). Transcriptomic profiling of adaptive responses to ocean acidification. *Mol. Ecol.* 26, 5974–5988. doi: 10.1111/mec.14333

Griffiths, J. S., Pan, T.-C. F., and Kelly, M. W. (2019). Differential responses to ocean acidification between populations of *Balanophyllia elegans* corals from high and low upwelling environments. *Mol. Ecol.* 28, 2715–2730. doi: 10.1111/mec.15050

Guinotte, J. M., and Fabry, V. J. (2008). Ocean acidification and its potential effects on marine ecosystems. *Ann. N. Y. Acad. Sci.* 1134, 320–342. doi: 10.1196/annals.1439.013

Helm, M. M., and Bourne, N. (2004). *Hatchery Culture of Bivalves: A Practical Manual*. Food & Agriculture Organization. Available online at: https://books.google.com/books/about/Hatchery_Culture_of_Bivalves.html?hl=&id=hFUbAQAAIAAJ

Hofmann, G. E. (2017). Ecological epigenetics in marine metazoans. *Front. Mar. Sci.* 4, 1–7. doi: 10.3389/fmars.2017.00004

Holcomb, M., Venn, A. A., Tambutt,é, E., Tambutt,é, S., Allemand, D., Trotter, J., et al. (2014). Coral calcifying fluid pH dictates response to ocean acidification. *Sci. Rep.* 4:5207. doi: 10.1038/srep05207

Hothorn, T., Bretz, F., and Westfall, P. (2008). Simultaneous inference in general parametric models. *Biom. J.* 50, 346–363. doi: 10.1002/bimj.200810425

Huh, I., Zeng, J., Park, T., and Yi, S. V. (2013). DNA methylation and transcriptional noise. *Epigenet. Chromatin* 6:9. doi: 10.1186/1756-8935-6-9

Hüning, A. K., Melzner, F., Thomsen, J., Gutowska, M. A., Krämer, L., Frickenhaus, S., et al. (2013). Impacts of seawater acidification on mantle gene expression patterns of the Baltic Sea blue mussel: implications for shell formation and energy metabolism. *Mar. Biol.* 160, 1845–1861. doi: 10.1007/s00227-012-1930-9

Intergovernmental Panel on Climate Change (2007). *Climate change 2007 - Mitigation of Climate Change: Working Group III Contribution to the Fourth Assessment Report of the IPCC*. Cambridge University Press. Available online at: https://play.google.com/store/books/details?id=U_4ltxID60UC

Ivanina, A. V., Dickinson, G. H., Matoo, O. B., Bagwe, R., Dickinson, A., Beniash, E., et al. (2013). Interactive effects of elevated temperature and CO_2 levels on energy metabolism and biomineralization of marine bivalves *Crassostrea virginica* and *Mercenaria mercenaria*. *Comp. Biochem. Physiol. A Mol. Integr. Physiol.* 166, 101–111. doi: 10.1016/j.cbpa.2013.05.016

Jablonka, E., and Lamb, M. J. (2002). The changing concept of epigenetics. *Ann. N. Y. Acad. Sci.* 981, 82–96. doi: 10.1111/j.1749-6632.2002.tb04913.x

Johnson, K. M., and Hofmann, G. E. (2017). Transcriptomic response of the Antarctic pteropod *Limacina helicina* antarctica to ocean acidification. *BMC Genomics* 18:812. doi: 10.1186/s12864-017-4161-0

Jombart, T., Devillard, S., and Balloux, F. (2010). Discriminant analysis of principal components: a new method for the analysis of genetically structured populations. *BMC Genet.* 11:94. doi: 10.1186/1471-2156-11-94

Kaniewska, P., Campbell, P. R., Kline, D. I., Rodriguez-Lanetty, M., Miller, D. J., Dove, S., et al. (2012). Major cellular and physiological impacts of ocean acidification on a reef building coral. *PLoS ONE* 7:e34659. doi: 10.1371/journal.pone.0034659

Köhler-Rink, S., and Kühl, M. (2000). Microsensor studies of photosynthesis and respiration in larger symbiotic foraminifera. I The physicochemical microenvironment of *Marginopora vertebralis*, *Amphistegina lobifera* and *Amphisorus hemprichii*. *Mar. Biol.* 137, 473–486. doi: 10.1007/s002270000335

Kroeker, K. J., Kordas, R. L., Crim, R. N., and Singh, G. G. (2010). Meta-analysis reveals negative yet variable effects of ocean acidification on marine organisms. *Ecol. Lett.* 13, 1419–1434. doi: 10.1111/j.1461-0248.2010.01518.x

Krueger, F., and Andrews, S. R. (2011). *Bismark*: a flexible aligner and methylation caller for Bisulfite-Seq applications. *Bioinformatics* 27, 1571–1572. doi: 10.1093/bioinformatics/btr167

Kuznetsova, A., Brockhoff, P. B., and Christensen, R. H. B. (2017). *lmerTest* package: tests in linear mixed effects models. *J. Stat. Softw.* 82, 1–26. doi: 10.18637/jss.v082.i13

Langfelder, P., and Horvath, S. (2008). *WGCNA:* an R package for weighted correlation network analysis. *BMC Bioinformatics* 9, 1–13. doi: 10.1186/1471-2105-9-559

Láruson, Á. J., Yeaman, S., and Lotterhos, K. E. (2020). The importance of genetic redundancy in evolution. *Trend. Ecol. Evol.* 35, 809–822. doi: 10.1016/j.tree.2020.04.009

Li, B., and Dewey, C. N. (2011). *RSEM*: accurate transcript quantification from RNA-Seq data with or without a reference genome. *BMC Bioinformatics* 12:323. doi: 10.1186/1471-2105-12-323

Li, S., Liu, C., Huang, J., Liu, Y., Zhang, S., Zheng, G., et al. (2016). Transcriptome and biomineralization responses of the pearl oyster *Pinctada fucata* to elevated CO_2 and temperature. *Sci. Rep.* 6:18943. doi: 10.1038/srep18943

Liew, Y. J., Zoccola, D., Li, Y., Tambutt,é, E., Venn, A. A., Michell, C. T., et al. (2018). Epigenome-associated phenotypic acclimatization to ocean acidification in a reef-building coral. *Sci. Adv.* 4:eaar8028. doi: 10.1126/sciadv.aar8028

Liu, Y.-W., Eagle, R. A., Aciego, S. M., Gilmore, R. E., and Ries, J. B. (2018). A coastal coccolithophore maintains pH homeostasis and switches carbon sources in response to ocean acidification. *Nat. Commun.* 9:2857. doi: 10.1038/s41467-018-04463-7

Liu, Y.-W., Sutton, J. N., Ries, J. B., and Eagle, R. A. (2020). Regulation of calcification site pH is a polyphyletic but not always governing response to ocean acidification. *Sci Adv* 6:eaax1314. doi: 10.1126/sciadv.aax1314

Lyko, F., Foret, S., Kucharski, R., Wolf, S., Falckenhayn, C., and Maleszka, R. (2010). The honey bee epigenomes: differential methylation of brain DNA in queens and workers. *PLoS Biol.* 8:e1000506. doi: 10.1371/journal.pbio.1000506

Malik, A. A., Swenson, T., Weihe, C., Morrison, E. W., Martiny, J. B. H., Brodie, E. L., et al. (2020). Drought and plant litter chemistry alter microbial gene expression and metabolite production. *ISME J.* 14, 2236–2247. doi: 10.1038/s41396-020-0683-6

Martin, M. (2011). *Cutadapt* removes adapter sequences from high-throughput sequencing reads. *EMBnet.J.* 17, 10–12. doi: 10.14806/ej.17.1.200

Matoo, O. B., Ivanina, A. V., Ullstad, C., Beniash, E., and Sokolova, I. M. (2013). Interactive effects of elevated temperature and CO_2 levels on metabolism and oxidative stress in two common marine bivalves (*Crassostrea virginica* and *Mercenaria mercenaria*). *Comp. Biochem. Physiol. A Mol. Integr. Physiol.* 164, 545–553. doi: 10.1016/j.cbpa.2012.12.025

McCulloch, M., Falter, J., Trotter, J., and Montagna, P. (2012). Coral resilience to ocean acidification and global warming through pH up-regulation. *Nat. Clim. Chang.* 2, 623–627. doi: 10.1038/nclimate1473

Melatunan, S., Calosi, P., Rundle, S. D., Widdicombe, S., and Moody, A. J. (2013). Effects of ocean acidification and elevated temperature on shell plasticity and its energetic basis in an intertidal gastropod. *Mar. Ecol. Prog. Ser.* 472, 155–168. doi: 10.3354/meps10046

Michaelidis, B., Haas, D., and Grieshaber, M. K. (2005). Extracellular and intracellular acid-base status with regard to the energy metabolism in the oyster Crassostrea gigas during exposure to air. *Physiol. Biochem. Zool.* 78, 373–383. doi: 10.1086/430223

Miller, A. W., Reynolds, A. C., Sobrino, C., and Riedel, G. F. (2009). Shellfish face uncertain future in high CO_2 world: influence of acidification on oyster larvae calcification and growth in estuaries. *PLoS ONE* 4:e5661. doi: 10.1371/journal.pone.0005661

Murtagh, F., and Legendre, P. (2014). Ward's hierarchical agglomerative clustering method: which algorithms implement ward's criterion? *J. Classif.* 31, 274–295. doi: 10.1007/s00357-014-9161-z

Olson, C. E., and Roberts, S. B. (2014). Genome-wide profiling of DNA methylation and gene expression in *Crassostrea gigas* male gametes. *Front. Physiol.* 5:224. doi: 10.3389/fphys.2014.00224

Orr, J. C., Fabry, V. J., Aumont, O., Bopp, L., Doney, S. C., Feely, R. A., et al. (2005). Anthropogenic ocean acidification over the twenty-first century and its impact on calcifying organisms. *Nature* 437, 681–686. doi: 10.1038/nature04095

Pierrot, D. E., Wallace, D. W. R., and Lewis, E. (2011). *MS Excel Program Developed for CO_2 System Calculations*. Oak Ridge, TN: Carbon Dioxide Information Analysis Center, Oak Ridge National Laboratory, US Department of Energy. doi: 10.3334/cdiac/otg.co2sys_xls_cdiac105a

Pritchard, J. K., Pickrell, J. K., and Coop, G. (2010). The genetics of human adaptation: hard sweeps, soft sweeps, and polygenic adaptation. *Curr. Biol.* 20, R208–R215. doi: 10.1016/j.cub.2009.11.055

Putnam, H. M., Davidson, J. M., and Gates, R. D. (2016). Ocean acidification influences host DNA methylation and phenotypic plasticity in environmentally susceptible corals. *Evol. Appl.* 9, 1165–1178. doi: 10.1111/eva.12408

Rajan, K. C., and Vengatesen, T. (2020). Molecular adaptation of molluscan biomineralisation to high-CO_2 oceans – The known and the unknown. *Mar. Environ. Res.* 155:104883. doi: 10.1016/j.marenvres.2020.104883

Ramesh, K., Hu, M. Y., Thomsen, J., Bleich, M., and Melzner, F. (2017). Mussel larvae modify calcifying fluid carbonate chemistry to promote calcification. *Nat. Commun.* 8:1709. doi: 10.1038/s41467-017-01806-8

Reum, J. C. P., Alin, S. R., Feely, R. A., Newton, J., Warner, M., and McElhany, P. (2014). Seasonal carbonate chemistry covariation with temperature, oxygen, and salinity in a fjord estuary: Implications for the design of ocean acidification experiments. *PLoS ONE* 9:e89619. doi: 10.1371/journal.pone.0089619

Richards, E. J. (2006). Inherited epigenetic variation–revisiting soft inheritance. *Nat. Rev. Genet.* 7, 395–401. doi: 10.1038/nrg1834

Richards, M. L. (2018). *The Impact of CO_2-Related Ocean Acidification on the Molecular Regulation of Shell Development in the Eastern Oyster (Crassostrea virginica)* Dissertation/master's thesis. Baton Rouge, LA: Louisiana State University.

Ries, J. B. (2011). A physicochemical framework for interpreting the biological calcification response to CO_2-induced ocean acidification. *Geochim. Cosmochim. Acta* 75, 4053–4064. doi: 10.1016/j.gca.2011.04.025

Ries, J. B., Cohen, A. L., and McCorkle, D. C. (2009). Marine calcifiers exhibit mixed responses to CO_2-induced ocean acidification. *Geology* 37, 1131–1134. doi: 10.1130/G30210A.1

Ries, J. B., Ghazaleh, M. N., Connolly, B., Westfield, I., and Castillo, K. D. (2016). Impacts of seawater saturation state (ΩA= 0.4–4.6) and temperature

(10, 25°C) on the dissolution kinetics of whole-shell biogenic carbonates. *Geochimi. Cosmochim. Acta* 192, 318–337. doi: 10.1016/j.gca.2016.07.001

Rink, S., Kühl, M., Bijma, J., and Spero, H. J. (1998). Microsensor studies of photosynthesis and respiration in the symbiotic foraminifer *Orbulina universa*. *Mar. Biol.* 131, 583–595. doi: 10.1007/s002270050350

Ritchie, M. E., Phipson, B., Wu, D., Hu, Y., Law, C. W., Shi, W., et al. (2015). *limma* powers differential expression analyses for RNA-sequencing and microarray studies. *Nucl. Acids Res.* 43:e47. doi: 10.1093/nar/gkv007

Salisbury, J. E., Vandemark, D., Hunt, C. W., Campbell, J. W., McGillis, W. R., and McDowell, W. H. (2008). Seasonal observations of surface waters in two Gulf of Maine estuary-plume systems - relationships between watershed attributes, optical measurements and surface pCO_2. *Estuar. Coast. Shelf Sci.* 77, 245–252. doi: 10.1016/j.ecss.2007.09.033

Schübeler, D. (2015). Function and information content of DNA methylation. *Nature* 517, 321–326. doi: 10.1038/nature14192

Seger, J., and Brockmann, H. J. (1987). What is bet-hedging? *Oxford Surveys in Evolutionary Biology* 4, 182–211.

Starrfelt, J., and Kokko, H. (2012). Bet-hedging—a triple trade-off between means, variances and correlations. *Biol. Rev. Camb. Philos. Soc.* 87, 742–755. doi: 10.1111/j.1469-185X.2012.00225.x

Strader, M. E., Wong, J. M., and Hofmann, G. E. (2020). Ocean acidification promotes broad transcriptomic responses in marine metazoans: a literature survey. *Front. Zool.* 17:7. doi: 10.1186/s12983-020-0350-9

Sutton, J. N., Liu, Y.-W., Ries, J. B., Guillermic, M., Ponzevera, E., and Eagle, R. A. (2018). δ11B as monitor of calcification site pH in divergent marine calcifying organisms. *Biogeosciences* 15, 1447–1467. doi: 10.5194/bg-15-1447-2018

Talmage, S. C., and Gobler, C. J. (2009). The effects of elevated carbon dioxide concentrations on the metamorphosis, size, and survival of larval Hard clams (*Mercenaria mercenaria*), Bay scallops (*Argopecten irradians*), and Eastern oysters (*Crassostrea virginica*). *Limnol. Oceanogr.* 54, 2072–2080. doi: 10.4319/lo.2009.54.6.2072

Talmage, S. C., and Gobler, C. J. (2010). Effects of past, present, and future ocean carbon dioxide concentrations on the growth and survival of larval shellfish. *Proc. Natl. Acad. Sci. U.S.A.* 107, 17246–17251. doi: 10.1073/pnas.0913804107

Todgham, A. E., and Hofmann, G. E. (2009). Transcriptomic response of sea urchin larvae *Strongylocentrotus purpuratus* to CO_2-driven seawater acidification. *J. Exp. Biol.* 212, 2579–2594. doi: 10.1242/jeb.032540

Tomanek, L., Zuzow, M. J., Ivanina, A. V., Beniash, E., and Sokolova, I. M. (2011). Proteomic response to elevated pCO_2 level in Eastern oysters, *Crassostrea virginica*: evidence for oxidative stress. *J. Exp. Biol.* 214, 1836–1844. doi: 10.1242/jeb.055475

Venkataraman, Y. R., Downey-Wall, A. M., Ries, J., Westfield, I., White, S. J., Roberts, S. B., et al. (2020). General DNA methylation patterns and environmentally-induced differential methylation in the Eastern oyster (*Crassostrea virginica*). *Front. Mar. Sci.* 7, 1–14. doi: 10.1101/2020.01.07.897934

Venn, A., Tambutté, E., Holcomb, M., Allemand, D., and Tambutté, S. (2011). Live tissue imaging shows reef corals elevate pH under their calcifying tissue relative to seawater. *PLoS ONE* 6:e20013. doi: 10.1371/journal.pone.0020013

Wagner, A. (2005). Energy constraints on the evolution of gene expression. *Mol. Biol. Evol.* 22, 1365–1374. doi: 10.1093/molbev/msi126

Waldbusser, G. G., and Salisbury, J. E. (2014). Ocean acidification in the coastal zone from an organism's perspective: multiple system parameters, frequency domains, and habitats. *Ann. Rev. Mar. Sci.* 6, 221–247. doi: 10.1146/annurev-marine-121211-172238

Waldbusser, G. G., Steenson, R. A., and Green, M. A. (2011a). Oyster shell dissolution rates in estuarine waters: effects of pH and shell legacy. *J. Shellfish Res.* 30, 659–669. doi: 10.2983/035.030.0308

Waldbusser, G. G., Voigt, E. P., Bergschneider, H., Green, M. A., and Newell, R. I. E. (2011b). Biocalcification in the Eastern oyster (*Crassostrea virginica*) in relation to long-term trends in Chesapeake Bay pH. *Estuaries Coasts* 34, 221–231. doi: 10.1007/s12237-010-9307-0

Wallace, R. B., Baumann, H., Grear, J. S., Aller, R. C., and Gobler, C. J. (2014). Coastal ocean acidification: The other eutrophication problem. *Estuar. Coast. Shelf Sci.* 148, 1–13. doi: 10.1016/j.ecss.2014.05.027

Wang, Q., Cao, R., Ning, X., You, L., Mu, C., Wang, C., et al. (2016). Effects of ocean acidification on immune responses of the Pacific oyster *Crassostrea gigas*. *Fish Shellfish Immunol.* 49, 24–33. doi: 10.1016/j.fsi.2015.12.025

Weiße, A. Y., Oyarzún, D. A., Danos, V., and Swain, P. S. (2015). Mechanistic links between cellular trade-offs, gene expression, and growth. *Proc. Natl. Acad. Sci. U.S.A.* 112, E1038–E1047. doi: 10.1073/pnas.1416533112

Whitlock, M., and Schluter, D. (2014). *The Analysis of Biological Data*. Roberts & Company. Available online at: https://books.google.com/books/about/The_Analysis_of_Biological_Data.html?hl=&id=Wm__oAEACAAJ

Wong, J. M., Johnson, K. M., Kelly, M. W., and Hofmann, G. E. (2018). Transcriptomics reveal transgenerational effects in purple sea urchin embryos: adult acclimation to upwelling conditions alters the response of their progeny to differential pCO_2 levels. *Mol. Ecol.* 27, 1120–1137. doi: 10.1111/mec.14503

Wood, H. L., Spicer, J. I., and Widdicombe, S. (2008). Ocean acidification may increase calcification rates, but at a cost. *Proc. Biol. Sci.* 275, 1767–1773. doi: 10.1098/rspb.2008.0343

Wright, R. M., Aglyamova, G. V., Meyer, E., and Matz, M. V. (2015). Gene expression associated with white syndromes in a reef building coral, *Acropora hyacinthus*. *BMC Genomics* 16:371. doi: 10.1186/s12864-015-1540-2

Wu, C.-Y., Alexander Rolfe, P., Gifford, D. K., and Fink, G. R. (2010). Control of transcription by cell size. *PLoS Biol.* 8:e1000523. doi: 10.1371/journal.pbio.1000523

Xu, X., Li, G., Li, C., Zhang, J., Wang, Q., Simmons, D. K., et al. (2019). Evolutionary transition between invertebrates and vertebrates via methylation reprogramming in embryogenesis. *Nat. Sci. Rev.* 6, 993–1003. doi: 10.1093/nsr/nwz064

Yeaman, S. (2015). Local adaptation by alleles of small effect. *Am. Nat.* 186(Suppl. 1), S74–S89. doi: 10.1086/682405

Yong-Villalobos, L., González-Morales, S. I., Wrobel, K., Gutiérrez-Alanis, D., Cervantes-Peréz, S. A., Hayano-Kanashiro, C., et al. (2015). Methylome analysis reveals an important role for epigenetic changes in the regulation of the *Arabidopsis* response to phosphate starvation. *Proc. Natl. Acad. Sci. U.S.A.* 112, E7293–E7302. doi: 10.1073/pnas.1522301112

Zemach, A., McDaniel, I. E., Silva, P., and Zilberman, D. (2010). Genome-wide evolutionary analysis of eukaryotic DNA methylation. *Science* 328, 916–919. doi: 10.1126/science.1186366

Zhang, H., Lang, Z., and Zhu, J.-K. (2018). Dynamics and function of DNA methylation in plants. *Nat. Rev. Mol. Cell Bio.* 19, 489–506. doi: 10.1038/s41580-018-0016-z

Zhang, J., Luo, S., Gu, Z., Deng, Y., and Jiao, Y. (2020). Genome-wide DNA methylation analysis of mantle edge and mantle central from *Pearl oyster Pinctada fucata martensii*. *Mar. Biotechnol.* 22, 380–390. doi: 10.1007/s10126-020-09957-4

Zilberman, D., Gehring, M., Tran, R. K., Ballinger, T., and Henikoff, S. (2007). Genome-wide analysis of *Arabidopsis thaliana* DNA methylation uncovers an interdependence between methylation and transcription. *Nat. Genet.* 39, 61–69. doi: 10.1038/ng1929

Conflict of Interest: The authors declare that the research was conducted in the absence of any commercial or financial relationships that could be construed as a potential conflict of interest.

frontiers in Marine Science

ORIGINAL RESEARCH
published: 14 January 2021
doi: 10.3389/fmars.2020.604878

DNA Methylation Dynamics in Atlantic Salmon (*Salmo salar*) Challenged With High Temperature and Moderate Hypoxia

Anne Beemelmanns[1], Laia Ribas[2], Dafni Anastasiadi[2], Javier Moraleda-Prados[2], Fábio S. Zanuzzo[1], Matthew L. Rise[1] and A. Kurt Gamperl[1]*

[1] Department of Ocean Sciences, Memorial University, St. John's, NL, Canada, [2] Department of Renewable Marine Resources, Institut de Ciències del Mar, Consejo Superior de Investigaciones Científicas (CSIC), Barcelona, Spain

The marine environment is predicted to become warmer and more hypoxic, and these conditions may become a challenge for marine fish species. Phenotypically plastic responses facilitating acclimatization to changing environments can be mediated by DNA methylation through the modulation of gene expression. To investigate whether temperature and hypoxia exposure induce DNA methylation changes, we challenged post-smolt Atlantic salmon (*Salmo salar*) to increasing temperatures (12 → 20°C, 1°C week^{-1}) under normoxia or moderate hypoxia (~70% air saturation) and compared responses in the liver after 3 days or 4 weeks at 20°C. DNA methylation was studied in six genes related to temperature stress (*cirbp, serpinh1*), oxidative stress (*prdx6*, *ucp2*), apoptosis (*jund*), and metabolism (*pdk3*). Here, we report that exposure to high temperature, alone or combined with hypoxia, affected the methylation of CpG sites within different genomic regulatory elements around the transcription start of these temperature/hypoxia biomarker genes. Yet, we uncovered distinct CpG methylation profiles for each treatment group, indicating that each environmental condition may induce different epigenetic signatures. These CpG methylation responses were strongly dependent on the duration of stress exposure, and we found reversible, but also persistent, CpG methylation changes after 4 weeks of exposure to 20°C. Further, several of these changes in CpG methylation correlated with transcriptional changes, and thus, can be considered as regulatory epigenetic marks (epimarkers). Our study provides insights into the dynamic associations between CpG methylation and transcript expression in Atlantic salmon, and suggests that this epigenetic mechanism may mediate physiological acclimation to short-term and long-term environmental changes.

Keywords: DNA methylation, high temperature, low oxygen, environmental changes, acclimatization, epigenetic marks, biomarkers, aquaculture

OPEN ACCESS

Edited by:
Jose M. Eirin-Lopez, Florida International University, United States

Reviewed by:
Mikko Juhani Nikinmaa, University of Turku, Finland
Daniel Garcia-Souto, University of Vigo, Spain
Malthe Hvas, Norwegian Institute of Marine Research (IMR), Norway

****Correspondence:***
Anne Beemelmanns
abeemelmanns@mun.ca

Specialty section:
This article was submitted to Marine Molecular Biology and Ecology, a section of the journal Frontiers in Marine Science

Received: *10 September 2020*
Accepted: *16 November 2020*
Published: *14 January 2021*

Citation:
Beemelmanns A, Ribas L, Anastasiadi D, Moraleda-Prados J, Zanuzzo FS, Rise ML and Gamperl AK (2021) DNA Methylation Dynamics in Atlantic Salmon (Salmo salar) Challenged With High Temperature and Moderate Hypoxia. Front. Mar. Sci. 7:604878. doi: 10.3389/fmars.2020.604878

INTRODUCTION

Increasing temperatures and deoxygenation (hypoxia) of the oceans associated with global warming (Breitburg et al., 2018; Claret et al., 2018; IPCC, 2019) can affect the physiology of marine organisms resulting in shifts in phenotypic traits (Somero, 2010; Crozier and Hutchings, 2014). Aquatic ectotherms, such as fish, are especially sensitive to variations in temperature and hypoxia,

as these conditions have lasting effects on their development, growth, metabolism, immunity and reproduction (Brett, 1956, 1971; Hughes, 1973; Currie and Schulte, 2014; Abdel-Tawwab et al., 2019). Phenotypic plasticity, by which prolonged or repeated stress exposure leads to changes in phenotypic responses that optimize physiological performance, has been observed in fishes and this allows them to survive in rapidly changing environments (Crozier and Hutchings, 2014; Seebacher et al., 2015; Beaman et al., 2016). Many fish species have evolved molecular mechanisms and strategies that operate at the transcript level, and enable them to respond and adapt to these environmental stressors (Hazel and Prosser, 1974; Larsen et al., 2011). Although it is still not well-understood how signals of environmental stressors are perceived and integrated into the genome, there is growing evidence that epigenetic mechanisms (e.g., DNA methylation) play an essential role in facilitating this phenotypic plasticity through the modulation of gene expression (Jaenisch and Bird, 2003; Turner, 2009; Eirin-Lopez and Putnam, 2019; McCaw et al., 2020; Ryu et al., 2020; Venney et al., 2020).

Epigenetic modifications are a dynamic combination of DNA methylation, histone modifications, and non-coding RNAs that regulate gene expression (Bird, 2002; Best et al., 2018; Eirin-Lopez and Putnam, 2019). DNA methylation is the reversible addition of a methyl group (CH_3) to the 5′ carbon end of cytosine (5mC) nucleotides catalyzed by specific DNA methyltransferases (Edwards et al., 2017). The best characterized process in animals is the methylation of cytosine-phosphate-guanine (CpG) dinucleotides that provides a signal for the activation or deactivation of gene transcription (Jones, 2001, 2012; Edwards et al., 2017). Classically, the hyper-methylation of CpG-rich promoters has been associated with gene silencing through the blockage of the transcription initiation machinery (Jones, 2001, 2012; Bird, 2002; Edwards et al., 2017). However, DNA methylation patterns are far more dynamic and context-dependent than originally thought (Jones, 2012; Baubec and Schübeler, 2014; Ambrosi et al., 2017). For example, increasing evidence also suggests that promoter hyper-methylation is associated with gene activation (Smith et al., 2020). Further, DNA methylation changes appear in a variety of genomic elements that contribute to transcriptional regulation: e.g., within the 5′ upstream (promoter) region (Campos et al., 2013; McGaughey et al., 2014; Han et al., 2016; Wang et al., 2016; Moghadam et al., 2017; Zheng et al., 2017; Uren Webster et al., 2018; Veron et al., 2018), specifically at transcription factor binding sites and enhancers (Bogdanović et al., 2016; Li et al., 2017), as well as in exons (Ball et al., 2009; McGaughey et al., 2014; Li et al., 2017; Moghadam et al., 2017; Uren Webster et al., 2018) and introns of the gene body (Anastasiadi et al., 2018a). These DNA methylation changes can be rapidly induced in response to environmental cues (Angers et al., 2010) and can persist through cell division within generations, but also across multiple generations (Jablonka and Raz, 2009; Nelson et al., 2013; Mirbahai and Chipman, 2014; Szyf, 2015; Wang et al., 2016; Ryu et al., 2018, 2020; Valdivieso et al., 2020; Venney et al., 2020). Consequently, the temporal relationship between environmentally induced DNA methylation changes and gene expression appears to be complex, and thus, additional research is needed before we can fully understand epigenetic processes that modulate phenotypic variation in response to changing environments.

The most challenging environmental stressors faced by fishes include seasonal changes in water temperature (Brett, 1956, 1971; Madeira et al., 2016; Wade et al., 2019) and low water oxygen levels (hypoxia) (Hughes, 1973; Burt et al., 2013; Abdel-Tawwab et al., 2019), and these stressors are predicted to become a greater risk with global warming (Breitburg et al., 2018; Claret et al., 2018; IPCC, 2019). Coastal ecosystems are particularly vulnerable to extreme seasonal temperature increases and hypoxia events, and marine heatwaves are predicted to occur with higher frequency and duration in the future (Frölicher et al., 2018; Oliver et al., 2018). Marine aquaculture species, like Atlantic salmon (*Salmo salar*), are confined in coastal sea-cages and exposed to increasing temperatures that co-occur with hypoxia for prolonged periods during the summer months, and cannot relocate to more favorable conditions (Burt et al., 2012; Stehfest et al., 2017; Wade et al., 2019; Burke et al., 2020). For instance, water temperatures in Atlantic salmon sea-cages in Tasmania have already exceeded 22–23°C in the summer, while in the Northern Atlantic water temperatures can reach 18–20°C, and oxygen levels often drop to 60–70% of air saturation during these periods (Burt et al., 2012; Stehfest et al., 2017; Wade et al., 2019; Burke et al., 2020). Yet, Atlantic salmon have an optimal growth performance between 10 and 14°C and significant mortalities (∼30%) are observed if temperatures reach 22–23°C (Hvas et al., 2017; Gamperl et al., 2020). As a consequence, these extreme and suboptimal environmental conditions negatively affect their physiological and growth performance (Wade et al., 2019; Gamperl et al., 2020), and they were recently identified as the primary cause of a mass mortality event at cage-sites in Newfoundland in the summer of 2019 (Burke et al., 2020). Thus, this is raising concerns worldwide with respect to salmon health and welfare as the climate warms. Our research has already shown that elevated temperatures (20°C) alone, or in combination with moderate hypoxia (∼70% air saturation), results in large-scale transcriptional changes in the liver of Atlantic salmon, and that the expression of genes related to the heat-shock response, apoptosis and immune defense were up-regulated, whereas those connected to oxidative stress and various metabolic processes were largely suppressed (Beemelmanns et al., 2020). However, it is still not clear how resilient fish are to long-term exposure to elevated temperatures (alone or in combination with hypoxia), and it is important to understand the epigenetic mechanisms regulating these changes in gene expression, and consequently, how they mediate physiological plasticity and acclimatization responses.

Recent research provides compelling evidence that teleost DNA methylation is influenced in various ways by thermal challenges (Campos et al., 2013; Han et al., 2016; Anastasiadi et al., 2017; Burgerhout et al., 2017; Metzger and Schulte, 2017; Ryu et al., 2018, 2020; Uren Webster et al., 2018; McCaw et al., 2020; Valdivieso et al., 2020). Nonetheless, the role of DNA methylation in regulating gene expression during or following hypoxic stress is still largely unexplored (Wang et al., 2016; Veron et al., 2018). Epigenetic marks established during early

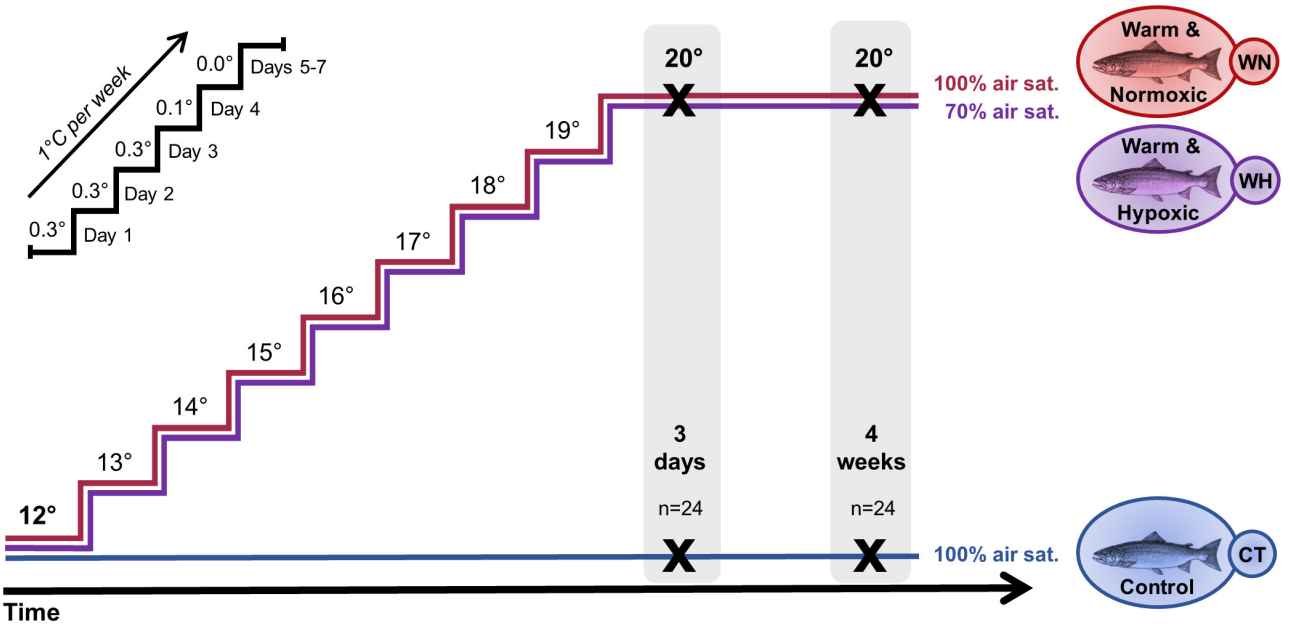

FIGURE 1 | Design of the temperature and hypoxia challenge with Atlantic salmon. Post-smolt salmon were either exposed to: (i) a temperature increase from 12 → 20°C and normoxia (~100% air saturation) (Warm & Normoxic, WN); (ii) a temperature increase from 12 → 20°C and moderate hypoxia (~70% air sat.) (Warm & Hypoxic, WH); or (iii) a constant water temperature of 12°C and normoxia (~100% air sat.) (Control, CT). The temperature was increased by 1°C week^{-1}, following the temperature regimen shown in the upper left portion of the figure. Liver samples were collected 3 days and 4 weeks after the temperature reached 20°C (n = 8 per treatment/time point, N = 48 total) and used to measure gene expression (qPCR, Fluidigm Biomark^{TM}) and to examine CpG methylation (Multiplex Bisulfite Sequencing, MBS) in a ~500 bp region around the transcription start site.

development are known to be sensitive to environmental cues due to the high rate of mitotic cell division (Faulk and Dolinoy, 2011; Toraño et al., 2016; Pérez et al., 2019). On the contrary, it is still unclear whether environmental stressors experienced at older life-stages (i.e., immature juveniles and adults) can also induce DNA methylation changes that are integrated into the genome as epigenetic marks and facilitate physiological acclimation (reversible or permanent). Given that DNA methylation changes of specific CpGs are sensitive to environmental influences, and can be stably associated with a particular phenotypic response, they can be applied as epigenetic biomarkers (epimarkers). For example, DNA methylation markers are utilized in medicine as non-invasive diagnostic tools for the prognosis of cancer and other diseases (Mikeska and Craig, 2014). Epimarkers have also been used to construct clocks capable of accurately estimating age in humans (Horvath, 2013) and in other vertebrates, including fish (Polanowski et al., 2014; De Paoli-Iseppi et al., 2019; Anastasiadi and Piferrer, 2020). The development of epimarkers to detect past environmental stress exposure in marine organisms gives us the ability to identify early exposures to detrimental stressors, and this will enhance biomonitoring and conservation as well as aquaculture management efforts (Gavery and Roberts, 2017; Beal et al., 2018; Best et al., 2018; Eirin-Lopez and Putnam, 2019). Recently, epigenetic markers were developed to predict sex in fish species, and this will improve sex-control programs in aquaculture (Anastasiadi et al., 2018b; Piferrer, 2018). Further, epigenetic footprinting (epigenetic memory) of lifetime stressors allows for the detection of anthropogenic pollutants, toxins, or even changes in temperature in the marine environment (Beal et al., 2018; Anastasiadi et al., in press).

In this study, we employed Multiplex Bisulfite Sequencing (MBS) to measure CpG methylation within a ~500 bp region around the transcription start sites of six thermal/hypoxia biomarker genes in the liver of post-smolt Atlantic salmon following short-term (3 days) and prolonged (4 weeks) exposure to (i) high temperature (20°C) and normoxia (~100% air saturation) (Warm & Normoxic—WN) or (ii) high temperature (20°C) and moderate hypoxia (~70% air saturation) (Warm & Hypoxic—WH), as compared to (iii) control conditions (12°C, normoxia) (Control—CT) (**Figure 1**). The biomarker genes used in this study were selected based on previous microarray and qPCR studies on liver tissue from the same experimental fish, and they exhibited stress-induced mRNA expression changes that were associated with physiological performance (Beemelmanns et al., 2020). These target genes are known to be important regulators of temperature (*cirbp, serpinh1*) (Ishida and Nagata, 2011; Zhong and Huang, 2017; Akbarzadeh et al., 2018; Houde et al., 2019) and oxidative stress (*prdx6*, *ucp2*) (Brand and Esteves, 2005; Ambruso, 2013), apoptosis (*jund*) (Weitzman et al., 2000), and glucose metabolism (*pdk3*) (Kuntz and Harris, 2018; **Table 1**). By using this gene-specific locus approach, we aimed to identify epigenetic marks within important genomic regulatory elements [i.e., the 5′ upstream region (including putative TATA-box or Polymerase II (POL-II) promoter sequences), 5′ UTR, first coding exon, and first intron] (**Figure 2**). We hypothesized that epigenetic modifications are induced by environmental

TABLE 1 | Overview of genes used for Multiplex Bisulfite Sequencing (MBS).

Gene[a]	Gene name[a]	Ensembl gene ID[a]	Functional category[b]	Expression change[c]	Chr[d]	Position (start/end)[e]	Size (bp)[f]	No. of CpGs[g]	CpGs per 100 (bp)[g]	5′ up-stream (bp)[h]	Promoter motifs (bp)[h]	5′ UTR (bp)[h]	Exon (bp)[h]	Intron (bp)[h]
serpinh1	Serpin H1	ENSSSAG00000032055	Temperature stress	↑	ssa 09	121,686,950 121,687,410	460	8	1.7	0	0	37	210	213
jund	Transcription factor Jun-D	ENSSSAG00000077483	Apoptosis	↑	ssa 03	13,688,204 13,688,672	468	16	3.4	268	9	178	13	0
pdk3	Pyruvate dehydrogenase kinase isozyme 3	ENSSSAG00000001825	Metabolism	↑	ssa 04	35,435,799 35,436,262	463	18	3.9	0	0	6	103	354
cirbp	Cold-inducible RNA-binding protein	ENSSSAG00000039849	Temperature stress, hypoxia	↓	ssa 16	37,941,668 37,942,151	483	23	4.8	19	0	36	0	428
prdx6	Peroxiredoxin 6	ENSSSAG00000073907	Oxidative stress	↓	ssa 14	33,502,535 33,503,013	478	14	2.9	222	7	67	92	90
ucp2	Mitochondrial uncoupling protein 2	ENSSSAG00000044701	Oxidative stress	↓	ssa 04	44,947,084 44,947,566	482	15	3.1	93	7	203	0	179
						Average	**474.9**	**15.3**	**3.2**					

[a]Refers to the identity of the genes identified through BLASTn searches against NCBI and Ensembl nr/nt databases. [b]Refers to the broader functional category of the protein (Beemelmanns et al., 2020). [c]Indicated is the direction of the transcript expression response (↑up- or ↓down-regulation) to high temperature and hypoxia (Beemelmanns et al., 2020). [d]Chromosome number according to Salmo salar assembly (ssa) ICSASG_V2 (GCF_000233375.1). [e]Start and end position in base pairs (bp) of targeted amplicon within the specific Atlantic salmon chromosomes. [f]The total size of the sequenced amplicon in base pairs (bp). [g]The total number and frequency of CpGs per 100 base pairs (bp) within the amplicon. [h]Coverage of the 5′ upstream region, putative promoter (TATA-box motif), 5′ UTR, first coding exon, and first intron within the amplicon in base pairs (bp).

stressors, that these epigenetic marks are important in mediating physiological plasticity and acclimatization responses, and that they may be applicable as epimarkers to predict environmental stress exposure and/or tolerance.

RESULTS

CpG Methylation Dynamics

To examine the methylation profiles of salmon exposed to the WN or WH conditions at 20°C for 3 days or 4 weeks, in comparison to CT fish (**Figure 1**), we performed Principal Component Analysis (PCA) using the methylation values of CpGs that responded to the treatment with a change in their methylation levels (thereafter called 'treatment responsive CpGs') (**Table 2**). These PCA analyses were separated into up- (**Figure 3**) and down-regulated (**Figure 4**) genes so that the direction of the response was considered. Overall, we detected different CpG methylation profiles for WN and WH fish (**Figures 3**, **4** and **Supplementary Table S1**). However, these CpG methylation responses were gene-specific, context-specific and exposure time-dependent, suggesting temporal changes within different genomic elements (**Figures 2–4** and **Table 2**).

CpG Methylation Dynamics of Up-Regulated Genes

In the first coding exon of *serpinh1*, four CpGs (No. 1–4) were responsive in the WN and WH groups after 3 days of exposure to 20°C (**Figure 2A** and **Table 2**). Based on their collective methylation values, we found similar, but distinct, profiles between WN and WH fish as compared to CT fish, as shown by a clear cluster separation along with the first Principal Component (PC-1: $F = 6.1$, $p = 0.007$; CT vs. WN $p = 0.046$, CT vs. WH $p = 0.007$, WN vs. WH $p = 0.624$; 61.5% variation; **Figure 3A** and **Supplementary Table S1**). However, the effects for these same CpGs diminished after exposure to 20°C for 4 weeks, as evidenced by the overlapping ellipses for all three treatment groups in the PCA (PC-1: $F = 1.3$, $p = 0.292$; **Figure 3B** and **Supplementary Table S1**).

Different CpG methylation profiles were also found based on three responsive CpGs (No. 7, 10, and 13) located within the 5′ upstream region close to the putative promoter site (TATA-box) of the gene *jund* (**Figure 2B** and **Table 2**) in fish exposed to WN or WH conditions at 20°C for 3 days as compared to the CT group (PC-2: $F = 10.7$, $p = 4.9e\text{-}4$; CT vs. WN $p = 0.008$, CT vs. WH $p < 0.0001$, WN vs. WH $p = 0.384$; 32.4% variation; **Figure 3C** and **Supplementary Table S1**). However, after 4 weeks of exposure to 20°C, the methylation of a different set of three responsive CpGs (No. 10, 12, and 15) located in the same 5′ upstream region (**Figure 2B** and **Table 2**) only resulted in a significant separation of the WH group from the CT group (PC-1: $F = 3.7$, $p = 0.038$; CT vs. WH $p = 0.033$; 47.1% variance; **Figure 3D** and **Supplementary Table S1**).

For *pdk3*, we only found weak effects for the combined responses of three CpGs (No. 5, 7, and 12) situated in the first intron (**Figure 2C** and **Table 2**) upon short-term exposure to 20°C (PC-1: $F = 3.3$, $p = 0.054$; **Figure 3E** and **Supplementary Table S1**). However, we did not observe significantly different

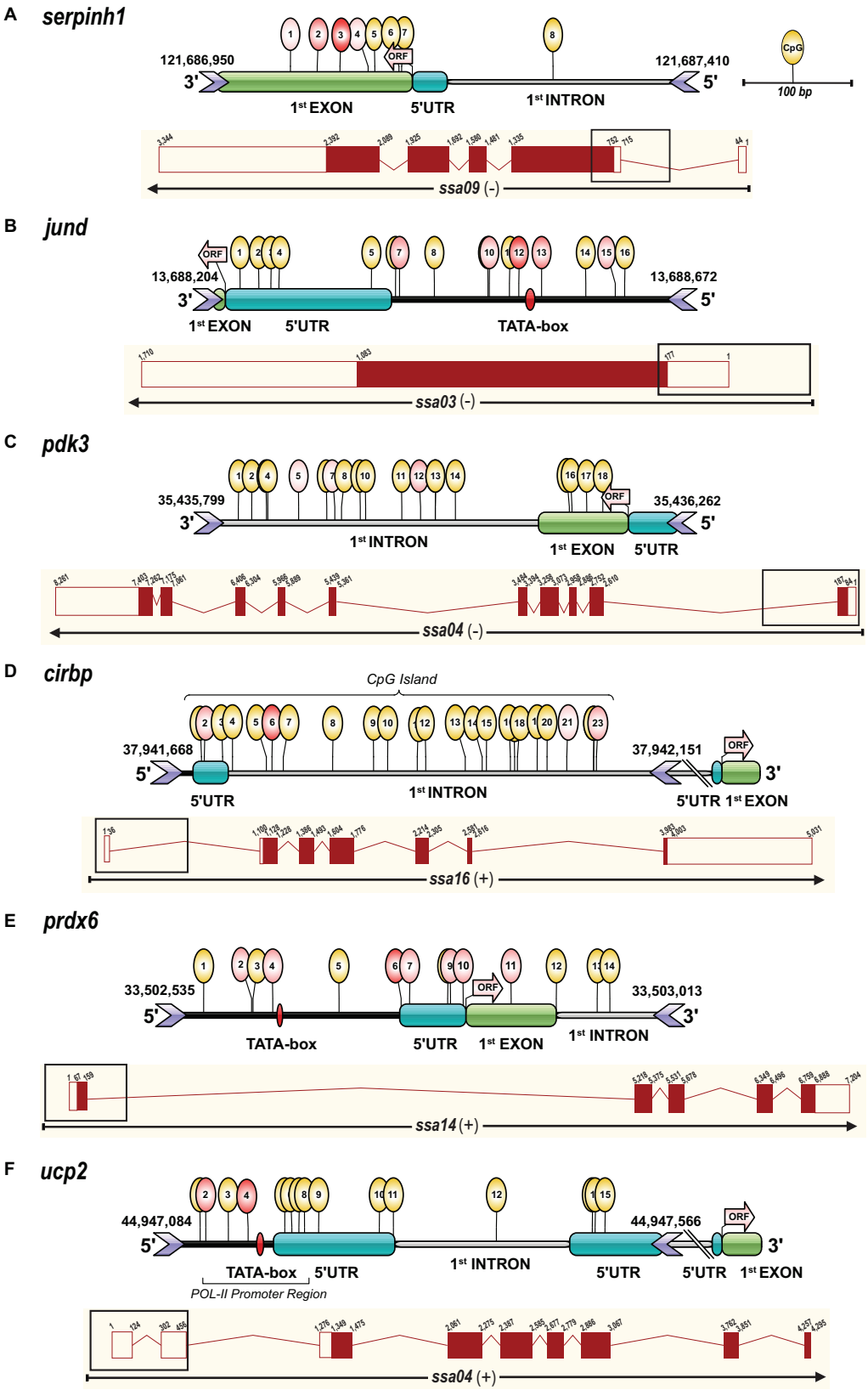

FIGURE 2 | Continued

FIGURE 2 | Gene transcript and amplicon structure (∼500 bp) including CpG methylation marks. Each panel contains an illustration representing the targeted amplicon sequence structure including CpG methylation marks assessed by Methylation Bisulfite Sequencing (MBS) and a complete transcript diagram for the genes **(A)** *serpinh1*, **(B)** *jund*, **(C)** *pdk3*, **(D)** *cirbp*, **(E)** *prdx6*, and **(F)** *ucp2*. The amplicon structure illustration was performed with IBS software (Liu et al., 2015) and shows the genomic regions (5′ upstream, 5′ UTR, first coding exon and first intron) and CpG methylation marks determined based on the Atlantic salmon (*Salmo salar*) genome assembly (*ssa*) version ICSASG_v2 available on NCBI and Ensembl. The identification of putative promoter regions (TATA-box, POL-II promoter sequence) and CpG islands was performed *in silico* with promoter prediction tools (www.softberry.com). The start codon and the beginning of the open reading frame (ORF) are indicated by an arrow in light red. The exact chromosome location of the sequenced region, including genomic start and end positions, is given in base pairs (bp) on top of the location of the forward and reverse primers (> <icons) for each gene (**Table 1**). The positions for the detected methylated cytosines in a CpG context are illustrated by yellow circular marks on top of the genomic elements. The treatment responsive CpG methylation sites are indicated in red and the intensity of this color corresponds to the significance of the response (**Table 2**). The transcript diagrams below the amplicon structure for each gene were obtained and modified from the Ensembl database (http://useast.ensembl.org/index.html), and show exons as red boxes and introns as lines. Filled boxes are protein-coding exon sequences and unfilled boxes are untranslated regions (UTRs), and for each of them, the cumulative size is indicated in bp. The black rectangular box on top of each transcript diagram represents the genomic area (∼500 bp) that was targeted for the MBS approach.

methylation profiles for this gene between the two treatment groups (WN, WH) and the CT group at either of the exposure time points (**Figures 3E,F** and **Supplementary Table S1**).

CpG Methylation Dynamics of Down-Regulated Genes

For the gene *cirbp*, we identified one responsive CpG in the first part of the 5′ UTR (No. 2) and three CpGs in the intron (1,074 bp) that interrupts the 5′ UTR (No. 6, 21, and 23) upon short-term WN and WH exposure at 20°C (**Figure 2D** and **Table 2**). Based on their collective responses, the WN fish displayed the strongest difference in CpG methylation as compared to the CT group along PC-1 (F = 6.9, p = 0.004; CT vs. WN p = 0.005, WN vs. WH p = 0.031; 48.3% variance; **Figure 4A** and **Supplementary Table S1**). In contrast, the WH group showed a trend for a greater cluster separation from the CT group with regards to PC-2 (F = 3.4, p = 0.051; CT vs. WH p = 0.041; 25.4% variance; **Figure 4A** and **Supplementary Table S1**). When comparing the same set of CpGs after 4 weeks of exposure to 20°C, the CpG methylation profiles were similar between all three groups (PC-1: F = 2.3, p = 0.118; **Figure 4B** and **Supplementary Table S1**).

The gene *prdx6* had two responsive CpGs located in the 5′ upstream region in close proximity to the putative TATA-box site (Nos. 2 and 4) and one CpG within the 5′ UTR (No. 7) (**Figure 2E** and **Table 2**) that differentiated the WN group from the CT group, but also from the WH group, after short-term exposure to 20°C (PC-1: F = 6.5, p = 0.004; CT vs. WN p = 0.041, WN vs. WH p = 0.004; 49.9% variance; **Figure 4C** and **Supplementary Table S1**). In contrast, after long-term exposure to 20°C, we identified a different set of four responsive CpGs within the 5′ UTR (No. 6, 9, and 10) and the first coding exon (No. 11) (**Figure 2E** and **Table 2**). Based on these CpGs the WH group clustered differently from the CT group, but also from the WN group, along PC-1 (F = 5.3, p = 0.013; CT vs. WH p = 0.041, WN vs. WH p = 0.017; 37.5% variance; **Figure 4D** and **Supplementary Table S1**); while the WN group clustered apart from the CT group along PC-2 (F = 5.7, p = 9.6e-3; CT vs. WN p = 0.008; 31.8% variance; **Figure 4D** and **Supplementary Table S1**).

Finally, *ucp2* had two highly responsive CpGs (Nos. 2 and 4) located in the 5′ upstream region in close proximity to the putative TATA-box and POL-II motif (**Figure 2F** and **Table 2**) that differentiated the WN and WH groups from the CT group after short- and long-term exposure to 20°C (3-days/PC-1: F = 14.6, p = 7.2e-5; 52.6% variation; 4-weeks/PC-1: F = 27.2, p = 6.8e-7; 66.9% variation; **Figures 4E,F** and **Supplementary Table S1**). Interestingly, WH fish displayed a more pronounced separation from CT fish after 3 days of exposure to 20°C (3-days/PC-1: CT vs. WN p = 0.011, CT vs. WH p < 0.0001, WN vs. WH p = 0.061; **Figure 4E** and **Supplementary Table S1**), whereas the methylation levels were more strongly affected in WN fish after 4 weeks at this temperature (4-weeks/PC-1: CT vs. WN p < 0.0001, CT vs. WH p = 0.017, WN vs. WH p = 0.001; **Figure 4F** and **Supplementary Table S1**).

Correlation Analyses Between Global CpG Methylation and Transcript Expression Changes

The collective responses of all significantly affected (p < 0.05) CpGs (**Table 2**) and the overall relative transcript expression levels (RQ) were investigated in a global PCA approach for short-term (3 days) (**Figures 5A,B**) and long-term (4 weeks) WN or WH exposure to 20°C (**Figures 5D,E** and **Supplementary Table S1**). The association between collective CpG methylation and transcript expression responses was estimated by correlating the extracted scores from the PC-1 of the global CpG methylation and the transcript expression PCAs using Pearson correlation coefficients (R) (**Figures 5C,F**).

Global CpG Methylation and Transcript Expression Changes After 3 Days at 20°C

The effects of short-term exposure to 20°C in WN and WH fish were evident in the collective CpG methylation and transcript expression profiles of the six genes (**Figures 5A,B**). Salmon of all three treatment groups could be clearly distinguished from each other given their distinct methylation profiles when all 12 significantly affected CpGs (**Table 2**) were considered (PC-1: F = 14.7, p = 6.8e-5; CT vs. WN p = 0.020, CT vs. WH p < 0.0001, WN vs. WH p = 0.026; 24.3% variation; PC-2: F = 29.8, p = 5.9e-4; CT vs. WN p = 0.001; WN vs. WH p = 0.004; 20.1% variation; **Figure 5A** and **Supplementary Table S1**). The transcript expression of the corresponding six target genes in both WN and WH fish

TABLE 2 | CpG methylation and relationship to the transcript expression of six genes (*cirbp*, *jund*, *pdk3*, *prdx6*, *serpinh1*, and *ucp2*) assessed by linear mixed-effect models (*lmer*) and correlation analyses.

CpG methylation per gene					Treatment effect[d]								Correlation[g]	
Gene[a]		**Time**	**CpG no. chr. position[b]**	**Genomic element[c]**	**F-val.**	**Pr(>F)**		**WN vs. CT[e]**	**WH vs. CT[e]**	**WN vs. WH[e]**	**WN vs. CT[f]**	**WH vs. CT[f]**	**WN vs. WH[f]**	**Pr (>F)**	**R**
serpinh1	Up ↑	3 days	CpG.1.121687029	1st exon	2.8	*0.082*	∼							**6.0e-4**	**+0.650**
			CpG.2.121687058	1st exon	3.9	**0.032**	*	↑	↑		*0.057*	*0.055*	1.000	0.147	+0.305
			CpG.3.121687082♦	1st exon	5.9	**0.008**	**	↑	↑		**0.038**	**0.009**	0.746	**0.008**	**+0.528**
			CpG.4.121687112	1st exon	2.8	*0.081*	∼							0.151	+0.302
		4 weeks	CpG.1.121687029	1st exon	1.2	0.332								0.565	-0.124
			CpG.2.121687058	1st exon	1.1	0.339								0.323	+0.211
			CpG.3.121687082	1st exon	1.4	0.274								0.167	-0.292
			CpG.4.121687112	1st exon	0.01	0.991								0.465	-0.157
jund	Up ↑	3 days	CpG.7.13688404	5′ upstream	5.7	**0.009**	**	↑			**0.007**	0.219	0.250	0.139	+0.311
			CpG.10.13688501	5′ upstream	7.0	**0.004**	**		↑	↓↑	0.239	**0.002**	*0.075*	0.317	+0.213
			CpG.13.13688555	Promoter	4.1	**0.029**	*	↓			**0.026**	0.602	0.181	0.436	-0.167
		4 weeks	CpG.10.13688501	5′ upstream	3.1	*0.062*	∼							0.632	-0.103
			CpG.12.13688533♦	Promoter	7.1	**0.004**	**	↓	↓		**0.008**	**0.012**	1.000	**0.034**	**-0.434**
			CpG.15.13688637	5′ upstream	3.4	**0.049**	*		↓	↑↓	0.988	*0.065*	*0.086*	0.955	+0.012
pdk3	Up ↑	3 days	CpG.5.35435889	1st intron	2.8	*0.081*	∼							0.613	+0.109
			CpG.7.35435928	1st intron	3.0	*0.066*	∼							0.375	+0.190
			CpG.12.35436020	1st intron	3.6	**0.044**	*			↑↓	0.343	0.491	**0.035**	0.342	+0.203
		4 weeks	CpG.5.35435889	1st intron	0.8	0.459								0.968	+0.009
			CpG.7.35435928	1st intron	0.5	0.642								0.920	-0.022
			CpG.12.35436020	1st intron	1.9	0.168								0.651	-0.097

(Continued)

TABLE 2 | Continued

CpG methylation per gene					Treatment effect[d]								Correlation[g]	
Gene[a]		**Time**	**CpG no. chr. position[b]**	**Genomic element[c]**	**F-val.**	**Pr(>F)**		**WN vs. CT[e]**	**WH vs. CT[e]**	**WN vs. WH[e]**	**WN vs. CT[f]**	**WH vs. CT[f]**	**WN vs. WH[f]**	**Pr (>F)**	**R**
cirbp	Down ↓	3 days	CpG.2.37941700	5′ UTR	5.6	**0.010**	*			↑↓	0.205	0.317	**0.008**	0.862	-0.037
			CpG.6.37941770♦	1st intron	3.6	**0.042**	*	↑	↑		**0.048**	*0.051*	0.946	**0.026**	**-0.455**
			CpG.21.37942071	1st intron	2.9	*0.076*	∼							0.160	+0.296
			CpG.23.37942102	1st intron	4.0	**0.033**	*	↑			**0.036**	0.824	0.118	0.292	-0.224
		4 weeks	CpG.2.37941700	5′ UTR	2.5	0.100								0.198	-0.272
			CpG.6.37941770	1st intron	1.0	0.392								0.968	-0.009
			CpG.21.37942071	1st intron	2.1	0.139								0.100	+0.344
			CpG.23.37942102	1st intron	2	0.163								0.454	-0.160
prdx6	Down ↓	3 days	CpG.2.33502611	5′ upstream	2.9	*0.077*	∼							*0.056*	*+0.395*
			CpG.4.33502632	Promoter	5.2	**0.013**	*			↓↑	0.155	0.476	**0.011**	0.713	+0.079
			CpG.7.33502773	5′ UTR	3.4	*0.050*	∼							0.391	+0.183
		4 weeks	CpG.6.33502764♦	5′ UTR	3.5	**0.046**	*	↑			**0.043**	0.194	0.797	*0.097*	-0.357
			CpG.9.33502814	5′ UTR	3.3	*0.056*	∼							0.616	-0.108
			CpG.10.33502827	5′ UTR	3.0	*0.068*	∼							0.828	+0.047
			CpG.11.33502876	1st exon	4.0	**0.032**	*			↑↓	0.162	0.624	**0.030**	0.308	-0.217
ucp2	Down ↓	3 days	CpG.2.44947115	Promoter	8.1	**0.002**	**		↓	↑↓	0.738	**0.003**	**0.011**	0.175	+0.286
			CpG.4.44947155♦	Promoter	6.3	**0.006**	**	↓	↓		**0.018**	**0.010**	0.940	*0.058*	*+0.392*
		4 weeks	CpG.2.44947115	Promoter	7.0	**0.004**	**	↓		↓↑	**0.011**	0.968	**0.009**	0.267	+0.294
			CpG.4.44947155♦	Promoter	35.4	**6.9e-8**	***	↓	↓	↓↑	**<0.0001**	**<0.0001**	**0.038**	**1.7e-4**	**+0.623**

*[a]Indicated is the direction of the transcript expression response (↑up-regulation, ↓down-regulation) upon high temperature and/or hypoxia exposure (**Table 1**; Beemelmanns et al., 2020). [b]The name of each CpG consists of a given numerical number (i.e., CpG.1) followed by the chromosomal position (i.e., CpG.1.44947115) in base pairs. [c]The location of each CpG within the different regulatory genomic elements of interest (**Figure 2**). [d]Linear mixed-effect models (lmer) were performed on CpG methylation values to assess the effects of the fixed factors "treatment" (CT, Control; WN, Warm & Normoxic; WH, Warm & Hypoxic) and "sex" (Female vs. Male), and "tank" was included as a random term. Significant p-values are marked in bold letters ($p < 0.001$***, $p < 0.01$**, $p < 0.05$*) and trends in italics ($0.05 < p < 0.10$) with an "∼" symbol. The complete results for all 94 CpGs are given in **Supplementary Table S2**. [e]The arrows indicate the direction of CpG methylation responses (↑hyper-methylated, ↓hypo-methylated) and represent the results of least square means (lsmeans) post-hoc tests to differentiate between treatment groups. Bold arrows illustrate the direction of significant differences between CT vs. WN, CT vs. WH, and WN vs. WH groups ($p < 0.001$***, $p < 0.01$**, $p < 0.05$*), while narrow arrows indicate trends ($0.05 < p < 0.10$) (see **Supplementary Table S2**). [f]The p-values of the lsmeans post-hoc test used for differentiating between CT, WN vs. WH groups (see **Supplementary Table S2**). [g]Spearman's rank correlation coefficients (R) and corresponding p-values to estimate the overall association between CpG methylation (%) and transcript expression (RQ) in the treatment groups (see **Supplementary Table S2**). ♦The diamond symbol indicates CpGs with significant changes in methylation that correlated with transcript expression.*

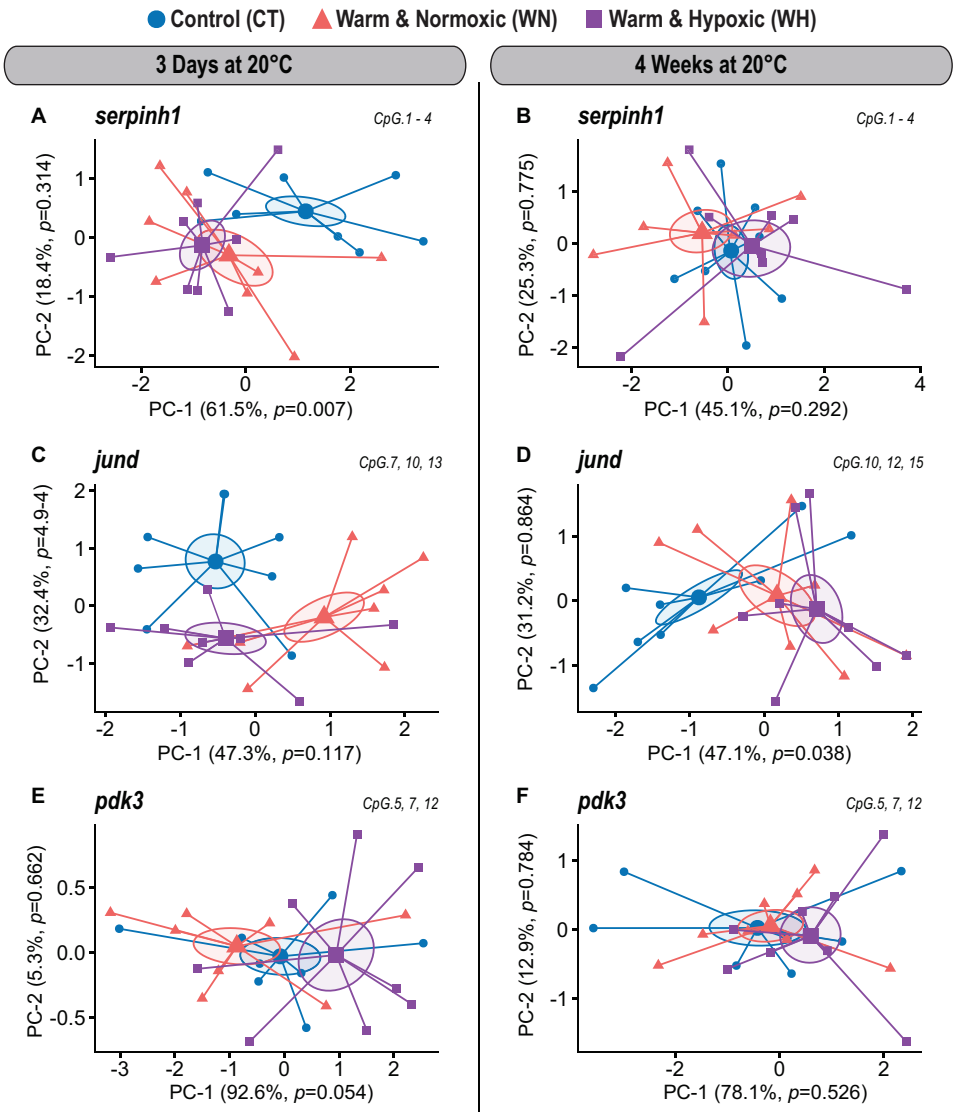

FIGURE 3 | DNA methylation dynamics of responsive CpGs in three genes up-regulated in Atlantic salmon exposed to high temperature and hypoxia. Principal Component Analysis (PCA) on DNA methylation percentages (%) for treatment responsive CpGs from three up-regulated target genes (*serpinh1*, *jund*, and *pdk3*) measured in the liver of Atlantic salmon exposed to high temperature alone (WN: 20°C, ∼100% air saturation) or combined with hypoxia (WH: 20°C, ∼70% air sat.) for 3 days or 4 weeks, as compared to control conditions (CT: 12°C, ∼100% air sat.) (n = 8 per treatment/time point, N = 48 total). PCAs are illustrated separately for each up-regulated gene and exposure time point [*serpinh1* **(A,B)**; *jund* **(C,D)**, *pdk3* **(E,F)**]. PCAs show cluster distribution between the CT, WN, and WH groups with ellipses demonstrating the dispersion of variance and enlarged symbols indicating the center of the distribution for each group. The variance explained by PC-1 and PC-2 are specified in percentage values (%). The p-values represent the treatment effect obtained by applying linear mixed-effect models on the extracted scores of PC-1 and PC-2. Each PCA was based on a specific selection of treatment responsive CpGs as indicated in the upper right corner (see **Table 2**).

was highly dysregulated, but both treatment groups showed a similar separation in comparison to the CT fish (PC-1: F = 248.0, p = 2.0e-16; CT vs. WN p < 0.0001, CT vs. WH p < 0.0001, WN vs. WH p = 0.478; 71.8% variation; **Figure 5B** and **Supplementary Table S1**). Nevertheless, the significant positive correlation between the PC-1 scores of the global CpG methylation and the transcript expression PCAs (Spearman R = 0.53, p = 0.007; **Figure 5C**) indicates a similar cluster distribution and an association between these responses.

Global Methylation and Transcript Expression Changes After 4 Weeks at 20°C

After WN and WH exposure to 20°C for 4 weeks, the effects on CpG methylation were less pronounced, with only six significantly affected CpGs amongst three genes (*jund*, *prdx6*, and *ucp2*) (**Table 2**). However, we still observed a significant segregation between all three treatment groups in the PCA based on their collective CpG responses (PC-1: F = 26.1, p = 9.7e-7; CT vs. WN p < 0.0001, CT vs. WH p < 0.0001, WN vs. WH p = 0.026; 34.4% variation; **Figure 5D** and **Supplementary Table S1**). Also,

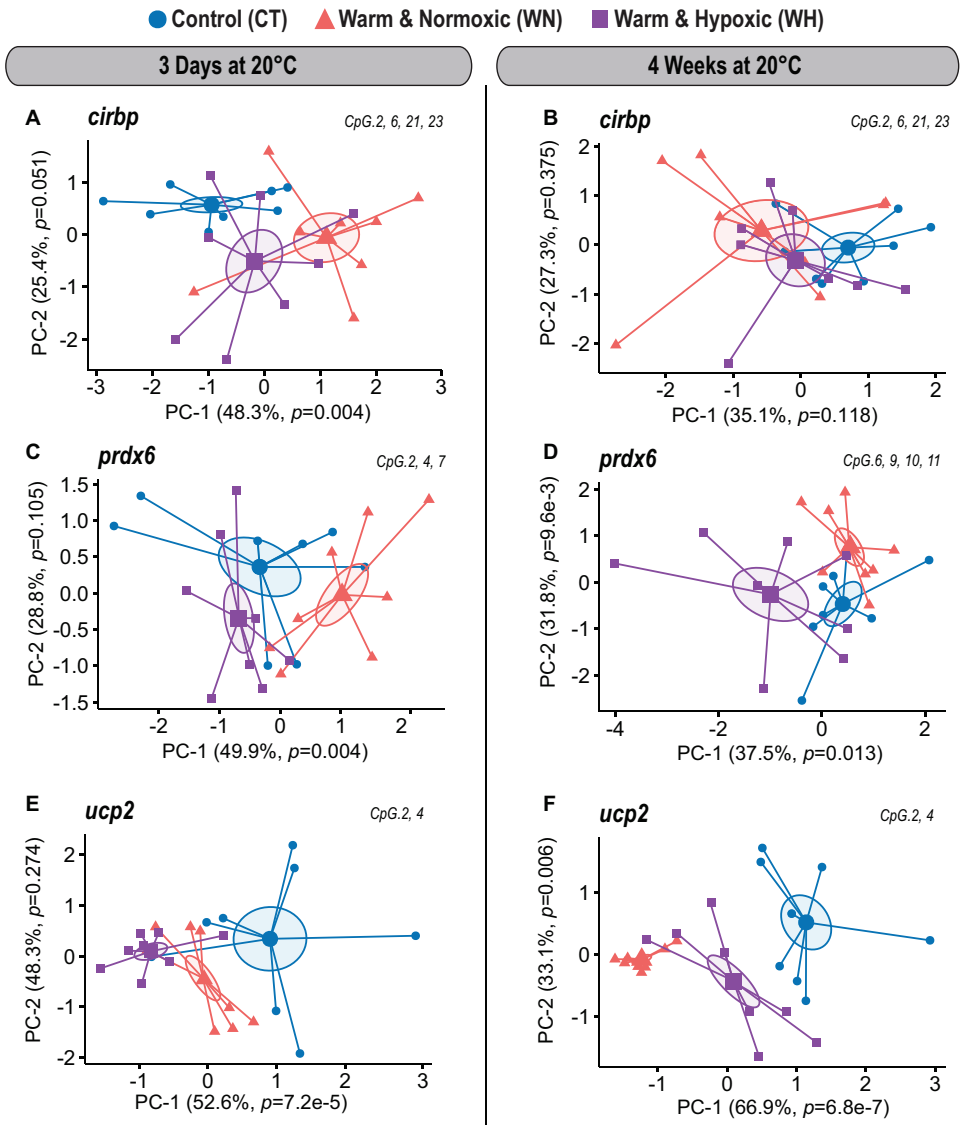

FIGURE 4 | DNA methylation dynamics of responsive CpGs in three genes down-regulated in Atlantic salmon exposed to high temperature and hypoxia. Principal Component Analysis (PCA) on DNA methylation percentages (%) for treatment responsive CpGs from three down-regulated target genes (*cirbp*, *prdx6*, and *ucp2*) measured in the liver of Atlantic salmon exposed to high temperature alone (WN: 20°C, ∼100% air saturation) or combined with hypoxia (WH: 20°C, ∼70% air sat.) for 3 days or 4 weeks, as compared to control conditions (CT: 12°C, ∼100% air sat.) (n = 8 per treatment/time point, N = 48 total). PCAs are illustrated separately for each down-regulated gene and exposure time point [*cirbp* **(A,B)**; *prdx6* **(C,D)**, *ucp2* **(E,F)**]. PCAs show cluster distribution between the CT, WN, and WH groups with ellipses demonstrating the dispersion of variance and enlarged symbols indicating the center of the distribution for each group. The variances explained by PC-1 and PC-2 are specified in percentage values (%). The p-values represent the treatment effect obtained by applying linear mixed-effect models on the extracted scores of PC-1 and PC-2. Each PCA was based on a specific selection of treatment responsive CpGs as indicated in the upper right corner (see **Table 2**).

the transcript expression of these three genes was similarly dysregulated in the WN and WH fish after 4 weeks at 20°C as compared to the CT fish at 12°C (PC-1: $F = 82.5$, $p = 1.8e\text{-}11$; CT vs. WN $p < 0.0001$, CT vs. WH $p < 0.0001$, WN vs. WH $p = 0.067$; 77.0% variation; **Figure 5E** and **Supplementary Table S1**). When overlaying the PCA cluster of the global CpG methylation and transcript expression responses after 4 weeks at 20°C, a similar distribution along PC-1 was evident, and this was reflected in a highly significant positive correlation between their PC-1 scores (Spearman $R = 0.74$, $p = 4.1e\text{-}5$, **Figure 5F**).

Correlations Between CpG Methylation and Transcript Expression Responses

The association between the methylation of significantly affected CpGs and transcript expression was examined in component maps, which segregated all variables according to their specific responses in a 2-dimensional space (i.e., response variables that cluster on opposing directions alongside Component 1 "CP-1" or Component 2 "CP-2" have an inverse correlation). First, we described the general relationship between CpG

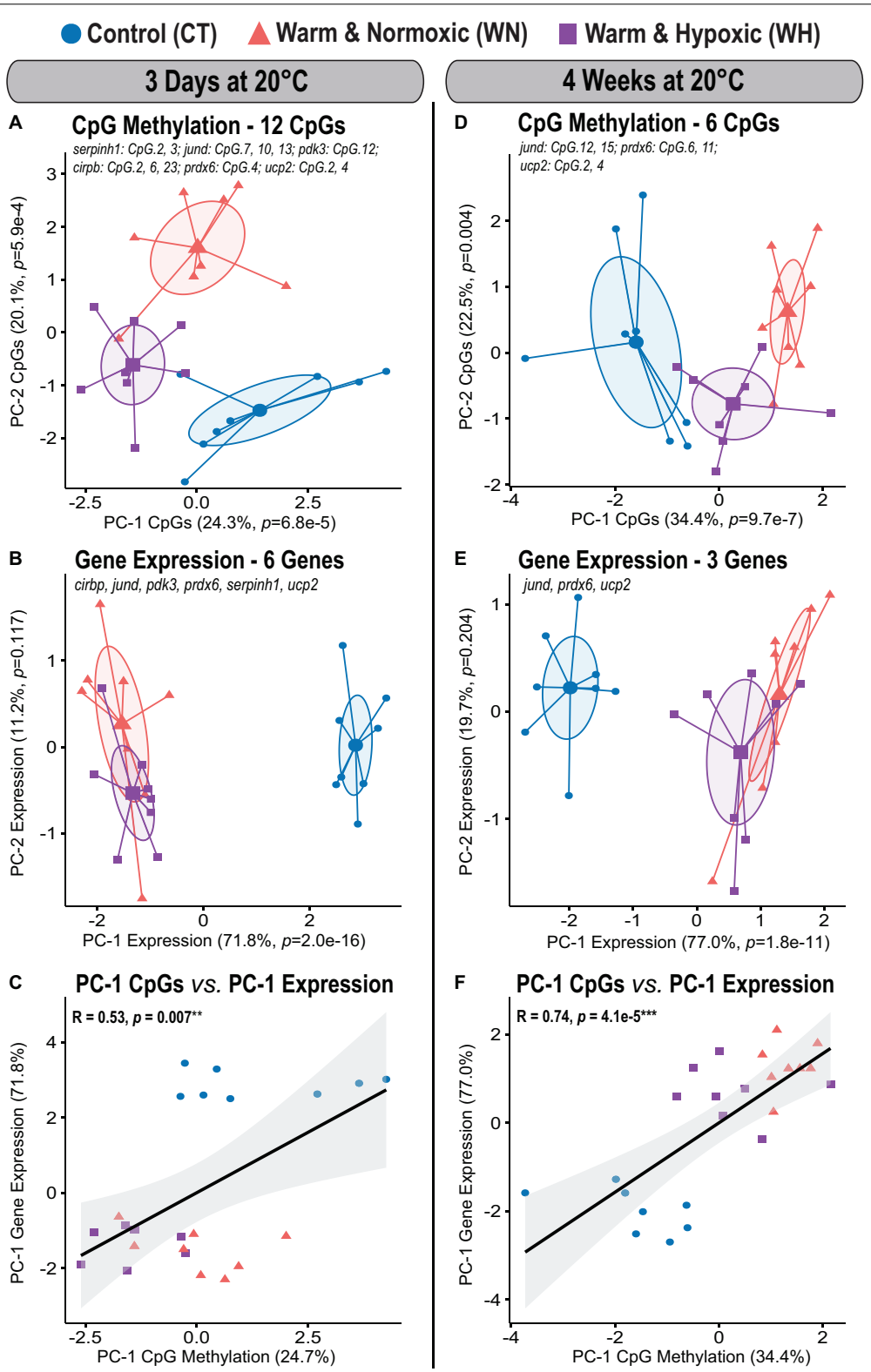

FIGURE 5 | Global DNA methylation changes in Atlantic salmon exposed to high temperature and hypoxia, and their relationship to transcript expression. Principal Component Analysis (PCA) for all significantly affected CpGs and corresponding transcript expression in the liver of Atlantic salmon exposed to high temperature alone (WN: 20°C, ~100% air saturation) or combined with hypoxia (WH: 20°C, ~70% air sat.) for 3 days or 4 weeks as compared to control conditions (CT: 12°C, ~100% air sat.) (n = 8 per treatment/time point, N = 48 total). **(A)** PCA based on 12 significantly affected CpGs after 3 days at 20°C and **(B)** the corresponding transcript expression PCA of six genes (*serpinh1*, *jund*, *pdk3 cirbp*, *prdx6*, and *ucp2*). PCAs show cluster distribution between the CT, WN, and WH groups,

(Continued)

FIGURE 5 | Continued
with ellipses demonstrating the dispersion of variance and enlarged symbols indicating the center of the distribution for each group. The variance explained by PC-1 and PC-2 are specified as percentage values (%). The *p*-values represent the treatment effect on CpG methylation obtained by applying linear mixed-effect models to the extracted scores of PC-1 and PC-2. **(C)** Correlation between the extracted PC-1 scores of the transcript expression PCA and the PC-1 scores of the CpG methylation PCAs. **(D)** PCA based on six significantly affected CpGs after 4 weeks at 20°C and **(E)** the corresponding transcript expression PCA for three genes (*jund*, *prdx6*, and *ucp2*). **(F)** Correlation between the extracted PC-1 scores of the transcript expression PCA and the PC-1 scores of the CpG methylation PCAs. In **(C,F)**, the strength of the correlation is indicated by the Pearson correlation coefficient (R) and the corresponding level of significance ($p < 0.001^{***}$, $p < 0.01^{**}$). The transcript expression data for the six genes (*serpinh1*, *jund*, *pdk3*, *cirbp*, *prdx6*, and *ucp2*) from the short-term exposure time point (3 days at 20°C) were previously published as part of an initial transcriptome study by Beemelmanns et al. (2020), and included herein to specifically investigate the correlation between transcript expression and DNA methylation responses.

methylation and transcript expression reflected in the component maps (**Figure 6**). Second, we analyzed more specifically the methylation level of individual CpGs that: (i) were identified within the component maps as high contributors; (ii) were significantly affected by the treatments; and; (iii) showed strong correlations with transcript expression (**Figure 7**, **Table 2**, and **Supplementary Table S2**).

CpG Methylation and Corresponding Transcript Expression Responses After 3 Days at 20°C

The first component map is based on the methylation values of 12 significantly affected CpGs and the corresponding relative expression (RQ) of six genes from salmon exposed for 3 days at 20°C with and without hypoxia (**Figure 6A**). The six genes segregated according to their responses into up-regulated (*serpinh1*, *jund*, and *pdk3*) and down-regulated genes (*cirbp*, *prdx6*, and *ucp2*) on opposing directions along CP-1 (35.9%, $p = 0.001$) (**Figure 6A**). Eight CpGs (*serpinh1-CpG.2*, *serpinh1-CpG.3*, *jund-CpG.7*, *jund-CpG.10*, *cirbp-CpG.2*, *cirbp-CpG.6*, *cirbp-CpG.23*, and *pdk3-CpG.12*) clustered along with up-regulated genes (**Figure 6A**), indicating higher methylation levels (i.e., they were hyper-methylated when compared to the control group) (**Table 2**). On the contrary, four CpGs (*jund-CpG.13*, *prdx6-CpG.4*, *ucp2-CpG.2,* and *ucp2-CpG.4*) clustered together with the down-regulated genes in the component map, and thus, this suggested that they had lower methylation levels (i.e., they were hypo-methylated) (**Figure 6A** and **Table 2**).

The two *serpinh1*-specific CpGs (*serpinh1-CpG.2* and *serpinh1-CpG.3*), both located in the first coding exon (**Figure 2A**), clustered very closely to the up-regulated gene itself, reflecting a positive association between their responses (**Figure 6A**). After exposure to WN and WH for 3 days at 20°C, we found a strong trend of hyper-methylation for *serpinh1-CpG.2* ($F = 3.9$, $p = 0.032$; CT vs. WN $p = 0.057$, CT vs. WH $p = 0.055$; **Table 2**) and a significant effect for *serpinh1-CpG.3* ($F = 5.9$, $p = 0.008$; CT vs. WN $p = 0.038$, CT vs. WH $p = 0.009$; **Figure 7A** and **Table 2**). Specifically, *serpinh1-CpG.3* had a significant positive correlation with up-regulated *serpinh1* expression (Spearman $R = 0.53$, $p = 0.008$; **Figure 7A** and **Table 2**).

Two *jund*-specific CpGs (*jund-CpG.7* and *jund-CpG.10*) located in the 5′ upstream region had a positive association with the up-regulated gene *jund*, whereas it was the opposite for *jund-CpG.13* situated in close proximity (∼7 bp) to the putative promoter site (TATA-box) (**Figures 2B**, **6A**). The site *jund-CpG.7* was more highly methylated in WN fish as compared to CT fish after 3 days at 20°C ($F = 5.7$ $p = 0.009$; CT vs. WN $p = 0.007$; **Table 2**), while *jund-CpG.10* showed increased methylation in WH fish ($F = 7.1$, $p = 0.004$; CT vs. WH $p = 0.002$; **Table 2**). In contrast, the methylation of *jund-CpG.13* was reduced in fish exposed to the WN challenge after 3 days at 20°C as compared to CT fish ($F = 4.1$, $p = 0.029$; CT vs. WN $p = 0.026$; **Table 2**). However, for none of these three CpG sites were the methylation levels significantly correlated with *jund* expression (**Table 2**).

All three responsive CpGs located in the 5′ UTR or first intron of the down-regulated gene *cirbp* (*cirbp-CpG.2*, *cirbp-CpG.6*, and *cirbp-CpG.23*) (**Figure 2D** and **Table 2**) clustered on the opposite side of the component map as compared to its transcript expression (**Figure 6A**). Interestingly, *cirbp-CpG.6*, situated in the first intron (**Figure 2D**), clustered along CP-1 in the opposite direction to *cirbp* expression, reflecting their strong negative association (**Figure 6A**). The site *cirbp-CpG.6* was more highly methylated in WN salmon exposed to 20°C for 3 days as compared to CT fish, and there was a similar trend for WH fish ($F = 3.6$, $p = 0.042$; CT vs. WN $p = 0.048$, CT vs. WH $p = 0.051$; **Figure 7B** and **Table 2**). Yet, there was a significant negative correlation between the hyper-methylation of *cirbp-CpG.6* and the down-regulation of *cirbp* expression (Spearman $R = -0.45$, $p = 0.026$; **Figure 7B** and **Table 2**).

For the down-regulated gene *ucp2*, both analyzed CpG sites (*ucp2-CpG.2* and *ucp2-CpG.4*) were located within the putative promoter region (**Figure 2F**) and positively correlated with *ucp2* expression, although the relationship was stronger for *ucp2-CpG.4* (**Figure 6A** and **Table 2**). The methylation level of *ucp2-CpG.4*, located ∼12 bp 5′ upstream of the TATA-box (**Figure 2F**), was significantly lower upon short-term exposure to WN and WH in comparison to CT ($F = 6.3$, $p = 0.006$; CT vs. WN $p = 0.018$; CT vs. WH $p = 0.010$; **Figure 7C** and **Table 2**), and showed a strong tendency for a positive correlation with down-regulated *ucp2* expression (Spearman $R = 0.39$, $p = 0.058$; **Figure 7C** and **Table 2**).

CpG Methylation and Corresponding Transcript Expression Responses After 4 Weeks at 20°C

The second component map is based on the methylation of six significantly affected CpGs and the corresponding relative expression of three genes from salmon exposed to the WN and WH treatments at 20°C for 4 weeks (**Figure 6B**). The genes separated according to their responses into up-regulated (*jund*) and down-regulated (*prdx6*, *ucp2*) genes along Component 1 (CP-1, 42.2%, $p = 0.001$) (**Figure 6B**). Two CpG sites were more highly methylated (*prdx6-CpG.6* and *prdx6-CpG.11*), while four

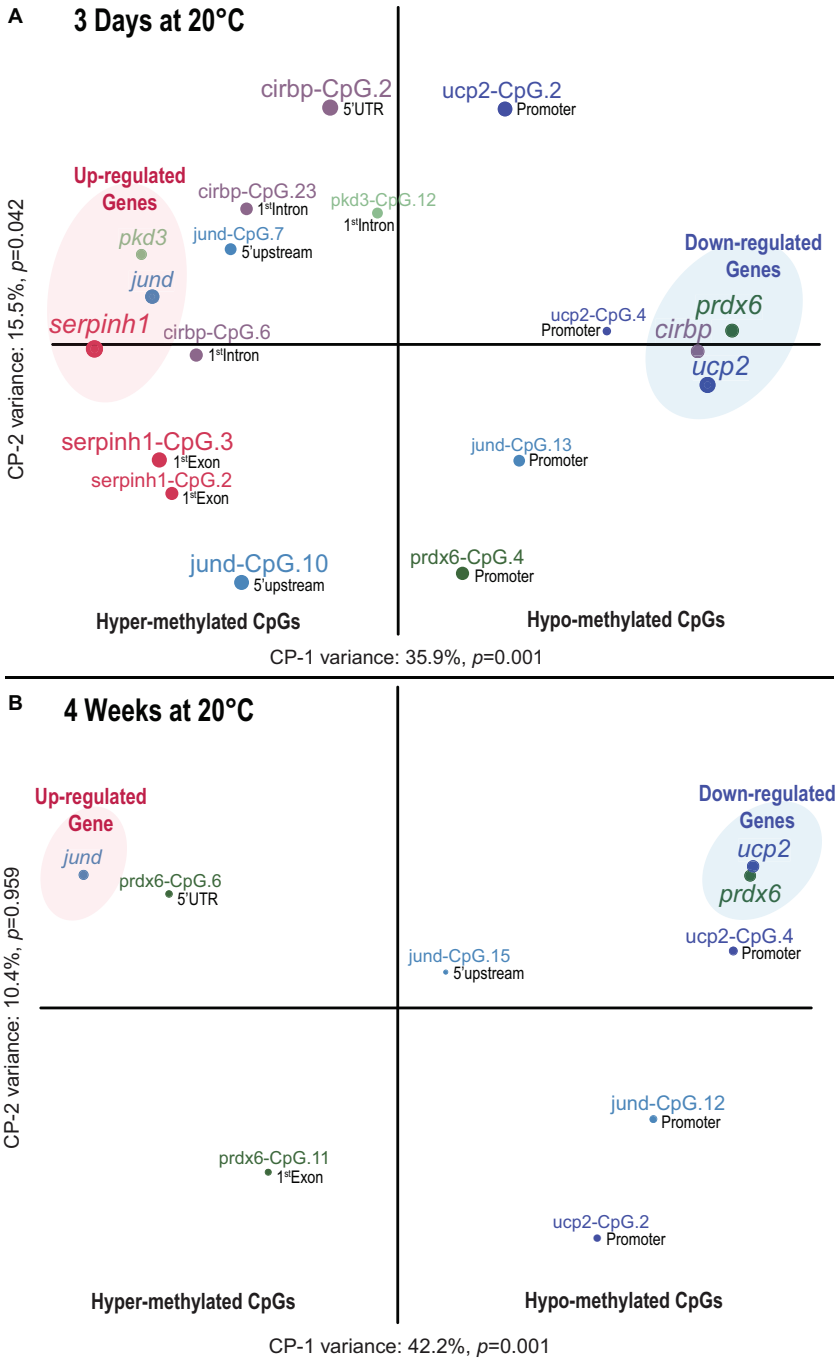

FIGURE 6 | Time dependent association between CpG methylation and transcript expression in Atlantic salmon exposed to high temperature and hypoxia. **(A)** Component map based on 12 significantly affected CpGs and the transcript expression of six genes (*serpinh1*, *jund*, *pdk3 cirbp*, *prdx6*, and *ucp2*) in the liver of Atlantic salmon challenged for 3 days to 20°C with and without hypoxia (~70% air saturation). **(B)** Component map based on six significantly affected CpGs and the corresponding transcript expression for three genes (*jund*, *prdx6*, and *ucp2*) in the liver of Atlantic salmon challenged for 4 weeks to 20°C with and without hypoxia (~70% air saturation) (n = 8 per treatment/time point, N = 48 total). Each component map illustrates the relationship between CpG methylation and the transcript expression response. The results of the battery of inference permutation test indicate which components are significantly affected ($p < 0.05$). The circle and label size correspond with the magnitude of the component scores obtained for each response variable, and the label color associates CpGs with corresponding genes. The terms hyper- and hypo-methylation relate to the direction of the respective CpG methylation response (see **Table 2**). The genomic location (promoter, 5′ upstream, 5′ UTR, first coding exon and first intron) of each CpG is indicated next to the circles (see **Figure 2**). The CpGs indicated by "promoter" were located close to (i.e., within < 25 bp) or within the putative promoter motif (TATA-box, POL-II promoter sequence) (see **Figure 2**). The transcript expression data for the six genes (*serpinh1*, *jund*, *pdk3*, *cirbp*, *prdx6*, and *ucp2*) from the short-term exposure time point (3 days at 20°C) were previously published as part of an initial transcriptome study by Beemelmanns et al. (2020), and were included herein to specifically investigate the correlation between transcript expression and DNA methylation responses.

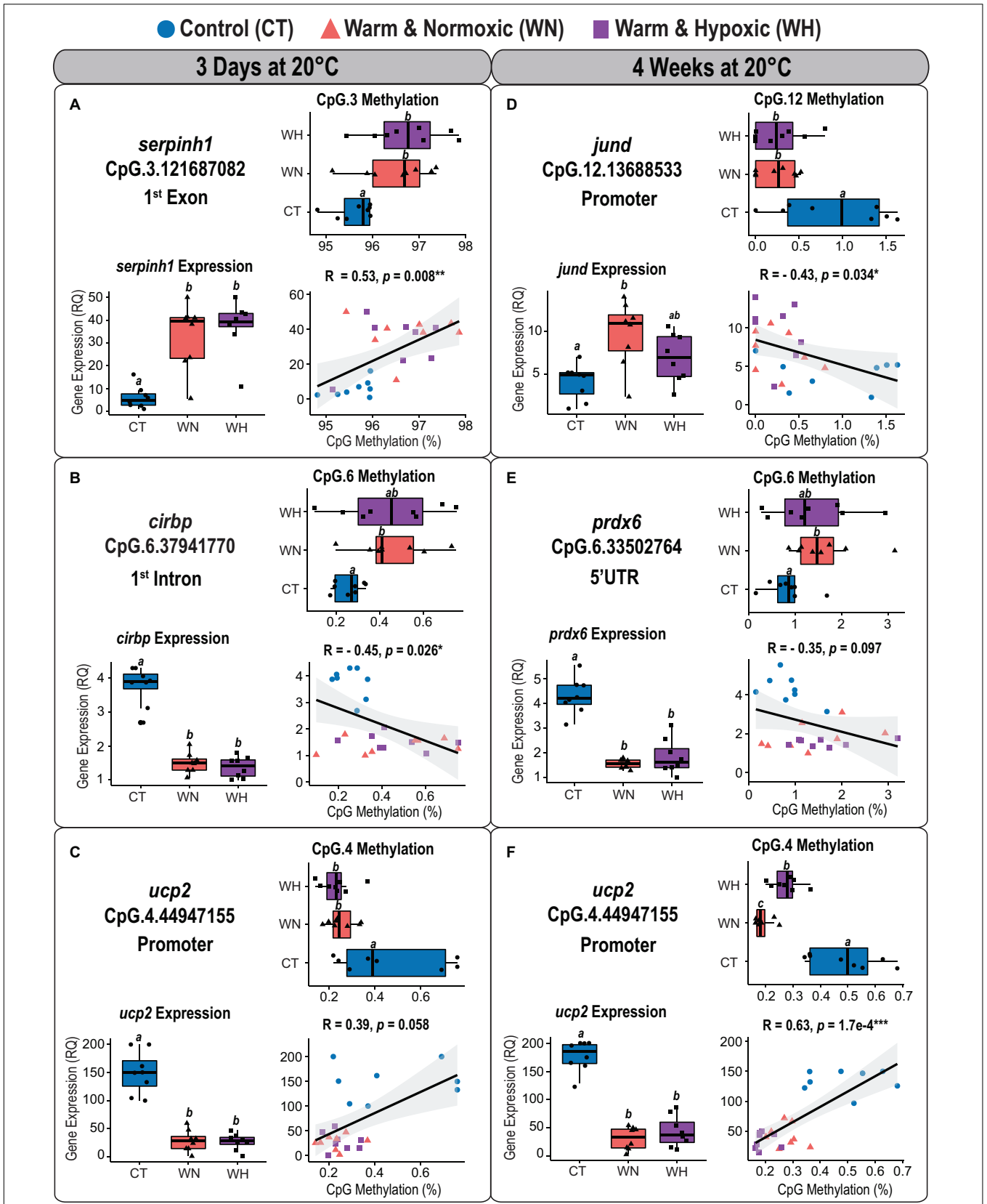

FIGURE 7 | Continued

FIGURE 7 | Correlation analyses between CpG methylation and transcript expression in Atlantic salmon exposed to high temperature and hypoxia. Each panel contains a graph showing the correlation between CpG methylation percentage (%) and transcript expression (RQ) measured in the liver of Atlantic salmon exposed to high temperature alone (WN: 20°C, ∼100% air saturation) or combined with hypoxia (WH: 20°C, ∼70% air sat.) for 3 days or 4 weeks, as compared to control conditions (CT: 12°C, ∼100% air sat.) (n = 8 per treatment/time point, N = 48 total). Spearman's rank correlation coefficients (R) and the level of significance ($p < 0.001$***, $p < 0.01$**, $p < 0.05$*) are indicated for each relationship. Also contained within each panel are boxplots displaying the percentage of CpG methylation (%) and transcript expression (relative quantity, RQ) for fish of the three treatment groups. Dissimilar letters in the box plots indicate groups that are significantly different (determined using least square means *post-hoc* tests). The left panel shows the correlation analyses between **(A)** *serpinh1* vs. CpG.3, **(B)** *cirbp* vs. CpG.6, and **(C)** *ucp2* vs. CpG.4 measured after 3 days at 20°C. The right panel shows the correlation analyses between **(D)** *jund* vs. CpG.12, **(E)** *prdx6* vs. CpG.6, and **(F)** *ucp2* vs. CpG.4 measured after 4 weeks at 20°C (see **Table 2** and **Supplementary Table S2**). The transcript expression data for the three genes (*serpinh1*, *cirbp*, and *ucp2*) from the short-term time point (3 days at 20°C) were previously published as part of an initial transcriptome study by Beemelmanns et al. (2020), and included herein to specifically investigate the correlation between transcript expression and DNA methylation responses.

exhibited lower methylation (*jund-CpG.12*, *jund-CpG.15*, *ucp2-CpG.2,* and *ucp2-CpG.4*) (**Figure 6B** and **Table 2**).

Based on the component map, there was a negative association between the up-regulated gene *jund* and the methylation levels of *jund-CpG.12* and *jund-CpG.15* (**Figure 6B** and **Table 2**) located in the 5′ upstream/promoter region (**Figure 2B**). Interestingly, the site *jund-CpG.12* which is located in close proximity to the putative TATA-box (∼6 bp) (**Figure 2B**) had a significantly lower level of methylation in WN and WH salmon exposed to 20°C for 4 weeks as compared to CT fish (F = 7.1, p = 0.004; CT vs. WN p = 0.008, CT vs. WH p = 0.012; **Figure 7D** and **Table 2**), and was negatively correlated with *jund* expression (Spearman R = −0.43, p = 0.034; **Figure 7D** and **Table 2**).

The expression levels of the down-regulated gene *prdx6* were inversely related to the methylation levels of *prdx6-CpG.6* and *prdx6-CpG.11* (**Figure 6B** and **Table 2**). The site *prdx6-CpG.6*, which is located in the 5′ UTR region (**Figure 2E**), had a significantly higher methylation level in fish from the WN group after exposure to 20°C for 4 weeks as compared to the CT group, and a similar trend was observed for the WH group (F = 3.5, p = 0.046, CT vs. WN p = 0.043, CT vs. WH p = 0.094; **Figure 7E** and **Table 2**). However, the negative relationship between down-regulated *prdx6* transcript expression and *prdx6-CpG.6* hyper-methylation level fell short of being significant (Spearman R = −0.35, p = 0.097; **Figure 7E** and **Table 2**).

Finally, the two *ucp2* specific CpGs located in close proximity to the putative promoter region (**Figure 2F**) remained hypo-methylated, and were positively correlated with expression of the down-regulated gene *ucp2* after 4 weeks at 20°C (**Figure 6B** and **Table 2**). This suggests that there were persistent and long-lasting changes in CpG methylation. Specifically, *ucp2-CpG.4* stayed close to *ucp2* expression in the component map, possibly reflecting their time-persistent positive association (**Figure 6B**). The *ucp2-CpG.4* site still had a lower level of methylation in WN and WH fish after long-term exposure to 20°C as compared to fish in the CT group (F = 35.4, p = 6.9e-8; CT vs. WN $p < 0.0001$; CT vs. WH $p < 0.0001$; **Figure 7F** and **Table 2**), and showed a positive correlation with *ucp2* expression (Spearman R = 0.623, p = 1.7e-4; **Figure 7F** and **Table 2**).

Sex Effects on DNA Methylation

In our statistical analyses we included sex as a factor in the linear mixed models to account for potential sex-specific influences on DNA methylation levels. Remarkably, we found evidence for sex-specific effects on DNA methylation when all significantly affected CpGs were considered for both exposure time points (3-days/PC-1: F = 6.4, p = 0.018; 4-weeks/PC-2: F = 5.7, p = 0.026; **Supplementary Table S1**). More specifically, we identified sex effects on CpG methylation for the genes *jund* (3-days/PC-2: F = 7.9, p = 0.009; **Supplementary Table S1**), *pdk3* (3-days/PC-2: F = 4.5, p = 0.044; **Supplementary Table S1**), *prdx6* (4-weeks/PC-2: F = 7.3, p = 0.012; **Supplementary Table S1**), and *ucp2* (3-days/PC-2: F = 7.9, p = 0.010; 4-weeks/PC-2: F = 5.3, p = 0.030; **Supplementary Table S1**).

DISCUSSION

DNA Methylation Responses to High Temperature Alone or Combined With Moderate Hypoxia

In this study, we report that high temperature alone, and in combination with moderate hypoxia, induced dynamic DNA methylation changes in five treatment-responsive genes in the liver of post-smolt Atlantic salmon that are involved in the heat shock response (*serpinh1*) (Ishida and Nagata, 2011), the regulation of mRNA stability (*cirbp*) (Zhong and Huang, 2017), the cellular oxidative stress response (*prdx6*, *ucp2*) (Brand and Esteves, 2005; Ambruso, 2013), and apoptosis (*jund*) (Weitzman et al., 2000). Remarkably, the collective CpG methylation changes in these genes revealed distinct methylation profiles in ∼1.5 year-old fish exposed to each environmental condition (i.e., WN vs. WH) for 3 days and 4 weeks, that were associated with global transcript expression changes. These results suggest that each environmental condition (temperature, hypoxia) experienced during a salmon's lifetime may leave a different signature (footprint) on DNA methylation that is important for the regulation of gene expression responses. Further, it indicates that environmentally induced changes in DNA methylation are not exclusively manifested during early life-history stages (i.e., embryos and larvae) in fishes. These are novel and important findings for the following two reasons.

First, the integration of epigenomic changes during an organism's lifetime is still not well-understood even in mammals (Aguilera et al., 2010; Pérez et al., 2019), and it is generally thought that epigenetic marks are mainly sensitive to environmental cues during the early life-stages of development when the rate of mitotic cell division is high and epigenetic marks are in the process of being established (Faulk and Dolinoy, 2011; Toraño et al., 2016). This is based on previously published

studies that have primarily examined DNA methylation changes when fish were exposed to elevated temperatures during early developmental stages (i.e., embryo to larvae) (Campos et al., 2013; Han et al., 2016; Anastasiadi et al., 2017; Burgerhout et al., 2017; McCaw et al., 2020). For instance, Anastasiadi et al. (2017) demonstrated that temperature increases of only +2°C during the early developmental stages (i.e., 0–15 days post-fertilization) but not in later stages (i.e., 20–60 dpf) of the European sea bass (*Dicentrarchus labrax*) resulted in global DNA methylation changes of many genomic loci and alterations in the expression of environmental stress-relevant genes.

Second, the effects of hypoxia on DNA methylation remain largely unexplored, as so far only two studies have examined the effect of this environmental stressor on DNA methylation (Wang et al., 2016; Veron et al., 2018). For example, rainbow trout (*Oncorhynchus mykiss*) embryos exposed to acute hypoxia (∼22% air saturation for 24 h) had hypo- and hyper-methylated CpGs within the proximal promoters of the up-regulated gene paralogs *bnip3a* and *bnip3lb1* (Bcl-2/E1B-19 K interacting protein 3), which are involved in mitochondrial-mediated apoptosis and/or mitochondrial autophagy (Veron et al., 2018).

In our study, we report that high temperatures, and exposure to this condition in combination with moderate hypoxia, can induce DNA methylation changes in fish long after early development has been completed and epigenetic marks are established. Collectively, our results indicate that environmental challenges experienced later in life can be differentially integrated into the genome as epigenetic marks, and thus, regulate gene expression responses that can alter the fish's phenotype. Hence, these epigenetic changes could be advantageous for individual fish as they allow for immediate and flexible adjustments of transcript expression to environmental pressures, and facilitate phenotypic plasticity.

Exposure Time-Dependent CpG Methylation and Acclimatization Responses

The DNA methylation changes reported in this study were highly dependent on the duration of stress exposure, and this agrees with what has recently been shown for Atlantic salmon larvae subjected to acute vs. chronic stress (Uren Webster et al., 2018). In the treatment groups exposed to the environmental challenges (at 20°C) for only 3 days, we found induced DNA methylation responses in 12 CpGs located in six genes (*serpinh1*, *jund*, *cirbp*, *pdk3*, *prdx6,* and *ucp2*) when compared to control fish held at 12°C. On the contrary, these effects were weaker after prolonged stress (at 20°C) for 4 weeks, with differential DNA methylation observed for only six CpGs in three genes (*jund*, *prdx6*, and *ucp2*). Interestingly, the average amplicon methylation levels in four out of the six studied genes with significant treatment effects were quite low (less than 3%). However, this is similar to trans-generational effects reported in humans where methylation differences were ∼5% (Heijmans et al., 2008), and in zebrafish (*Danio rerio*) where sexual dimorphic methylation profiles differed by ∼2% (Caballero-Huertas et al., 2020). Hence, these findings suggest that small changes in DNA methylation levels at CpG sites can be drivers for the epigenetic regulation of gene expression.

Reversible CpG methylation changes were found for five genes (*serpinh1*, *jund*, *cirbp*, *pdk3,* and *prdx6*) while only one gene (*ucp2*) showed lasting changes in CpG methylation. These findings indicate that there were two types of DNA methylation-mediated responses to the applied stressors: (i) a stronger rapid response to short-term stress that can be reversed; and (ii) a weaker, but more persistent, response that may be permanent. The second type of response, involving epigenetic regulatory adjustments over an extended period of thermal stress, is very likely to coincide with the acclimatization response of individuals (Metzger and Schulte, 2017). Acclimatization is the ability of individuals to maintain and remodel physiological processes repeatedly throughout their lifetime to compensate for the negative effects of changing environments (Seebacher et al., 2015; Beaman et al., 2016). In comparison to DNA-based mutations, dynamic epigenetic changes, such as DNA methylation, can mediate quick and plastic phenotypic responses and facilitate "reversible plasticity" or acclimatization that is crucial for coping with variable environments (Jaenisch and Bird, 2003; Turner, 2009; Beaman et al., 2016), such as those associated with climate change-related events (Claret et al., 2018; Frölicher et al., 2018; IPCC, 2019). Some studies have shown that epigenetic changes in histone variants occur with seasonal temperature acclimation in fish (Araya et al., 2010; Simonet et al., 2013). However, our knowledge about the role that DNA methylation plays beyond developmental plasticity (i.e., during the embryonic and larval stages) in teleost fish species is limited to one study in three-spine sticklebacks (*Gasterosteus aculeatus*), in which it was demonstrated that both developmental temperature and adult acclimation temperature can have long-lasting effects on the epigenome (Metzger and Schulte, 2017). Hence, our findings of persistent CpG methylation changes for the down-regulated gene *ucp2* (which encodes for Mitochondrial uncoupling protein 2) suggest that this epigenetic change could be important in regulating the coupling of mitochondrial respiration to ATP synthesis in cells during chronic high temperature exposure (Brand and Esteves, 2005). Under stressful conditions, mitochondrial coupling may be enhanced partly through a lower expression of *ucp2*, and this would have the added benefit of decreasing ROS synthesis. This may be an important mechanism for cell protection against oxidative stress (Laskowski et al., 2016), and for the long-term survival of Atlantic salmon at high temperatures (Gamperl et al., 2020). Indeed, Gerber et al. (2020) have shown that long-term acclimation of salmon to 20 vs. 12°C increases the respiratory coupling ratio (RCR) and decreases mitochondrial ROS release when tested at 20°C.

These temporal dynamics, but also persistent associations between stress-induced changes in CpG methylation and gene expression, may be important epigenetic regulatory mechanisms facilitating acclimatization responses that enable Atlantic salmon to cope with climate change-related challenges, such as predicted increases in temperature and the frequency and severity of hypoxic episodes (Breitburg et al., 2018; Claret et al., 2018; IPCC, 2019). A putative fixation of these environmentally

induced epigenetic marks ("epi-mutations") may create an "epigenetic memory" that could prime individuals throughout their lifetime (Mirbahai and Chipman, 2014; Ryu et al., 2020), and possibly across generations (i.e., confer non-genetic inheritance) (Jablonka and Raz, 2009; Nelson et al., 2013; Szyf, 2015; Wang et al., 2016; Ryu et al., 2018; Venney et al., 2020) given that these epigenetic marks would have been integrated into the germline and skipped epigenetic reprogramming (Seisenberger et al., 2013). In the context of global warming, transgenerational epigenetic inheritance is increasingly being accepted as relevant with regards to the survival of species, as it enables organisms to adjust their phenotype to a warmer future environment over multiple generations (trans-generational acclimatization) (Jablonka and Raz, 2009; Veilleux et al., 2015; Ryu et al., 2018, 2020; McCaw et al., 2020). This has been suggested to lead to an epigenetic buffering at the population level that may allow species to alter their phenotype to react to the immediate impacts of changing environments, and it would ultimately provide sufficient time for genetic adaptations to occur (O'Dea et al., 2016).

CpG Methylation Changes and Their Relation to Transcript Expression Responses

In this study, we found differences in the CpG methylation profiles between salmon exposed to the WN vs. WH challenges, whereas the transcript expression profiles for both treatment groups were similarly dysregulated as compared to the CT group (i.e., based on global CpG methylation and transcript expression profiles; **Figures 5A,B,D,E**). These findings might be due to complex interactions between several layers of epigenetic regulatory mechanisms. In fish, temperature can also induce changes in histone modifications and variants (Araya et al., 2010; Simonet et al., 2013) as well as changes in the levels of non-coding RNAs [e.g., microRNAs (miRNAs)], and these are also known to play an essential role in temperature-driven processes (Campos et al., 2014; Zhang et al., 2017). Likewise, exposure to hypoxia alters the regulation of miRNAs in different tissues (Lau et al., 2014; Huang et al., 2015) and results in histone-dependent chromatin modifications (Hancock et al., 2015). Consequently, in the current study, it is likely that histone modifications and changes in the levels of non-coding RNAs contributed to the observed gene expression response, and this may explain the herein observed differences between DNA methylation and gene expression profiles. Clearly, understanding the interactive effects of different epigenetic regulatory mechanisms is an area of research that deserves further attention.

We measured DNA methylation levels in the liver, however, different responses might have occurred in other tissues. For instance, in adult European sea bass (3 years old) that were exposed to +3.6°C from 7 to 63 days-post-fertilization, a larger number of differentially methylated regions (DMRs) were found in testis and muscle, while the lowest number of DMRs was observed in the liver (Anastasiadi et al., in press). When considering that the liver is a core metabolic organ in fishes (Tierney et al., 2013) with rather narrow margins for epigenetic plasticity (i.e., DNA methylation) (Anastasiadi et al., in press), it is noteworthy that we were able to determine differences in CpGs methylation in these liver samples from post-smolt (400–600 g) salmon (Gamperl et al., 2020).

In this study, we also report that sex (female/male) had a significant effect on the variation of DNA methylation levels, and this is consistent with previous studies in other fish species (Zhang et al., 2013; Anastasiadi et al., 2018b; Podgorniak et al., 2019; Caballero-Huertas et al., 2020). Remarkably, we found sex-specific effects on CpG methylation for the target genes *jund*, *pdk3*, *prdx6*, and *ucp2* in the liver of these maturing Atlantic salmon. Similar results were described in zebrafish gonads showing sexually dimorphic methylation patterns of immune-related genes (Caballero-Huertas et al., 2020) and also after an immune-stimulation during early stages of development (Moraleda-Prados et al., 2021). The exposure of maturing zebrafish to high temperature resulted in sex ratio shifts with lasting transgenerational changes of their testicular epigenome (Valdivieso et al., 2020). In addition, genetic background may directly affect DNA methylation patterns, and there is increasing evidence for strong associations between the epigenome and genetics (i.e., a family effect) (Burgerhout et al., 2017; Cheung et al., 2017).

Collectively, our findings suggest that the relationship between environmentally induced DNA methylation and transcript expression changes involve complex interactions between several layers of epigenetic regulatory mechanisms that are likely to be tissue-specific and depend on the sex of the fish. Based on our results, we hypothesize that males and females may activate distinct epigenetic regulatory mechanisms to acclimate to high temperature and/or hypoxia exposure, and this question should be addressed in future research.

CpG Methylation in Different Genomic Elements Regulate Transcript Expression

In this study, we used the MBS method to identify highly context-dependent DNA methylation changes for a particular genomic region of ∼500 bp that included parts of the 5′ upstream region (i.e., including putative promoter sequences, the 5′ UTR, the first coding exon and/or the first intron) of six treatment-responsive genes (see **Figure 2**). The assessed amplicons which contained parts of the 5′ upstream region with putative TATA-box and/or POL-II sequences of genes, such as *jund*, *prdx6*, and *ucp2* consistently displayed differential methylation patterns in the global CpG analysis (i.e., when considering all responsive CpGs per gene amplicon) after short-term (3 days) and long-term (4 weeks) WN and WH exposure at 20°C. For instance, a hyper-methylated promoter CpG site of the gene *jund*, which encodes the transcription factor JunD that regulates the protection of cells from p53-dependent senescence and apoptosis (Weitzman et al., 2000), was inversely correlated with up-regulated *jund* expression. The hypo-methylation of CpG sites in promoter regions is well documented to mediate the activation of gene expression upon environmental perturbations in salmonids (Burgerhout et al., 2017; Veron et al., 2018) and other fish species (Campos et al., 2013; Wang et al., 2016; Zheng et al., 2017). Also,

in domesticated mouse lines, a reduction of a single CpG within the promoter which is specifically located at the putative binding site of transcription factor USF1 (Upstream Stimulatory Factor 1) was associated with up-regulated *mup* (Major urinary protein) transcript expression (Nelson et al., 2013).

On the contrary, hypo-methylated promoter CpG sites of the gene *ucp2* (Mitochondrial uncoupling protein 2) were positively correlated with down-regulated *ucp2* expression. These findings are in contrast to the classical model of gene regulation by DNA methylation in which gene silencing is regulated by promoter hyper-methylation (Jones, 2001, 2012; Bird, 2002; Edwards et al., 2017). However, increasing evidence suggests that DNA methylation patterns are far more dynamic and context-dependent than originally thought (Jones, 2012; Baubec and Schübeler, 2014; Ambrosi et al., 2017), and that promoter hyper-methylation can be positively associated with high transcriptional activity (Smith et al., 2020). For instance, Veron et al. (2018) found hyper- and hypo-methylated CpG sites in the promoter region of *bnip3a* and *bnip3lb1*, and suggested that there was a positive correlation with mRNA changes in rainbow trout fry with a hypoxic history. Clearly, the possibility that hypo-methylation of CpGs within the promoter region could be related to gene suppression deserves further investigation and calls for a more context-dependent view of epigenetic transcriptional regulation.

The methylation levels of the first coding exon might also be linked to the epigenetic regulation of transcript expression responses upon temperature and hypoxic stress in Atlantic salmon. For instance, the up-regulation of the gene *serpinh1* (encoding Serpin H1 alias HSP47) in WN and WH fish, a chaperone with an important function in collagen biosynthesis and maintenance during temperature stress (Ishida and Nagata, 2011), was positively correlated with the hyper-methylation of CpGs located within the first coding exon. This is in agreement with the findings of Wang et al. (2016) who showed that the F0 and F2 generations of hypoxia exposed marine medaka (1.4 ± 0.2 mg L^{-1} DO, 120 days post-hatch) had a higher number of differentially methylated regions in exons (as compared to the promoter) and that the exonic region of the transcription factor encoding gene *foxp2* (Forkheadbox P2) was hyper-methylated. Furthermore, McGaughey et al. (2014) postulated that exon methylation (in particular in the last coding exon) is an even better predictor of mRNA expression levels than promoter methylation in zebrafish, and reported an association between increasing exon methylation of genes (hyper-methylation) and higher transcription activity.

Interestingly, the down-regulation of the gene *prdx6* [which encodes for Peroxiredoxin 6; an important mediator of cell protection against oxidative stress (Ambruso, 2013)] in WN and WH fish, was inversely correlated with the hyper-methylation of a CpG site within the 5′ UTR. Consequently, DNA methylation of the 5′ UTR appears to be another regulatory mechanism of gene expression in Atlantic salmon, since similar percentages of differentially methylated CpGs were discovered in the 5′ UTR (4%) and putative promoter (6%) after chronic stress exposure (cold-shock and air-exposure) during early larval development (Moghadam et al., 2017). Also, Cortese et al. (2008) reported an inverse correlation between the 5′ UTR methylation profiles and the expression of nine target genes in cancer cells, suggesting that these genes were at least partially regulated by 5′ UTR methylation changes. However, our understanding of the impacts of DNA methylation changes within the 5′ UTR of a gene is limited and requires additional research.

Finally, WN and WH fish had hyper-methylated CpGs located in the first intron of *cirbp* (as part of a CpG island), and this change was inversely correlated with *cirbp* down-regulation; a gene encoding for a cold-inducible RNA-binding protein involved in the regulation of mRNA stability during temperature and hypoxic stress (Zhong and Huang, 2017). This pattern agrees with the recent findings of Anastasiadi et al. (2018a), who demonstrated inverse correlations between DNA methylation of the first intron and gene expression across tissues and species.

Collectively, our findings reinforce that environmental stressor-induced DNA methylation changes appear in a variety of different genomic elements, and result in a highly complex and context-dependent regulation of the expression of genes with different functions.

CONCLUSION

We demonstrated that elevated temperature (20°C) as a single stressor, or combined with moderate hypoxia (∼70% air sat.), induced methylation changes at several CpG sites within different genomic elements around the transcription start site of five biomarker genes (*cirbp, serpinh1*, *prdx6*, *ucp2,* and *jund*), and that these methylation changes correlated with gene expression responses. These CpG methylation changes were also highly dependent on the duration of the stress, with some being reversible (*cirbp*, *serpinh1*, *prdx6,* and *jund*) whereas others were persistent (*ucp2*). These temporal, context-dependent and dynamic associations between stress-induced CpG methylation changes and gene expression may be an important epigenetic regulatory mechanism facilitating physiological plasticity and acclimatization, that allows fish species to cope with climate change-related challenges, such as predicted increases in temperature and the frequency and severity of hypoxic episodes. These responsive CpG methylation marks could be considered as putative predictors of gene expression changes, and this is important in the context of aquaculture and the development of epigenetic markers (epimarkers) to predict phenotypic traits. To date, the study of epigenetics and its application in aquaculture is in its infancy, and epimarkers hold significant promise as predictors of tissue development, growth rates, sex ratios, reproduction, disease resistance and stress tolerance (Gavery and Roberts, 2017; Best et al., 2018; Granada et al., 2018). As several epigenetic marks of the five thermal/hypoxia-responsive genes (*serpinh1*, *jund*, *cirbp*, *prdx6,* and *ucp2*) were firmly linked to differential expression, and subsequently physiological changes (Beemelmanns et al., 2020), they have potential as tools to detect: (i) past exposure to either acute or chronic temperature/hypoxia stress; (ii) early responses to sub-lethal stressors; and (iii) to predict thermal and/or hypoxia tolerance in salmonid fishes. Hence, our data suggest that the detected

epigenetic marks associated with these biomarker genes could potentially be used not only in aquaculture breeding programs, but also for conservation and ecological surveys of wild populations. Future genome-wide methylation studies should focus on effects at different developmental stages (i.e., larvae, juvenile and adult), within and across generations, to generate age-specific DNA methylation profiles and to identify stably induced epigenetic marks. These would have significant potential for the prediction of thermal and/or hypoxia tolerance in the context of climate change-related challenges faced by wild and aquaculture fish populations.

MATERIALS AND METHODS

This experiment was performed as part of the "Mitigating the Impacts of Climate-Related Challenges on Salmon Aquaculture (MICCSA)" project. A detailed description of the experimental protocol is published in Gamperl et al. (2020). All experimental procedures described herein were approved by the Institutional Animal Care Committee of Memorial University (NL, Canada) (Protocol #16-90-KG), and followed guidelines set by the Canadian Council on Animal Care. All parts of this study adhere to the ARRIVE Guidelines for reporting animal research (Kilkenny et al., 2010), and a completed ARRIVE guidelines checklist is provided in the **Supplementary Material**.

Animal Husbandry

The experiment was performed from March-August 2017 in the "Laboratory for Atlantic Salmon and Climate Change Research" (LASCCR) at Memorial University, St. John's, NL, Canada. Three hundred and sixty post-smolt (∼1.5 year-old fish, immature) Atlantic salmon with a starting mass of 137.6 ± 1.3 g (mean ± SE) were randomly distributed into six 2.2 m^3 circular indoor fiberglass tanks (60 fish $tank^{-1}$) supplied with seawater (32 ppt salinity) at 15 L min^{-1} (flow-through system) that were initially maintained at 12°C and 100% air saturation with a photoperiod of 14 h light: 10 h dark. These fish were mixed offspring from an aquaculture company's commercial brood-stock (of St. John River strain) to capture as much genetic variation as possible. The fish were fed a daily ration of 1% body weight day^{-1} with a commercial salmon feed (5 mm, EWOS Dynamic S, EWOS Canada Ltd, Surrey, BC, Canada). All fish in this experiment were implanted with Passive Integrated Transponder (PIT) tags (Loligo® Systems ISO 11784 certified PIT tags, Viborg, Denmark) approximately 2 months before the experiment.

Experimental Design

For the experiment, we assigned two tanks randomly to one of three treatments: (i) Warm & Normoxic (WN) fish were challenged with an incremental increase in water temperature (from 12 to 20°C at 1°C $week^{-1}$) at ∼100% air saturation, and then 20°C for an additional 4 weeks; (ii) Warm & Hypoxic (WH) fish were exposed to the same temperature regimen (as in i), but simultaneously exposed to moderate hypoxia (O_2 level of ∼70% air saturation) throughout the experiment; whereas (iii) Control (CT) fish were maintained at 12°C and ∼100% air saturation (**Figure 1**). The weekly temperature increases in the tanks of the WN and WH treatment groups were 0.3°C (from days 1 to 3), 0.1°C on day 4, and then no change from days 5 to 7. The temperature and dissolved oxygen level in the tanks were monitored daily (YSI, ProODO, Yellow Springs, OH, United States) and ammonia and nitrite levels in the tanks were measured weekly (LaMotte test kit, Chestertown, MD, United States). During the experiment, salmon were carefully fed by hand to satiation twice daily (at 9:00 and 15:00) (see Gamperl et al., 2020 for additional experimental details).

For sampling, eight fish per group (four fish per tank duplicate) were periodically netted individually out of the tanks and euthanized in an aerated seawater bath (∼10 L) containing a lethal dose (0.4 g L^{-1}) of the central nervous system depressant MS-222 (tricaine methanesulphonate; Syndel Laboratories, Nanaimo, BC, Canada) followed by cerebral concussion (blow to the head between the eyes). We recorded physiological growth parameters as described and reported in Gamperl et al. (2020), and determined the sex of the fish by visual inspection of the gonads. For the current study, a 200 mg piece of liver was collected from WN and WH fish subjected to 20°C for 3 days and 4 weeks, and from CT fish at 12°C at the same sampling points (n = 8 fish per group/sampling point, N = 48 fish in total); then flash-frozen in liquid nitrogen, and stored at −80°C until further processing. The number of samples per exposure time point (i.e., 24) was based on prior experiments with similar designs and treatments (Gamperl et al., 2020), and was considered as sufficient to achieve statistical robustness and power (80%) to detect a significant effect ($p < 0.05$) with an estimated medium-large effect size (43%), according to *a priori* power calculations (Beemelmanns et al., 2020).

Multiplex Bisulfite Sequencing (MBS)

DNA Extraction and Bisulfite Conversion

Multiplex Bisulfite Sequencing (MBS) was performed in principle according to the protocol developed by Anastasiadi et al. (2018b). In the first step, we extracted DNA from 10 mg of liver tissue using the Wizard Genomic DNA Purification Kit (Promega, Madison, WI, United States) following the instruction manual. In addition, a total of 10 μg of genomic DNA per sample was precipitated in 0.2 M NaCl and 70% ethanol and washed 2× with 70% ethanol to remove any salt contaminants. The quantity and purity of the DNA samples before and after purification were measured with a ND-100 spectrophotometer (NanoDrop Technologies, Wilmington, DE, United States), and the integrity of DNA samples was examined on 1% agarose gels. For each sample, 1 μg of DNA was bisulfite converted with the EZ DNA Methylation-Direct™ Kit (D5020; Zymo Research, Irvine, CA, United States) following the manufacturer's manual with minor adjustments. To ensure a high bisulfite conversion ratio, we extended the desulphonation time to 30 min, and performed the elution of the bisulfite converted DNA twice with 40 μL of Milli-Q autoclaved H_2O to reach a theoretical concentration of 25 ng μL^{-1} of bisulfite converted DNA.

Gene Selection for MBS

The selection of target genes was based on a previous transcriptomic (44K microarray and qPCR validation) study, and we chose genes that were differentially expressed in the liver of identical experimental fish exposed to the same WN and WH treatments (Beemelmanns et al., 2020). For the current DNA methylation study, we picked six target genes that fulfilled the following conditions: (i) were significantly up-regulated (*jund*, *pdk3,* and *serpinh1*) or down-regulated (*cirbp*, *prdx6,* and *ucp2*) upon exposure to 20°C and hypoxia; (ii) had significant correlations with physiological and growth parameters; and (iii) showed functional associations with the heat-shock response, oxidative stress, apoptosis and/or metabolism (Beemelmanns et al., 2020; **Table 1**). For each target gene, we determined the chromosome location and size (bp) of the 5′ and 3′ untranslated regions (UTRs) of exons, protein-coding exonic regions (exons), non-coding intronic regions (introns) and individual CpG sites based on the Atlantic salmon genome assembly (*ssa*) ICSASG_V2 (Lien et al., 2016) available on-line on "NCBI[1]," "SalmoBase[2]," and "Ensembl[3]". We determined putative promoter regions [TATA-box motif, Polymerase II (POL-II) promoter sequence] within the 5′ upstream region of each gene *in silico* using the promoter site prediction software "Promoter.2.0" (Knudsen, 1999), and "TSSW" as well as "TSSG" online tools available on http://www.softberry.com (Solovyev et al., 2010). CpG islands were identified with the online tool "CpG Finder[4]."

Primer Design and Amplicon Sequence Structure

The primers were designed to encompass important genomic elements that regulate gene expression, such as the 5′ upstream region (including putative promoter), the 5′ UTR, the first coding exon and the first intron (**Figure 2** and **Table 1**). Primers were developed using "MethPrimer" with the incorporated "Plus CpG Islands Prediction" algorithm (Li and Dahiya, 2002) to locate the primers in regions with a high CpG frequency (**Supplementary Table S3**). In addition, an *in silico* test was conducted with "Primer3" (Untergasser et al., 2012) to validate the binding capacity of the primers to the bisulfite converted target region. Forward and reverse adapters were added to the 5′ ends of the primers, as described in the Illumina protocol for 16S metagenomics library preparation (**Supplementary Table S3**). For an individual gene, the number of CpGs ranged from a minimum of 8 to a maximum of 23, and a total of 94 CpGs were covered with an average of 15.3 CpGs per gene and a frequency of 3.2 CpGs per 100 base pairs (**Table 1** and **Supplementary Table S4**). The gene structure and CpG methylation marks of the sequenced regions (∼500 bp) were illustrated for each gene using the IBS software (Liu et al., 2015; **Figure 2**).

PCR Amplification

The PCR amplification with 25 ng of bisulfite converted DNA as template was completed in a 26 μL reaction volume with 5X Green GoTaq Flexi Buffer (Promega, Madison, WI, United States), 2.5 U of GoTaq G2 Hot Start polymerase (Promega), 2.5 mM of $MgCl_2$ (Promega), 0.8 mM of dNTPs (Promega) and 0.4 μM of each forward and reverse primer (Tecknocroma, Barcelona, Spain). The PCR reactions were performed using 7 min at 95°C, followed by 40 cycles of [1 min at 95°C, 2 min at the primer-pair specific annealing temperature (**Supplementary Table S3**), and 65°C for 2 min], and a final incubation step of 10 min at 65°C. The presence and size of all PCR amplicons were verified by 1% agarose gel electrophoresis. Sanger sequencing of the PCR amplicons (Center for Research of Agricultural Genomics CRAG, Bellaterra, Spain) and BLASTn searches against NCBI nr/nt databases (January 2019) were also carried out before Illumina sequencing to validate the sequence identities and primer specificity.

PCR Amplicon Purification and Normalization

Magnetic bead-based normalization and size selection of the DNA quantities across all PCR amplicons were conducted with Sera-mag SpeedBeads (Fisher 09981123; Waltham, MA, United States) following a customized protocol described in Anastasiadi et al. (2018b) which was modified from Rohland and Reich (2012) and Hosomichi et al. (2014). For the final bead-based normalization procedure, the cleaned PCR amplicons were incubated in equal volumes with 20-fold diluted magnetic beads (20% PEG-8000, 2.5 M NaCl) and 20 μL of isopropanol for 5 min (room temperature), and then washed with 70% fresh ethanol on a magnetic stand. The normalized PCR amplicons were eluted in 13 μL of Milli-Q autoclaved H_2O to obtain an equal quantity of DNA (in picomoles). In a final step, we combined 4 μL of the size-selected and normalized amplicons of each gene to obtain pools of 48 samples.

Indexing of Amplicons and Sequencing

Each sample (PCR amplicon) was indexed with a unique Nextera XT code combination according to a dual-index strategy using i7 and i5 indices from the Nextera XT index Kit Set A (Illumina®-Nextera™, San Diego, CA, United States) according to Illumina's protocol for 16S metagenomic library preparation. After indexing, the target amplicons were cleaned using a 0.6× Sera-mag SpeedBeads size-selection strategy (Fisher 09981123; Waltham, United States) and eluted in 22 μL of Milli-Q autoclaved H_2O. For each sample, a high-sensitivity DNA assay was carried out with a Bioanalyzer (Agilent 2100, Santa Clara, CA, United States) to determine the concentration, molarity, and the exact amplicon size. A final amplicon library pool of 40 nM was prepared by combining each sample in an equimolar manner. The amplicon library was sequenced with 300 bp paired-end Illumina Mi-seq v3 (Illumina, San Diego, CA, United States) at the National Genome Analysis Center (CNAG, Barcelona, Spain).

Bioinformatics and Data Acquisition

De-multiplexed fastq raw sequence files per forward and reverse reads were provided by CNAG. The total number of Illumina read-pairs for all 48 samples ranged between 172,495 and 1,993,577 with an average of 402,849 ± 54,069 (mean ± SEM) (**Supplementary Table S5**). We trimmed adapters and low-quality reads with default settings (Phred score < 20) of paired-end reads with Trim Galore! (v.0.4.4_dev,

[1]https://www.ncbi.nlm.nih.gov/assembly/GCF_000233375.1

[2]https://salmobase.org/genome_browser

[3]https://uswest.ensembl.org/Salmo_salar/Info/Index

[4]http://www.softberry.com

Babraham Bioinformatics) (Krueger, 2018), and checked the quality with MultiQC (v.1.9) (Ewels et al., 2016). We utilized Bismark (v.0.20.0) to generate an *in silico* bisulfite converted Atlantic salmon genome reference with the *bismark_genome_preparation* command (Krueger and Andrews, 2011). Specifically, we concatenated the genome sequences of five chromosomes that contain the loci of the six target genes (ssa03/NC_027302.1, ssa04/NC_027303.1, ssa09/NC_027308.1, ssa14/NC_027313.1, and ssa16/NC_027315.1; downloaded from NCBI in January 2019) to obtain a shorter bisulfite converted genome reference and minimize the alignment processing time. The trimmed reads were aligned against this customized bisulfite converted genome reference using Bismark (Krueger and Andrews, 2011). The alignment performed was un-directional for paired-end reads using a minimum alignment function of "*f(x) = 0 + −0.4*x (x = read length)*." Mapping efficiencies were 79% on average, with a total average number of 245,102 ± 5,507 (mean ± SEM) mapped read-pairs for all samples (**Supplementary Table S5**). Finally, we extracted the methylation values with the *bismark_methylation_extractor* (v0.19.0) tool. The bisulfite conversion ratios were within the necessary range of 99.2–99.5% (**Supplementary Table S5**). Further calculations were performed in R (*v3.6.0.*) (R Core Team, 2018). The coverage per CpG position was calculated as "Σ *methylated Cs + non-methylated Cs*" and reads with a coverage of <5 were filtered out. The percentage of methylation (%) for each CpG position was determined using the equation "*CpG methylation (%) = (methylated Cs/coverage) *100*." To localize the exact position of the 94 CpGs within each chromosome, we utilized the *GenomicRanges* package (v3.8 Bioconductor) in R (Lawrence et al., 2013; **Figure 2** and **Supplementary Table S4**). We achieved a high coverage with an average of 35,983 ± 2071 reads over all genes (**Supplementary Table S6**), which was evenly distributed across samples (**Supplementary Figure S1**) but more variable across genes (**Supplementary Figure S2**). Overall, gene methylation levels ranged between 0 and 100%. The genes s*erpinh1* (92.3 ± 0.17%) and *pdk3* (26.6 ± 0.69%) had high average methylation percentages, while *jund* (0.7 ± 0.02%), *ucp2* (0.5 ± 0.02%), *cirbp* (0.5 ± 0.01%), and *prdx6* (1.4 ± 0.07%) showed low DNA methylation levels (**Supplementary Figure S3** and **Supplementary Table S6**).

Gene Expression Data Acquisition

The precise methods used for RNA extraction, cDNA synthesis and gene expression analysis can be found in Beemelmanns et al. (2020) (see **Supplementary Methods** and **Supplementary Table S7**), and were conducted according to previous established protocols (Xu et al., 2013; Booman et al., 2014; Caballero-Solares et al., 2017; Eslamloo et al., 2017). The mRNA transcript levels of six target genes (*cirbp*, *jund*, *pdk3*, *prdx6, serpinh1*, and *ucp2*) and two normalizer genes [60S ribosomal protein L32 (*rpl32*, BT043656); eukaryotic translation initiation factor 3 subunit D (*eif3d,* GE777139)] (Xue et al., 2015; Eslamloo et al., 2017) were obtained using the Fluidigm Biomark^{TM} HD system (96.96 dynamic arrays) according to the protocol described in Beemelmanns and Roth (2016) and Beemelmanns et al. (2020) (**Supplementary Methods** and **Supplementary Table S7**). For the current study, we re-used the mean threshold cycle (C_T) values of these 8 genes from 48 liver samples of the same experimental fish (Fish ID: $^{\#}$73–$^{\#}$120) that were measured previously as part of the larger MICCSA project (Beemelmanns et al., 2020). This dataset which contains the C_T values for all samples, including those of the current study, is accessible on-line at https://doi.org/10.1594/PANGAEA.913696. In our previous geNorm analysis with qBase+ (Hellemans et al., 2007) the two reference genes *rpl32* (geNorm M = 0.302) and *eif3d* (geNorm M = 0.313) were determined as a stable combination for normalization purposes of this dataset (geNorm V = 0.115) (Beemelmanns et al., 2020; **Supplementary Methods** and **Supplementary Table S7**). Hence, the relative quantity (RQ) of expression was determined for each target gene through the normalization to the geometric mean (C_T values) of the endogenous reference genes *rpl32* and *eif3d*, including the primer amplification efficiencies (Beemelmanns et al., 2020; **Supplementary Methods**), and setting the sample with the lowest expression level as the calibrator (RQ = 1.0) (Hellemans et al., 2007).

Statistical Analyses

Univariate Statistics

All statistical tests and visualizations were performed in the R environment (*v3.6.0.*) (R Core Team, 2018). The differences in CpG methylation levels between the treatment groups were assessed using linear mixed-effect models by applying the *lmer* function implemented in the *lme4* (Bates et al., 2014) and *lmerTest* packages of R (Kuznetsova et al., 2017). Our statistical models were computed to test the effects of "treatment" and "sex" (fixed factors) on the DNA methylation of individual CpGs. We included "tank" as a random term to account for variation between tank replicates (tank effect) and to consider the mixed genetic background (unknown kinship) of randomly assigned fish among tanks. For each *lmer*, the residual distribution and the fit were examined, and values were $\log_2$ or arcsine transformed to fulfill assumptions for normality when necessary. Finally, models that identified significant effects were followed by a least square means *post-hoc* test with Tukey's method for p-value adjustment for multiple comparisons by applying the *lsmeans* function in R (Lenth, 2016).

Multivariate Statistics

To compare the CpG methylation, and the corresponding transcript expression profiles, of fish from the CT, WN, and WH groups at the two exposure time points, we performed PCAs using the *ade4* package in R (Dray et al., 2015). During the univariate statistical analysis, we identified CpGs that were responsive to the treatment and defined as significantly affected at $p < 0.05$ or showed a trend with $0.05 < p < 0.10$ for either of the exposure time points (**Table 2** and **Supplementary Table S2**). We only included the values of a selection of responsive CpGs to draw PCAs for each gene and exposure time point individually, since we found different sets of responsive CpGs depending on the exposure time (**Figures 3**, **4**, and **Table 2**). Finally, PCAs were projected based on the methylation levels of all significantly affected CpGs ($p < 0.05$), as well as for all corresponding transcript expression levels [relative quantity–(RQ)] for both exposure time points (**Figure 5** and **Table 2**). We considered

the approach of dimensionality reduction via the PCA method as the most appropriate way to deal with our high-dimensional data because of its potential to reduce noise while preserving the global structure (Nguyen and Holmes, 2019). Accordingly, for each PCA, we plotted the PC-1 and PC-2 that accounted for most of the model variation to obtain a projection of the whole dataset onto a small dimension. To statistically test differences in cluster distribution between the treatments within the PCA, we extracted the scores of PC-1 and PC-2, and fitted for each of them a linear mixed-effect model as described in the previous paragraph (see **Supplementary Table S1**).

Correlation Analysis

To investigate the effects of DNA methylation on the regulation of gene expression, we followed three different statistical approaches. First, we performed a PCA based on the overall relative transcript expression values (RQ) for the six genes and correlated the extracted score values with those of the global CpG methylation PCAs using Pearson correlation coefficients (R). Specifically, the PC-1 scores from the global CpG methylation PCA were correlated with PC-1 scores of the transcript expression PCA for both time points (**Figures 5C,F**). Second, we applied the *epPCA.inference.battery* command of the package *InPosition* in R (Beaton et al., 2014), which allows for the simultaneous assessment of the relationship between CpG methylation and transcript expression responses in component maps (**Figure 6**). The incorporated battery of inference permutation tests calculated the significance of the components, and the magnitude of component scores per response variable was visualized through circle and label size (Beaton et al., 2014). Finally, we estimated significant positive or negative correlations between individual CpG methylation and RQ-values for each gene (*cirbp*, *jund*, *pdk3*, *prdx6*, *serpinh1*, and *ucp2*) with Spearman's rank correlation coefficients (R) (**Figure 7**, **Table 2**, and **Supplementary Table S2**).

DATA AVAILABILITY STATEMENT

The datasets generated for this study can be found in the online repositories. The names of the repository/repositories and accession number(s) can be found below: https://www.ncbi.nlm.nih.gov/geo/, GSE153343; https://doi.org/10.1594/PANGAEA.913696.

ETHICS STATEMENT

The animal study was reviewed and approved by the Institutional Animal Care Committee of Memorial University (NL, Canada) (Protocol #16-90-AG).

AUTHOR CONTRIBUTIONS

AB carried out the experiment and samplings, performed the MBS protocol and bioinformatic sequence analysis, conducted statistical data analyses, interpreted results, and wrote the manuscript. LR contributed to the MBS protocol, provided reagents, and interpreted results. DA assisted with the MBS protocol, supported the bioinformatic sequence and statistical data analyses, and interpreted results. JM-P supported the bioinformatic sequence analysis. FZ contributed to the design of the experiment and carried out the experiment and samplings. MR contributed to the experimental design and the interpretation of the results. AKG conceived the study, designed the experiment, provided reagents, and interpreted results. All authors contributed intellectually, revised, and approved the final manuscript.

FUNDING

Funding for this research was provided to AKG by the Ocean Frontier Institute, through an award from the Canada First Research Excellence Fund (20181007) and was supported by the Spanish Ministry of Science Grants AGL2015-73864-JIN "Ambisex" and RYC2018-024017-I, and an "Interomics" Grant (202030E004) from the Spanish National Research Council (CSIC) to LR. This research was conducted on samples collected through the "Mitigating the Impact of Climate-Related Challenges on Salmon Aquaculture (MICCSA)" project. MICCSA funding was provided by the Atlantic Canada Opportunities Agency (781-9658-205222), Innovate NL (5404-1209-104), and Innovate PEI to AKG.

ACKNOWLEDGMENTS

We thank Brian Dixon for suggesting this pan-Atlantic collaboration and are very grateful to Francesc Piferrer for his collaboration in this project and the use of his lab facility and supplies for MBS library preparation at the Institute of Marine Sciences (ICM) in Barcelona, Spain. We thank the staff of the Dr. Joe Brown Aquatic Research Building (JBARB, Memorial University of Newfoundland, Canada) for assistance with fish husbandry. We are grateful to Rebeccah Sandrelli, MacGregor Parent, Olufemi Ajiboye, Tasha Harrold, and Gord Nash for assistance with sampling, and to Tasha Harrold for her help in managing the "Mitigating the Impact of Climate-Related Challenges on Salmon Aquaculture (MICCSA)" project and Module J2 of the Ocean Frontier Institute. We thank Sílvia Joly and Núria Sánchez-Baizán for their kind assistance in performing the MBS protocol, and Alejandro Valdivieso Muñoz for his intellectual support during MBS data assessment.

SUPPLEMENTARY MATERIAL

The Supplementary Material for this article can be found online at: https://www.frontiersin.org/articles/10.3389/fmars.2020.604878/full#supplementary-material

REFERENCES

Abdel-Tawwab, M., Monier, M. N., Hoseinifar, S. H., and Faggio, C. (2019). Fish response to hypoxia stress: growth, physiological, and immunological biomarkers. *Fish Physiol. Biochem.* 45, 997–1013. doi: 10.1007/s10695-019-00614-9

Aguilera, O., Fernández, A. F., Muñoz, A., and Fraga, M. F. (2010). Epigenetics and environment: a complex relationship. *J. Appl. Physiol.* 109, 243–251. doi: 10.1152/japplphysiol.00068.2010

Akbarzadeh, A., Günther, O. P., Houde, A. L., Li, S., Ming, T. J., Jeffries, K. M., et al. (2018). Developing specific molecular biomarkers for thermal stress in salmonids. *BMC Genomics* 19:749. doi: 10.1186/s12864-018-5108-9

Ambrosi, C., Manzo, M., and Baubec, T. (2017). Dynamics and context-dependent roles of DNA methylation. *J. Mol. Biol.* 429, 1459–1475. doi: 10.1016/j.jmb.2017.02.008

Ambruso, D. R. (2013). Peroxiredoxin-6 and NADPH oxidase activity. *Hydrog. Peroxide Cell Signal. Pt B* 527, 145–167. doi: 10.1016/B978-0-12-405882-8.00008-8

Anastasiadi, D., Díaz, N., and Piferrer, F. (2017). Small ocean temperature increases elicit stage-dependent changes in DNA methylation and gene expression in a fish, the European sea bass. *Sci. Rep.* 7, 1–12. doi: 10.1038/s41598-017-10861-6

Anastasiadi, D., Esteve-Codina, A., and Piferrer, F. (2018a). Consistent inverse correlation between DNA methylation of the first intron and gene expression across tissues and species. *Epigenet. Chromatin* 11:37. doi: 10.1186/s13072-018-0205-1

Anastasiadi, D., Vandeputte, M., Sánchez-Baizán, N., Allal, F., and Piferrer, F. (2018b). Dynamic epimarks in sex-related genes predict gonad phenotype in the European sea bass, a fish with mixed genetic and environmental sex determination. *Epigenetics* 13, 988–1011. doi: 10.1080/15592294.2018.1529504

Anastasiadi, D., and Piferrer, F. (2020). A clockwork fish: age prediction using DNA methylation-based biomarkers in the European seabass. *Mol. Ecol. Resour.* 20, 387–397. doi: 10.1111/1755-0998.13111

Anastasiadi, D., Shao, C., Chen, S., and Piferrer, F. (in press). Footprints of global change in marine life: inferring past developmental temperature based on DNA methylation and gene expression marks. *Mol. Ecol.* doi: 10.1111/mec.15764

Angers, B., Castonguay, E., and Rachel, M. (2010). Environmentally induced phenotypes and DNA methylation: how to deal with unpredictable conditions until the next generation and after. *Mol. Ecol.* 19, 1283–1295. doi: 10.1111/j.1365-294X.2010.04580.x

Araya, I., Nardocci, G., Morales, J. P., Vera, M. I., Molina, A., and Alvarez, M. (2010). MacroH2A subtypes contribute antagonistically to the transcriptional regulation of the ribosomal cistron during seasonal acclimatization of the carp fish. *Epigenet. Chromatin* 3:14. doi: 10.1186/1756-8935-3-14

Ball, M. P., Li, J. B., Gao, Y., Lee, J.-H., LeProust, E. M., Park, I.-H., et al. (2009). Targeted and genome-scale strategies reveal gene-body methylation signatures in human cells. *Nat. Biotechnol.* 27:361. doi: 10.1038/nbt.1533

Bates, D., Maechler, M., Bolker, B., and Walker, S. (2014). *lme4: Linear Mixed-Effects Models Using Eigen and S4. R Packag. Version 1, 1–23.*

Baubec, T., and Schübeler, D. (2014). Genomic patterns and context specific interpretation of DNA methylation. *Curr. Opin. Genet. Dev.* 25, 85–92. doi: 10.1016/j.gde.2013.11.015

Beal, A., Rodriguez-Casariego, J., Rivera-Casas, C., Suarez-Ulloa, V., and Eirin-Lopez, J. M. (2018). "Environmental epigenomics and its applications in marine organisms," in *Population Genomics: Marine Organisms*, eds M. F. Oleksiak and O. P. Rajora (Berlin: Springer), 325–359. doi: 10.1007/13836_2018_28

Beaman, J. E., White, C. R., and Seebacher, F. (2016). Evolution of plasticity: mechanistic link between development and reversible acclimation. *Trends Ecol. Evol.* 31, 237–249. doi: 10.1016/j.tree.2016.01.004

Beaton, D., Chin Fatt, C. R., and Abdi, H. (2014). An ExPosition of multivariate analysis with the singular value decomposition in R. *Comput. Stat. Data Anal.* 72, 176–189. doi: 10.1016/j.csda.2013.11.006

Beemelmanns, A., and Roth, O. (2016). Biparental immune priming in the pipefish *Syngnathus typhle*. *Zoology* 119, 262–272. doi: 10.1016/j.zool.2016.06.002

Beemelmanns, A., Zanuzzo, F. S., Xue, X., Sandrelli, R. M., Rise, M. L., and Gamperl, A. K. (2020). Transcriptomic responses of Atlantic salmon (*Salmo salar*) to high temperature stress alone, or in combination with moderate hypoxia. *ResearchSquare* [Preprint]. Available online at: https://www.researchsquare.com/article/rs-38228/v1

Best, C., Ikert, H., Kostyniuk, D. J., Craig, P. M., Navarro-Martin, L., Marandel, L., et al. (2018). Epigenetics in teleost fish: from molecular mechanisms to physiological phenotypes. *Comp. Biochem. Physiol. Part B Biochem. Mol. Biol.* 224, 210–244. doi: 10.1016/j.cbpb.2018.01.006

Bird, A. (2002). DNA methylation patterns and epigenetic memory. *Genes Dev.* 16, 6–21. doi: 10.1101/gad.947102.6

Bogdanović, O., Smits, A. H., de la Calle Mustienes, E., Tena, J. J., Ford, E., Williams, R., et al. (2016). Active DNA demethylation at enhancers during the vertebrate phylotypic period. *Nat. Genet.* 48, 417–426. doi: 10.1038/ng.3522

Booman, M., Xu, Q., and Rise, M. L. (2014). Evaluation of the impact of camelina oil-containing diets on the expression of genes involved in the innate anti-viral immune response in Atlantic cod (*Gadus morhua*). *Fish Shellfish Immunol.* 41, 52–63. doi: 10.1016/j.fsi.2014.05.017

Brand, M. D., and Esteves, T. C. (2005). Physiological functions of the mitochondrial uncoupling proteins UCP2 and UCP3. *Cell Metab.* 2, 85–93. doi: 10.1016/j.cmet.2005.06.002

Breitburg, D., Levin, L. A., Oschlies, A., Grégoire, M., Chavez, F. P., Conley, D. J., et al. (2018). Declining oxygen in the global ocean and coastal waters. *Science* 359:eaam7240. doi: 10.1126/science.aam7240

Brett, J. R. (1956). Some principles in the thermal requirements of fishes. *Q. Rev. Biol.* 31, 75–87. doi: 10.1086/401257

Brett, J. R. (1971). Energetic responses of salmon to temperature. A study of some thermal relations in the physiology and freshwater ecology of sockeye salmon (*Oncorhynchus nerkd*). *Am. Zool.* 11, 99–113. doi: 10.1093/icb/11.1.99

Burgerhout, E., Mommens, M., Johnsen, H., Aunsmo, A., Santi, N., and Andersen, Ø. (2017). Genetic background and embryonic temperature affect DNA methylation and expression of myogenin and muscle development in Atlantic salmon (*Salmo salar*). *PLoS One* 12:e0179918. doi: 10.1371/journal.pone.0179918

Burke, H., Gardner, I., and Farrell, A. P. (2020). *A review of the 2019 Newfoundland and Labrador South Coast cultured Atlantic salmon mortality event*. Department of Fisheries and Land Resources, Government of Newfoundland and Labrador, *Special Studies and Reports*. Available online at: https://www.gov.nl.ca/ffa/files/publications-pdf-2019-salmon-review-final-report.pdf

Burt, K., Hamoutene, D., Mabrouk, G., Lang, C., Puestow, T., Drover, D., et al. (2012). Environmental conditions and occurrence of hypoxia within production cages of Atlantic salmon on the south coast of Newfoundland. *Aquac. Res.* 43, 607–620. doi: 10.1111/j.1365-2109.2011.02867.x

Burt, K., Hamoutene, D., Perez-Casanova, J., Gamperl, A. K., and Volkoff, H. (2013). The effect of intermittent hypoxia on growth, appetite and some aspects of the immune response of Atlantic salmon (*Salmo salar*). *Aquac. Res.* 45, 124–137. doi: 10.1111/j.1365-2109.2012.03211.x

Caballero-Huertas, M., Moraleda-Prados, J., Joly, S., and Ribas, L. (2020). Immune genes, *IL1β* and *Casp9*, show sexual dimorphic methylation patterns in zebrafish gonads. *Fish Shellfish Immunol.* 97, 648–655. doi: 10.1016/j.fsi.2019.12.013

Caballero-Solares, A., Hall, J. R., Xue, X., Eslamloo, K., Taylor, R. G., Parrish, C. C., et al. (2017). The dietary replacement of marine ingredients by terrestrial animal and plant alternatives modulates the antiviral immune response of Atlantic salmon (*Salmo salar*). *Fish Shellfish Immunol.* 64, 24–38. doi: 10.1016/j.fsi.2017.02.040

Campos, C., Sundaram, A. Y., Valente, L. M., Conceição, L. E., Engrola, S., and Fernandes, J. M. (2014). Thermal plasticity of the miRNA transcriptome during Senegalese sole development. *BMC Genomics* 15:525. doi: 10.1186/1471-2164-15-525

Campos, C., Valente, L., Conceição, L., Engrola, S., and Fernandes, J. (2013). Temperature affects methylation of the myogenin putative promoter, its expression and muscle cellularity in Senegalese sole larvae. *Epigenetics* 8, 389–397. doi: 10.4161/epi.24178

Cheung, W. A., Shao, X., Morin, A., Siroux, V., Kwan, T., Ge, B., et al. (2017). Functional variation in allelic methylomes underscores a strong genetic contribution and reveals novel epigenetic alterations in the human epigenome. *Genome Biol.* 18:50. doi: 10.1186/s13059-017-1173-7

Claret, M., Galbraith, E. D., Palter, J. B., Bianchi, D., Fennel, K., Gilbert, D., et al. (2018). Rapid coastal deoxygenation due to ocean circulation shift in the

northwest Atlantic. *Nat. Clim. Chang.* 8, 868–872. doi: 10.1038/s41558-018-0263-1

Cortese, R., Hartmann, O., Berlin, K., and Eckhardt, F. (2008). Correlative gene expression and DNA methylation profiling in lung development nominate new biomarkers in lung cancer. *Int. J. Biochem. Cell Biol.* 40, 1494–1508. doi: 10.1016/j.biocel.2007.11.018

Crozier, L. G., and Hutchings, J. A. (2014). Plastic and evolutionary responses to climate change in fish. *Evol. Appl.* 7, 68–87. doi: 10.1111/eva.12135

Currie, S., and Schulte, P. M. (2014). *Thermal Stress*, 4th Edn. Raton, FL: CRC Press.

De Paoli-Iseppi, R., Deagle, B. E., Polanowski, A. M., McMahon, C. R., Dickinson, J. L., Hindell, M. A., et al. (2019). Age estimation in a long-lived seabird (*Ardenna tenuirostris*) using DNA methylation-based biomarkers. *Mol. Ecol. Resour.* 19, 411–425. doi: 10.1111/1755-0998.12981

Dray, S., Dufour, A. B., and Thioulouse, J. (2015). *ade4: Analysis of Ecological Data: Exploratory and Euclidean Methods in Environmental Sciences. R Package Version 1.7–2.*

Edwards, J. R., Yarychkivska, O., Boulard, M., and Bestor, T. H. (2017). DNA methylation and DNA methyltransferases. *Epigenet. Chromatin* 10:23. doi: 10.1186/s13072-017-0130-8

Eirin-Lopez, J. M., and Putnam, H. M. (2019). Marine environmental epigenetics. *Ann. Rev. Mar. Sci.* 11, 335–368. doi: 10.1146/annurev-marine-010318-095114

Eslamloo, K., Xue, X., Hall, J. R., Smith, N. C., Caballero-Solares, A., Parrish, C. C., et al. (2017). Transcriptome profiling of antiviral immune and dietary fatty acid dependent responses of Atlantic salmon macrophage-like cells. *BMC Genomics* 18:706. doi: 10.1186/s12864-017-4099-2

Ewels, P., Magnusson, M., Lundin, S., and Käller, M. (2016). MultiQC: summarize analysis results for multiple tools and samples in a single report. *Bioinformatics* 32, 3047–3048. doi: 10.1093/bioinformatics/btw354

Faulk, C., and Dolinoy, D. C. (2011). Timing is everything: the when and how of environmentally induced changes in the epigenome of animals. *Epigenetics* 6, 791–797. doi: 10.4161/epi.6.7.16209

Frölicher, T. L., Fischer, E. M., and Gruber, N. (2018). Marine heatwaves under global warming. *Nature* 560, 360–364. doi: 10.1038/s41586-018-0383-9

Gamperl, A. K., Ajiboye, O. O., Zanuzzo, F. S., Sandrelli, R. M., Peroni, E. F. C., and Beemelmanns, A. (2020). The impacts of increasing temperature and moderate hypoxia on the production characteristics, cardiac morphology and haematology of Atlantic Salmon (*Salmo salar*). *Aquaculture* 519:734874. doi: 10.1016/j.aquaculture.2019.734874

Gavery, M. R., and Roberts, S. B. (2017). Epigenetic considerations in aquaculture. *PeerJ* 5:e4147. doi: 10.7717/peerj.4147

Gerber, L., Clow, K. A., Mark, F. C., and Gamperl, A. K. (2020). Improved mitochondrial function in salmon (*Salmo salar*) following high temperature acclimation suggests that there are cracks in the proverbial 'ceiling'. *Sci. Rep.* doi: 10.1038/s41598-020-78519-4

Granada, L., Lemos, M. F. L., Cabral, H. N., Bossier, P., and Novais, S. C. (2018). Epigenetics in aquaculture – the last frontier. *Rev. Aquac.* 10, 994–1013. doi: 10.1111/raq.12219

Han, B., Li, W., Chen, Z., Xu, Q., Luo, J., Shi, Y., et al. (2016). Variation of DNA methylome of zebrafish cells under cold pressure. *PLoS One* 11:e0160358. doi: 10.1371/journal.pone.0160358

Hancock, R. L., Dunne, K., Walport, L. J., Flashman, E., and Kawamura, A. (2015). Epigenetic regulation by histone demethylases in hypoxia. *Epigenomics* 7, 791–811. doi: 10.2217/epi.15.24

Hazel, J. R., and Prosser, C. L. (1974). Molecular mechanisms of temperature compensation in poikilotherms. *Physiol. Rev.* 54, 620–677. doi: 10.1152/physrev.1974.54.3.620

Heijmans, B. T., Tobi, E. W., Stein, A. D., Putter, H., Blauw, G. J., Susser, E. S., et al. (2008). Persistent epigenetic differences associated with prenatal exposure to famine in humans. *Proc. Natl. Acad. Sci. U.S.A.* 105, 17046–17049. doi: 10.1073/pnas.0806560105

Hellemans, J., Mortier, G., De Paepe, A., Speleman, F., and Vandesompele, J. (2007). qBase relative quantification framework and software for management and automated analysis of real-time quantitative PCR data. *Genome Biol.* 8:R19. doi: 10.1186/gb-2007-8-2-r19

Horvath, S. (2013). DNA methylation age of human tissues and cell types. *Genome Biol.* 14:R115. doi: 10.1186/gb-2013-14-10-r115

Hosomichi, K., Mitsunaga, S., Nagasaki, H., and Inoue, I. (2014). A Bead-based Normalization for Uniform Sequencing depth (BeNUS) protocol for multi-samples sequencing exemplified by HLA-B. *BMC Genomics* 15:645. doi: 10.1186/1471-2164-15-645

Houde, A. L. S., Akbarzadeh, A., Günther, O. P., Li, S., Patterson, D. A., Farrell, A. P., et al. (2019). Salmonid gene expression biomarkers indicative of physiological responses to changes in salinity and temperature, but not dissolved oxygen. *J. Exp. Biol.* 222:jeb198036. doi: 10.1242/jeb.198036

Huang, C., Chen, N., Wu, X.-J., Huang, C.-H., He, Y., Tang, R., et al. (2015). The zebrafish miR-462/miR-731 cluster is induced under hypoxic stress via hypoxia-inducible factor 1α and functions in cellular adaptations. *FASEB J.* 29, 4901–4913. doi: 10.1096/fj.14-267104

Hughes, G. M. (1973). Respiratory responses to hypoxia in fish. *Am. Zool.* 13, 475–489. doi: 10.1093/icb/13.2.475

Hvas, M., Folkedal, O., Imsland, A., and Oppedal, F. (2017). The effect of thermal acclimation on aerobic scope and critical swimming speed in Atlantic salmon, *Salmo salar*. *J. Exp. Biol.* 220, 2757–2764. doi: 10.1242/jeb.154021

IPCC (2019). "Summary for policymakers," in *IPCC Special Report on the Ocean and Cryosphere in a Changing Climate*, eds H.-O. Pörtner, D. C. Roberts, V. Masson-Delmotte, P. Zhai, M. Tignor, E. Poloczanska, et al. (Geneva: IPCC).

Ishida, Y., and Nagata, K. (2011). "Hsp47 as a collagen-specific molecular chaperon," in *Methods in Enzymology*, eds J. Abelson, M. Simon, G. Verdine, and A. Pyle (Cambridge, MA: Academic Press), 167–182. doi: 10.1016/b978-0-12-386471-0.00009-2

Jablonka, E., and Raz, G. (2009). Transgenerational epigenetic inheritance: prevalence, mechanisms, and implications for the study of heredity and evolution. *Q. Rev. Biol.* 84, 131–176. doi: 10.1086/598822

Jaenisch, R., and Bird, A. (2003). Epigenetic regulation of gene expression: how the genome integrates intrinsic and environmental signals. *Nat. Genet.* 33, 245–254. doi: 10.1038/ng1089

Jones, P. A. (2001). The role of DNA methylation in mammalian epigenetics. *Science* 293, 1068–1070. doi: 10.1126/science.1063852

Jones, P. A. (2012). Functions of DNA methylation: islands, start sites, gene bodies and beyond. *Nat. Rev. Genet.* 13, 484–492. doi: 10.1038/nrg3230

Kilkenny, C., Browne, W. J., Cuthill, I. C., Emerson, M., and Altman, D. G. (2010). Improving bioscience research reporting: the ARRIVE guidelines for reporting animal research. *PLoS Biol.* 8:e1000412. doi: 10.1371/journal.pbio.1000412

Knudsen, S. (1999). Promoter2.0: for the recognition of PolII promoter sequences. *Bioinformatics* 15, 356–361. doi: 10.1093/bioinformatics/15.5.356

Krueger, F. (2018). *Trim Galore, Babraham Bioinformatics*. Available online at: http://www.bioinformatics.babraham.ac.uk/projects/trim_galore/ (accessed January, 2019).

Krueger, F., and Andrews, S. R. (2011). Bismark: a flexible aligner and methylation caller for Bisulfite-Seq applications. *Bioinformatics* 27, 1571–1572. doi: 10.1093/bioinformatics/btr167

Kuntz, M. J., and Harris, R. A. (2018). "Pyruvate dehydrogenase kinase," in *Encyclopedia of Signaling Molecules*, ed. S. Choi (New York, NY: Springer). doi: 10.1007/978-1-4614-6438-9_101636-2

Kuznetsova, A., Brockhoff, P. B., and Christensen, R. H. B. (2017). lmerTest package: tests in linear mixed effects models. *J. Stat. Softw.* 82, 1–26. doi: 10.18637/jss.v082.i13

Larsen, P. F., Schulte, P. M., and Nielsen, E. E. (2011). Gene expression analysis for the identification of selection and local adaptation in fishes. *J. Fish Biol.* 78, 1–22. doi: 10.1111/j.1095-8649.2010.02834.x

Laskowski, M., Augustynek, B., Kulawiak, B., Koprowski, P., Bednarczyk, P., Jarmuszkiewicz, W., et al. (2016). What do we not know about mitochondrial potassium channels? *Biochim. Biophys. Acta Bioenerg.* 1857, 1247–1257. doi: 10.1016/j.bbabio.2016.03.007

Lau, K., Lai, K. P., Bao, J. Y. J., Zhang, N., Tse, A., Tong, A., et al. (2014). Identification and expression profiling of MicroRNAs in the brain, liver and gonads of marine medaka (*Oryzias melastigma*) and in response to hypoxia. *PLoS One* 9:e110698. doi: 10.1371/journal.pone.0110698

Lawrence, M., Huber, W., Pagès, H., Aboyoun, P., Carlson, M., Gentleman, R., et al. (2013). Software for computing and annotating genomic ranges. *PLoS Comput. Biol.* 9:e1003118. doi: 10.1371/journal.pcbi.1003118

Lenth, R. V. (2016). Least-squares means: the R package lsmeans. *J. Stat. Sofw.* 69, 1–33.

Li, L.-C., and Dahiya, R. (2002). MethPrimer: designing primers for methylation PCRs. *Bioinformatics* 18, 1427–1431. doi: 10.1093/bioinformatics/18.11.1427

Li, S., He, F., Wen, H., Li, J., Si, Y., Liu, M., et al. (2017). Low salinity affects cellularity, DNA methylation, and mRNA expression of igf1 in the liver of half smooth tongue sole (*Cynoglossus semilaevis*). *Fish Physiol. Biochem.* 43, 1587–1602. doi: 10.1007/s10695-017-0395-7

Lien, S., Koop, B. F., Sandve, S. R., Miller, J. R., Kent, M. P., Nome, T., et al. (2016). The Atlantic salmon genome provides insights into rediploidization. *Nature* 533, 200–205. doi: 10.1038/nature17164

Liu, W., Xie, Y., Ma, J., Luo, X., Nie, P., Zuo, Z., et al. (2015). IBS: an illustrator for the presentation and visualization of biological sequences. *Bioinformatics* 31, 3359–3361. doi: 10.1093/bioinformatics/btv362

Madeira, D., Vinagre, C., and Diniz, M. S. (2016). Are fish in hot water? Effects of warming on oxidative stress metabolism in the commercial species *Sparus aurata*. *Ecol. Indic.* 63, 324–331. doi: 10.1016/j.ecolind.2015.12.008

McCaw, B., Stevenson, T. J., and Lancaster, L. T. (2020). Epigenetic responses to temperature and climate. *Integr. Comp. Biol.* 1–12. doi: 10.1093/icb/icaa049

McGaughey, D. M., Abaan, H. O., Miller, R. M., Kropp, P. A., and Brody, L. C. (2014). Genomics of CpG methylation in developing and developed zebrafish. *G3 Genes Genomes Genet.* 4, 861–869. doi: 10.1534/g3.113.009514

Metzger, D. C. H., and Schulte, P. M. (2017). Persistent and plastic effects of temperature on DNA methylation across the genome of threespine stickleback (*Gasterosteus aculeatus*). *Proc. R. Soc. B Biol. Sci.* 284:20171667. doi: 10.1098/rspb.2017.1667

Mikeska, T., and Craig, J. (2014). DNA methylation biomarkers: cancer and beyond. *Genes* 5, 821–864. doi: 10.3390/genes5030821

Mirbahai, L., and Chipman, J. K. (2014). Epigenetic memory of environmental organisms: a reflection of lifetime stressor exposures. *Mutat. Res. Genet. Toxicol. Environ. Mutagen.* 76, 10–17. doi: 10.1016/j.mrgentox.2013.10.003

Moghadam, H. K., Johnsen, H., Robinson, N., Andersen, Ø, Jørgensen, E. H., Johnsen, H. K., et al. (2017). Impacts of early life stress on the methylome and transcriptome of atlantic salmon. *Sci. Rep.* 7, 1–11. doi: 10.1038/s41598-017-05222-2

Moraleda-Prados, J., Caballero-Huertas, M., Valdivieso, V., Joly, S., Ji, J., Roher, N., et al. (2021). Immune stimulation during sex differentiation alters epigenetics and can induce feminization in a dose-dependent manner in fish. *Dev. Comp. Immunol.* 114:103848. doi: 10.1016/j.dci.2020.103848

Nelson, A. C., Cauceglia, J. W., Merkley, S. D., Youngson, N. A., Oler, A. J., Nelson, R. J., et al. (2013). Reintroducing domesticated wild mice to sociality induces adaptive transgenerational effects on MUP expression. *Proc. Natl. Acad. Sci. U.S.A.* 110, 19848–19853. doi: 10.1073/pnas.1310427110

Nguyen, L. H., and Holmes, S. (2019). Ten quick tips for effective dimensionality reduction. *PLoS Comput. Biol.* 15:e1006907. doi: 10.1371/journal.pcbi.1006907

O'Dea, R. E., Noble, D. W. A., Johnson, S. L., Hesselson, D., and Nakagawa, S. (2016). The role of non-genetic inheritance in evolutionary rescue: epigenetic buffering, heritable bet hedging and epigenetic traps. *Environ. Epigenetics* 2:1. doi: 10.1093/eep/dvv014

Oliver, E. C. J., Donat, M. G., Burrows, M. T., Moore, P. J., Smale, D. A., Alexander, L. V., et al. (2018). Longer and more frequent marine heatwaves over the past century. *Nat. Commun.* 9:1324. doi: 10.1038/s41467-018-03732-9

Pérez, R. F., Santamarina, P., Tejedor, J. R., Urdinguio, R. G., Álvarez-Pitti, J., Redon, P., et al. (2019). Longitudinal genome-wide DNA methylation analysis uncovers persistent early-life DNA methylation changes. *J. Transl. Med.* 17:15. doi: 10.1186/s12967-018-1751-9

Piferrer, F. (2018). "Epigenetics of sex determination and differentiation in fish," in *Sex Control in Aquaculture*, eds H. Wang, S. Chen, Z.-G. Shen, and F. Piferrer (Chichester, UK: John Wiley & Sons, Ltd), 65–83. doi: 10.1002/9781119127291.ch3

Podgorniak, T., Brockmann, S., Konstantinidis, I., and Fernandes, J. M. O. (2019). Differences in the fast muscle methylome provide insight into sex-specific epigenetic regulation of growth in Nile tilapia during early stages of domestication. *Epigenetics* 14, 818–836. doi: 10.1080/15592294.2019.1618164

Polanowski, A. M., Robbins, J., Chandler, D., and Jarman, S. N. (2014). Epigenetic estimation of age in humpback whales. *Mol. Ecol. Resour.* 14, 976–987. doi: 10.1111/1755-0998.12247

R Core Team (2018). *R: A Language and Environment for Statistical Computing*. Available online at: http://www.r-project.org/ (accessed January, 2019).

Rohland, N., and Reich, D. (2012). Cost-effective, high-throughput DNA sequencing libraries for multiplexed target capture. *Genome Res.* 22, 939–946. doi: 10.1101/gr.128124.111

Ryu, T., Veilleux, H. D., Donelson, J. M., Munday, P. L., and Ravasi, T. (2018). The epigenetic landscape of transgenerational acclimation to ocean warming. *Nat. Clim. Chang.* 8, 504–509. doi: 10.1038/s41558-018-0159-0

Ryu, T., Veilleux, H. D., Munday, P. L., Jung, I., Donelson, J. M., and Ravasi, T. (2020). An epigenetic signature for within-generational plasticity of a reef fish to ocean warming. *Front. Mar. Sci.* 7:284. doi: 10.3389/fmars.2020.00284

Seebacher, F., White, C. R., and Franklin, C. E. (2015). Physiological plasticity increases resilience of ectothermic animals to climate change. *Nat. Clim. Chang.* 5, 61–66. doi: 10.1038/nclimate2457

Seisenberger, S., Peat, J. R., Hore, T. A., Santos, F., Dean, W., and Reik, W. (2013). Reprogramming DNA methylation in the mammalian life cycle: building and breaking epigenetic barriers. *Philos. Trans. R. Soc. B Biol. Sci.* 368:20110330. doi: 10.1098/rstb.2011.0330

Simonet, N., Reyes, M., Nardocci, G., Molina, A., and Alvarez, M. (2013). Epigenetic regulation of the ribosomal cistron seasonally modulates enrichment of H2A.Z and H2A.Zub in response to different environmental inputs in carp (*Cyprinus carpio*). *Epigenet. Chromatin* 6:22. doi: 10.1186/1756-8935-6-22

Smith, J., Sen, S., Weeks, R. J., Eccles, M. R., and Chatterjee, A. (2020). Promoter DNA hypermethylation and paradoxical gene activation. *Trends Cancer* 6, 392–406. doi: 10.1016/j.trecan.2020.02.007

Solovyev, V. V., Shahmuradov, I. A., and Salamov, A. A. (2010). *Identification of Promoter Regions and Regulatory Sites*. Cham: Springer.

Somero, G. N. (2010). The physiology of climate change: how potentials for acclimatization and genetic adaptation will determine "winners" and "losers.". *J. Exp. Biol.* 213, 912–920. doi: 10.1242/jeb.037473

Stehfest, K. M., Carter, C. G., McAllister, J. D., Ross, J. D., and Semmens, J. M. (2017). Response of Atlantic salmon *Salmo salar* to temperature and dissolved oxygen extremes established using animal-borne environmental sensors. *Sci. Rep.* 7:4545. doi: 10.1038/s41598-017-04806-2

Szyf, M. (2015). Nongenetic inheritance and transgenerational epigenetics. *Trends Mol. Med.* 21, 134–144. doi: 10.1016/j.molmed.2014.12.004

Tierney, K. B., Farrell, A. P., and Brauner, C. J. (2013). *Fish Physiology: Organic Chemical Toxicology of Fishes*. Cambridge, MA: Academic Press.

Toraño, E. G., García, M. G., Fernández-Morera, J. L., Niño-García, P., and Fernández, A. F. (2016). The impact of external factors on the epigenome: in utero and over lifetime. *Biomed Res. Int.* 2016, 1–17. doi: 10.1155/2016/2568635

Turner, B. M. (2009). Epigenetic responses to environmental change and their evolutionary implications. *Philos. Trans. R. Soc. B Biol. Sci.* 364, 3403–3418. doi: 10.1098/rstb.2009.0125

Untergasser, A., Cutcutache, I., Koressaar, T., Ye, J., Faircloth, B. C., Remm, M., et al. (2012). Primer3–new capabilities and interfaces. *Nucleic Acids Res.* 40:e115. doi: 10.1093/nar/gks596

Uren Webster, T. M., Rodriguez-Barreto, D., Martin, S. A. M., Van Oosterhout, C., Orozco-terWengel, P., Cable, J., et al. (2018). Contrasting effects of acute and chronic stress on the transcriptome, epigenome, and immune response of Atlantic salmon. *Epigenetics* 13, 1191–1207. doi: 10.1080/15592294.2018.1554520

Valdivieso, A., Ribas, L., Monleón-Getino, A., Orbán, L., and Piferrer, F. (2020). Exposure of zebrafish to elevated temperature induces sex ratio shifts and alterations in the testicular epigenome of unexposed offspring. *Environ. Res.* 186:109601. doi: 10.1016/j.envres.2020.109601

Veilleux, H. D., Ryu, T., Donelson, J. M., van Herwerden, L., Seridi, L., Ghosheh, Y., et al. (2015). Molecular processes of transgenerational acclimation to a warming ocean. *Nat. Clim. Chang.* 5, 1074–1078. doi: 10.1038/nclimate2724

Venney, C. J., Wellband, K. W., and Heath, D. D. (2020). Rearing environment affects the genetic architecture and plasticity of DNA methylation in Chinook salmon. *Heredity* doi: 10.1038/s41437-020-0346-4. [Epub ahead of print].

Veron, V., Marandel, L., Liu, J., Vélez, E. J., Lepais, O., Panserat, S., et al. (2018). DNA methylation of the promoter region of *bnip3* and *bnip3l* genes induced by metabolic programming. *BMC Genomics* 19:677. doi: 10.1186/s12864-018-5048-4

Wade, N. M., Clark, T. D., Maynard, B. T., Atherton, S., Wilkinson, R. J., Smullen, R. P., et al. (2019). Effects of an unprecedented summer heatwave on the growth performance, flesh colour and plasma biochemistry of marine cage-farmed

Atlantic salmon (*Salmo salar*). *J. Therm. Biol.* 80, 64–74. doi: 10.1016/j.jtherbio.2018.12.021

Wang, S. Y., Lau, K., Lai, K.-P., Zhang, J.-W., Tse, A. C.-K., Li, J.-W., et al. (2016). Hypoxia causes transgenerational impairments in reproduction of fish. *Nat. Commun.* 7:12114. doi: 10.1038/ncomms12114

Weitzman, J. B., Fiette, L., Matsuo, K., and Yaniv, M. (2000). JunD protects cells from p53-dependent senescence and apoptosis. *Mol. Cell* 6, 1109–1119. doi: 10.1016/S1097-2765(00)00109-X

Xu, Q., Feng, C. Y., Hori, T. S., Plouffe, D. A., Buchanan, J. T., and Rise, M. L. (2013). Family-specific differences in growth rate and hepatic gene expression in juvenile triploid growth hormone (GH) transgenic Atlantic salmon (*Salmo salar*). *Comp. Biochem. Physiol. Pt D Genomics Proteomics* 8, 317–333. doi: 10.1016/j.cbd.2013.09.002

Xue, X., Hixson, S. M., Hori, T. S., Booman, M., Parrish, C. C., Anderson, D. M., et al. (2015). Atlantic salmon (*Salmo salar*) liver transcriptome response to diets containing *Camelina sativa* products. *Comp. Biochem. Physiol. D Genomics Proteomics* 14, 1–15. doi: 10.1016/j.cbd.2015.01.005

Zhang, C., Tong, C., Tian, F., and Zhao, K. (2017). Integrated mRNA and microRNA transcriptome analyses reveal regulation of thermal acclimation in *Gymnocypris przewalskii*: a case study in Tibetan Schizothoracine fish. *PLoS One* 12:e0186433. doi: 10.1371/journal.pone.0186433

Zhang, Y., Zhang, S., Liu, Z., Zhang, L., and Zhang, W. (2013). Epigenetic modifications during sex change repress gonadotropin stimulation of *cyp19a1a* in a teleost ricefield eel (*Monopterus albus*). *Endocrinology* 154, 2881–2890. doi: 10.1210/en.2012-2220

Zheng, J.-L., Guo, S.-N., Yuan, S.-S., Xia, H., Zhu, Q.-L., and Lv, Z.-M. (2017). Preheating mitigates cadmium toxicity in zebrafish livers: evidence from promoter demethylation, gene transcription to biochemical levels. *Aquat. Toxicol.* 190, 104–111. doi: 10.1016/j.aquatox.2017.06.022

Zhong, P., and Huang, H. (2017). Recent progress in the research of cold-inducible RNA-binding protein. *Futur. Sci. OA* 3:FSO246. doi: 10.4155/fsoa-2017-0077

Conflict of Interest: The authors declare that the research was conducted in the absence of any commercial or financial relationships that could be construed as a potential conflict of interest.

Advantages of publishing in Frontiers

OPEN ACCESS
Articles are free to read for greatest visibility and readership

FAST PUBLICATION
Around 90 days from submission to decision

HIGH QUALITY PEER-REVIEW
Rigorous, collaborative, and constructive peer-review

TRANSPARENT PEER-REVIEW
Editors and reviewers acknowledged by name on published articles

Frontiers
Avenue du Tribunal-Fédéral 34
1005 Lausanne | Switzerland

Visit us: www.frontiersin.org
Contact us: frontiersin.org/about/contact

REPRODUCIBILITY OF RESEARCH
Support open data and methods to enhance research reproducibility

DIGITAL PUBLISHING
Articles designed for optimal readership across devices

FOLLOW US
@frontiersin

IMPACT METRICS
Advanced article metrics track visibility across digital media

EXTENSIVE PROMOTION
Marketing and promotion of impactful research

LOOP RESEARCH NETWORK
Our network increases your article's readership